UNIVERSITY OF OKLAHOMA

GRADUATE COLLEGE

IDENTIFICATION OF PIECEWISE FLEXURAL RIGIDITY OF A PRESTRESSED CONCRETE BRIDGE GIRDER

A THESIS

SUBMITTED TO THE GRADUATE FACULTY

in partial fulfillment of the requirements for

the degree of

MASTER OF SCIENCE

By

JOHN M. TOSHIMA
Norman, Oklahoma
2019

IDENTIFICATION OF PIECEWISE FLEXURAL RIGIDITY OF A PRESTRESSED CONCRETE BRIDGE GIRDER

A THESIS APPROVED FOR THE
SCHOOL OF CIVIL ENGINEERING AND ENVIRONMENTAL SCIENCE

BY THE COMMITTEE CONSISTING OF

Dr. Royce W. Floyd, Co-chair

Dr. Jin-Song Pei, Co-chair

Dr. Jeffery S. Volz

To my family and friends

Thank you for packing my parachute

the love, prayers, support, guidance,
and motivation you have given me,
have held me high.
Thank you!

ACKNOWLEDGMENTS

This study was sponsored by the Oklahoma Department of Transportation (ODOT) SPR project 2280 entitled "Development of Rating Tool for Prestressed Concrete Bridges Vulnerable to Shear".

TABLE OF CONTENTS

LIST OF TABLES

LIST OF FIGURES

Abstract

Aging infrastructure calls for structural health monitoring for recommendations on load postings, retrofitting, or replacements. Flexural rigidity identification has been used to monitor aging precast pretensioned concrete bridge girders with suitable datasets collected from laboratory testing of a prestressed girder in previous studies. These former studies utilized classical beam theory focusing on the physical phenomenon of bending under a point load. A significant issue persisted in the previous studies' inverse problem where data analysis using the standard linear least-squares method led to negative identified flexural rigidity values. Thus, the inverse problem is completely reformulated in this study. An intuitive illustrative example is first provided for comprehension of the least-squares approach; a Bayesian analytical approach is also introduced in plain words. This approach in this study was contributed by an outside researcher, while the programming, implementation, and result analysis were performed at the University of Oklahoma in a process of learning Bayesian analysis through numerical exercises and contrasting its performance to the least-squares method. The values of critical user-defined parameters are systematically decided and thoroughly discussed to discover any limitations. Objective decisions regarding data removal are also automated through learning and exercising concepts from Computer Science. Possible idealizations of piecewise divisions are explored for their effect on model efficacy. Identified flexural rigidity values from Bayesian analysis are then compared against functional flexural rigidity values for the girder. Identifications are consistent with end region corrosion over the course of the girder's 40+ years of service-life justifying the usefulness of Bayesian analysis. This study has also led to an improved Bayesian analysis formulation. The two methodologies, previously programmed into MATLAB, were streamlined and debugged throughout this study. The original MATLAB code was used to further expand the coding suite to include numerous utility functions to expedite this study and future expansion. Validation of the code and Bayesian methodology was carried out using demonstration problems (i.e., problems with known solutions).

Keywords: Prestressed concrete, Flexural rigidity, Bayesian analysis, Linear least-squares method, Linear system identification

Nomenclature

b	y-intercept
E_{ACI}	Young's modulus of concrete calculated from American Concrete Institute (ACI) formulas
E_c	Young's modulus of concrete
EI	Flexural rigidity
EI_0	Nominal flexural rigidity of Girder A
$h_{jk}^{(i)}$	Unit response function
$\mathbf{H}$	Theoretical deflections (scaled up by ideal incremental loads and normalized unit response function)
$\hat{\mathbf{H}}$	Theoretical deflections (scaled up by real-world test loads and normalized unit response function)
I	Moment of inertia
$\mathbf{I}$	Identity matrix
I_{cr}	Cracked moment of inertia calculated from Precast/Prestressed Concrete Institute (PCI) formulas
I_{tr}	Conservative transformed moment of inertia
J	Number of active (not including those at supports) LVDTs (linear variable displacement transducers)
K	Number of incremental loads in loading scheme
L	Total beam length
m	Bending moment distribution caused by virtual unit point load
M	Bending moment distribution caused by real unit point load
N	Number of substructures (segments) dividing beam
p	True probability distribution of a dataset
P	Load increment at a given time
q	Probability distribution describing true distribution "p"
s	Slope
$S_{\max}$	Location of pin support
$S_{\min}$	Location of roller support
$\mathbf{S}$ or Σ	Posterior covariance matrix
t	Time
$\mathbf{x}_{EI}$	Vector containing coordinates defining piecewise EI divisions which include $S_{\min}$ and $S_{\max}$
x_P	Scalar defining coordinate for the application of the real load
$\mathbf{x}_{\text{unique}}$	Vector containing every uniquely defined point along girder
x_δ	Scalar defining coordinate of the application of the virtual load
$\mathbf{x}_{\boldsymbol{\Delta}}$	Vector specifying the coordinates of LVDTs, both active and inactive
α	Posterior COV (coefficient of variation)
δ	Deflection at a given active LVDT
$\boldsymbol{\Delta}$	Elastic deflections (simulated by some beam model)
$\hat{\boldsymbol{\Delta}}$	Elastic deflections (measured from testing Girder A)
ε	Model prediction errors

μ	Mean value
σ	Prediction error standard deviation
σ_i	Posterior standard deviation
$\sigma_{\text{init.}}$	Initial value for objective function maximization
σ_0	Prior standard deviation
$\boldsymbol{\theta}$	Flexural rigidity identified from linear least squares
$\boldsymbol{\theta}_0$	Nominal values of $\boldsymbol{\theta}$
$\bar{\boldsymbol{\theta}}$	Posterior mean

1. INTRODUCTION

1.1. Motivations and Technical Challenges

As time passes, the state of Oklahoma's bridge infrastructure ages and has the potential to worsen. Limited funding to address this and other concerns require solutions to properly maintain current infrastructure. This is where the need for structural health monitoring (SHM) of existing bridge structures is realized. SHM can be employed through identifying flexural rigidity conveying information on both material and cross-sectional properties for a given prestressed structural element to infer possible damages caused by strand corrosion among other reasons. Inferences regarding damage can then be made by comparing identified values against some nominal (undamaged) value. Inferring damages across structural elements, recommendations for load postings, retrofitting, or replacements could then be facilitated.

In this study, previously obtained load-deflection data from a precast pretensioned concrete bridge girder, termed "Girder A" - a common design by the Oklahoma Department of Transportation (ODOT) - are used for identification. Identification methodologies from previous studies are revamped in the current study in an effort to establish a correct method for such structural elements.

A well-established challenge in the system identification of prestressed concrete beams is defined and reaffirmed in numerous studies utilizing modal analyses - modal parameters are relatively unchanged between damage states due to the prestress force effect in prestressed concrete beams after load removal. This study utilizes a statics-based approach to construct an inverse approach for system identification of a precast pretensioned concrete bridge girder, termed "Girder A", effectively bypassing the challenges in modal analyses. This inverse approach identifies flexural rigidity in a piecewise manner as the assumption of a constant flexural rigidity along the span may not hold due to strand harping, varying reinforcement

layouts, and unknown damage. Defining a piecewise manner by which Girder A may be best characterized requires the exploration of different piecewise idealizations, which was initiated in this study.

Girder A, in service for 40+ years, was removed from service before laboratory testing commenced. Due to time-dependent effects (creep) of concrete, loss of prestressing force before and during testing, damage during testing, and corrosion at the end regions, larger (than normal) deflections are theoretically expected in test data and must be accounted for. Pinpointing any damage along the span of Girder A would also require a determination of a functional flexural rigidity value against which comparisons and inferences of performance may be made.

Two methodologies are proposed and contrasted in this study. The first is a linear least-squares analysis, a commonly applied approach in numerous studies. The second is Bayesian analysis, an otherwise advanced topic that is not included in typical collegiate curriculum, which is learned throughout this study in parallel with its application. While systematic and comprehensive analyses are carried out leading to reasonable results, several afterthoughts are included in analyses and discussions to reflect the continuously improved understanding of the Bayesian methodology throughout this study. To highlight a key feature of this study, implementation of Bayesian analysis requires the specification of user-defined model parameters which the success of the analysis relies on. These user-defined parameters occupy a large parameter space making them difficult to estimate.

1.2. Intended Contributions

This study presents a significant step towards using flexural rigidity identification for SHM proposed in previous studies. For the first time, meaningful results are obtained using Bayesian analysis, a state-of-the-art identification technique. Additionally, a statics-based approach is utilized in contrast to the vast amount of existing modal analytical methods

for system identification of reinforced and prestressed concrete beam elements. This study vividly demonstrates the usefulness of Bayesian analysis in contrast with a linear least-squares method for SHM of precast pretensioned concrete bridge girders. Additionally, an intuitive illustrative example and plainly-worded educational materials are provided for the least-squares and Bayesian methodologies, respectively.

The Bayesian analytical approach was contributed by Professor James L. Beck, a researcher at the California Institute of Technology, while the programming, implementation, and result analysis were performed at the University of Oklahoma in a process of learning Bayesian analysis through numerical exercises. Continuously improved understanding of the Bayesian methodology has led to an intuitive understanding of the theory. This study has also led to an improved Bayesian analysis formulation.

The Bayesian analytical solution requires the specification of user-defined model parameters which occupy a large parameter space. For this reason, an empirical approach is exercised to narrow the range of these parameters and eventually decide specific values for use in this study. This systematic exercise and complimentary extensive reasoning manifest both learning and contribution to research using Bayesian analysis.

Entropy concepts from Computer Science are learned and exercised to automate the removal of linear variable displacement transducer (LVDT) data with questionable quality in an objective manner. The application of concepts from Computer Science to structural engineering serve as an example of their potential in benefitting SHM.

The piecewise identification of Girder A requires a segmentation be specified to characterize the beam to localize possible reductions of flexural rigidity. Furthermore, utilizing piecewise divisions, localized reductions in flexural rigidity may be seen. A non-exhaustive exploration of idealized divisions for analysis is conducted for this purpose. Identified results are also compared against functional flexural rigidity values for Girder A which are obtained from

a previous study and conservative estimations through MATLAB programming. Utilizing these functional flexural rigidity values, comparisons and inferences of girder performance may be made.

The methodology proposed was coded in an extensive MATLAB file suite for the analysis and illustration of identified results. Through MATLAB, a unique perspective is offered augmenting theoretical equations with validated coding processes. The original MATLAB code, compiled by Dr. Jin-Song Pei of the University of Oklahoma, was used as a foundation to further expand the coding suite to include numerous utility functions to expedite this study and future expansion.

1.3. Structure of this Thesis

After the introduction and literature review in Sections 1 and 2, Section 3 elucidates the methodologies in the problem formulation and implemented coding suites. An accompanying example is provided in Appendix A to illustrate the problem formulation. Section 4 uses demonstration problems (i.e., problems with known solutions) to validate the programmed solver and the proposed methodologies. Section 5 outlines the data preprocessing required for the real-world laboratory data measurements. Section 6 makes sense of the processed results and concluding remarks are made in Section 7. Processed results are provided in Appendix B, Appendix C, and Appendix D.

2. LITERATURE REVIEW

2.1. Structural Health Monitoring

Structural health monitoring (SHM) as defined by Housner et al. (1997), "refers to the use of in-situ, nondestructive sensing and analysis of structural characteristics, including the structural response, for the purpose of detecting changes that may indicate damage or degradation." SHM started with the ideas and theories that govern structural control and has grown into a very productive research area of its own. Research in structural control related to system identification has grown exponentially since the mid-1900s. These innovations, pioneered by the structural engineering community, have played a pivotal role in the construction and monitoring of structures designed to be safe-life and/or damage tolerant. Many bodies of authority have established codes for building and infrastructure design optimized for safe-life construction, however, it is well know that structures that stand the test of time will not maintain their original characteristics (e.g., capacity, stiffness, or functionality). It is here that the need for SHM is realized. In an effort to assess expected or unexpected damages in damage tolerant designs, general steps have been established to monitor such damage endured by a structure during its lifespan. These steps are listed as follows (Worden et al. 2007):

1. Establishing the existence of damage,
2. Damage location(s),
3. Type(s) of damage, and
4. The damage severity.

Worden et al. (2007) further states starting points for SHM in a "non-exhaustive" list of fundamental Axioms listed in Table 1:

Table 1. Fundamental Axioms in structural health monitoring (SHM) as put by Worden et al. (2007)

Axiom	**Description**
Axiom I	All materials have inherent flaws or defects
Axiom II	The assessment of damage requires a comparison between two system states
Axiom III	Identifying the existence and location of damage can be done in an unsupervised learning mode, but identifying the type of damage present and the damage severity can generally only be done in a supervised learning mode
Axiom IVa	Sensors cannot measure damage. Feature extraction through signal processing and statistical classification is necessary to convert sensor data into damage information
Axiom IVb	Without intelligent feature extraction, the more sensitive a measurement is to damage, the more sensitive it is to changing operational and environmental conditions
Axiom V	The length- and time-scales associated with damage initiation and evolution dictate the required properties of the SHM sensing system
Axiom VI	There is a trade-off between the sensitivity to damage of an algorithm and its noise rejection capability
Axiom VII	The size of damage that can be detected from changes in system dynamics is inversely proportional to the frequency range of excitation

Of the Axioms found in Table 1, this study focuses on Axioms I, II, IVa, and IVb.

In accordance with Axiom I, the discussion of damage and damage detection in a structure is better understood after specifying what constitutes "damage." A fundamental truth of all materials is that they consist of inherent flaws or defects that are accounted for by manufacturers in production and also by engineers in design (Worden et al. 2007). In this sense, all material is damaged before being used as a part of a structural system, therefore this is not the damage that is most important to structural engineers. The type of damage that is meaningful to engineers is the detectable damage (e.g., cracking, yielding, or rupture) that will negatively affect the safety of structures. As such, structural control research into damage detection modeling aims to assess the state of current structures.

Seo et al. (2015) provides a comprehensive summary of damage detection methodologies in SHM as they are applied to highway bridges. The review discusses Department of Transportation (DOT) inspection and rating frequency of the structural integrity of bridges occurring

at least once every two years. With highway bridges experiencing recurring loading and exposure to environmental stresses, they should be monitored with more frequency. Despite the need to further inspect bridge conditions throughout their lifespan, state agencies have limited resources and funding to accomplish this. Therefore, it is necessary to make the most out of these periodic checks through monitoring structural characteristic parameters which are functions of physical properties of a structural system.

2.2. Prior Work Related to System Modeling

Highway bridges in America are primarily constructed with reinforced concrete. Concrete is a brittle material that alone does not suffice for constructing bridge spans without steel reinforcement. When concrete is damaged from external loading or time-dependent effects, it inevitably cracks; this is a critical phenomenon that adversely affects bending members in bridges. The cracking of concrete can happen both internally and externally meaning damage may not always be apparent. Cracks may also manifest in a manner that are difficult to diagnose visually. In an effort to detect damage in concrete bridge structures, many methods have been established to identify structural parameters that help to infer information related to these damages.

One such characteristic that is extensively researched is flexural rigidity (EI). By identifying flexural rigidity, information regarding cross-sectional and material properties can then be gleaned. From the constituents of flexural rigidity: Young's modulus (E_c) and moment of inertia (I), the cross section of a given segment of a bridge can be analyzed for possible damages based on reductions in flexural rigidity. In line with Axiom II, flexural rigidity reduction is relative to some state of the system where it is functional. Here, the viability and importance of system identification for flexural rigidity in association with highway bridge structures are realized.

Flexural rigidity identification research has been conducted on both prestressed concrete

(PC) and reinforced concrete (RC) beams where methods of analysis are shared between the two beam designs. A variety of methodologies are reviewed as an introduction to the research proposed in this study.

With various SHM methodologies implemented in damage detection it is important to refer to Axioms IVa and IVb in Table 1; these Axioms state that sensors cannot directly measure damage but instead "measure the response of a system to its operational and environmental input" (Worden et al. 2007). Because sensors do not measure damage, this review focuses on research methodologies. Inverse methodologies based on physical measurements as used in the current research are not commonplace in flexural rigidity identification, therefore the analysis techniques discussed are a mix of forward and inverse modeling based on modal data. Here, the reviewed studies using modal analyses are focused on identifying element stiffness which is a function of E_c, I, member length, and boundary conditions. There is also a stark contrast to the existing amount of literature involving PC beams in relation to RC beams with the majority focusing on the latter - with this in mind, both will be reviewed.

2.2.1. Kato and Shimada (1986)

The imbalance in research efforts between PC and RC beams may be attributed to difficulties in testing PC structures as found by Kato and Shimada (1986). This study sought to investigate ambient vibration testing (AVT) as a method in measuring bridge safety. The AVT procedure was employed to measure small horizontal and vertical structural vibrations during the application of incremental static loadings forcing failure of a PC bridge. Assuming the effects of creep and shrinkage had taken their maximum toll after 5 years, the AVT data were filtered to remove aliasing effects and resolved into natural frequencies and damping constants. Monitoring changes in the vibrational characteristics of the bridge before and after failure (characterized by yielding of the prestressed steel reinforcement), it was determined that "little change in vibrational characteristics occurred while the prestressed steel

wires were in the elastic state [and the] sudden change in vibrational characteristics may have followed after the wires exceeded the elastic limit" (Kato and Shimada 1986). Kato and Shimada (1986) concluded that the closing of cracks due to effective prestressing after load removal caused small decrements in the natural frequencies before failure. Observing this post-tensioning effect in the PC bridge, the possibility of discovering weaknesses through vibrational testing once the tendons reached their plastic limit was stated.

2.2.2. Huth et al. (2005)

Since the study by Kato and Shimada (1986), vibration-based analyses of concrete structures for stiffness identification have been increasingly employed. As invariants of structures, modal parameters can be used to determine changes associated with a given structure without destructive testing. Their "global character" does not confine them to the location of damage (Huth et al. 2005).

Despite the appeal for vibrational testing, the difficulty in identifying early-stage damage in PC bridges is reaffirmed by Huth et al. (2005). This study describes various damage detection, localization, and quantification methods revolving around modal analyses. The first analysis method was chosen by directly comparing three separate methods of output-only system identification algorithms in combination with ambient excitation sources. These methods aimed to model both the dynamics of the physical system and how the measured output is related to state variables of the system resulting in natural frequencies, modal damping, and mode shapes. Notably, over an 8 month span, ambient temperature was monitored to determine its effect on natural frequencies. A comparison of the natural frequencies and the mode shapes before and after damage steps exhibited small changes.

A secondary modal analysis method called the modal assurance criterion (MAC) method, measuring the correlation existing between two mode shapes, followed suit with the former analysis indicating poor sensitivity to damage. With the MAC model showing little promise

of analyzing the mode shapes, a new analysis method is introduced: the mode shape area index. This analysis method requires that the bridge be partitioned into several spans whose mode shapes' areas are monitored for changes during damage evolution. The mode shape area index revealed higher sensitivity to changes in the mode shape than the MAC method. Huth et al. (2005) moves forward with further modal analyses by employing flexibility difference, a method proposed by Pandey and Biswas (1995). The flexibility difference method offers localized damage detection in a structure based on changes in the flexibility matrices between an assumed healthy and damaged structure states.

Utilizing select modal parameters obtained from previous tests, a finite element (FE) model is created and updated continuously to determine changes in Young's moduli across elements of the bridge deck. Tuning the model updating method iteratively, changes in Young's moduli are obtained resulting in ambiguous damage localization and quantification. This is thought to be caused by ill-conditioning of the updating method.

The final method discussed is the direct stiffness calculation (DSC). Much like the FE updating model, DSC also uses mode shapes to locate and quantify damage. DSC returned ambiguous damage related results which are attributed to the modal estimation errors. The research by Huth et al. (2005) was unsuccessful in reliably detecting, localizing, or quantifying early-stage damage on PC bridges through modal analyses due to the post-tensioning effects of the PC element, as found by Kato and Shimada (1986), even with the evolution of significant cracking.

2.2.3. Unger et al. (2006)

Another study by Unger et al. (2006), addressing the difficulties due to the post-tensioning effects stated by Kato and Shimada (1986), aimed to localize and quantify stiffness reductions in PC beams through the use of updating FE models. Three FE models were programmed in ANSYS, utilizing mode shape information, to result in analytical modal parameters in

an effort to match those which were measured. Comparing the analytical and measured parameters resulted in the need for updating the FE models to further simulate the beam specimen accurately. Using the updating method, damage patterns are identified after simulating damage on the linear beam model. Similar to methods by Huth et al. (2005), Young's modulus is used to quantify the stiffness reduction. To optimize the FE programming, nonlinear least-squares regression of the objective function was iterated upon to fall within a standard trust region. Further optimization involved weighting frequencies and mode shapes to balance damage detection localization with distribution. Unger et al. (2006) concluded that the methodology allowed a clear damage localization and quantification when 80% of the failure load was reached. Difficulties remain in early damage detection on PC beams despite the methods proposed in this research.

The methodologies reviewed up to this point have focused on modal analytical techniques of PC beams. In an effort to review similar as well as other methods of damage detection and stiffness identification, research on RC beams are included.

2.2.4. Maeck et al. (2000)

Two previously discussed techniques by Huth et al. (2005) were used in a study by Maeck et al. (2000) on damage detection in RC beams: FE updating and direct stiffness. Similar to the other FE updating methods discussed, iterative minimizations between experimental and numerical modal data were employed to estimate stiffness. Through the "degradation of stiffness," monitored by a reduction in Young's modulus, the location as well as severity of damage to the RC beam was inferred (Maeck et al. 2000). The second technique pursued did not rely on establishing a numerical model but instead utilized bending moments and dense measurements of curvature, both being functions of stiffness. Maeck et al. (2000) determined that the direct stiffness method would allow for the best damage detection but would require a "rather dense measurement grid" to be able to capture curvature. The

direct stiffness method, though not requiring a numerical model, did not seem to be a well-automated system of analysis. The research identifies a disadvantage to this method when penalty factors must be incorporated "in an allowable range: large enough to be effective and not too large to avoid numerical difficulties" (Maeck et al. 2000).

It should also be noted that the formulation of the FE model in this research assumes symmetric damage under experimentation of one static damage scenario where symmetric damage is expected. This paper addresses the possibility of non-symmetric damage patterns but does not investigate this further. The study goes on to address the large number of updating parameters needed to properly describe stiffness variations and aims to model damage as a reduction in Young's modulus through only a few representative parameters. Though not included as a parameter, the authors mention the possibility of time-dependent effects of concrete (creep) influencing test results.

2.2.5. Impollonia et al. (2016)

Another FE updating model applied to RC beams was constructed by Impollonia et al. (2016) where a statistical moment-based damage detection method was employed. Second-order moments of FE nodal responses, explicitly related to stiffness and modal damping, are found. This method, much like the methodology by Maeck et al. (2000) involves simulating damage through reductions in Young's modulus without considering time-dependent effects in concrete.

The FE updating method is validated by identifying a damaged region in the FE beam model and subdividing the damaged region multiple times to localize the detected damage location(s). The Euler-type beam model assumes constant stiffness in undamaged regions and those surrounding the damaged segment, but this simplification may not hold in real structures. The research by Impollonia et al. (2016) is only used to analyze FE models of beams and panels and is not applied to physical experiments. By using a simulated FE modeled

beam, the original stiffness properties are imparted to the simulation and changes in stiffness are the desired phenomena. Though large departures from the nominal stiffness values have the ability to indicate damage location and severity, there is something to be said about a threshold value at which damage cannot and/or should not be detected. Investigations into a minimum stiffness value or a range of stiffness indicating system functionality should be pursued for a more robust damage detection system.

2.2.6. Song et al. (2007)

Research has also been conducted in crack sensing methodologies focusing solely on damage detection through physical measurements, taking for example, work by Song et al. (2007). The authors specify the limitations of their crack sensing method to predicting onsets of surface cracks and structural failure but not being able to offer detailed crack information in terms of location, width, length or orientation. Comparing a physical methodology for damage against research in stiffness identification, a parameter-based methodology: determining reduced stiffness values across a given RC or PC beam does not constitute the determination of detailed crack dimensions or orientation either, yet has the potential to offer insight into crack location and magnitude which may be enough to recommend repair procedures.

2.3. Background of This Study

2.3.1. Pei et al. (2008)

Research carried out by Pei et al. (2008) sought to study methods of rating precast prestressed concrete bridges, a typical design in Oklahoma, for their shear capacities in order to aid Oklahoma Department of Transportation (ODOT) engineers on recommendations of load postings and/or retrofittings. The girders involved in the study had been designed in the 1960s and 1970s using outdated AASHTO Standard Specifications, and their shear capacities relating to newer standards were in question.

One girder from the 2008 study was recovered from the I-244 Bridge over the Arkansas River in Tulsa after being in service for over 40 years. The girders on this bridge showing minor damages were retrofitted with glass fiber reinforced polymer (GFRP) or replaced if the damage was extensive. The recovered girder, referred to as the "Old Girder" herein, suffered severe end corrosion and was retrofitted with GFRP and used to glean information on the performance of the reinforcement.

Through a parametric study of nominal shear capacity comparing both the ACI and LRFD design codes it was apparent that the capacity was sensitive to effective prestressing stress (Pei et al. 2008). To calculate shear capacity it was necessary to accurately estimate the prestressing stress in the girder after 40 years in service and being decommissioned due to major damages. The report states that, "[a]lthough there are methods for determining long-term prestress losses, they apply to a wide variety of structural members and do not necessarily reflect the condition of the real-world girder and the uncertainties studied here" (Pei et al. 2008).

Therefore, to identify the actual (effective) prestressing stress of the girder, the report details the construction of an inverse problem based on mechanics and real-world measurements to indirectly estimate properties related to said prestressing stress. Camber measurements in conjunction with accurate estimations of the flexural rigidity distribution along the length of the girder were required to ultimately identify the effective prestressing stress. The flexural rigidity along the length of the beam was assumed to be piecewise constant due to the aging of the girder as well as the GFRP retrofitted end. Flexural rigidity distributions were identified through flexural (load-deflection) testing.

Preliminary analysis estimating prestressing stress showed a significant influence from the time-dependent behavior of prestressed concrete including creep and bond loss (relaxation of reinforcement) and suggested for a further analytical study of these effects on the inverse problem formulation (Pei et al. 2008). Due to difficulties arising from the measurement

procedures, asymmetrical strand profiles of the old girder used in this study as well as time-dependent effects of concrete (creep), the idea to utilize camber measurements in the estimation of prestressing stress was abandoned.

2.3.2. Floyd et al. (2016)

In later research by Floyd et al. (2016) the flexural rigidity identification process was revisited for improvement through two different girders, dubbed "A" and "C" obtained from the same bridge as in Pei et al. (2008) before its demolition in 2013. The recovered girders were subjected to both flexural and other destructive testing to identify their system properties. Concerns regarding the original inverse problem formulation are addressed and suggestions for improvement are included. Problems arising from the original problem formulation included the necessity of "double regression" and its effect on the validity of the study, contradictions in the original problem formulation, and the issue of reformulating the original inverse problem. Suggested improvements to the problem formulation addressed in this report included a better mathematical foundation, better result interpretations based on data processing through programming, and the tying in of time-dependent effects of concrete.

2.4. Application of Bayesian Analysis in Structural Engineering

2.4.1. A Brief Overview

Here, structural engineering applications of Bayesian analyses are briefly reviewed. A broad summary of the Bayesian analytical approach is given by van de Schoot et al. (2014), where this approach "allows researchers to incorporate background knowledge into their analyses instead of testing essentially the same null hypothesis over and over again, ignoring the lessons of previous studies." This summary is useful in the comprehension of analyses utilizing the Bayesian approach for SHM purposes.

Quoting "Nonlinear System Identification in Structural Dynamics: 10 More Years of Progress" by Noël and Kerschen (2017): "An important change of paradigm has blossomed over the past few years in the third step of this process, as researchers have progressively recognised the importance of quantifying uncertainties in nonlinear system identification. This has given rise to methods estimating parameters together with, e.g., confidence bounds or distributions. In this context, the Bayesian framework put forward by Jim Beck and his collaborators is currently drawing noticeable attention in the community." Similarly, in Green and Worden (2015), it states that "To date, the most systematic and extensive development of Bayesian SI is the result of the work of James L. Beck and his various collaborators." Here, Professor Beck directly contributed to this project through his formulation of a linear system identification problem.

Indeed, there is a large body of literature contributing to applying Bayesian analysis in SHM. The literature reviewed in this section is not meant to exhaust the allowable applications of Bayesian analysis in structural engineering nor is the depth of the research in the subsequent papers fully understood. This section is instead used as an information gathering tool in an effort to conceptualize the implementation of the Bayesian probabilistic approach in practice. The latest literature review is entitled "State-of-the-art review on Bayesian inference in structural system identification and damage assessment" in Huang et al. (2019).

2.4.2. Vanik et al. (2000)

Beginning with a study by Vanik et al. (2000) where a Bayesian probabilistic methodology is utilized in SHM: in this research, localized stiffness losses are used to identify damage based on changes in modal data. Unlike other modal inverse analyses discussed previously, this SHM system continuously monitors modal data to separate systematic changes from random fluctuations while also filtering out noise to some degree. Bayesian analysis is used here to account for ill-conditioning of the problem formulation from "unavoidable uncer-

tainties" such as model errors and measurement noise. In doing so, Vanik et al. (2000) addresses the question: "Based on the available modal data and acknowledging the unavoidable uncertainties, what is the probability that the current model stiffness parameters are less than a specified fraction of the corresponding undamaged stiffness parameters?" Illustrative examples are provided in the research for the proposed method's application in a 10 degree-of-freedom (DOF) shear structure model.

2.4.3. Huang and Beck (2013)

Another research effort featuring Bayesian analysis was conducted by Huang and Beck (2013) where a "new sparse Bayesian probabilistic approach [is presented using] noisy incomplete modal data from before and after possible damage" to compute the probability of localized reductions in stiffness. Current limitations in SHM, such as the need to establish typical thresholds for damage indication or the need for dense sensor measurements, are first explored. The model formulation is reported, utilizing sparse Bayesian learning from prior research, employing an optimization methodology iterating between "groups of modal parameters and hyperpameters" to obtain sparse stiffness reductions and their uncertainties Huang and Beck (2013). Where hyperparameters are "parameters of the prior distribution" (van de Schoot et al. 2014). Lastly, validation of the proposed model is conducted through simulated data from the "IASC-ASCE Phase II Benchmark structure [which is a] four-story, two-bay by two-bay steel braced-frame model" (Huang and Beck 2013). Results from the validation procedure showed that "no threshold [was] needed for issuing a damage alarm and the occurrence of false-positive and false-negative damage detection in the presence of modeling error [was] clearly suppressed" (Huang and Beck 2013).

2.4.4. Capellari et al. (2018)

The Bayesian approach as used in SHM is not limited to uncertainty quantification of structural parameters but can also be applied to optimize data acquisition. Capellari et al. (2018) explores the optimization of sensor placement by maximizing the expected information gain between the prior and posterior using a Monte Carlo sampling approach. The optimal placement in turn relates to "the maximal amount of information in terms of the parameters to be identified" (Capellari et al. 2018). To apply this approach to large computationally demanding structures, two surrogate models are compared to replace full-order models which are more expensive. Choosing the surrogate model that appropriately captured the response of high-order DOF systems then allowed for the procedural testing for optimal design of a sensor network for Milan's Pirelli Tower. The approach was found to be "very effective in matching the full-order model response", however, limitations of the model are subsequently addressed. In addition to constraints imposed on the orientation, type, and number of the sensors - with the last two constraints directly affecting project effort costs - Capellari et al. (2018) states that unique optimal network configurations may not exist for large measurement errors on a given system as the noise for each possible solution hides the expected information.

2.5. Entropy in Analysis

Here, a brief overview is provided on information theory and entropy and their uses in this study. From Gray (1990), "Information theory [has] two primary goals: The first is the development of the fundamental theoretical limit on the achievable performance when communicating a given information source over a given communications channel using coding schemes from within a prescribed class. The second goal is the development of coding schemes that provide performance that is reasonably good in comparison with the optimal performance given by the theory."

Focusing on the second goal, entropy and its use in rationalizing data is discussed. Entropy can be referred to as the degree of chaos or disorder in a given system. Entropy can also be referred to as missing information. Applying this concept in the information theory context, insight can be gained regarding the system's information content. Through entropy, events can be identified relating information about the true probability distribution of a system, especially when combined with intuition. As such, the entropic calculations in Section 6.4 are paired with suspicions of LVDT L1 malfunctioning during the last testing day.

A demonstration is also provided in Table 3 contrasting the KL divergence values when switching "Uncorrected" and "L1 Corrected" as the "true", distribution. It is seen that the commutative property does not hold when comparing $KL(p_1, p_2)$ and $KL(p_2, p_1)$. The expected disagreement between the KL divergences indicate that the data in either category are not well represented by the data in the remaining category. Conversely, this is why $KL(p_1, p_1) = KL(p_2, p_2) = 0$, informing that the distributions match exactly. Additionally, the non-negative nature of the calculations is expected and can be proved with a variety of methods including Gibb's or Jensen's inequalities (Bishop 2006).

The values of KL are used as "a measure of how much 'predictive power' or 'evidence' each sample will on average bring [when] trying to distinguish $p(x)$ from $q(x)$, [when] sampling from $p(x)$. If $p(x)$ and $q(x)$ are very similar then each individual sample will bring little 'evidence' to the table. On the other hand, if $p(x)$ and $q(x)$ are very different then each sample will bring a lot of evidence showcasing that $q(x)$ is not a good representation of $p(x)$" (Cotra 2017). Coupling the explanation by (Cotra 2017) with the knowledge of L1 malfunctioning on the last testing day, a cutoff value for KL is established for LVDT L1's removal.

2.6. Literature Review Summary

The research methodologies, relating to system modeling, included in the literature review are predominantly forward and inverse modal analytical methods that aim to identify differences in modal parameters and/or stiffness between healthy and damaged PC or RC beams. In contrast, the methodology proposed in this study utilizes a statics-based approach to construct an inverse problem identifying piecewise constant flexural rigidity in PC beams using static test data. By determining the adequacy of the methods proposed in this study, it is desired that recommendations be made in the assessment of PC bridge members in Oklahoma. Table 2 lists summaries of the literature review relating to system modeling to be used for comparison with the research conducted in this study.

Table 2. Summaries of literature review relating to system modeling

Kato and Shimada (1986)	• Ambient Vibration Testing (AVT) – Comparing modal parameters before and after bridge failure • Incremental static loading process with AVT after every increment • Assumed time-dependent effects of concrete had taken maximum toll in 5 years • Digital signal processing to remove aliasing effects • Damage detection difficulty if prestressed tendons did not yield
Maeck et al. (2000)	• Monitoring changes in Young's modulus for stiffness reduction using FE model updating • Assuming symmetrical damage patterns • Not accounting for time-dependent effects of concrete • Direct stiffness calculation (DSC) – Quantification of damage using mode shapes • Best damage detection requires a dense measurement grid

Huth et al. (2005)	• Not accounting for time-dependent effects of concrete • Output-only system identification algorithms – Comparing modal parameters before and after bridge failure • Modeling dynamics of physical system and relating outputs to state variables of system • 8 month monitoring of ambient temperature • Modal assurance criterion (MAC) – Measuring correlation between two mode shapes • Mode shape area index – Monitoring mode shape areas for change between damage steps • Bridge partitioned into several spans for analysis • Flexibility difference – Comparing changes in flexibility matrices of a healthy and damage structure • Localized damage detection • FE updating – Monitoring changes in Young's modulus for stiffness reduction • Ambiguous damage localization and quantification caused by ill-conditioned methodology • Direct stiffness calculation (DSC) – Quantification of damage using mode shapes • Ambiguous damage related results attributed to modal estimation errors
Unger et al. (2006)	• Not accounting for time-dependent effects of concrete • FE updating – Monitoring changes in Young's modulus for stiffness reduction • Non-linear least-squares optimization • Weighting modal parameters • Clear damage localization and quantification at 80% failure load
Song et al. (2007)	• Sensing crack formation at concrete surface • Offering no detailed crack information (location, width, length, orientation)
Pei et al. (2008)	• Inverse problem – Using physical measurements to identify piecewise constant flexural rigidity • Static loading • Linear least-squares optimization • Non-unique solutions inherent to inverse problem • Not accounting for time-dependent effects of concrete

Impollonia et al. (2016)	• FE updating - Monitoring changes in Young's modulus for stiffness reduction • Not accounting for time-dependent effects of concrete • Methodology not applied to physical experiments • Questionable damage detection based on threshold stiffness value
Floyd et al. (2016)	• Flexural rigidity identification process revisited - Concerns and suggestions • Necessity of double regression's effect on validity of study • Time-dependent effects of concrete • Contradiction in original problem formulation

Basing the problem formulation on the physical phenomenon of bending under a point load, this study effectively bypasses difficulties in PC beam damage detection due to post-tensioning effects as found by Kato and Shimada (1986) and reaffirmed by Huth et al. (2005) and Unger et al. (2006). Revisiting the flexural rigidity identification formulation originally proposed by Pei et al. (2008) and drawing in concerns and suggestions addressed in the report by Floyd et al. (2016), the overall effect of time-dependent effects of concrete would be in the identified results. Creep will undoubtedly affect the results of the research and with few studies from Table 2 accounting for time-dependent effects, this factor is a necessary inclusion in SHM of RC and PC bridge girders.

Research using FE and other modal analyses model damage as a reduction in Young's modulus when flexural rigidity (EI) is a function of both Young's modulus (E_c) and the moment of inertia (I). Therefore, conservative calculations of I for both undamaged and damaged girder cross sections will be included in addition to a variations of E_c with respect to time-dependent effects and location (in member). Similar to the flexibility difference used by Pandey and Biswas (1995) and Huth et al. (2005), this study compares identified stiffness (flexural rigidity) values of a potentially damaged girder to those of an undamaged girder.

To increase the identification accuracy of the model, the given girder is partitioned into increasingly shorter segments as in FE studies by Impollonia et al. (2016) and other methods

using flexibility difference. The segmentation of the beam for flexural rigidity identification offers "a good compromise between the complexity of the unknown condition and properties of [a] real-world girder and the idealization for the purpose of theoretical studies" (Pei et al. 2008). Furthermore, segmenting the beam in such a manner also offers the capability of localizing flexural rigidity reductions, which may allow for improved inferences to be made of damaged portions of the beam. Automation of the solution is performed by programming the research methodologies in MATLAB. The coding is extensively validated to ensure that the results obtained can be interpreted with minimal ambiguity.

3. METHODOLOGIES AND CODING

3.1. Organization of Coding

The analyses in this study are automated through suites of files constructed in MATLAB; the individual files will be referred to as *m-files* hereafter due to their naming (filename.m). The processes of the m-files run by MATLAB are separated into two unique parts: Main and Preprocessing. Flowcharts in Figs. 1 and 2 provide overviews of the input/ouput processes of the m-files created for this study. The processes automated by of each of these suites is concisely summarized thereafter.

Following Fig. 1, the datasets are loaded and preprocessed in MATLAB.

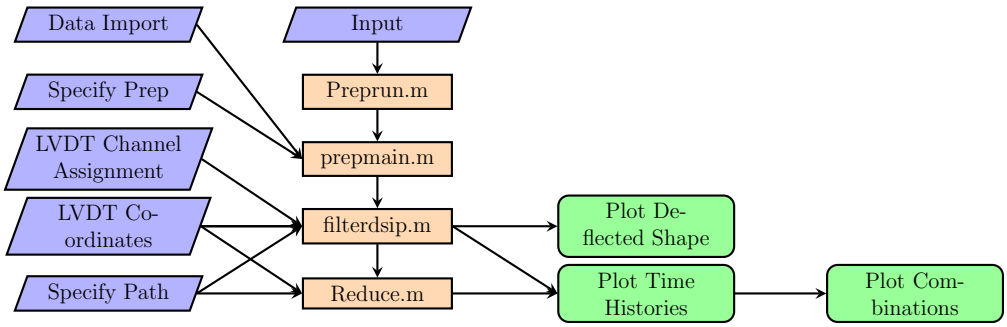

Fig. 1. A flowchart of the involved additional preprocessing

By specifying the inputs of the Main suite in Fig. 2, the coding of the m-files found in this suite function to import a dataset(s) that has been preprocessed by the Preprocessing suite to test certain beam configuration case(s) to identify flexural rigidity.

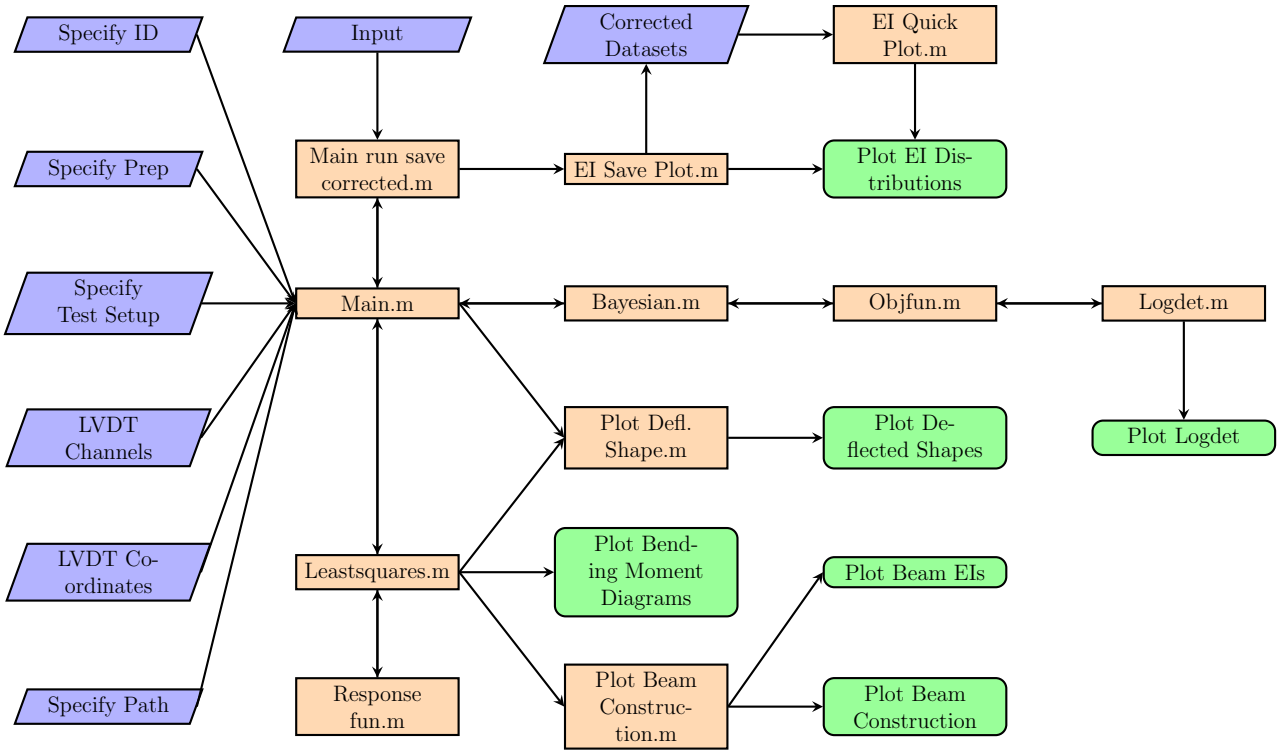

Fig. 2. A flowchart of the involved programming

The processes that are automated by the MATLAB code associated with the m-files in Figs. 1 and 2 are listed:

Preprocessing: Real-world data preprocessing

- Data truncation
- High frequency noise filtering
- Data quality check
- Data reduction

Main: Ordinary least-squares solution

- Rigid body motion correction
- Unit response function construction

- Scaling and normalization
- Ordinary least-squares regression
- Pseudo-inverse algorithm application

Main: Bayesian solution

- Introduction of uncertainty to problem formulation
- Maximizing objective function
- Parametric study of user-defined parameters
- Identifying most probable solution

The code is extensively and intensively validated. In particular, simulations through beam theory for the testing of a simply-supported beam and a simply-supported beam with an overhang will be reported in addition to various testing cases utilizing matrix structural analysis. For efficiency in understanding and clarity in presentation the problem formulation is first provided with a complimentary illustrative example to glean the goal of this study.

3.2. Model Overview

The assumption of a constant flexural rigidity (EI) across the beam does not hold for the given real-world girder(s) in this project due to strand harping, varying reinforcement layouts, and unknown damage, therefore it is necessary to divide the span of the beam into N smaller segments imparting a piecewise constant flexural rigidity along the length of the beam. The nature of the problem of identifying the assumed piecewise flexural rigidities (EI) requires an inverse approach where measured deflections will be used to solve for the rigidity; the forward approach would use the rigidities to solve for deflections. Using this inverse approach, the piecewise flexural rigidities will be indirectly estimated by first solving for flexibility ($1/EI$), which is inversely proportional to the flexural rigidity. The linear

flexural testing data obtained from the study by Floyd et al. (2016) allows the indirect solving of EI using a linear least square solution as opposed to a non-linear least square solution.

Utilizing the system's response to K applied loading schemes, the measured deflections across J active degrees of freedom can be formulated into a math problem to solve for system flexural rigidities through the equation:

$$\underbrace{\mathbf{H}}_{JK\times N}\ \underbrace{\boldsymbol{\theta}}_{N\times 1} = \underbrace{\boldsymbol{\Delta}}_{JK\times 1} \tag{1}$$

where $\mathbf{H}$ is a $JK \times N$ matrix of the response function that is scaled up and normalized by the nominal EI value, found in Appendix A.2. $\boldsymbol{\Delta}$ is a column vector of length JK housing the elastic deflections that are induced by an incremental loading scheme, and its construction is found in Appendix A.3. Lastly, $\boldsymbol{\theta}$, see Appendix A.5, denotes a vector of normalized parameter values $\boldsymbol{\theta} = \frac{EI_0}{EI_i}$. Because $JK > N$, the ordinary least-squares solution to Eq. (1) is required. There are N elements $\boldsymbol{\theta}_i$, each representing one of N segments of the beam. These segments are herein referred to as substructures, these substructures do not refer to the physical supporting structures of a bridge (i.e., piers and abutments). For each substructure the value of $\boldsymbol{\theta}_i$ is approximately equal to 1 because of the normalization by the nominal value EI_0 in the definition of $\boldsymbol{\theta}_i$. From the $\boldsymbol{\theta}_i$ values in the least-squares solution of Eq. (1), $EI_i = \frac{EI_0}{\boldsymbol{\theta}_i}, i = 1, \ldots, N$ is obtained, as the EI rigidities that produce the deflections through beam theory to best match the measured deflections in $\boldsymbol{\Delta}$. A prediction can then be made for the anticipated deflections of the beam undergoing incremental loading schemes. The solution for $\boldsymbol{\theta}$ can then be compared against anticipated ranges of EI to infer possible damages. An illustration of the full construction of Eq. (1) begins in Appendix A.

3.3. Bayesian Analysis: Theory

Professor James L. Beck directly contributed to this project to formulate a linear system identification problem, it is given first as follows:

Eq. (1) describes a deterministic forward model that comes from beam theory or some other model. Here, a methodology is introduced to arrive at a probabilistic result for the inverse analysis of Eq. (1) that models uncertainty from deterministic model errors and deflection measurement errors. The problem formulation as expressed previously now accounts for model prediction errors $\boldsymbol{\varepsilon}$ as:

$$\boldsymbol{\Delta} = \hat{\mathbf{H}}\boldsymbol{\theta} + \boldsymbol{\varepsilon} \tag{2}$$

where $\hat{\mathbf{H}}$ contains the measured loading from physical testing. The uncertain prediction error $\boldsymbol{\varepsilon}$ represents a combined modeling error and measurement error, thereby encompassing the uncertainties in this project (Beck 2018). The uncertainty in $\boldsymbol{\varepsilon}$ is modeled by a multi-dimensional Gaussian (Normal) probability distribution which maximizes Shannon entropy to produce the maximum uncertainty subject to statistical moment constraints of zero mean and covariance matrix $\sigma^2\mathbf{I}_{JK}$, where σ^2 is the prediction-error variance whose value is uncertain and must be learned from the data (Beck 2018).

Eq. (2) with Guassian $\boldsymbol{\varepsilon}$ determines the probability of obtaining the *measured* deflections in $\hat{\boldsymbol{\Delta}}$. In addition, a prior distribution is required to quantify the a priori uncertainty about the values of the parameters $\boldsymbol{\theta}$. The prior distribution for $\boldsymbol{\theta}$ is chosen as a multi-dimensional Gaussian with mean $\boldsymbol{\theta}_0$ and covariance matrix $\sigma_0^2\mathbf{I}_N$ for some chosen prior variance σ_0^2 (Beck 2018). Several sources of uncertainties that are desired to be captured in $\boldsymbol{\varepsilon}$ through σ_0 are examined in Section 6.1.

The Bayesian solution in this study is derived analytically. In short, analysis starts with

the prior probability distribution and end with the posterior probability distribution. With an analytical derivation, the solution can be programmed in MATLAB for computation. Examining the posterior properties that can be generated by the code:

(1) Posterior covariance:

$$\mathbf{S} = \left[\sigma_0^{-2}\mathbf{I}_N + \sigma^{-2}\hat{\mathbf{H}}^T\hat{\mathbf{H}}\right]^{-1} \in \mathbb{R}^{N\times N} \tag{3}$$

This is a square matrix of $N \times N$ dimensions, where N is the number of the parameters to be identified. For example, when one substructure (segment) is specified $N = 1$, for three substructures $N = 3$. The diagonal elements of $\mathbf{S}, \sigma_i^2, i = 1, \ldots, N$ are the posterior variances.

(2) Posterior mean:

$$\bar{\boldsymbol{\theta}} = \sigma^{-2}\mathbf{S}\hat{\mathbf{H}}^T\hat{\boldsymbol{\Delta}} + \sigma_0^{-2}\mathbf{S}\boldsymbol{\theta}_0 \ \in \mathbb{R}^N \tag{4}$$

In general, this vector contains the most probable value of flexural rigidity based on the data where $\boldsymbol{\theta}_0$ is a column vector of N elements housing nominal $\boldsymbol{\theta}_0$ of unity because of the chosen normalization of the parameter vector $\boldsymbol{\theta}$.

3.4. Bayesian Analysis: Implementation and Practical Tips

Even though Professor James L. Beck derived a closed-form solution to the specified problem, there are critical user-defined parameters to be decided and tuned in the process. The understanding gained from his work is given as follows:

Through least-squares analysis, data is solely utilized in learning. In Bayesian analysis, fitting data is not the only ingredient as it is also necessary to assume the expectation for the desired unknown parameters. This expectation is called the *prior* of the parameter; the Bayesian process involves using both the data and the prior. The outcome of the Bayesian process is

the *posterior* of the parameter. Both the prior and posterior are not fixed values. In fact, each is defined by a Gaussian distribution. Recall that a Gaussian distribution is defined using its mean and standard deviation (or equivalently, the variance).

The mean of the prior, in this study, is assumed to be one given the attempt to identify normalized flexural rigidity and drastic variations of this value along the span are not anticipated. The variance of the prior is unknown, and will be treated as a user-defined parameter. The mean and variance of the posterior will be obtained through Bayesian analysis.

Another distinct feature of Bayesian analysis is in Eq. (2): the prediction error is explicitly introduced into the equation. This prediction error is also not a fixed value. It is assumed to have a Gaussian distribution with zero mean. The variance, however, is not assumed. Rather, it will be "learned" from the data.

Descriptions for the user-defined parameters are given as follows:

1. σ_0^2: This is the variance of the prior (prior distribution). For the piecewise EI identification problem, in general, the prior has a mean vector and covariance matrix. While the mean is a vector of one(s), the covariance matrix is $\sigma_0^2\mathbf{I}_N$. This means that the normalized EI values are assumed to be independent of each other in the beginning of Bayesian analysis.

   After performing Bayesian analysis the posterior Gaussian distribution is obtained with a mean vector of $\bar{\boldsymbol{\theta}}$ in Eq. (4) and covariance matrix of $\mathbf{S}$ in Eq. (3). Here, the mean vector contains the most probable values of the piecewise EI that are sought, while the covariance matrix measures the uncertainty in these most probable values.

   Determining σ_0^2 is important: When $\sigma_0^2 = 0$, there is no uncertainty, meaning that the prior has the fixed value of $\boldsymbol{\theta}_0 = \mathbf{1}$. When $\sigma_0^2 \to \infty$, the Bayesian analysis approaches the least-squares results. This specific prior is called a "non-informative" or "flat" prior.

Mathematically, yielding:

$$\bar{\boldsymbol{\theta}} \rightarrow \left(\hat{\mathbf{H}}^T\hat{\mathbf{H}}\right)^{-1}\hat{\mathbf{H}}^T\hat{\boldsymbol{\Delta}} \tag{5}$$

In summary, a value of σ_0^2 is desired that is not too large or too small. Hence, parametric study of σ_0^2 is performed in Section 6.3. In implementation, a small value is first used and gradually increased to see how the identified values are affected.

2. $\sigma^2_{\text{init.}}$: This is the initial value for the optimization of σ^2 in Eq. (2), the variance of the prediction error. This optimization is how the variance of the prediction error is "learned" from the data. This happens during Bayesian analysis. Another parametric study for $\sigma_{\text{init.}}$ is performed later under Section 6.3.

   The objective function, in fact (the equation for which is not provided in this thesis), is a sum of two terms with one increasing and the other, decreasing, with respect to σ^2. Obtaining a peak/valley is anticipated indicating optimality. However, sometimes this did not occur in this study, instead the optimization returned a negative σ, the reason for which is still being investigated. This issue nevertheless is documented in this thesis. When this happens, the identification is terminated and the result is not reported.

There are three distinct methods for tuning these user-defined parameters from the most to least theoretical and efficient:

Problem reformulation

Most recently, a new formulation was proposed by Professor James L. Beck to reduce the number of user-defined parameters to only one.

Evidence maximization

Often the data is not sufficiently informative, and so the pseudo-inverse in Eq. (5) then becomes ill-conditioned as σ_0^2 increases. A procedure called "maximization of the

evidence" in Bayesian analysis can be carried out for σ_0^2.

Empirical exercise

See Section 6.3 for details related to the experimental data. All validation cases followed a similar treatment.

Overall, these are the two focuses in Bayesian analysis:

1. Learning from: Data only? Or, data plus prior information?

   If learning from data alone, that is the least-squares approach. If opening to both data and the prior information, it is Bayesian. The least squares is a special or limiting case of Bayesian. When tuning a certain parameter (σ_0), Bayesian analysis can behave just like least squares.

2. Deterministic vs. indeterministic

   That is, a fixed identification through least-squares analysis for previously obtained datasets vs. a distribution of all possible values due to the identification employing both data and an assumed variance.

4. DEMONSTRATION (VALIDATION) PROBLEMS

4.1. Overview

Model validation is necessary to ensure that the identified results from real-world data processing are reliable to reach definitive conclusions. Validation of the Bayesian methodology and programming in MATLAB were conducted (i) through the generation of deflection data based on beam theory and matrix structural analysis, and (ii) in contrast with the least-squares solutions. For relevancy, the validation cases were made to mimic the experimental loading and boundary conditions. The flexural data obtained from Floyd et al. (2016) featured two support conditions: a simply-supported span throughout and a simply-supported span with only one overhang of varying length.

Two test configurations were employed to produce deflection data with beam theory: a simple beam (SS - a simply-supported beam span) and a simple beam with an overhang (SO - a simply-supported beam with overhanging span) assuming a constant EI throughout the span. The matrix structural analysis (MSA) beam data was obtained using simply supported spans with and without overhangs, much like the SS and SO cases from the beam theory model, but with piecewise constant EIs throughout the span. The generation of data for both beam models simulate real-world testing by including uniformly distributed noise - versus the assumed Gaussian prediction error in the Bayesian problem formulation - of 5% for beam theory and 15% for MSA. Every validation case was analyzed using three and six substructures, however, only the three-substructure cases' results are reported in this section for brevity. Further subdivisions are explored in Section 6.2 for real-world data processing.

Utilizing the deflection data generated by these two models, the datasets were processed through the Main suite. Recovering the original flexural rigidity values using both beam models would validate the correctness of the MATLAB coding, thereby validating the proposed Bayesian methodology and allowing comparison with the least-squares method. Each

simulation case is discussed in detail.

4.2. SS and SO

The SS and SO deflection datasets were simulated by the application of a point load on a beam. The point load for the SS case was located at midspan whereas the load location for the SO case was at the end of the overhanging span (a special case not tested in the real-world data).

For both beams, uniform flexural rigidity values were specified and data were generated in MATLAB by programming well-established equations for the deflections and looping the programming from a starting load of 0 force units and ending at 16 force units, incrementally increasing the load by 10% of the maximum load.

As shown in Figs. 3 and 4, respectively, the SS deflections were obtained at 9 points along the length of the span and the SO deflections at 14 points along the span, as the lengths of the spans differ by 50%. After the data was generated, a uniform distribution of 5% noise was added to the data. This simulated flexural testing data was then input into the Main suite for flexural rigidity identification.

The beams' spans were segmented for EI identification and LVDT coordinates were specified to coincide with the locations of the deflections.

The results for the SS case are shown in Fig. 3:

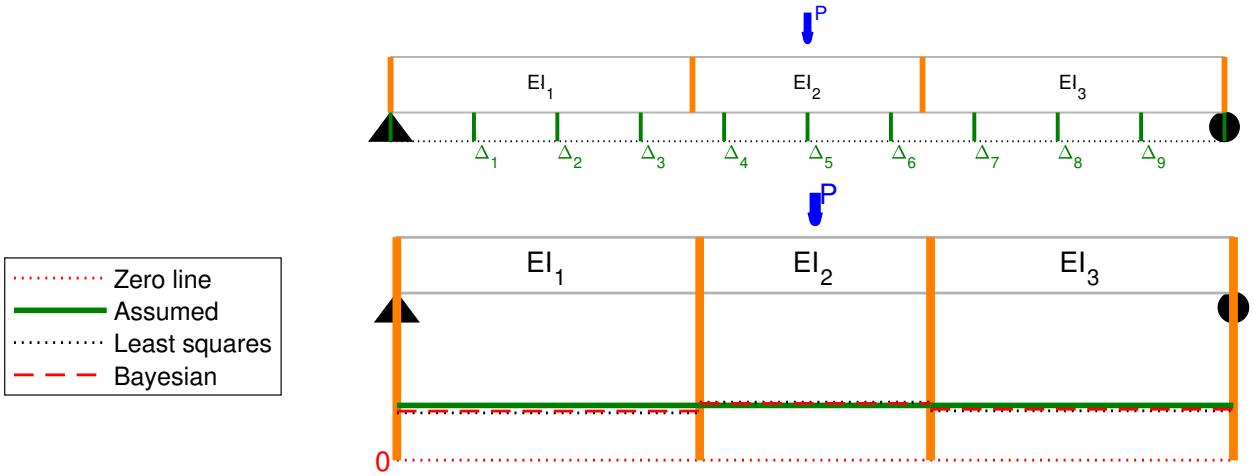

Anticipated $\boldsymbol{\theta}$:	1.00	1.00	1.00
Least squares:	1.07	0.97	1.05
Bayesian:	1.05	0.98	1.03
Anticipated EI (x10^8 kip-in^2):	2.00	2.00	2.00
Least squares (x10^8 kip-in^2):	1.88	2.06	1.91
Bayesian (x10^8 kip-in^2):	1.90	2.04	1.93

Fig. 3. Validation of the least-squares and Bayesian methodologies using a simple beam with uniform piecewise constant EIs and uniformly distributed addition of 5% noise

For each substructure of the SS case, the Bayesian analysis ($\boldsymbol{\theta}$) and least-squares ($\bar{\boldsymbol{\theta}}$) parameter values are nearly 1.00, meaning that the identified EIs for each span are roughly those used to generate the deflection data.

These results are replicated in the SO case, Fig. 4.

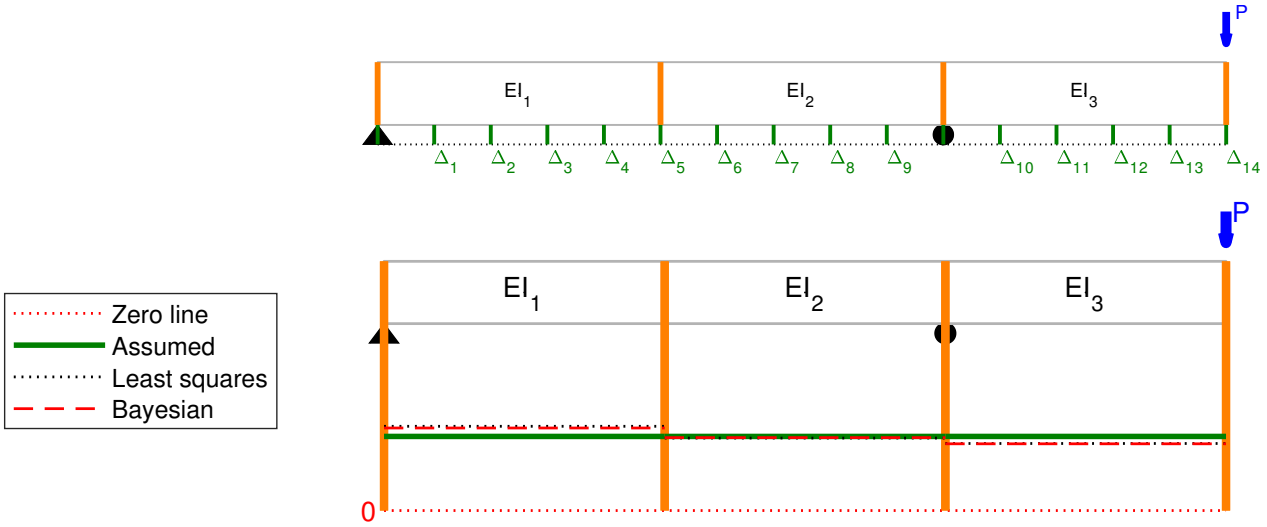

Anticipated $\boldsymbol{\theta}$:	1.00	1.00	1.00
Least squares:	0.91	1.01	1.06
Bayesian:	0.93	1.01	1.07
Anticipated EI (x10^8 kip-in^2):	2.00	2.00	2.00
Least squares (x10^8 kip-in^2):	2.20	1.97	1.88
Bayesian (x10^8 kip-in^2):	2.16	1.98	1.88

Fig. 4. Validation of the least-squares and Bayesian methodologies using a simple beam with one overhang with uniform piecewise constant EIs and uniformly distributed addition of 5% noise

Note that the least-squares and Bayesian analysis results are rather similar for the SS and SO validation cases, for which two possibilities arise: Either the data is not perturbed enough to cause difficulty in fitting or that the chosen prior is already considered a flat prior for this amount of noise added to an ideal dataset. To test these possibilities the SS and SO identifications are repeated with 10% uniformly distributed noise added to the data - the perturbed data begins to resemble measured data.

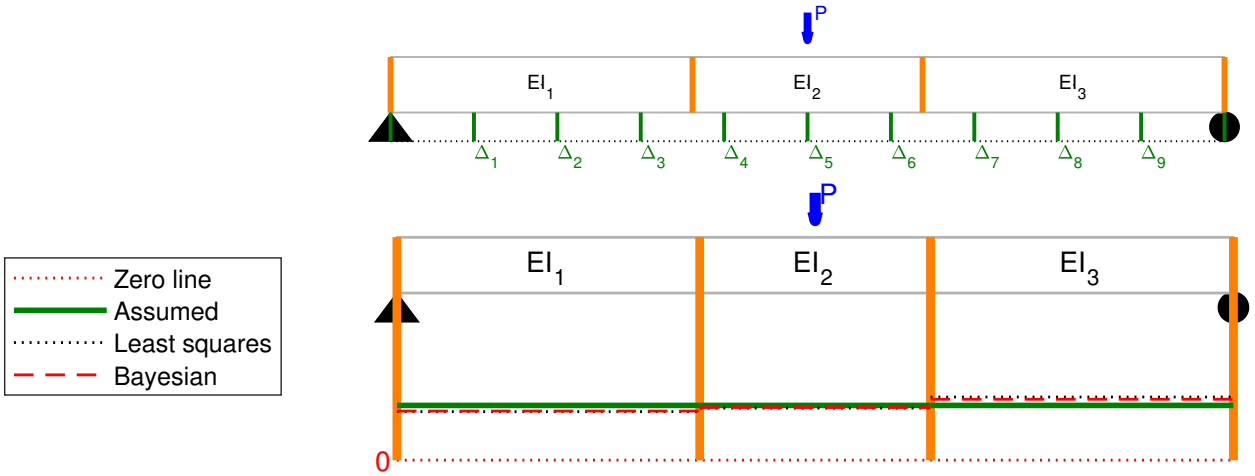

Anticipated $\boldsymbol{\theta}$:	1.00	1.00	1.00
Least squares:	1.06	1.02	0.93
Bayesian:	1.05	1.02	0.95
Anticipated EI (x10^8 kip-in^2):	2.00	2.00	2.00
Least squares (x10^8 kip-in^2):	1.90	1.95	2.16
Bayesian (x10^8 kip-in^2):	1.90	1.96	2.12

Fig. 5. Validation of the least-squares and Bayesian methodologies using a simple beam with uniform piecewise constant EIs and uniformly distributed addition of 10% noise

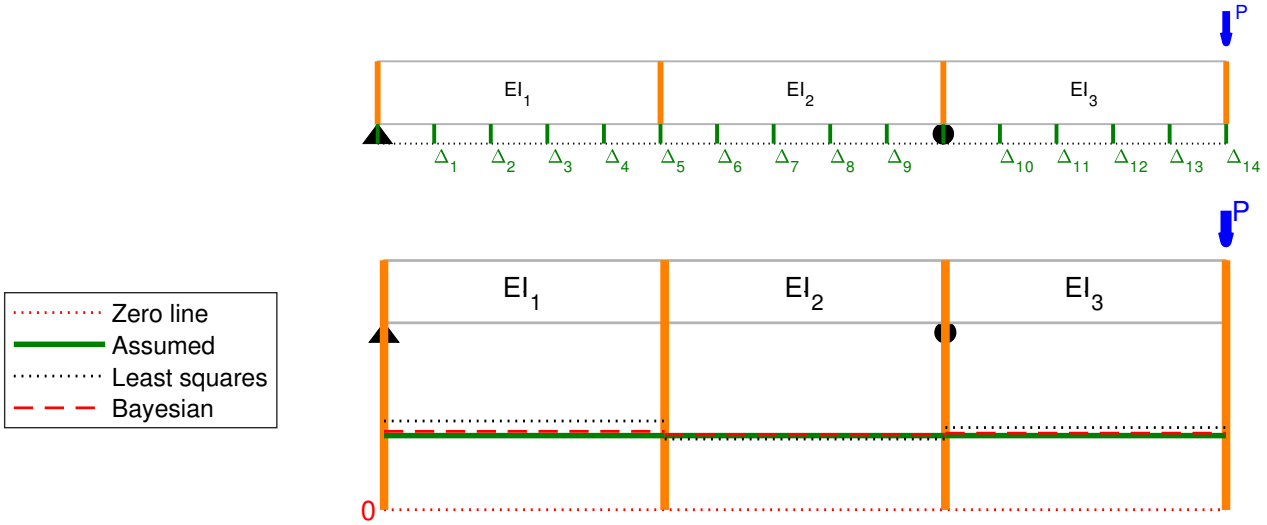

Anticipated $\boldsymbol{\theta}$:	1.00	1.00	1.00
Least squares:	0.87	1.03	0.93
Bayesian:	0.96	0.99	0.98
Anticipated EI (x10^8 kip-in^2):	2.00	2.00	2.00
Least squares (x10^8 kip-in^2):	2.30	1.94	2.15
Bayesian (x10^8 kip-in^2):	2.08	2.01	2.04

Fig. 6. Validation of the least-squares and Bayesian methodologies using a simple beam with one overhang with uniform piecewise constant EIs and uniformly distributed addition of 10% noise

With 10% uniformly distributed noise added, the imperfect Bayesian analysis results are still similar to the least-squares identifications. This can be explained by the choice of the prior for validation $\sigma_0 = 0.1$ (and testing, see Section 6.3) encompassing deviations within 10% of the nominal parameter values. Thus, the addition of more noise into the dataset is explored to conclusively validate the proposed Bayesian methodology.

4.3. Piecewise Beam

Utilizing beam theory, deflections were generated across each substructure assuming one constant EI value. Due to the variability of the damage states along the span of the girder used in this study, it was deemed necessary to study the effects of piecewise constant EI identification with different values. To do this, a MSA model was created allowing the assignment of distinct piecewise constant EI values based on the desired number of substructures. This beam model was created in a manner that allowed it to mimic any of the 17 testing configurations used in this study, for brevity, the setups of tests 1, 10, and 15 are reported here. To distinguish between the real-world testing and MSA validation, these cases are denoted "# MSA" (# - test configuration number). For all MSA datasets, 15% uniformly distributed noise is added to address the need for more noise from the SS and SO cases.

The 1 MSA dataset features piecewise constant EIs that are uniformly chosen to mimic the SS and SO cases. The value of the uniform EI is somewhat arbitrarily chosen to be in the range expected for Girder A. The results, as seen from Fig. 7, show that the proposed methods are able to reasonably identify each substructure's flexural rigidity.

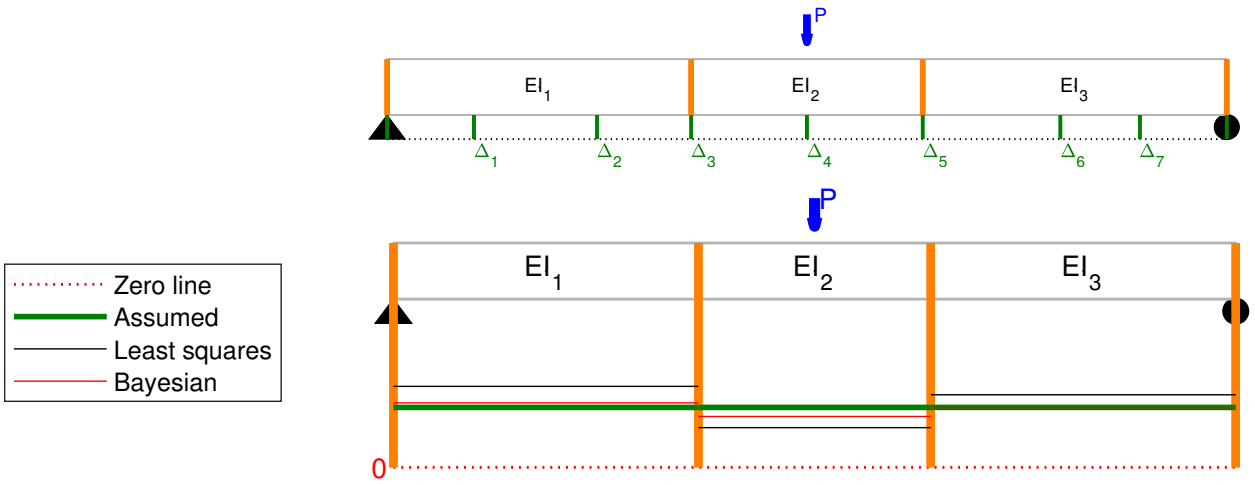

Anticipated $\boldsymbol{\theta}$:	1.00	1.00	1.00
Least squares:	0.81	1.19	0.88
Bayesian:	0.96	1.08	1.00
Anticipated EI (x10^8 kip-in^2):	3.50	3.50	3.50
Least squares (x10^8 kip-in^2):	4.34	2.95	3.96
Bayesian (x10^8 kip-in^2):	3.65	3.23	3.49

Fig. 7. Validation of the least-squares and Bayesian methodologies using a simple beam with uniform piecewise constant EIs and uniformly distributed addition of 15% noise, for the test 1 setup

Similarly, the 10 and 15 MSA datasets are processed in Figs. 8 and 9; the difference here being that the EI values arbitrarily chosen to simulate the deflections are not uniformly specified across the length of the beam. Note that the anticipated $\boldsymbol{\theta}$ values for these two cases are not the same 1.00 as specified in previous validation cases. Though the anticipated EIs are used to simulate the deflections in Figs. 8 and 9, normalization of the anticipated parameter $\boldsymbol{\theta} = \frac{EI_0}{EI_i}$ is done with a constant value (i.e., the same EI_i is not anticipated across each span likewise, the same $\boldsymbol{\theta}_i$ is not anticipated). Thus, EI_0 is taken to be the mean of the anticipated EIs.

Reasonable flexural rigidity values approximating the original flexural rigidities are recovered by Bayesian analysis in all MSA datasets, even with the addition of 15% uniformly distributed noise, thus validating the proposed Bayesian analysis model. Unreasonable identifications are seen by the least-squares methodology basically finding that the beam is twice as rigid than simulated in some sections.

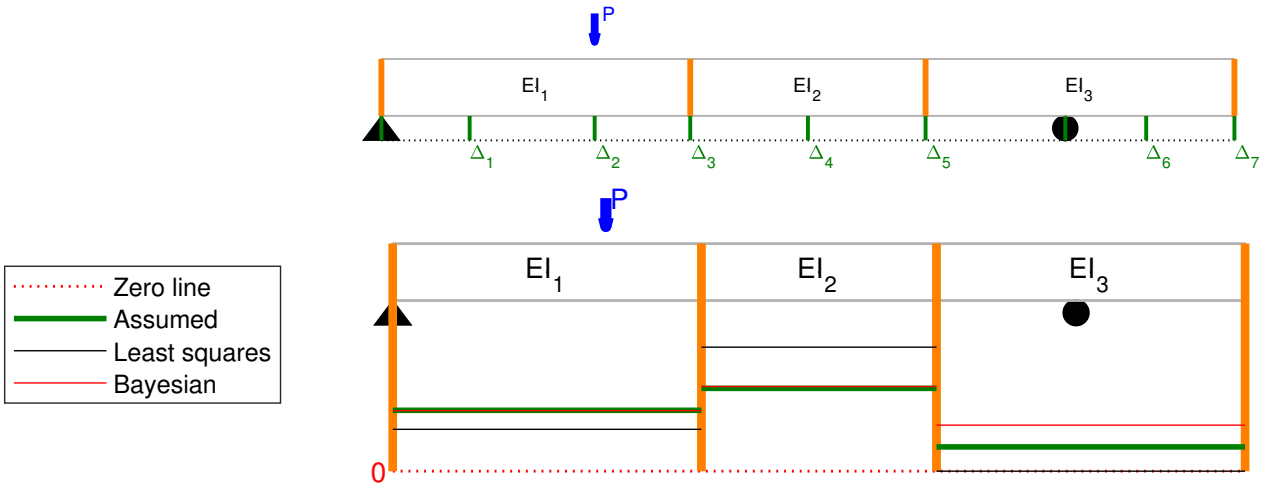

Anticipated $\boldsymbol{\theta}$:	1.00	0.80	1.33
Least squares:	1.17	0.42	2.74
Bayesian:	1.00	0.78	1.14
Anticipated EI (x10^8 kip-in^2):	4.00	4.00	4.00
Least squares (x10^8 kip-in^2):	3.41	9.42	1.46
Bayesian (x10^8 kip-in^2):	3.99	5.11	3.52

Fig. 8. Validation of the Bayesian methodology using a simple beam - with varying piecewise constant EIs and uniformly distributed addition of 15% noise, for the test 10 setup

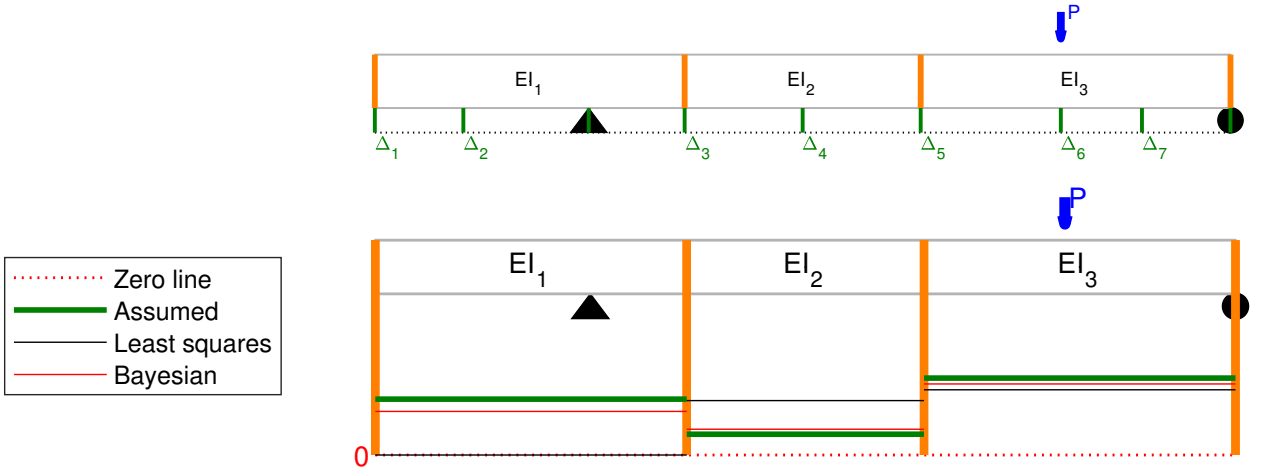

Anticipated $\boldsymbol{\theta}$:	1.00	1.33	0.80
Least squares:	4.14	1.01	0.91
Bayesian:	1.12	1.29	0.86
Anticipated EI (x10^8 kip-in^2):	4.00	4.00	4.00
Least squares (x10^8 kip-in^2):	9.66e+07	3.95	4.39
Bayesian (x10^8 kip-in^2):	3.58	3.11	4.67

Fig. 9. Validation of the Bayesian methodology using a simple beam - with varying piecewise constant EIs and uniformly distributed addition of 15% noise, for the test 15 setup. Note that all EIs are $\times 10^8$ kip-in^2 unless otherwise shown across each span.

Validating the proposed Bayesian methodology through the MSA datasets showcases its

robust identification capability and promising identification of real-world data, with the least-squares methodology providing adequate identifications only for uniformly rigid beam cases, of which are not expected in this study.

After introducing the problem formulation coded in the Main suite and validating the code through demonstration problems, focus returns to the preprocessing methodology in the Preprocessing suite. A brief review of the data acquisition setup and methods from Floyd et al. (2016) are provided. Thereafter, the preprocessing methodology is discussed and applied to large amounts of data.

5. DATA PREPROCESSING

5.1. Obtaining Data: A Review

The data acquisition system consisted of a "National Instruments (NI) CompactDAQ 8-slot USB chassis, an NI 9205 analog input module, and an NI 9219 universal analog input module" (Floyd et al. 2016). Additionally, LabVIEW (.vi) files were written specifically to test and calibrate the instruments. Prior to any testing, "the load cells were calibrated using the Fears Lab Baldwin Universal Testing machine that is externally calibrated once each year [and all] LVDTs were calibrated using a micrometer" (Floyd et al. 2016). After preparing the girder surface for loading, a battery of testing commenced.

5.2. Preprocessing Methodology

A total of 27 datasets were obtained from prior research and stored as Excel (.csv) files. The datasets encompass the 17 testing configurations conducted by Floyd et al. (2016), see Fig. 10. Tests where data acquisition issues were suspected to have occurred warranted additional testing and are distinguished in this study by letters "a" and "b" following the test configuration number.

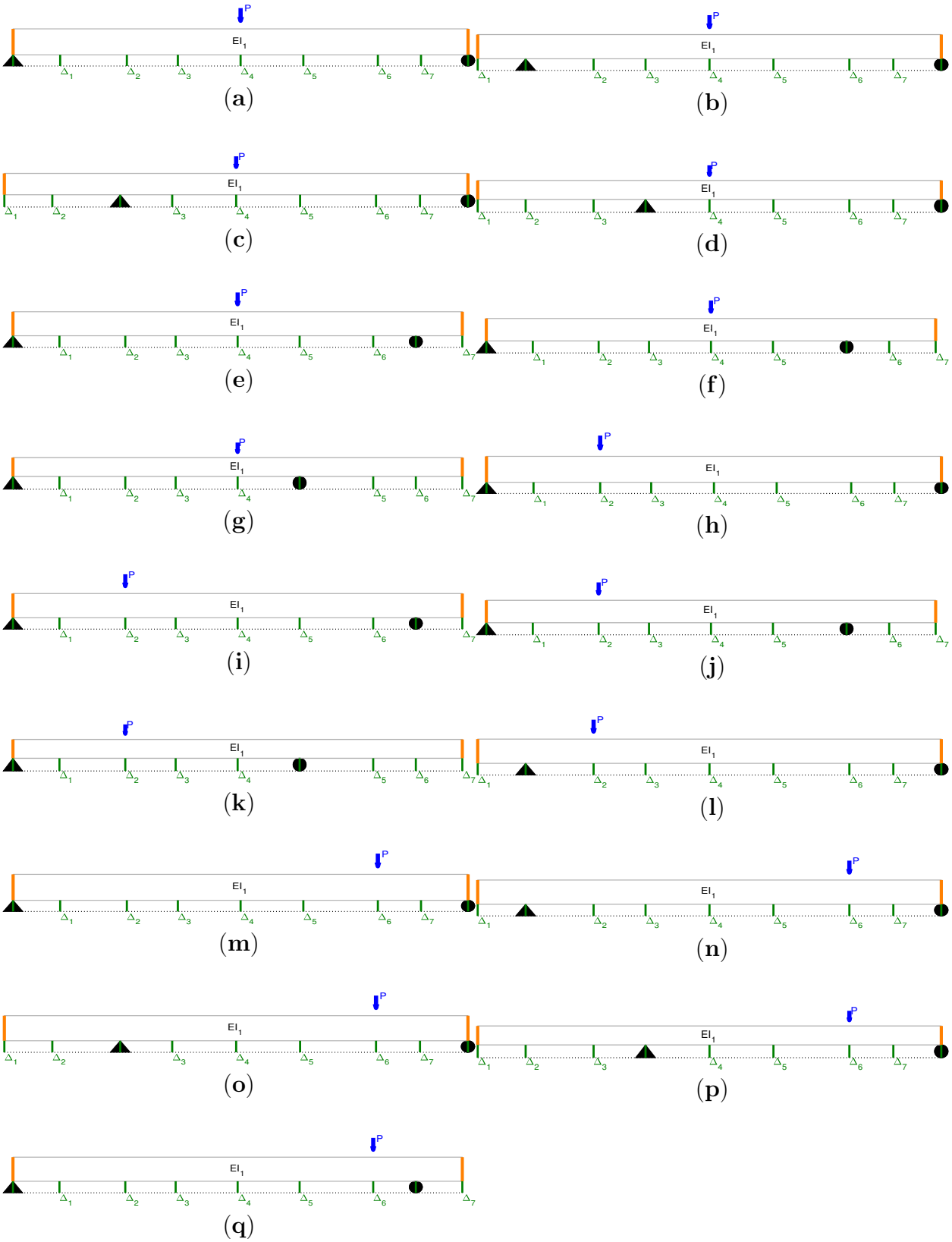

Fig. 10. Test configurations 1 (a) through 17 (q) utilized for flexural testing of Girder A

The Preprocessing suite in Fig. 1 is looped for the 27 datasets to automate filtering, quality checks, truncation, and reduction of the data. The deflection dataset's time histories were first truncated to remove the irrelevant data, shown in Fig. 11, before testing commenced.

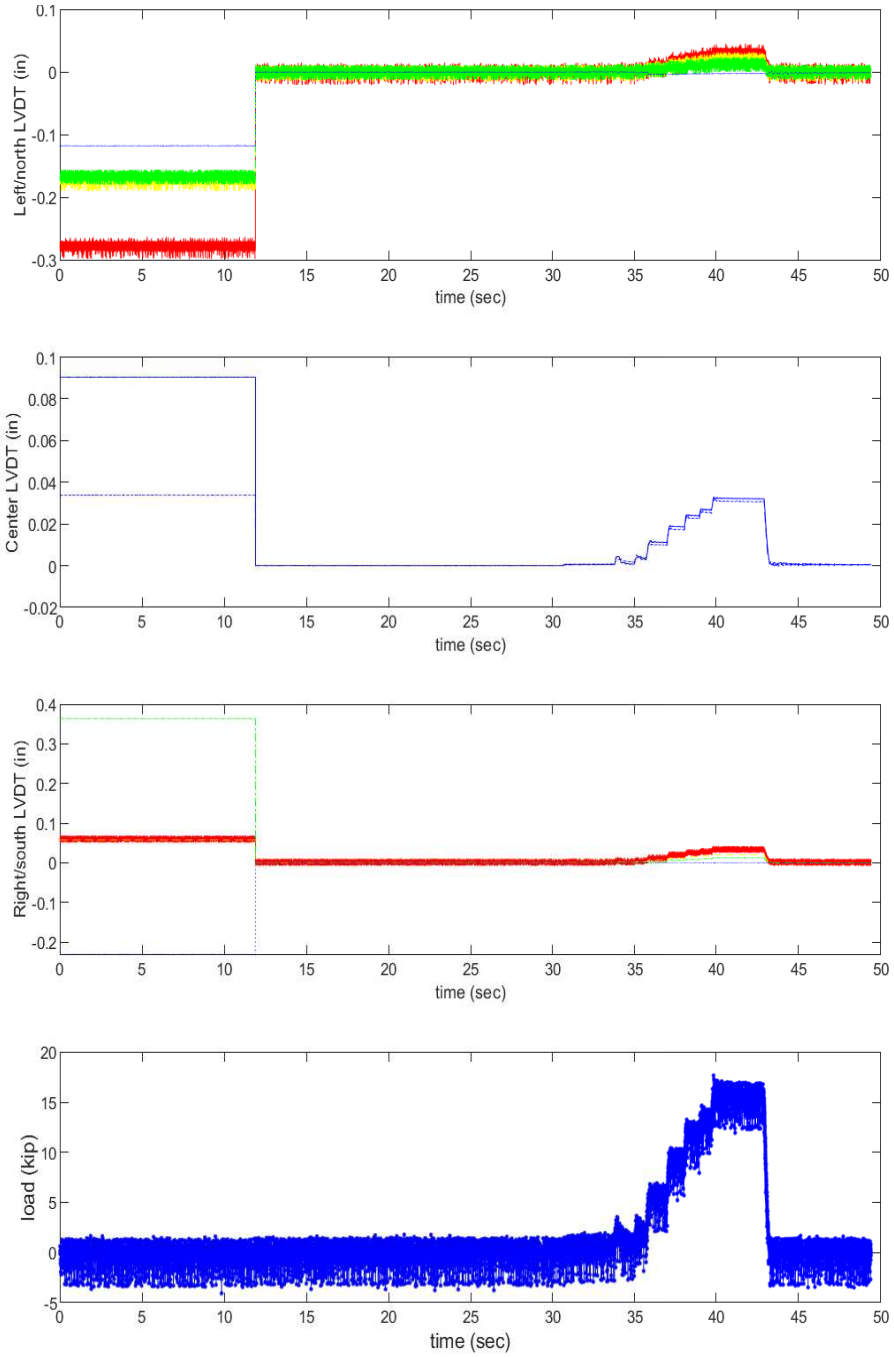

Fig. 11. Raw load/displacement vs. time history of a typical test including irrelevant data

The high frequency noise in Fig. 11 is then filtered utilizing MATLAB's butter and filter

commands. The second-order Butterworth digital filter is designed with a cutoff frequency of 0.01. The one-dimensional, lowpass filter designed by butter is then carried out by filter to produce the following typical load-deflection graphs for all LVDTs.

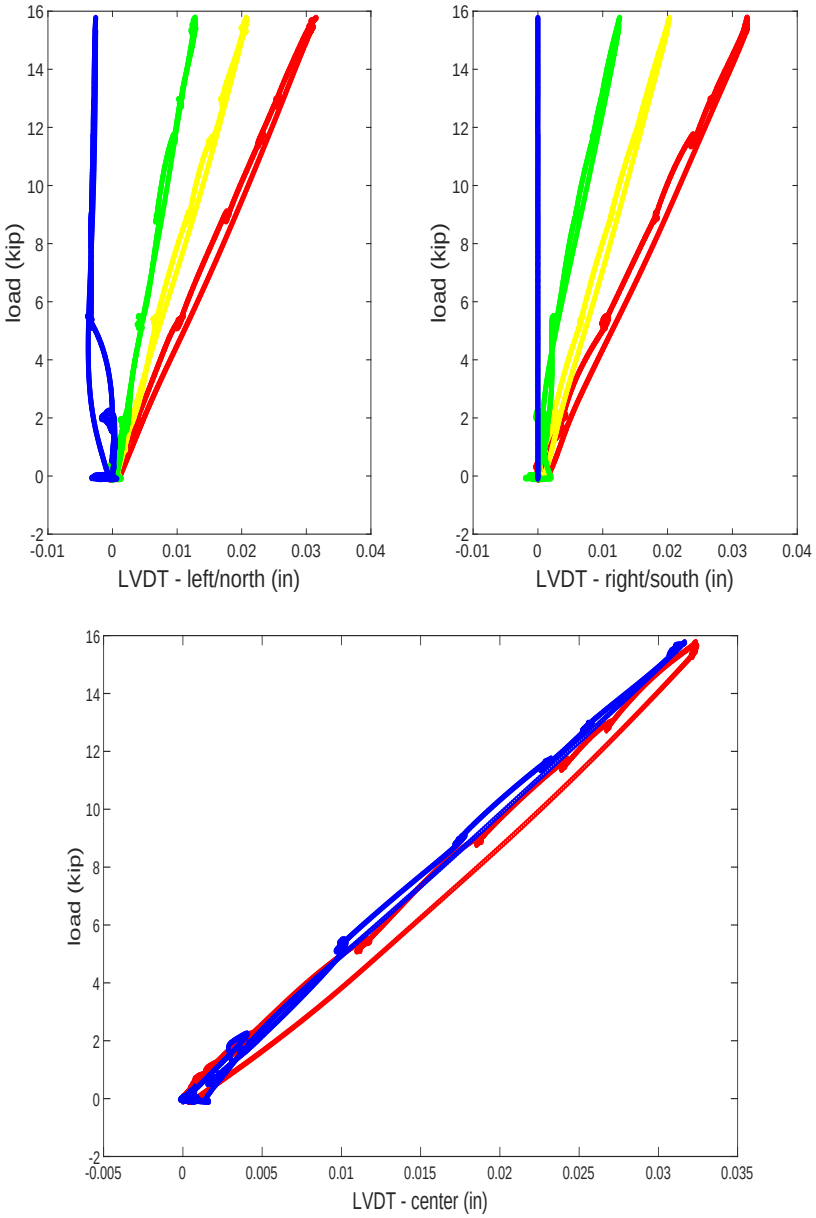

Fig. 12. Filtered (with a low-pass filter) multi-channel data measurements in terms of load-displacement. For the upper left panel, LVDTs L1 to L4 are shown from right to left. For the upper right panel, LVDTs R1 to R4 shown from right to left. For the lower panel, LVDTs C1 and C2 are shown from right to left.

Next, the filtered load-deflection data quality is observed utilizing LVDTs C1 and C2, each

located 5in from center line in opposing directions, shown in the lower panel of Fig. 13. These LVDTs were spaced approximately 10in apart and 3in off of the longitudinal centerline of the beam to account for torsional displacements during testing (Floyd et al. 2016). Additionally, from the top panel, it is evident that support settlement due to rigid body motion is captured by the filtered data.

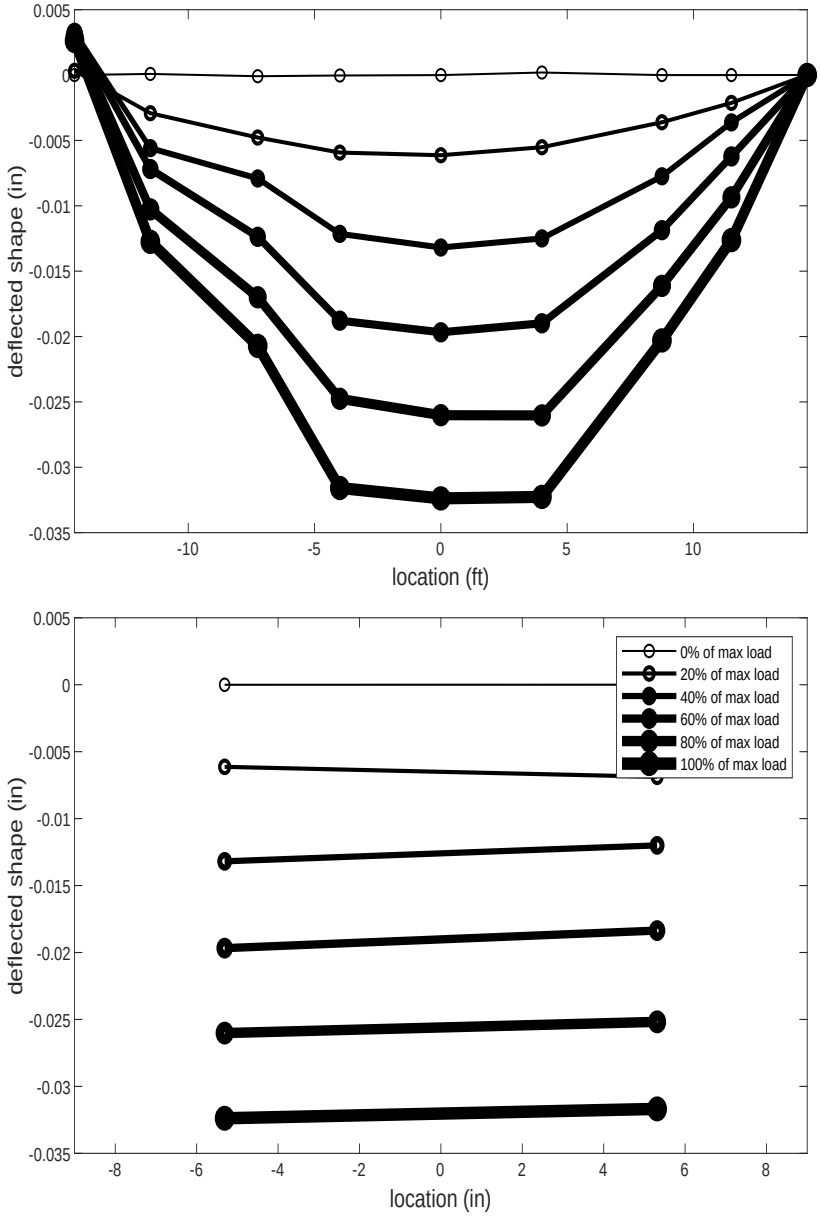

Fig. 13. Filtered (with a low-pass filter) and linearly interpolated multi-channel data measurements in terms of deflected shape and cross-sectional rotation to assess the data quality

Finally, the load-deflection datasets are reduced to include only the data points denoted by the circle markers in Fig. 14 - points least affected by the vibrations caused during loading (and unloading) of the beam. The identified points are further reduced by specifying the minimum peak distance between points and truncating the dataset once more to manually exclude time instances at the ends of the time histories where corresponding deflections are

not accurately captured.

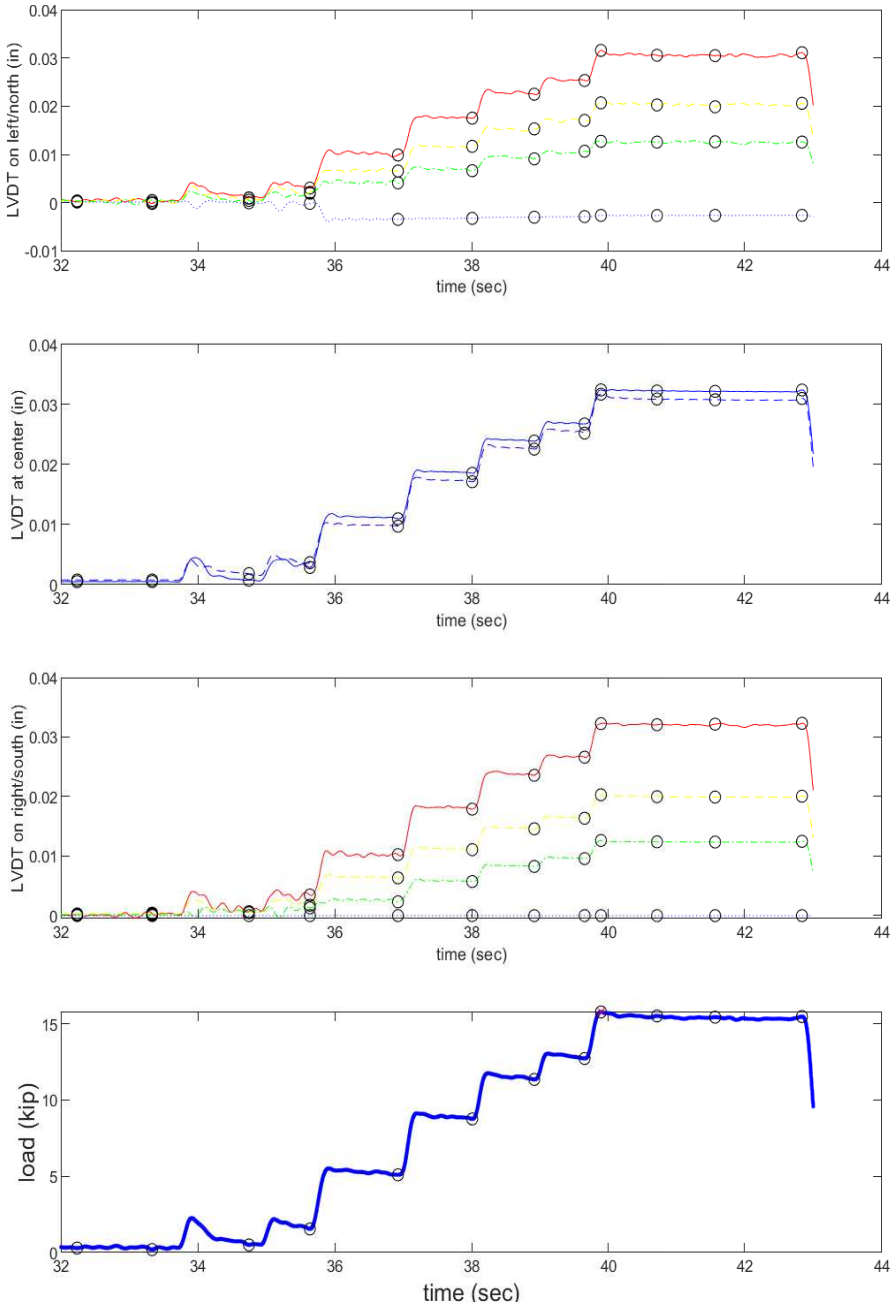

Fig. 14. Filtered (with a low-pass filter) and reduced (as shown in circles) multi-channel data measurements for further analysis using the proposed least-squares and Bayesian approach

The preprocessed datasets, consisting only of the filtered and reduced data, are then saved for piecewise EI identification through the Main suite.

6. RESULTS AND ANALYSIS

6.1. Uncertainties in Measurements and Modeling

Uncertainties in the modeling of deflection can be attributed to the following non-exhaustive categories:

Category 1: Environmental Effects stemming from ambient conditions such as temperature or humidity

Category 2: Material Properties Variations in moment of inertia I along the length as well as those in Young's modulus E_c along both span and depth of the member, are considered accordingly. Additionally, prior damage and testing damage experienced by Girder A in terms of steel debonding and crack formations between tests

Category 3: Experimental Variability in the data acquisition system from the load cell or LVDTs

Category 4: Modeling Numerical uncertainties and model-form uncertainties

Through this discussion insight is sought on the potential impacts on flexural rigidity identification stemming from the uncertainties under these categories.

6.1.1. Environmental

External factors in the form of ambient interference from temperature and humidity are first discussed. Not accounting for the curing of the concrete in any harsh conditions, focus is shifted to the effects of Category 1 on flexural testing. A vast amount of literature exists on temperature and moisture effects on the curing of concrete; however, relatively little exists (or is available) in terms of their effects on flexural testing. Shoukry et al. (2009)

determined an inverse correlation in both concrete strength and Young's modulus when related to temperature and moisture content.

Testing of Girder A occurred at Fears Structural Lab at the University of Oklahoma during the summer season, over the course of several days. The testing of Girder A in a laboratory setting allows for minimal effects in concrete strength reduction in terms of the research by Shoukry et al. (2009), who tested their specimens at upwards of 90% moisture content and 38°C (100°F). Though not a direct comparison to flexural testing, it is assumed that perhaps the impacts of ambient conditions are negligible and their minimal effects may be encompassed by the chosen prior standard deviation for other categories.

6.1.2. Material Properties

Variations in material property are inherently included in the current research or accounted for in later sections. A brief investigation of the variation of I along Girder A's length and the effects of debonding are conducted in Section 6.6. Additionally, issues related to debonding and data acquisition errors are touched on in Sections 6.2 and 6.4, respectively.

The value of Young's modulus as determined by Cranor (2015) encompasses the variability of E_c to describe the beam. Two determinations of Young's modulus are conducted for Girder A: through testing concrete cores and flexural rigidity testing. The concrete cores were taken at varying depths and span locations to find an average E_c. Of the cores taken, only 6 samples were retained due to sampling issues, however, spread is still seen in the determination of Young's modulus for the cores. The spread in sampling can also be attributed to time-dependent decreases, such as creep, after Girder A's 40 years of service. The average value for E_c determined by the concrete cores was 4750 ksi. Flexural rigidity testing averages lowered E_c. Though the cores represent discrete points along the length and depth of Girder A with some variation, the flexural rigidity testing average has a higher potential for fluctuation between tests based on procedure and measurement errors. The representative E_c for Girder

A, based on the largest value of E_c from flexural rigidity testing by Cranor (2015), is taken as 4150 ksi. This E_c value adopted in this study is an option that was later thought to not be as reliable as that found from the coring average. For normalization purposes EI_0 is taken to be 3.88×10^8 kip-in^2 from Table 4.14 of Cranor (2015) as determined from flexural testing, noting that this value is a product of E_c and I from flexural testing averages and should be reexamined.

6.1.3. Experimental

Mentioned previously, data acquisition errors occurred in the prior research. These matters will be discussed in detail in subsequent sections, however, it is beneficial to discuss the elements from which uncertainties may arise. High resolution measurements are made by the load cell and LVDTs for loading and deflections. Error is inherent to the measurements despite the accuracy of these instruments. The Interface model 1252 load cell's static error band (maximum error) is ±0.10 %FS (FS - Full Scale). Meanwhile, the LVDTs were able to accurately detect changes of approximately 0.001in, with typical errors on the order of 0.5% when compared to a calibrated micrometer.

Another potentially large source of error is attributed to movements in the support condition and possible imperfections in vertical alignment of the LVDTs. The testing of Girder A was conducted over the course of several days and repeated for certain tests where data quality was questionable. The instruments were calibrated for each non-repeated test but repositioning of the LVDTs was necessary between tests with different test configurations and those tests with questionable data quality, denoted by "a" and "b" in the test name. Repositioning the LVDTs on the underside of Girder A was found to be difficult at times.

When set for testing, LVDTs should contact the soffit of the girder at a perpendicular angle - otherwise, measurement errors may arise from the angle at which the LVDT contacts the girder. Deflections are relatively small near supports, this measurement error should not

drastically affect identification here but will have the potential to do so near the midspan of the beam where supports are not located. In addition to the potential for calibration errors between tests, calibration of the instruments may have varied over the 5 testing days. As such, there may exist some difference in prediction errors according to test day as well as between tests.

The testing conducted by Floyd et al. (2016) utilized 17 different test configurations. These configurations can be characterized into distinct three conditions: a simply supported beam (without overhanging spans), a simply supported beam (with an overhang on the left/north side of the beam), and a simply supported beam (with an overhang on the right/south side of the beam). The concern here is whether more error is associated with any of the three support conditions.

In data acquisition, the LVDT readings are thought to be influenced by uncertainties the most. Uncertainties and their impact through the act of flexural testing and test setup must be learned through the data. Inherent equipment accuracy error paired with the prior knowledge of the occurrence of data acquisition errors incites the necessity to account for these variabilities through σ_0.

6.1.4. Modeling

Uncertainties in modeling are based mostly on the assumptions in the problem formulation (model-form uncertainty) as well as observed numerical performance. An assumption made in the problem formulation is the assumed linear-elastic behavior of the beam. Built on the foundations of beam theory and applied to many substructures, piecewise constant flexural rigidity is to be identified. With loads that are not expected to cause yielding, data is collected for inverse identification of EI. For sections of the beam having pre-existing damage (debonded end sections due to corrosion), it is difficult to quantify the effects on data acquisition without an undamaged dataset comparison. Through piecewise constant flexural

rigidity localizations, damages are expected in the form of reduced EI values and functional threshold(s) of flexural rigidity may be defined/assumed to properly characterize "damage."

The issue of numerical uncertainties are normally addressed through the verification and validation process, where verification is the determination of whether the mathematical model is correctly solved and validation is the assessment of accuracy of the model simulation for its application domain. Roache (1998) simplifies these definitions as "solving the equations right" and "solv[ing] the right equations." Freitas (2002) further expands on validation to "solving the right model equations with the right methods" to disassociate numerical errors that arise between a given model and methodology to arrive at a solution. For this study, only validation is focused on. Intensive validations of the code and identified results are carried out by using demonstration problems with known solutions.

The objective of this process is to minimize error in code and model equations and then establish uncertainty bounds for a simulation (Freitas 2002). This process is followed by using demonstration cases (to minimize errors) as well as tuning user-defined parameters based on a coupled parametric study and comparing deflection predictions to physical measurements to quantify uncertainty in physical observations.

6.2. EI Distributions

Different piecewise divisions (substructures) were explored to determine possible idealizations of EI distribution and efficacy of the model. Idealized distributions consist of a small number of piecewise constant EI substructures required for consistency in identification. For example, a beam segmented into three substructures will return three EI values. Each of the three substructures is then further subdivided in half to give six substructures to examine if the EIs obtained are consistent with those of the three substructure beam. See Fig. 15. It is important to note that these divisions are not exhaustive but an initial exercise.

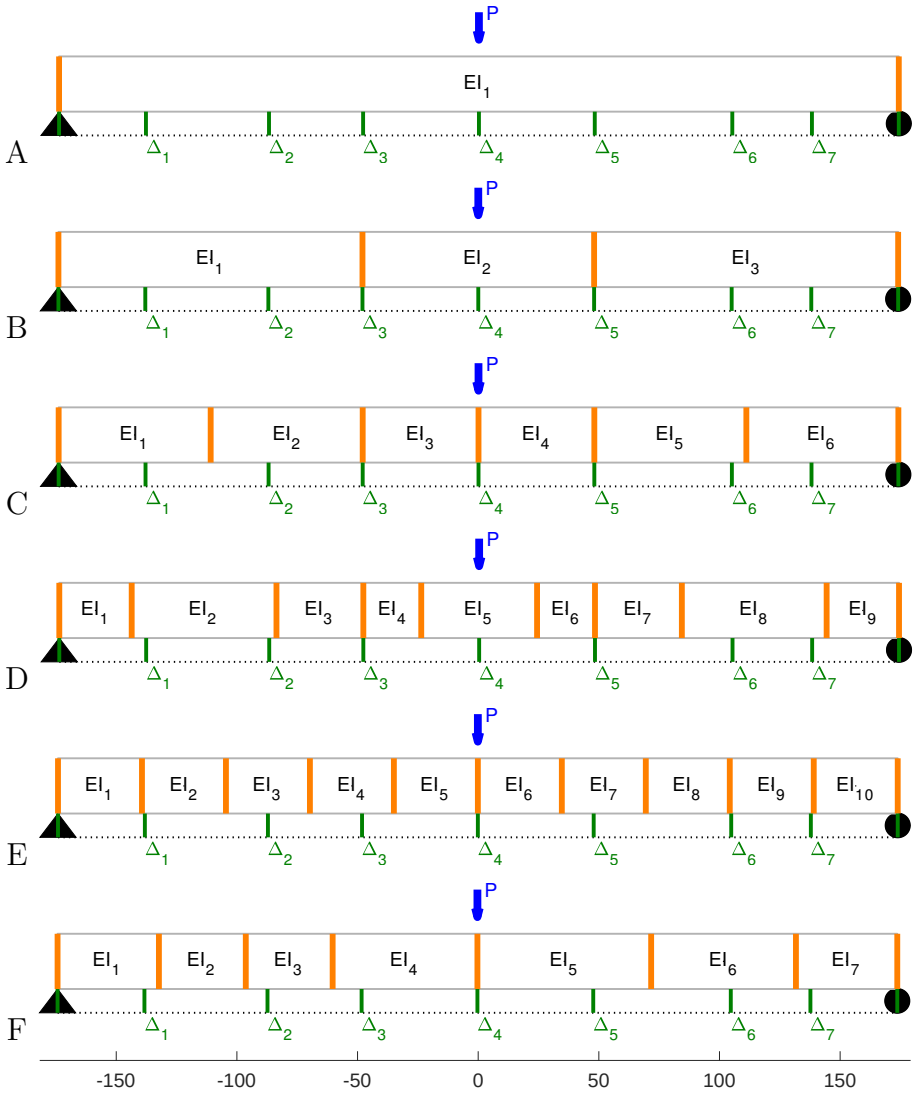

Fig. 15. 1, 3, 6, 9, 10, and an example arbitrary substructure divisions applied to a simulated Girder A

The following *EI* division substructures are used as shown in Fig. 15:

(A) "One substructure": No division in the beam with one uniform value of *EI* throughout

(B) "Three substructures": Three divisions with separation at the harping points (approximately 4ft from centerline)

(C) "Six substructures": Subdivisions are made to see if the results are consistent with those under "B"

(D) "Nine substructures": Further divisions made to see if the results are consistent with those under "C"

(E) "Ten substructure": Division of the beam into ten segments for damage detection localization

(F) "Arbitrary substructure": One realization of an arbitrary segmentation of the beam to explore robustness of model (a minimum span of 3ft is specified for identification clarity)

From Fig. 15, the substructure of panel A returns an EI value that characterizes the beam in a manner consistent with beam theory. The identified value in this case should return an average EI value that can properly describe the deflection behavior of the beam along its whole length. However, idealizing the beam into a single flexural rigidity span has the potential to produce a high degree of uncertainty as this uniform value must describe regions of variable damage (localized reductions in flexural rigidity). This would also suggest that uniform flexural rigidity would be a poor estimate by which recommendations on remaining capacity and/or retrofitting may not be appropriate.

This is where the significance of substructure "B" is realized. Three distinct sections can be identified by characterizing the beam based on the layout of the flexural reinforcement strands using the harping points as cutoffs (approximately 4ft on each side of the beam centerline). The three-substructure case balances the idealized constant EI for a given substructure with the variability of the cross-sectional properties and potential for damages along the beam. Determining the idealized EI distribution that may properly characterize Girder A requires further subdivisions of the substructures to ensure consistency in identification. "C" and "D" will be utilized for this purpose.

Substructure idealizations are subsequently referred to as "lower" or "higher-order" based on the number of substructures utilized. For example, case "A" is a lower-order substructure when compared to "B", which in this instance would be a higher-order substructure.

Notice, that the six substructure's EI divisions are at the midpoints of the three substructure's spans. Further subdividing the beam into nine substructures, it is evident that this segmentation does not follow suit. This is due to the six substructures' division points occurring at the minimum reasonable increment in inches. The subdivision of panel D shifts the division points to the nearest foot for clarity.

Evenly-spaced substructures are found in case "E". The use of ten substructures is determined to be beneficial for system identification after observing localization trends in higher-order substructures.

Finally, a randomized division is also made in the beam to determine the robustness of the proposed model. This arbitrary division is chosen one time so data can be analyzed for a given division. An additional substructure case was proposed with the intention of capturing the actual failure pattern(s) of Girder A from Floyd et al. (2016), however, the failures of the girder occurred in the inelastic loading range. This, along with a data acquisition error resulting in the loss of deflection data recorded during testing exhibiting strand-slip, led to using an arbitrary substructure as an alternative. With other available deflection data, there were concerns that the resolution and accuracy of the data in the elastic range would not be sufficient to characterize the beam when bond-loss occurred.

6.3. Parametric Study of User-Defined Parameters: Empirical Exercise

A parametric study for the values of σ_0 and $\sigma_{\text{init.}}$ can be seen in tabulated results in Appendix B, where an empirical approach is exercised.

As a motivating example and by using one typical set of experimental data, a case study is presented to better understand the choice of the user-defined parameter σ_0. See Fig. 16. The parameter values are chosen to be 0.01, 0.1, 1, 5 to vividly show the effect of the prior of being too small (not learning from data), just right, too large (only learning from data as in

least squares), and again too large (only learning from data as in least squares), respectively. For this reason, $\sigma_0 = 0.1$ could be used as an approximate number, which will be explained more shortly after.

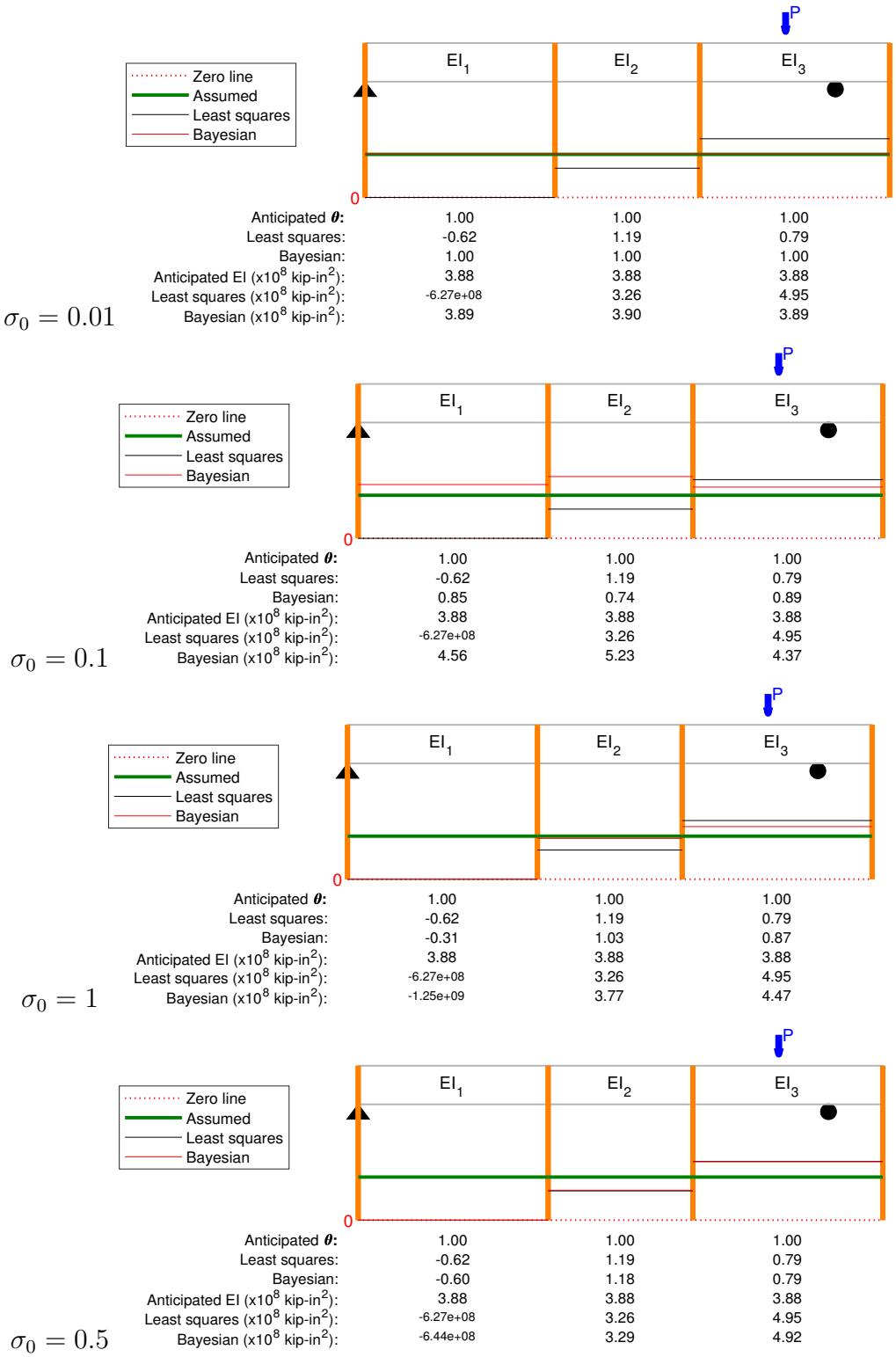

Fig. 16. Determining the upper limit of σ_0 as 1, where the Bayesian solution approach the least-squares solution, indicating a flatter prior. Tested priors are: 0.01 (top), 0.1, 1, and 5 (bottom) for a test 17a.

To start the empirical exercise, five different values of $\sigma_{\text{init.}}$ are chosen for each value of σ_0. $\sigma_{\text{init.}}$ was exercised in a large range by using 0.0001, 0.001, 0.01, 0.1, and 5. It was found that $\sigma_{\text{init.}} = 1$ never worked for any optimization, the reason of which is not understood. Thus, $\sigma_{\text{init.}} = 1$ is not used in this study.

A practical approach was adopted by monitoring the performance of the optimization; a unified value for $\sigma_{\text{init.}}$ for all test data is desired. The only problem with the optimization being the occasional negative σ outcome that still being investigated. To move on, the criterion of deciding a unified value for $\sigma_{\text{init.}}$ for all test data is to avoid this problem as often as possible. From Tables B.9 to B.13, for the one-substructure case, three $\sigma_{\text{init.}}$ values were highlighted with the lowest quantity of negative values for every σ_0 revealing that $\sigma_{\text{init.}} = 0.1$ consistently returned the least quantity of negative σ values, perhaps indicating that it is the optimal value in the given range. This same observation is made across the three, six, and nine-substructure cases but is not tested with the arbitrary-substructure case based on the significant computational resources already used for the results in Appendix B. Other values of $\sigma_{\text{init.}}$ between the orders of magnitude in the range specified are not tested as virtually every value of $\sigma_{\text{init.}}$ returns at least one negative σ across all substructures.

An afterthought stemming from Eq. (2) suggests that a reasonable σ and $\sigma_{\text{init.}}$ should be consistent with the range of $\mathbf{\Delta}$, typically about 0.03in, see Appendix D. This means that, very likely, σ would not be in the range of 0.1 let alone 5. $\sigma_{\text{init.}}$, the initial value for σ optimization could follow this analysis: Using 5 would be a waste of computational resources; using 0.1 may or may not be close enough to the optimized σ value.

After $\sigma_{\text{init.}}$, σ_0 is tuned with the obtained results from the one, three, six, and nine-substructure cases. The values chosen for the prior are 0.0001, 0.001, 0.01, 0.1, and 1, which differs than that used in the motivating example above. To decide σ_0, minimization of $\sigma_i, i = 1, \ldots, N$, the posterior standard deviation, is sought. This was done in an approximate manner through picking the lowest value of the posterior coefficient(s) of variation

(COV), α_i, which is defined as:

$$\alpha_i = \frac{\sigma_i}{\bar{\boldsymbol{\theta}}_i} \tag{6}$$

where σ_i are the square rooted diagonal elements of $\mathbf{S}$. The posterior COV is minimized through the choice of σ_0^2 and $\sigma_{\text{init.}}^2$ in maximizing the objective function (evidence), which acts as a likelihood for σ_0^2. This empirical approach, was initially thought to be rational, however, it was later learned that this approach suffered from a limitation: Eqs. (3) and (4) may be sensitive to more than σ_0^2. Nonetheless, the results based on this empirical approach in this study are reported.

From Tables B.9 to B.13, it can be seen that all α_i (COV) values become the prior values when $\sigma_0 = 0.0001,\ 0.001$, indicating that these prior values are too small so that the numerator in Eq. (6) is not updated, while the denominator is not updated as well, being σ_0 and 1, respectively. The motivating example above indicates that $\sigma_0 = 1$ is too large as the Bayesian results behave like that of least squares. Now, there are two values remaining: 0.01 and 0.1 for σ_0. Focus then shifts to $\sigma_0 = 0.01$, where changes in the COV for the one-substructure case are now seen. However, even at this magnitude, the COV values tend to be equal to the prior in the higher-order substructures. Eventually $\sigma_0 = 0.1$ turns out to be reasonable for the prior, based on the COV values which rarely agree with $\sigma_0 = 0.1$. These findings for the one-substructure case are corroborated by the three, six, and nine-substructure cases.

Though $\sigma_0 = 0.1$ is specified, true optimization of σ_0 may still lie at a value between 0.1 and 1. This is because the empirical exercise is manually done at discrete values. Nonetheless, both unified approximate values $\sigma_{\text{init.}} = 0.1$ and $\sigma_0 = 0.1$ were obtained through an extensive examination, increasing confidence in these two important user-defined parameter values.

In fact, $\sigma_0 = 0.1$ does make sense from another viewpoint. This is 10% of 1, the mean of the prior distribution of $\bar{\boldsymbol{\theta}}$. This could be a reasonable guess for the variation expected of $\bar{\boldsymbol{\theta}}$. On the other hand, when $\sigma_{\text{init.}} = 0.1$, σ varies between 3 to 5% of the maximum value of

the measured deflection for reasonable identification results as in test 1, versus 26% for an unreasonable identification result as in test 14b.

6.4. "Good" and "Bad" Data

A total of 27 tests, with 17 test configurations, were conducted on Girder A. The quality and condition of the measurement devices were questioned throughout this study, even at the laboratory when the data was collected. Proper functioning of LVDTs were questioned even after calibration and examinations; this was the rationale for repeating most of the test configurations. Despite these efforts, the collected data was re-examined when questions arose regarding measurements by specific LVDT(s) in some tests. Here, LVDT L1 is discussed only to illuminate the challenge.

The preprocessed data was first examined in terms of time histories, force-displacement and deflected shape plots regarding measurements by all LVDTs in all tests, see Figs. 11 to 13. A few LVDT's measurements were in question from time to time, even after excluding the effects of rigid body motion, where the resulting elastic curves are shown in Fig. 17.

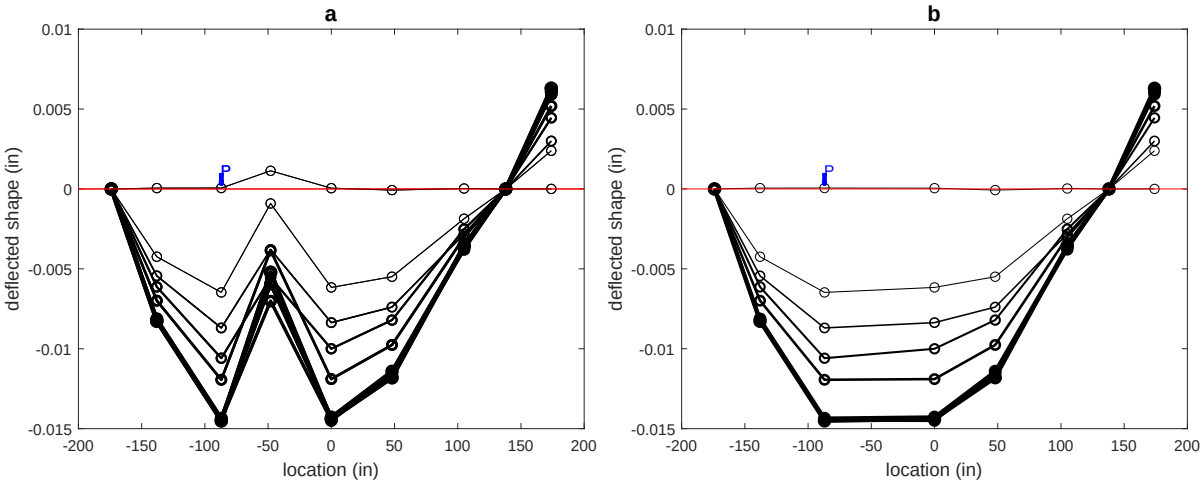

Fig. 17. Panel (a) depicts test 9a, a typical test result involving LVDT L1 (located left of center at about 50 in) that is most likely malfunctioning. Panel (b) provides strategy adopted to remove all readings from the possibly unreliable L1.

In principle, an elastic curve is obtained through the so-called double-integration of $\frac{M(x)}{EI(x)}$. $M(x)$ is known to be piecewise linear, and $EI(x)$ is assumed to be piecewise constant. Since the piecewise constant EI being drastically different is not anticipated, the elastic curve should not differ fundamentally from the counterpart of one constant EI value, which is known based on structural analysis.

For the test configuration shown in Fig. 17, inflection points are not anticipated. With this said, the "spikes" caused by LVDT L1 (located at about -50in) are questionable. This then raises concern of whether and how much the readings of any suspicious LVDTs would impact the identified piecewise EI values. Carefully examining the elastic curves led to the conclusion that not all LVDTs performed reasonably at all times. In other words, some elastic curves were deemed reasonable, while others were not, see Fig. 18.

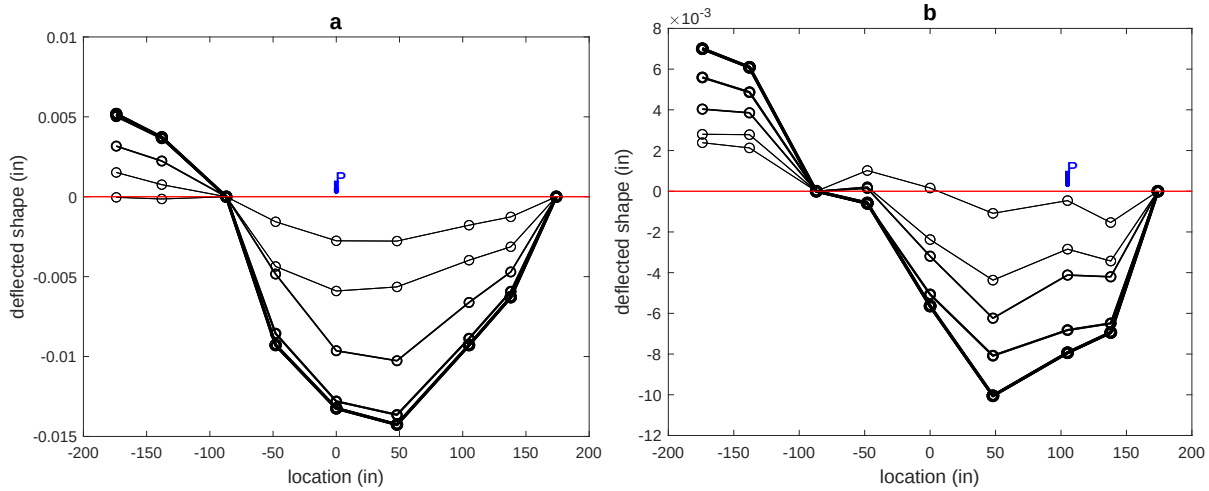

Fig. 18. Panel (a) depicts test 3, a typical test exhibiting overall reasonable LVDT performance. Panel (b) depicts test 15a, a typical test exhibiting overall unreasonable LVDT performance.

Confirming that some LVDT readings were questionable, taking L1 as the most evident situation based on Fig. 17, it was then necessary to remove the data associated with the specific LVDT so that the identified results were not corrupted. In the case of Fig. 17, the drastic decrease in deflection at the "spiked" reading artificially stiffens the beam (less deflection implying stiffer section); removing LVDT L1 from this case should decrease the

identified flexural rigidity. Panel (b) of Fig. 17 shows the removal of L1 from all loading history associated with the test resulting in a smoother curve consistent with the loading. In this instance, the malfunctioning LVDT is seemingly obvious to identify. On a case-by-case basis it can be increasingly difficult to identify a malfunctioning LVDT, as shown in panel (b) of Fig. 18. It is evident that some method is required to determine which tests were affected by a possible malfunction. For this purpose, exercises are performed to calculate the entropy of each test's prediction error and identified posterior parameters to quantify L1's effect. The concept of entropy will be discussed in the following section.

With the questionable nature of some of the collected data, attempts were made to identify the tests where L1 may be kept and those where L1 must to be removed for the sake of an unbiased identified result. Two strategies/options for each test were assessed to reduce the subjectiveness in removing the affected data: the first, using all datasets and the second, using all but L1 datasets - even though it is suspected that other LVDTs could have malfunctioned as well. Here, information entropy concepts are exercised including both differential entropy and relative entropy (i.e., KL distance including forward and backward KL), where a lower entropy means less uncertainty, while a higher entropy means more uncertainty. As such, the identified results with reduced uncertainty (i.e., lower entropy), are preferred. Nonetheless, how low is considered low is unknown, which needs to be determined using a cutoff value.

The posterior means and variances for the univariate and multivariate Gaussian entropies were evaluated, the variance of the prediction error for the univariate Gaussian entropy is also exercised upon. The calculated results are fairly scattered from test to test making the decision on the cutoff value ambiguous. To supplement the numbers, the deflected shapes are assessed by using structural analysis, based on which a cutoff value for KL distance is proposed, below which L1 data may be accepted. The calculations involved (i) L1 kept in all tests, and (ii) L1 removed from all tests. Recommendations were also made regarding (iii) L1 removed from some tests.

6.4.1. Univariate Entropy Exercise

Entropy is most easiest compared for the one substructure case, the lowest-order substructure. Two categories were then created and named intuitively: "Uncorrected" and "L1 Corrected". "Uncorrected" houses all 27 datasets which include all LVDTs and all data associated. "L1 Corrected" also includes the same 27 test datasets however, the readings of L1 are removed from all tests with the exception of tests 4a, 4b, and 16a. This is due to the location of the support coinciding with L1 during these tests.

The univariate Gaussian entropies are then calculated for the 27 tests in the "Uncorrected" and "L1 Corrected" categories as so (Bishop 2006):

$$H_u = \frac{1}{2}\ln\left(2\pi e\sigma_{1,u}^2\right) \ , \ H_c = \frac{1}{2}\ln\left(2\pi e\sigma_{1,c}^2\right) \tag{7}$$

where H_u and H_c represent the "Uncorrected" and "L1 Corrected" univariate Gaussian entropies of the prediction error, respectively. Recall, σ^2 is the variance of the Gaussian prediction error, which is a continuous variable. For a continuous variable, a higher entropy indicates more uncertainty in the variable. Thus, larger values of H can relay more information about the effect of L1 on EI results in terms of uncertainty. H_u is compared with H_c to rule out the necessity of excluding L1. That is, if $H_u > H_c$, then L1 readings are excluded. If $H_u < H_c$, then L1 readings are kept.

For this purpose, the entropy ratio is calculated, $ER = \frac{H_u}{H_c}$. All H_u, H_c, and ER are given in Table 3 under Columns 4, 5, and 6, respectively. The test days are grouped chronologically such that the top section of Table 3 is the first day of testing. All elastic curves for the last day of testing exhibit issues with L1 similar to panel (a) of Fig. 17. Entropy, however, cannot precisely determine that L1 is actually malfunctioning. Comparing the entropies for every test in both categories, H_u and H_c describe information about the underlying Gaussian probability distribution, not about the meaning of an event itself (Cotra 2017, Thomas 2019).

Entropy can be used to determine how well the test's results are described by the probability distributions of "Uncorrected" and "L1 Corrected" then infer L1's effects.

Table 3. Differential (H) and relative (KL) univariate Gaussian entropies calculated to infer the effects of L1 on EI identification

TestDay	Test	TestSetup	"Uncorrected" (H_u)	"L1 Corrected" (H_c)	ER	KL Fwd.	KL Rev.
1	1	SS	3.188	3.012	1.059	0.259	0.364
	5a	SO South	3.208	3.119	1.029	1.882	2.250
	5b	SO South	NaN	NaN	NaN	NaN	NaN
2	2a	SO North	2.308	2.170	1.064	0.402	0.528
	2b	SO North	2.049	1.901	1.078	0.162	0.215
	4a	SO North	2.521	2.521	-	-	-
	4b	SO North	1.460	1.460	-	-	-
	6a	SO South	1.877	1.713	1.096	0.182	0.249
	6b	SO South	1.333	1.227	1.087	0.144	0.178
	7	SO South	1.150	1.165	0.987	0.150	0.146
3	3	SO North	1.554	1.519	1.023	0.060	0.064
4	8	SS	2.801	2.724	1.028	2.248	2.622
	13a	SS	2.665	2.830	0.942	3.483	2.508
	13b	SS	2.771	3.291	0.842	7.193	2.599
	14a	SO North	1.691	1.573	1.075	0.013	0.016
	14b	SO North	2.776	2.836	0.979	1.059	0.939
	15a	SO North	1.701	1.661	1.024	0.065	0.070
	15b	SO North	1.910	2.034	0.939	0.264	0.207
	16a	SO North	1.260	1.260	-	-	-
	17a	SO South	1.995	2.004	0.995	1.386	1.362
	17b	SO South	1.914	1.807	1.059	0.618	0.764
5	9a	SO South	2.003	2.989	0.670	51.460	7.425
	9b	SO South	2.046	3.133	0.653	65.720	7.803
	10	SO South	1.411	1.443	0.978	2.767	2.596
	11	SO South	1.266	1.353	0.936	1.167	0.982
	12a	SO North	2.269	2.621	0.866	6.747	3.356
	12b	SO North	2.521	3.249	0.776	37.705	8.930

Table 3 depicts an ambiguous result: A majority of tests indicate an unclear trend with ER being close to one. Surprisingly, the last day of testing indicates that keeping L1 is better than removing it. Table 4 is designed for examining all σ; it is found that Test 5b's σ is not meaningful thus its entropy is excluded in Table 3 by using "NaN". Additionally in Table 3,

the data of the entries reported as **"-"** remain unchanged due to the location of the supports coinciding with L1, thereby revealing no information (i.e., zero entropy).

Table 4. Checking signs of univariate Gaussian σ from the maximized objective function for data inclusion/exclusion. † denotes tests with negative σ values.

Test	$\sigma_{1,u}$	$\sigma_{1,c}$
1	0.0017	0.0018
2a	0.0023	0.0024
2b	0.0035	0.0037
3	0.0033	0.0033
4a	0.0007	0.0007
4b	0.0017	0.0017
5a	0.0010	0.0009
5b†	-0.0019	-0.0020
6a	0.0024	0.0025
6b	0.0044	0.0047
7	0.0034	0.0031
8	0.0014	0.0013
9a	0.0028	0.0008
9b	0.0026	0.0007
10	0.0043	0.0034
11	0.0042	0.0033
12a	0.0011	0.0007
12b	0.0013	0.0006
13a	0.0015	0.0011
13b	0.0009	0.0005
14a	0.0032	0.0035
14b	0.0009	0.0008
15a	0.0026	0.0026
15b	0.0015	0.0013
16a	0.0040	0.0040
17a	0.0008	0.0007
17b	0.0011	0.0011

Given this unclear outcome using the univariate Gaussian entropy, another entropy measure is employed. The Kullback-Leibler divergence (KL), also known as relative entropy, is calculated between two univariate Gaussian distributions p_1 and p_2 with μ_1 and μ_2, and σ_1 and

σ_2 as the means and standard deviations, respectively.

$$KL(p_1, p_2) \;=\; \log \frac{\sigma_2}{\sigma_1} + \frac{\sigma_1^2 + (\mu_1 - \mu_2)^2}{2\sigma_2^2} - \frac{1}{2} \tag{8}$$

where larger KL values provide more "evidence" distinguishing the two categories, see 2.5 for a concise explanation of the significance of the KL divergence. The KL distance is applied to the identified parameter values, which are Gaussian variables with mean $\boldsymbol{\theta}$ and variances $\mathbf{S}$ as given earlier; the KL distance will not be applied to the two prediction-error distributions with $\sigma_{1,u}$ and $\sigma_{1,c}$ as the variances, respectively. In application, there are two options: (i) the Forward (Fwd.) KL calculation where p_1, the "Uncorrected" data, is assigned as the "true" probability distribution (described in Eq. (8)) and (ii) the Reverse (Rev.) KL calculations where p_2, the "L1 Corrected" data, is assigned as the "true" probability distribution (Eq. (8) where all subscripts are reversed). Assuming a "true" probability distribution, the KL divergence value indicates how closely the remaining distribution describes the true distribution; larger values indicate more divergence ("evidence") separating the two distributions. The non-commutative property of KL divergence will show the Forward and Reverse KL calculations to be unequal, see the last two columns of Table 3 for results.

In the last testing day, relatively high Forward (Fwd.) KL values were determined, with respect to other KL values in the same column, which are consistent with the suspicions of L1 malfunctioning during all tests during this day. This also explains why similar numerical performance is seen in the same tests for the Reverse (Rev.) calculations. From column "KL Rev." only slightly increased values of KL are seen relative to the rest of the tests - this is due to the difference in the shape of the probability distribution function of the modeled "true" Gaussian distribution. The same evidence trends are determined from the Forward and Reverse KL calculations. Hereafter, only the Forward calculation of KL is reported for ease in comprehension in terms of the "evidence" discussed above.

Unfortunately the values of KL divergence do not seem to unambiguously determine the necessity of L1's removal, thus a cutoff value for KL is defined to determine whether a test is likely to be influenced by L1. To do so, each test's KL value is paired with their deflected shapes. A low enough KL value with a deflected shape that unambiguously indicates the need for L1 removal (i.e., "unreasonable") is sought. Among six typical tests given in Table 5 and depicted in Figs. 19 to 21, it can be seen that test 11 pinpoints the cut off value which is 1.167. Table 3 shows the values of tests 9a and 9b are exceptionally high when compared to other tests, hinting a consistent necessity of L1 removal for both tests. Furthermore, Fig. 20 illustrates reasonable elastic curves that are seemingly not affected by L1. With low KL values for both tests in conjunction with the elastic curves, it is determined that L1 does not affect these tests. However, observing L2 (at approximately -100in) in test 2a, there is potential for identification improvement. The high KL values for tests 13a and 9b, Fig. 21, stem from the evident obfuscating of the elastic curves by L1. Test 14b in panel (a) of Fig. 19 is not selected as the cutoff due to its ambiguous deflected shape.

Table 5. KL values representing the spread obtained from analysis of the univariate case

Test	KL Fwd.	Classifications	Deflected Shape
3	0.060	Very low	Reasonable
2a	0.402	Low	Reasonable
14b	1.059	Potential alternative cutoff	Ambiguous
11	1.167	Assumed cutoff	Unreasonable
13a	3.483	High	Fairly Reasonable
9b	65.720	Very high	Unreasonable

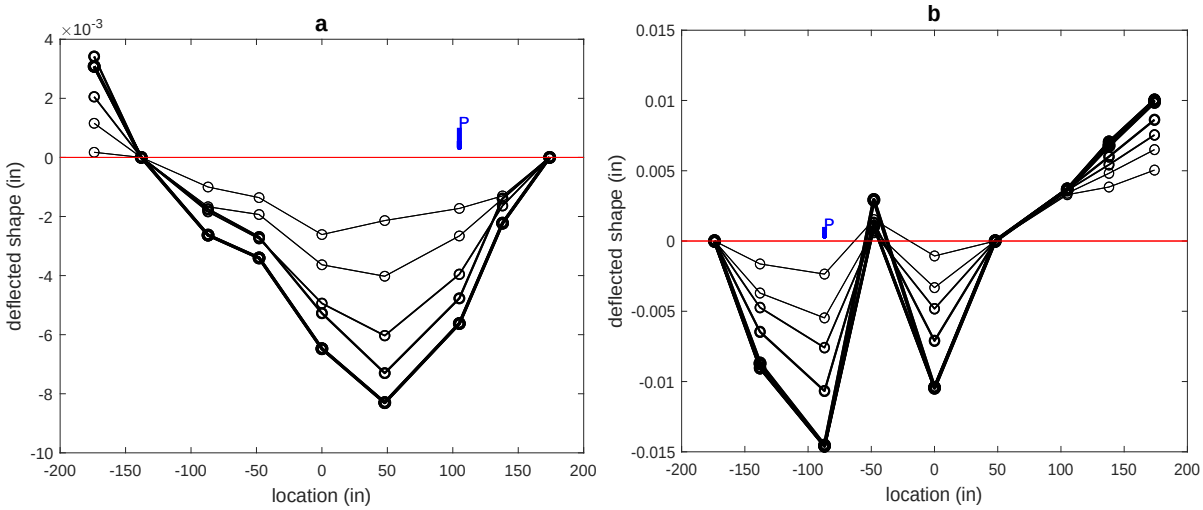

Fig. 19. Panel (a) depicts test 14b's deflected shape and panel (b) is test 11's deflected shape. These deflected shapes are used to determine the criteria for the cutoff point of KL.

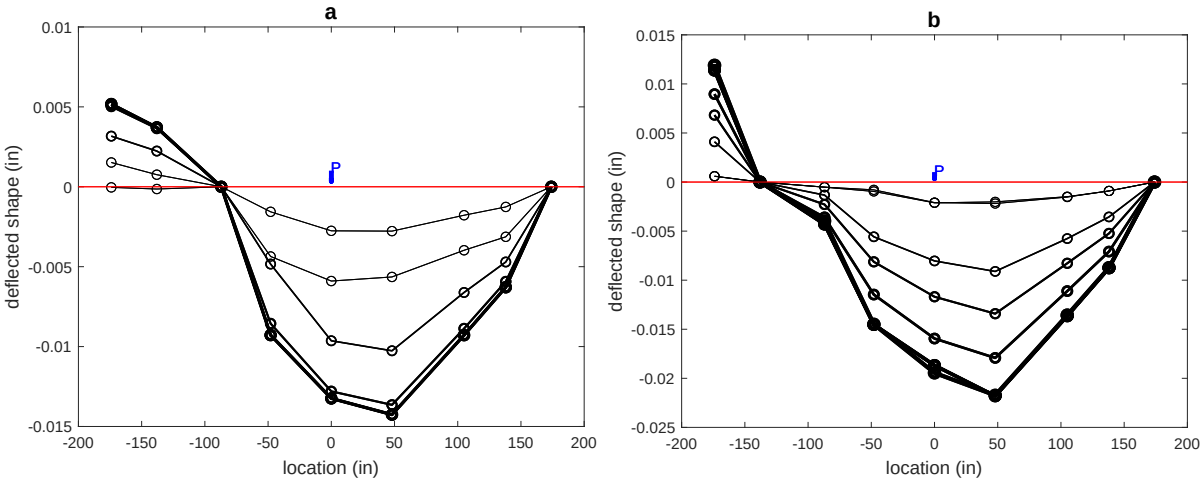

Fig. 20. Panel (a) depicts test 3's deflected shape and panel (b) is test 2a's deflected shape. These deflected shapes are examples of elastic curves with acceptable L1 readings.

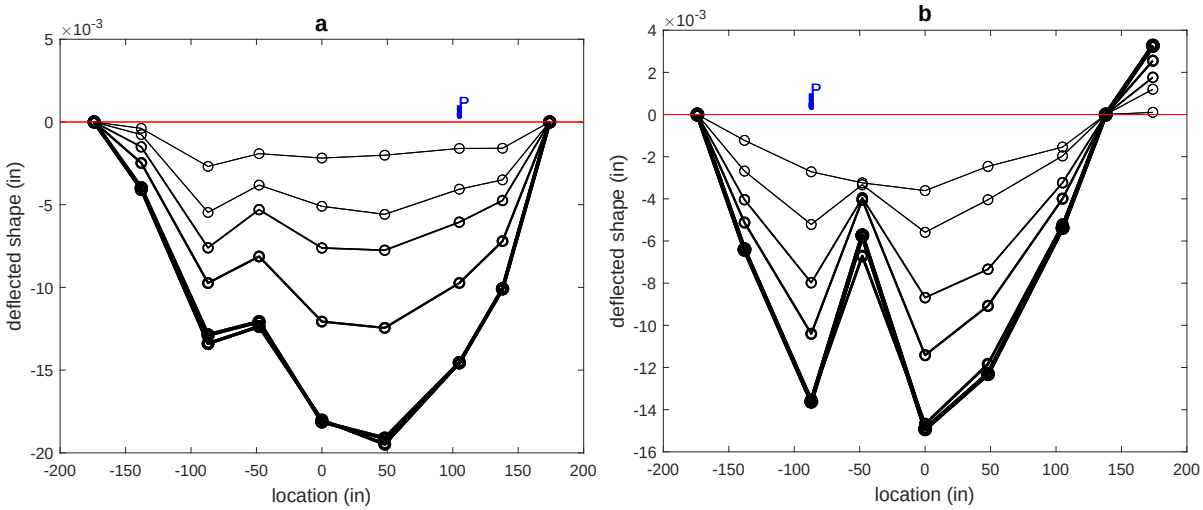

Fig. 21. Panel (a) depicts test 13a's deflected shape and panel (b) is test 9b's deflected shape. These deflected shapes are examples of elastic curves with unacceptable L1 readings.

The idea of employing a cutoff related only to L1's entire removal does not seem to work from time to time. First, two close KL values may correspond to two drastically different deflected shapes in terms of being reasonable or not. For example, tests 14b and 11 have comparable KL values but refer to Fig. 19 for their deflected shapes. Next, 13a's KL value falls between those of tests 11 and 9b, both of which have comparatively more unreasonable deflected shapes. The deflected shape of test 13a as in panel (a) of Fig. 21, however, is fairly reasonable. In summary, it does not seem that the KL divergence is a comprehensive measure for this purpose.

6.4.2. Multivariate Entropy Exercise

The operating assumption throughout this study entails that a beam theory model consisting of a constant EI does not properly characterize the properties of Girder A. Therefore, different substructure idealizations are explored. $\boldsymbol{\theta}$ contains N number of unknown parameters (i.e., normalized piecewise EIs corresponding to the number of substructures). Now, with a multivariate problem formulation, it is necessary to accordingly determine entropies between multivariate Gaussian distributions using:

$$KL(p_1, p_2) \;=\; \frac{1}{2}\left[\log\frac{|\Sigma_2|}{|\Sigma_1|} - d + tr\{\Sigma_2^{-1}\Sigma_1\} + (\mu_2 - \mu_1)^T\Sigma_2^{-1}(\mu_2 - \mu_1)\right] \tag{9}$$

where Σ_1 and Σ_2 are the posterior covariance matrices for the "Uncorrected" and "L1 Corrected" datasets, respectively and μ_1 and μ_2 are their means. d, the dimension of μ, corresponds to the number of substructures utilized. As before, the Bayesian analysis results are excluded when the σ values are unreasonable, see Table 6. Note that test 4b overlaps exclusions based on support location and improper objective function maximization. See Table 7 for the KL Divergence of the three, six, and nine-substructure cases.

Table 6. 3+ substructure σ values from the maximized objective function for "Uncorrected" (σ_1) and "L1 Corrected" (σ_2) for use in data inclusion/exclusion. "x" indicates tests excluded for analysis.

Test	σ_1	σ_2	Observ.	σ_1	σ_2	Observ.	σ_1	σ_2	Observ.
	3 Substruct.			6 Substruct.			6 Substruct.		
1	0.0017	0.0017		0.0017	0.0017		0.0017	0.0017	
5a	0.0009	0.0009		0.0009	0.0009		0.0009	0.0009	
5b	-0.0019	-0.0020	x	-0.0019	-0.0020	x	-0.0019	-0.0020	x
2a	0.0022	0.0024		0.0023	0.0024		0.0023	0.0024	
2b	0.0034	0.0036		0.0034	0.0036		0.0034	0.0036	
4a	0.0007	0.0007		0.0007	0.0007		0.0007	0.0007	
4b	0.0017	0.0017		-0.0019	-0.0019	x	-0.0019	-0.0019	x
6a	0.0023	0.0025		0.0023	0.0025		0.0023	0.0025	
6b	0.0044	0.0046		0.0044	0.0046		0.0044	0.0046	
7	0.0034	0.0031		0.0034	0.0031		0.0034	0.0031	
3	0.0033	0.0033		0.0034	0.0035		0.0034	0.0035	
8	0.0013	0.0012		0.0013	0.0013		0.0014	0.0013	
13a	0.0014	0.0011		0.0014	0.0011		0.0015	0.0011	
13b	0.0008	0.0004		0.0009	0.0004		0.0009	0.0004	
14a	0.0032	0.0034		0.0032	0.0035		0.0032	0.0035	
14b	0.0010	0.0008		0.0013	0.0010		0.0034	0.0033	
15a	0.0024	0.0024		0.0025	0.0025		0.0024	0.0025	
15b	0.0015	0.0012		0.0015	0.0013		0.0015	0.0013	
16a	0.0041	0.0041		0.0042	0.0042		0.0043	0.0043	
17a	0.0008	0.0007		0.0009	0.0007		0.0009	0.0008	
17b	0.0012	0.0011		0.0012	0.0012		0.0012	0.0012	
9a	0.0028	0.0007		0.0029	0.0007		0.0031	0.0007	
9b	0.0027	0.0007		0.0027	0.0007		0.0029	0.0007	
10	0.0043	0.0034		0.0043	0.0034		0.0043	0.0034	
11	0.0042	0.0032		0.0042	0.0033		0.0042	0.0033	
12a	0.0011	0.0007		0.0011	0.0007		0.0011	0.0007	
12b	0.0013	0.0005		0.0012	0.0005		0.0013	0.0005	

Table 7. 3+ Substructure multivariate KL divergence (relative entropy) and observations where KL values $\geq$ cutoff value

Test	Test Setup	3 Substruct.	Observ.	6 Substruct.	Observ.	9 Substruct.	Observ.
1	SS	0.513		0.589		0.514	
5a	SO South	1.824	x	2.123	x	1.921	x
5b	SO South	NaN		NaN		NaN	
2a	SO North	0.540		0.690		0.697	x
2b	SO North	0.189		0.183		0.164	
4a	SO North	-		-		-	
4b	SO North	-		NaN		NaN	
6a	SO South	0.140		0.117		0.095	
6b	SO South	0.111		0.087		0.070	
7	SO South	0.092		0.071		0.052	
3	SO North	0.042		0.011		0.006	
8	SS	2.708	x	2.857	x	2.777	x
13a	SS	3.473	x	2.993	x	2.282	x
13b	SS	7.602	x	5.433	x	3.004	x
14a	SO North	0.021		0.018		0.019	
14b	SO North	1.441	x	0.384		0.162	
15a	SO North	0.085		0.052		0.044	
15b	SO North	0.142		0.069		0.036	
16a	SO North	-		-		-	
17a	SO South	1.139	x	0.720		0.418	
17b	SO South	0.669		0.579		0.513	
9a	SO South	51.961	x	26.677	x	13.625	x
9b	SO South	37.204	x	19.585	x	6.679	x
10	SO South	2.158	x	1.749	x	1.312	x
11	SO South	1.112	x	0.854	x	0.640	x
12a	SO North	5.112	x	4.218	x	2.777	x
12b	SO North	34.403	x	29.174	x	21.400	x

Here, similar numerical performance is found to the one-substructure case where the "Observations" (Observ.) highlight the tests where KL values are greater than or equal to test 11's KL, the cutoff KL, with respect to their substructure case. There are variances between substructure orders where tests' KL values exceed or fall short of the cutoff. This is expected as further discretization of the beam utilizes more localized deflection data to solve for $\bar{\boldsymbol{\theta}}$. Some localized substructures will house measured data that is not easily fit by Bayesian analysis causing lower identification of $\boldsymbol{\theta}_i$, whereas other substructures will experience a localized increase in the identification of $\bar{\boldsymbol{\theta}}_i$ as ill-fitting data leaves the lower-order

substructure. For those tests which are sensitive to the arbitrary subdivision of the beam, it is not recommended that L1 be removed but, that L1 be removed from those tests with KL values consistently at or above the cutoff threshold.

It is here that another category is created encompassing all 27 test. This category, "L1-KL Corrected", will remove L1 readings in accordance with the consistently high KL values. The identified EI results will be explored in Section 6.5.

Other instances of LVDT malfunctions are evident when observing the elastic curves of all 27 tests in Appendix D. However, it is difficult to determine LVDTs that consistently malfunction in a manner similar to L1. Due to the improved performance of the remaining LVDTs relative to L1 it is difficult to establish an objective procedure for removing other LVDTs in conjunction with L1. For this reason, only LVDT L1 is removed to improve the EI identification. A flowchart of the method for rationalizing the removal of L1 is provided for summary:

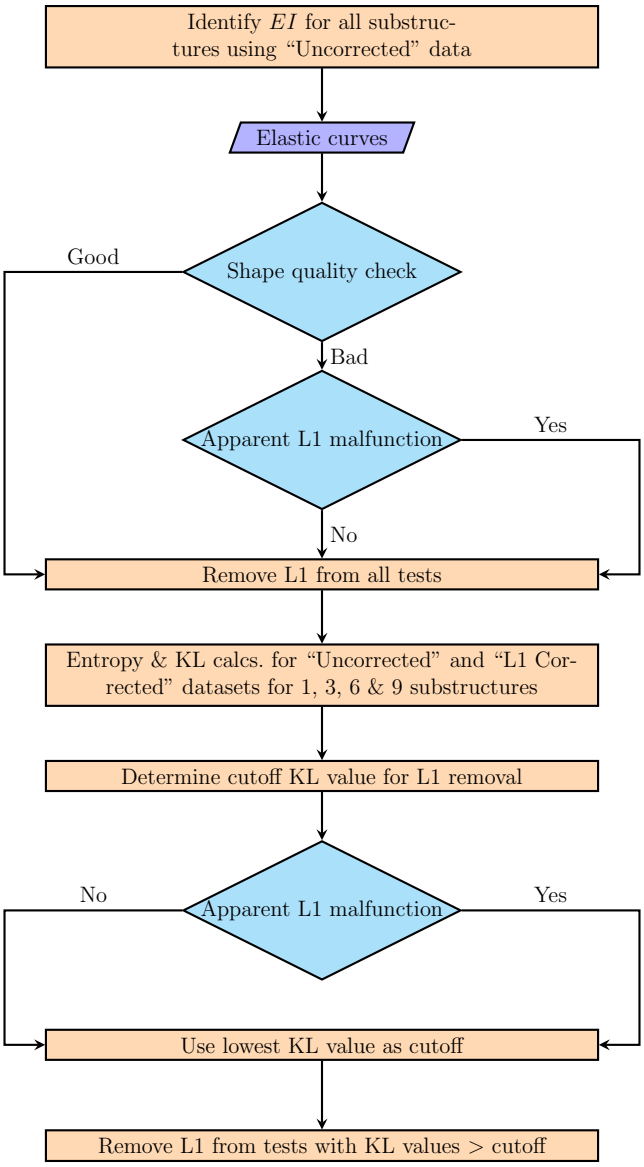

Fig. 22. A flowchart summarizing the removal of LVDT L1

6.5. Results

6.5.1. L1 Removal: Test Specific Results

EI divisions of the data categories listed below are focused on, hereafter.

Category 1: "Uncorrected" All LVDT readings were used

Category 2: "L1 Corrected" All L1 readings were removed

Category 3: "L1-KL Corrected" Relative entropies (KL divergence) were used as criteria in L1 removal

Individual results are first obtained and plotted on a test-by-test basis for each category to determine if consistency exists in identification between higher and lower-order substructures.

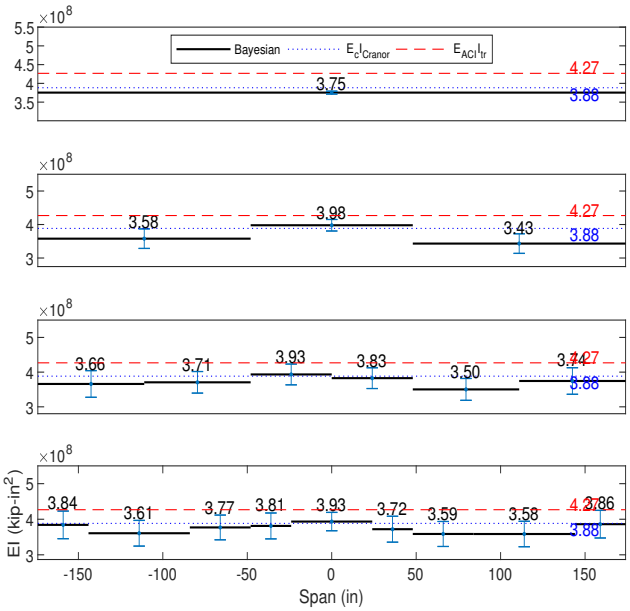

Fig. 23. Test 1 "Uncorrected" identification for substructures 1 (top) to 9 (bottom)

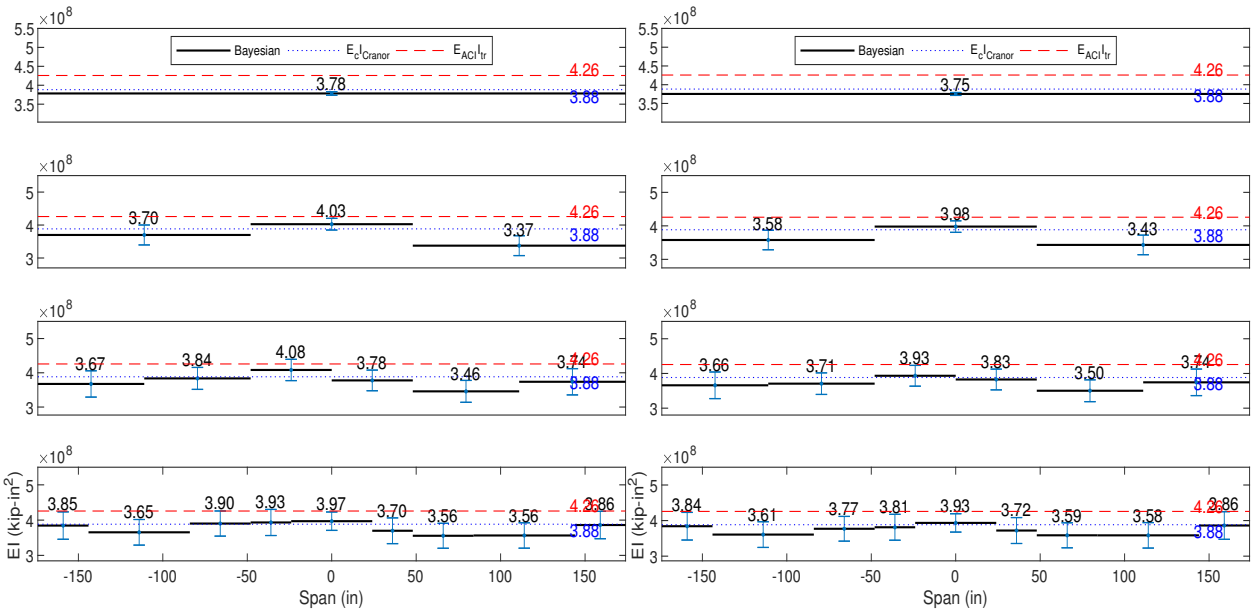

Fig. 24. Test 1 "L1 Corrected" identification for substructures 1 (top) to 9 (bottom)

Fig. 25. Test 1 "L1-KL Corrected" identification for substructures 1 (top) to 9 (bottom)

From Fig. 23, the lower-order EIs - if simplified as averages of the higher-order, show agreement in identification between substructures for the "Uncorrected" data. True averages are not obtained as this simplification ignores the fitting of data within individual substructures; higher-order substructure cases partition (good and/or bad) data into smaller sections, affecting data fit and producing localized increases/decreases in flexural rigidity. As a result of partitioning, higher standard deviations in higher-order substructure identifications are found. This increase in standard deviation is expected as the higher-order substructures indicate a larger number of substructures for the same amount of data. These trends are also exhibited in Figs. 24 and 25 when the identification was carried out with the full or partial removal of LVDT L1 readings.

These EI distributions also feature additional EI lines establishing functional flexural rigidity values to describe Girder A. The constant value of 3.88×10^8 kip-in^2 is determined from a battery of flexural rigidity tests by Cranor (2015). This constant value is taken, from Table 4.14 in Cranor (2015), for granted. The second EI distribution of 4.26×10^8 kip-in^2 is

calculated using the transformed moment of inertia I_{tr} for a typical AASHTO type II girder and E_{ACI} from ACI formulas, details of calculating EI_{tr} are found in Section 6.6.

As illustrated in Section 6.2, a limited number of possible substructure idealizations are utilized for identification purposes. Here, Fig. 26 provides a glimpse of the consistent identification results among substructures. In this study, the identification is stopped at the ten-substructure case.

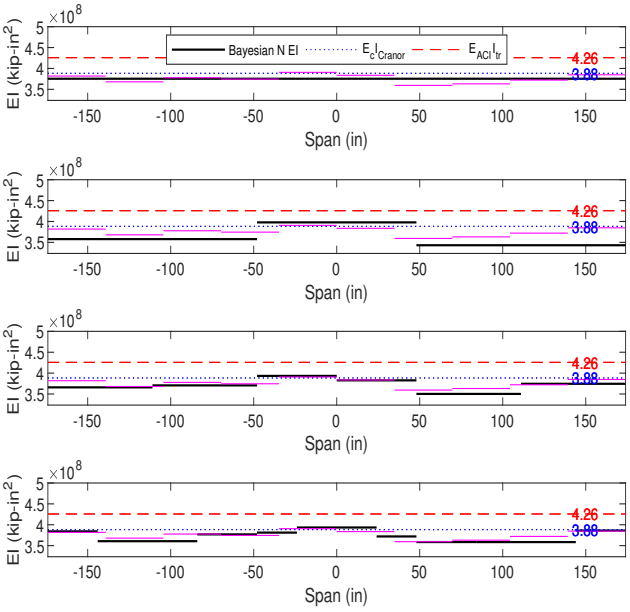

Fig. 26. Test 1 "Uncorrected" identification for substructures 1 (top), 3, 6, and 9 (bottom), vs. the 10 substructure identification case, shown in purple, to illustrate consistent identifications across substructures

Following Figs. 23 to 25, the individual test values are plotted across the range of all 27 tests in the subsequent section. Individual test's flexural rigidity identification results can be found in Appendix D.9.

6.5.2. L1 Removal: Mean Test Results

In Fig. 27, for the one substructure EI identification using Bayesian analysis, all three categories are plotted for each test according to testing day. Each test day is denoted by

a grey-scale section, chronological test progression is from left to right. Each category's respective mean and standard deviation are shown below the corresponding data marker in the legend.

Comparing the location of the markers between categories, it is evident that L1 indeed affects EI identification, especially for those tests encompassed in the last day of testing. Note that most tests in "L1 Corrected" and "L1-KL Corrected" suffered a reduction in flexural rigidity, addressing the artificial stiffening by the removal of L1, nonetheless, the mean values of EI decreased minimally while also reducing standard deviations. Fig. 27 illustrates that the entropic calculations in Section 6.4 do not accurately encompass which tests are affected by L1, taking for example test 5a of the one-substructure case where an increase in flexural rigidity is seen.

Utilizing higher-order substructures may hold the potential for more accurate identifications by providing new information on the tests affected by L1. It must be noted that tests with objective functions that were not properly maximized are intentionally left blank (e.g., test 5b across all substructure cases, test 4b in the six and higher-order substructure cases, and test 14b in the arbitrary substructure case) and are excluded from the mean value calculations in this section. Additionally, the identified results of test 14b are unusually high for the one, three, and six-substructure cases, the reason for which being the high prediction error mentioned at the end of Section 6.3.

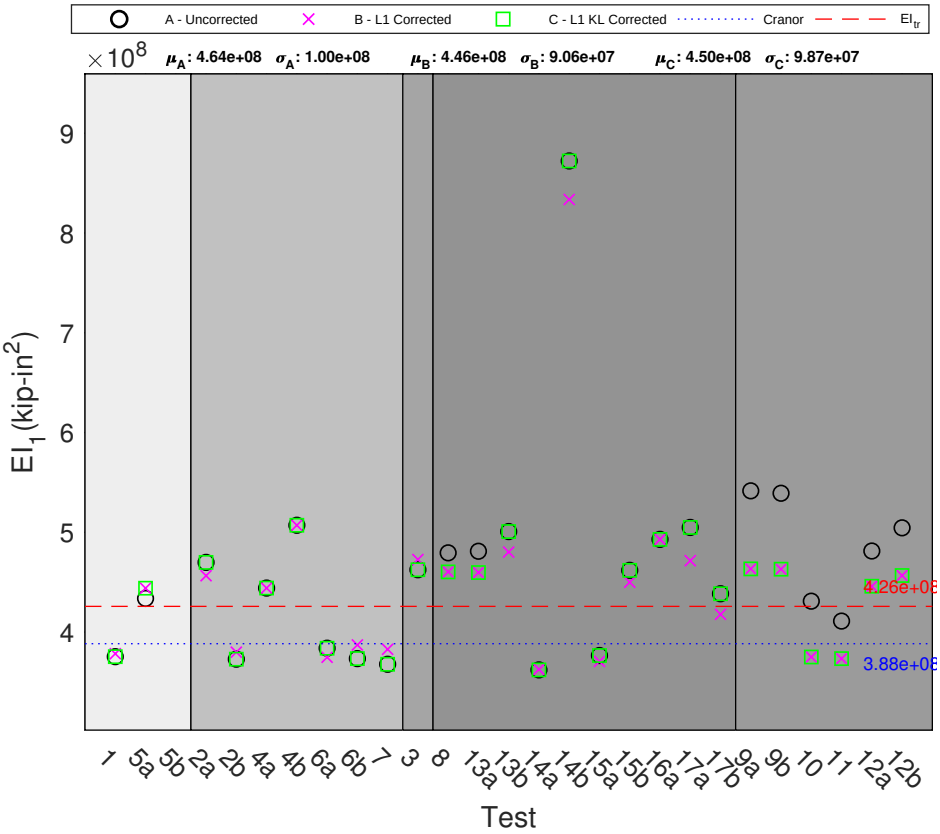

Fig. 27. One EI value for Girder A when Bayesian analysis was applied: Distribution of EI identification for each test based on category

The effects of L1 are again seen in the plotting of the three substructure identification using Bayesian analysis in Fig. 28. Each panel describes a substructure of the beam and the three data categories are plotted for each substructure. Here, mixed results are found when comparing L1's effects on each span. For the first substructure EI_1, trends in mean and standard deviation between categories are found resembling the one substructure identification; this finding also holds for the second substructure. The third substructure, however, displays improved identification after the removal of L1 with an increase in standard deviation for category "L1 Corrected" and the opposite for "L1-KL Corrected".

To understand this occurrence, the effect of removing L1 at the test level across substructures is compared. From Fig. 27, it was determined that the KL values used to rationalize the partial removal of L1 may not produce consistent adjustments in identification. Focusing

this discussion in the framework of the three-substructure case in Fig. 28, the removal of L1 seems to inversely affects EI_3 as it does EI_1 and EI_2. It is expected that the spans closest to the malfunctioning LVDT will exhibit the greatest flexural rigidity decreases from LVDT removal. The seemingly inverse effect L1's removal has on the furthest substructure may be explained by the partitioning of data into smaller substructures for Bayesian fitting, as mentioned in the previous section. This partitioning effect is illustrated in EI_2 which exhibits less flexural rigidity reduction than EI_1.

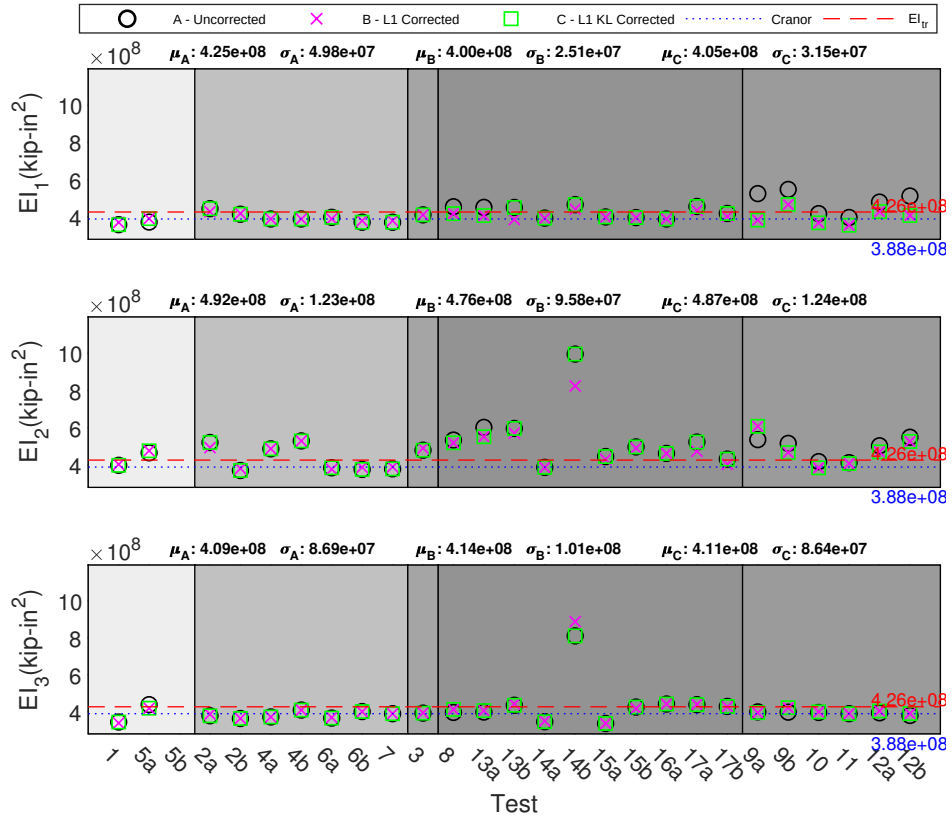

Fig. 28. Three EI values for Girder A when Bayesian analysis was applied: Distribution of EI identification for each test based on category

With improved identification in EI_3, this substructure's standard deviation under "L1-KL Corrected" supports the removal of L1 based on relative entropy. Comparing the standard deviation of "L1-KL Corrected" with "L1 Corrected" in EI_3, a noticeable difference can be seen that seems to suggest that blindly removing L1 data from all tests may affect the identification reliability in substructures not immediately surrounding the removed LVDT.

Identification under "L1-KL Corrected" in EI_2 shows an increase in standard deviation when compared to "Uncorrected" indicating there may exist a trade-off in result accuracy between spans experiencing LVDT removal and the adjacent span not undergoing LVDT removal.

Further subdivision of the beam is required to determine whether "L1-KL Corrected" will produce the least negatively impacted identified results. Fig. 29 subdivides Girder A into six substructures for EI identification.

The results of the six-substructure case are consistent with results for the three and one-substructure cases. As before, removal of L1 decreases the identified results of the immediately surrounding substructures in either category of L1 removal. With a higher-order substructure it is again seen that "L1 Corrected" typically has lower means with lower standard deviations near the location of the removed LVDT than "L1-KL Corrected". However, at locations further away from L1, the means between both categories are nearly identical but higher standard deviations are more commonly found in "L1 Corrected".

Category "L1 Corrected" seems to show marked reduction in identified results near L1 while simultaneously minimizing the identification spread. Though the spread of data increases in substructures further from L1 under this category, the majority of substructures show smaller standard deviations relative to "L1-KL Corrected". In other words, the benefits to identification by removing L1 from all datasets may outweigh the increased spread in data away from the removal location.

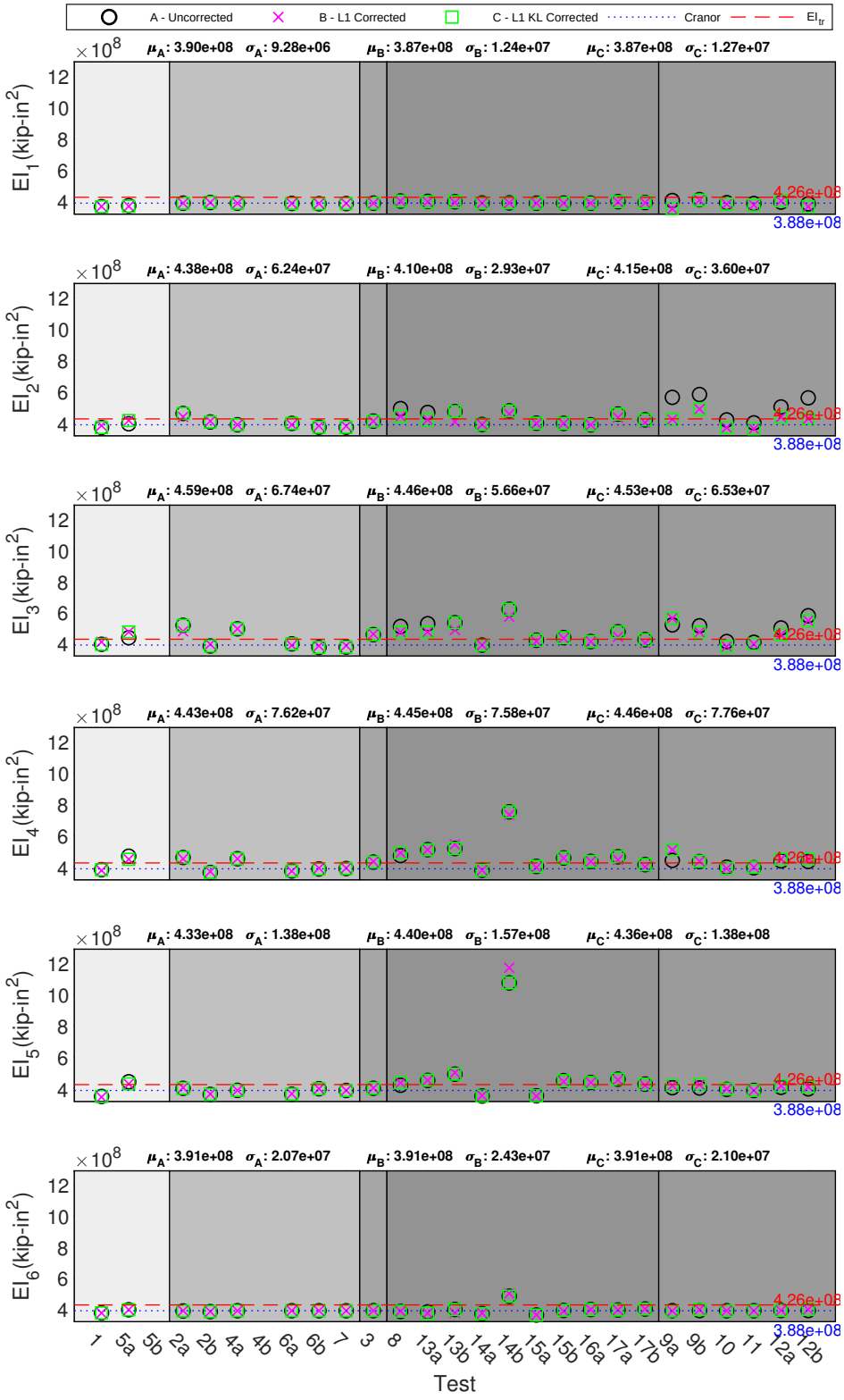

Fig. 29. Six EI values for Girder A when Bayesian analysis was applied: Distribution of EI identification for each test based on category

The formulaic segmentation of the beam thus far has returned consistent mean flexural rigidity identifications. Similar performance is obtained by utilizing one realization of an arbitrary substructure to analyze Girder A in Fig. 30. Segmenting Girder A in this manner, localized increases/decreases in flexural rigidity are again seen with the partitioning of good and/or bad data into higher-order substructure elements. The effects of removing L1 are increasingly pronounced in the substructure where L1 is located. Agreement is again seen when comparing the flexural rigidity values from the arbitrary substructures with flexural rigidity values obtained from lower-order substructures.

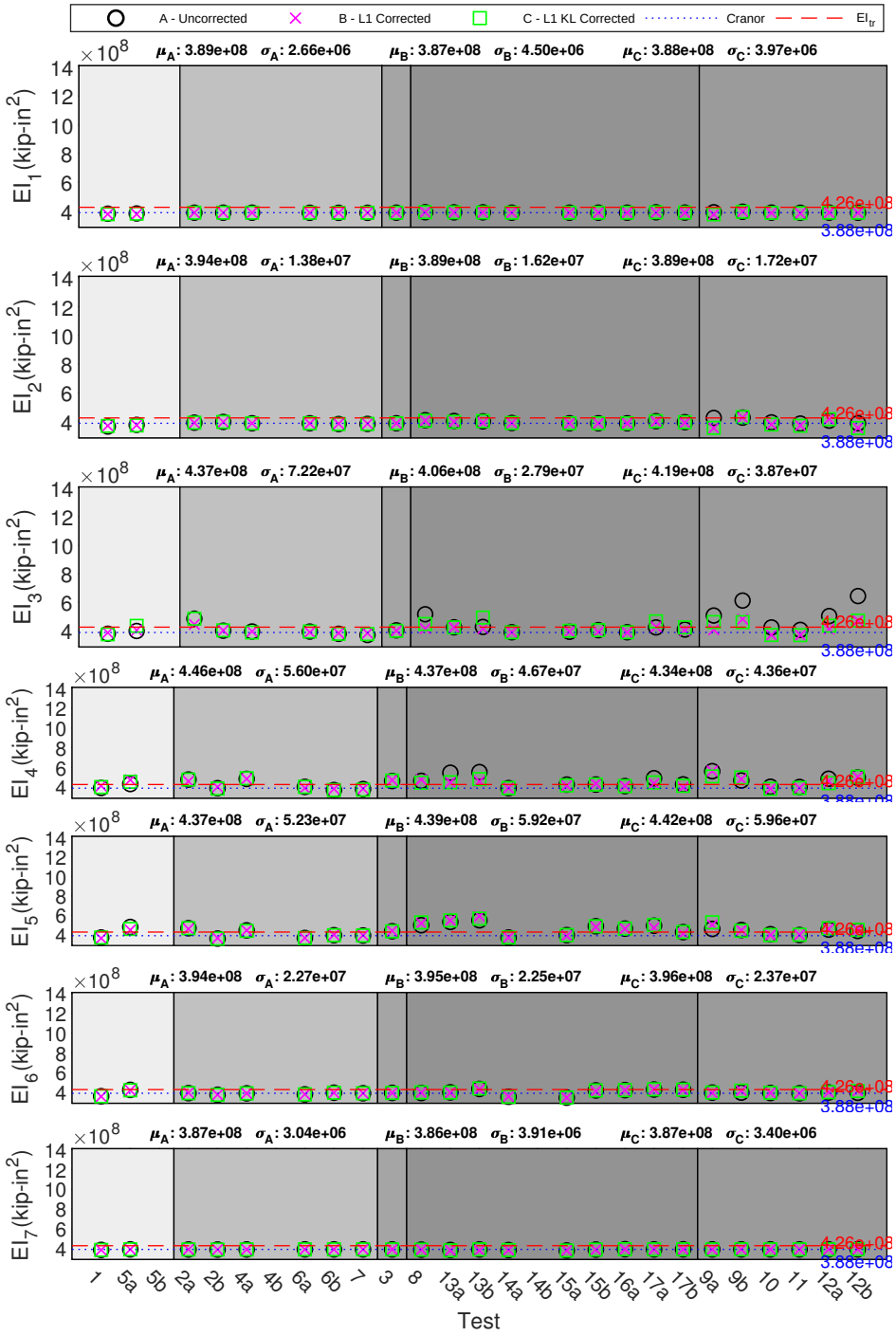

Fig. 30. Seven arbitrary EI values for Girder A when Bayesian analysis was applied: Distribution of EI identification for each test based on category

Increasing substructures in Figs. 31 and 32, minuscule changes are seen in mean identification in substructures further away from L1 across all categories, even with L1 removal. This

further reaffirms that L1 indeed impacts flexural rigidity identification in regions surrounding it and that removing L1 from all datasets was a necessary step. Combining higher-order substructures and L1's removal from all datasets, further identification decreases are seen across substructures while also minimizing standard deviation in regions close to L1. Under the ten-substructure case, "L1 Corrected" shows minimal increases in standard deviation in areas away from L1. This increase in standard deviation using "L1 Corrected" is said to be minimal in the sense that it is typically less than that for "L1-KL Corrected". Notably, by partitioning the beam under these higher-order substructures, drastic reduction to the flexural rigidity identification of test 14b is seen, as compared to Figs. 27 to 30.

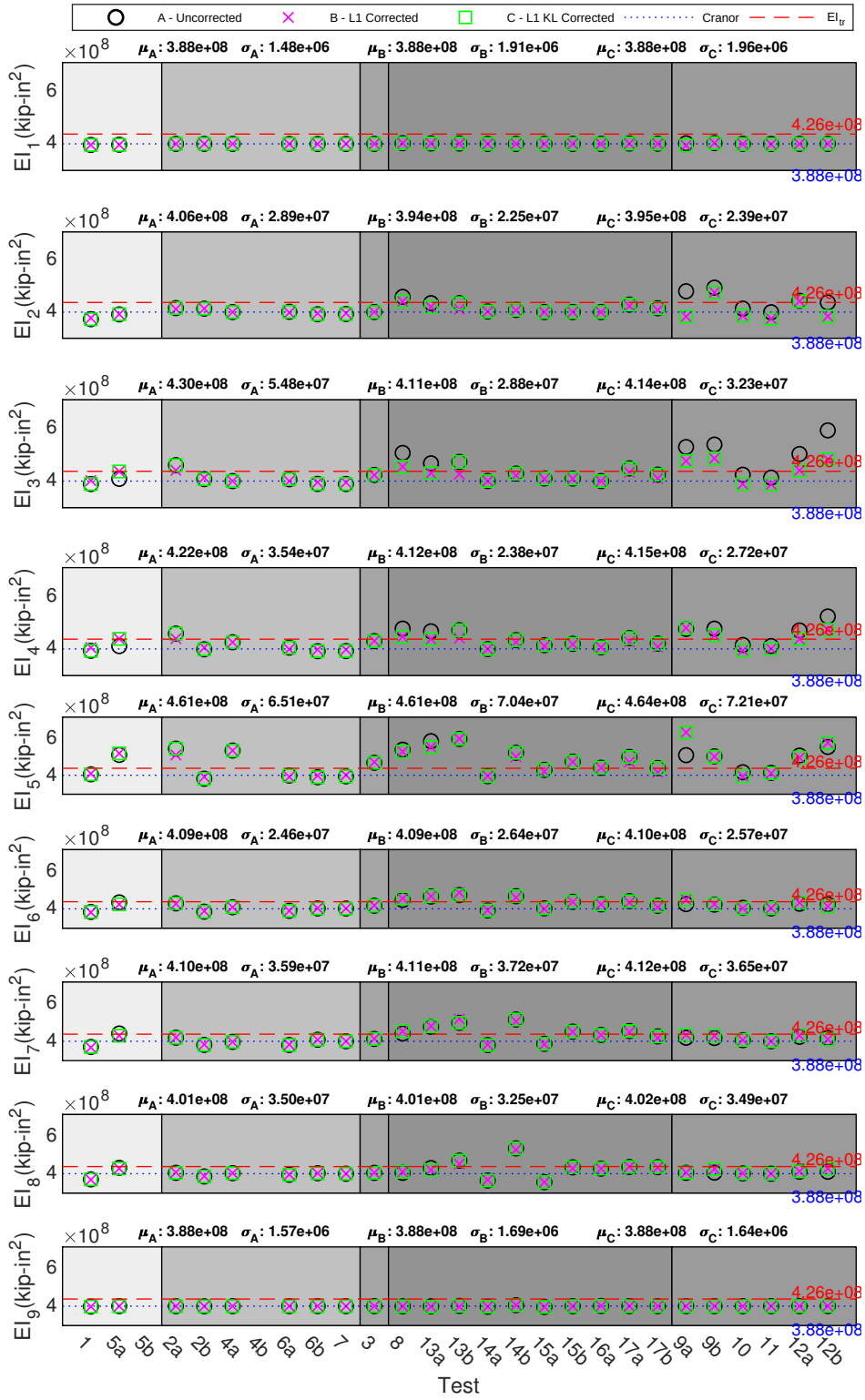

Fig. 31. Nine EI values for Girder A when Bayesian analysis was applied: Distribution of EI identification for each test based on category

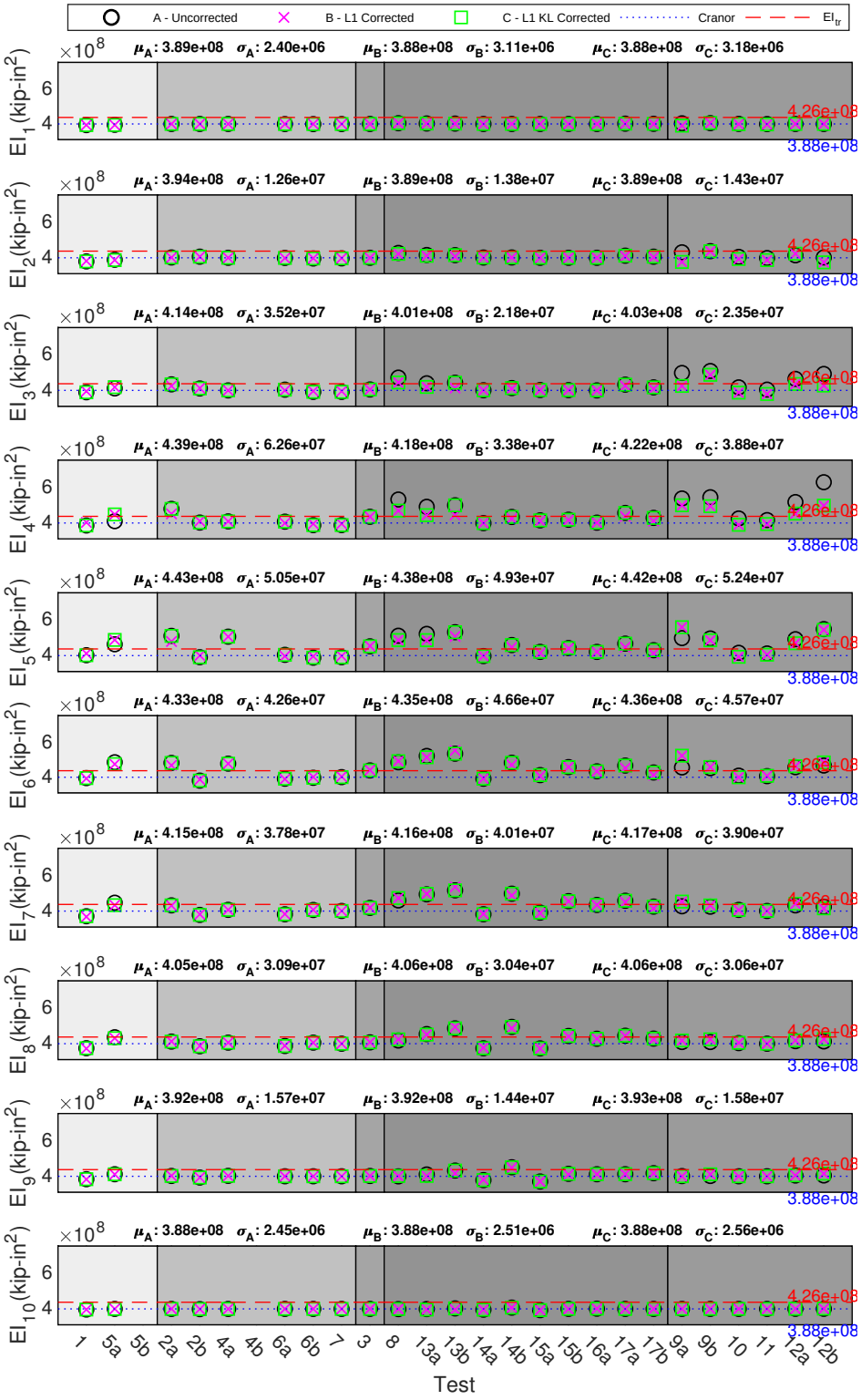

Fig. 32. Ten *EI* values for Girder A when Bayesian analysis was applied: Distribution of *EI* identification for each test based on category

Figs. 33 to 35 are counterparts to Figs. 27 to 29, respectively, using least-squares analysis. When the three and six substructure identifications are used, least squares returns negative as well as infinite EI values, which can be seen clearly in Figs. 34 and 35 under all three categories. Interestingly, the one-substructure case exhibits similar identification performance to its Bayesian counterpart. Nevertheless, the mean values are strongly tinted by the negative EI values making the mean values untrustworthy. For this reason, the results of the least-squares method for the one, three, and six substructures are reported but analyses of these results are not conducted. Note that the least-squares results minimize the root mean square error (RMSE) as the data fit relies solely on the data, unlike in Bayesian analysis. Despite the minimization of the RMSE through least squares, unreasonable parameter values are still identified. Hereafter, Bayesian analysis results are used to draw conclusions.

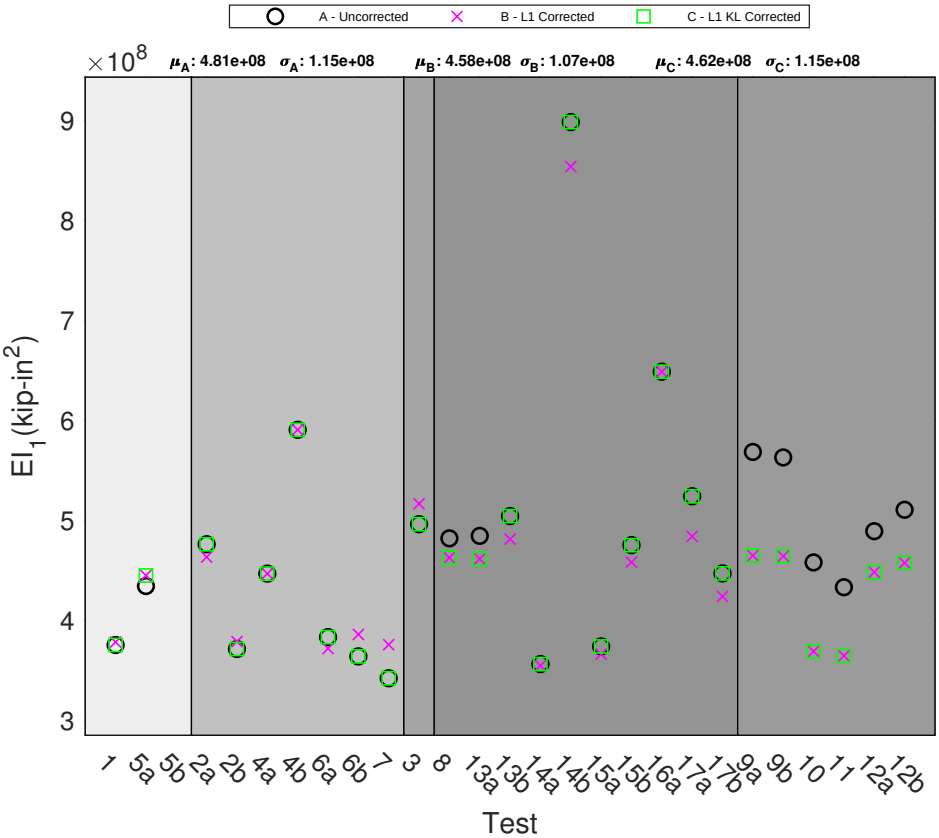

Fig. 33. One EI value for Girder A when least-squares analysis was applied: Distribution of EI identification for each test based on category

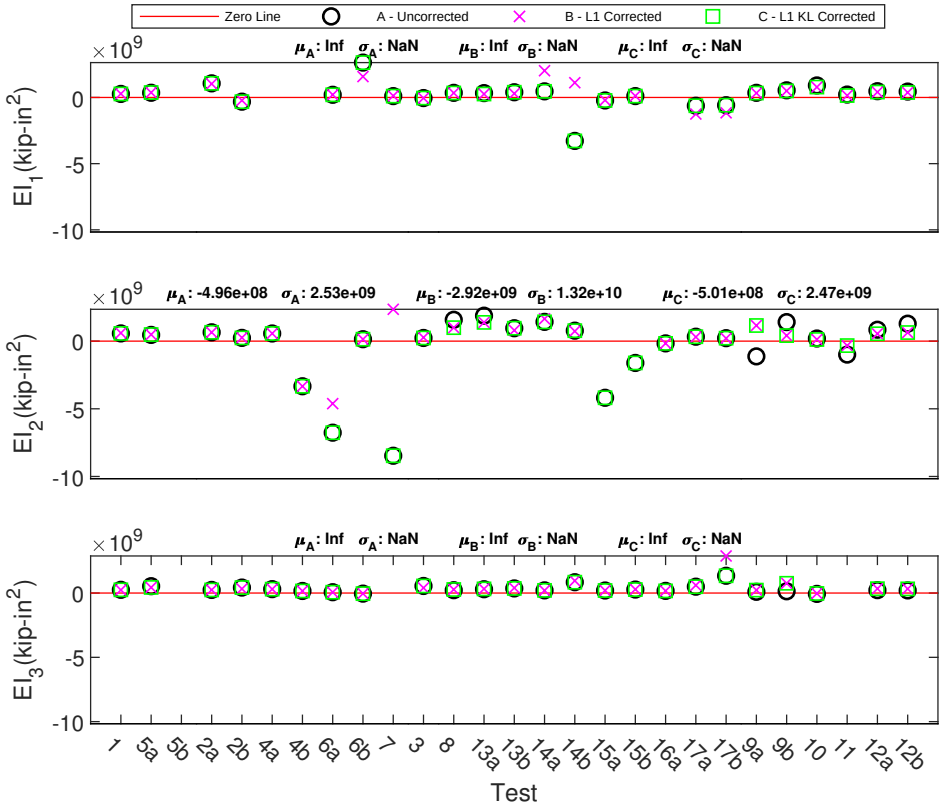

Fig. 34. Three EI values for Girder A when least-squares analysis was applied: Distribution of EI identification for each test based on category

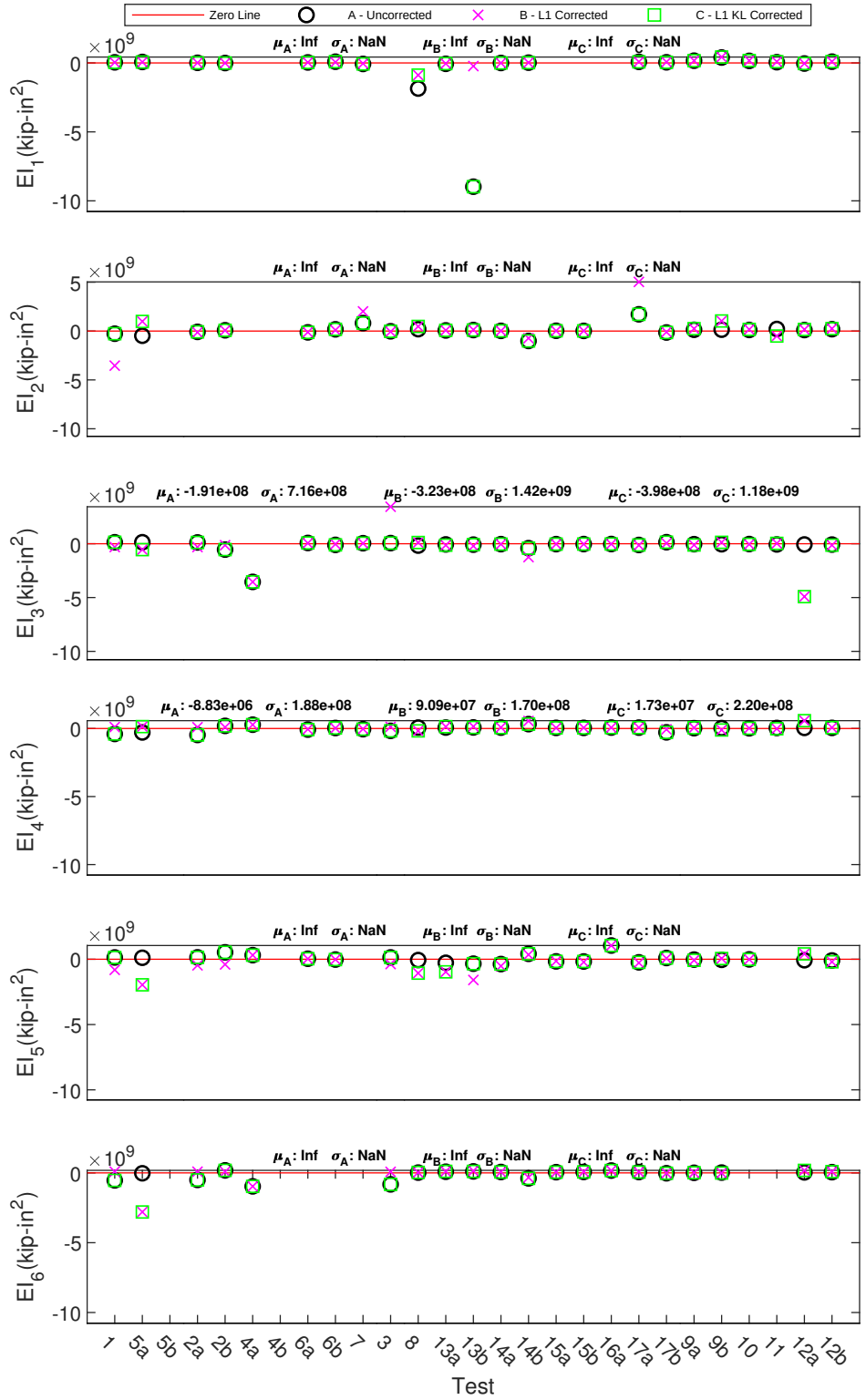

Fig. 35. Six EI values for Girder A when least-squares analysis was applied: Distribution of EI identification for each test based on category

6.6. Discussions

6.6.1. Moment of Inertia Calculations and Damage Detection Efforts

Fig. 36 assumes an uncracked section with a perfect bond returning a minimum inertia of roughly 1.014×10^5 in^4. The minimum value differs by 0.3% from the maximum. Thus, the bond is taken to be imperfect, and no contribution from the steel due to cracking of the concrete (though unrealistic until failure occurs) is assumed; a constant I_{tr} of 9.924×10^4 in^4 was established - only differing from the maximum by 2.4% but yielding a more conservative estimate. Utilizing E_{ACI}, the modulus of elasticity obtained from ACI equations using the compressive strength specified for Girder A (5000psi), yields the upper bound, EI_{tr}, for a functional Girder A at or above which damage is assumed to be negligible.

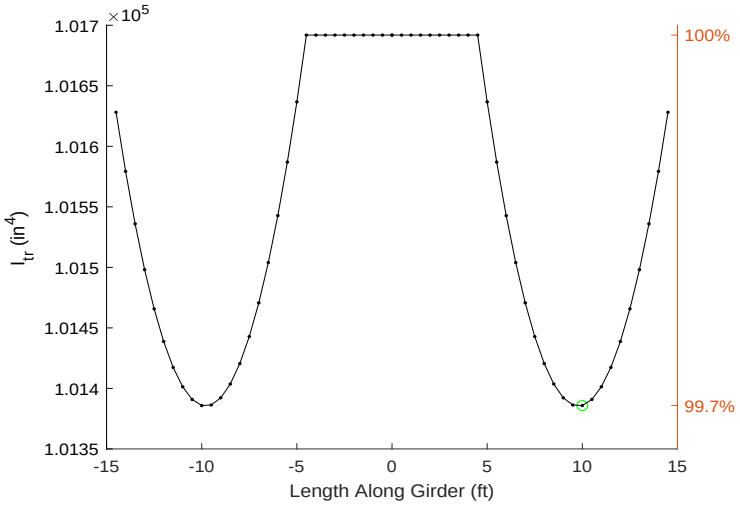

Fig. 36. Distribution of I_{tr} along beam span

The establishment of a damage threshold (lower bound) flexural rigidity can help to determine whether the identification results from this study imply damage. To explore this difficult topic, a determination of the cracked moment of inertia I_{cr} for a prestressed concrete beam is made. From MATLAB programming, the conservative estimate of approximately 1.1×10^4 in^4, or roughly 11% of I_{tr}, was determined as the lowest bound of the moment of inertia for Girder A. The value of I_{cr} used is from the unharped section to narrow the assumed

functional range of flexural rigidity, the end values fall within 6 to 8% of I_{tr}.

Utilizing E_c, the minimum flexural rigidity EI_{cr} of 4.57×10^7 kip-in^2 is found for Girder A. This minimum is to be taken as the point at which Girder A is no longer functional and should be replaced. This minimum threshold was not approached when plotting the distribution of identified values of flexural rigidity in Sections 6.5.1 and 6.5.2 and is overly conservative. Additional studies are necessary to improve quantification of a threshold flexural rigidity value for quantitative damage detection purposes.

This process could be done by determining the neutral axis of the cracked section and iterating on the height of the assumed crack to increase I_{cr} to a more reasonable value, thus establishing a damage threshold or undamaged range of flexural rigidity. This process is not conducted in the current research as it is subjective to an assumed crack height, however, current m-files can be modified to accommodate this functionality in future studies.

Additionally, I_{cr} could be refined utilizing the "Severe II" and "Severe III" ratings from Harries et al. (2012), however, this refinement would require an extensive parametric study into the original properties of Girder A and the loss of section required for the complete loss of camber, not to mention the maximum 0.5% deflection of the girder. Other issues non-exhaustively include: inaccurate camber measurements obtained due to the unevenness of the girder soffit, difficulty characterizing creep coefficients, and the estimation of effective prestressing (Pei et al. 2008). Note that ratings in Harries et al. (2012) assumed damage caused by impact; the ratings are provided simply to assist future research. At this time, damage detection is not a possibility for Girder A.

6.6.2. Other Uncertainties: Rearranging Results by Test Configuration

Here, experimental uncertainties discussed in Section 6.1 are addressed. With interest in determining whether different test configurations affect flexural rigidity identification, the

test configurations are grouped into three general categories:

Category 1: *SO Left* A simply-supported beam with an overhang on the left/north side of the beam

Category 2: *SS* A fully simply supported beam

Category 3: *SO Right* A simply supported beam with an overhang on the right/south side of the beam

The mean test results found previously are rearranged in Fig. D.131 to D.136 accommodating the three categories listed above, with *SO Left* shown on the left grey-scale and *SO Right* shown on the right. By visual inspection, no apparent trend seems to exist that would indicate one general test configuration impacting the identified flexural rigidities more than another.

Here the increasingly consistent identification of flexural rigidity at the end substructures is noted with the increase in substructures. With the finest subdivisions, Fig. D.136 exhibits an almost uniform identification across EI_1 and EI_{10}. These substructures would suggest that the test configuration has little bearing on the performance of the Bayesian analytical model as the end spans are either supported or unsupported for a given test configuration. Additionally, this uniform identification is also seen in Fig. 32 when the tests are arranged by chronological test day, further supporting this.

6.6.3. Comparing Identification Permutations

The figures in Section 6.5.2 provide average EI values for the beam based on the results of the 27 tests. As these tests occur on the same beam, it is expected that the identified piecewise flexural rigidity values show consistency between lower and higher-order substructures. Thus far, this is the case and similar values of EI are indeed obtained.

In an exercise attempting to measure the robustness of the proposed identification suite, the methodology from Section 6.4 is applied to the results of the "Uncorrected" data to create 27x27 matrices containing KL values for all permutations of test pairs. These matrices are created for the one, three, six, and nine-substructure cases to determine the difference between identified $\bar{\boldsymbol{\theta}}$ values between tests and perhaps provide a measure of success (or failure) of the proposed methodology of identifying consistent EIs.

Beginning with Table 6.6.3 for the one-substructure case, data solely from category "Uncorrected" is used to determine the KL divergence of all test permutations. Note that data from the other categories could have also been used, however, it is vital that the KL divergence is measured between data from the same category. In Section 6.4, the KL values were determined between categories "Uncorrected" - "L1 Corrected" and "Uncorrected" - "L1-KL Corrected" for LVDT L1 removal. Here, it is necessary to compare the same categories to establish KL values uninfluenced by data changes. Test pairings along the diagonals have been removed from the results as their KL values are zero. In Table 6.6.3, the highlighted values correspond to the test pairings with KL values greater than or equal to the cutoff that is found from analysis in Section 6.4 for the one-substructure case.

Table 8. 27x27 matrix of KL values from test pairings of data from "Uncorrected" for the one-substructure case. These values are compared against the cutoff value found in Section 6.4 to determine flexural rigidity identification agreement.

555/702 $Pairs \geq KL\ Cutoff$ | 1 Substructure | $KL\ Cutoff = 1.167$

Tests	1	2a	2b	3	4a	4b	5a	5b	6a	6b	7	8	9a
1	-	218.901	3.488	201.771	129.557	376.246	97.281	34.123	7.686	18.217	29.241	253.417	509.864
2a	37.830	-	39.989	1.154	2.019	4.556	4.577	13.830	29.869	41.357	48.868	0.415	10.453
2b	0.716	23.828	-	21.303	14.529	39.610	11.691	4.340	0.489	0.877	1.726	27.923	54.127
3	8.412	0.398	7.967	-	0.770	1.050	1.766	3.115	5.743	7.721	9.160	0.957	3.024
4a	34.221	3.085	37.252	3.589	-	18.198	0.896	8.107	25.612	39.929	49.499	5.548	33.121
4b	12.669	1.022	12.267	0.870	2.486	-	3.918	6.280	9.700	11.903	13.438	1.184	0.588
5a	101.260	26.421	115.077	27.754	3.091	101.973	-	17.516	76.105	128.121	162.968	38.319	170.061
5b	12.387	29.027	14.993	26.268	11.123	67.301	6.141	-	7.536	19.386	28.031	36.907	101.425
6a	1.037	12.662	0.350	10.937	7.165	22.299	5.807	1.680	-	0.730	1.629	15.353	31.699
6b	1.371	6.145	0.335	4.973	4.103	9.249	3.955	1.818	0.310	-	0.070	7.493	13.114
7	1.586	5.194	0.499	4.114	3.713	7.251	3.764	1.964	0.511	0.052	-	6.325	10.230
8	116.870	0.978	125.111	6.347	9.694	9.991	17.004	47.083	95.975	129.861	151.543	-	21.169
9a	47.981	5.691	49.347	7.322	11.797	1.554	15.653	26.305	40.717	49.600	55.242	4.448	-
9b	51.179	5.825	52.750	7.629	12.307	1.590	16.381	27.856	43.451	53.095	59.212	4.480	0.007
10	3.851	1.278	3.111	0.560	0.766	2.628	1.316	1.189	1.922	2.777	3.530	2.112	5.107
11	2.299	2.108	1.393	1.257	1.328	3.475	1.715	0.949	0.740	0.977	1.344	3.011	5.926
12a	41.897	0.308	44.028	1.731	3.691	2.563	6.767	17.080	33.716	45.191	52.631	0.212	6.535
12b	93.007	4.310	97.965	8.451	14.474	2.637	21.176	44.213	78.083	100.201	114.213	2.207	4.063
13a	91.256	0.814	97.326	4.847	7.956	6.900	13.886	37.209	74.813	100.757	117.378	0.030	15.080
13b	146.228	5.959	154.956	12.937	21.358	5.273	31.424	68.266	123.075	159.140	181.928	2.590	8.493
14a	1.383	15.462	0.342	13.638	10.282	23.684	8.920	4.168	0.957	0.430	0.502	17.972	31.815
14b	763.910	319.989	782.861	346.147	405.107	231.184	445.752	566.072	707.381	784.782	831.130	292.610	163.572
15a	1.015	11.028	0.123	9.459	6.743	18.165	5.780	2.143	0.127	0.194	0.610	13.233	25.429
15b	15.436	0.203	15.706	0.163	0.698	2.467	1.996	5.242	11.379	15.948	19.057	0.845	5.969
16a	7.897	0.768	7.220	0.357	1.596	0.086	2.686	3.828	5.581	6.747	7.641	1.117	0.887
17a	33.226	1.596	34.218	2.557	5.307	0.428	8.104	15.828	27.154	34.531	39.309	1.175	1.253
17b	9.500	1.498	9.536	1.000	0.306	5.924	0.869	2.126	6.228	9.841	12.408	2.722	11.167

555/702 $Pairs \geq KL\ Cutoff$ 1 Substructure $KL\ Cutoff = 1.167$

Tests	9b	10	11	12a	12b	13a	13b	14a	14b	15a	15b	16a	17a	17b
1	499.238	104.699	61.396	261.947	352.837	259.718	337.206	15.201	1744.244	7.848	193.208	326.909	357.406	115.840
2a	9.820	6.406	14.552	0.333	2.819	0.420	2.405	52.810	125.637	36.814	0.387	3.810	2.959	3.235
2b	53.055	10.796	5.919	28.340	38.138	28.465	36.721	0.656	183.147	0.207	20.737	34.222	38.138	12.498
3	2.901	0.743	2.213	0.540	1.473	0.865	1.546	10.371	30.488	7.045	0.102	0.619	1.097	0.509
4a	31.720	3.934	10.951	6.095	14.476	5.968	12.980	53.167	243.587	33.855	2.079	14.376	15.044	0.748
4b	0.569	2.895	5.109	0.676	0.624	1.022	0.862	14.918	17.114	11.207	1.042	0.122	0.208	2.430
5a	163.688	16.068	34.640	42.732	83.266	40.973	75.356	172.264	1059.379	104.896	20.486	82.632	87.195	5.354
5b	98.571	9.367	6.639	38.732	60.685	38.297	56.907	28.197	467.149	13.334	23.740	55.888	61.827	9.155
6a	31.021	4.774	2.221	15.428	21.647	15.640	20.839	1.384	117.586	0.176	10.664	18.895	21.481	5.794
6b	12.892	2.376	1.117	7.187	9.706	7.518	9.559	0.232	44.441	0.116	5.109	7.817	9.305	3.159
7	10.080	2.103	1.066	5.958	7.883	6.308	7.842	0.233	32.924	0.269	4.315	6.137	7.445	2.841
8	19.645	25.368	50.805	0.439	3.845	0.037	2.755	162.464	308.064	116.405	3.777	10.008	5.062	14.845
9a	0.007	16.409	25.253	3.844	1.497	4.113	1.977	59.317	35.014	46.426	7.185	3.314	1.273	13.344
9b	-	17.349	26.863	3.879	1.420	4.135	1.901	63.553	39.017	49.628	7.443	3.456	1.225	14.012
10	4.969	-	0.298	1.721	3.140	2.057	3.156	4.284	30.740	2.510	0.705	1.867	2.737	0.219
11	5.803	0.225	-	2.614	4.089	2.961	4.109	1.890	27.859	0.951	1.444	2.648	3.660	0.659
12a	6.054	8.503	17.401	-	1.157	0.123	0.973	56.834	104.691	40.747	1.083	2.547	1.229	5.126
12b	3.554	25.786	44.904	1.901	-	1.883	0.097	122.432	139.301	91.767	7.258	4.902	0.407	18.363
13a	13.960	19.881	39.633	0.208	2.509	-	1.793	125.980	231.179	90.517	2.986	7.074	3.305	11.842
13b	7.545	40.035	70.513	2.508	0.146	2.213	-	194.700	237.490	145.228	10.713	8.581	1.171	27.870
14a	31.263	7.476	4.338	17.952	23.447	18.209	22.792	-	99.493	0.423	13.526	20.607	23.186	8.802
14b	167.297	462.727	557.053	288.052	231.687	288.326	239.895	867.919	-	758.329	345.554	266.482	231.882	428.180
15a	24.932	4.463	2.183	13.159	17.983	13.422	17.430	0.432	88.798	-	9.361	15.490	17.715	5.484
15b	5.671	1.771	4.879	0.550	2.223	0.802	2.109	20.949	61.375	14.196	-	1.777	2.004	0.787
16a	0.874	1.381	2.614	0.614	0.836	0.976	1.051	8.735	13.492	6.442	0.584	-	0.387	1.306
17a	1.105	8.545	15.144	0.720	0.201	0.972	0.400	42.537	48.792	31.824	2.373	1.100	-	6.274
17b	10.753	0.455	2.045	2.538	5.532	2.775	5.212	13.730	76.560	8.374	0.792	4.454	5.335	-

In terms of the same KL cutoff determined for the one-substructure case in Table 3 it can be said that: The cutoff KL value equates to the minimum difference in flexural rigidity that is deemed unacceptable (i.e., the difference in flexural rigidity found when correcting L1 LVDT is the largest deviation desired). This equating is rational recalling that L1 was removed from datasets to determine its effect on the identified EIs. KL values between tests that are equal to, or higher, than the cutoff indicate disparity in identified results corresponding to inaccurate or perhaps non-conservative identifications. From 27^2 results (less the 27 tests due to diagonals that have KL values of zero) for the one-substructure case, it is determined that 555 pairs are at or above the cutoff. In other words, approximately 80% of the test pairs' identified EI values exhibit a difference too large to constitute agreement in identification. A graphical representation of Table 6.6.3 is shown below:

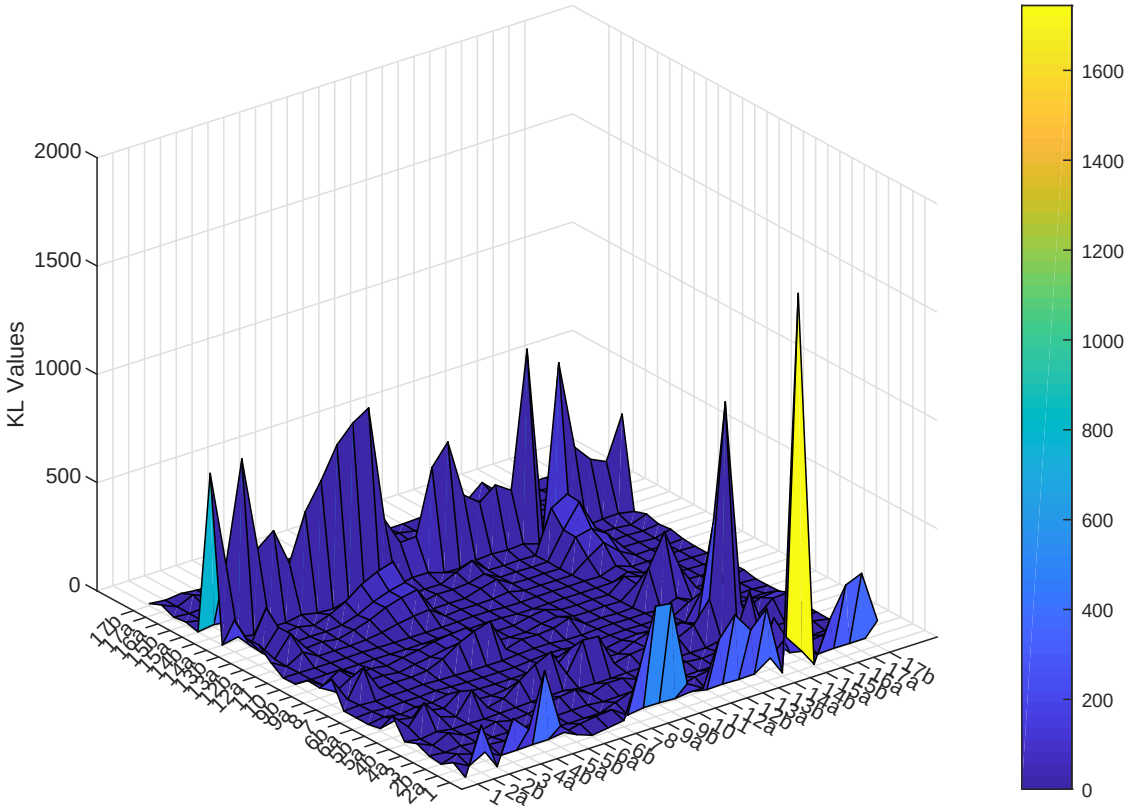

Fig. 37. A graphical representation of the KL values found between pairing of the data from "Uncorrected" for the one-substructure case

The results of Table 6.6.3 are replicated for the three, six, and nine-substructure cases and

are reported in Appendix C. The tables for the higher-order substructures show even higher percentages of test pair identification disagreement, on the order of 90%. These pairings show increased disparity in identification between tests as the number of substructures increase.

With results obtained from Table 6.6.3 and in Appendix C indicating an almost complete disparity between identified results of individual test permutations, this suggests that the KL divergence applied in this aspect is too stringent of a criteria to base the success or failure of the study upon. Permutations aside, the mean test values illustrated in Section 6.5.2 indicate the usefulness of Bayesian analysis and frequent agreement in identification between all three test data categories in substructures further away from L1's removal location under higher-order substructures. As such, KL divergence applied in this context to is deemed too stringent for the purposes of this study.

6.6.4. Complexity and Limitation of this Study

The complexity of the problem in this study lies in the complexity of precast pretensioned concrete and bridge girder systems. The variability of the constituent material is first observed. Concrete is a non-homogenous material whose behavior can be more complex than that of a homogenous, isotropic material such as steel. This complex behavior can impact flexural rigidity identification. This leads to the variability in E_c and I as discussed in Section 6.1. Additionally, for continuous bridges, creep can lead to cracking at joints which will also affect flexural rigidity. Flexural rigidity varies within the transfer length at the end spans for a pretensioned concrete girder. Adequately encompassing these and other potential reductions in flexural rigidity is limited with the proposed identification formulation.

Towards the end of this study, it remains unsolved why σ has the potential to return negative optimized values. A future investigation is required to determine the cause. For $\sigma_{\text{init.}} = 0.1$, 4.4 to 7.4%, the lowest percentage, of the optimizations for σ were found to be negative based on the results of the substructure idealizations utilized, where the occurrence of im-

proper optimizations increased with the number of substructures. The highest percentage of improper optimizations was found to be 57.8 to 59.3% when $\sigma_{\text{init.}} = 0.01$. 8.9 to 13.3% of the optimizations were found to be negative using the remaining $\sigma_{\text{init.}}$ values. Again, the identified values associated with the negative σ values were not used in this study.

Two values need to be reexamined in this study: EI_0, which used in Bayesian analysis, and one of the EI lines first seen in Figs. 23 to 25. Both values are chosen to be 3.88×10^8 kip-in^2 from Cranor (2015). The value of EI_0 could be reexamined using the average Young's modulus from cored samples in Section 6.1.2 and perhaps I_{tr} from a transformed section calculation of Girder A in Section 6.6.1. A parametric study should then be conducted varying EI_0 in Bayesian analysis.

Limited exercises are conducted in this study when the girder is divided into one, three, six, nine, and ten substructures as well as an additional arbitrarily generated substructure. The assumed flexibility in the developed methodology and code remains to be explored and exploited. For example, in a future study, it remains to be seen if more substructures would benefit the identified results.

7. CONCLUSIONS

Aging infrastructure requires structural health monitoring for recommendations on load posting, retrofitting, or replacements. Flexural rigidity has been used to monitor the aging of precast pretensioned concrete bridge girders with suitable datasets collected from laboratory testing in previous studies. These studies utilized classical beam theory focusing on the physical phenomenon of bending under a point load. A significant issue persisted in the previous studies' inverse problem formulation, where data analysis using the standard linear least-squares method led to negative identified flexural rigidity values. Problem reformation for the inverse problem is thus carried out in this study. An intuitive illustrative example is provided for comprehension of the least-squares approach; a Bayesian analytical approach is also introduced in plain words.

The Bayesian analytical approach was contributed by an outside researcher, while the programming, implementation, and result analysis were performed at the University of Oklahoma in a process of learning Bayesian analysis through numerical exercises and in contrast with the performance of the least-squares method. Least-squares analysis, a common solution applied in numerous studies, relies solely on data for fitting. However, Bayesian analysis utilizes both data and user-defined parameters quantifying expected uncertainty for fitting.

This study facilitated a just-in-time learning experience of Bayesian analysis, an otherwise advanced topic that is not included in typical collegiate curriculum. In this regard, an intuitive understanding of the theory was achieved in this study. Several afterthoughts are included in analyses and discussions that reflect a continuously improved understanding of the Bayesian methodology throughout this study.

Through navigating a large parameter space, reasonable values are pinned down for the two user-defined parameters, $\sigma_{\text{init.}}$ and σ_0, that are critical for the success of Bayesian analysis. Specifically, the Bayesian solution is sensitive to one of the parameters, σ_0, and can lead

to meaningless results if extreme values are chosen. For this reason, a parametric study is conducted to narrow the range of the user-defined parameters and eventually decide specific values for use in this study; the parametric study for user-defined parameter determination is a coupled process in which the posterior COV is minimized. This systematic exercise and complimentary extensive reasoning manifest both learning and contribution to research using Bayesian analysis.

The range of the values tested for both user-defined parameters turns out to be similar. A constant value of $\sigma_{\text{init.}} = 0.1$ is first decided from the parametric study to be used for all test analyses and substructure idealizations, where $\sigma_{\text{init.}}$ is the initial value for the optimized objective function at σ. An afterthought suggests that a smaller, more suitable value of $\sigma_{\text{init.}}$ may exist.

The prior standard deviation of the Gaussian distribution of $\boldsymbol{\theta}$, specified as $\sigma_0 = 0.1$, is then decided for all test analyses and substructure idealizations in an empirical manner minimizing the posterior COV. Noting the vast parameter space between discrete choices of σ_0, absolute confidence in this parameter value is not held. The estimate of $\sigma_0 = 0.1$ cannot be further optimized through the proposed exercise, noting an improved value could exist.

The collected data's quality was not taken for granted throughout this project. The raw data required digital signal preprocessing to filter out high-frequency noise and methodically downsample the large amount of data. Further data processing was utilized to correct for rigid body motion. Yet, unreasonable deflected shapes resulted from the processed data requiring the removal of some of the LVDT data to avoid unreasonable/inaccurate identified results. To make objective decisions regarding LVDT reading removal and in order to automate this process, concepts from Computer Science were learned and exercised. Calculating differential and relative entropy, the results (when paired with unreasonable deflected shape determinations) indicated that LVDT L1 indeed affected identification efforts. As such, LVDT L1 is removed from specific tests. Though Computer Science concepts were exercised for LVDT

data removal, mixed feelings are held about their application - specifically whether entropy is being used in the most efficient manner.

Three categories of test data are then created and their results are compared: (i) L1 kept in all tests, (ii) L1 removed from all tests, and (iii) L1 removed from some tests. For each test data category, possible idealizations of piecewise divisions (substructures) are explored for their effect on the model's efficacy. The Bayesian analysis identified results are generally found to be consistent between substructure idealizations. More conservative identifications and agreement between the three test data categories are seen as more substructures are utilized. The ten-substructure case, at approximately 3ft per substructure, holds potential for improved flexural rigidity identification when compared to the other subdivisions used in this study. Utilizing this idealized beam division with the three test data categories, it is determined that category (ii) seems to balance the flexural rigidity correction due to LVDT removal with localized increases in standard deviation. Thus, removal of L1 from specific tests under category (iii) did not prove as useful as initially thought.

Identified flexural rigidity values from the Bayesian methodology are then compared against functional flexural rigidity values for the girder, where a constant flexural rigidity determined by Cranor (2015) accurately characterizes the two end spans. The end span identifications are consistent with the end region corrosion seen as a result of the girder's 40+ years of service-life justifying the usefulness of Bayesian analysis. The end span flexural rigidity reductions are roughly 94% of a conservative estimate for an undamaged girder. Conversely, the largest identified midspan flexural rigidity value is 106% of the conservative estimate. Least-squares regression identified results are immediately removed from consideration as they are often found to be negative numbers, zero, or generally meaningless in terms of physical insights to Girder A.

At this time, quantitative damage detection is not possible despite promising flexural rigidity identifications through Bayesian analysis. Damage detection efforts are briefly discussed

highlighting the need to specify a functional flexural rigidity range for the girder in this study to properly characterize what constitutes "damage".

In addition to the contribution to the Bayesian analysis and data quality examination, the two methodologies, previously programmed into MATLAB, were streamlined and debugged throughout this study. Validation of the code and Bayesian methodology was carried out using demonstration problems (i.e., problems with known solutions), which were simulated through beam theory and matrix structural analysis, in this study. The validation cases illustrate the usefulness of Bayesian analysis; contrasting Bayesian analysis results with that of least squares, it is found that the least-squares methodology can return meaningless results. The original MATLAB code was used as a foundation to further expand the coding suite to include numerous utility functions to expedite this study and future expansion such as: improving result reporting, storing data outputs, calculating cross-sectional properties, and calculating entropy.

8. REFERENCES

Attaway, S., 1981. MATLAB A Practical Introduction to Programming and Problem Solving. Butterworth–Heinemann Publications.

Beck, J.L., 2018. Project Notes on the Bayesian Method for EI Determination from Beam Deflection Data. Notes.

Bishop, C.M., 2006. Pattern Recognition and Machine Learning. Springer.

Capellari, G., Chatzi, E., Mariani, S., 2018. Structural Health Monitoring Sensor Network Optimization Through Bayesian Experimental Design. Article.

Cotra, M., 2017. Making sense of the kullback-leibler (kl) divergence. https://medium.com/@cotra.marko/making-sense-of-the-kullback-leibler-kl-divergence-b0d57ee10e0a.

Cranor, B.N., 2015. Analysis And Experimental Testing For Shear Behavior Of An Aashto Type Ii Girder In Service For Several Decades. Report. The University of Oklahoma, School Of Civil Engineering And Environmental Science.

Floyd, R.W., Pei, J.S., Murray, C.D., Cranor, B., Tang, P.F., 2016. Understanding the Behavior of Prestressed Girders after Years of Service. Report. Oklahoma Department of Transportation Office of Research and Implementation.

Freitas, C.J., 2002. The Issue of Numerical Uncertainty. Report. Southwest Research Institute.

Gray, R.M., 1990. Entropy and Information Theory. Springer Science + Business Media, LLC.

Green, P.L., Worden, K., 2015. Bayesian and markov chain monte carlo methods for identifying nonlinear systems in the presence of uncertainty. Philosophical Transactions A 373.

Harries, K.A., Kasan, J., Miller, R., Brinkman, R., 2012. Guide to recommended practice for the repair of impact-damaged prestressed concrete bridge girders. http://onlinepubs.trb.org/onlinepubs/nchrp/docs/NCHRP20-07(307)_AppendixA-GUIDE.pdf.

Housner, G.W., Bergman, L.A., Caughey, T.K., Chassiakos, A.G., Claus, R.O., Masri, S.F., Skelton, R.E., Soong, T.T., Spencer, B.F., Yao, J.T.P., 1997. Structural Control: Past, Present, And Future. Report. Journal of Engineering Mechanics.

Huang, Y., Beck, J.L., 2013. Novel Sparse Bayesian Learning For Structural Health Monitoring Using Incomplete Modal Data. Article.

Huang, Y., Shao, C., Wu, B., Beck, J.L., Li, H., 2019. State-of-the-art review on bayesian inference in structural system identification and damage assessment. Advances in Structural Engineering 22, 1329–1351.

Huth, O., Feltrin, G., Maeck, J., Kilic, N., Motavalli, M., 2005. Damage identification using modal data: Experiences on a prestressed concrete bridge. Journal of Structural Engineering 131. doi:10.1061/(ASCE)0733-9445(2005)131:12(1898).

Impollonia, N., Failla, I., Ricciardi, G., 2016. Parametric statistical moment method for damage detection and health monitoring. ASCE-ASME Journal of Risk and Uncertainty in Engineering Systems, Part A: Civil Engineering 2. doi:https://iopscience.iop.org/article/10.1088/0964-1726/16/4/003/meta.

Kato, M., Shimada, S., 1986. Vibration of pc bridge during failure process. Journal of Structural Engineering 112. doi:https://doi.org/10.1061/(ASCE)0733-9445(1986)112:7(1692).

Maeck, J., Wahab, M.A., Peeters, B., Roeck, G.D., Visscher, J.D., Wilde, W.P.D., Ndambi, J.M., Vantomme, J., 2000. Damage identification in reinforced concrete structures by dynamic stiffness determination. Engineering Structures 22. doi:https://doi.org/10.1016/S0141-0296(99)00074-7.

Noël, J.P., Kerschen, G., 2017. Nonlinear system identification in structural dynamics: 10 more years of progress. Mechanical Systems and Signal Progressing 83, 2–35.

Pandey, A.K., Biswas, M., 1995. Experimental verification of flexibility difference method for locating damage in structures. Journal of Sound ad Vibration 184. doi:https://doi.org/10.1006/jsvi.1995.0319.

Pei, J.S., Martin, R., Sandburg, C., Kang, T.H.K., 2008. Rating Precast Prestressed Concrete Bridges for Shear. Report. Oklahoma Department of Transportation Office of Research and Implementation.

Roache, P., 1998. Verification and Validation in Computational Science and Engineering. Article.

van de Schoot, R., Kaplan, D., Denissen, J., Asendorpf, J.B., Neyer, F.J., van Aken, M.A., 2014. A Gentle Introduction to Bayesian Analysis: Applications to Developmental Research. Article.

Seo, J., Hu, J.W., Lee, J., 2015. Summary review of structural health monitoring applications for highway bridges. Journal of Performance of Constructed Facilities 30. doi:https://doi.org/10.1061/(ASCE)CF.1943-5509.0000824.

Shoukry, S., William, G.W., Riad, M.Y., Downie, B., 2009. Effect of Moisture and Temperature on the Mechanical Properties of Concrete. Report. West Virginia University.

Song, G., Gu, H., Mo, Y.L., Hsu, T.T.C., Dhonde, H., 2007. Concrete structural health monitoring using embedded piezoceramic transducers. Smart Materials and Structures 16.

Thomas, A., 2019. An introduction to entropy, cross entropy and kl divergence in machine learning. https://adventuresinmachinelearning.com/cross-entropy-kl-divergence/.

Unger, J.F., Teughels, A., Roeck, G.D., 2006. System identification and damage detection of a prestressed concrete beam. Journal of Structural Engineering 132. doi:10.1061/(ASCE)0733-9445(2006)132:11(1691).

Vanik, M.W., Beck, J.L., Au, S.K., 2000. Bayesian Probabilistic Approach To Structural Health Monitoring. Article.

Worden, K., Farrar, C.R., Mason, G., Park, G., 2007. The fundamental axioms of structural health monitoring. Report. The Royal Society.

Appendix A. ILLUSTRATIVE EXAMPLE

Appendix A.1. Motivation

Programming in MATLAB of the two methodologies discussed in Section 3.2 were mainly developed by Dr. Jin-Song Pei, however, no written or oral explanation was given for their development process. As such, the matching narrative is provided for the least-squares method in the form of an illustrative example; the Bayesian analysis narrative is plainly explained in Section 3.4. Debugging of the extensive original coding suite was possible through the understanding gained from these narratives.

Appendix A.2. Formulation of Scaled and Normalized Response Function - **H**

The piecewise constant EI values along the span of the beam are to ultimately be identified through Eq. (1). The subsequent sections impart physical meaning to the elements in this equation, thereby building a foundation for comprehension.

The construction of **H** begins with a deflection response of the beam which is then scaled up - to determine deflections, it is necessary to involve the use of the principle of virtual work. The principle of virtual work is well established as follows:

$$\Delta = \int_L \frac{Mm}{EI} dx \tag{A.1}$$

where Δ is the deflection of the beam at the point of interest, M refers to the real bending moment diagram caused by the application of the physical load and m refers to the virtual bending moment diagram caused by the application of a virtual load.

To achieve a thorough understanding of this problem formulation, a specific example is given as follows where $N = 3$, $J = 4$ and $K = 1$ meaning that three piecewise values for EI (over

L_1, L_2 and L_3) are assumed, measurements from four active LVDTs are used, and the data of only one time step (incremental load) is considered.

For the case of a simply supported beam, the following bending moment diagrams can be constructed through Eq. (A.1) in response to a generically applied a point load as in Fig. A.38. The moment distribution colored in blue signifies the real bending moment diagram produced by a unit point load whereas the moment distribution colored in red signify those produced by unit virtual loads. It must be noted that virtual loads are not illustrated in Fig. A.38 as they do not actually exist. Virtual load application points for a given test are defined by the principle of virtual work as the locations of the measured deflections in $\mathbf{\Delta}$, corresponding to the number of active degrees of freedom in J.

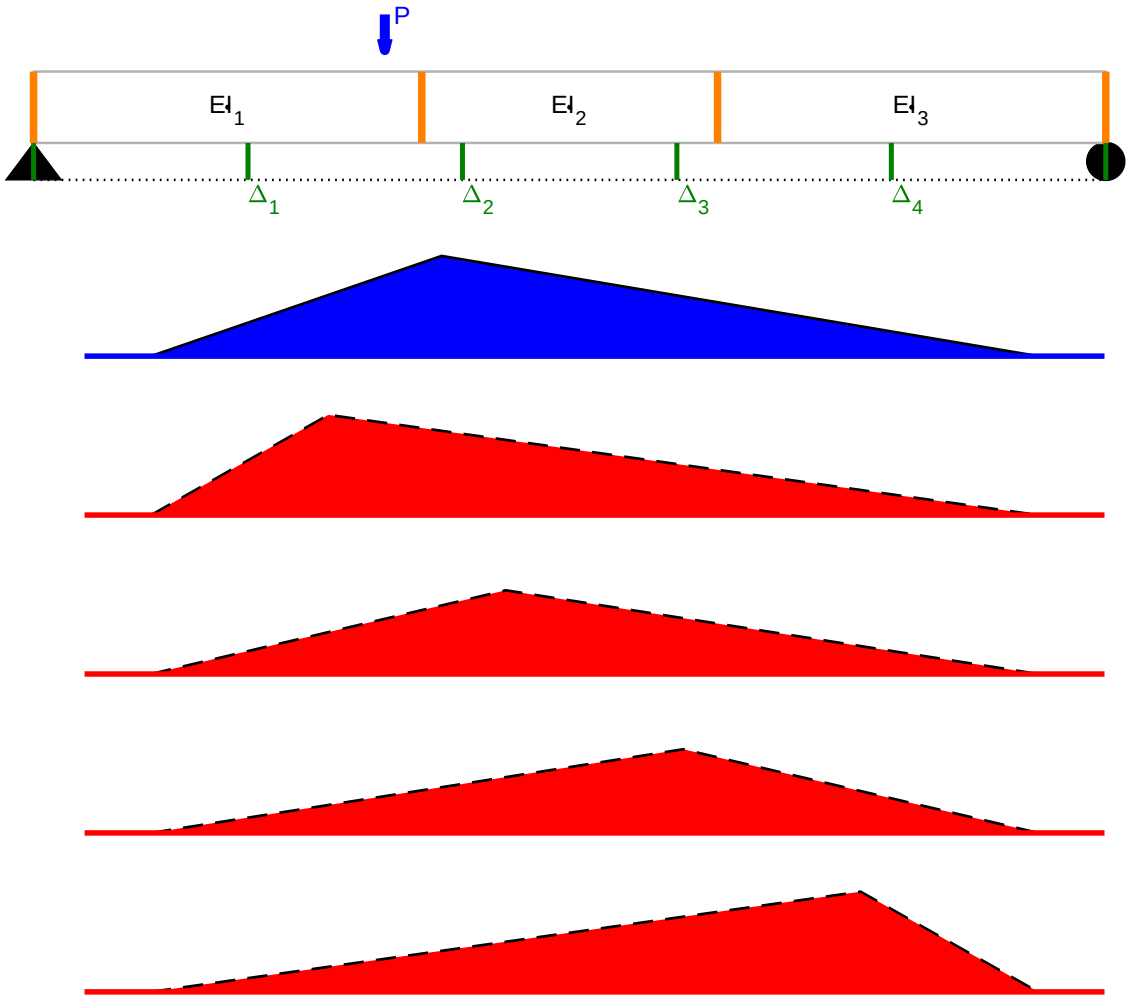

Fig. A.38. An illustrative example using $N = 3$, $J = 4$ and $K = 1$: Test setup, and real and virtual bending moment diagrams utilized in Leastsquares.m

Utilizing the bending moment diagrams in Fig. A.38 theoretical expressions for the deflections, by Eq. (A.1), experienced at the active LVDTs are as follows:

$$\Delta_1 = \int_{L_1} \frac{Mm_1}{EI_1} dx + \int_{L_2} \frac{Mm_1}{EI_2} dx + \int_{L_3} \frac{Mm_1}{EI_3} dx \tag{A.2}$$

$$\Delta_2 = \int_{L_1} \frac{Mm_2}{EI_1} dx + \int_{L_2} \frac{Mm_2}{EI_2} dx + \int_{L_3} \frac{Mm_2}{EI_3} dx \tag{A.3}$$

$$\Delta_3 = \int_{L_1} \frac{Mm_3}{EI_1} dx + \int_{L_2} \frac{Mm_3}{EI_2} dx + \int_{L_3} \frac{Mm_3}{EI_3} dx \tag{A.4}$$

$$\Delta_4 = \int_{L_1} \frac{Mm_4}{EI_1} dx + \int_{L_2} \frac{Mm_4}{EI_2} dx + \int_{L_3} \frac{Mm_4}{EI_3} dx \tag{A.5}$$

Eqs. (A.2) to (A.5) can be separated into their constituent vectors which equate with the original equations through the use of vector inner product (dot product):

$$\Delta_1 = \begin{bmatrix} \int_{L_1} Mm_1 dx & \int_{L_2} Mm_1 dx & \int_{L_3} Mm_1 dx \end{bmatrix} \begin{bmatrix} \frac{1}{EI_1} \\ \frac{1}{EI_2} \\ \frac{1}{EI_3} \end{bmatrix} \tag{A.6}$$

$$\Delta_2 = \begin{bmatrix} \int_{L_1} Mm_2 dx & \int_{L_2} Mm_2 dx & \int_{L_3} Mm_2 dx \end{bmatrix} \begin{bmatrix} \frac{1}{EI_1} \\ \frac{1}{EI_2} \\ \frac{1}{EI_3} \end{bmatrix} \tag{A.7}$$

$$\Delta_3 = \begin{bmatrix} \int_{L_1} Mm_3 dx & \int_{L_2} Mm_3 dx & \int_{L_3} Mm_3 dx \end{bmatrix} \begin{bmatrix} \frac{1}{EI_1} \\ \frac{1}{EI_2} \\ \frac{1}{EI_3} \end{bmatrix} \tag{A.8}$$

$$\Delta_4 = \begin{bmatrix} \int_{L_1} Mm_4 dx & \int_{L_2} Mm_4 dx & \int_{L_3} Mm_4 dx \end{bmatrix} \begin{bmatrix} \frac{1}{EI_1} \\ \frac{1}{EI_2} \\ \frac{1}{EI_3} \end{bmatrix} \tag{A.9}$$

where the row vectors containing the products of the integrations of the real and virtual

bending moment diagrams are the unit response functions to be scaled up in **H**. Combining these four equations into a linear system produces the following:

$$\begin{bmatrix} \Delta_1 \\ \Delta_2 \\ \Delta_3 \\ \Delta_4 \end{bmatrix} = \begin{bmatrix} \int_{L_1} M m_1 dx & \int_{L_2} M m_1 dx & \int_{L_3} M m_1 dx \\ \int_{L_1} M m_2 dx & \int_{L_2} M m_2 dx & \int_{L_3} M m_2 dx \\ \int_{L_1} M m_3 dx & \int_{L_2} M m_3 dx & \int_{L_3} M m_3 dx \\ \int_{L_1} M m_4 dx & \int_{L_2} M m_4 dx & \int_{L_3} M m_4 dx \end{bmatrix} \begin{bmatrix} \frac{1}{EI_1} \\ \frac{1}{EI_2} \\ \frac{1}{EI_3} \end{bmatrix} \tag{A.10}$$

Normalization by EI_0 is then introduced in Eq. (A.11) to obtain a better numerical performance:

$$\begin{bmatrix} \Delta_1 \\ \Delta_2 \\ \Delta_3 \\ \Delta_4 \end{bmatrix} = \frac{1}{EI_0} \begin{bmatrix} \int_{L_1} M m_1 dx & \int_{L_2} M m_1 dx & \int_{L_3} M m_1 dx \\ \int_{L_1} M m_2 dx & \int_{L_2} M m_2 dx & \int_{L_3} M m_2 dx \\ \int_{L_1} M m_3 dx & \int_{L_2} M m_3 dx & \int_{L_3} M m_3 dx \\ \int_{L_1} M m_4 dx & \int_{L_2} M m_4 dx & \int_{L_3} M m_4 dx \end{bmatrix} \begin{bmatrix} \frac{EI_0}{EI_1} \\ \frac{EI_0}{EI_2} \\ \frac{EI_0}{EI_3} \end{bmatrix} \tag{A.11}$$

The above is for one generic time step. Utilizing the data of multiple time steps:

$$\begin{bmatrix} \Delta_{1k} \\ \Delta_{2k} \\ \Delta_{3k} \\ \Delta_{4k} \end{bmatrix} = \frac{1}{EI_0} \begin{bmatrix} \int_{L_1} M_k m_1 dx & \int_{L_2} M_k m_1 dx & \int_{L_3} M_k m_1 dx \\ \int_{L_1} M_k m_2 dx & \int_{L_2} M_k m_2 dx & \int_{L_3} M_k m_2 dx \\ \int_{L_1} M_k m_3 dx & \int_{L_2} M_k m_3 dx & \int_{L_3} M_k m_3 dx \\ \int_{L_1} M_k m_4 dx & \int_{L_2} M_k m_4 dx & \int_{L_3} M_k m_4 dx \end{bmatrix} \begin{bmatrix} \frac{EI_0}{EI_1} \\ \frac{EI_0}{EI_2} \\ \frac{EI_0}{EI_3} \end{bmatrix} \tag{A.12}$$

For example, considering $N = 3$, $J = 4$ and $K = 2$ yields:

$$\begin{bmatrix} \Delta_{11} \\ \Delta_{21} \\ \Delta_{31} \\ \Delta_{41} \\ \Delta_{12} \\ \Delta_{22} \\ \Delta_{32} \\ \Delta_{42} \end{bmatrix} = \frac{1}{EI_0} \begin{bmatrix} \int_{L_1} M_1 m_1 dx & \int_{L_2} M_1 m_1 dx & \int_{L_3} M_1 m_1 dx \\ \int_{L_1} M_1 m_2 dx & \int_{L_2} M_1 m_2 dx & \int_{L_3} M_1 m_2 dx \\ \int_{L_1} M_1 m_3 dx & \int_{L_2} M_1 m_3 dx & \int_{L_3} M_1 m_3 dx \\ \int_{L_1} M_1 m_4 dx & \int_{L_2} M_1 m_4 dx & \int_{L_3} M_1 m_4 dx \\ \int_{L_1} M_2 m_1 dx & \int_{L_2} M_2 m_1 dx & \int_{L_3} M_2 m_1 dx \\ \int_{L_1} M_2 m_2 dx & \int_{L_2} M_2 m_2 dx & \int_{L_3} M_2 m_2 dx \\ \int_{L_1} M_2 m_3 dx & \int_{L_2} M_2 m_3 dx & \int_{L_3} M_2 m_3 dx \\ \int_{L_1} M_2 m_4 dx & \int_{L_2} M_2 m_4 dx & \int_{L_3} M_2 m_4 dx \end{bmatrix} \begin{bmatrix} \frac{EI_0}{EI_1} \\ \frac{EI_0}{EI_2} \\ \frac{EI_0}{EI_3} \end{bmatrix} \tag{A.13}$$

Despite multiple time steps, the bending moment response does not change in shape, only magnitude. Given the fact that $M_k = M_0 P_k$, where M_0 is the moment response of the beam under a unit load and P_k is the scaling time step then gives:

$$\begin{bmatrix} \Delta_{11} \\ \Delta_{21} \\ \Delta_{31} \\ \Delta_{41} \\ \Delta_{12} \\ \Delta_{22} \\ \Delta_{32} \\ \Delta_{42} \end{bmatrix} = \begin{bmatrix} \frac{\left(\int_{L_1} M_0 m_1 dx\right) P_1}{EI_0} & \frac{\left(\int_{L_2} M_0 m_1 dx\right) P_1}{EI_0} & \frac{\left(\int_{L_3} M_0 m_1 dx\right) P_1}{EI_0} \\ \frac{\left(\int_{L_1} M_0 m_2 dx\right) P_1}{EI_0} & \frac{\left(\int_{L_2} M_0 m_2 dx\right) P_1}{EI_0} & \frac{\left(\int_{L_3} M_0 m_2 dx\right) P_1}{EI_0} \\ \frac{\left(\int_{L_1} M_0 m_3 dx\right) P_1}{EI_0} & \frac{\left(\int_{L_2} M_0 m_3 dx\right) P_1}{EI_0} & \frac{\left(\int_{L_3} M_0 m_3 dx\right) P_1}{EI_0} \\ \frac{\left(\int_{L_1} M_0 m_4 dx\right) P_1}{EI_0} & \frac{\left(\int_{L_2} M_0 m_4 dx\right) P_1}{EI_0} & \frac{\left(\int_{L_3} M_0 m_4 dx\right) P_1}{EI_0} \\ \frac{\left(\int_{L_1} M_0 m_1 dx\right) P_2}{EI_0} & \frac{\left(\int_{L_2} M_0 m_1 dx\right) P_2}{EI_0} & \frac{\left(\int_{L_3} M_0 m_1 dx\right) P_2}{EI_0} \\ \frac{\left(\int_{L_1} M_0 m_2 dx\right) P_2}{EI_0} & \frac{\left(\int_{L_2} M_0 m_2 dx\right) P_2}{EI_0} & \frac{\left(\int_{L_3} M_0 m_2 dx\right) P_2}{EI_0} \\ \frac{\left(\int_{L_1} M_0 m_3 dx\right) P_2}{EI_0} & \frac{\left(\int_{L_2} M_0 m_3 dx\right) P_2}{EI_0} & \frac{\left(\int_{L_3} M_0 m_3 dx\right) P_2}{EI_0} \\ \frac{\left(\int_{L_1} M_0 m_4 dx\right) P_2}{EI_0} & \frac{\left(\int_{L_2} M_0 m_4 dx\right) P_2}{EI_0} & \frac{\left(\int_{L_3} M_0 m_4 dx\right) P_2}{EI_0} \end{bmatrix} \begin{bmatrix} \frac{EI_0}{EI_1} \\ \frac{EI_0}{EI_2} \\ \frac{EI_0}{EI_3} \end{bmatrix} \tag{A.14}$$

Defining the unit response functions as constituent pieces of $\mathbf{H}$, thus giving them the designation of "h", the elements are redefined as $h_{jk}^{(i)}$. Denoting that the response functions in $\mathbf{H}$ are only functions of their location and scaling these unit response functions leads to the construction of $\mathbf{H}$. Following this notation:

$$\begin{bmatrix} \int_{L_1} Mm_1 dx & \int_{L_2} Mm_1 dx & \int_{L_3} Mm_1 dx \\ \int_{L_1} Mm_2 dx & \int_{L_2} Mm_2 dx & \int_{L_3} Mm_2 dx \\ \int_{L_1} Mm_3 dx & \int_{L_2} Mm_3 dx & \int_{L_3} Mm_3 dx \\ \int_{L_1} Mm_4 dx & \int_{L_2} Mm_4 dx & \int_{L_3} Mm_4 dx \end{bmatrix} = \begin{bmatrix} h_{11}^{(1)} & h_{11}^{(2)} & h_{11}^{(3)} \\ h_{21}^{(1)} & h_{21}^{(2)} & h_{21}^{(3)} \\ h_{31}^{(1)} & h_{31}^{(2)} & h_{31}^{(3)} \\ h_{41}^{(1)} & h_{41}^{(2)} & h_{41}^{(3)} \end{bmatrix} \tag{A.15}$$

Substituting the unit response functions To be scaled up by P_k:

$$\begin{bmatrix} \Delta_{11} \\ \Delta_{21} \\ \Delta_{31} \\ \Delta_{41} \\ \Delta_{12} \\ \Delta_{22} \\ \Delta_{32} \\ \Delta_{42} \end{bmatrix} = \begin{bmatrix} \frac{h_{11}^{(1)} P_1}{EI_0} & \frac{h_{11}^{(2)} P_1}{EI_0} & \frac{h_{11}^{(3)} P_1}{EI_0} \\ \frac{h_{21}^{(1)} P_1}{EI_0} & \frac{h_{21}^{(2)} P_1}{EI_0} & \frac{h_{21}^{(3)} P_1}{EI_0} \\ \frac{h_{31}^{(1)} P_1}{EI_0} & \frac{h_{31}^{(2)} P_1}{EI_0} & \frac{h_{31}^{(3)} P_1}{EI_0} \\ \frac{h_{41}^{(1)} P_1}{EI_0} & \frac{h_{41}^{(2)} P_1}{EI_0} & \frac{h_{41}^{(3)} P_1}{EI_0} \\ \frac{h_{12}^{(1)} P_2}{EI_0} & \frac{h_{12}^{(2)} P_2}{EI_0} & \frac{h_{12}^{(3)} P_2}{EI_0} \\ \frac{h_{22}^{(1)} P_2}{EI_0} & \frac{h_{22}^{(2)} P_2}{EI_0} & \frac{h_{22}^{(3)} P_2}{EI_0} \\ \frac{h_{32}^{(1)} P_2}{EI_0} & \frac{h_{32}^{(2)} P_2}{EI_0} & \frac{h_{32}^{(3)} P_2}{EI_0} \\ \frac{h_{42}^{(1)} P_2}{EI_0} & \frac{h_{42}^{(2)} P_2}{EI_0} & \frac{h_{42}^{(3)} P_2}{EI_0} \end{bmatrix} \begin{bmatrix} \frac{EI_0}{EI_1} \\ \frac{EI_0}{EI_2} \\ \frac{EI_0}{EI_3} \end{bmatrix} \tag{A.16}$$

Manipulating **H** using MATLAB's built-in command reshape, effectively forgoing the usage of looping:

$$\mathbf{H} = \frac{1}{EI_0} \begin{bmatrix} h_{11}^{(1)} P_1 & h_{11}^{(2)} P_1 & h_{11}^{(3)} P_1 \\ h_{21}^{(1)} P_1 & h_{21}^{(2)} P_1 & h_{21}^{(3)} P_1 \\ & \vdots & \\ h_{32}^{(1)} P_2 & h_{32}^{(2)} P_2 & h_{32}^{(3)} P_2 \\ h_{42}^{(1)} P_2 & h_{42}^{(2)} P_2 & h_{42}^{(3)} P_2 \end{bmatrix} \tag{A.17}$$

This matrix manipulation was implemented using element-wise operations (versus looping) in programming for efficiency (Attaway 1981).

Given Eq. (A.17), it is evident that the response functions $h_{jk}^{(i)}$, given the definition, do not depend on the time step K. The response function only has to do with the location of the one unit point load and where node j is. Here the scalability property of a linear system is utilized by factoring out the incremental load from the response function:

$$\mathbf{H} = \begin{bmatrix} \frac{h_{11}^{(1)} P_1}{EI_0} & \frac{h_{11}^{(2)} P_1}{EI_0} & \frac{h_{11}^{(3)} P_1}{EI_0} \\ \frac{h_{21}^{(1)} P_1}{EI_0} & \frac{h_{21}^{(2)} P_1}{EI_0} & \frac{h_{21}^{(3)} P_1}{EI_0} \\ \frac{h_{31}^{(1)} P_1}{EI_0} & \frac{h_{31}^{(2)} P_1}{EI_0} & \frac{h_{31}^{(3)} P_1}{EI_0} \\ \frac{h_{41}^{(1)} P_1}{EI_0} & \frac{h_{41}^{(2)} P_1}{EI_0} & \frac{h_{41}^{(3)} P_1}{EI_0} \\ \frac{h_{12}^{(1)} P_2}{EI_0} & \frac{h_{12}^{(2)} P_2}{EI_0} & \frac{h_{12}^{(3)} P_2}{EI_0} \\ \frac{h_{22}^{(1)} P_2}{EI_0} & \frac{h_{22}^{(2)} P_2}{EI_0} & \frac{h_{22}^{(3)} P_2}{EI_0} \\ \frac{h_{32}^{(1)} P_2}{EI_0} & \frac{h_{32}^{(2)} P_2}{EI_0} & \frac{h_{32}^{(3)} P_2}{EI_0} \\ \frac{h_{42}^{(1)} P_2}{EI_0} & \frac{h_{42}^{(2)} P_2}{EI_0} & \frac{h_{42}^{(3)} P_2}{EI_0} \end{bmatrix} = \left[\begin{array}{ccc} \frac{h_{11}^{(1)} P_1}{EI_0} & \frac{h_{11}^{(2)} P_1}{EI_0} & \frac{h_{11}^{(3)} P_1}{EI_0} \\ \frac{h_{21}^{(1)} P_1}{EI_0} & \frac{h_{21}^{(2)} P_1}{EI_0} & \frac{h_{21}^{(3)} P_1}{EI_0} \\ \frac{h_{31}^{(1)} P_1}{EI_0} & \frac{h_{31}^{(2)} P_1}{EI_0} & \frac{h_{31}^{(3)} P_1}{EI_0} \\ \frac{h_{41}^{(1)} P_1}{EI_0} & \frac{h_{41}^{(2)} P_1}{EI_0} & \frac{h_{41}^{(3)} P_1}{EI_0} \\ \hline \frac{h_{12}^{(1)} P_2}{EI_0} & \frac{h_{12}^{(2)} P_2}{EI_0} & \frac{h_{12}^{(3)} P_2}{EI_0} \\ \frac{h_{22}^{(1)} P_2}{EI_0} & \frac{h_{22}^{(2)} P_2}{EI_0} & \frac{h_{22}^{(3)} P_2}{EI_0} \\ \frac{h_{32}^{(1)} P_2}{EI_0} & \frac{h_{32}^{(2)} P_2}{EI_0} & \frac{h_{32}^{(3)} P_2}{EI_0} \\ \frac{h_{42}^{(1)} P_2}{EI_0} & \frac{h_{42}^{(2)} P_2}{EI_0} & \frac{h_{42}^{(3)} P_2}{EI_0} \end{array}\right] = \left[\begin{array}{c} \mathbf{H}_{11} \\ \hline \mathbf{H}_{21} \\ \hline \mathbf{H}_{31} \\ \hline \mathbf{H}_{41} \\ \hline \mathbf{H}_{12} \\ \hline \mathbf{H}_{22} \\ \hline \mathbf{H}_{32} \\ \hline \mathbf{H}_{42} \end{array}\right] \tag{A.18}$$

Thus, decomposing the first time step of $\mathbf{H}$ gives:

$$\mathbf{H}_{11} = \frac{1}{EI_0} \begin{bmatrix} P_1 \end{bmatrix} \begin{bmatrix} h_1^{(1)} & h_1^{(2)} & h_1^{(3)} \end{bmatrix} \tag{A.19}$$

$$\mathbf{H}_{21} = \frac{1}{EI_0} \begin{bmatrix} P_1 \end{bmatrix} \begin{bmatrix} h_2^{(1)} & h_2^{(2)} & h_2^{(3)} \end{bmatrix} \tag{A.20}$$

$$\mathbf{H}_{31} = \frac{1}{EI_0} \begin{bmatrix} P_1 \end{bmatrix} \begin{bmatrix} h_3^{(1)} & h_3^{(2)} & h_3^{(3)} \end{bmatrix} \tag{A.21}$$

$$\mathbf{H}_{41} = \frac{1}{EI_0} \begin{bmatrix} P_1 \end{bmatrix} \begin{bmatrix} h_4^{(1)} & h_4^{(2)} & h_4^{(3)} \end{bmatrix} \tag{A.22}$$

Similarly, the second time step of $\mathbf{H}$ is also decomposed. The unit response function can then be coded separately utilizing its independence from the time step:

$$\mathbf{h} = \begin{bmatrix} h_{11}^{(1)} & h_{11}^{(2)} & h_{11}^{(3)} \\ h_{21}^{(1)} & h_{21}^{(2)} & h_{21}^{(3)} \\ h_{31}^{(1)} & h_{31}^{(2)} & h_{31}^{(3)} \\ h_{41}^{(1)} & h_{41}^{(2)} & h_{41}^{(3)} \end{bmatrix} \tag{A.23}$$

Further information regarding the construction of the unit response function can be found in Appendix A.6.

Coding the response function matrix alone to later be scaled by an incremental load grid and normalized by EI_0 can effectively minimize the use of for-end loops in the coding process. The use of vectorization (versus looping) is instrumental in recreating $\mathbf{H}$ from $\mathbf{h}$.

Rearranging $\mathbf{h}$ into h_{row}, a row vector consisting of JN elements:

$$h_{row} = \begin{bmatrix} h_{11}^{(1)} & h_{11}^{(2)} & h_{11}^{(3)} & \dots & h_{41}^{(1)} & h_{41}^{(2)} & h_{41}^{(3)} \end{bmatrix} \tag{A.24}$$

Then finding the outer product of h_{row} with a column vector of ones to replicate said row vector $K = 2$ times allows for vectorization to create the unit response function matrix, H:

$$H = \begin{bmatrix} 1 \\ 1 \end{bmatrix} \begin{bmatrix} h_{11}^{(1)} & h_{11}^{(2)} & h_{11}^{(3)} & \dots & h_{41}^{(1)} & h_{41}^{(2)} & h_{41}^{(3)} \end{bmatrix} = \begin{bmatrix} h_{11}^{(1)} & h_{11}^{(2)} & h_{11}^{(3)} & \dots & h_{41}^{(1)} & h_{41}^{(2)} & h_{41}^{(3)} \\ h_{11}^{(1)} & h_{11}^{(2)} & h_{11}^{(3)} & \dots & h_{41}^{(1)} & h_{41}^{(2)} & h_{41}^{(3)} \end{bmatrix} \tag{A.25}$$

To reconstruct Eq. (A.18) a load grid is created through matrix multiplication comprising of K incremental loads. The matrix of ones will house the same JN elements as h_{row}:

$$P_{grid} = \begin{bmatrix} P_1 \\ P_2 \end{bmatrix} \begin{bmatrix} 1 & 1 & 1 & \dots & 1 & 1 & 1 \end{bmatrix} = \begin{bmatrix} P_1 & P_1 & P_1 & \dots & P_1 & P_1 & P_1 \\ P_2 & P_2 & P_2 & \dots & P_2 & P_2 & P_2 \end{bmatrix} \tag{A.26}$$

Vectorization can now occur:

$$H. * P_{grid} = \underbrace{\begin{bmatrix} h_{11}^{(1)} & h_{11}^{(2)} & h_{11}^{(3)} & \dots & h_{41}^{(1)} & h_{41}^{(2)} & h_{41}^{(3)} \\ h_{11}^{(1)} & h_{11}^{(2)} & h_{11}^{(3)} & \dots & h_{41}^{(1)} & h_{41}^{(2)} & h_{41}^{(3)} \end{bmatrix}}_{K \times JN} \underbrace{\begin{bmatrix} P_1 & P_1 & P_1 & \dots & P_1 & P_1 & P_1 \\ P_2 & P_2 & P_2 & \dots & P_2 & P_2 & P_2 \end{bmatrix}}_{K \times JN} \tag{A.27}$$

Transposing Eq. (A.27) and reshaping it into a column vector composed of JKN elements yields:

$$HP = \underbrace{\begin{bmatrix} h_{11}^{(1)} & h_{11}^{(2)} & h_{11}^{(3)} & h_{21}^{(1)} & h_{21}^{(2)} & h_{21}^{(3)} & \dots & h_{32}^{(1)} & h_{32}^{(2)} & h_{32}^{(3)} & h_{42}^{(1)} & h_{42}^{(2)} & h_{42}^{(3)} \\ P_1 & P_1 & P_1 & P_1 & P_1 & P_1 & \dots & P_2 & P_2 & P_2 & P_2 & P_2 & P_2 \end{bmatrix}^T}_{1 \times JKN} \tag{A.28}$$

Reshaping and transposing Eq. (A.28) and normalizing this scaled up response function matrix by EI_0 results in $\mathbf{H}$ from Eq. (A.17). With $\mathbf{H}$ constructed, Eq. (1) requires only $\boldsymbol{\Delta}$ to be constructed before the ordinary least-squares regression for $\boldsymbol{\theta}$.

Appendix A.3. Formulation of Measured Deflection Matrix - $\boldsymbol{\Delta}$

The values of $\boldsymbol{\theta}$ are realized after the construction of $\boldsymbol{\Delta}$, a matrix comprising of the elastic deflections obtained from real load-deflection test data of the given girder. EI values to be identified for the $N = 3$ piecewise substructures of the beam only affect elastic deformation, as such, the predicted deflections that can be calculated after resolution of Eq. (1) will be purely elastic. For this reason, inverse identification of the EI values across the piecewise spans of the beam require that the measured deflections in $\boldsymbol{\Delta}$, by LVDTs, be purely elastic to ensure the EI values could produce the forward model predictions.

Under non-ideal conditions, the deflections that constitute $\boldsymbol{\Delta}$ are not elastic. Deflections are measured at the supports when the incremental loading schemes are applied to the beam

(i.e., support settlement occurs). Treating the beam as a rigid body, support settlement introduces both translational and rotational motion to the entire beam, also known as rigid body motion. In general, the settlements at the supports are not equal in magnitude and/or direction causing both translational and rotational movements.

For the same beam, taking the measured deflections at each LVDT along the length of the girder for each time step and storing them in a matrix forms the following:

$$dataset\_measured = \begin{bmatrix} \delta_{11} & \delta_{21} & \delta_{31} & \delta_{41} & \delta_{51} & \delta_{61} \\ \delta_{12} & \delta_{22} & \delta_{32} & \delta_{42} & \delta_{52} & \delta_{62} \end{bmatrix} \tag{A.29}$$

And for better visualization in accordance with the example:

$$dataset\_measured = \begin{bmatrix} P_1 \\ P_2 \end{bmatrix} \begin{bmatrix} \delta_{Smin} & \delta_1 & \delta_2 & \delta_3 & \delta_4 & \delta_{Smax} \end{bmatrix} \tag{A.30}$$

where δ_{Smin} and δ_{Smax} correspond to the deflections experienced at the left support ($S_{\min}$) and the right support ($S_{\max}$) of the girder. Loading this dataset into MATLAB via the load function allows for its manipulation to produce the elastic deflections in Fig. A.39.

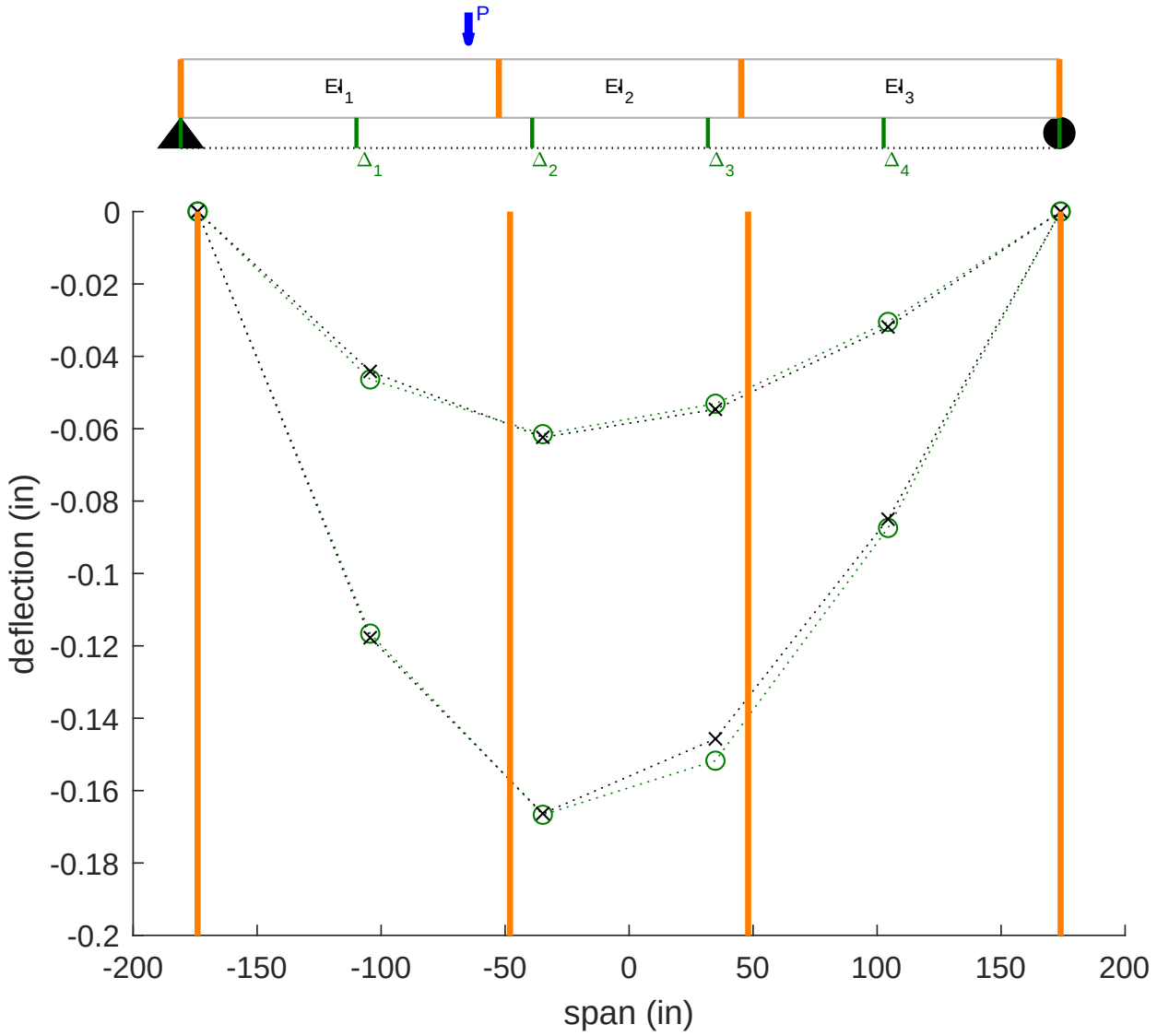

Fig. A.39. An illustrative example using $N = 3$, $J = 4$ and $K = 2$: Test setup, measured and predicted sample deflected shapes using the identified piecewise EI values

In Fig. A.39, the elastic deflections are indicated by the circled markers for each time step and the anticipated deflections can be produced following identification of the solution to Eq. (1). The predicted values of the deflections are shown by the crosses.

Discounting the rigid body motion from the displacement measurements in $\mathbf{\Delta}$ results in purely elastic deflections. The undesirable effects on the beam were accounted for by calculating the contribution from the rigid body motion based on the support settlement, where small angle rotations are assumed.

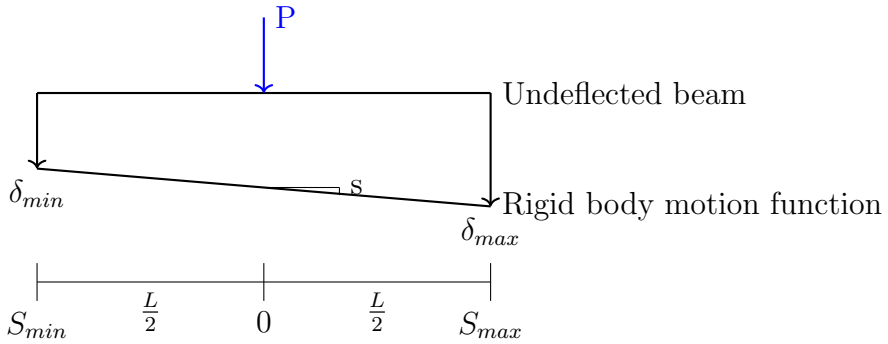

Fig. A.40. Effects of rigid body motion on Girder A

From Fig. A.40 it can be seen that the beam remains straight with vertical movements at both supports. If the support settlements are equal, then there is only translational motion. If the movements are not equal, then there are both translational and small angle rotational motions.

The support settlements being algebraic quantities coupled with the fact that the beam remains a straight line defined by two end points after their respective movements, the rigid body motion correction can be calculated by utilizing the trapezoid shown in Fig. A.40. Such a straight line can be assumed of having the following function form:

$$y \;=\; sx + b \tag{A.31}$$

where x and y denote the distance along the beam and the rigid body motion to be corrected, respectively. The slope (s) can be solved by using the two support settlements and their

locations as follows:

$$s = \frac{\delta_{Smax} - \delta_{Smin}}{S_{\max} - S_{\min}} \tag{A.32}$$

creating a column vector of slopes based on the two incremental loads:

$$\begin{bmatrix} s_1 \\ s_2 \end{bmatrix} \tag{A.33}$$

The y-intercept (b) of the bottom chord of the trapezoid is determined as follows:

$$b = \frac{S_{\max} d_{\min} - S_{\min} d_{\max}}{S_{\max} - S_{\min}} \tag{A.34}$$

subsequently forming the column vector:

$$\begin{bmatrix} b_1 \\ b_2 \end{bmatrix} \tag{A.35}$$

To use element-wise operations to discount the effects of rigid body motion, it is be necessary to create matrices of the same size as the measured responses in Eq. (A.29). To do this Eqs. (A.33) and (A.35) were replicated across $J = 6$ columns as shown:

$$s = \begin{bmatrix} s_1 \\ s_2 \end{bmatrix} \begin{bmatrix} 1 & \dots & 1 \end{bmatrix} = \begin{bmatrix} s_1 & s_1 & s_1 & s_1 & s_1 & s_1 \\ s_2 & s_2 & s_2 & s_2 & s_2 & s_2 \end{bmatrix} \tag{A.36}$$

Following Eq. (A.31), the application of a position matrix comprising of the locations of all

LVDTs would then be created to complete all necessary components of the rigid body motion function. The position matrix is created through by replicating a row vector containing all LVDT locations (δ_x), K=2 times:

$$\delta_x = \begin{bmatrix} 1 \\ 1 \end{bmatrix} \begin{bmatrix} S_{\min} & \dots & S_{\max} \end{bmatrix} = \begin{bmatrix} S_{\min} & x_1 & x_2 & x_3 & x_4 & S_{\max} \\ S_{\min} & x_1 & x_2 & x_3 & x_4 & S_{\max} \end{bmatrix} \tag{A.37}$$

Through element-wise multiplication, Eqs. (A.36) and (A.37) are multiplied and with the addition of Eq. (A.35), the rigid body motion function is completed:

$$y = \begin{bmatrix} s_1 & s_1 & s_1 & s_1 & s_1 & s_1 \\ s_2 & s_2 & s_2 & s_2 & s_2 & s_2 \end{bmatrix} \begin{bmatrix} S_{\min} & x_1 & x_2 & x_3 & x_4 & S_{\max} \\ S_{\min} & x_1 & x_2 & x_3 & x_4 & S_{\max} \end{bmatrix} + \begin{bmatrix} b_1 & b_1 & b_1 & b_1 & b_1 & b_1 \\ b_2 & b_2 & b_2 & b_2 & b_2 & b_2 \end{bmatrix} \tag{A.38}$$

Element-wise subtraction of Eqs. (A.31) from Eq. (A.29) yields:

$$dataset\_deflection = \begin{bmatrix} \mathbf{\Delta}_{Smin1} & \mathbf{\Delta}_{11} & \mathbf{\Delta}_{21} & \mathbf{\Delta}_{31} & \mathbf{\Delta}_{41} & \mathbf{\Delta}_{Smax1} \\ \mathbf{\Delta}_{Smin2} & \mathbf{\Delta}_{22} & \mathbf{\Delta}_{32} & \mathbf{\Delta}_{42} & \mathbf{\Delta}_{52} & \mathbf{\Delta}_{Smax2} \end{bmatrix} \tag{A.39}$$

where the resulting elastic deflections found at $S_{\min}$ and $S_{\max}$ are now zero. Removing the deformations at the supports which will ideally always be zero, and reshaping Eq. (A.39) into a column vector consisting of JK elements yields $\mathbf{\Delta}$:

$$\mathbf{\Delta} = \underbrace{\begin{bmatrix} \Delta_{11} & \Delta_{21} & \Delta_{31} & \Delta_{41} & \Delta_{12} & \Delta_{22} & \Delta_{32} & \Delta_{42} \end{bmatrix}^T}_{1 \times JK} \tag{A.40}$$

After discounting the effects of rigid body motion of the beam the deflections measured by the LVDTs reflect only the elastic deformations caused by the application of the incremental loadings.

Appendix A.5. Least-squares Solution - $\boldsymbol{\theta}$

With the inverse problem well-conditioned, $\boldsymbol{\theta}$ is then found through the Moore-Penrose Pseudoinverse:

$$\boldsymbol{\Delta} = \mathbf{H}\boldsymbol{\theta} \tag{A.41}$$

$$[(\mathbf{H}^T\mathbf{H})^{-1}\mathbf{H}^T]\boldsymbol{\Delta} = [(\mathbf{H}^T\mathbf{H})^{-1}\mathbf{H}^T]\mathbf{H}\boldsymbol{\theta} \tag{A.42}$$

$$[(\mathbf{H}^T\mathbf{H})^{-1}\mathbf{H}^T]\boldsymbol{\Delta} = \boldsymbol{\theta} \tag{A.43}$$

Resulting in $\boldsymbol{\theta}$:

$$\boldsymbol{\theta} = \underbrace{\begin{bmatrix} \frac{EI_0}{EI_1} \\ \frac{EI_0}{EI_2} \\ \frac{EI_0}{EI_3} \end{bmatrix}}_{N\times 1} \tag{A.44}$$

Reintroducing $\boldsymbol{\theta}$ into the problem formulation by matrix multiplication with $\mathbf{H}$ produces the predicted elastic deflections of the girder illustrated in Fig. A.39. The sensitivity of problem formulation's solution is checked through a measure of its condition number. Through normalization by EI_0, introduced in Eq. (A.11), the condition number is minimized.

Appendix A.6. Formulation of Unit Response Function Matrix - $\boldsymbol{h}$

To properly construct Eq. (A.23), the partial formulation of Eq. (A.10), bending moments responses must first be induced by real and virtual loads. Taking the beam from Appendix A.2:

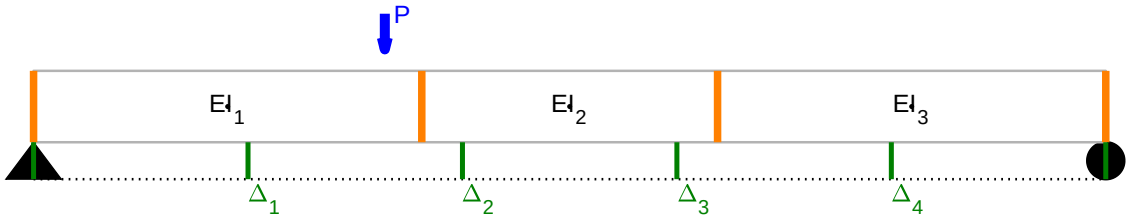

Fig. A.41. Beam used in illustrative example using $N = 3$, $J = 4$ and $K = 1$

representing all 27 tests which were limited to a single point load loading configuration and simply-supported boundary conditions with or without overhang(s).

The beam is first defined by control points used for MATLAB programming. Listing these points will aid in the theoretical construction of Eq. (A.23).

1. Vector $[S_{\min}, S_{\max}]$ containing the coordinates of the simple supports left (pin) and right (roller), respectively
2. Vector $\mathbf{x}_{EI}$ contains the coordinates of the piecewise EI divisions which include $S_{\min}$ and $S_{\max}$
3. Scalar x_P defines the coordinate for the application of the real load
4. Vector $\mathbf{x}_{\boldsymbol{\Delta}}$ specifies the coordinates of the LVDTs, both active and inactive
5. Scalar x_δ defines the coordinate of the virtual load - the locations of the active degrees of freedom in $\mathbf{x}_{\boldsymbol{\Delta}}$

The list of inputs given define the parameters necessary for calculations at those predefined points along the length of the beam which ultimately result in the unit response function. Specifying the boundary conditions of a beam along with the placement of a real unit load, a real maximum moment can be identified through beam theory. The bending moment diagram of a simply-supported beam with or without overhang(s) subjected to one point load

is piecewise linear, therefore linear interpolation can then be used to find the distribution along the entire span of the beam.

Utilizing the bending moment diagrams, the principle of virtual work is then employed to determine the unit response functions. The need is then seen to be able to systematically define where and how these responses are to be calculated along the beam's length for any configuration in accordance with the set boundary conditions in this study.

Appendix A.6.1. Response Function Construction: Obtaining Real and Virtual Bending Moment Diagrams

The application of the real load at x_P and the virtual loads at active LVDTs creates bending moment responses as in Fig. A.42. For a beam setup defined by the constraints of this project, the applied load will either act between or outside of the two supports. These mutually exclusive cases were accounted for in MATLAB to differentiate the overhang case(s) thus allowing the calculation of the maximum moment caused by a unit load.

In the set up of a simply-supported beam, featuring a pin and roller (located at $S_{\min}$ and $S_{\max}$, respectively), there are a total of three possibilities for where load coordinates x_P and x_δ lie: To the left of the pin ($x_P < S_{\min}$), to the right of the roller ($x_P > S_{\max}$) or in between the supports ($S_{\min} < x_P < S_{\max}$). These three situations are described below:

Situation 1: $x_P < S_{\min}$

Situation 1 describes one instance of the simply-supported beam with overhang(s) where the real load is applied on the overhang on the left side of the beam. The applied load causes a negative moment along the length of the beam which in turn deflects the beam such that the top fibers of the beam experience tension and conversely, compression in the bottom fibers. An example of bending moment distribution responses to the unit loads are shown in Fig. A.42, where the real load causes the blue moment

distribution and the red moment distributions are caused by virtual loads.

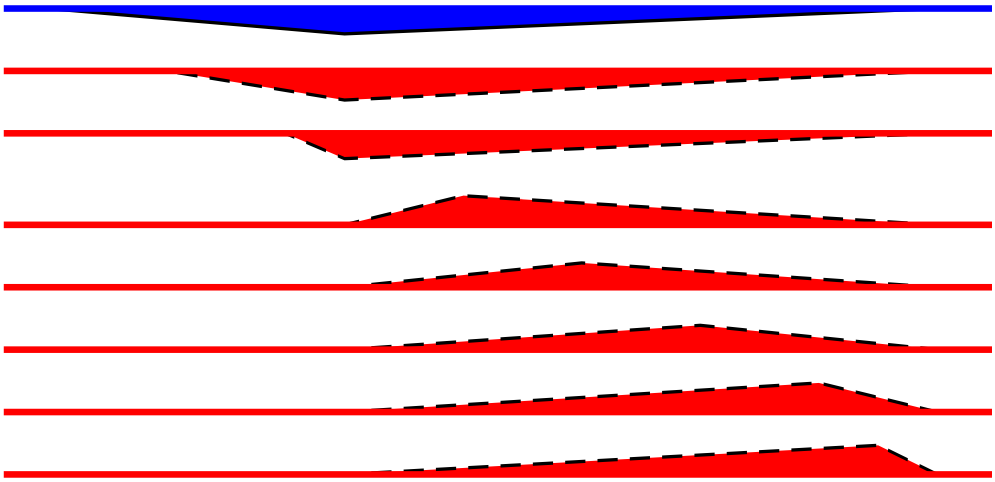

Fig. A.42. Situation 1 - Real and virtual bending moment diagrams

This bending moment diagram reaches its largest hogging moment at S_{min}. At the ends of the beam the bending moment is zero; the diagram is piecewise linear. The largest moment response for Situation 1 is then calculated as so:

$$M_{max} = Pc \tag{A.45}$$

where P is the unit load and c is the distance between the x_P and S_{min}. Substituting Eq. (A.45) with the specified parameters:

$$M_{max} = x_P - S_{\text{min}} \tag{A.46}$$

Calculating this negative moment identifies the peak of the bending moment diagram in Fig. A.42 which will later be used as a control point, along with the moments at the ends of the beam, to produce the distribution of moment along the length of the beam.

Situation 2: $x_P > S_{\text{max}}$

Situation 2 describes the second instance of the simply-supported beam with overhang(s) where the real load is applied on the overhang on the right side of the beam. In a similar manner to Situation 1, Situation 2's bending moment diagram reaches its most negative hogging moment value at the closest support to the load, $S_{\max}$. The bending moment diagram for Situation 2 is not illustrated as it is the mirrored image response of Situation 1 (assuming the same testing configuration for simplicity).

The value of the mirrored moment response is calculated similarly to the first situation following Eq. (A.45) however, the distance defined by c is now the difference between the location of x_P and $S_{\max}$:

$$M_{max} = S_{\max} - x_P \tag{A.47}$$

The applied real unit load for Situation 2, like Situation 1, also causes a downward concavity in the beam.

Situation 3: $S_{\min} < x_P < S_{\max}$

Situation 3 describes a simply-supported span of a beam with or without overhang(s) where the applied real unit load lies along the span between the supports. In this configuration the bending moment diagram will consist of positive values as shown in Fig. A.43. Due to the positive bending moment distribution along the length of the beam, the top fibers of the beam will experience a compressive stress and the bottom fibers of the beam will see a tensile stress.

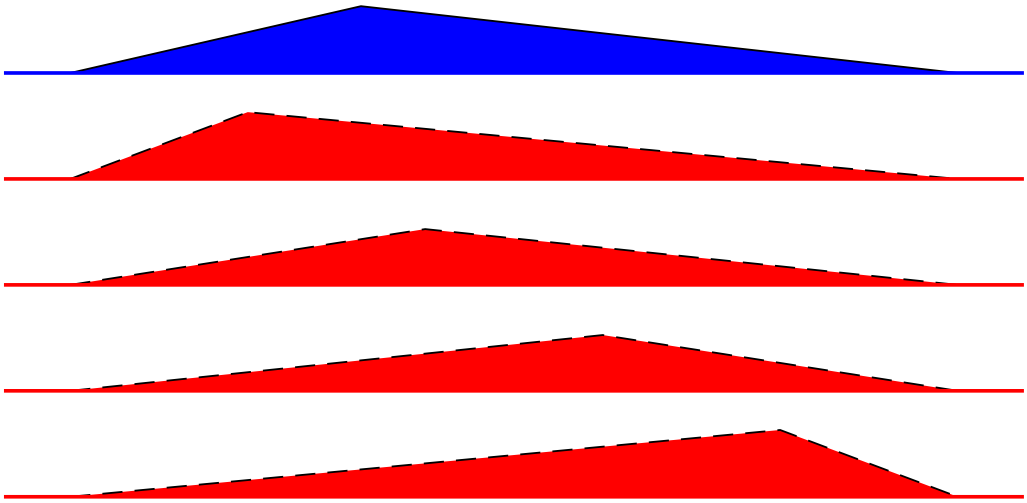

Fig. A.43. Situation 3 - Real and virtual bending moment diagrams

The bending moment diagram will reach its maximum value at the point of application of the unit load. This maximum value is calculated along the span of the beam between the two supports as so:

$$M_{\max} = \frac{Pab}{L} \tag{A.48}$$

where P is the magnitude of the point load, a is the distance from the left support to the point load, b is the distance from the right support to the point load, and L is the length of the beam. Following the notation of control points, the formula is as follows:

$$M_{\max} = \frac{(x_P - S_{\min})(S_{\max} - x_P)}{(S_{\max} - S_{\min})} \tag{A.49}$$

As in the computation of the moments for Situations 1 and 2, identifying the maximum sagging moment for Situation 3 allows for the construction of the bending moment diagram through the use of control points.

The control points for the piecewise linear bending moment diagrams consist only of maximum and zero moment values. Utilizing MATLAB's interp1 command, linear interpolation

between the maximum and zero bending moment values return the values for the diagrams seen for each situation above. Interpolation points used in the creation of the moment distributions were to be a robust set of points that could be defined easily for every test configuration.

To do this, a concatenated vector $\mathbf{x}_{\text{unique}}$ was defined containing every unique point in a given test setup. $\mathbf{x}_{\text{unique}}$ then defines the finest subdivisions of any given beam allowing for accurate intermediate interpolations of the bending moment diagrams for both the real and virtual load cases. The values of the real bending moment distribution interpolated along the points in $\mathbf{x}_{\text{unique}}$ are then contained in $\mathbf{M}$.

The bending moment distribution values for the virtual load are calculated in the same manner as the real load following the three situations defined previously. However, it is to be noted that the application point of the virtual unit load was shifted J times along the length of the beam at LVDTs representing active degrees of freedom in $\mathbf{x}_{\boldsymbol{\Delta}}$. Moving the virtual unit load across x_δ, different situations will control the intensity of M_{max} and the shape of the diagrams; these interpolated virtual bending moment distributions were stored in the vector $\mathbf{m}$.

The moment distributions contained in $\mathbf{M}$ and $\mathbf{m}$ are plotted against $\mathbf{x}_{\text{unique}}$ to produce the real and virtual bending moment distributions.

Calculating the bending moment distributions along the length of the beam allow for the construction of the response function as defined in Eq. (A.15).

Appendix A.6.2. Response function construction: Final Computation

With the moment distributions stored in $\mathbf{M}$ and $\mathbf{m}$, the calculation of the response function only required a numerical integration. Recall that all of the experiments involved were simply-supported and subjected to a single point load resulting in piecewise linear bending moment

diagrams. This piecewise linear behavior allowed for the exact calculation of the integrals to be carried out using the well established formula as follows:

$$\int_L \mathbf{Mm}dx \;=\; \frac{1}{6}[m_1(2M_1 + M_2) + m_2(M_1 + 2M_2)]L \tag{A.50}$$

The integration boundaries were constructed between the coordinates in $\mathbf{x}_{\text{unique}}$ that constituted the length of the beam, offering the finest segmentation of the beam and allowing for the versatility of calculating the response functions for any test setup where inputs are closely or widely spaced. Eq. (A.50) is an effective method of calculating the integral of piecewise linear bending moment diagrams as it can calculate the exact areas of not only trapezoids but also that of triangles.

With the value of the responses known at the finest subdivisions of the beam, it is necessary to recall that identification of EI is done across N spans of the beam. Therefore, the responses are summed across individual EI spans, separated by points in $\mathbf{x}_{EI}$, as in Eqs. (A.2) to (A.5) thereby forming the unit response functions defined in Eq. (A.15). Summations across each piecewise span are stored in $\mathbf{h}$, see Eq. (A.15).

Appendix B. USER-DEFINED PARAMETER VALUES

Appendix B.1. 1 Substructure

Table B.9. Parametric analysis to define optimal values for $\sigma_{\text{init.}}$ and σ_0 for Bayesian analysis. Negative σ sensitivity is returned by varying $\sigma_{\text{init.}}$ and COV (α) minimization is based on Bayesian prior, σ_0.

	1 Substructure								σ_0 **(Prior) = 0.0001**					
Test	$\sigma_{\text{init.}}$	$-\sigma$	α	$\sigma_{\text{init.}}$	$-\sigma$	α	$\sigma_{\text{init.}}$	$-\sigma$	α	$\sigma_{\text{init.}}$	$-\sigma$	α	$\sigma_{\text{init.}}$	$-\sigma$	α
1			0.0001			0.0001			0.0001			0.0001			0.0001
2a			0.0001		x	0.0001		x	0.0001			0.0001			0.0001
2b			0.0001		x	0.0001		x	0.0001			0.0001			0.0001
3			0.0001		x	0.0001		x	0.0001			0.0001			0.0001
4a		x	0.0001			0.0001			0.0001			0.0001		x	0.0001
4b			0.0001			0.0001		x	0.0001			0.0001			0.0001
5a			0.0001			0.0001			0.0001			0.0001			0.0001
5b			0.0001			0.0001			0.0001		x	0.0001			0.0001
6a			0.0001			0.0001			0.0001			0.0001			0.0001
6b			0.0001			0.0001		x	0.0001			0.0001			0.0001
7			0.0001			0.0001		x	0.0001			0.0001			0.0001
8		x	0.0001			0.0001		x	0.0001			0.0001			0.0001
9a			0.0001			0.0001		x	0.0001			0.0001			0.0001
9b	**0.0001**		0.0001	0.001		0.0001	0.01	x	0.0001	**0.1**		0.0001	**5**		0.0001
10			0.0001			0.0001		x	0.0001			0.0001			0.0001
11			0.0001			0.0001		x	0.0001			0.0001			0.0001
12a			0.0001			0.0001			0.0001			0.0001			0.0001
12b			0.0001			0.0001			0.0001			0.0001			0.0001
13a			0.0001			0.0001		x	0.0001			0.0001			0.0001
13b			0.0001			0.0001		x	0.0001			0.0001			0.0001
14a			0.0001			0.0001		x	0.0001			0.0001			0.0001
14b			0.0001			0.0001		x	0.0001			0.0001			0.0001
15a			0.0001			0.0001		x	0.0001			0.0001			0.0001
15b			0.0001			0.0001			0.0001			0.0001			0.0001
16a			0.0001			0.0001		x	0.0001			0.0001			0.0001
17a			0.0001			0.0001			0.0001			0.0001			0.0001
17b			0.0001			0.0001			0.0001			0.0001			0.0001

Table B.10. Parametric analysis to define optimal values for $\sigma_{\text{init.}}$ and σ_0 for Bayesian analysis. Negative σ sensitivity is returned by varying $\sigma_{\text{init.}}$ and COV (α) minimization is based on Bayesian prior, σ_0.

	1 Substructure						σ_0 **(Prior) = 0.001**					
Test	$\sigma_{\text{init.}}$	$-\sigma$	α	$\sigma_{\text{init.}}$	$-\sigma$	α	$\sigma_{\text{init.}}$	$-\sigma$	α	$\sigma_{\text{init.}}$	$-\sigma$	α	$\sigma_{\text{init.}}$	$-\sigma$	α
1			0.0010			0.0010			0.0010			0.0010			0.0010
2a			0.0010			0.0010		x	0.0010			0.0010			0.0010
2b			0.0010		x	0.0010		x	0.0010			0.0010			0.0010
3			0.0010		x	0.0010		x	0.0010			0.0010			0.0010
4a		x	0.0010			0.0010			0.0010			0.0010		x	0.0010
4b			0.0010			0.0010		x	0.0010			0.0010			0.0010
5a			0.0010			0.0010			0.0010			0.0010			0.0010
5b			0.0010			0.0010			0.0010		x	0.0010			0.0010
6a			0.0010			0.0010			0.0010			0.0010			0.0010
6b			0.0010			0.0010		x	0.0010			0.0010			0.0010
7			0.0010			0.0010		x	0.0010			0.0010			0.0010
8			0.0010			0.0010		x	0.0010			0.0010			0.0010
9a			0.0010			0.0010		x	0.0010			0.0010			0.0010
9b	**0.0001**		0.0010	0.001		0.0010	0.01	x	0.0010	**0.1**		0.0010	**5**		0.0010
10			0.0010			0.0010		x	0.0010			0.0010			0.0010
11			0.0010			0.0010		x	0.0010			0.0010			0.0010
12a			0.0010			0.0010			0.0010			0.0010			0.0010
12b			0.0010			0.0010			0.0010			0.0010			0.0010
13a			0.0010			0.0010		x	0.0010			0.0010			0.0010
13b			0.0010			0.0010		x	0.0010			0.0010			0.0010
14a			0.0010			0.0010		x	0.0010			0.0010			0.0010
14b			0.0010			0.0010		x	0.0010			0.0010			0.0010
15a			0.0010			0.0010		x	0.0010			0.0010			0.0010
15b			0.0010			0.0010			0.0010			0.0010			0.0010
16a			0.0010			0.0010		x	0.0010			0.0010			0.0010
17a			0.0010			0.0010			0.0010			0.0010			0.0010
17b			0.0010			0.0010			0.0010			0.0010			0.0010

Table B.11. Parametric analysis to define optimal values for $\sigma_{\text{init.}}$ and σ_0 for Bayesian analysis. Negative σ sensitivity is returned by varying $\sigma_{\text{init.}}$ and COV (α) minimization is based on Bayesian prior, σ_0.

	1 Substructure						σ_0 **(Prior) = 0.01**					
Test	$\sigma_{\text{init.}}$	$-\sigma$	α	$\sigma_{\text{init.}}$	$-\sigma$	α	$\sigma_{\text{init.}}$	$-\sigma$	α	$\sigma_{\text{init.}}$	$-\sigma$	α	$\sigma_{\text{init.}}$	$-\sigma$	α
1			0.0070			0.0070			0.0070			0.0070			0.0070
2a			0.0097			0.0097		x	0.0097			0.0097			0.0097
2b			0.0096			0.0095		x	0.0095			0.0095			0.0095
3			0.0099		x	0.0099		x	0.0099			0.0099			0.0099
4a			0.0095			0.0095			0.0095			0.0095		x	0.0095
4b			0.0100			0.0100		x	0.0100			0.0100			0.0100
5a		x	0.0082			0.0082			0.0082			0.0082			0.0082
5b			0.0088			0.0088			0.0088		x	0.0088			0.0088
6a			0.0097			0.0097			0.0097			0.0097			0.0097
6b			0.0099			0.0099		x	0.0099			0.0099			0.0099
7			0.0100			0.0100		x	0.0100			0.0100			0.0100
8			0.0096			0.0096		x	0.0096			0.0096			0.0096
9a			0.0099		x	0.0099		x	0.0099			0.0099			0.0099
9b	**0.0001**		0.0099	0.001		0.0099	0.01	x	0.0099	**0.1**		0.0099	**5**		0.0099
10			0.0099			0.0099		x	0.0099			0.0099			0.0099
11			0.0100			0.0100		x	0.0100			0.0100			0.0100
12a			0.0098			0.0098			0.0098			0.0098			0.0098
12b			0.0097			0.0097			0.0097		x	0.0097			0.0097
13a			0.0097			0.0097		x	0.0097			0.0097			0.0097
13b			0.0098			0.0098		x	0.0098			0.0098			0.0098
14a			0.0098		x	0.0098		x	0.0098			0.0098			0.0098
14b			0.0100		x	0.0100		x	0.0100			0.0100			0.0100
15a			0.0098			0.0098		x	0.0098			0.0098			0.0098
15b			0.0099			0.0099			0.0099			0.0099			0.0099
16a			0.0100			0.0100		x	0.0100			0.0100			0.0100
17a			0.0099			0.0099			0.0099			0.0099			0.0099
17b		x	0.0098			0.0098			0.0098			0.0098			0.0098

Table B.12. Parametric analysis to define optimal values for $\sigma_{\text{init.}}$ and σ_0 for Bayesian analysis. Negative σ sensitivity is returned by varying $\sigma_{\text{init.}}$ and COV (α) minimization is based on Bayesian prior, σ_0.

	1 Substructure						σ_0 **(Prior) = 0.1**							
Test	$\sigma_{\text{init.}}$		$-\sigma$	α	$\sigma_{\text{init.}}$	$-\sigma$	α	$\sigma_{\text{init.}}$	$-\sigma$	α	$\sigma_{\text{init.}}$	$-\sigma$	α	$\sigma_{\text{init.}}$	$-\sigma$	α
1				0.0096			0.0096			0.0096			0.0096			0.0096
2a				0.0291			0.0291		x	0.0291			0.0291			0.0291
2b				0.0304			0.0299		x	0.0299			0.0299			0.0299
3				0.0605			0.0609		x	0.0609			0.0609			0.0609
4a				0.0222			0.0222			0.0222			0.0222		x	0.0222
4b				0.0734			0.0734		x	0.0734			0.0734			0.0734
5a			x	0.0109			0.0109			0.0109			0.0109		x	0.0109
5b				0.0175			0.0174			0.0174		x	0.0174			0.0174
6a				0.0365			0.0366		x	0.0366			0.0366			0.0366
6b				0.0601			0.0613		x	0.0613			0.0613			0.0613
7				0.0728			0.0725		x	0.0725			0.0725			0.0725
8				0.0181			0.0181			0.0181			0.0181			0.0181
9a				0.0458			0.0455		x	0.0455			0.0455			0.0455
9b	**0.0001**			0.0434	**0.001**		0.0434	0.01	x	0.0434	**0.1**		0.0434	5		0.0434
10				0.0656			0.0655		x	0.0655			0.0655			0.0655
11				0.0731			0.0722		x	0.0722			0.0722			0.0722
12a			x	0.0310			0.0310			0.0310			0.0310			0.0310
12b				0.0253			0.0253			0.0253			0.0253			0.0253
13a				0.0209			0.0209			0.0209			0.0209			0.0209
13b				0.0195			0.0195			0.0195			0.0195		x	0.0195
14a				0.0412			0.0416		x	0.0416			0.0416			0.0416
14b				0.0339			0.0339		x	0.0339			0.0339		x	0.0339
15a				0.0428			0.0428		x	0.0428			0.0428			0.0428
15b				0.0426			0.0426			0.0426			0.0426			0.0426
16a				0.0868			0.0871		x	0.0871			0.0871			0.0871
17a				0.0428			0.0428			0.0428			0.0428		x	0.0428
17b			x	0.0403			0.0403			0.0403			0.0403			0.0403

Table B.13. Parametric analysis to define optimal values for $\sigma_{\text{init.}}$ and σ_0 for Bayesian analysis. Negative σ sensitivity is returned by varying $\sigma_{\text{init.}}$ and COV (α) minimization is based on Bayesian prior, σ_0.

	1 Substructure			σ_0 **(Prior) = 1**										
Test	$\sigma_{\text{init.}}$	$-\sigma$	α	$\sigma_{\text{init.}}$	$-\sigma$	α	$\sigma_{\text{init.}}$	$-\sigma$	α	$\sigma_{\text{init.}}$	$-\sigma$	α	$\sigma_{\text{init.}}$	$-\sigma$	α
1			0.0097			0.0097			0.0097			0.0097			0.0097
2a			0.0303			0.0303			0.0303			0.0303			0.0303
2b			0.0319		x	0.0314		x	0.0314			0.0314			0.0314
3			0.0742			0.0752		x	0.0752			0.0752			0.0752
4a			0.0228			0.0228			0.0228			0.0228		x	0.0228
4b			0.0986			0.0986			0.0986			0.0986			0.0986
5a		x	0.0110			0.0110			0.0110			0.0110			0.0110
5b			0.0177			0.0177			0.0177		x	0.0177			0.0177
6a			0.0392			0.0393		x	0.0393			0.0393			0.0393
6b			0.0748			0.0776		x	0.0776			0.0776			0.0776
7			0.1055			0.1046		x	0.1046			0.1046			0.1046
8			0.0184			0.0184			0.0184			0.0184			0.0184
9a			0.0504			0.0501		x	0.0501			0.0501			0.0501
9b	0.0001	x	0.0475	**0.001**		0.0473	0.01	x	0.0473	**0.1**		0.0473	**5**		0.0473
10			0.0860			0.0857		x	0.0857			0.0857			0.0857
11			0.1061			0.1036		x	0.1036			0.1036			0.1036
12a		x	0.0325			0.0325			0.0325			0.0325			0.0325
12b			0.0260			0.0260			0.0260			0.0260			0.0260
13a			0.0213			0.0213			0.0213			0.0213			0.0213
13b		x	0.0199			0.0199			0.0199			0.0199		x	0.0199
14a			0.0451		x	0.0457		x	0.0457			0.0457			0.0457
14b			0.0350			0.0350			0.0350			0.0350		x	0.0350
15a			0.0474			0.0474		x	0.0474			0.0474			0.0474
15b			0.0467			0.0468			0.0468			0.0468			0.0468
16a			0.1507		x	0.1493		x	0.1493			0.1493			0.1493
17a			0.0466			0.0466			0.0466			0.0466		x	0.0466
17b		x	0.0439			0.0439			0.0439			0.0439			0.0439

Appendix B.2.1. SS Substructure

Table B.14. Parametric analysis to define optimal values for $\sigma_{\text{init.}}$ and σ_0 for Bayesian analysis. Negative σ sensitivity is returned by varying $\sigma_{\text{init.}}$ and COV (α) minimization is based on Bayesian prior, σ_0.

3 Substructures σ_0 **(Prior) = 0.0001**

Test	$\sigma_{\text{init.}}$	$-\sigma$	α			$\sigma_{\text{init.}}$	$-\sigma$	α			$\sigma_{\text{init.}}$	$-\sigma$	α		
SS	0.0001	x	0.0001	0.0001	0.0001	**0.001**		0.0001	0.0001	0.0001	**0.01**		0.0001	0.0001	0.0001
SS	**0.1**		0.0001	0.0001	0.0001	5	x	0.0001	0.0001	0.0001					

3 Substructures σ_0 **(Prior) = 0.001**

Test	$\sigma_{\text{init.}}$	$-\sigma$	α			$\sigma_{\text{init.}}$	$-\sigma$	α			$\sigma_{\text{init.}}$	$-\sigma$	α		
SS	0.0001	x	0.0010	0.0010	0.0010	**0.001**		0.0010	0.0010	0.0010	**0.01**		0.0010	0.0010	0.0010
SS	**0.1**		0.0010	0.0010	0.0010	5	x	0.0010	0.0010	0.0010					

3 Substructures σ_0 **(Prior) = 0.01**

Test	$\sigma_{\text{init.}}$	$-\sigma$	α			$\sigma_{\text{init.}}$	$-\sigma$	α			$\sigma_{\text{init.}}$	$-\sigma$	α		
SS	0.0001	x	0.0090	0.0055	0.0090	**0.001**		0.0090	0.0055	0.0090	**0.01**		0.0090	0.0055	0.0090
SS	**0.1**		0.0090	0.0055	0.0090	5	x	0.0090	0.0055	0.0090					

3 Substructures σ_0 **(Prior) = 0.1**

Test	$\sigma_{\text{init.}}$	$-\sigma$	α			$\sigma_{\text{init.}}$	$-\sigma$	α			$\sigma_{\text{init.}}$	$-\sigma$	α		
SS	0.0001	x	0.0308	0.0207	0.0320	**0.001**		0.0308	0.0207	0.0320	**0.01**		0.0308	0.0207	0.0320
SS	**0.1**		0.0308	0.0207	0.0320	5	x	0.0308	0.0207	0.0320					

3 Substructures σ_0 **(Prior) = 1**

Test	$\sigma_{\text{init.}}$	$-\sigma$	α			$\sigma_{\text{init.}}$	$-\sigma$	α			$\sigma_{\text{init.}}$	$-\sigma$	α		
SS	0.0001	x	0.0335	0.0229	0.0349	**0.001**		0.0335	0.0229	0.0349	**0.01**		0.0335	0.0229	0.0349
SS	**0.1**		0.0335	0.0229	0.0349	5	x	0.0335	0.0229	0.0349					

Table B.15. Parametric analysis to define optimal values for $\sigma_{\text{init.}}$ and σ_0 for Bayesian analysis. Negative σ sensitivity is returned by varying $\sigma_{\text{init.}}$ and COV (α) minimization is based on Bayesian prior, σ_0.

3 Substructures σ_0 **(Prior) = 0.0001**

Test	$\sigma_{\text{init.}}$	$-\sigma$	α			$\sigma_{\text{init.}}$	$-\sigma$	α			$\sigma_{\text{init.}}$	$-\sigma$	α		
SO	**0.0001**		0.0001	0.0001	0.0001	**0.001**		0.0001	0.0001	0.0001	0.01	x	0.0001	0.0001	0.0001
SO	**0.1**		0.0001	0.0001	0.0001	**5**		0.0001	0.0001	0.0001					

3 Substructures σ_0 **(Prior) = 0.001**

Test	$\sigma_{\text{init.}}$	$-\sigma$	α			$\sigma_{\text{init.}}$	$-\sigma$	α			$\sigma_{\text{init.}}$	$-\sigma$	α		
SO	**0.0001**		0.0010	0.0010	0.0010	**0.001**		0.0010	0.0010	0.0010	0.01	x	0.0010	0.0010	0.0010
SO	**0.1**		0.0010	0.0010	0.0010	**5**		0.0010	0.0010	0.0010					

3 Substructures σ_0 **(Prior) = 0.01**

Test	$\sigma_{\text{init.}}$	$-\sigma$	α			$\sigma_{\text{init.}}$	$-\sigma$	α			$\sigma_{\text{init.}}$	$-\sigma$	α		
SO	**0.0001**		0.0097	0.0063	0.0092	**0.001**		0.0097	0.0064	0.0092	0.01	x	0.0097	0.0064	0.0092
SO	**0.1**		0.0097	0.0064	0.0092	**5**		0.0097	0.0064	0.0092					

3 Substructures σ_0 **(Prior) = 0.1**

Test	$\sigma_{\text{init.}}$	$-\sigma$	α			$\sigma_{\text{init.}}$	$-\sigma$	α			$\sigma_{\text{init.}}$	$-\sigma$	α		
SO	**0.0001**		0.0542	0.0234	0.0389	**0.001**		0.0551	0.0238	0.0396	0.01	x	0.0551	0.0238	0.0396
SO	**0.1**		0.0551	0.0238	0.0396	**5**		0.0551	0.0238	0.0396					

3 Substructures σ_0 **(Prior) = 1**

Test	$\sigma_{\text{init.}}$	$-\sigma$	α			$\sigma_{\text{init.}}$	$-\sigma$	α			$\sigma_{\text{init.}}$	$-\sigma$	α		
SO	**0.0001**		0.0696	0.0289	0.0471	**0.001**		0.0715	0.0297	0.0484	0.01	x	0.0715	0.0297	0.0484
SO	**0.1**		0.0715	0.0297	0.0484	**5**		0.0715	0.0297	0.0484					

Table B.16. Parametric analysis to define optimal values for $\sigma_{\text{init.}}$ and σ_0 for Bayesian analysis. Negative σ sensitivity is returned by varying $\sigma_{\text{init.}}$ and COV (α) minimization is based on Bayesian prior, σ_0.

3 Substructures σ_0 **(Prior) = 0.0001**

Test	$\sigma_{\text{init.}}$	$-\sigma$	α			$\sigma_{\text{init.}}$	$-\sigma$	α			$\sigma_{\text{init.}}$	$-\sigma$	α		
1 MSA	**0.0001**		0.0001	0.0001	0.0001	0.001		0.0001	0.0001	0.0001	0.01	x	0.0001	0.0001	0.0001
1 MSA	**0.1**		0.0001	0.0001	0.0001	**5**		0.0001	0.0001	0.0001					

3 Substructures σ_0 **(Prior) = 0.001**

Test	$\sigma_{\text{init.}}$	$-\sigma$	α			$\sigma_{\text{init.}}$	$-\sigma$	α			$\sigma_{\text{init.}}$	$-\sigma$	α		
1 MSA	**0.0001**		0.0010	0.0010	0.0010	0.001	x	0.0010	0.0010	0.0010	0.01	x	0.0010	0.0010	0.0010
1 MSA	**0.1**		0.0010	0.0010	0.0010	**5**		0.0010	0.0010	0.0010					

3 Substructures σ_0 **(Prior) = 0.01**

Test	$\sigma_{\text{init.}}$	$-\sigma$	α			$\sigma_{\text{init.}}$	$-\sigma$	α			$\sigma_{\text{init.}}$	$-\sigma$	α		
1 MSA	**0.0001**		0.0097	0.0086	0.0098	0.001		0.0097	0.0085	0.0098	0.01	x	0.0097	0.0085	0.0098
1 MSA	**0.1**		0.0097	0.0085	0.0098	**5**		0.0097	0.0085	0.0098					

3 Substructures σ_0 **(Prior) = 0.1**

Test	$\sigma_{\text{init.}}$	$-\sigma$	α			$\sigma_{\text{init.}}$	$-\sigma$	α			$\sigma_{\text{init.}}$	$-\sigma$	α		
1 MSA	**0.0001**		0.0656	0.0433	0.0765	0.001		0.0656	0.0433	0.0765	0.01	x	0.0656	0.0433	0.0765
1 MSA	**0.1**		0.0656	0.0433	0.0765	**5**		0.0656	0.0433	0.0765					

3 Substructures σ_0 **(Prior) = 1**

Test	$\sigma_{\text{init.}}$	$-\sigma$	α			$\sigma_{\text{init.}}$	$-\sigma$	α			$\sigma_{\text{init.}}$	$-\sigma$	α		
1 MSA	**0.0001**		0.1055	0.0941	0.1360	0.001		0.1055	0.0941	0.1360	0.01	x	0.1055	0.0941	0.1360
1 MSA	**0.1**		0.1055	0.0941	0.1360	**5**		0.1055	0.0941	0.1360					

Table B.17. Parametric analysis to define optimal values for $\sigma_{\text{init.}}$ and σ_0 for Bayesian analysis. Negative σ sensitivity is returned by varying $\sigma_{\text{init.}}$ and COV (α) minimization is based on Bayesian prior, σ_0.

3 Substructures σ_0 **(Prior) = 0.0001**

Test	$\sigma_{\text{init.}}$	$-\sigma$	α			$\sigma_{\text{init.}}$	$-\sigma$	α			$\sigma_{\text{init.}}$	$-\sigma$	α		
10 MSA	**0.0001**		0.0001	0.0001	0.0001	**0.001**		0.0001	0.0001	0.0001	**0.01**		0.0001	0.0001	0.0001
10 MSA	**0.1**		0.0001	0.0001	0.0001	5	x	0.0001	0.0001	0.0001					

3 Substructures σ_0 **(Prior) = 0.001**

Test	$\sigma_{\text{init.}}$	$-\sigma$	α			$\sigma_{\text{init.}}$	$-\sigma$	α			$\sigma_{\text{init.}}$	$-\sigma$	α		
10 MSA	**0.0001**		0.0010	0.0010	0.0010	**0.001**		0.0010	0.0010	0.0010	**0.01**		0.0010	0.0010	0.0010
10 MSA	**0.1**		0.0010	0.0010	0.0010	5	x	0.0010	0.0010	0.0010					

3 Substructures σ_0 **(Prior) = 0.01**

Test	$\sigma_{\text{init.}}$	$-\sigma$	α			$\sigma_{\text{init.}}$	$-\sigma$	α			$\sigma_{\text{init.}}$	$-\sigma$	α		
10 MSA	**0.0001**		0.0090	0.0093	0.0100	**0.001**		0.0090	0.0093	0.0100	**0.01**		0.0090	0.0093	0.0100
10 MSA	**0.1**		0.0090	0.0093	0.0100	5	x	0.0090	0.0093	0.0100					

3 Substructures σ_0 **(Prior) = 0.1**

Test	$\sigma_{\text{init.}}$	$-\sigma$	α			$\sigma_{\text{init.}}$	$-\sigma$	α			$\sigma_{\text{init.}}$	$-\sigma$	α		
10 MSA	**0.0001**		0.0400	0.0460	0.0913	**0.001**		0.0399	0.0460	0.0913	**0.01**		0.0399	0.0460	0.0913
10 MSA	**0.1**		0.0399	0.0460	0.0913	5	x	0.0399	0.0460	0.0913					

3 Substructures σ_0 **(Prior) = 1**

Test	$\sigma_{\text{init.}}$	$-\sigma$	α			$\sigma_{\text{init.}}$	$-\sigma$	α			$\sigma_{\text{init.}}$	$-\sigma$	α		
10 MSA	**0.0001**		0.0544	0.0899	0.2340	**0.001**		0.0544	0.0899	0.2340	**0.01**		0.0544	0.0899	0.2340
10 MSA	**0.1**		0.0544	0.0899	0.2340	5	x	0.0544	0.0899	0.2340					

Table B.18. Parametric analysis to define optimal values for $\sigma_{\text{init.}}$ and σ_0 for Bayesian analysis. Negative σ sensitivity is returned by varying $\sigma_{\text{init.}}$ and COV (α) minimization is based on Bayesian prior, σ_0.

3 Substructures σ_0 **(Prior) = 0.0001**

Test	$\sigma_{\text{init.}}$	$-\sigma$	α			$\sigma_{\text{init.}}$	$-\sigma$	α			$\sigma_{\text{init.}}$	$-\sigma$	α		
15 MSA	**0.0001**		0.0001	0.0001	0.0001	**0.001**		0.0001	0.0001	0.0001	**0.01**		0.0001	0.0001	0.0001
15 MSA	**0.1**		0.0001	0.0001	0.0001	5	x	0.0001	0.0001	0.0001					

3 Substructures σ_0 **(Prior) = 0.001**

Test	$\sigma_{\text{init.}}$	$-\sigma$	α			$\sigma_{\text{init.}}$	$-\sigma$	α			$\sigma_{\text{init.}}$	$-\sigma$	α		
15 MSA	**0.0001**		0.0010	0.0010	0.0010	**0.001**		0.0010	0.0010	0.0010	**0.01**		0.0010	0.0010	0.0010
15 MSA	**0.1**		0.0010	0.0010	0.0010	5	x	0.0010	0.0010	0.0010					

3 Substructures σ_0 **(Prior) = 0.01**

Test	$\sigma_{\text{init.}}$	$-\sigma$	α			$\sigma_{\text{init.}}$	$-\sigma$	α			$\sigma_{\text{init.}}$	$-\sigma$	α		
15 MSA	**0.0001**		0.0100	0.0092	0.0088	**0.001**		0.0100	0.0092	0.0088	**0.01**		0.0100	0.0092	0.0088
15 MSA	**0.1**		0.0100	0.0092	0.0088	5	x	0.0100	0.0092	0.0088					

3 Substructures σ_0 **(Prior) = 0.1**

Test	$\sigma_{\text{init.}}$	$-\sigma$	α			$\sigma_{\text{init.}}$	$-\sigma$	α			$\sigma_{\text{init.}}$	$-\sigma$	α		
15 MSA	**0.0001**		0.1029	0.0424	0.0315	**0.001**		0.1029	0.0424	0.0315	**0.01**		0.1029	0.0424	0.0315
15 MSA	**0.1**		0.1029	0.0424	0.0315	5	x	0.1029	0.0424	0.0315					

3 Substructures σ_0 **(Prior) = 1**

Test	$\sigma_{\text{init.}}$	$-\sigma$	α			$\sigma_{\text{init.}}$	$-\sigma$	α			$\sigma_{\text{init.}}$	$-\sigma$	α		
15 MSA	**0.0001**		4.5927	0.0701	0.0423	**0.001**		4.5952	0.0701	0.0422	**0.01**		4.5949	0.0701	0.0422
15 MSA	**0.1**		4.5947	0.0701	0.0422	5	x	4.5948	0.0701	0.0422					

Table B.19. Parametric analysis to define optimal values for $\sigma_{\text{init.}}$ and σ_0 for Bayesian analysis. Negative σ sensitivity is returned by varying $\sigma_{\text{init.}}$ and COV (α) minimization is based on Bayesian prior, σ_0.

	3 Substructure					σ_0 **(Prior) = 0.0001**									
Test	$\sigma_{\text{init.}}$	$-\sigma$		α		$\sigma_{\text{init.}}$	$-\sigma$		α		$\sigma_{\text{init.}}$	$-\sigma$		α	
1			0.0001	0.0001	0.0001			0.0001	0.0001	0.0001			0.0001	0.0001	0.0001
2a			0.0001	0.0001	0.0001		x	0.0001	0.0001	0.0001		x	0.0001	0.0001	0.0001
2b			0.0001	0.0001	0.0001		x	0.0001	0.0001	0.0001		x	0.0001	0.0001	0.0001
3			0.0001	0.0001	0.0001		x	0.0001	0.0001	0.0001		x	0.0001	0.0001	0.0001
4a		x	0.0001	0.0001	0.0001			0.0001	0.0001	0.0001			0.0001	0.0001	0.0001
4b			0.0001	0.0001	0.0001			0.0001	0.0001	0.0001		x	0.0001	0.0001	0.0001
5a			0.0001	0.0001	0.0001			0.0001	0.0001	0.0001			0.0001	0.0001	0.0001
5b			0.0001	0.0001	0.0001			0.0001	0.0001	0.0001			0.0001	0.0001	0.0001
6a			0.0001	0.0001	0.0001			0.0001	0.0001	0.0001			0.0001	0.0001	0.0001
6b			0.0001	0.0001	0.0001			0.0001	0.0001	0.0001		x	0.0001	0.0001	0.0001
7			0.0001	0.0001	0.0001			0.0001	0.0001	0.0001		x	0.0001	0.0001	0.0001
8		x	0.0001	0.0001	0.0001			0.0001	0.0001	0.0001		x	0.0001	0.0001	0.0001
9a			0.0001	0.0001	0.0001			0.0001	0.0001	0.0001		x	0.0001	0.0001	0.0001
9b	**0.0001**		0.0001	0.0001	0.0001	0.001		0.0001	0.0001	0.0001	0.01	x	0.0001	0.0001	0.0001
10			0.0001	0.0001	0.0001			0.0001	0.0001	0.0001		x	0.0001	0.0001	0.0001
11			0.0001	0.0001	0.0001			0.0001	0.0001	0.0001		x	0.0001	0.0001	0.0001
12a			0.0001	0.0001	0.0001			0.0001	0.0001	0.0001			0.0001	0.0001	0.0001
12b			0.0001	0.0001	0.0001			0.0001	0.0001	0.0001			0.0001	0.0001	0.0001
13a			0.0001	0.0001	0.0001			0.0001	0.0001	0.0001		x	0.0001	0.0001	0.0001
13b			0.0001	0.0001	0.0001			0.0001	0.0001	0.0001		x	0.0001	0.0001	0.0001
14a			0.0001	0.0001	0.0001			0.0001	0.0001	0.0001		x	0.0001	0.0001	0.0001
14b			0.0001	0.0001	0.0001			0.0001	0.0001	0.0001		x	0.0001	0.0001	0.0001
15a			0.0001	0.0001	0.0001			0.0001	0.0001	0.0001		x	0.0001	0.0001	0.0001
15b			0.0001	0.0001	0.0001			0.0001	0.0001	0.0001			0.0001	0.0001	0.0001
16a			0.0001	0.0001	0.0001			0.0001	0.0001	0.0001		x	0.0001	0.0001	0.0001
17a			0.0001	0.0001	0.0001			0.0001	0.0001	0.0001			0.0001	0.0001	0.0001
17b			0.0001	0.0001	0.0001			0.0001	0.0001	0.0001			0.0001	0.0001	0.0001

3 Substructure σ_0 **(Prior) = 0.0001**

Test	$\sigma_{\text{init.}}$	$-\sigma$	α			$\sigma_{\text{init.}}$	$-\sigma$	α		
1			0.0001	0.0001	0.0001			0.0001	0.0001	0.0001
2a			0.0001	0.0001	0.0001			0.0001	0.0001	0.0001
2b			0.0001	0.0001	0.0001			0.0001	0.0001	0.0001
3			0.0001	0.0001	0.0001			0.0001	0.0001	0.0001
4a			0.0001	0.0001	0.0001		x	0.0001	0.0001	0.0001
4b			0.0001	0.0001	0.0001			0.0001	0.0001	0.0001
5a			0.0001	0.0001	0.0001			0.0001	0.0001	0.0001
5b		x	0.0001	0.0001	0.0001			0.0001	0.0001	0.0001
6a			0.0001	0.0001	0.0001			0.0001	0.0001	0.0001
6b			0.0001	0.0001	0.0001			0.0001	0.0001	0.0001
7			0.0001	0.0001	0.0001			0.0001	0.0001	0.0001
8			0.0001	0.0001	0.0001			0.0001	0.0001	0.0001
9a			0.0001	0.0001	0.0001			0.0001	0.0001	0.0001
9b	**0.1**		0.0001	0.0001	0.0001	**5**		0.0001	0.0001	0.0001
10			0.0001	0.0001	0.0001			0.0001	0.0001	0.0001
11			0.0001	0.0001	0.0001			0.0001	0.0001	0.0001
12a			0.0001	0.0001	0.0001			0.0001	0.0001	0.0001
12b			0.0001	0.0001	0.0001			0.0001	0.0001	0.0001
13a			0.0001	0.0001	0.0001			0.0001	0.0001	0.0001
13b			0.0001	0.0001	0.0001			0.0001	0.0001	0.0001
14a			0.0001	0.0001	0.0001			0.0001	0.0001	0.0001
14b			0.0001	0.0001	0.0001			0.0001	0.0001	0.0001
15a			0.0001	0.0001	0.0001			0.0001	0.0001	0.0001
15b			0.0001	0.0001	0.0001			0.0001	0.0001	0.0001
16a			0.0001	0.0001	0.0001			0.0001	0.0001	0.0001
17a			0.0001	0.0001	0.0001			0.0001	0.0001	0.0001
17b			0.0001	0.0001	0.0001			0.0001	0.0001	0.0001

Table B.20. Parametric analysis to define optimal values for $\sigma_{\text{init.}}$ and σ_0 for Bayesian analysis. Negative σ sensitivity is returned by varying $\sigma_{\text{init.}}$ and COV (α) minimization is based on Bayesian prior, σ_0.

	3 Substructure					σ_0 **(Prior) = 0.001**									
Test	$\sigma_{\text{init.}}$	$-\sigma$		α			$\sigma_{\text{init.}}$	$-\sigma$		α			$\sigma_{\text{init.}}$	$-\sigma$		α	
1			0.0010	0.0010	0.0010			0.0010	0.0010	0.0010			0.0010	0.0010	0.0010
2a			0.0010	0.0010	0.0010		x	0.0010	0.0010	0.0010		x	0.0010	0.0010	0.0010
2b			0.0010	0.0010	0.0010		x	0.0010	0.0010	0.0010		x	0.0010	0.0010	0.0010
3			0.0010	0.0010	0.0010		x	0.0010	0.0010	0.0010		x	0.0010	0.0010	0.0010
4a		x	0.0010	0.0010	0.0010			0.0010	0.0010	0.0010			0.0010	0.0010	0.0010
4b			0.0010	0.0010	0.0010			0.0010	0.0010	0.0010		x	0.0010	0.0010	0.0010
5a			0.0010	0.0010	0.0010			0.0010	0.0010	0.0010			0.0010	0.0010	0.0010
5b			0.0010	0.0010	0.0010			0.0010	0.0010	0.0010			0.0010	0.0010	0.0010
6a			0.0010	0.0010	0.0010			0.0010	0.0010	0.0010			0.0010	0.0010	0.0010
6b			0.0010	0.0010	0.0010			0.0010	0.0010	0.0010		x	0.0010	0.0010	0.0010
7			0.0010	0.0010	0.0010			0.0010	0.0010	0.0010		x	0.0010	0.0010	0.0010
8			0.0010	0.0010	0.0010			0.0010	0.0010	0.0010		x	0.0010	0.0010	0.0010
9a			0.0010	0.0010	0.0010		x	0.0010	0.0010	0.0010		x	0.0010	0.0010	0.0010
9b	**0.0001**		0.0010	0.0010	0.0010	0.001		0.0010	0.0010	0.0010	0.01	x	0.0010	0.0010	0.0010
10			0.0010	0.0010	0.0010			0.0010	0.0010	0.0010		x	0.0010	0.0010	0.0010
11			0.0010	0.0010	0.0010			0.0010	0.0010	0.0010		x	0.0010	0.0010	0.0010
12a			0.0010	0.0010	0.0010			0.0010	0.0010	0.0010			0.0010	0.0010	0.0010
12b			0.0010	0.0010	0.0010			0.0010	0.0010	0.0010			0.0010	0.0010	0.0010
13a			0.0010	0.0010	0.0010			0.0010	0.0010	0.0010		x	0.0010	0.0010	0.0010
13b			0.0010	0.0010	0.0010			0.0010	0.0010	0.0010		x	0.0010	0.0010	0.0010
14a			0.0010	0.0010	0.0010			0.0010	0.0010	0.0010		x	0.0010	0.0010	0.0010
14b			0.0010	0.0010	0.0010			0.0010	0.0010	0.0010		x	0.0010	0.0010	0.0010
15a			0.0010	0.0010	0.0010			0.0010	0.0010	0.0010		x	0.0010	0.0010	0.0010
15b			0.0010	0.0010	0.0010			0.0010	0.0010	0.0010			0.0010	0.0010	0.0010
16a			0.0010	0.0010	0.0010			0.0010	0.0010	0.0010		x	0.0010	0.0010	0.0010
17a			0.0010	0.0010	0.0010			0.0010	0.0010	0.0010			0.0010	0.0010	0.0010
17b			0.0010	0.0010	0.0010			0.0010	0.0010	0.0010			0.0010	0.0010	0.0010

3 Substructure σ_0 **(Prior) = 0.001**

Test	$\sigma_{\text{init.}}$	$-\sigma$	α			$\sigma_{\text{init.}}$	$-\sigma$	α		
1			0.001	0.001	0.001			0.001	0.001	0.001
2a			0.001	0.001	0.001			0.001	0.001	0.001
2b			0.001	0.001	0.001			0.001	0.001	0.001
3			0.001	0.001	0.001			0.001	0.001	0.001
4a			0.001	0.001	0.001		x	0.001	0.001	0.001
4b			0.001	0.001	0.001			0.001	0.001	0.001
5a			0.001	0.001	0.001			0.001	0.001	0.001
5b		x	0.001	0.001	0.001			0.001	0.001	0.001
6a			0.001	0.001	0.001			0.001	0.001	0.001
6b			0.001	0.001	0.001			0.001	0.001	0.001
7			0.001	0.001	0.001			0.001	0.001	0.001
8			0.001	0.001	0.001			0.001	0.001	0.001
9a			0.001	0.001	0.001			0.001	0.001	0.001
9b	**0.1**		0.001	0.001	0.001	**5**		0.001	0.001	0.001
10			0.001	0.001	0.001			0.001	0.001	0.001
11			0.001	0.001	0.001			0.001	0.001	0.001
12a			0.001	0.001	0.001			0.001	0.001	0.001
12b			0.001	0.001	0.001			0.001	0.001	0.001
13a			0.001	0.001	0.001			0.001	0.001	0.001
13b			0.001	0.001	0.001			0.001	0.001	0.001
14a			0.001	0.001	0.001			0.001	0.001	0.001
14b			0.001	0.001	0.001			0.001	0.001	0.001
15a			0.001	0.001	0.001			0.001	0.001	0.001
15b			0.001	0.001	0.001			0.001	0.001	0.001
16a			0.001	0.001	0.001			0.001	0.001	0.001
17a			0.001	0.001	0.001			0.001	0.001	0.001
17b			0.001	0.001	0.001			0.001	0.001	0.001

Table B.21. Parametric analysis to define optimal values for $\sigma_{\text{init.}}$ and σ_0 for Bayesian analysis. Negative σ sensitivity is returned by varying $\sigma_{\text{init.}}$ and COV (α) minimization is based on Bayesian prior, σ_0.

3 Substructure												σ_0 **(Prior) = 0.01**				
Test	$\sigma_{\text{init.}}$	$-\sigma$		α		$\sigma_{\text{init.}}$	$-\sigma$		α		$\sigma_{\text{init.}}$	$-\sigma$		α	
1			0.0098	0.0087	0.0098			0.0098	0.0087	0.0098			0.0098	0.0087	0.0098
2a			0.0100	0.0099	0.0100			0.0100	0.0099	0.0100		x	0.0100	0.0099	0.0100
2b			0.0100	0.0098	0.0100			0.0100	0.0098	0.0100		x	0.0100	0.0098	0.0100
3			0.0100	0.0100	0.0100		x	0.0100	0.0100	0.0100		x	0.0100	0.0100	0.0100
4a			0.0100	0.0098	0.0100			0.0100	0.0098	0.0100			0.0100	0.0098	0.0100
4b			0.0100	0.0100	0.0100			0.0100	0.0100	0.0100		x	0.0100	0.0100	0.0100
5a		x	0.0099	0.0095	0.0100			0.0099	0.0095	0.0100			0.0099	0.0095	0.0100
5b			0.0099	0.0095	0.0100			0.0099	0.0095	0.0100			0.0099	0.0095	0.0100
6a			0.0100	0.0099	0.0100			0.0100	0.0099	0.0100			0.0100	0.0099	0.0100
6b			0.0100	0.0100	0.0100			0.0100	0.0100	0.0100		x	0.0100	0.0100	0.0100
7			0.0100	0.0100	0.0100			0.0100	0.0100	0.0100		x	0.0100	0.0100	0.0100
8			0.0100	0.0100	0.0100			0.0100	0.0100	0.0100		x	0.0100	0.0100	0.0100
9a			0.0100	0.0100	0.0100			0.0100	0.0100	0.0100		x	0.0100	0.0100	0.0100
9b	0.0001		0.0100	0.0100	0.0100	0.001		0.0100	0.0100	0.0100	0.01	x	0.0100	0.0100	0.0100
10			0.0100	0.0100	0.0100			0.0100	0.0100	0.0100		x	0.0100	0.0100	0.0100
11			0.0100	0.0100	0.0100			0.0100	0.0100	0.0100		x	0.0100	0.0100	0.0100
12a		x	0.0100	0.0100	0.0100			0.0100	0.0100	0.0100			0.0100	0.0100	0.0100
12b			0.0100	0.0100	0.0100			0.0100	0.0100	0.0100			0.0100	0.0100	0.0100
13a			0.0100	0.0100	0.0100		x	0.0100	0.0100	0.0100		x	0.0100	0.0100	0.0100
13b			0.0100	0.0100	0.0100			0.0100	0.0100	0.0100		x	0.0100	0.0100	0.0100
14a			0.0100	0.0100	0.0099		x	0.0100	0.0100	0.0099		x	0.0100	0.0100	0.0099
14b		x	0.0100	0.0100	0.0100		x	0.0100	0.0100	0.0100		x	0.0100	0.0100	0.0100
15a			0.0100	0.0100	0.0099			0.0100	0.0100	0.0099		x	0.0100	0.0100	0.0099
15b			0.0100	0.0100	0.0100			0.0100	0.0100	0.0100			0.0100	0.0100	0.0100
16a			0.0100	0.0100	0.0100			0.0100	0.0100	0.0100		x	0.0100	0.0100	0.0100
17a			0.0100	0.0100	0.0100			0.0100	0.0100	0.0100			0.0100	0.0100	0.0100
17b		x	0.0100	0.0100	0.0100			0.0100	0.0100	0.0100			0.0100	0.0100	0.0100

3 Substructure σ_0 **(Prior) = 0.01**

Test	$\sigma_{\text{init.}}$	$-\sigma$	α			$\sigma_{\text{init.}}$	$-\sigma$	α		
1			0.0098	0.0087	0.0098			0.0098	0.0087	0.0098
2a			0.01	0.0099	0.01			0.01	0.0099	0.01
2b			0.01	0.0098	0.01			0.01	0.0098	0.01
3			0.01	0.01	0.01			0.01	0.01	0.01
4a			0.01	0.0098	0.01		x	0.01	0.0098	0.01
4b			0.01	0.01	0.01			0.01	0.01	0.01
5a			0.0099	0.0095	0.01			0.0099	0.0095	0.01
5b		x	0.0099	0.0095	0.01			0.0099	0.0095	0.01
6a			0.01	0.0099	0.01			0.01	0.0099	0.01
6b			0.01	0.01	0.01			0.01	0.01	0.01
7			0.01	0.01	0.01			0.01	0.01	0.01
8			0.01	0.01	0.01			0.01	0.01	0.01
9a			0.01	0.01	0.01			0.01	0.01	0.01
9b	**0.1**		0.01	0.01	0.01	**5**		0.01	0.01	0.01
10			0.01	0.01	0.01			0.01	0.01	0.01
11			0.01	0.01	0.01			0.01	0.01	0.01
12a			0.01	0.01	0.01			0.01	0.01	0.01
12b			0.01	0.01	0.01			0.01	0.01	0.01
13a			0.01	0.01	0.01			0.01	0.01	0.01
13b			0.01	0.01	0.01			0.01	0.01	0.01
14a			0.01	0.01	0.0099			0.01	0.01	0.0099
14b			0.01	0.01	0.01			0.01	0.01	0.01
15a			0.01	0.01	0.0099			0.01	0.01	0.0099
15b			0.01	0.01	0.01			0.01	0.01	0.01
16a			0.01	0.01	0.01			0.01	0.01	0.01
17a			0.01	0.01	0.01			0.01	0.01	0.01
17b			0.01	0.01	0.01			0.01	0.01	0.01

Table B.22. Parametric analysis to define optimal values for $\sigma_{\text{init.}}$ and σ_0 for Bayesian analysis. Negative σ sensitivity is returned by varying $\sigma_{\text{init.}}$ and COV (α) minimization is based on Bayesian prior, σ_0.

3 Substructure						σ_0 **(Prior) = 0.1**									
Test	$\sigma_{\text{init.}}$	$-\sigma$	α			$\sigma_{\text{init.}}$	$-\sigma$	α			$\sigma_{\text{init.}}$	$-\sigma$	α		
1			0.0691	0.0453	0.0665			0.0692	0.0453	0.0665			0.0692	0.0453	0.0665
2a			0.1084	0.0679	0.0846			0.1084	0.0679	0.0846		x	0.1084	0.0679	0.0846
2b			0.1026	0.0545	0.0846		x	0.1028	0.0543	0.0844		x	0.1028	0.0543	0.0844
3			0.1052	0.0871	0.0940			0.1052	0.0871	0.0940		x	0.1052	0.0871	0.0940
4a		x	0.1000	0.0487	0.0728			0.1000	0.0487	0.0728			0.1000	0.0487	0.0728
4b			0.1000	0.0983	0.0988			0.1000	0.0983	0.0988		x	0.1000	0.0983	0.0988
5a			0.0640	0.0453	0.0958		x	0.0640	0.0453	0.0958			0.0640	0.0453	0.0958
5b			0.0835	0.0478	0.0990			0.0835	0.0478	0.0990			0.0835	0.0478	0.0990
6a			0.0922	0.0600	0.0925			0.0922	0.0600	0.0925			0.0922	0.0600	0.0925
6b			0.0913	0.0779	0.1025			0.0914	0.0782	0.1024		x	0.0914	0.0782	0.1024
7			0.0930	0.0849	0.1000			0.0929	0.0847	0.1000		x	0.0929	0.0847	0.1000
8			0.0732	0.0839	0.0910			0.0732	0.0839	0.0910			0.0732	0.0839	0.0910
9a			0.1006	0.1044	0.1010			0.1006	0.1044	0.1010		x	0.1006	0.1044	0.1010
9b	0.0001		0.1035	0.0993	0.1006	**0.001**		0.1035	0.0993	0.1006	0.01	x	0.1035	0.0993	0.1006
10			0.0909	0.0956	0.1015			0.0910	0.0956	0.1015		x	0.0910	0.0956	0.1015
11			0.0880	0.0989	0.1000			0.0875	0.0989	0.1000		x	0.0875	0.0989	0.1000
12a		x	0.0993	0.0806	0.0933			0.0993	0.0806	0.0933			0.0993	0.0806	0.0933
12b			0.0985	0.0813	0.0869			0.0985	0.0813	0.0869			0.0985	0.0813	0.0869
13a			0.1047	0.0971	0.0613			0.1047	0.0971	0.0613		x	0.1047	0.0971	0.0613
13b			0.1037	0.0944	0.0652			0.1037	0.0944	0.0652			0.1037	0.0944	0.0652
14a			0.1002	0.0824	0.0698			0.1002	0.0823	0.0696		x	0.1002	0.0823	0.0696
14b		x	0.1150	0.1609	0.1154			0.1150	0.1609	0.1154		x	0.1150	0.1609	0.1154
15a			0.1026	0.0958	0.0602			0.1026	0.0958	0.0603		x	0.1026	0.0958	0.0603
15b			0.1017	0.1032	0.0716			0.1017	0.1032	0.0716			0.1017	0.1032	0.0716
16a			0.1000	0.1123	0.0967			0.1000	0.1124	0.0967		x	0.1000	0.1124	0.0967
17a			0.1110	0.0942	0.0952			0.1110	0.0942	0.0952			0.1110	0.0942	0.0952
17b		x	0.1023	0.0792	0.0941			0.1023	0.0792	0.0941			0.1023	0.0792	0.0941

	3 Substructure					σ_0 **(Prior) = 0.1**				
Test	$\sigma_{\text{init.}}$	$-\sigma$		α		$\sigma_{\text{init.}}$	$-\sigma$		α	
1			0.0692	0.0453	0.0665			0.0692	0.0453	0.0665
2a			0.1084	0.0679	0.0846			0.1084	0.0679	0.0846
2b			0.1028	0.0543	0.0844			0.1028	0.0543	0.0844
3			0.1052	0.0871	0.094			0.1052	0.0871	0.094
4a			0.1	0.0487	0.0728		x	0.1	0.0487	0.0728
4b			0.1	0.0983	0.0988			0.1	0.0983	0.0988
5a			0.064	0.0453	0.0958		x	0.064	0.0453	0.0958
5b		x	0.0835	0.0478	0.099			0.0835	0.0478	0.099
6a			0.0922	0.06	0.0925			0.0922	0.06	0.0925
6b			0.0914	0.0782	0.1024			0.0914	0.0782	0.1024
7			0.0929	0.0847	0.1			0.0929	0.0847	0.1
8			0.0732	0.0839	0.091			0.0732	0.0839	0.091
9a			0.1006	0.1044	0.101			0.1006	0.1044	0.101
9b	**0.1**		0.1035	0.0993	0.1006	**5**		0.1035	0.0993	0.1006
10			0.091	0.0956	0.1015			0.091	0.0956	0.1015
11			0.0875	0.0989	0.1			0.0875	0.0989	0.1
12a			0.0993	0.0806	0.0933			0.0993	0.0806	0.0933
12b			0.0985	0.0813	0.0869			0.0985	0.0813	0.0869
13a			0.1047	0.0971	0.0613			0.1047	0.0971	0.0613
13b			0.1037	0.0944	0.0652		x	0.1037	0.0944	0.0652
14a			0.1002	0.0823	0.0696			0.1002	0.0823	0.0696
14b			0.115	0.1609	0.1154			0.115	0.1609	0.1154
15a			0.1026	0.0958	0.0603			0.1026	0.0958	0.0603
15b			0.1017	0.1032	0.0716			0.1017	0.1032	0.0716
16a			0.1	0.1124	0.0967			0.1	0.1124	0.0967
17a			0.111	0.0942	0.0952		x	0.111	0.0942	0.0952
17b			0.1023	0.0792	0.0941			0.1023	0.0792	0.0941

Table B.23. Parametric analysis to define optimal values for $\sigma_{\text{init.}}$ and σ_0 for Bayesian analysis. Negative σ sensitivity is returned by varying $\sigma_{\text{init.}}$ and COV (α) minimization is based on Bayesian prior, σ_0.

	3 Substructure					σ_0 **(Prior) = 1**									
Test	$\sigma_{\text{init.}}$	$-\sigma$		α		$\sigma_{\text{init.}}$	$-\sigma$		α		$\sigma_{\text{init.}}$	$-\sigma$		α	
1			0.0955	0.1315	0.0899			0.0954	0.1313	0.0898			0.0954	0.1313	0.0898
2a			0.9181	0.2676	0.1499			0.9165	0.2670	0.1495		x	0.9165	0.2670	0.1495
2b			-0.6855	0.1398	0.2769			-0.6756	0.1387	0.2755		x	-0.6756	0.1387	0.2755
3			-0.2614	0.2272	0.1729			-0.2614	0.2272	0.1729		x	-0.2615	0.2272	0.1729
4a		x	1.0000	0.0848	0.1005		x	1.0000	0.0848	0.1005			1.0000	0.0848	0.1005
4b		x	1.0000	-3.9151	0.1395			1.0000	-3.9133	0.1395			1.0000	-3.9130	0.1395
5a			0.1004	0.0922	0.2600			0.1005	0.0922	0.2600			0.1005	0.0922	0.2600
5b			0.2387	0.1166	0.8311			0.2382	0.1164	0.8302			0.2382	0.1164	0.8302
6a			0.1638	0.4882	0.1174			0.1638	0.4882	0.1173		x	0.1638	0.4882	0.1173
6b			0.2939	0.2257	-0.4105			0.2938	0.2255	-0.4097		x	0.2938	0.2255	-0.4097
7			0.2097	0.6686	1.0000			0.2096	0.6687	1.0000		x	0.2096	0.6687	1.0000
8			0.1044	0.5388	0.1606			0.1043	0.5387	0.1605			0.1043	0.5387	0.1605
9a		x	0.2192	1.6206	0.2854			0.2201	1.6073	0.2865		x	0.2201	1.6073	0.2865
9b	0.0001		0.3172	0.4744	0.3600	**0.001**		0.3172	0.4744	0.3600	0.01	x	0.3172	0.4744	0.3600
10			0.3411	0.4790	4.4711			0.3393	0.4758	4.7003		x	0.3393	0.4758	4.7003
11			0.2005	-14.9811	1.0000			0.2030	-19.7647	1.0000		x	0.2030	-19.7729	1.0000
12a		x	0.2548	0.3923	0.2120			0.2548	0.3923	0.2120			0.2548	0.3923	0.2120
12b			0.1791	0.4494	0.1437			0.1791	0.4494	0.1436			0.1791	0.4494	0.1436
13a			0.2399	0.6599	0.0768			0.2399	0.6599	0.0768			0.2399	0.6599	0.0768
13b			0.2785	0.3653	0.0912			0.2784	0.3653	0.0912			0.2784	0.3653	0.0912
14a			1.0011	0.8556	0.1264			1.0009	0.8555	0.1263		x	1.0009	0.8555	0.1263
14b			8.5983	0.3168	0.1791			8.5886	0.3169	0.1792			8.5890	0.3169	0.1792
15a			9.4076	-0.6093	0.0525			9.5285	-0.6089	0.0524		x	9.5286	-0.6089	0.0524
15b			0.6057	2.1960	0.0979			0.6056	2.1967	0.0978			0.6056	2.1966	0.0978
16a			1.0000	-0.1252	0.0721			1.0000	-0.1253	0.0722		x	1.0000	-0.1253	0.0722
17a		x	-1.3442	0.2378	0.2568			-1.3444	0.2378	0.2568			-1.3444	0.2378	0.2568
17b		x	-2.6077	0.1835	0.5546			-2.6142	0.1836	0.5547			-2.6129	0.1836	0.5547

	3 Substructure					σ_0 **(Prior) = 1**				
Test	$\sigma_{\text{init.}}$	$-\sigma$		α		$\sigma_{\text{init.}}$	$-\sigma$		α	
1			0.0954	0.1313	0.0898			0.0954	0.1313	0.0898
2a		x	0.9165	0.267	0.1495			0.9165	0.267	0.1495
2b			-0.676	0.1387	0.2755			-0.676	0.1387	0.2755
3			-0.261	0.2272	0.1729			-0.261	0.2272	0.1729
4a			1	0.0848	0.1005		x	1	0.0848	0.1005
4b			1	-3.913	0.1395			1	-3.913	0.1395
5a			0.1005	0.0922	0.26		x	0.1005	0.0922	0.26
5b		x	0.2382	0.1164	0.8302			0.2382	0.1164	0.8302
6a			0.1638	0.4882	0.1173			0.1638	0.4882	0.1173
6b			0.2938	0.2255	-0.41			0.2938	0.2255	-0.41
7			0.2096	0.6687	1			0.2096	0.6687	1
8			0.1043	0.5387	0.1605			0.1043	0.5387	0.1605
9a			0.2201	1.6073	0.2865			0.2201	1.6073	0.2865
9b	**0.1**		0.3172	0.4744	0.36	**5**		0.3172	0.4744	0.36
10			0.3393	0.4758	4.7003			0.3393	0.4758	4.7002
11			0.203	-19.76	1			0.203	-19.77	1
12a			0.2548	0.3923	0.212			0.2548	0.3923	0.212
12b			0.1791	0.4494	0.1436			0.1791	0.4494	0.1436
13a			0.2399	0.6599	0.0768			0.2399	0.6599	0.0768
13b			0.2784	0.3653	0.0912		x	0.2784	0.3653	0.0912
14a			1.0009	0.8555	0.1263			1.0009	0.8555	0.1263
14b			8.5879	0.3169	0.1792		x	8.5878	0.3169	0.1792
15a			9.5282	-0.609	0.0524			9.528	-0.609	0.0524
15b			0.6056	2.1967	0.0978			0.6056	2.1967	0.0978
16a		x	1	-0.125	0.0722			1	-0.125	0.0722
17a			-1.344	0.2378	0.2568		x	-1.344	0.2378	0.2568
17b			-2.613	0.1836	0.5547			-2.613	0.1836	0.5547

Appendix B.3.1. SS

Table B.24. Parametric analysis to define optimal values for $\sigma_{\text{init.}}$ and σ_0 for Bayesian analysis. Negative σ sensitivity is returned by varying $\sigma_{\text{init.}}$ and COV (α) minimization is based on Bayesian prior, σ_0.

6 Substructures																	σ_0 **(Prior) = 0.0001**
Test	$\sigma_{\text{init.}}$	$-\sigma$	α						$\sigma_{\text{init.}}$	$-\sigma$	α						
SS	0.0001	x	0.0001	0.0001	0.0001	0.0001	0.0001	0.0001	**0.001**		0.0001	0.0001	0.0001	0.0001	0.0001	0.0001	
SS	**0.01**		0.0001	0.0001	0.0001	0.0001	0.0001	0.0001	**0.1**		0.0001	0.0001	0.0001	0.0001	0.0001	0.0001	
SS	5	x	0.0001	0.0001	0.0001	0.0001	0.0001	0.0001									

6 Substructures																	σ_0 **(Prior) = 0.001**
Test	$\sigma_{\text{init.}}$	$-\sigma$	α						$\sigma_{\text{init.}}$	$-\sigma$	α						
SS	0.0001	x	0.0010	0.0010	0.0010	0.0010	0.0010	0.0010	**0.001**		0.0010	0.0010	0.0010	0.0010	0.0010	0.0010	
SS	**0.01**		0.0010	0.0010	0.0010	0.0010	0.0010	0.0010	**0.1**		0.0010	0.0010	0.0010	0.0010	0.0010	0.0010	
SS	5	x	0.0010	0.0010	0.0010	0.0010	0.0010	0.0010									

6 Substructures																	σ_0 **(Prior) = 0.01**
Test	$\sigma_{\text{init.}}$	$-\sigma$	α						$\sigma_{\text{init.}}$	$-\sigma$	α						
SS	0.0001	x	0.0100	0.0090	0.0083	0.0084	0.0091	0.0100	**0.001**		0.0100	0.0090	0.0083	0.0084	0.0091	0.0100	
SS	**0.01**		0.0100	0.0090	0.0083	0.0084	0.0091	0.0100	**0.1**		0.0100	0.0090	0.0083	0.0084	0.0091	0.0100	
SS	5	x	0.0100	0.0090	0.0083	0.0084	0.0091	0.0100									

6 Substructures																	σ_0 **(Prior) = 0.1**
Test	$\sigma_{\text{init.}}$	$-\sigma$	α						$\sigma_{\text{init.}}$	$-\sigma$	α						
SS	0.0001	x	0.0918	0.0476	0.0597	0.0552	0.0513	0.0944	**0.001**		0.0918	0.0476	0.0597	0.0552	0.0513	0.0944	
SS	**0.01**		0.0918	0.0476	0.0597	0.0552	0.0513	0.0944	**0.1**		0.0918	0.0476	0.0597	0.0552	0.0513	0.0944	
SS	5	x	0.0918	0.0476	0.0597	0.0552	0.0513	0.0944									

6 Substructures																	σ_0 **(Prior) = 1**
Test	$\sigma_{\text{init.}}$	$-\sigma$	α						$\sigma_{\text{init.}}$	$-\sigma$	α						
SS	0.0001	x	0.3716	0.1021	0.1352	0.0977	0.1283	0.3214	**0.001**		0.3716	0.1021	0.1352	0.0977	0.1283	0.3215	
SS	**0.01**		0.3717	0.1021	0.1352	0.0977	0.1283	0.3215	**0.1**		0.3716	0.1021	0.1352	0.0977	0.1283	0.3215	
SS	5	x	0.3716	0.1021	0.1352	0.0977	0.1283	0.3215									

Table B.25. Parametric analysis to define optimal values for $\sigma_{\text{init.}}$ and σ_0 for Bayesian analysis. Negative σ sensitivity is returned by varying $\sigma_{\text{init.}}$ and COV (α) minimization is based on Bayesian prior, σ_0.

6 Substructures — σ_0 **(Prior) = 0.0001**

Test	$\sigma_{\text{init.}}$	$-\sigma$	α						$\sigma_{\text{init.}}$	$-\sigma$	α					
SO	**0.0001**		0.0001	0.0001	0.0001	0.0001	0.0001	0.0001	0.001		0.0001	0.0001	0.0001	0.0001	0.0001	0.0001
SO	0.01	x	0.0001	0.0001	0.0001	0.0001	0.0001	0.0001	**0.1**		0.0001	0.0001	0.0001	0.0001	0.0001	0.0001
SO	**5**		0.0001	0.0001	0.0001	0.0001	0.0001	0.0001								

6 Substructures — σ_0 **(Prior) = 0.001**

Test	$\sigma_{\text{init.}}$	$-\sigma$	α						$\sigma_{\text{init.}}$	$-\sigma$	α					
SO	**0.0001**		0.0010	0.0010	0.0010	0.0010	0.0010	0.0010	0.0010		0.0010	0.0010	0.0010	0.0010	0.0010	0.0010
SO	0.01	x	0.0010	0.0010	0.0010	0.0010	0.0010	0.0010	**0.1**		0.0010	0.0010	0.0010	0.0010	0.0010	0.0010
SO	**5**		0.0010	0.0010	0.0010	0.0010	0.0010	0.0010								

6 Substructures — σ_0 **(Prior) = 0.01**

Test	$\sigma_{\text{init.}}$	$-\sigma$	α						$\sigma_{\text{init.}}$	$-\sigma$	α					
SO	**0.0001**		0.0100	0.0098	0.0092	0.0083	0.0092	0.0100	0.001		0.0100	0.0098	0.0092	0.0083	0.0093	0.0100
SO	0.01	x	0.0100	0.0098	0.0092	0.0083	0.0093	0.0100	**0.1**		0.0100	0.0098	0.0092	0.0083	0.0093	0.0100
SO	**5**		0.0100	0.0098	0.0092	0.0083	0.0093	0.0100								

6 Substructures — σ_0 **(Prior) = 0.1**

Test	$\sigma_{\text{init.}}$	$-\sigma$	α						$\sigma_{\text{init.}}$	$-\sigma$	α					
SO	**0.0001**		0.0986	0.0747	0.0530	0.0538	0.0559	0.0949	0.001	x	0.0987	0.0751	0.0535	0.0543	0.0565	0.0951
SO	0.01	x	0.0987	0.0751	0.0535	0.0543	0.0565	0.0951	**0.1**		0.0987	0.0751	0.0535	0.0543	0.0565	0.0951
SO	**5**		0.0987	0.0751	0.0535	0.0543	0.0565	0.0951								

6 Substructures — σ_0 **(Prior) = 1**

Test	$\sigma_{\text{init.}}$	$-\sigma$	α						$\sigma_{\text{init.}}$	$-\sigma$	α					
SO	**0.0001**		0.4383	0.3210	0.1006	0.1253	0.1145	0.4056	0.001	x	0.4474	0.3253	0.1028	0.1279	0.1170	0.4132
SO	0.01	x	0.4474	0.3253	0.1028	0.1279	0.1170	0.4132	**0.1**		0.4474	0.3253	0.1028	0.1279	0.1170	0.4132
SO	**5**		0.4474	0.3253	0.1028	0.1279	0.1170	0.4132								

Table B.26. Parametric analysis to define optimal values for $\sigma_{\text{init.}}$ and σ_0 for Bayesian analysis. Negative σ sensitivity is returned by varying $\sigma_{\text{init.}}$ and COV (α) minimization is based on Bayesian prior, σ_0.

6 Substructures — σ_0 **(Prior) = 0.0001**

Test	$\sigma_{\text{init.}}$	$-\sigma$	α						$\sigma_{\text{init.}}$	$-\sigma$	α					
1 MSA	0.0001		0.0001	0.0001	0.0001	0.0001	0.0001	0.0001	**0.001**		0.0001	0.0001	0.0001	0.0001	0.0001	0.0001
1 MSA	0.01	x	0.0001	0.0001	0.0001	0.0001	0.0001	0.0001	**0.1**		0.0001	0.0001	0.0001	0.0001	0.0001	0.0001
1 MSA	**5**		0.0001	0.0001	0.0001	0.0001	0.0001	0.0001								

6 Substructures — σ_0 **(Prior) = 0.001**

Test	$\sigma_{\text{init.}}$	$-\sigma$	α						$\sigma_{\text{init.}}$	$-\sigma$	α					
1 MSA	0.0001		0.0010	0.0010	0.0010	0.0010	0.0010	0.0010	**0.001**		0.0010	0.0010	0.0010	0.0010	0.0010	0.0010
1 MSA	0.01	x	0.0010	0.0010	0.0010	0.0010	0.0010	0.0010	**0.1**		0.0010	0.0010	0.0010	0.0010	0.0010	0.0010
1 MSA	**5**		0.0010	0.0010	0.0010	0.0010	0.0010	0.0010								

6 Substructures — σ_0 **(Prior) = 0.01**

Test	$\sigma_{\text{init.}}$	$-\sigma$	α						$\sigma_{\text{init.}}$	$-\sigma$	α					
1 MSA	0.0001		0.0100	0.0098	0.0095	0.0096	0.0098	0.0100	**0.001**		0.0100	0.0098	0.0095	0.0096	0.0098	0.0100
1 MSA	0.01	x	0.0100	0.0098	0.0095	0.0096	0.0098	0.0100	**0.1**		0.0100	0.0098	0.0095	0.0096	0.0098	0.0100
1 MSA	**5**		0.0100	0.0098	0.0095	0.0096	0.0098	0.0100								

6 Substructures — σ_0 **(Prior) = 0.1**

Test	$\sigma_{\text{init.}}$	$-\sigma$	α						$\sigma_{\text{init.}}$	$-\sigma$	α					
1 MSA	0.0001		0.0978	0.0710	0.0689	0.0817	0.0814	0.0967	**0.001**		0.0978	0.0710	0.0689	0.0817	0.0814	0.0967
1 MSA	0.01	x	0.0978	0.0710	0.0689	0.0817	0.0814	0.0967	**0.1**		0.0978	0.0710	0.0689	0.0817	0.0814	0.0967
1 MSA	**5**		0.0978	0.0710	0.0689	0.0817	0.0814	0.0967								

6 Substructures — σ_0 **(Prior) = 1**

Test	$\sigma_{\text{init.}}$	$-\sigma$	α						$\sigma_{\text{init.}}$	$-\sigma$	α					
1 MSA	0.0001	x	0.7251	0.6797	0.1405	-0.5150	0.2056	0.5888	**0.001**		0.7239	0.6807	0.1403	-0.5133	0.2054	0.5890
1 MSA	0.01	x	0.7239	0.6807	0.1403	-0.5133	0.2054	0.5890	**0.1**		0.7239	0.6807	0.1403	-0.5133	0.2054	0.5890
1 MSA	**5**		0.7239	0.6807	0.1403	-0.5133	0.2054	0.5890								

Table B.27. Parametric analysis to define optimal values for $\sigma_{\text{init.}}$ and σ_0 for Bayesian analysis. Negative σ sensitivity is returned by varying $\sigma_{\text{init.}}$ and COV (α) minimization is based on Bayesian prior, σ_0.

6 Substructures — σ_0 **(Prior) = 0.0001**

Test	$\sigma_{\text{init.}}$	$-\sigma$	α						$\sigma_{\text{init.}}$	$-\sigma$	α					
10 MSA	**0.0001**		0.0001	0.0001	0.0001	0.0001	0.0001	0.0001	**0.001**		0.0001	0.0001	0.0001	0.0001	0.0001	0.0001
10 MSA	**0.01**		0.0001	0.0001	0.0001	0.0001	0.0001	0.0001	**0.1**		0.0001	0.0001	0.0001	0.0001	0.0001	0.0001
10 MSA	5	x	0.0001	0.0001	0.0001	0.0001	0.0001	0.0001								

6 Substructures — σ_0 **(Prior) = 0.001**

Test	$\sigma_{\text{init.}}$	$-\sigma$	α						$\sigma_{\text{init.}}$	$-\sigma$	α					
10 MSA	**0.0001**		0.0010	0.0010	0.0010	0.0010	0.0010	0.0010	**0.001**		0.0010	0.0010	0.0010	0.0010	0.0010	0.0010
10 MSA	**0.01**		0.0010	0.0010	0.0010	0.0010	0.0010	0.0010	**0.1**		0.0010	0.0010	0.0010	0.0010	0.0010	0.0010
10 MSA	5	x	0.0010	0.0010	0.0010	0.0010	0.0010	0.0010								

6 Substructures — σ_0 **(Prior) = 0.01**

Test	$\sigma_{\text{init.}}$	$-\sigma$	α						$\sigma_{\text{init.}}$	$-\sigma$	α					
10 MSA	**0.0001**		0.0100	0.0093	0.0097	0.0099	0.0100	0.0100	**0.001**		0.0100	0.0093	0.0097	0.0099	0.0100	0.0100
10 MSA	**0.01**		0.0100	0.0093	0.0097	0.0099	0.0100	0.0100	**0.1**		0.0100	0.0093	0.0097	0.0099	0.0100	0.0100
10 MSA	5	x	0.0100	0.0093	0.0097	0.0099	0.0100	0.0100								

6 Substructures — σ_0 **(Prior) = 0.1**

Test	$\sigma_{\text{init.}}$	$-\sigma$	α						$\sigma_{\text{init.}}$	$-\sigma$	α					
10 MSA	**0.0001**		0.0923	0.0542	0.0783	0.0794	0.0908	0.1000	**0.001**		0.0923	0.0542	0.0783	0.0794	0.0908	0.1000
10 MSA	**0.01**		0.0923	0.0542	0.0783	0.0794	0.0908	0.1000	**0.1**		0.0923	0.0542	0.0783	0.0794	0.0908	0.1000
10 MSA	5	x	0.0923	0.0542	0.0783	0.0794	0.0908	0.1000								

6 Substructures — σ_0 **(Prior) = 1**

Test	$\sigma_{\text{init.}}$	$-\sigma$	α						$\sigma_{\text{init.}}$	$-\sigma$	α					
10 MSA	**0.0001**		0.2608	0.2018	0.3206	0.4455	0.3681	1.0000	**0.001**		0.2608	0.2018	0.3205	0.4455	0.3680	1.0000
10 MSA	**0.01**		0.2608	0.2018	0.3206	0.4455	0.3681	1.0000	**0.1**		0.2608	0.2018	0.3206	0.4455	0.3681	1.0000
10 MSA	5	x	0.2608	0.2018	0.3206	0.4455	0.3681	1.0000								

Table B.28. Parametric analysis to define optimal values for $\sigma_{\text{init.}}$ and σ_0 for Bayesian analysis. Negative σ sensitivity is returned by varying $\sigma_{\text{init.}}$ and COV (α) minimization is based on Bayesian prior, σ_0.

6 Substructures — σ_0 **(Prior) = 0.0001**

Test	$\sigma_{\text{init.}}$	$-\sigma$	α						$\sigma_{\text{init.}}$	$-\sigma$	α					
15 MSA	0.0001		0.0001	0.0001	0.0001	0.0001	0.0001	0.0001	**0.001**		0.0001	0.0001	0.0001	0.0001	0.0001	0.0001
15 MSA	**0.01**		0.0001	0.0001	0.0001	0.0001	0.0001	0.0001	**0.1**		0.0001	0.0001	0.0001	0.0001	0.0001	0.0001
15 MSA	5		0.0001	0.0001	0.0001	0.0001	0.0001	0.0001								

6 Substructures — σ_0 **(Prior) = 0.001**

Test	$\sigma_{\text{init.}}$	$-\sigma$	α						$\sigma_{\text{init.}}$	$-\sigma$	α					
15 MSA	0.0001	x	0.0010	0.0010	0.0010	0.0010	0.0010	0.0010	**0.001**		0.0010	0.0010	0.0010	0.0010	0.0010	0.0010
15 MSA	**0.01**		0.0010	0.0010	0.0010	0.0010	0.0010	0.0010	**0.1**		0.0010	0.0010	0.0010	0.0010	0.0010	0.0010
15 MSA	5		0.0010	0.0010	0.0010	0.0010	0.0010	0.0010								

6 Substructures — σ_0 **(Prior) = 0.01**

Test	$\sigma_{\text{init.}}$	$-\sigma$	α						$\sigma_{\text{init.}}$	$-\sigma$	α					
15 MSA	0.0001		0.0100	0.0100	0.0099	0.0098	0.0094	0.0099	**0.001**		0.0100	0.0100	0.0099	0.0098	0.0094	0.0099
15 MSA	**0.01**		0.0100	0.0100	0.0099	0.0098	0.0094	0.0099	**0.1**		0.0100	0.0100	0.0099	0.0098	0.0094	0.0099
15 MSA	5		0.0100	0.0100	0.0099	0.0098	0.0094	0.0099								

6 Substructures — σ_0 **(Prior) = 0.1**

Test	$\sigma_{\text{init.}}$	$-\sigma$	α						$\sigma_{\text{init.}}$	$-\sigma$	α					
15 MSA	0.0001	x	0.1000	0.0988	0.0835	0.0679	0.0414	0.0907	**0.001**		0.1000	0.0988	0.0835	0.0679	0.0414	0.0907
15 MSA	**0.01**		0.1000	0.0988	0.0835	0.0679	0.0414	0.0907	**0.1**		0.1000	0.0988	0.0835	0.0679	0.0414	0.0907
15 MSA	5	x	0.1000	0.0988	0.0835	0.0679	0.0414	0.0907								

6 Substructures — σ_0 **(Prior) = 1**

Test	$\sigma_{\text{init.}}$	$-\sigma$	α						$\sigma_{\text{init.}}$	$-\sigma$	α					
15 MSA	0.0001	x	1.0000	0.3912	-8.1170	0.1970	0.1753	0.4723	**0.001**		1.0000	0.3912	-8.1096	0.1970	0.1753	0.4723
15 MSA	**0.01**		1.0000	0.3912	-8.1114	0.1970	0.1753	0.4723	**0.1**		1.0000	0.3912	-8.1115	0.1970	0.1753	0.4723
15 MSA	5	x	1.0000	0.3912	-8.1108	0.1970	0.1753	0.4723								

Table B.29. Parametric analysis to define optimal values for $\sigma_{\text{init.}}$ and σ_0 for Bayesian analysis. Negative σ sensitivity is returned by varying $\sigma_{\text{init.}}$ and COV (α) minimization is based on Bayesian prior, σ_0.

	6 Substructure								σ_0 **(Prior) = 0.0001**							
Test	$\sigma_{\text{init.}}$	$-\sigma$	α						$\sigma_{\text{init.}}$	$-\sigma$	α					
1			0.0001	0.0001	0.0001	0.0001	0.0001	0.0001			0.0001	0.0001	0.0001	0.0001	0.0001	0.0001
2a			0.0001	0.0001	0.0001	0.0001	0.0001	0.0001		x	0.0001	0.0001	0.0001	0.0001	0.0001	0.0001
2b			0.0001	0.0001	0.0001	0.0001	0.0001	0.0001		x	0.0001	0.0001	0.0001	0.0001	0.0001	0.0001
3			0.0001	0.0001	0.0001	0.0001	0.0001	0.0001		x	0.0001	0.0001	0.0001	0.0001	0.0001	0.0001
4a		x	0.0001	0.0001	0.0001	0.0001	0.0001	0.0001			0.0001	0.0001	0.0001	0.0001	0.0001	0.0001
4b			0.0001	0.0001	0.0001	0.0001	0.0001	0.0001			0.0001	0.0001	0.0001	0.0001	0.0001	0.0001
5a			0.0001	0.0001	0.0001	0.0001	0.0001	0.0001			0.0001	0.0001	0.0001	0.0001	0.0001	0.0001
5b			0.0001	0.0001	0.0001	0.0001	0.0001	0.0001			0.0001	0.0001	0.0001	0.0001	0.0001	0.0001
6a			0.0001	0.0001	0.0001	0.0001	0.0001	0.0001			0.0001	0.0001	0.0001	0.0001	0.0001	0.0001
6b			0.0001	0.0001	0.0001	0.0001	0.0001	0.0001			0.0001	0.0001	0.0001	0.0001	0.0001	0.0001
7			0.0001	0.0001	0.0001	0.0001	0.0001	0.0001			0.0001	0.0001	0.0001	0.0001	0.0001	0.0001
8		x	0.0001	0.0001	0.0001	0.0001	0.0001	0.0001			0.0001	0.0001	0.0001	0.0001	0.0001	0.0001
9a			0.0001	0.0001	0.0001	0.0001	0.0001	0.0001			0.0001	0.0001	0.0001	0.0001	0.0001	0.0001
9b	**0.0001**		0.0001	0.0001	0.0001	0.0001	0.0001	0.0001	0.001		0.0001	0.0001	0.0001	0.0001	0.0001	0.0001
10			0.0001	0.0001	0.0001	0.0001	0.0001	0.0001			0.0001	0.0001	0.0001	0.0001	0.0001	0.0001
11			0.0001	0.0001	0.0001	0.0001	0.0001	0.0001			0.0001	0.0001	0.0001	0.0001	0.0001	0.0001
12a			0.0001	0.0001	0.0001	0.0001	0.0001	0.0001			0.0001	0.0001	0.0001	0.0001	0.0001	0.0001
12b			0.0001	0.0001	0.0001	0.0001	0.0001	0.0001			0.0001	0.0001	0.0001	0.0001	0.0001	0.0001
13a			0.0001	0.0001	0.0001	0.0001	0.0001	0.0001			0.0001	0.0001	0.0001	0.0001	0.0001	0.0001
13b			0.0001	0.0001	0.0001	0.0001	0.0001	0.0001			0.0001	0.0001	0.0001	0.0001	0.0001	0.0001
14a			0.0001	0.0001	0.0001	0.0001	0.0001	0.0001			0.0001	0.0001	0.0001	0.0001	0.0001	0.0001
14b			0.0001	0.0001	0.0001	0.0001	0.0001	0.0001			0.0001	0.0001	0.0001	0.0001	0.0001	0.0001
15a			0.0001	0.0001	0.0001	0.0001	0.0001	0.0001			0.0001	0.0001	0.0001	0.0001	0.0001	0.0001
15b			0.0001	0.0001	0.0001	0.0001	0.0001	0.0001			0.0001	0.0001	0.0001	0.0001	0.0001	0.0001
16a			0.0001	0.0001	0.0001	0.0001	0.0001	0.0001			0.0001	0.0001	0.0001	0.0001	0.0001	0.0001
17a			0.0001	0.0001	0.0001	0.0001	0.0001	0.0001			0.0001	0.0001	0.0001	0.0001	0.0001	0.0001
17b			0.0001	0.0001	0.0001	0.0001	0.0001	0.0001			0.0001	0.0001	0.0001	0.0001	0.0001	0.0001

6 Substructure σ_0 **(Prior) = 0.0001**

Test	$\sigma_{\text{init.}}$	$-\sigma$	α						$\sigma_{\text{init.}}$	$-\sigma$	α					
1			0.0001	0.0001	0.0001	0.0001	0.0001	0.0001			0.0001	0.0001	0.0001	0.0001	0.0001	0.0001
2a		x	0.0001	0.0001	0.0001	0.0001	0.0001	0.0001			0.0001	0.0001	0.0001	0.0001	0.0001	0.0001
2b		x	0.0001	0.0001	0.0001	0.0001	0.0001	0.0001			0.0001	0.0001	0.0001	0.0001	0.0001	0.0001
3		x	0.0001	0.0001	0.0001	0.0001	0.0001	0.0001			0.0001	0.0001	0.0001	0.0001	0.0001	0.0001
4a			0.0001	0.0001	0.0001	0.0001	0.0001	0.0001			0.0001	0.0001	0.0001	0.0001	0.0001	0.0001
4b		x	0.0001	0.0001	0.0001	0.0001	0.0001	0.0001			0.0001	0.0001	0.0001	0.0001	0.0001	0.0001
5a			0.0001	0.0001	0.0001	0.0001	0.0001	0.0001			0.0001	0.0001	0.0001	0.0001	0.0001	0.0001
5b			0.0001	0.0001	0.0001	0.0001	0.0001	0.0001		x	0.0001	0.0001	0.0001	0.0001	0.0001	0.0001
6a			0.0001	0.0001	0.0001	0.0001	0.0001	0.0001			0.0001	0.0001	0.0001	0.0001	0.0001	0.0001
6b		x	0.0001	0.0001	0.0001	0.0001	0.0001	0.0001			0.0001	0.0001	0.0001	0.0001	0.0001	0.0001
7		x	0.0001	0.0001	0.0001	0.0001	0.0001	0.0001			0.0001	0.0001	0.0001	0.0001	0.0001	0.0001
8		x	0.0001	0.0001	0.0001	0.0001	0.0001	0.0001			0.0001	0.0001	0.0001	0.0001	0.0001	0.0001
9a		x	0.0001	0.0001	0.0001	0.0001	0.0001	0.0001			0.0001	0.0001	0.0001	0.0001	0.0001	0.0001
9b	0.01	x	0.0001	0.0001	0.0001	0.0001	0.0001	0.0001	**0.1**		0.0001	0.0001	0.0001	0.0001	0.0001	0.0001
10		x	0.0001	0.0001	0.0001	0.0001	0.0001	0.0001			0.0001	0.0001	0.0001	0.0001	0.0001	0.0001
11		x	0.0001	0.0001	0.0001	0.0001	0.0001	0.0001			0.0001	0.0001	0.0001	0.0001	0.0001	0.0001
12a			0.0001	0.0001	0.0001	0.0001	0.0001	0.0001			0.0001	0.0001	0.0001	0.0001	0.0001	0.0001
12b			0.0001	0.0001	0.0001	0.0001	0.0001	0.0001			0.0001	0.0001	0.0001	0.0001	0.0001	0.0001
13a		x	0.0001	0.0001	0.0001	0.0001	0.0001	0.0001			0.0001	0.0001	0.0001	0.0001	0.0001	0.0001
13b		x	0.0001	0.0001	0.0001	0.0001	0.0001	0.0001			0.0001	0.0001	0.0001	0.0001	0.0001	0.0001
14a		x	0.0001	0.0001	0.0001	0.0001	0.0001	0.0001			0.0001	0.0001	0.0001	0.0001	0.0001	0.0001
14b		x	0.0001	0.0001	0.0001	0.0001	0.0001	0.0001			0.0001	0.0001	0.0001	0.0001	0.0001	0.0001
15a		x	0.0001	0.0001	0.0001	0.0001	0.0001	0.0001			0.0001	0.0001	0.0001	0.0001	0.0001	0.0001
15b			0.0001	0.0001	0.0001	0.0001	0.0001	0.0001			0.0001	0.0001	0.0001	0.0001	0.0001	0.0001
16a		x	0.0001	0.0001	0.0001	0.0001	0.0001	0.0001			0.0001	0.0001	0.0001	0.0001	0.0001	0.0001
17a			0.0001	0.0001	0.0001	0.0001	0.0001	0.0001			0.0001	0.0001	0.0001	0.0001	0.0001	0.0001
17b			0.0001	0.0001	0.0001	0.0001	0.0001	0.0001			0.0001	0.0001	0.0001	0.0001	0.0001	0.0001

6 Substructure σ_0 **(Prior) = 0.0001**

Test	$\sigma_{\text{init.}}$	$-\sigma$	α					
1			0.0001	0.0001	0.0001	0.0001	0.0001	0.0001
2a			0.0001	0.0001	0.0001	0.0001	0.0001	0.0001
2b			0.0001	0.0001	0.0001	0.0001	0.0001	0.0001
3			0.0001	0.0001	0.0001	0.0001	0.0001	0.0001
4a		x	0.0001	0.0001	0.0001	0.0001	0.0001	0.0001
4b			0.0001	0.0001	0.0001	0.0001	0.0001	0.0001
5a			0.0001	0.0001	0.0001	0.0001	0.0001	0.0001
5b			0.0001	0.0001	0.0001	0.0001	0.0001	0.0001
6a			0.0001	0.0001	0.0001	0.0001	0.0001	0.0001
6b			0.0001	0.0001	0.0001	0.0001	0.0001	0.0001
7			0.0001	0.0001	0.0001	0.0001	0.0001	0.0001
8			0.0001	0.0001	0.0001	0.0001	0.0001	0.0001
9a			0.0001	0.0001	0.0001	0.0001	0.0001	0.0001
9b	**5**		0.0001	0.0001	0.0001	0.0001	0.0001	0.0001
10			0.0001	0.0001	0.0001	0.0001	0.0001	0.0001
11			0.0001	0.0001	0.0001	0.0001	0.0001	0.0001
12a			0.0001	0.0001	0.0001	0.0001	0.0001	0.0001
12b			0.0001	0.0001	0.0001	0.0001	0.0001	0.0001
13a			0.0001	0.0001	0.0001	0.0001	0.0001	0.0001
13b			0.0001	0.0001	0.0001	0.0001	0.0001	0.0001
14a			0.0001	0.0001	0.0001	0.0001	0.0001	0.0001
14b			0.0001	0.0001	0.0001	0.0001	0.0001	0.0001
15a			0.0001	0.0001	0.0001	0.0001	0.0001	0.0001
15b			0.0001	0.0001	0.0001	0.0001	0.0001	0.0001
16a			0.0001	0.0001	0.0001	0.0001	0.0001	0.0001
17a			0.0001	0.0001	0.0001	0.0001	0.0001	0.0001
17b			0.0001	0.0001	0.0001	0.0001	0.0001	0.0001

Table B.30. Parametric analysis to define optimal values for $\sigma_{\text{init.}}$ and σ_0 for Bayesian analysis. Negative σ sensitivity is returned by varying $\sigma_{\text{init.}}$ and COV (α) minimization is based on Bayesian prior, σ_0.

	6 Substructure								σ_0 **(Prior) = 0.001**							
Test	$\sigma_{\text{init.}}$	$-\sigma$	α						$\sigma_{\text{init.}}$	$-\sigma$	α					
1			0.0010	0.0010	0.0010	0.0010	0.0010	0.0010			0.0010	0.0010	0.0010	0.0010	0.0010	0.0010
2a			0.0010	0.0010	0.0010	0.0010	0.0010	0.0010		x	0.0010	0.0010	0.0010	0.0010	0.0010	0.0010
2b			0.0010	0.0010	0.0010	0.0010	0.0010	0.0010		x	0.0010	0.0010	0.0010	0.0010	0.0010	0.0010
3			0.0010	0.0010	0.0010	0.0010	0.0010	0.0010		x	0.0010	0.0010	0.0010	0.0010	0.0010	0.0010
4a		x	0.0010	0.0010	0.0010	0.0010	0.0010	0.0010			0.0010	0.0010	0.0010	0.0010	0.0010	0.0010
4b			0.0010	0.0010	0.0010	0.0010	0.0010	0.0010			0.0010	0.0010	0.0010	0.0010	0.0010	0.0010
5a			0.0010	0.0010	0.0010	0.0010	0.0010	0.0010			0.0010	0.0010	0.0010	0.0010	0.0010	0.0010
5b			0.0010	0.0010	0.0010	0.0010	0.0010	0.0010			0.0010	0.0010	0.0010	0.0010	0.0010	0.0010
6a			0.0010	0.0010	0.0010	0.0010	0.0010	0.0010			0.0010	0.0010	0.0010	0.0010	0.0010	0.0010
6b			0.0010	0.0010	0.0010	0.0010	0.0010	0.0010			0.0010	0.0010	0.0010	0.0010	0.0010	0.0010
7			0.0010	0.0010	0.0010	0.0010	0.0010	0.0010			0.0010	0.0010	0.0010	0.0010	0.0010	0.0010
8			0.0010	0.0010	0.0010	0.0010	0.0010	0.0010			0.0010	0.0010	0.0010	0.0010	0.0010	0.0010
9a			0.0010	0.0010	0.0010	0.0010	0.0010	0.0010		x	0.0010	0.0010	0.0010	0.0010	0.0010	0.0010
9b	**0.0001**		0.0010	0.0010	0.0010	0.0010	0.0010	0.0010	0.001		0.0010	0.0010	0.0010	0.0010	0.0010	0.0010
10			0.0010	0.0010	0.0010	0.0010	0.0010	0.0010			0.0010	0.0010	0.0010	0.0010	0.0010	0.0010
11			0.0010	0.0010	0.0010	0.0010	0.0010	0.0010			0.0010	0.0010	0.0010	0.0010	0.0010	0.0010
12a			0.0010	0.0010	0.0010	0.0010	0.0010	0.0010			0.0010	0.0010	0.0010	0.0010	0.0010	0.0010
12b			0.0010	0.0010	0.0010	0.0010	0.0010	0.0010			0.0010	0.0010	0.0010	0.0010	0.0010	0.0010
13a			0.0010	0.0010	0.0010	0.0010	0.0010	0.0010			0.0010	0.0010	0.0010	0.0010	0.0010	0.0010
13b			0.0010	0.0010	0.0010	0.0010	0.0010	0.0010			0.0010	0.0010	0.0010	0.0010	0.0010	0.0010
14a			0.0010	0.0010	0.0010	0.0010	0.0010	0.0010			0.0010	0.0010	0.0010	0.0010	0.0010	0.0010
14b			0.0010	0.0010	0.0010	0.0010	0.0010	0.0010			0.0010	0.0010	0.0010	0.0010	0.0010	0.0010
15a			0.0010	0.0010	0.0010	0.0010	0.0010	0.0010			0.0010	0.0010	0.0010	0.0010	0.0010	0.0010
15b			0.0010	0.0010	0.0010	0.0010	0.0010	0.0010			0.0010	0.0010	0.0010	0.0010	0.0010	0.0010
16a			0.0010	0.0010	0.0010	0.0010	0.0010	0.0010			0.0010	0.0010	0.0010	0.0010	0.0010	0.0010
17a			0.0010	0.0010	0.0010	0.0010	0.0010	0.0010			0.0010	0.0010	0.0010	0.0010	0.0010	0.0010
17b			0.0010	0.0010	0.0010	0.0010	0.0010	0.0010			0.0010	0.0010	0.0010	0.0010	0.0010	0.0010

6 Substructure σ_0 **(Prior) = 0.001**

Test	$\sigma_{\text{init.}}$	$-\sigma$	α						$\sigma_{\text{init.}}$	$-\sigma$	α					
1			0.0010	0.0010	0.0010	0.0010	0.0010	0.0010			0.0010	0.0010	0.0010	0.0010	0.0010	0.0010
2a		x	0.0010	0.0010	0.0010	0.0010	0.0010	0.0010			0.0010	0.0010	0.0010	0.0010	0.0010	0.0010
2b		x	0.0010	0.0010	0.0010	0.0010	0.0010	0.0010			0.0010	0.0010	0.0010	0.0010	0.0010	0.0010
3		x	0.0010	0.0010	0.0010	0.0010	0.0010	0.0010			0.0010	0.0010	0.0010	0.0010	0.0010	0.0010
4a			0.0010	0.0010	0.0010	0.0010	0.0010	0.0010			0.0010	0.0010	0.0010	0.0010	0.0010	0.0010
4b		x	0.0010	0.0010	0.0010	0.0010	0.0010	0.0010			0.0010	0.0010	0.0010	0.0010	0.0010	0.0010
5a			0.0010	0.0010	0.0010	0.0010	0.0010	0.0010			0.0010	0.0010	0.0010	0.0010	0.0010	0.0010
5b			0.0010	0.0010	0.0010	0.0010	0.0010	0.0010		x	0.0010	0.0010	0.0010	0.0010	0.0010	0.0010
6a			0.0010	0.0010	0.0010	0.0010	0.0010	0.0010			0.0010	0.0010	0.0010	0.0010	0.0010	0.0010
6b		x	0.0010	0.0010	0.0010	0.0010	0.0010	0.0010			0.0010	0.0010	0.0010	0.0010	0.0010	0.0010
7		x	0.0010	0.0010	0.0010	0.0010	0.0010	0.0010			0.0010	0.0010	0.0010	0.0010	0.0010	0.0010
8		x	0.0010	0.0010	0.0010	0.0010	0.0010	0.0010			0.0010	0.0010	0.0010	0.0010	0.0010	0.0010
9a		x	0.0010	0.0010	0.0010	0.0010	0.0010	0.0010			0.0010	0.0010	0.0010	0.0010	0.0010	0.0010
9b	0.01	x	0.0010	0.0010	0.0010	0.0010	0.0010	0.0010	**0.1**		0.0010	0.0010	0.0010	0.0010	0.0010	0.0010
10		x	0.0010	0.0010	0.0010	0.0010	0.0010	0.0010			0.0010	0.0010	0.0010	0.0010	0.0010	0.0010
11		x	0.0010	0.0010	0.0010	0.0010	0.0010	0.0010			0.0010	0.0010	0.0010	0.0010	0.0010	0.0010
12a			0.0010	0.0010	0.0010	0.0010	0.0010	0.0010			0.0010	0.0010	0.0010	0.0010	0.0010	0.0010
12b			0.0010	0.0010	0.0010	0.0010	0.0010	0.0010			0.0010	0.0010	0.0010	0.0010	0.0010	0.0010
13a		x	0.0010	0.0010	0.0010	0.0010	0.0010	0.0010			0.0010	0.0010	0.0010	0.0010	0.0010	0.0010
13b		x	0.0010	0.0010	0.0010	0.0010	0.0010	0.0010			0.0010	0.0010	0.0010	0.0010	0.0010	0.0010
14a		x	0.0010	0.0010	0.0010	0.0010	0.0010	0.0010			0.0010	0.0010	0.0010	0.0010	0.0010	0.0010
14b		x	0.0010	0.0010	0.0010	0.0010	0.0010	0.0010			0.0010	0.0010	0.0010	0.0010	0.0010	0.0010
15a		x	0.0010	0.0010	0.0010	0.0010	0.0010	0.0010			0.0010	0.0010	0.0010	0.0010	0.0010	0.0010
15b			0.0010	0.0010	0.0010	0.0010	0.0010	0.0010			0.0010	0.0010	0.0010	0.0010	0.0010	0.0010
16a		x	0.0010	0.0010	0.0010	0.0010	0.0010	0.0010			0.0010	0.0010	0.0010	0.0010	0.0010	0.0010
17a			0.0010	0.0010	0.0010	0.0010	0.0010	0.0010			0.0010	0.0010	0.0010	0.0010	0.0010	0.0010
17b			0.0010	0.0010	0.0010	0.0010	0.0010	0.0010			0.0010	0.0010	0.0010	0.0010	0.0010	0.0010

6 Substructure σ_0 **(Prior) = 0.001**

Test	$\sigma_{\text{init.}}$	$-\sigma$	α					
1			0.0010	0.0010	0.0010	0.0010	0.0010	0.0010
2a			0.0010	0.0010	0.0010	0.0010	0.0010	0.0010
2b			0.0010	0.0010	0.0010	0.0010	0.0010	0.0010
3			0.0010	0.0010	0.0010	0.0010	0.0010	0.0010
4a		x	0.0010	0.0010	0.0010	0.0010	0.0010	0.0010
4b			0.0010	0.0010	0.0010	0.0010	0.0010	0.0010
5a			0.0010	0.0010	0.0010	0.0010	0.0010	0.0010
5b			0.0010	0.0010	0.0010	0.0010	0.0010	0.0010
6a			0.0010	0.0010	0.0010	0.0010	0.0010	0.0010
6b			0.0010	0.0010	0.0010	0.0010	0.0010	0.0010
7			0.0010	0.0010	0.0010	0.0010	0.0010	0.0010
8			0.0010	0.0010	0.0010	0.0010	0.0010	0.0010
9a			0.0010	0.0010	0.0010	0.0010	0.0010	0.0010
9b	**5**		0.0010	0.0010	0.0010	0.0010	0.0010	0.0010
10			0.0010	0.0010	0.0010	0.0010	0.0010	0.0010
11			0.0010	0.0010	0.0010	0.0010	0.0010	0.0010
12a			0.0010	0.0010	0.0010	0.0010	0.0010	0.0010
12b			0.0010	0.0010	0.0010	0.0010	0.0010	0.0010
13a			0.0010	0.0010	0.0010	0.0010	0.0010	0.0010
13b			0.0010	0.0010	0.0010	0.0010	0.0010	0.0010
14a			0.0010	0.0010	0.0010	0.0010	0.0010	0.0010
14b			0.0010	0.0010	0.0010	0.0010	0.0010	0.0010
15a			0.0010	0.0010	0.0010	0.0010	0.0010	0.0010
15b			0.0010	0.0010	0.0010	0.0010	0.0010	0.0010
16a			0.0010	0.0010	0.0010	0.0010	0.0010	0.0010
17a			0.0010	0.0010	0.0010	0.0010	0.0010	0.0010
17b			0.0010	0.0010	0.0010	0.0010	0.0010	0.0010

Table B.31. Parametric analysis to define optimal values for $\sigma_{\text{init.}}$ and σ_0 for Bayesian analysis. Negative σ sensitivity is returned by varying $\sigma_{\text{init.}}$ and COV (α) minimization is based on Bayesian prior, σ_0.

6 Substructure									σ_0 **(Prior) = 0.01**							
Test	$\sigma_{\text{init.}}$	$-\sigma$	α						$\sigma_{\text{init.}}$	$-\sigma$	α					
1			0.0100	0.0098	0.0096	0.0096	0.0098	0.0100			0.0100	0.0098	0.0096	0.0096	0.0098	0.0100
2a			0.0100	0.0100	0.0100	0.0100	0.0100	0.0100			0.0100	0.0100	0.0100	0.0100	0.0100	0.0100
2b			0.0100	0.0100	0.0100	0.0099	0.0100	0.0100		x	0.0100	0.0100	0.0100	0.0099	0.0100	0.0100
3			0.0100	0.0100	0.0100	0.0100	0.0100	0.0100		x	0.0100	0.0100	0.0100	0.0100	0.0100	0.0100
4a			0.0100	0.0100	0.0100	0.0100	0.0100	0.0100			0.0100	0.0100	0.0100	0.0100	0.0100	0.0100
4b			0.0100	0.0100	0.0100	0.0100	0.0100	0.0100			0.0100	0.0100	0.0100	0.0100	0.0100	0.0100
5a		x	0.0100	0.0100	0.0099	0.0100	0.0100	0.0100			0.0100	0.0100	0.0099	0.0100	0.0100	0.0100
5b			0.0100	0.0099	0.0099	0.0099	0.0100	0.0100			0.0100	0.0099	0.0099	0.0099	0.0100	0.0100
6a			0.0100	0.0100	0.0100	0.0100	0.0100	0.0100			0.0100	0.0100	0.0100	0.0100	0.0100	0.0100
6b			0.0100	0.0100	0.0100	0.0100	0.0100	0.0100			0.0100	0.0100	0.0100	0.0100	0.0100	0.0100
7			0.0100	0.0100	0.0100	0.0100	0.0100	0.0100			0.0100	0.0100	0.0100	0.0100	0.0100	0.0100
8			0.0100	0.0100	0.0100	0.0100	0.0100	0.0100			0.0100	0.0100	0.0100	0.0100	0.0100	0.0100
9a			0.0100	0.0100	0.0100	0.0100	0.0100	0.0100			0.0100	0.0100	0.0100	0.0100	0.0100	0.0100
9b	0.0001		0.0100	0.0100	0.0100	0.0100	0.0100	0.0100	0.001		0.0100	0.0100	0.0100	0.0100	0.0100	0.0100
10			0.0100	0.0100	0.0100	0.0100	0.0100	0.0100			0.0100	0.0100	0.0100	0.0100	0.0100	0.0100
11			0.0100	0.0100	0.0100	0.0100	0.0100	0.0100			0.0100	0.0100	0.0100	0.0100	0.0100	0.0100
12a			0.0100	0.0100	0.0100	0.0100	0.0100	0.0100			0.0100	0.0100	0.0100	0.0100	0.0100	0.0100
12b			0.0100	0.0100	0.0100	0.0100	0.0100	0.0100			0.0100	0.0100	0.0100	0.0100	0.0100	0.0100
13a			0.0100	0.0100	0.0100	0.0100	0.0100	0.0100			0.0100	0.0100	0.0100	0.0100	0.0100	0.0100
13b			0.0100	0.0100	0.0100	0.0100	0.0100	0.0100			0.0100	0.0100	0.0100	0.0100	0.0100	0.0100
14a			0.0100	0.0100	0.0100	0.0100	0.0100	0.0100			0.0100	0.0100	0.0100	0.0100	0.0100	0.0100
14b			0.0100	0.0100	0.0100	0.0100	0.0100	0.0100			0.0100	0.0100	0.0100	0.0100	0.0100	0.0100
15a			0.0100	0.0100	0.0100	0.0100	0.0099	0.0100			0.0100	0.0100	0.0100	0.0100	0.0099	0.0100
15b			0.0100	0.0100	0.0100	0.0100	0.0100	0.0100			0.0100	0.0100	0.0100	0.0100	0.0100	0.0100
16a			0.0100	0.0100	0.0100	0.0100	0.0100	0.0100			0.0100	0.0100	0.0100	0.0100	0.0100	0.0100
17a			0.0100	0.0100	0.0100	0.0100	0.0100	0.0100			0.0100	0.0100	0.0100	0.0100	0.0100	0.0100
17b		x	0.0100	0.0100	0.0100	0.0100	0.0100	0.0100			0.0100	0.0100	0.0100	0.0100	0.0100	0.0100

6 Substructure σ_0 **(Prior) = 0.01**

Test	$\sigma_{\text{init.}}$	$-\sigma$	α						$\sigma_{\text{init.}}$	$-\sigma$	α					
1			0.0100	0.0098	0.0096	0.0096	0.0098	0.0100			0.0100	0.0098	0.0096	0.0096	0.0098	0.0100
2a		x	0.0100	0.0100	0.0100	0.0100	0.0100	0.0100			0.0100	0.0100	0.0100	0.0100	0.0100	0.0100
2b		x	0.0100	0.0100	0.0100	0.0099	0.0100	0.0100			0.0100	0.0100	0.0100	0.0099	0.0100	0.0100
3		x	0.0100	0.0100	0.0100	0.0100	0.0100	0.0100			0.0100	0.0100	0.0100	0.0100	0.0100	0.0100
4a			0.0100	0.0100	0.0100	0.0100	0.0100	0.0100			0.0100	0.0100	0.0100	0.0100	0.0100	0.0100
4b		x	0.0100	0.0100	0.0100	0.0100	0.0100	0.0100			0.0100	0.0100	0.0100	0.0100	0.0100	0.0100
5a			0.0100	0.0100	0.0099	0.0100	0.0100	0.0100			0.0100	0.0100	0.0099	0.0100	0.0100	0.0100
5b			0.0100	0.0099	0.0099	0.0099	0.0100	0.0100		x	0.0100	0.0099	0.0099	0.0099	0.0100	0.0100
6a			0.0100	0.0100	0.0100	0.0100	0.0100	0.0100			0.0100	0.0100	0.0100	0.0100	0.0100	0.0100
6b		x	0.0100	0.0100	0.0100	0.0100	0.0100	0.0100			0.0100	0.0100	0.0100	0.0100	0.0100	0.0100
7		x	0.0100	0.0100	0.0100	0.0100	0.0100	0.0100			0.0100	0.0100	0.0100	0.0100	0.0100	0.0100
8		x	0.0100	0.0100	0.0100	0.0100	0.0100	0.0100			0.0100	0.0100	0.0100	0.0100	0.0100	0.0100
9a		x	0.0100	0.0100	0.0100	0.0100	0.0100	0.0100			0.0100	0.0100	0.0100	0.0100	0.0100	0.0100
9b	0.01	x	0.0100	0.0100	0.0100	0.0100	0.0100	0.0100	**0.1**		0.0100	0.0100	0.0100	0.0100	0.0100	0.0100
10		x	0.0100	0.0100	0.0100	0.0100	0.0100	0.0100			0.0100	0.0100	0.0100	0.0100	0.0100	0.0100
11		x	0.0100	0.0100	0.0100	0.0100	0.0100	0.0100			0.0100	0.0100	0.0100	0.0100	0.0100	0.0100
12a			0.0100	0.0100	0.0100	0.0100	0.0100	0.0100			0.0100	0.0100	0.0100	0.0100	0.0100	0.0100
12b			0.0100	0.0100	0.0100	0.0100	0.0100	0.0100			0.0100	0.0100	0.0100	0.0100	0.0100	0.0100
13a		x	0.0100	0.0100	0.0100	0.0100	0.0100	0.0100			0.0100	0.0100	0.0100	0.0100	0.0100	0.0100
13b			0.0100	0.0100	0.0100	0.0100	0.0100	0.0100			0.0100	0.0100	0.0100	0.0100	0.0100	0.0100
14a		x	0.0100	0.0100	0.0100	0.0100	0.0100	0.0100			0.0100	0.0100	0.0100	0.0100	0.0100	0.0100
14b		x	0.0100	0.0100	0.0100	0.0100	0.0100	0.0100			0.0100	0.0100	0.0100	0.0100	0.0100	0.0100
15a		x	0.0100	0.0100	0.0100	0.0100	0.0099	0.0100			0.0100	0.0100	0.0100	0.0100	0.0099	0.0100
15b			0.0100	0.0100	0.0100	0.0100	0.0100	0.0100			0.0100	0.0100	0.0100	0.0100	0.0100	0.0100
16a		x	0.0100	0.0100	0.0100	0.0100	0.0100	0.0100			0.0100	0.0100	0.0100	0.0100	0.0100	0.0100
17a			0.0100	0.0100	0.0100	0.0100	0.0100	0.0100			0.0100	0.0100	0.0100	0.0100	0.0100	0.0100
17b			0.0100	0.0100	0.0100	0.0100	0.0100	0.0100			0.0100	0.0100	0.0100	0.0100	0.0100	0.0100

6 Substructure						σ_0 **(Prior) = 0.01**		
Test	$\sigma_{\text{init.}}$	$-\sigma$			α			
1			0.0100	0.0098	0.0096	0.0096	0.0098	0.0100
2a			0.0100	0.0100	0.0100	0.0100	0.0100	0.0100
2b			0.0100	0.0100	0.0100	0.0099	0.0100	0.0100
3			0.0100	0.0100	0.0100	0.0100	0.0100	0.0100
4a		x	0.0100	0.0100	0.0100	0.0100	0.0100	0.0100
4b			0.0100	0.0100	0.0100	0.0100	0.0100	0.0100
5a			0.0100	0.0100	0.0099	0.0100	0.0100	0.0100
5b			0.0100	0.0099	0.0099	0.0099	0.0100	0.0100
6a			0.0100	0.0100	0.0100	0.0100	0.0100	0.0100
6b			0.0100	0.0100	0.0100	0.0100	0.0100	0.0100
7			0.0100	0.0100	0.0100	0.0100	0.0100	0.0100
8			0.0100	0.0100	0.0100	0.0100	0.0100	0.0100
9a			0.0100	0.0100	0.0100	0.0100	0.0100	0.0100
9b	**5**		0.0100	0.0100	0.0100	0.0100	0.0100	0.0100
10			0.0100	0.0100	0.0100	0.0100	0.0100	0.0100
11			0.0100	0.0100	0.0100	0.0100	0.0100	0.0100
12a			0.0100	0.0100	0.0100	0.0100	0.0100	0.0100
12b			0.0100	0.0100	0.0100	0.0100	0.0100	0.0100
13a			0.0100	0.0100	0.0100	0.0100	0.0100	0.0100
13b			0.0100	0.0100	0.0100	0.0100	0.0100	0.0100
14a			0.0100	0.0100	0.0100	0.0100	0.0100	0.0100
14b			0.0100	0.0100	0.0100	0.0100	0.0100	0.0100
15a			0.0100	0.0100	0.0100	0.0100	0.0099	0.0100
15b			0.0100	0.0100	0.0100	0.0100	0.0100	0.0100
16a			0.0100	0.0100	0.0100	0.0100	0.0100	0.0100
17a			0.0100	0.0100	0.0100	0.0100	0.0100	0.0100
17b			0.0100	0.0100	0.0100	0.0100	0.0100	0.0100

Table B.32. Parametric analysis to define optimal values for $\sigma_{\text{init.}}$ and σ_0 for Bayesian analysis. Negative σ sensitivity is returned by varying $\sigma_{\text{init.}}$ and COV (α) minimization is based on Bayesian prior, σ_0.

6 Substructure									σ_0 **(Prior) = 0.1**							
Test	$\sigma_{\text{init.}}$	$-\sigma$	α						$\sigma_{\text{init.}}$	$-\sigma$	α					
1			0.0931	0.0763	0.0781	0.0760	0.0731	0.0950			0.0931	0.0763	0.0781	0.0760	0.0731	0.0950
2a			0.0999	0.1118	0.1106	0.0960	0.0918	0.0990			0.0999	0.1118	0.1106	0.0960	0.0918	0.0990
2b			0.1011	0.1001	0.0850	0.0790	0.0855	0.0981			0.1011	0.1002	0.0849	0.0789	0.0853	0.0981
3			0.1000	0.1055	0.1085	0.0991	0.0977	0.0999			0.1000	0.1055	0.1085	0.0991	0.0977	0.0999
4a			0.1000	0.1000	0.1045	0.0814	0.0822	0.0988			0.1000	0.1000	0.1045	0.0814	0.0822	0.0988
4b			0.1000	0.1000	0.1111	0.1065	0.1026	0.1006			0.1000	0.1000	0.1111	0.1065	0.1026	0.1006
5a			0.0942	0.0758	0.0829	0.0892	0.0985	0.1015			0.0942	0.0758	0.0829	0.0892	0.0986	0.1015
5b			0.0987	0.0876	0.0820	0.0834	0.0978	0.1018			0.0987	0.0876	0.0820	0.0834	0.0978	0.1018
6a			0.0993	0.0928	0.0857	0.0855	0.0921	0.1000			0.0993	0.0928	0.0857	0.0855	0.0921	0.1000
6b			0.0990	0.0924	0.0895	0.0952	0.1023	0.1000			0.0990	0.0925	0.0896	0.0952	0.1022	0.1000
7			0.0993	0.0938	0.0916	0.0982	0.1000	0.1000			0.0993	0.0938	0.0916	0.0982	0.1000	0.1000
8			0.1012	0.0860	0.1096	0.1065	0.0990	0.0983			0.1012	0.0860	0.1096	0.1065	0.0990	0.0983
9a			0.1031	0.1128	0.1189	0.1078	0.1029	0.1001			0.1031	0.1128	0.1188	0.1078	0.1029	0.1001
9b	**0.0001**		0.1045	0.1148	0.1169	0.1056	0.1023	0.1002	**0.001**	x	0.1045	0.1148	0.1169	0.1056	0.1023	0.1002
10			0.1002	0.0951	0.1004	0.1009	0.1016	0.1000			0.1002	0.0952	0.1004	0.1009	0.1016	0.1000
11			0.0989	0.0924	0.1004	0.1010	0.1000	0.1000			0.0988	0.0921	0.1005	0.1011	0.1000	0.1000
12a		x	0.1015	0.1025	0.1090	0.1007	0.0980	0.1000			0.1015	0.1025	0.1090	0.1007	0.0980	0.1000
12b			0.0986	0.1062	0.1227	0.0969	0.0929	0.0998			0.0986	0.1062	0.1227	0.0969	0.0929	0.0998
13a		x	0.1025	0.1105	0.1199	0.1118	0.0815	0.0944			0.1025	0.1105	0.1199	0.1118	0.0815	0.0944
13b			0.1020	0.1109	0.1205	0.1128	0.0872	0.0979			0.1020	0.1109	0.1205	0.1128	0.0872	0.0979
14a			0.1003	0.0995	0.0963	0.0902	0.0759	0.0937			0.1003	0.0995	0.0963	0.0903	0.0761	0.0938
14b			0.1005	0.1194	0.1467	0.1674	0.1948	0.1196			0.1005	0.1194	0.1467	0.1674	0.1948	0.1196
15a			0.1000	0.1024	0.1049	0.0958	0.0716	0.0907			0.1000	0.1024	0.1049	0.0958	0.0716	0.0907
15b			0.1000	0.1020	0.1083	0.1068	0.0865	0.0976			0.1000	0.1020	0.1083	0.1068	0.0865	0.0976
16a			0.1000	0.1000	0.1054	0.1088	0.1027	0.1011		x	0.1000	0.1000	0.1054	0.1088	0.1027	0.1011
17a		x	0.1023	0.1123	0.1126	0.1068	0.1012	0.1009			0.1023	0.1123	0.1126	0.1068	0.1012	0.1009
17b			0.1010	0.1033	0.1007	0.0954	0.0944	0.1026			0.1010	0.1033	0.1007	0.0954	0.0944	0.1026

6 Substructure σ_0 **(Prior) = 0.1**

Test	$\sigma_{\text{init.}}$	$-\sigma$	α						$\sigma_{\text{init.}}$	$-\sigma$	α					
1			0.0931	0.0763	0.0781	0.0760	0.0731	0.0950			0.0931	0.0763	0.0781	0.0760	0.0731	0.0950
2a		x	0.0999	0.1118	0.1106	0.0960	0.0918	0.0990			0.0999	0.1118	0.1106	0.0960	0.0918	0.0990
2b		x	0.1011	0.1002	0.0849	0.0789	0.0853	0.0981			0.1011	0.1002	0.0849	0.0789	0.0853	0.0981
3		x	0.1000	0.1055	0.1086	0.0991	0.0977	0.0999			0.1000	0.1055	0.1086	0.0991	0.0977	0.0999
4a			0.1000	0.1000	0.1045	0.0814	0.0822	0.0988			0.1000	0.1000	0.1045	0.0814	0.0822	0.0988
4b		x	0.1000	0.1000	0.1111	0.1065	0.1026	0.1006		x	0.1000	0.1000	0.1111	0.1065	0.1026	0.1006
5a			0.0942	0.0758	0.0829	0.0892	0.0985	0.1015			0.0942	0.0758	0.0829	0.0892	0.0985	0.1015
5b			0.0987	0.0876	0.0820	0.0834	0.0978	0.1018		x	0.0987	0.0876	0.0820	0.0834	0.0978	0.1018
6a			0.0993	0.0928	0.0857	0.0855	0.0921	0.1000			0.0993	0.0928	0.0857	0.0855	0.0921	0.1000
6b		x	0.0990	0.0925	0.0896	0.0952	0.1022	0.1000			0.0990	0.0925	0.0896	0.0952	0.1022	0.1000
7		x	0.0993	0.0938	0.0916	0.0982	0.1000	0.1000			0.0993	0.0938	0.0916	0.0982	0.1000	0.1000
8		x	0.1012	0.0860	0.1096	0.1065	0.0990	0.0983			0.1012	0.0860	0.1096	0.1065	0.0990	0.0983
9a		x	0.1031	0.1128	0.1188	0.1078	0.1029	0.1001			0.1031	0.1128	0.1188	0.1078	0.1029	0.1001
9b	0.01	x	0.1045	0.1148	0.1169	0.1056	0.1023	0.1002	**0.1**		0.1045	0.1148	0.1169	0.1056	0.1023	0.1002
10		x	0.1002	0.0952	0.1004	0.1009	0.1016	0.1000			0.1002	0.0952	0.1004	0.1009	0.1016	0.1000
11		x	0.0988	0.0921	0.1005	0.1011	0.1000	0.1000			0.0988	0.0921	0.1005	0.1011	0.1000	0.1000
12a			0.1015	0.1025	0.1090	0.1007	0.0980	0.1000			0.1015	0.1025	0.1090	0.1007	0.0980	0.1000
12b			0.0986	0.1062	0.1227	0.0969	0.0929	0.0998			0.0986	0.1062	0.1227	0.0969	0.0929	0.0998
13a		x	0.1025	0.1105	0.1199	0.1118	0.0815	0.0944			0.1025	0.1105	0.1199	0.1118	0.0815	0.0944
13b		x	0.1020	0.1109	0.1205	0.1128	0.0872	0.0979			0.1020	0.1109	0.1205	0.1128	0.0872	0.0979
14a		x	0.1003	0.0995	0.0963	0.0903	0.0761	0.0938			0.1003	0.0995	0.0963	0.0903	0.0761	0.0938
14b			0.1005	0.1194	0.1467	0.1674	0.1948	0.1196			0.1005	0.1194	0.1467	0.1674	0.1948	0.1196
15a		x	0.1000	0.1024	0.1049	0.0958	0.0716	0.0907			0.1000	0.1024	0.1049	0.0958	0.0716	0.0907
15b			0.1000	0.1020	0.1083	0.1068	0.0865	0.0976			0.1000	0.1020	0.1083	0.1068	0.0865	0.0976
16a		x	0.1000	0.1000	0.1054	0.1088	0.1027	0.1011			0.1000	0.1000	0.1054	0.1088	0.1027	0.1011
17a			0.1023	0.1123	0.1126	0.1068	0.1012	0.1009			0.1023	0.1123	0.1126	0.1068	0.1012	0.1009
17b			0.1010	0.1033	0.1007	0.0954	0.0944	0.1026			0.1010	0.1033	0.1007	0.0954	0.0944	0.1026

6 Substructure σ_0 **(Prior) = 0.1**

Test	$\sigma_{\text{init.}}$	$-\sigma$	α					
1			0.0931	0.0763	0.0781	0.0760	0.0731	0.0950
2a			0.0999	0.1118	0.1106	0.0960	0.0918	0.0990
2b			0.1011	0.1002	0.0849	0.0789	0.0853	0.0981
3			0.1000	0.1055	0.1086	0.0991	0.0977	0.0999
4a		x	0.1000	0.1000	0.1045	0.0814	0.0822	0.0988
4b			0.1000	0.1000	0.1111	0.1065	0.1026	0.1006
5a		x	0.0942	0.0758	0.0829	0.0892	0.0985	0.1015
5b			0.0987	0.0876	0.0820	0.0834	0.0978	0.1018
6a			0.0993	0.0928	0.0857	0.0855	0.0921	0.1000
6b			0.0990	0.0925	0.0896	0.0952	0.1022	0.1000
7			0.0993	0.0938	0.0916	0.0982	0.1000	0.1000
8			0.1012	0.0860	0.1096	0.1065	0.0990	0.0983
9a			0.1031	0.1128	0.1188	0.1078	0.1029	0.1001
9b	5		0.1045	0.1148	0.1169	0.1056	0.1023	0.1002
10			0.1002	0.0952	0.1004	0.1009	0.1016	0.1000
11			0.0988	0.0921	0.1005	0.1011	0.1000	0.1000
12a			0.1015	0.1025	0.1090	0.1007	0.0980	0.1000
12b			0.0986	0.1062	0.1227	0.0969	0.0929	0.0998
13a			0.1025	0.1105	0.1199	0.1118	0.0815	0.0944
13b		x	0.1020	0.1109	0.1205	0.1128	0.0872	0.0979
14a			0.1003	0.0995	0.0963	0.0903	0.0761	0.0938
14b		x	0.1005	0.1194	0.1467	0.1674	0.1948	0.1196
15a			0.1000	0.1024	0.1049	0.0958	0.0716	0.0907
15b			0.1000	0.1020	0.1083	0.1068	0.0865	0.0976
16a			0.1000	0.1000	0.1054	0.1088	0.1027	0.1011
17a		x	0.1023	0.1123	0.1126	0.1068	0.1012	0.1009
17b			0.1010	0.1033	0.1007	0.0954	0.0944	0.1026

Table B.33. Parametric analysis to define optimal values for $\sigma_{\text{init.}}$ and σ_0 for Bayesian analysis. Negative σ sensitivity is returned by varying $\sigma_{\text{init.}}$ and COV (α) minimization is based on Bayesian prior, σ_0.

	6 Substructure								σ_0 **(Prior) = 1**							
Test	$\sigma_{\text{init.}}$	$-\sigma$	α						$\sigma_{\text{init.}}$	$-\sigma$	α					
1			0.1510	0.8630	0.2953	0.9014	0.2110	0.6811			0.1508	0.8655	0.2950	0.9024	0.2109	0.6811
2a		x	0.4913	0.9630	22.6095	0.4210	0.3451	0.7632			0.4912	0.9628	22.6849	0.4209	0.3450	0.7631
2b			-35.1196	-0.9291	0.3581	0.5639	0.3946	0.8113		x	-35.1090	-0.9291	0.3581	0.5639	0.3946	0.8113
3			1.0000	-0.3959	-1.2001	0.2674	0.5111	0.7477			1.0000	-0.3958	-1.2003	0.2674	0.5112	0.7477
4a		x	1.0000	1.0000	-7.9817	0.2664	0.3788	1.8727		x	1.0000	1.0000	-7.9807	0.2664	0.3788	1.8727
4b			1.0000	1.0000	-0.1905	0.2163	0.4239	0.9187			1.0000	1.0000	-0.1905	0.2163	0.4238	0.9188
5a		x	0.2052	0.6516	0.2723	0.5211	0.3581	55.6407			0.2052	0.6516	0.2723	0.5211	0.3581	55.6714
5b			0.4279	0.5176	0.6663	0.3045	1.7459	-2.2050			0.4279	0.5176	0.6663	0.3045	1.7459	-2.2049
6a		x	0.3834	0.3889	1.0088	1.7744	0.1424	1.0000			0.3834	0.3889	1.0086	1.7758	0.1423	1.0000
6b			0.7577	0.4613	0.3571	1.0403	-0.4785	1.0000		x	0.7575	0.4613	0.3570	1.0393	-0.4776	1.0000
7			0.9326	0.2751	0.3930	-0.7246	1.0000	1.0000			0.9331	0.2749	0.3926	-0.7219	1.0000	1.0000
8			0.7631	0.2480	1.6772	1.0624	0.4653	0.2996			0.7631	0.2480	1.6772	1.0625	0.4653	0.2996
9a			0.2489	0.4221	-0.3400	0.2302	0.4901	0.9513			0.2489	0.4221	-0.3399	0.2302	0.4902	0.9513
9b	0.0001		0.3510	0.5182	-0.4772	0.2206	0.7024	1.2753	**0.001**		0.3509	0.5180	-0.4769	0.2206	0.7026	1.2756
10			0.5504	0.6140	1.1995	0.5880	12.1354	1.0000			0.5512	0.6141	1.1987	0.5889	11.7245	1.0000
11			0.4348	0.3473	-4.4579	1.0075	1.0000	1.0000			0.4415	0.3503	-5.1022	1.0193	1.0000	1.0000
12a		x	3.7181	0.2263	-0.7463	0.3252	0.4861	0.8057			3.7183	0.2263	-0.7463	0.3252	0.4861	0.8057
12b			0.1462	0.0838	-0.0771	0.0614	-0.3000	0.3271		x	0.1462	0.0838	-0.0771	0.0614	-0.3000	0.3271
13a			1.2766	0.2386	-0.4546	0.2898	0.6829	0.2304			1.2766	0.2386	-0.4546	0.2898	0.6829	0.2304
13b		x	0.5449	0.2544	-0.3700	0.2133	1.1982	0.2524		x	0.5449	0.2544	-0.3700	0.2133	1.1980	0.2524
14a			1.4395	1.0496	1.1359	1.9243	0.2956	0.3850			1.4395	1.0496	1.1359	1.9242	0.2956	0.3850
14b			0.5512	0.4313	-0.4034	0.3567	0.3248	-0.5875		x	0.5512	0.4313	-0.4034	0.3567	0.3248	-0.5874
15a		x	1.0000	2.2553	-0.3361	0.3135	0.4507	0.1430			1.0000	2.2556	-0.3361	0.3135	0.4507	0.1430
15b			1.0000	0.6526	-7.6383	0.9878	0.4654	0.3297			1.0000	0.6526	-7.6366	0.9878	0.4654	0.3297
16a		x	1.0000	1.0000	-0.2301	-0.4386	0.1680	0.6557			1.0000	1.0000	-0.2301	-0.4386	0.1680	0.6557
17a			0.7649	-3.0807	-5.7374	0.2794	0.6228	0.8862		x	0.7649	-3.0805	-5.7346	0.2794	0.6228	0.8862
17b			0.8079	4.7439	3.2267	0.2721	0.5695	-0.8373			0.8079	4.7441	3.2278	0.2721	0.5694	-0.8371

6 Substructure σ_0 **(Prior) = 1**

Test	$\sigma_{\text{init.}}$	$-\sigma$	α						$\sigma_{\text{init.}}$	$-\sigma$	α					
1			0.1508	0.8655	0.2950	0.9023	0.2109	0.6811			0.1508	0.8655	0.2950	0.9023	0.2109	0.6811
2a		x	0.4912	0.9628	22.6845	0.4209	0.3450	0.7631		x	0.4912	0.9628	22.6834	0.4209	0.3450	0.7631
2b		x	-35.1077	-0.9291	0.3581	0.5639	0.3946	0.8113			-35.1078	-0.9291	0.3581	0.5639	0.3946	0.8113
3		x	1.0000	-0.3958	-1.2003	0.2674	0.5112	0.7477		x	1.0000	-0.3958	-1.2003	0.2674	0.5112	0.7477
4a			1.0000	1.0000	-7.9815	0.2664	0.3788	1.8727			1.0000	1.0000	-7.9811	0.2664	0.3788	1.8727
4b			1.0000	1.0000	-0.1905	0.2163	0.4239	0.9187			1.0000	1.0000	-0.1905	0.2163	0.4238	0.9188
5a			0.2052	0.6516	0.2723	0.5211	0.3581	55.6179			0.2052	0.6515	0.2723	0.5211	0.3581	55.5489
5b			0.4279	0.5176	0.6662	0.3045	1.7459	-2.2046			0.4279	0.5176	0.6663	0.3045	1.7459	-2.2049
6a		x	0.3834	0.3889	1.0086	1.7758	0.1423	1.0000			0.3834	0.3889	1.0086	1.7757	0.1423	1.0000
6b		x	0.7575	0.4613	0.3570	1.0393	-0.4776	1.0000			0.7575	0.4613	0.3570	1.0393	-0.4776	1.0000
7		x	0.9331	0.2748	0.3926	-0.7219	1.0000	1.0000			0.9331	0.2748	0.3926	-0.7219	1.0000	1.0000
8			0.7631	0.2480	1.6772	1.0625	0.4653	0.2996			0.7631	0.2480	1.6772	1.0625	0.4653	0.2996
9a		x	0.2489	0.4221	-0.3399	0.2302	0.4902	0.9513		x	0.2489	0.4221	-0.3399	0.2302	0.4902	0.9513
9b	0.01	x	0.3509	0.5181	-0.4769	0.2206	0.7026	1.2755	**0.1**		0.3509	0.5181	-0.4769	0.2206	0.7026	1.2755
10		x	0.5512	0.6141	1.1987	0.5889	11.7244	1.0000			0.5512	0.6141	1.1987	0.5889	11.7239	1.0000
11		x	0.4415	0.3503	-5.1022	1.0193	1.0000	1.0000			0.4415	0.3503	-5.1022	1.0193	1.0000	1.0000
12a			3.7184	0.2263	-0.7463	0.3252	0.4861	0.8057			3.7129	0.2263	-0.7468	0.3253	0.4861	0.8057
12b			0.1462	0.0838	-0.0771	0.0614	-0.3000	0.3271			0.1462	0.0838	-0.0771	0.0614	-0.3000	0.3271
13a			1.2766	0.2386	-0.4546	0.2898	0.6829	0.2304			1.2766	0.2386	-0.4546	0.2898	0.6829	0.2304
13b			0.5449	0.2544	-0.3701	0.2133	1.1979	0.2524			0.5449	0.2544	-0.3701	0.2133	1.1979	0.2524
14a		x	1.4395	1.0496	1.1359	1.9243	0.2956	0.3850			1.4395	1.0496	1.1359	1.9243	0.2956	0.3850
14b			0.5512	0.4313	-0.4034	0.3567	0.3248	-0.5875			0.5512	0.4313	-0.4034	0.3567	0.3248	-0.5875
15a		x	1.0000	2.2556	-0.3361	0.3135	0.4507	0.1430			1.0000	2.2557	-0.3361	0.3135	0.4507	0.1430
15b			1.0000	0.6526	-7.6430	0.9879	0.4654	0.3297			1.0000	0.6524	-7.6159	0.9874	0.4654	0.3297
16a		x	1.0000	1.0000	-0.2301	-0.4386	0.1680	0.6557		x	1.0000	1.0000	-0.2301	-0.4386	0.1680	0.6557
17a			0.7649	-3.0807	-5.7369	0.2794	0.6228	0.8862			0.7649	-3.0807	-5.7373	0.2794	0.6228	0.8862
17b			0.8079	4.7441	3.2278	0.2721	0.5694	-0.8371			0.8079	4.7437	3.2260	0.2721	0.5695	-0.8374

6 Substructure σ_0 **(Prior) = 1**

Test	$\sigma_{\text{init.}}$	$-\sigma$	α					
1			0.1508	0.8655	0.2950	0.9023	0.2109	0.6811
2a			0.4912	0.9628	22.6832	0.4209	0.3450	0.7631
2b			-35.1116	-0.9291	0.3581	0.5639	0.3946	0.8113
3			1.0000	-0.3958	-1.2003	0.2674	0.5112	0.7477
4a		x	1.0000	1.0000	-7.9811	0.2664	0.3788	1.8727
4b		x	1.0000	1.0000	-0.1905	0.2163	0.4238	0.9188
5a		x	0.2052	0.6515	0.2723	0.5211	0.3581	55.5753
5b			0.4279	0.5176	0.6663	0.3045	1.7459	-2.2049
6a			0.3834	0.3889	1.0086	1.7757	0.1423	1.0000
6b			0.7575	0.4613	0.3570	1.0393	-0.4776	1.0000
7			0.9331	0.2748	0.3926	-0.7219	1.0000	1.0000
8			0.7631	0.2480	1.6772	1.0625	0.4653	0.2996
9a			0.2489	0.4221	-0.3399	0.2302	0.4902	0.9513
9b	5		0.3509	0.5181	-0.4769	0.2206	0.7026	1.2755
10			0.5512	0.6141	1.1987	0.5889	11.7240	1.0000
11			0.4415	0.3503	-5.1023	1.0193	1.0000	1.0000
12a		x	3.7182	0.2263	-0.7463	0.3252	0.4861	0.8057
12b		x	0.1462	0.0838	-0.0771	0.0614	-0.3000	0.3271
13a			1.2766	0.2386	-0.4546	0.2898	0.6829	0.2304
13b		x	0.5449	0.2544	-0.3701	0.2133	1.1979	0.2524
14a			1.4395	1.0496	1.1359	1.9243	0.2956	0.3850
14b		x	0.5512	0.4313	-0.4034	0.3567	0.3248	-0.5875
15a			1.0000	2.2557	-0.3361	0.3135	0.4507	0.1430
15b			1.0000	0.6526	-7.6372	0.9878	0.4654	0.3297
16a			1.0000	1.0000	-0.2301	-0.4386	0.1680	0.6557
17a		x	0.7649	-3.0807	-5.7372	0.2794	0.6228	0.8862
17b		x	0.8079	4.7441	3.2277	0.2721	0.5694	-0.8371

Table B.34. Parametric analysis to define optimal values for $\sigma_{\text{init.}}$ and σ_0 for Bayesian analysis. Negative σ sensitivity is returned by varying $\sigma_{\text{init.}}$ and COV (α) minimization is based on Bayesian prior, σ_0.

9 Substructure							σ_0 **(Prior) = 0.0001**				
Test	$\sigma_{\text{init.}}$	$-\sigma$					α				
1			0.0001	0.0001	0.0001	0.0001	0.0001	0.0001	0.0001	0.0001	0.0001
2a			0.0001	0.0001	0.0001	0.0001	0.0001	0.0001	0.0001	0.0001	0.0001
2b			0.0001	0.0001	0.0001	0.0001	0.0001	0.0001	0.0001	0.0001	0.0001
3			0.0001	0.0001	0.0001	0.0001	0.0001	0.0001	0.0001	0.0001	0.0001
4a		x	0.0001	0.0001	0.0001	0.0001	0.0001	0.0001	0.0001	0.0001	0.0001
4b			0.0001	0.0001	0.0001	0.0001	0.0001	0.0001	0.0001	0.0001	0.0001
5a			0.0001	0.0001	0.0001	0.0001	0.0001	0.0001	0.0001	0.0001	0.0001
5b			0.0001	0.0001	0.0001	0.0001	0.0001	0.0001	0.0001	0.0001	0.0001
6a			0.0001	0.0001	0.0001	0.0001	0.0001	0.0001	0.0001	0.0001	0.0001
6b			0.0001	0.0001	0.0001	0.0001	0.0001	0.0001	0.0001	0.0001	0.0001
7			0.0001	0.0001	0.0001	0.0001	0.0001	0.0001	0.0001	0.0001	0.0001
8		x	0.0001	0.0001	0.0001	0.0001	0.0001	0.0001	0.0001	0.0001	0.0001
9a			0.0001	0.0001	0.0001	0.0001	0.0001	0.0001	0.0001	0.0001	0.0001
9b	**0.0001**		0.0001	0.0001	0.0001	0.0001	0.0001	0.0001	0.0001	0.0001	0.0001
10			0.0001	0.0001	0.0001	0.0001	0.0001	0.0001	0.0001	0.0001	0.0001
11			0.0001	0.0001	0.0001	0.0001	0.0001	0.0001	0.0001	0.0001	0.0001
12a			0.0001	0.0001	0.0001	0.0001	0.0001	0.0001	0.0001	0.0001	0.0001
12b			0.0001	0.0001	0.0001	0.0001	0.0001	0.0001	0.0001	0.0001	0.0001
13a			0.0001	0.0001	0.0001	0.0001	0.0001	0.0001	0.0001	0.0001	0.0001
13b			0.0001	0.0001	0.0001	0.0001	0.0001	0.0001	0.0001	0.0001	0.0001
14a			0.0001	0.0001	0.0001	0.0001	0.0001	0.0001	0.0001	0.0001	0.0001
14b			0.0001	0.0001	0.0001	0.0001	0.0001	0.0001	0.0001	0.0001	0.0001
15a			0.0001	0.0001	0.0001	0.0001	0.0001	0.0001	0.0001	0.0001	0.0001
15b			0.0001	0.0001	0.0001	0.0001	0.0001	0.0001	0.0001	0.0001	0.0001
16a			0.0001	0.0001	0.0001	0.0001	0.0001	0.0001	0.0001	0.0001	0.0001
17a			0.0001	0.0001	0.0001	0.0001	0.0001	0.0001	0.0001	0.0001	0.0001
17b			0.0001	0.0001	0.0001	0.0001	0.0001	0.0001	0.0001	0.0001	0.0001

9 Substructure σ_0 **(Prior) = 0.0001**

Test	$\sigma_{\text{init.}}$	$-\sigma$	α								
1			0.0001	0.0001	0.0001	0.0001	0.0001	0.0001	0.0001	0.0001	0.0001
2a		x	0.0001	0.0001	0.0001	0.0001	0.0001	0.0001	0.0001	0.0001	0.0001
2b		x	0.0001	0.0001	0.0001	0.0001	0.0001	0.0001	0.0001	0.0001	0.0001
3		x	0.0001	0.0001	0.0001	0.0001	0.0001	0.0001	0.0001	0.0001	0.0001
4a			0.0001	0.0001	0.0001	0.0001	0.0001	0.0001	0.0001	0.0001	0.0001
4b			0.0001	0.0001	0.0001	0.0001	0.0001	0.0001	0.0001	0.0001	0.0001
5a			0.0001	0.0001	0.0001	0.0001	0.0001	0.0001	0.0001	0.0001	0.0001
5b			0.0001	0.0001	0.0001	0.0001	0.0001	0.0001	0.0001	0.0001	0.0001
6a			0.0001	0.0001	0.0001	0.0001	0.0001	0.0001	0.0001	0.0001	0.0001
6b			0.0001	0.0001	0.0001	0.0001	0.0001	0.0001	0.0001	0.0001	0.0001
7			0.0001	0.0001	0.0001	0.0001	0.0001	0.0001	0.0001	0.0001	0.0001
8			0.0001	0.0001	0.0001	0.0001	0.0001	0.0001	0.0001	0.0001	0.0001
9a			0.0001	0.0001	0.0001	0.0001	0.0001	0.0001	0.0001	0.0001	0.0001
9b	0.001		0.0001	0.0001	0.0001	0.0001	0.0001	0.0001	0.0001	0.0001	0.0001
10			0.0001	0.0001	0.0001	0.0001	0.0001	0.0001	0.0001	0.0001	0.0001
11			0.0001	0.0001	0.0001	0.0001	0.0001	0.0001	0.0001	0.0001	0.0001
12a			0.0001	0.0001	0.0001	0.0001	0.0001	0.0001	0.0001	0.0001	0.0001
12b			0.0001	0.0001	0.0001	0.0001	0.0001	0.0001	0.0001	0.0001	0.0001
13a			0.0001	0.0001	0.0001	0.0001	0.0001	0.0001	0.0001	0.0001	0.0001
13b			0.0001	0.0001	0.0001	0.0001	0.0001	0.0001	0.0001	0.0001	0.0001
14a			0.0001	0.0001	0.0001	0.0001	0.0001	0.0001	0.0001	0.0001	0.0001
14b			0.0001	0.0001	0.0001	0.0001	0.0001	0.0001	0.0001	0.0001	0.0001
15a			0.0001	0.0001	0.0001	0.0001	0.0001	0.0001	0.0001	0.0001	0.0001
15b			0.0001	0.0001	0.0001	0.0001	0.0001	0.0001	0.0001	0.0001	0.0001
16a			0.0001	0.0001	0.0001	0.0001	0.0001	0.0001	0.0001	0.0001	0.0001
17a			0.0001	0.0001	0.0001	0.0001	0.0001	0.0001	0.0001	0.0001	0.0001
17b			0.0001	0.0001	0.0001	0.0001	0.0001	0.0001	0.0001	0.0001	0.0001

9 Substructure σ_0 **(Prior) = 0.0001**

Test	$\sigma_{\text{init.}}$	$-\sigma$	α								
1			0.0001	0.0001	0.0001	0.0001	0.0001	0.0001	0.0001	0.0001	0.0001
2a		x	0.0001	0.0001	0.0001	0.0001	0.0001	0.0001	0.0001	0.0001	0.0001
2b		x	0.0001	0.0001	0.0001	0.0001	0.0001	0.0001	0.0001	0.0001	0.0001
3		x	0.0001	0.0001	0.0001	0.0001	0.0001	0.0001	0.0001	0.0001	0.0001
4a			0.0001	0.0001	0.0001	0.0001	0.0001	0.0001	0.0001	0.0001	0.0001
4b		x	0.0001	0.0001	0.0001	0.0001	0.0001	0.0001	0.0001	0.0001	0.0001
5a			0.0001	0.0001	0.0001	0.0001	0.0001	0.0001	0.0001	0.0001	0.0001
5b			0.0001	0.0001	0.0001	0.0001	0.0001	0.0001	0.0001	0.0001	0.0001
6a			0.0001	0.0001	0.0001	0.0001	0.0001	0.0001	0.0001	0.0001	0.0001
6b		x	0.0001	0.0001	0.0001	0.0001	0.0001	0.0001	0.0001	0.0001	0.0001
7		x	0.0001	0.0001	0.0001	0.0001	0.0001	0.0001	0.0001	0.0001	0.0001
8		x	0.0001	0.0001	0.0001	0.0001	0.0001	0.0001	0.0001	0.0001	0.0001
9a		x	0.0001	0.0001	0.0001	0.0001	0.0001	0.0001	0.0001	0.0001	0.0001
9b	0.01	x	0.0001	0.0001	0.0001	0.0001	0.0001	0.0001	0.0001	0.0001	0.0001
10		x	0.0001	0.0001	0.0001	0.0001	0.0001	0.0001	0.0001	0.0001	0.0001
11		x	0.0001	0.0001	0.0001	0.0001	0.0001	0.0001	0.0001	0.0001	0.0001
12a			0.0001	0.0001	0.0001	0.0001	0.0001	0.0001	0.0001	0.0001	0.0001
12b			0.0001	0.0001	0.0001	0.0001	0.0001	0.0001	0.0001	0.0001	0.0001
13a		x	0.0001	0.0001	0.0001	0.0001	0.0001	0.0001	0.0001	0.0001	0.0001
13b		x	0.0001	0.0001	0.0001	0.0001	0.0001	0.0001	0.0001	0.0001	0.0001
14a		x	0.0001	0.0001	0.0001	0.0001	0.0001	0.0001	0.0001	0.0001	0.0001
14b		x	0.0001	0.0001	0.0001	0.0001	0.0001	0.0001	0.0001	0.0001	0.0001
15a		x	0.0001	0.0001	0.0001	0.0001	0.0001	0.0001	0.0001	0.0001	0.0001
15b			0.0001	0.0001	0.0001	0.0001	0.0001	0.0001	0.0001	0.0001	0.0001
16a		x	0.0001	0.0001	0.0001	0.0001	0.0001	0.0001	0.0001	0.0001	0.0001
17a			0.0001	0.0001	0.0001	0.0001	0.0001	0.0001	0.0001	0.0001	0.0001
17b			0.0001	0.0001	0.0001	0.0001	0.0001	0.0001	0.0001	0.0001	0.0001

9 Substructure σ_0 **(Prior) = 0.0001**

Test	$\sigma_{\text{init.}}$	$-\sigma$	α								
1			0.0001	0.0001	0.0001	0.0001	0.0001	0.0001	0.0001	0.0001	0.0001
2a			0.0001	0.0001	0.0001	0.0001	0.0001	0.0001	0.0001	0.0001	0.0001
2b			0.0001	0.0001	0.0001	0.0001	0.0001	0.0001	0.0001	0.0001	0.0001
3			0.0001	0.0001	0.0001	0.0001	0.0001	0.0001	0.0001	0.0001	0.0001
4a			0.0001	0.0001	0.0001	0.0001	0.0001	0.0001	0.0001	0.0001	0.0001
4b			0.0001	0.0001	0.0001	0.0001	0.0001	0.0001	0.0001	0.0001	0.0001
5a			0.0001	0.0001	0.0001	0.0001	0.0001	0.0001	0.0001	0.0001	0.0001
5b		x	0.0001	0.0001	0.0001	0.0001	0.0001	0.0001	0.0001	0.0001	0.0001
6a			0.0001	0.0001	0.0001	0.0001	0.0001	0.0001	0.0001	0.0001	0.0001
6b			0.0001	0.0001	0.0001	0.0001	0.0001	0.0001	0.0001	0.0001	0.0001
7			0.0001	0.0001	0.0001	0.0001	0.0001	0.0001	0.0001	0.0001	0.0001
8			0.0001	0.0001	0.0001	0.0001	0.0001	0.0001	0.0001	0.0001	0.0001
9a			0.0001	0.0001	0.0001	0.0001	0.0001	0.0001	0.0001	0.0001	0.0001
9b	**0.1**		0.0001	0.0001	0.0001	0.0001	0.0001	0.0001	0.0001	0.0001	0.0001
10			0.0001	0.0001	0.0001	0.0001	0.0001	0.0001	0.0001	0.0001	0.0001
11			0.0001	0.0001	0.0001	0.0001	0.0001	0.0001	0.0001	0.0001	0.0001
12a			0.0001	0.0001	0.0001	0.0001	0.0001	0.0001	0.0001	0.0001	0.0001
12b			0.0001	0.0001	0.0001	0.0001	0.0001	0.0001	0.0001	0.0001	0.0001
13a			0.0001	0.0001	0.0001	0.0001	0.0001	0.0001	0.0001	0.0001	0.0001
13b			0.0001	0.0001	0.0001	0.0001	0.0001	0.0001	0.0001	0.0001	0.0001
14a			0.0001	0.0001	0.0001	0.0001	0.0001	0.0001	0.0001	0.0001	0.0001
14b			0.0001	0.0001	0.0001	0.0001	0.0001	0.0001	0.0001	0.0001	0.0001
15a			0.0001	0.0001	0.0001	0.0001	0.0001	0.0001	0.0001	0.0001	0.0001
15b			0.0001	0.0001	0.0001	0.0001	0.0001	0.0001	0.0001	0.0001	0.0001
16a			0.0001	0.0001	0.0001	0.0001	0.0001	0.0001	0.0001	0.0001	0.0001
17a			0.0001	0.0001	0.0001	0.0001	0.0001	0.0001	0.0001	0.0001	0.0001
17b			0.0001	0.0001	0.0001	0.0001	0.0001	0.0001	0.0001	0.0001	0.0001

9 Substructure σ_0 **(Prior) = 0.0001**

Test	$\sigma_{\text{init.}}$	$-\sigma$	α								
1			0.0001	0.0001	0.0001	0.0001	0.0001	0.0001	0.0001	0.0001	0.0001
2a			0.0001	0.0001	0.0001	0.0001	0.0001	0.0001	0.0001	0.0001	0.0001
2b			0.0001	0.0001	0.0001	0.0001	0.0001	0.0001	0.0001	0.0001	0.0001
3			0.0001	0.0001	0.0001	0.0001	0.0001	0.0001	0.0001	0.0001	0.0001
4a		x	0.0001	0.0001	0.0001	0.0001	0.0001	0.0001	0.0001	0.0001	0.0001
4b			0.0001	0.0001	0.0001	0.0001	0.0001	0.0001	0.0001	0.0001	0.0001
5a			0.0001	0.0001	0.0001	0.0001	0.0001	0.0001	0.0001	0.0001	0.0001
5b			0.0001	0.0001	0.0001	0.0001	0.0001	0.0001	0.0001	0.0001	0.0001
6a			0.0001	0.0001	0.0001	0.0001	0.0001	0.0001	0.0001	0.0001	0.0001
6b			0.0001	0.0001	0.0001	0.0001	0.0001	0.0001	0.0001	0.0001	0.0001
7			0.0001	0.0001	0.0001	0.0001	0.0001	0.0001	0.0001	0.0001	0.0001
8			0.0001	0.0001	0.0001	0.0001	0.0001	0.0001	0.0001	0.0001	0.0001
9a			0.0001	0.0001	0.0001	0.0001	0.0001	0.0001	0.0001	0.0001	0.0001
9b	**5**		0.0001	0.0001	0.0001	0.0001	0.0001	0.0001	0.0001	0.0001	0.0001
10			0.0001	0.0001	0.0001	0.0001	0.0001	0.0001	0.0001	0.0001	0.0001
11			0.0001	0.0001	0.0001	0.0001	0.0001	0.0001	0.0001	0.0001	0.0001
12a			0.0001	0.0001	0.0001	0.0001	0.0001	0.0001	0.0001	0.0001	0.0001
12b			0.0001	0.0001	0.0001	0.0001	0.0001	0.0001	0.0001	0.0001	0.0001
13a			0.0001	0.0001	0.0001	0.0001	0.0001	0.0001	0.0001	0.0001	0.0001
13b			0.0001	0.0001	0.0001	0.0001	0.0001	0.0001	0.0001	0.0001	0.0001
14a			0.0001	0.0001	0.0001	0.0001	0.0001	0.0001	0.0001	0.0001	0.0001
14b			0.0001	0.0001	0.0001	0.0001	0.0001	0.0001	0.0001	0.0001	0.0001
15a			0.0001	0.0001	0.0001	0.0001	0.0001	0.0001	0.0001	0.0001	0.0001
15b			0.0001	0.0001	0.0001	0.0001	0.0001	0.0001	0.0001	0.0001	0.0001
16a			0.0001	0.0001	0.0001	0.0001	0.0001	0.0001	0.0001	0.0001	0.0001
17a			0.0001	0.0001	0.0001	0.0001	0.0001	0.0001	0.0001	0.0001	0.0001
17b			0.0001	0.0001	0.0001	0.0001	0.0001	0.0001	0.0001	0.0001	0.0001

Table B.35. Parametric analysis to define optimal values for $\sigma_{\text{init.}}$ and σ_0 for Bayesian analysis. Negative σ sensitivity is returned by varying $\sigma_{\text{init.}}$ and COV (α) minimization is based on Bayesian prior, σ_0.

9 Substructure							σ_0 **(Prior) = 0.001**				
Test	$\sigma_{\text{init.}}$	$-\sigma$				α					
1			0.0010	0.0010	0.0010	0.0010	0.0010	0.0010	0.0010	0.0010	0.0010
2a			0.0010	0.0010	0.0010	0.0010	0.0010	0.0010	0.0010	0.0010	0.0010
2b			0.0010	0.0010	0.0010	0.0010	0.0010	0.0010	0.0010	0.0010	0.0010
3			0.0010	0.0010	0.0010	0.0010	0.0010	0.0010	0.0010	0.0010	0.0010
4a		x	0.0010	0.0010	0.0010	0.0010	0.0010	0.0010	0.0010	0.0010	0.0010
4b			0.0010	0.0010	0.0010	0.0010	0.0010	0.0010	0.0010	0.0010	0.0010
5a			0.0010	0.0010	0.0010	0.0010	0.0010	0.0010	0.0010	0.0010	0.0010
5b			0.0010	0.0010	0.0010	0.0010	0.0010	0.0010	0.0010	0.0010	0.0010
6a			0.0010	0.0010	0.0010	0.0010	0.0010	0.0010	0.0010	0.0010	0.0010
6b			0.0010	0.0010	0.0010	0.0010	0.0010	0.0010	0.0010	0.0010	0.0010
7			0.0010	0.0010	0.0010	0.0010	0.0010	0.0010	0.0010	0.0010	0.0010
8			0.0010	0.0010	0.0010	0.0010	0.0010	0.0010	0.0010	0.0010	0.0010
9a			0.0010	0.0010	0.0010	0.0010	0.0010	0.0010	0.0010	0.0010	0.0010
9b	**0.0001**		0.0010	0.0010	0.0010	0.0010	0.0010	0.0010	0.0010	0.0010	0.0010
10			0.0010	0.0010	0.0010	0.0010	0.0010	0.0010	0.0010	0.0010	0.0010
11			0.0010	0.0010	0.0010	0.0010	0.0010	0.0010	0.0010	0.0010	0.0010
12a			0.0010	0.0010	0.0010	0.0010	0.0010	0.0010	0.0010	0.0010	0.0010
12b			0.0010	0.0010	0.0010	0.0010	0.0010	0.0010	0.0010	0.0010	0.0010
13a			0.0010	0.0010	0.0010	0.0010	0.0010	0.0010	0.0010	0.0010	0.0010
13b			0.0010	0.0010	0.0010	0.0010	0.0010	0.0010	0.0010	0.0010	0.0010
14a			0.0010	0.0010	0.0010	0.0010	0.0010	0.0010	0.0010	0.0010	0.0010
14b			0.0010	0.0010	0.0010	0.0010	0.0010	0.0010	0.0010	0.0010	0.0010
15a			0.0010	0.0010	0.0010	0.0010	0.0010	0.0010	0.0010	0.0010	0.0010
15b			0.0010	0.0010	0.0010	0.0010	0.0010	0.0010	0.0010	0.0010	0.0010
16a			0.0010	0.0010	0.0010	0.0010	0.0010	0.0010	0.0010	0.0010	0.0010
17a			0.0010	0.0010	0.0010	0.0010	0.0010	0.0010	0.0010	0.0010	0.0010
17b			0.0010	0.0010	0.0010	0.0010	0.0010	0.0010	0.0010	0.0010	0.0010

9 Substructure σ_0 **(Prior) = 0.001**

Test	$\sigma_{\text{init.}}$	$-\sigma$	α								
1			0.0010	0.0010	0.0010	0.0010	0.0010	0.0010	0.0010	0.0010	0.0010
2a		x	0.0010	0.0010	0.0010	0.0010	0.0010	0.0010	0.0010	0.0010	0.0010
2b		x	0.0010	0.0010	0.0010	0.0010	0.0010	0.0010	0.0010	0.0010	0.0010
3		x	0.0010	0.0010	0.0010	0.0010	0.0010	0.0010	0.0010	0.0010	0.0010
4a			0.0010	0.0010	0.0010	0.0010	0.0010	0.0010	0.0010	0.0010	0.0010
4b			0.0010	0.0010	0.0010	0.0010	0.0010	0.0010	0.0010	0.0010	0.0010
5a			0.0010	0.0010	0.0010	0.0010	0.0010	0.0010	0.0010	0.0010	0.0010
5b			0.0010	0.0010	0.0010	0.0010	0.0010	0.0010	0.0010	0.0010	0.0010
6a			0.0010	0.0010	0.0010	0.0010	0.0010	0.0010	0.0010	0.0010	0.0010
6b			0.0010	0.0010	0.0010	0.0010	0.0010	0.0010	0.0010	0.0010	0.0010
7			0.0010	0.0010	0.0010	0.0010	0.0010	0.0010	0.0010	0.0010	0.0010
8			0.0010	0.0010	0.0010	0.0010	0.0010	0.0010	0.0010	0.0010	0.0010
9a			0.0010	0.0010	0.0010	0.0010	0.0010	0.0010	0.0010	0.0010	0.0010
9b	0.001		0.0010	0.0010	0.0010	0.0010	0.0010	0.0010	0.0010	0.0010	0.0010
10			0.0010	0.0010	0.0010	0.0010	0.0010	0.0010	0.0010	0.0010	0.0010
11			0.0010	0.0010	0.0010	0.0010	0.0010	0.0010	0.0010	0.0010	0.0010
12a			0.0010	0.0010	0.0010	0.0010	0.0010	0.0010	0.0010	0.0010	0.0010
12b			0.0010	0.0010	0.0010	0.0010	0.0010	0.0010	0.0010	0.0010	0.0010
13a			0.0010	0.0010	0.0010	0.0010	0.0010	0.0010	0.0010	0.0010	0.0010
13b			0.0010	0.0010	0.0010	0.0010	0.0010	0.0010	0.0010	0.0010	0.0010
14a			0.0010	0.0010	0.0010	0.0010	0.0010	0.0010	0.0010	0.0010	0.0010
14b			0.0010	0.0010	0.0010	0.0010	0.0010	0.0010	0.0010	0.0010	0.0010
15a			0.0010	0.0010	0.0010	0.0010	0.0010	0.0010	0.0010	0.0010	0.0010
15b			0.0010	0.0010	0.0010	0.0010	0.0010	0.0010	0.0010	0.0010	0.0010
16a			0.0010	0.0010	0.0010	0.0010	0.0010	0.0010	0.0010	0.0010	0.0010
17a			0.0010	0.0010	0.0010	0.0010	0.0010	0.0010	0.0010	0.0010	0.0010
17b			0.0010	0.0010	0.0010	0.0010	0.0010	0.0010	0.0010	0.0010	0.0010

9 Substructure σ_0 **(Prior) = 0.001**

Test	$\sigma_{\text{init.}}$	$-\sigma$	α								
1			0.0010	0.0010	0.0010	0.0010	0.0010	0.0010	0.0010	0.0010	0.0010
2a		x	0.0010	0.0010	0.0010	0.0010	0.0010	0.0010	0.0010	0.0010	0.0010
2b		x	0.0010	0.0010	0.0010	0.0010	0.0010	0.0010	0.0010	0.0010	0.0010
3		x	0.0010	0.0010	0.0010	0.0010	0.0010	0.0010	0.0010	0.0010	0.0010
4a			0.0010	0.0010	0.0010	0.0010	0.0010	0.0010	0.0010	0.0010	0.0010
4b		x	0.0010	0.0010	0.0010	0.0010	0.0010	0.0010	0.0010	0.0010	0.0010
5a			0.0010	0.0010	0.0010	0.0010	0.0010	0.0010	0.0010	0.0010	0.0010
5b			0.0010	0.0010	0.0010	0.0010	0.0010	0.0010	0.0010	0.0010	0.0010
6a			0.0010	0.0010	0.0010	0.0010	0.0010	0.0010	0.0010	0.0010	0.0010
6b		x	0.0010	0.0010	0.0010	0.0010	0.0010	0.0010	0.0010	0.0010	0.0010
7		x	0.0010	0.0010	0.0010	0.0010	0.0010	0.0010	0.0010	0.0010	0.0010
8		x	0.0010	0.0010	0.0010	0.0010	0.0010	0.0010	0.0010	0.0010	0.0010
9a		x	0.0010	0.0010	0.0010	0.0010	0.0010	0.0010	0.0010	0.0010	0.0010
9b	0.01	x	0.0010	0.0010	0.0010	0.0010	0.0010	0.0010	0.0010	0.0010	0.0010
10		x	0.0010	0.0010	0.0010	0.0010	0.0010	0.0010	0.0010	0.0010	0.0010
11		x	0.0010	0.0010	0.0010	0.0010	0.0010	0.0010	0.0010	0.0010	0.0010
12a			0.0010	0.0010	0.0010	0.0010	0.0010	0.0010	0.0010	0.0010	0.0010
12b			0.0010	0.0010	0.0010	0.0010	0.0010	0.0010	0.0010	0.0010	0.0010
13a		x	0.0010	0.0010	0.0010	0.0010	0.0010	0.0010	0.0010	0.0010	0.0010
13b		x	0.0010	0.0010	0.0010	0.0010	0.0010	0.0010	0.0010	0.0010	0.0010
14a		x	0.0010	0.0010	0.0010	0.0010	0.0010	0.0010	0.0010	0.0010	0.0010
14b		x	0.0010	0.0010	0.0010	0.0010	0.0010	0.0010	0.0010	0.0010	0.0010
15a		x	0.0010	0.0010	0.0010	0.0010	0.0010	0.0010	0.0010	0.0010	0.0010
15b			0.0010	0.0010	0.0010	0.0010	0.0010	0.0010	0.0010	0.0010	0.0010
16a		x	0.0010	0.0010	0.0010	0.0010	0.0010	0.0010	0.0010	0.0010	0.0010
17a			0.0010	0.0010	0.0010	0.0010	0.0010	0.0010	0.0010	0.0010	0.0010
17b			0.0010	0.0010	0.0010	0.0010	0.0010	0.0010	0.0010	0.0010	0.0010

9 Substructure σ_0 **(Prior) = 0.001**

Test	$\sigma_{\text{init.}}$	$-\sigma$	α								
1			0.0010	0.0010	0.0010	0.0010	0.0010	0.0010	0.0010	0.0010	0.0010
2a			0.0010	0.0010	0.0010	0.0010	0.0010	0.0010	0.0010	0.0010	0.0010
2b			0.0010	0.0010	0.0010	0.0010	0.0010	0.0010	0.0010	0.0010	0.0010
3			0.0010	0.0010	0.0010	0.0010	0.0010	0.0010	0.0010	0.0010	0.0010
4a			0.0010	0.0010	0.0010	0.0010	0.0010	0.0010	0.0010	0.0010	0.0010
4b			0.0010	0.0010	0.0010	0.0010	0.0010	0.0010	0.0010	0.0010	0.0010
5a			0.0010	0.0010	0.0010	0.0010	0.0010	0.0010	0.0010	0.0010	0.0010
5b		x	0.0010	0.0010	0.0010	0.0010	0.0010	0.0010	0.0010	0.0010	0.0010
6a			0.0010	0.0010	0.0010	0.0010	0.0010	0.0010	0.0010	0.0010	0.0010
6b			0.0010	0.0010	0.0010	0.0010	0.0010	0.0010	0.0010	0.0010	0.0010
7			0.0010	0.0010	0.0010	0.0010	0.0010	0.0010	0.0010	0.0010	0.0010
8			0.0010	0.0010	0.0010	0.0010	0.0010	0.0010	0.0010	0.0010	0.0010
9a			0.0010	0.0010	0.0010	0.0010	0.0010	0.0010	0.0010	0.0010	0.0010
9b	**0.1**		0.0010	0.0010	0.0010	0.0010	0.0010	0.0010	0.0010	0.0010	0.0010
10			0.0010	0.0010	0.0010	0.0010	0.0010	0.0010	0.0010	0.0010	0.0010
11			0.0010	0.0010	0.0010	0.0010	0.0010	0.0010	0.0010	0.0010	0.0010
12a			0.0010	0.0010	0.0010	0.0010	0.0010	0.0010	0.0010	0.0010	0.0010
12b			0.0010	0.0010	0.0010	0.0010	0.0010	0.0010	0.0010	0.0010	0.0010
13a			0.0010	0.0010	0.0010	0.0010	0.0010	0.0010	0.0010	0.0010	0.0010
13b			0.0010	0.0010	0.0010	0.0010	0.0010	0.0010	0.0010	0.0010	0.0010
14a			0.0010	0.0010	0.0010	0.0010	0.0010	0.0010	0.0010	0.0010	0.0010
14b			0.0010	0.0010	0.0010	0.0010	0.0010	0.0010	0.0010	0.0010	0.0010
15a			0.0010	0.0010	0.0010	0.0010	0.0010	0.0010	0.0010	0.0010	0.0010
15b			0.0010	0.0010	0.0010	0.0010	0.0010	0.0010	0.0010	0.0010	0.0010
16a			0.0010	0.0010	0.0010	0.0010	0.0010	0.0010	0.0010	0.0010	0.0010
17a			0.0010	0.0010	0.0010	0.0010	0.0010	0.0010	0.0010	0.0010	0.0010
17b			0.0010	0.0010	0.0010	0.0010	0.0010	0.0010	0.0010	0.0010	0.0010

9 Substructure σ_0 **(Prior) = 0.001**

Test	$\sigma_{\text{init.}}$	$-\sigma$	α								
1			0.0010	0.0010	0.0010	0.0010	0.0010	0.0010	0.0010	0.0010	0.0010
2a			0.0010	0.0010	0.0010	0.0010	0.0010	0.0010	0.0010	0.0010	0.0010
2b			0.0010	0.0010	0.0010	0.0010	0.0010	0.0010	0.0010	0.0010	0.0010
3			0.0010	0.0010	0.0010	0.0010	0.0010	0.0010	0.0010	0.0010	0.0010
4a		x	0.0010	0.0010	0.0010	0.0010	0.0010	0.0010	0.0010	0.0010	0.0010
4b			0.0010	0.0010	0.0010	0.0010	0.0010	0.0010	0.0010	0.0010	0.0010
5a			0.0010	0.0010	0.0010	0.0010	0.0010	0.0010	0.0010	0.0010	0.0010
5b			0.0010	0.0010	0.0010	0.0010	0.0010	0.0010	0.0010	0.0010	0.0010
6a			0.0010	0.0010	0.0010	0.0010	0.0010	0.0010	0.0010	0.0010	0.0010
6b			0.0010	0.0010	0.0010	0.0010	0.0010	0.0010	0.0010	0.0010	0.0010
7			0.0010	0.0010	0.0010	0.0010	0.0010	0.0010	0.0010	0.0010	0.0010
8			0.0010	0.0010	0.0010	0.0010	0.0010	0.0010	0.0010	0.0010	0.0010
9a			0.0010	0.0010	0.0010	0.0010	0.0010	0.0010	0.0010	0.0010	0.0010
9b	**5**		0.0010	0.0010	0.0010	0.0010	0.0010	0.0010	0.0010	0.0010	0.0010
10			0.0010	0.0010	0.0010	0.0010	0.0010	0.0010	0.0010	0.0010	0.0010
11			0.0010	0.0010	0.0010	0.0010	0.0010	0.0010	0.0010	0.0010	0.0010
12a			0.0010	0.0010	0.0010	0.0010	0.0010	0.0010	0.0010	0.0010	0.0010
12b			0.0010	0.0010	0.0010	0.0010	0.0010	0.0010	0.0010	0.0010	0.0010
13a			0.0010	0.0010	0.0010	0.0010	0.0010	0.0010	0.0010	0.0010	0.0010
13b			0.0010	0.0010	0.0010	0.0010	0.0010	0.0010	0.0010	0.0010	0.0010
14a			0.0010	0.0010	0.0010	0.0010	0.0010	0.0010	0.0010	0.0010	0.0010
14b			0.0010	0.0010	0.0010	0.0010	0.0010	0.0010	0.0010	0.0010	0.0010
15a			0.0010	0.0010	0.0010	0.0010	0.0010	0.0010	0.0010	0.0010	0.0010
15b			0.0010	0.0010	0.0010	0.0010	0.0010	0.0010	0.0010	0.0010	0.0010
16a			0.0010	0.0010	0.0010	0.0010	0.0010	0.0010	0.0010	0.0010	0.0010
17a			0.0010	0.0010	0.0010	0.0010	0.0010	0.0010	0.0010	0.0010	0.0010
17b			0.0010	0.0010	0.0010	0.0010	0.0010	0.0010	0.0010	0.0010	0.0010

Table B.36. Parametric analysis to define optimal values for $\sigma_{\text{init.}}$ and σ_0 for Bayesian analysis. Negative σ sensitivity is returned by varying $\sigma_{\text{init.}}$ and COV (α) minimization is based on Bayesian prior, σ_0.

9 Substructure							σ_0 **(Prior) = 0.01**				
Test	$\sigma_{\text{init.}}$	$-\sigma$					α				
1			0.0100	0.0099	0.0099	0.0099	0.0095	0.0099	0.0099	0.0099	0.0100
2a			0.0100	0.0100	0.0100	0.0100	0.0100	0.0100	0.0100	0.0100	0.0100
2b			0.0100	0.0100	0.0100	0.0100	0.0099	0.0100	0.0100	0.0100	0.0100
3			0.0100	0.0100	0.0100	0.0100	0.0100	0.0100	0.0100	0.0100	0.0100
4a			0.0100	0.0100	0.0100	0.0100	0.0100	0.0100	0.0100	0.0100	0.0100
4b			0.0100	0.0100	0.0100	0.0100	0.0100	0.0100	0.0100	0.0100	0.0100
5a		x	0.0100	0.0100	0.0100	0.0100	0.0099	0.0100	0.0100	0.0100	0.0100
5b			0.0100	0.0100	0.0100	0.0100	0.0099	0.0100	0.0100	0.0100	0.0100
6a			0.0100	0.0100	0.0100	0.0100	0.0100	0.0100	0.0100	0.0100	0.0100
6b			0.0100	0.0100	0.0100	0.0100	0.0100	0.0100	0.0100	0.0100	0.0100
7			0.0100	0.0100	0.0100	0.0100	0.0100	0.0100	0.0100	0.0100	0.0100
8			0.0100	0.0100	0.0100	0.0100	0.0100	0.0100	0.0100	0.0100	0.0100
9a			0.0100	0.0100	0.0100	0.0100	0.0100	0.0100	0.0100	0.0100	0.0100
9b	**0.0001**		0.0100	0.0100	0.0100	0.0100	0.0100	0.0100	0.0100	0.0100	0.0100
10			0.0100	0.0100	0.0100	0.0100	0.0100	0.0100	0.0100	0.0100	0.0100
11			0.0100	0.0100	0.0100	0.0100	0.0100	0.0100	0.0100	0.0100	0.0100
12a			0.0100	0.0100	0.0100	0.0100	0.0100	0.0100	0.0100	0.0100	0.0100
12b			0.0100	0.0100	0.0100	0.0100	0.0100	0.0100	0.0100	0.0100	0.0100
13a			0.0100	0.0100	0.0100	0.0100	0.0100	0.0100	0.0100	0.0100	0.0100
13b			0.0100	0.0100	0.0100	0.0100	0.0100	0.0100	0.0100	0.0100	0.0100
14a			0.0100	0.0100	0.0100	0.0100	0.0100	0.0100	0.0100	0.0100	0.0100
14b			0.0100	0.0100	0.0100	0.0100	0.0100	0.0100	0.0100	0.0100	0.0100
15a			0.0100	0.0100	0.0100	0.0100	0.0100	0.0100	0.0100	0.0100	0.0100
15b			0.0100	0.0100	0.0100	0.0100	0.0100	0.0100	0.0100	0.0100	0.0100
16a			0.0100	0.0100	0.0100	0.0100	0.0100	0.0100	0.0100	0.0100	0.0100
17a		x	0.0100	0.0100	0.0100	0.0100	0.0100	0.0100	0.0100	0.0100	0.0100
17b		x	0.0100	0.0100	0.0100	0.0100	0.0100	0.0100	0.0100	0.0100	0.0100

9 Substructure σ_0 **(Prior) = 0.01**

Test	$\sigma_{\text{init.}}$	$-\sigma$	α								
1			0.0100	0.0099	0.0099	0.0099	0.0095	0.0099	0.0099	0.0099	0.0100
2a			0.0100	0.0100	0.0100	0.0100	0.0100	0.0100	0.0100	0.0100	0.0100
2b		x	0.0100	0.0100	0.0100	0.0100	0.0099	0.0100	0.0100	0.0100	0.0100
3		x	0.0100	0.0100	0.0100	0.0100	0.0100	0.0100	0.0100	0.0100	0.0100
4a			0.0100	0.0100	0.0100	0.0100	0.0100	0.0100	0.0100	0.0100	0.0100
4b			0.0100	0.0100	0.0100	0.0100	0.0100	0.0100	0.0100	0.0100	0.0100
5a			0.0100	0.0100	0.0100	0.0100	0.0099	0.0100	0.0100	0.0100	0.0100
5b			0.0100	0.0100	0.0100	0.0100	0.0099	0.0100	0.0100	0.0100	0.0100
6a			0.0100	0.0100	0.0100	0.0100	0.0100	0.0100	0.0100	0.0100	0.0100
6b			0.0100	0.0100	0.0100	0.0100	0.0100	0.0100	0.0100	0.0100	0.0100
7			0.0100	0.0100	0.0100	0.0100	0.0100	0.0100	0.0100	0.0100	0.0100
8			0.0100	0.0100	0.0100	0.0100	0.0100	0.0100	0.0100	0.0100	0.0100
9a			0.0100	0.0100	0.0100	0.0100	0.0100	0.0100	0.0100	0.0100	0.0100
9b	0.001	x	0.0100	0.0100	0.0100	0.0100	0.0100	0.0100	0.0100	0.0100	0.0100
10			0.0100	0.0100	0.0100	0.0100	0.0100	0.0100	0.0100	0.0100	0.0100
11			0.0100	0.0100	0.0100	0.0100	0.0100	0.0100	0.0100	0.0100	0.0100
12a			0.0100	0.0100	0.0100	0.0100	0.0100	0.0100	0.0100	0.0100	0.0100
12b			0.0100	0.0100	0.0100	0.0100	0.0100	0.0100	0.0100	0.0100	0.0100
13a			0.0100	0.0100	0.0100	0.0100	0.0100	0.0100	0.0100	0.0100	0.0100
13b			0.0100	0.0100	0.0100	0.0100	0.0100	0.0100	0.0100	0.0100	0.0100
14a			0.0100	0.0100	0.0100	0.0100	0.0100	0.0100	0.0100	0.0100	0.0100
14b			0.0100	0.0100	0.0100	0.0100	0.0100	0.0100	0.0100	0.0100	0.0100
15a		x	0.0100	0.0100	0.0100	0.0100	0.0100	0.0100	0.0100	0.0100	0.0100
15b			0.0100	0.0100	0.0100	0.0100	0.0100	0.0100	0.0100	0.0100	0.0100
16a			0.0100	0.0100	0.0100	0.0100	0.0100	0.0100	0.0100	0.0100	0.0100
17a			0.0100	0.0100	0.0100	0.0100	0.0100	0.0100	0.0100	0.0100	0.0100
17b			0.0100	0.0100	0.0100	0.0100	0.0100	0.0100	0.0100	0.0100	0.0100

9 Substructure σ_0 **(Prior) = 0.01**

Test	$\sigma_{\text{init.}}$	$-\sigma$	α								
1			0.0100	0.0099	0.0099	0.0099	0.0095	0.0099	0.0099	0.0099	0.0100
2a		x	0.0100	0.0100	0.0100	0.0100	0.0100	0.0100	0.0100	0.0100	0.0100
2b		x	0.0100	0.0100	0.0100	0.0100	0.0099	0.0100	0.0100	0.0100	0.0100
3		x	0.0100	0.0100	0.0100	0.0100	0.0100	0.0100	0.0100	0.0100	0.0100
4a			0.0100	0.0100	0.0100	0.0100	0.0100	0.0100	0.0100	0.0100	0.0100
4b		x	0.0100	0.0100	0.0100	0.0100	0.0100	0.0100	0.0100	0.0100	0.0100
5a			0.0100	0.0100	0.0100	0.0100	0.0099	0.0100	0.0100	0.0100	0.0100
5b			0.0100	0.0100	0.0100	0.0100	0.0099	0.0100	0.0100	0.0100	0.0100
6a			0.0100	0.0100	0.0100	0.0100	0.0100	0.0100	0.0100	0.0100	0.0100
6b		x	0.0100	0.0100	0.0100	0.0100	0.0100	0.0100	0.0100	0.0100	0.0100
7		x	0.0100	0.0100	0.0100	0.0100	0.0100	0.0100	0.0100	0.0100	0.0100
8		x	0.0100	0.0100	0.0100	0.0100	0.0100	0.0100	0.0100	0.0100	0.0100
9a		x	0.0100	0.0100	0.0100	0.0100	0.0100	0.0100	0.0100	0.0100	0.0100
9b	0.01	x	0.0100	0.0100	0.0100	0.0100	0.0100	0.0100	0.0100	0.0100	0.0100
10		x	0.0100	0.0100	0.0100	0.0100	0.0100	0.0100	0.0100	0.0100	0.0100
11		x	0.0100	0.0100	0.0100	0.0100	0.0100	0.0100	0.0100	0.0100	0.0100
12a			0.0100	0.0100	0.0100	0.0100	0.0100	0.0100	0.0100	0.0100	0.0100
12b			0.0100	0.0100	0.0100	0.0100	0.0100	0.0100	0.0100	0.0100	0.0100
13a		x	0.0100	0.0100	0.0100	0.0100	0.0100	0.0100	0.0100	0.0100	0.0100
13b			0.0100	0.0100	0.0100	0.0100	0.0100	0.0100	0.0100	0.0100	0.0100
14a		x	0.0100	0.0100	0.0100	0.0100	0.0100	0.0100	0.0100	0.0100	0.0100
14b		x	0.0100	0.0100	0.0100	0.0100	0.0100	0.0100	0.0100	0.0100	0.0100
15a		x	0.0100	0.0100	0.0100	0.0100	0.0100	0.0100	0.0100	0.0100	0.0100
15b			0.0100	0.0100	0.0100	0.0100	0.0100	0.0100	0.0100	0.0100	0.0100
16a		x	0.0100	0.0100	0.0100	0.0100	0.0100	0.0100	0.0100	0.0100	0.0100
17a			0.0100	0.0100	0.0100	0.0100	0.0100	0.0100	0.0100	0.0100	0.0100
17b			0.0100	0.0100	0.0100	0.0100	0.0100	0.0100	0.0100	0.0100	0.0100

9 Substructure σ_0 **(Prior) = 0.01**

Test	$\sigma_{\text{init.}}$	$-\sigma$	α								
1			0.0100	0.0099	0.0099	0.0099	0.0095	0.0099	0.0099	0.0099	0.0100
2a			0.0100	0.0100	0.0100	0.0100	0.0100	0.0100	0.0100	0.0100	0.0100
2b			0.0100	0.0100	0.0100	0.0100	0.0099	0.0100	0.0100	0.0100	0.0100
3			0.0100	0.0100	0.0100	0.0100	0.0100	0.0100	0.0100	0.0100	0.0100
4a			0.0100	0.0100	0.0100	0.0100	0.0100	0.0100	0.0100	0.0100	0.0100
4b			0.0100	0.0100	0.0100	0.0100	0.0100	0.0100	0.0100	0.0100	0.0100
5a			0.0100	0.0100	0.0100	0.0100	0.0099	0.0100	0.0100	0.0100	0.0100
5b		x	0.0100	0.0100	0.0100	0.0100	0.0099	0.0100	0.0100	0.0100	0.0100
6a			0.0100	0.0100	0.0100	0.0100	0.0100	0.0100	0.0100	0.0100	0.0100
6b			0.0100	0.0100	0.0100	0.0100	0.0100	0.0100	0.0100	0.0100	0.0100
7			0.0100	0.0100	0.0100	0.0100	0.0100	0.0100	0.0100	0.0100	0.0100
8			0.0100	0.0100	0.0100	0.0100	0.0100	0.0100	0.0100	0.0100	0.0100
9a			0.0100	0.0100	0.0100	0.0100	0.0100	0.0100	0.0100	0.0100	0.0100
9b	**0.1**		0.0100	0.0100	0.0100	0.0100	0.0100	0.0100	0.0100	0.0100	0.0100
10			0.0100	0.0100	0.0100	0.0100	0.0100	0.0100	0.0100	0.0100	0.0100
11			0.0100	0.0100	0.0100	0.0100	0.0100	0.0100	0.0100	0.0100	0.0100
12a			0.0100	0.0100	0.0100	0.0100	0.0100	0.0100	0.0100	0.0100	0.0100
12b			0.0100	0.0100	0.0100	0.0100	0.0100	0.0100	0.0100	0.0100	0.0100
13a			0.0100	0.0100	0.0100	0.0100	0.0100	0.0100	0.0100	0.0100	0.0100
13b			0.0100	0.0100	0.0100	0.0100	0.0100	0.0100	0.0100	0.0100	0.0100
14a			0.0100	0.0100	0.0100	0.0100	0.0100	0.0100	0.0100	0.0100	0.0100
14b			0.0100	0.0100	0.0100	0.0100	0.0100	0.0100	0.0100	0.0100	0.0100
15a			0.0100	0.0100	0.0100	0.0100	0.0100	0.0100	0.0100	0.0100	0.0100
15b			0.0100	0.0100	0.0100	0.0100	0.0100	0.0100	0.0100	0.0100	0.0100
16a			0.0100	0.0100	0.0100	0.0100	0.0100	0.0100	0.0100	0.0100	0.0100
17a			0.0100	0.0100	0.0100	0.0100	0.0100	0.0100	0.0100	0.0100	0.0100
17b			0.0100	0.0100	0.0100	0.0100	0.0100	0.0100	0.0100	0.0100	0.0100

9 Substructure σ_0 **(Prior) = 0.01**

Test	$\sigma_{\text{init.}}$	$-\sigma$	α								
1			0.0100	0.0099	0.0099	0.0099	0.0095	0.0099	0.0099	0.0099	0.0100
2a			0.0100	0.0100	0.0100	0.0100	0.0100	0.0100	0.0100	0.0100	0.0100
2b			0.0100	0.0100	0.0100	0.0100	0.0099	0.0100	0.0100	0.0100	0.0100
3			0.0100	0.0100	0.0100	0.0100	0.0100	0.0100	0.0100	0.0100	0.0100
4a		x	0.0100	0.0100	0.0100	0.0100	0.0100	0.0100	0.0100	0.0100	0.0100
4b			0.0100	0.0100	0.0100	0.0100	0.0100	0.0100	0.0100	0.0100	0.0100
5a			0.0100	0.0100	0.0100	0.0100	0.0099	0.0100	0.0100	0.0100	0.0100
5b			0.0100	0.0100	0.0100	0.0100	0.0099	0.0100	0.0100	0.0100	0.0100
6a			0.0100	0.0100	0.0100	0.0100	0.0100	0.0100	0.0100	0.0100	0.0100
6b			0.0100	0.0100	0.0100	0.0100	0.0100	0.0100	0.0100	0.0100	0.0100
7			0.0100	0.0100	0.0100	0.0100	0.0100	0.0100	0.0100	0.0100	0.0100
8			0.0100	0.0100	0.0100	0.0100	0.0100	0.0100	0.0100	0.0100	0.0100
9a			0.0100	0.0100	0.0100	0.0100	0.0100	0.0100	0.0100	0.0100	0.0100
9b	**5**		0.0100	0.0100	0.0100	0.0100	0.0100	0.0100	0.0100	0.0100	0.0100
10			0.0100	0.0100	0.0100	0.0100	0.0100	0.0100	0.0100	0.0100	0.0100
11			0.0100	0.0100	0.0100	0.0100	0.0100	0.0100	0.0100	0.0100	0.0100
12a			0.0100	0.0100	0.0100	0.0100	0.0100	0.0100	0.0100	0.0100	0.0100
12b			0.0100	0.0100	0.0100	0.0100	0.0100	0.0100	0.0100	0.0100	0.0100
13a			0.0100	0.0100	0.0100	0.0100	0.0100	0.0100	0.0100	0.0100	0.0100
13b			0.0100	0.0100	0.0100	0.0100	0.0100	0.0100	0.0100	0.0100	0.0100
14a			0.0100	0.0100	0.0100	0.0100	0.0100	0.0100	0.0100	0.0100	0.0100
14b			0.0100	0.0100	0.0100	0.0100	0.0100	0.0100	0.0100	0.0100	0.0100
15a			0.0100	0.0100	0.0100	0.0100	0.0100	0.0100	0.0100	0.0100	0.0100
15b			0.0100	0.0100	0.0100	0.0100	0.0100	0.0100	0.0100	0.0100	0.0100
16a			0.0100	0.0100	0.0100	0.0100	0.0100	0.0100	0.0100	0.0100	0.0100
17a			0.0100	0.0100	0.0100	0.0100	0.0100	0.0100	0.0100	0.0100	0.0100
17b			0.0100	0.0100	0.0100	0.0100	0.0100	0.0100	0.0100	0.0100	0.0100

Table B.37. Parametric analysis to define optimal values for $\sigma_{\text{init.}}$ and σ_0 for Bayesian analysis. Negative σ sensitivity is returned by varying $\sigma_{\text{init.}}$ and COV (α) minimization is based on Bayesian prior, σ_0.

9 Substructure							σ_0 **(Prior) = 0.1**				
Test	$\sigma_{\text{init.}}$	$-\sigma$					α				
1			0.0989	0.0864	0.0869	0.0920	0.0673	0.0898	0.0836	0.0850	0.0994
2a			0.1000	0.1033	0.1116	0.1109	0.1000	0.1025	0.0987	0.0975	0.1000
2b			0.1000	0.1030	0.0992	0.0967	0.0742	0.0925	0.0907	0.0938	0.0998
3			0.1000	0.1000	0.1055	0.1063	0.1023	0.1018	0.1003	0.0997	0.1000
4a			0.1000	0.1000	0.1000	0.1050	0.0770	0.0954	0.0899	0.0936	0.0999
4b			0.1000	0.1000	0.1000	0.1040	0.1099	0.1048	0.1033	0.1015	0.1001
5a			0.0991	0.0881	0.0886	0.0952	0.0793	0.1014	0.1013	0.1050	0.1000
5b			0.0998	0.0965	0.0947	0.0967	0.0735	0.0969	0.0984	0.1039	0.1000
6a			0.0999	0.0978	0.0968	0.0975	0.0798	0.0953	0.0937	0.0986	0.1000
6b			0.0999	0.0970	0.0953	0.0963	0.0896	0.0997	0.1017	0.1006	0.1000
7			0.0999	0.0976	0.0960	0.0969	0.0926	0.1003	0.1000	0.1000	0.1000
8		x	0.1006	0.0986	0.1089	0.1134	0.1093	0.1084	0.1055	0.0983	0.0998
9a			0.1005	0.1110	0.1209	0.1155	0.1158	0.1052	0.1038	0.1011	0.1000
9b	0.0001		0.1007	0.1137	0.1223	0.1156	0.1136	0.1045	0.1034	0.1012	0.1000
10			0.1001	0.0990	0.1011	0.1022	0.1004	0.1010	0.1014	0.1003	0.1000
11			0.0999	0.0961	0.0990	0.1014	0.1009	0.1005	0.1000	0.1000	0.1000
12a		x	0.1000	0.1063	0.1126	0.1125	0.1056	0.1040	0.1024	0.1006	0.1001
12b			0.1000	0.1025	0.1287	0.1243	0.1102	0.1025	0.0995	0.0995	0.1001
13a			0.1004	0.1065	0.1126	0.1139	0.1216	0.1109	0.1055	0.0869	0.0997
13b			0.1003	0.1063	0.1136	0.1148	0.1232	0.1126	0.1101	0.0941	0.1002
14a			0.1000	0.1005	0.0994	0.0991	0.0923	0.0955	0.0890	0.0828	0.0993
14b			0.1000	0.1021	0.1068	0.1080	0.1244	0.1148	0.1232	0.1252	0.1012
15a			0.1000	0.1000	0.1024	0.1031	0.1009	0.0980	0.0891	0.0772	0.0988
15b		x	0.1000	0.1000	0.1022	0.1043	0.1101	0.1060	0.1029	0.0920	0.0999
16a			0.1000	0.1000	0.1000	0.1016	0.1086	0.1051	0.1054	0.1017	0.1002
17a		x	0.1003	0.1064	0.1100	0.1087	0.1114	0.1069	0.1068	0.1045	0.1000
17b			0.1001	0.1027	0.1038	0.1033	0.0972	0.1008	0.0996	0.1040	0.1000

9 Substructure σ_0 **(Prior) = 0.1**

Test	$\sigma_{\text{init.}}$	$-\sigma$	α								
1			0.0989	0.0864	0.0869	0.0920	0.0673	0.0898	0.0836	0.0850	0.0994
2a			0.1000	0.1033	0.1116	0.1109	0.1000	0.1025	0.0987	0.0975	0.1000
2b			0.1000	0.1030	0.0992	0.0967	0.0742	0.0925	0.0907	0.0938	0.0998
3			0.1000	0.1000	0.1055	0.1063	0.1023	0.1018	0.1003	0.0997	0.1000
4a			0.1000	0.1000	0.1000	0.1050	0.0770	0.0954	0.0899	0.0936	0.0999
4b			0.1000	0.1000	0.1000	0.1040	0.1099	0.1048	0.1033	0.1015	0.1001
5a			0.0991	0.0881	0.0886	0.0952	0.0793	0.1014	0.1013	0.1050	0.1000
5b			0.0998	0.0965	0.0947	0.0967	0.0735	0.0969	0.0984	0.1039	0.1000
6a			0.0999	0.0978	0.0968	0.0975	0.0798	0.0953	0.0936	0.0986	0.1000
6b			0.0999	0.0970	0.0954	0.0963	0.0898	0.0997	0.1016	0.1006	0.1000
7			0.0999	0.0976	0.0960	0.0969	0.0926	0.1003	0.1000	0.1000	0.1000
8			0.1006	0.0986	0.1089	0.1134	0.1093	0.1084	0.1055	0.0983	0.0998
9a			0.1005	0.1110	0.1209	0.1155	0.1158	0.1052	0.1038	0.1011	0.1000
9b	**0.001**	x	0.1007	0.1137	0.1223	0.1156	0.1136	0.1045	0.1034	0.1012	0.1000
10			0.1001	0.0990	0.1011	0.1022	0.1004	0.1010	0.1013	0.1003	0.1000
11			0.0999	0.0960	0.0989	0.1015	0.1009	0.1005	0.1000	0.1000	0.1000
12a			0.1000	0.1063	0.1126	0.1125	0.1056	0.1040	0.1024	0.1006	0.1001
12b			0.1000	0.1025	0.1287	0.1243	0.1102	0.1025	0.0995	0.0995	0.1001
13a			0.1004	0.1065	0.1126	0.1139	0.1216	0.1109	0.1055	0.0869	0.0997
13b			0.1003	0.1063	0.1136	0.1148	0.1233	0.1126	0.1101	0.0941	0.1002
14a			0.1000	0.1005	0.0994	0.0991	0.0923	0.0955	0.0891	0.0829	0.0993
14b			0.1000	0.1021	0.1068	0.1080	0.1244	0.1148	0.1233	0.1252	0.1012
15a			0.1000	0.1000	0.1024	0.1031	0.1009	0.0980	0.0891	0.0772	0.0988
15b			0.1000	0.1000	0.1022	0.1043	0.1101	0.1060	0.1029	0.0920	0.0999
16a		x	0.1000	0.1000	0.1000	0.1016	0.1085	0.1050	0.1053	0.1017	0.1002
17a			0.1003	0.1064	0.1100	0.1087	0.1114	0.1069	0.1068	0.1045	0.1000
17b			0.1001	0.1027	0.1038	0.1033	0.0972	0.1008	0.0996	0.1040	0.1000

9 Substructure σ_0 **(Prior) = 0.1**

Test	$\sigma_{\text{init.}}$	$-\sigma$	α								
1			0.0989	0.0864	0.0869	0.0920	0.0673	0.0898	0.0836	0.0850	0.0994
2a		x	0.1000	0.1033	0.1116	0.1109	0.1000	0.1025	0.0987	0.0975	0.1000
2b		x	0.1000	0.1030	0.0992	0.0967	0.0742	0.0925	0.0907	0.0938	0.0998
3		x	0.1000	0.1000	0.1055	0.1063	0.1023	0.1018	0.1003	0.0997	0.1000
4a			0.1000	0.1000	0.1000	0.1050	0.0770	0.0954	0.0899	0.0936	0.0999
4b		x	0.1000	0.1000	0.1000	0.1040	0.1099	0.1048	0.1033	0.1015	0.1001
5a			0.0991	0.0881	0.0886	0.0952	0.0793	0.1014	0.1013	0.1050	0.1000
5b			0.0998	0.0965	0.0947	0.0967	0.0735	0.0969	0.0984	0.1039	0.1000
6a			0.0999	0.0978	0.0968	0.0975	0.0798	0.0953	0.0936	0.0986	0.1000
6b		x	0.0999	0.0970	0.0954	0.0963	0.0898	0.0997	0.1016	0.1006	0.1000
7		x	0.0999	0.0976	0.0960	0.0969	0.0926	0.1003	0.1000	0.1000	0.1000
8		x	0.1006	0.0986	0.1089	0.1134	0.1093	0.1084	0.1055	0.0983	0.0998
9a		x	0.1005	0.1110	0.1209	0.1155	0.1158	0.1052	0.1038	0.1011	0.1000
9b	0.01	x	0.1007	0.1137	0.1223	0.1156	0.1136	0.1045	0.1034	0.1012	0.1000
10		x	0.1001	0.0990	0.1011	0.1022	0.1004	0.1010	0.1013	0.1003	0.1000
11		x	0.0999	0.0960	0.0989	0.1015	0.1009	0.1005	0.1000	0.1000	0.1000
12a			0.1000	0.1063	0.1126	0.1125	0.1056	0.1040	0.1024	0.1006	0.1001
12b			0.1000	0.1025	0.1287	0.1243	0.1102	0.1025	0.0995	0.0995	0.1001
13a		x	0.1004	0.1065	0.1126	0.1139	0.1216	0.1109	0.1055	0.0869	0.0997
13b		x	0.1003	0.1063	0.1136	0.1148	0.1232	0.1126	0.1101	0.0941	0.1002
14a		x	0.1000	0.1005	0.0994	0.0991	0.0923	0.0955	0.0891	0.0829	0.0993
14b		x	0.1000	0.1021	0.1068	0.1080	0.1244	0.1148	0.1233	0.1252	0.1012
15a		x	0.1000	0.1000	0.1024	0.1031	0.1009	0.0980	0.0891	0.0772	0.0988
15b			0.1000	0.1000	0.1022	0.1043	0.1101	0.1060	0.1029	0.0920	0.0999
16a		x	0.1000	0.1000	0.1000	0.1016	0.1085	0.1050	0.1053	0.1017	0.1002
17a			0.1003	0.1064	0.1100	0.1087	0.1114	0.1069	0.1068	0.1045	0.1000
17b			0.1001	0.1027	0.1038	0.1033	0.0972	0.1008	0.0996	0.1040	0.1000

9 Substructure σ_0 **(Prior) = 0.1**

Test	$\sigma_{\text{init.}}$	$-\sigma$	α								
1			0.0989	0.0864	0.0869	0.0920	0.0673	0.0898	0.0836	0.0850	0.0994
2a			0.1000	0.1033	0.1116	0.1109	0.1000	0.1025	0.0987	0.0975	0.1000
2b			0.1000	0.1030	0.0992	0.0967	0.0742	0.0925	0.0907	0.0938	0.0998
3			0.1000	0.1000	0.1055	0.1063	0.1023	0.1018	0.1003	0.0997	0.1000
4a			0.1000	0.1000	0.1000	0.1050	0.0770	0.0954	0.0899	0.0936	0.0999
4b		x	0.1000	0.1000	0.1000	0.1040	0.1099	0.1048	0.1033	0.1015	0.1001
5a			0.0991	0.0881	0.0886	0.0952	0.0793	0.1014	0.1013	0.1050	0.1000
5b		x	0.0998	0.0965	0.0947	0.0967	0.0735	0.0969	0.0984	0.1039	0.1000
6a			0.0999	0.0978	0.0968	0.0975	0.0798	0.0953	0.0936	0.0986	0.1000
6b			0.0999	0.0970	0.0954	0.0963	0.0898	0.0997	0.1016	0.1006	0.1000
7			0.0999	0.0976	0.0960	0.0969	0.0926	0.1003	0.1000	0.1000	0.1000
8			0.1006	0.0986	0.1089	0.1134	0.1093	0.1084	0.1055	0.0983	0.0998
9a			0.1005	0.1110	0.1209	0.1155	0.1158	0.1052	0.1038	0.1011	0.1000
9b	**0.1**		0.1007	0.1137	0.1223	0.1156	0.1136	0.1045	0.1034	0.1012	0.1000
10			0.1001	0.0990	0.1011	0.1022	0.1004	0.1010	0.1013	0.1003	0.1000
11			0.0999	0.0960	0.0989	0.1015	0.1009	0.1005	0.1000	0.1000	0.1000
12a			0.1000	0.1063	0.1126	0.1125	0.1056	0.1040	0.1024	0.1006	0.1001
12b			0.1000	0.1025	0.1287	0.1243	0.1102	0.1025	0.0995	0.0995	0.1001
13a			0.1004	0.1065	0.1126	0.1139	0.1216	0.1109	0.1055	0.0869	0.0997
13b			0.1003	0.1063	0.1136	0.1148	0.1232	0.1126	0.1101	0.0941	0.1002
14a			0.1000	0.1005	0.0994	0.0991	0.0923	0.0955	0.0891	0.0829	0.0993
14b			0.1000	0.1021	0.1068	0.1080	0.1244	0.1148	0.1233	0.1252	0.1012
15a			0.1000	0.1000	0.1024	0.1031	0.1009	0.0980	0.0891	0.0772	0.0988
15b			0.1000	0.1000	0.1022	0.1043	0.1101	0.1060	0.1029	0.0920	0.0999
16a			0.1000	0.1000	0.1000	0.1016	0.1085	0.1050	0.1053	0.1017	0.1002
17a			0.1003	0.1064	0.1100	0.1087	0.1114	0.1069	0.1068	0.1045	0.1000
17b			0.1001	0.1027	0.1038	0.1033	0.0972	0.1008	0.0996	0.1040	0.1000

9 Substructure σ_0 **(Prior) = 0.1**

Test	$\sigma_{\text{init.}}$	$-\sigma$	α								
1			0.0989	0.0864	0.0869	0.0920	0.0673	0.0898	0.0836	0.0850	0.0994
2a			0.1000	0.1033	0.1116	0.1109	0.1000	0.1025	0.0987	0.0975	0.1000
2b			0.1000	0.1030	0.0992	0.0967	0.0742	0.0925	0.0907	0.0938	0.0998
3			0.1000	0.1000	0.1055	0.1063	0.1023	0.1018	0.1003	0.0997	0.1000
4a		x	0.1000	0.1000	0.1000	0.1050	0.0770	0.0954	0.0899	0.0936	0.0999
4b			0.1000	0.1000	0.1000	0.1040	0.1099	0.1048	0.1033	0.1015	0.1001
5a		x	0.0991	0.0881	0.0886	0.0952	0.0793	0.1014	0.1013	0.1050	0.1000
5b			0.0998	0.0965	0.0947	0.0967	0.0735	0.0969	0.0984	0.1039	0.1000
6a			0.0999	0.0978	0.0968	0.0975	0.0798	0.0953	0.0936	0.0986	0.1000
6b			0.0999	0.0970	0.0954	0.0963	0.0898	0.0997	0.1016	0.1006	0.1000
7			0.0999	0.0976	0.0960	0.0969	0.0926	0.1003	0.1000	0.1000	0.1000
8			0.1006	0.0986	0.1089	0.1134	0.1093	0.1084	0.1055	0.0983	0.0998
9a			0.1005	0.1110	0.1209	0.1155	0.1158	0.1052	0.1038	0.1011	0.1000
9b	**5**		0.1007	0.1137	0.1223	0.1156	0.1136	0.1045	0.1034	0.1012	0.1000
10			0.1001	0.0990	0.1011	0.1022	0.1004	0.1010	0.1013	0.1003	0.1000
11			0.0999	0.0960	0.0989	0.1015	0.1009	0.1005	0.1000	0.1000	0.1000
12a			0.1000	0.1063	0.1126	0.1125	0.1056	0.1040	0.1024	0.1006	0.1001
12b			0.1000	0.1025	0.1287	0.1243	0.1102	0.1025	0.0995	0.0995	0.1001
13a			0.1004	0.1065	0.1126	0.1139	0.1216	0.1109	0.1055	0.0869	0.0997
13b			0.1003	0.1063	0.1136	0.1148	0.1232	0.1126	0.1101	0.0941	0.1002
14a			0.1000	0.1005	0.0994	0.0991	0.0923	0.0955	0.0891	0.0829	0.0993
14b			0.1000	0.1021	0.1068	0.1080	0.1244	0.1148	0.1233	0.1252	0.1012
15a			0.1000	0.1000	0.1024	0.1031	0.1009	0.0980	0.0891	0.0772	0.0988
15b			0.1000	0.1000	0.1022	0.1043	0.1101	0.1060	0.1029	0.0920	0.0999
16a			0.1000	0.1000	0.1000	0.1016	0.1085	0.1050	0.1053	0.1017	0.1002
17a		x	0.1003	0.1064	0.1100	0.1087	0.1114	0.1069	0.1068	0.1045	0.1000
17b			0.1001	0.1027	0.1038	0.1033	0.0972	0.1008	0.0996	0.1040	0.1000

Table B.38. Parametric analysis to define optimal values for $\sigma_{\text{init.}}$ and σ_0 for Bayesian analysis. Negative σ sensitivity is returned by varying $\sigma_{\text{init.}}$ and COV (α) minimization is based on Bayesian prior, σ_0.

9 Substructure							σ_0 **(Prior) = 1**				
Test	$\sigma_{\text{init.}}$	$-\sigma$					α				
1			0.5396	0.1872	-1.7695	0.2889	3.0851	0.4804	0.4143	0.3628	0.8302
2a		x	1.0000	0.4047	-2.0125	1.7609	0.8776	0.5396	0.4616	0.5118	0.9396
2b		x	1.0000	-0.4805	1.4762	0.5451	0.4496	0.6353	0.5382	0.5640	0.9600
3			1.0000	1.0426	-0.3289	-0.9994	0.3880	0.5803	0.5633	0.5407	0.9509
4a			1.0000	1.0000	1.0000	0.5960	37.2252	0.3320	0.3609	-8.4929	0.8599
4b			1.0000	1.0000	1.0000	-1.0130	-0.8717	0.4365	0.3652	0.5485	0.9862
5a			0.5058	0.2117	-0.9085	0.1971	-2.0209	0.3769	0.5100	-0.9450	1.0000
5b			0.7913	0.4622	1.2656	0.5036	0.7125	0.3784	0.5056	-0.4849	1.0000
6a		x	0.8341	0.3436	1.0596	1.1111	1.2911	0.7119	0.1867	0.4535	1.0000
6b			0.9528	0.5614	0.5539	0.6265	0.3932	4.8751	-0.6853	3.4009	1.0000
7			0.9895	0.4913	0.3455	0.4877	2.0802	6.6347	1.0000	1.0000	1.0000
8			2.1195	0.2167	0.8901	-0.8313	0.2086	-0.9745	-1.1035	0.1501	0.7287
9a		x	1.0419	0.0979	-0.2855	-0.2942	0.2062	0.4602	0.5030	0.7674	1.0000
9b	**0.0001**		1.1241	0.1464	-0.4058	-0.4046	0.2201	0.4547	0.5751	2.2445	1.0000
10			0.9219	0.3659	-30.2497	4.1950	0.4621	1.0701	4.2771	1.3762	1.0000
11			0.8742	0.2466	-93.4909	-12.3517	0.9983	1.0962	1.0000	1.0000	1.0000
12a			1.0000	0.4017	0.9209	-1.0011	0.4356	0.7288	0.6482	0.5281	0.9759
12b			1.0000	0.0619	-2.4355	-0.1368	0.1031	0.2628	0.5697	-5.7912	0.6791
13a			1.1234	0.3658	0.9248	-1.2837	0.9941	0.7521	0.8718	0.2020	0.6781
13b			0.9971	0.2538	2.9882	-0.7129	0.5165	0.6499	0.8654	0.2466	0.6791
14a			1.0000	2.3912	0.8684	0.9563	2.3853	1.0930	0.7045	0.2225	0.8413
14b		x	1.0000	0.3318	-4.1907	-1.0676	14.1443	0.8206	0.3789	-1.4217	2.4513
15a			1.0000	1.0039	9.5142	-2.3683	-0.7525	0.6165	0.4799	0.1428	0.5180
15b			1.0000	0.9918	0.6748	1.4896	-2.1218	0.9297	0.6870	0.2565	0.7246
16a			1.0000	1.0000	1.0000	-1.6007	-0.1522	1.2730	0.3070	0.2123	0.9673
17a			0.9681	1.0685	-1.5350	-4.2608	0.5447	0.5847	0.5525	1.0519	1.0000
17b			0.9744	0.9584	-6.1646	10.4795	0.4835	0.5317	0.3728	-0.7650	1.0000

9 Substructure σ_0 **(Prior) = 1**

Test	$\sigma_{\text{init.}}$	$-\sigma$	α								
1			0.5396	0.1872	-1.7684	0.2889	3.0869	0.4803	0.4142	0.3628	0.8301
2a			1.0000	0.4047	-2.0123	1.7609	0.8776	0.5396	0.4616	0.5118	0.9396
2b			1.0000	-0.4805	1.4761	0.5451	0.4496	0.6353	0.5382	0.5640	0.9600
3			1.0000	1.0426	-0.3289	-0.9994	0.3880	0.5803	0.5633	0.5407	0.9509
4a		x	1.0000	1.0000	1.0000	0.5959	37.4591	0.3320	0.3609	-8.4845	0.8598
4b			1.0000	1.0000	1.0000	-1.0130	-0.8717	0.4365	0.3652	0.5485	0.9862
5a			0.5058	0.2117	-0.9084	0.1971	-2.0206	0.3769	0.5100	-0.9449	1.0000
5b			0.7911	0.4620	1.2666	0.5033	0.7129	0.3782	0.5053	-0.4843	1.0000
6a			0.8341	0.3436	1.0595	1.1111	1.2910	0.7118	0.1868	0.4535	1.0000
6b			0.9528	0.5615	0.5539	0.6265	0.3932	4.8735	-0.6855	3.3995	1.0000
7		x	0.9895	0.4913	0.3454	0.4876	2.0811	6.6416	1.0000	1.0000	1.0000
8			2.1196	0.2167	0.8901	-0.8313	0.2086	-0.9745	-1.1035	0.1501	0.7287
9a			1.0420	0.0979	-0.2854	-0.2941	0.2062	0.4602	0.5031	0.7674	1.0000
9b	**0.001**		1.1242	0.1463	-0.4057	-0.4045	0.2200	0.4547	0.5751	2.2460	1.0000
10			0.9218	0.3657	-29.2945	4.2067	0.4618	1.0701	4.2918	1.3767	1.0000
11			0.8739	0.2459	-63.6063	-11.8274	0.9955	1.0961	1.0000	1.0000	1.0000
12a			1.0000	0.4017	0.9209	-1.0012	0.4356	0.7288	0.6482	0.5281	0.9759
12b		x	1.0000	0.0619	-2.4364	-0.1368	0.1031	0.2628	0.5697	-5.7915	0.6791
13a			1.1234	0.3657	0.9247	-1.2830	0.9939	0.7521	0.8718	0.2020	0.6780
13b			0.9971	0.2538	2.9882	-0.7129	0.5165	0.6499	0.8654	0.2466	0.6791
14a			1.0000	2.3912	0.8684	0.9563	2.3853	1.0930	0.7045	0.2225	0.8413
14b		x	1.0000	0.3318	-4.1896	-1.0675	14.1300	0.8206	0.3789	-1.4216	2.4517
15a			1.0000	1.0039	9.5148	-2.3682	-0.7525	0.6165	0.4799	0.1428	0.5180
15b			1.0000	0.9918	0.6750	1.4896	-2.1230	0.9298	0.6871	0.2565	0.7247
16a			1.0000	1.0000	1.0000	-1.5990	-0.1521	1.2722	0.3068	0.2123	0.9673
17a			0.9681	1.0685	-1.5350	-4.2609	0.5447	0.5847	0.5525	1.0519	1.0000
17b			0.9744	0.9585	-6.1662	10.4750	0.4835	0.5317	0.3728	-0.7650	1.0000

9 Substructure σ_0 **(Prior) = 1**

Test	$\sigma_{\text{init.}}$	$-\sigma$					α				
1			0.5396	0.1872	-1.7685	0.2889	3.0867	0.4803	0.4142	0.3628	0.8302
2a		x	1.0000	0.4047	-2.0123	1.7609	0.8776	0.5396	0.4616	0.5118	0.9396
2b		x	1.0000	-0.4805	1.4761	0.5451	0.4496	0.6353	0.5382	0.5640	0.9600
3		x	1.0000	1.0426	-0.3289	-0.9994	0.3880	0.5803	0.5633	0.5407	0.9509
4a			1.0000	1.0000	1.0000	0.5959	37.4841	0.3320	0.3609	-8.4837	0.8598
4b			1.0000	1.0000	1.0000	-1.0130	-0.8717	0.4365	0.3652	0.5485	0.9862
5a			0.5058	0.2117	-0.9085	0.1971	-2.0208	0.3769	0.5100	-0.9450	1.0000
5b			0.7911	0.4620	1.2666	0.5033	0.7129	0.3782	0.5053	-0.4843	1.0000
6a		x	0.8341	0.3436	1.0595	1.1112	1.2910	0.7118	0.1868	0.4535	1.0000
6b		x	0.9528	0.5615	0.5539	0.6266	0.3932	4.8735	-0.6855	3.3995	1.0000
7		x	0.9895	0.4913	0.3454	0.4876	2.0811	6.6415	1.0000	1.0000	1.0000
8			2.1196	0.2167	0.8901	-0.8313	0.2086	-0.9745	-1.1035	0.1501	0.7287
9a		x	1.0420	0.0979	-0.2854	-0.2941	0.2062	0.4602	0.5031	0.7674	1.0000
9b	0.01	x	1.1242	0.1464	-0.4057	-0.4045	0.2200	0.4547	0.5751	2.2458	1.0000
10		x	0.9218	0.3657	-29.3153	4.2065	0.4618	1.0701	4.2915	1.3767	1.0000
11		x	0.8739	0.2459	-63.3558	-11.8212	0.9955	1.0961	1.0000	1.0000	1.0000
12a			1.0000	0.4017	0.9209	-1.0011	0.4356	0.7288	0.6482	0.5281	0.9759
12b			1.0000	0.0619	-2.4347	-0.1368	0.1031	0.2628	0.5697	-5.7908	0.6791
13a			1.1235	0.3657	0.9246	-1.2825	0.9938	0.7520	0.8719	0.2020	0.6780
13b			0.9971	0.2538	2.9882	-0.7129	0.5165	0.6499	0.8654	0.2466	0.6791
14a		x	1.0000	2.3912	0.8684	0.9563	2.3852	1.0930	0.7045	0.2225	0.8413
14b			1.0000	0.3318	-4.1903	-1.0676	14.1395	0.8206	0.3789	-1.4216	2.4515
15a		x	1.0000	1.0039	9.5150	-2.3682	-0.7525	0.6165	0.4799	0.1428	0.5180
15b			1.0000	0.9918	0.6750	1.4896	-2.1230	0.9298	0.6871	0.2565	0.7247
16a		x	1.0000	1.0000	1.0000	-1.5990	-0.1521	1.2722	0.3068	0.2123	0.9673
17a			0.9681	1.0685	-1.5350	-4.2609	0.5447	0.5847	0.5525	1.0519	1.0000
17b			0.9744	0.9585	-6.1659	10.4759	0.4835	0.5317	0.3728	-0.7650	1.0000

9 Substructure σ_0 **(Prior) = 1**

Test	$\sigma_{\text{init.}}$	$-\sigma$	α								
1			0.5396	0.1872	-1.7685	0.2889	3.0867	0.4803	0.4142	0.3628	0.8302
2a		x	1.0000	0.4047	-2.0124	1.7609	0.8776	0.5396	0.4616	0.5118	0.9396
2b			1.0000	-0.4805	1.4761	0.5451	0.4496	0.6353	0.5382	0.5640	0.9600
3		x	1.0000	1.0426	-0.3288	-0.9993	0.3879	0.5803	0.5633	0.5407	0.9509
4a			1.0000	1.0000	1.0000	0.5959	37.4784	0.3320	0.3609	-8.4839	0.8598
4b			1.0000	1.0000	1.0000	-1.0130	-0.8717	0.4365	0.3652	0.5485	0.9862
5a			0.5058	0.2117	-0.9085	0.1971	-2.0207	0.3769	0.5100	-0.9450	1.0000
5b			0.7911	0.4620	1.2665	0.5034	0.7129	0.3782	0.5053	-0.4843	1.0000
6a			0.8341	0.3436	1.0595	1.1111	1.2910	0.7118	0.1868	0.4535	1.0000
6b			0.9528	0.5615	0.5539	0.6266	0.3932	4.8735	-0.6855	3.3995	1.0000
7			0.9895	0.4913	0.3454	0.4876	2.0811	6.6415	1.0000	1.0000	1.0000
8			2.1191	0.2167	0.8902	-0.8316	0.2086	-0.9747	-1.1038	0.1502	0.7287
9a			1.0420	0.0979	-0.2854	-0.2941	0.2062	0.4602	0.5031	0.7674	1.0000
9b	**0.1**	x	1.1243	0.1463	-0.4057	-0.4044	0.2200	0.4547	0.5751	2.2464	1.0000
10			0.9218	0.3657	-29.3153	4.2065	0.4618	1.0701	4.2915	1.3767	1.0000
11			0.8739	0.2459	-63.3846	-11.8219	0.9955	1.0961	1.0000	1.0000	1.0000
12a			1.0000	0.4018	0.9213	-1.0021	0.4358	0.7289	0.6482	0.5282	0.9759
12b			1.0000	0.0619	-2.4352	-0.1368	0.1031	0.2628	0.5697	-5.7910	0.6791
13a			1.1234	0.3657	0.9247	-1.2830	0.9939	0.7521	0.8718	0.2020	0.6780
13b			0.9971	0.2538	2.9881	-0.7129	0.5165	0.6499	0.8654	0.2466	0.6791
14a			1.0000	2.3912	0.8684	0.9563	2.3853	1.0930	0.7045	0.2225	0.8413
14b			1.0000	0.3318	-4.1903	-1.0676	14.1391	0.8206	0.3789	-1.4216	2.4515
15a			1.0000	1.0039	9.5146	-2.3682	-0.7525	0.6165	0.4799	0.1428	0.5180
15b			1.0000	0.9918	0.6750	1.4896	-2.1230	0.9298	0.6871	0.2565	0.7247
16a		x	1.0000	1.0000	1.0000	-1.5990	-0.1521	1.2722	0.3068	0.2123	0.9673
17a			0.9681	1.0685	-1.5350	-4.2609	0.5447	0.5847	0.5525	1.0519	1.0000
17b			0.9745	0.9587	-6.1749	10.4500	0.4835	0.5317	0.3728	-0.7654	1.0000

9 Substructure σ_0 **(Prior) = 1**

Test	$\sigma_{\text{init.}}$	$-\sigma$					α				
1			0.5396	0.1872	-1.7688	0.2889	3.0862	0.4803	0.4142	0.3628	0.8302
2a			1.0000	0.4047	-2.0124	1.7609	0.8776	0.5396	0.4616	0.5118	0.9396
2b			1.0000	-0.4805	1.4761	0.5451	0.4496	0.6353	0.5382	0.5640	0.9600
3			1.0000	1.0426	-0.3289	-0.9994	0.3880	0.5803	0.5633	0.5407	0.9509
4a		x	1.0000	1.0000	1.0000	0.5959	37.5233	0.3320	0.3609	-8.4823	0.8598
4b			1.0000	1.0000	1.0000	-1.0130	-0.8717	0.4365	0.3652	0.5485	0.9862
5a		x	0.5058	0.2117	-0.9085	0.1971	-2.0207	0.3769	0.5100	-0.9450	1.0000
5b			0.7911	0.4620	1.2665	0.5034	0.7129	0.3782	0.5053	-0.4843	1.0000
6a			0.8341	0.3436	1.0595	1.1111	1.2910	0.7118	0.1868	0.4535	1.0000
6b			0.9528	0.5615	0.5539	0.6265	0.3932	4.8737	-0.6855	3.3997	1.0000
7			0.9895	0.4913	0.3454	0.4876	2.0810	6.6414	1.0000	1.0000	1.0000
8			2.1195	0.2167	0.8901	-0.8313	0.2086	-0.9745	-1.1035	0.1501	0.7287
9a			1.0420	0.0979	-0.2854	-0.2941	0.2062	0.4602	0.5031	0.7674	1.0000
9b	5		1.1242	0.1463	-0.4057	-0.4045	0.2200	0.4547	0.5751	2.2460	1.0000
10			0.9218	0.3657	-29.3073	4.2066	0.4618	1.0701	4.2916	1.3767	1.0000
11			0.8739	0.2459	-62.9946	-11.8122	0.9954	1.0961	1.0000	1.0000	1.0000
12a		x	1.0000	0.4017	0.9209	-1.0012	0.4356	0.7288	0.6482	0.5281	0.9759
12b		x	1.0000	0.0619	-2.4351	-0.1368	0.1031	0.2628	0.5697	-5.7910	0.6791
13a			1.1234	0.3657	0.9247	-1.2830	0.9939	0.7521	0.8718	0.2020	0.6780
13b		x	0.9971	0.2538	2.9881	-0.7129	0.5165	0.6499	0.8654	0.2466	0.6791
14a			1.0000	2.3912	0.8684	0.9563	2.3853	1.0930	0.7045	0.2225	0.8413
14b		x	1.0000	0.3318	-4.1903	-1.0676	14.1387	0.8206	0.3789	-1.4216	2.4515
15a			1.0000	1.0039	9.5136	-2.3684	-0.7525	0.6165	0.4799	0.1428	0.5180
15b			1.0000	0.9918	0.6750	1.4896	-2.1230	0.9298	0.6871	0.2565	0.7247
16a			1.0000	1.0000	1.0000	-1.5990	-0.1521	1.2722	0.3068	0.2123	0.9673
17a		x	0.9681	1.0685	-1.5350	-4.2609	0.5447	0.5847	0.5525	1.0519	1.0000
17b			0.9744	0.9585	-6.1659	10.4758	0.4835	0.5317	0.3728	-0.7650	1.0000

Appendix C. IDENTIFIED RESULT PERMUTATIONS

Table C.39. 27x27 matrix of KL values from test pairings of data from "Uncorrected" for the 3 Substructure case. These values are compared against the cutoff value found in Section 6.4 to determine flexural rigidity identification agreement.

$628/702 \geq KLCutoff$ | 3 Substructure | $KLCutoff = 1.112$

Tests	1	2a	2b	3	4a	4b	5a	5b	6a	6b	7	8	9a
1	-	211.109	5.091	134.492	103.167	210.600	108.208	36.556	7.345	13.963	16.184	266.745	345.594
2a	39.462	-	41.895	2.722	3.788	2.224	5.571	15.326	34.484	37.705	38.452	1.374	3.960
2b	2.332	25.025	-	16.408	14.668	28.183	18.148	5.629	0.531	1.969	1.939	31.940	38.198
3	7.871	1.025	7.811	-	0.924	1.005	2.315	2.657	5.757	6.145	6.102	2.102	3.575
4a	35.647	3.949	53.296	2.704	-	11.120	3.757	11.355	38.947	37.489	39.007	10.420	15.543
4b	11.511	1.552	13.252	0.994	1.891	-	2.383	5.432	10.272	9.781	9.789	1.938	3.729
5a	98.476	42.710	103.962	16.503	7.642	36.486	-	21.821	81.704	114.869	116.850	64.485	117.496
5b	11.499	37.064	10.939	16.575	12.154	32.380	7.649	-	7.118	13.590	14.432	49.186	72.846
6a	1.829	16.977	0.366	8.930	8.332	14.987	8.013	2.123	-	1.241	1.122	21.125	28.351
6b	2.804	9.996	1.395	5.157	5.786	7.765	4.979	1.805	0.919	-	0.058	11.861	15.585
7	2.446	8.079	1.225	4.041	4.733	6.201	4.511	1.741	0.718	0.057	-	9.675	12.728
8	128.914	3.251	97.194	18.497	28.346	13.843	33.318	52.552	92.204	120.041	121.382	-	7.456
9a	44.694	4.035	33.031	10.604	15.514	10.392	20.595	23.478	32.207	42.243	41.906	2.346	-
9b	49.195	4.872	35.862	12.205	17.639	12.306	23.179	25.889	35.268	46.490	46.156	2.984	0.100
10	4.729	3.550	1.802	1.061	2.323	2.657	2.958	1.043	1.313	2.270	2.167	4.628	7.367
11	3.177	4.250	1.330	1.389	2.292	2.778	2.854	1.006	0.712	1.060	0.915	5.444	8.526
12a	43.419	0.756	35.324	4.893	8.364	4.134	10.740	17.343	31.953	39.863	40.250	0.565	2.421
12b	101.642	5.760	87.206	19.744	26.806	14.299	31.361	49.304	80.635	96.690	97.471	2.404	0.854
13a	135.419	11.571	122.761	22.617	32.506	10.043	18.915	47.636	109.212	97.743	104.970	5.156	5.246
13b	192.989	26.805	176.136	41.920	57.442	20.705	32.712	75.230	158.590	141.039	150.964	14.347	11.509
14a	1.644	10.737	0.619	7.808	6.437	13.719	12.900	5.497	0.688	2.440	1.822	14.992	18.190
14b	657.629	341.724	638.181	366.842	409.994	291.909	316.002	430.802	602.422	543.947	565.083	292.766	275.743
15a	2.631	6.499	2.613	5.417	3.672	10.708	12.485	6.060	2.057	4.560	3.710	10.660	13.199
15b	20.461	2.697	18.720	1.800	3.975	0.617	1.877	4.815	15.426	10.793	12.126	2.372	4.248
16a	8.037	3.103	6.552	1.098	2.780	0.927	1.605	1.996	5.116	3.304	3.639	3.247	4.907
17a	30.612	2.302	26.745	4.041	7.292	2.175	5.878	11.274	23.454	23.261	24.246	1.332	1.491
17b	11.266	3.264	8.145	1.005	2.415	3.019	2.129	1.400	6.485	5.933	6.558	4.762	7.472

$628/702 \geq KLCutoff$						3 Substructure				$KLCutoff = 1.112$				
Tests	9b	10	11	12a	12b	13a	13b	14a	14b	15a	15b	16a	17a	17b
1	319.895	58.643	42.121	230.880	327.098	389.205	429.569	10.226	1487.700	42.893	180.244	135.261	300.112	89.532
2a	3.423	14.223	19.049	0.626	2.536	6.261	9.569	39.736	137.991	16.544	2.514	6.099	2.945	7.254
2b	34.706	6.382	4.831	25.989	36.783	47.296	52.814	0.781	193.906	5.720	23.900	18.455	35.692	11.089
3	3.738	1.698	2.307	1.472	3.547	4.380	5.484	6.902	49.364	2.925	0.813	1.001	2.205	1.030
4a	12.297	14.773	18.472	5.709	11.915	27.445	36.626	46.164	333.018	14.379	7.340	7.825	15.527	5.570
4b	4.656	4.718	5.305	2.428	3.770	2.447	2.855	11.624	35.263	6.068	0.464	1.276	1.437	3.022
5a	104.569	27.015	42.312	50.250	111.000	137.535	147.923	101.129	838.018	29.857	24.943	20.653	73.019	10.199
5b	66.566	4.574	4.837	40.395	71.107	84.174	89.019	12.111	368.685	7.359	24.043	14.419	52.260	5.660
6a	26.817	2.716	1.658	18.036	28.441	31.955	33.287	0.655	112.952	4.045	12.191	8.242	21.520	5.082
6b	15.376	1.959	1.134	10.540	16.135	16.656	16.855	1.614	55.031	4.411	6.315	3.960	11.113	3.032
7	12.703	1.547	0.812	8.605	13.232	13.495	13.725	1.198	45.903	3.515	5.126	3.283	9.035	2.619
8	7.673	41.892	61.285	0.902	5.101	5.343	7.391	105.195	156.977	53.692	16.392	30.708	3.080	27.536
9a	0.099	17.685	23.906	1.744	0.442	2.172	2.501	35.006	29.563	20.932	11.427	16.682	2.608	14.655
9b	-	19.562	26.498	2.109	0.621	3.013	3.362	38.341	32.440	23.227	13.262	18.940	3.313	16.306
10	7.586	-	0.240	3.904	7.735	7.596	7.877	2.108	37.702	2.086	2.034	1.325	4.231	0.555
11	8.923	0.215	-	4.950	8.798	8.171	8.493	1.255	36.409	1.851	2.275	1.392	5.095	0.992
12a	2.206	13.646	19.827	-	1.905	3.644	5.082	36.629	82.823	17.833	4.753	9.144	1.348	8.510
12b	0.950	41.704	55.181	3.043	-	2.033	3.461	89.505	102.017	48.681	17.183	28.770	3.471	29.376
13a	6.808	50.953	64.788	8.663	4.616	-	2.631	131.789	241.452	84.723	9.740	18.889	2.600	25.339
13b	14.692	80.509	99.139	20.709	13.804	2.946	-	188.697	220.768	129.321	20.205	31.993	5.141	43.775
14a	17.196	4.144	3.005	12.564	16.245	20.841	26.187	-	114.861	1.378	13.053	11.944	19.292	8.234
14b	292.774	449.599	482.527	320.058	300.887	238.548	190.009	661.346	-	570.522	291.680	310.690	235.191	360.867
15a	12.522	3.974	3.191	8.751	10.606	14.954	21.522	1.335	120.261	-	10.970	11.464	16.240	7.979
15b	5.013	5.600	7.018	2.785	4.573	2.659	3.714	20.175	77.481	14.198	-	0.710	1.579	1.732
16a	5.539	1.757	1.988	3.206	5.690	4.240	3.874	6.829	29.547	5.905	0.462	-	1.845	0.726
17a	1.965	10.264	13.589	1.469	2.025	1.524	1.584	27.810	52.447	17.006	2.149	4.143	-	5.372
17b	7.060	1.219	2.282	3.415	7.395	9.068	10.608	9.139	79.826	5.522	1.809	1.064	4.902	-

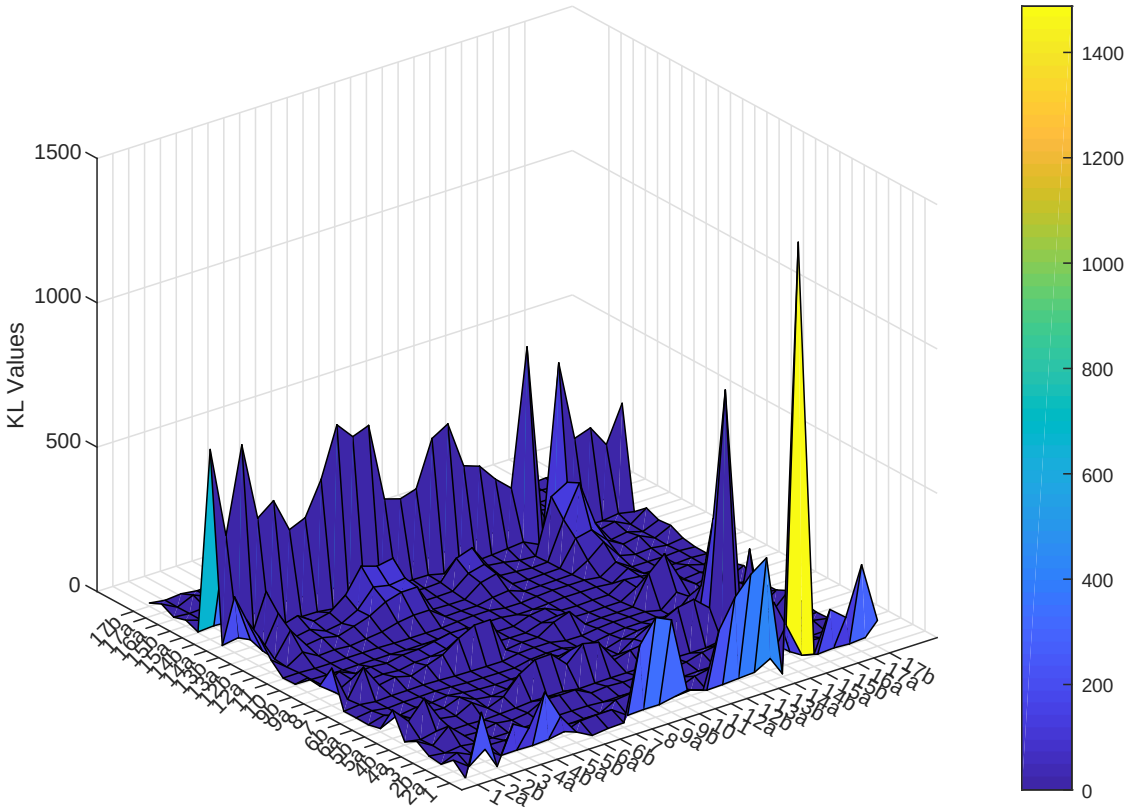

Fig. C.44. A graphical representation of the KL values found between pairing of the data from "Uncorrected" for the three-substructure case

Table C.40. 27x27 matrix of KL values from test pairings of data from "Uncorrected" for the 6 Substructure case. These values are compared against the cutoff value found in Section 6.44 to determine flexural rigidity identification agreement.

$638/702 \geq KLCutoff$ | 6 Substructure | $KLCutoff = 0.854$

Tests	1	2a	2b	3	4a	4b	5a	5b	6a	6b	7	8	9a
1	-	179.305	3.663	82.074	97.438	99.912	101.687	31.965	6.067	10.462	11.096	224.951	233.754
2a	36.646	-	36.393	4.840	3.235	4.212	4.452	13.255	30.200	31.072	31.535	1.181	2.144
2b	1.597	23.380	-	10.746	15.054	14.892	17.312	4.863	0.396	1.734	1.595	29.144	28.520
3	6.392	1.811	5.711	-	1.086	0.528	2.201	1.513	4.117	4.150	4.100	3.433	4.496
4a	37.728	2.617	46.765	3.271	-	2.572	3.211	11.179	36.013	29.353	30.202	6.764	7.795
4b	7.610	2.154	7.735	0.532	1.036	-	1.478	2.449	5.848	4.731	4.718	3.551	5.826
5a	99.599	27.587	97.743	9.772	6.112	9.318	-	21.946	77.477	94.924	96.016	44.633	60.528
5b	11.226	29.385	9.913	6.908	10.958	9.531	8.003	-	6.456	9.974	10.371	40.161	46.614
6a	1.483	15.993	0.303	5.715	8.845	7.538	8.861	2.103	-	1.213	1.030	20.389	22.782
6b	2.346	10.504	1.278	3.864	6.406	4.373	5.580	1.779	1.023	-	0.049	12.954	15.327
7	2.066	9.107	1.114	3.278	5.580	3.743	5.156	1.712	0.822	0.049	-	11.319	13.506
8	113.849	3.205	92.275	26.608	25.981	29.812	26.493	48.125	84.524	104.397	105.149	-	3.056
9a	36.600	3.040	28.656	11.217	12.945	14.176	15.340	18.623	26.780	34.613	34.355	1.497	-
9b	40.982	3.954	31.956	13.203	15.151	16.607	17.726	21.193	30.074	38.912	38.643	2.031	0.061
10	3.697	4.514	1.548	0.887	3.019	1.834	3.264	0.737	1.058	1.830	1.750	6.305	8.168
11	2.501	5.383	1.033	1.213	3.140	1.956	3.507	0.813	0.539	0.919	0.802	7.431	9.614
12a	38.174	0.676	31.794	7.000	7.623	8.604	8.535	14.849	28.054	34.499	34.736	0.768	1.513
12b	100.283	6.815	87.961	29.896	28.495	32.571	30.532	49.866	80.058	94.620	95.164	3.180	1.270
13a	107.635	8.353	99.113	25.475	22.498	18.738	13.457	40.327	88.269	75.497	79.983	4.050	8.326
13b	158.314	21.275	147.046	47.037	42.975	36.158	26.995	67.337	132.789	114.319	120.590	12.586	19.005
14a	1.313	12.218	0.407	5.954	7.951	8.632	11.989	4.202	0.493	1.834	1.387	16.151	16.013
14b	307.313	149.852	298.772	182.197	178.091	160.686	144.048	205.113	282.653	251.521	259.586	131.571	147.304
15a	1.986	8.014	1.478	3.795	5.003	6.414	10.167	3.613	1.087	2.659	2.129	11.624	11.259
15b	16.274	2.986	14.809	1.983	2.837	0.746	1.262	3.645	12.374	7.691	8.598	3.734	6.548
16a	6.145	3.934	4.921	1.050	2.673	0.674	1.725	1.320	3.890	1.964	2.202	5.045	7.356
17a	23.103	1.425	20.085	3.538	4.468	2.893	3.077	7.408	17.465	15.801	16.541	1.284	2.722
17b	9.382	3.628	6.989	0.607	2.425	1.269	2.323	0.997	5.539	4.473	4.914	5.662	6.819

638/702 $\geq$ $KLCutoff$					6 Substructure					$KLCutoff$ = 0.854				
Tests	9b	10	11	12a	12b	13a	13b	14a	14b	15a	15b	16a	17a	17b
1	227.727	36.750	25.249	176.268	259.302	290.046	344.081	6.519	1015.798	19.654	106.214	65.008	193.464	65.645
2a	2.548	14.764	19.102	0.672	2.583	3.926	7.825	35.382	96.335	20.667	4.404	9.615	1.458	7.485
2b	27.642	4.035	2.801	21.868	32.967	39.237	47.315	0.475	155.311	2.549	16.065	10.038	25.732	8.699
3	4.938	1.230	1.722	2.236	5.902	5.219	7.490	5.201	49.562	2.609	1.084	1.032	2.186	0.602
4a	8.294	16.511	19.939	4.222	7.533	15.572	25.130	41.455	222.389	21.327	3.482	6.281	6.474	6.224
4b	6.606	2.572	2.896	3.319	7.216	3.949	5.515	6.784	39.041	4.044	0.465	0.781	1.795	1.304
5a	59.392	30.714	45.885	28.386	76.176	70.935	92.405	96.994	471.243	45.198	8.301	19.966	25.745	11.349
5b	45.804	2.342	3.262	28.770	56.228	55.201	66.677	10.717	241.010	4.384	9.439	4.361	27.850	3.129
6a	22.800	1.741	0.931	15.822	27.033	25.850	30.208	0.501	93.043	1.575	8.106	4.564	15.518	4.270
6b	15.729	1.573	0.882	10.809	18.425	15.191	17.469	1.279	55.111	2.426	4.419	2.117	9.150	2.739
7	13.943	1.348	0.699	9.494	16.372	13.234	15.354	0.965	49.675	1.963	3.981	1.959	8.058	2.513
8	3.712	46.138	62.518	1.292	4.368	2.458	4.934	98.818	88.676	65.174	27.351	46.315	4.540	30.872
9a	0.060	16.179	21.161	1.257	0.756	3.215	4.095	30.490	32.869	21.439	14.076	19.400	4.365	13.100
9b	-	18.472	24.058	1.743	0.877	4.039	4.902	34.160	34.616	24.305	16.387	22.269	5.393	15.119
10	8.648	-	0.195	4.733	10.468	8.097	10.030	1.786	43.000	1.297	2.087	1.225	4.014	0.606
11	10.196	0.179	-	5.916	11.823	9.040	11.007	1.021	43.191	1.003	2.382	1.221	4.970	1.028
12a	1.769	14.069	19.509	-	2.899	3.154	5.587	33.515	62.848	20.991	8.241	14.150	1.637	8.848
12b	1.378	48.518	61.258	4.609	-	4.674	5.858	91.689	72.286	63.270	31.240	47.301	9.699	35.114
13a	9.691	47.796	58.550	9.630	7.372	-	2.259	103.506	153.974	75.591	12.836	25.968	3.213	24.535
13b	21.098	78.053	92.661	22.704	17.320	2.564	-	153.315	136.076	117.217	26.443	45.656	10.050	44.722
14a	15.934	2.772	1.864	12.320	18.067	21.844	28.128	-	106.875	0.736	10.678	7.393	15.913	6.443
14b	152.284	220.720	235.590	153.352	146.293	101.171	78.149	305.226	-	271.668	143.431	168.962	118.347	175.533
15a	11.301	2.086	1.550	8.418	12.563	16.904	23.544	0.716	108.412	-	8.873	6.548	12.734	5.245
15b	7.377	5.080	6.246	3.962	8.144	3.801	6.136	15.287	70.453	11.143	-	0.777	1.436	1.370
16a	8.016	1.438	1.572	4.565	9.447	5.370	6.584	4.899	37.609	3.987	0.465	-	2.393	0.578
17a	3.264	8.050	10.593	1.581	4.023	1.481	2.726	20.604	47.972	14.006	1.905	4.487	-	3.605
17b	7.060	1.200	2.139	3.638	8.869	8.629	11.894	7.533	73.728	4.596	1.183	0.657	3.559	-

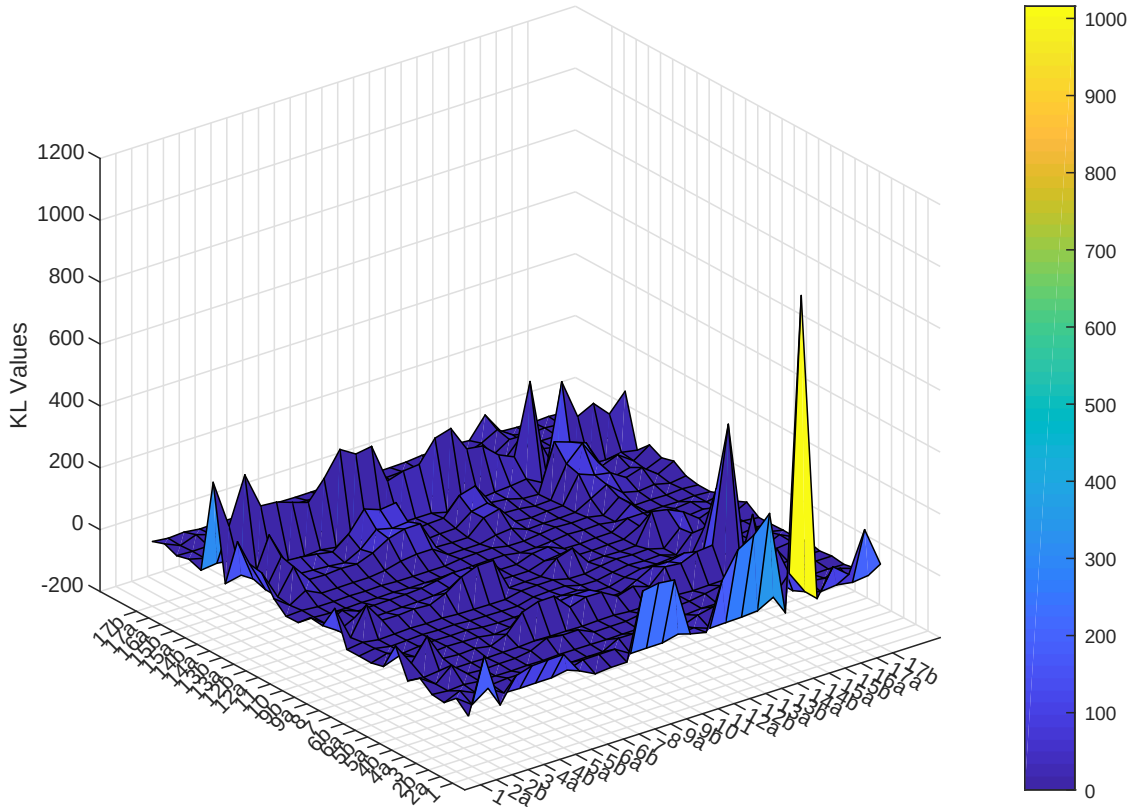

Fig. C.45. A graphical representation of the KL values found between pairing of the data from "Uncorrected" for the six-substructure case

Table C.41. 27x27 matrix of KL values from test pairings of data from "Uncorrected" for the 9 Substructure case. These values are compared against the cutoff value found in Section 6.4 to determine flexural rigidity identification agreement.

$651/702 \geq KLCutoff$	9 Substructure											$KLCutoff = 0.640$	
Tests	1	2a	2b	3	4a	4b	5a	5b	6a	6b	7	8	9a
1	-	156.878	3.498	64.065	81.697	81.068	97.106	30.511	6.411	8.840	9.496	222.063	188.190
2a	33.427	-	32.984	5.248	3.445	4.008	3.251	11.529	25.855	27.732	27.279	2.018	2.268
2b	1.683	22.263	-	8.876	13.556	12.496	16.923	4.643	0.476	1.229	1.171	30.466	24.632
3	5.882	2.094	5.061	-	1.417	0.512	2.154	1.133	3.252	3.559	3.364	5.179	4.590
4a	37.743	3.383	46.081	4.402	-	2.302	2.680	10.752	33.340	31.937	31.206	9.315	7.809
4b	7.218	1.942	7.083	0.529	0.974	-	1.332	2.029	4.965	4.636	4.412	5.140	5.560
5a	99.380	17.521	97.604	10.528	4.035	7.977	-	22.466	73.501	90.098	87.736	45.082	37.374
5b	11.197	23.996	9.710	4.243	8.273	6.837	8.248	-	5.586	8.754	8.474	41.562	34.536
6a	1.617	14.551	0.361	4.428	7.914	6.370	8.940	1.899	-	0.786	0.623	22.153	19.181
6b	2.236	9.930	0.918	3.219	6.191	4.140	6.201	1.772	0.673	-	0.037	14.851	13.715
7	1.999	8.694	0.807	2.719	5.421	3.546	5.652	1.617	0.514	0.037	-	13.179	12.213
8	111.148	6.520	89.481	32.459	30.391	32.753	27.041	47.487	79.874	94.437	93.299	-	1.432
9a	28.946	2.890	21.898	8.862	10.407	10.449	11.089	13.181	19.737	24.534	23.983	0.816	-
9b	32.651	3.855	24.652	10.687	12.321	12.483	13.049	15.289	22.458	27.855	27.264	1.096	0.062
10	3.659	4.634	1.367	0.843	3.338	1.895	3.743	0.731	0.805	1.325	1.211	8.197	7.397
11	2.566	5.317	0.968	1.059	3.411	2.003	3.935	0.822	0.406	0.674	0.552	9.362	8.738
12a	33.853	0.963	27.998	7.064	7.746	7.836	7.150	12.518	23.485	27.994	27.563	1.048	0.682
12b	91.765	9.017	80.991	31.295	29.622	31.911	27.364	45.326	71.131	81.434	80.520	2.478	3.519
13a	96.488	8.560	85.609	26.814	23.765	20.838	13.268	36.465	72.669	67.947	69.400	3.965	9.546
13b	136.821	20.352	122.884	46.448	42.256	37.642	25.685	58.776	106.389	99.450	101.512	11.614	20.557
14a	1.384	11.893	0.464	4.998	7.436	7.155	11.323	3.999	0.688	1.459	1.190	17.315	14.466
14b	25.810	7.012	22.509	8.794	10.100	7.050	5.489	10.528	19.116	16.641	17.100	7.514	9.812
15a	2.101	8.268	1.611	3.356	5.081	5.330	9.591	3.633	1.314	2.365	1.992	12.979	10.646
15b	14.107	2.537	11.772	1.679	2.877	0.884	1.320	2.782	8.893	6.664	6.997	5.043	5.950
16a	5.408	3.722	3.780	0.790	2.654	0.774	2.064	0.943	2.600	1.606	1.661	6.741	6.860
17a	17.820	1.123	14.537	2.516	3.710	2.130	2.254	4.868	11.689	11.414	11.500	2.192	2.581
17b	8.698	3.683	5.915	0.599	2.648	1.220	2.501	0.815	4.118	3.854	3.939	7.311	6.117

	$651/702 \geq KLCutoff$					9 Substructure					$KLCutoff = 0.640$			
Tests	9b	10	11	12a	12b	13a	13b	14a	14b	15a	15b	16a	17a	17b
1	188.673	28.866	20.776	164.151	260.650	269.150	318.983	5.973	217.955	17.592	87.844	48.330	146.644	55.870
2a	2.861	14.627	17.764	0.851	4.297	4.271	8.308	30.991	7.434	18.699	4.192	9.837	1.288	7.396
2b	24.670	3.147	2.301	21.977	36.646	38.926	47.059	0.523	35.918	2.582	13.733	7.395	20.570	7.674
3	5.204	1.151	1.484	2.874	8.093	6.577	9.391	4.504	7.670	2.360	0.993	0.811	1.859	0.595
4a	8.498	18.690	21.551	5.121	11.671	19.110	29.353	40.281	21.621	21.420	3.738	8.111	5.127	7.433
4b	6.379	2.580	2.834	3.580	8.816	4.980	7.183	6.171	5.634	3.723	0.595	0.938	1.555	1.314
5a	38.776	35.775	48.474	22.571	72.433	58.862	77.663	90.527	26.344	44.685	7.861	24.044	12.262	13.978
5b	35.275	2.088	3.077	26.120	56.571	50.303	60.983	9.475	30.823	4.094	6.805	2.776	18.177	2.178
6a	19.783	1.243	0.664	15.529	28.753	25.521	30.123	0.610	19.985	1.658	6.864	3.203	12.123	3.588
6b	14.398	1.211	0.680	10.967	20.153	15.941	18.845	1.088	12.951	2.181	4.181	1.733	7.775	2.557
7	12.885	1.011	0.515	9.720	18.129	14.148	16.904	0.867	12.082	1.807	3.771	1.560	6.899	2.304
8	1.657	49.760	62.875	2.293	2.845	2.326	4.245	91.555	13.255	64.424	30.072	48.775	9.245	33.946
9a	0.060	12.263	15.725	0.680	1.708	3.297	4.813	22.359	9.934	16.053	10.343	14.215	3.809	9.596
9b	-	14.256	18.165	1.122	1.824	3.990	5.469	25.313	11.264	18.479	12.279	16.574	4.818	11.322
10	8.054	-	0.160	5.265	12.242	9.268	11.786	1.546	8.866	1.294	2.089	0.942	3.517	0.700
11	9.496	0.150	-	6.341	13.438	10.161	12.708	1.004	9.547	1.087	2.351	0.941	4.314	1.063
12a	1.023	13.239	17.124	-	3.447	3.089	5.635	28.078	7.065	18.356	7.241	12.692	1.768	8.133
12b	3.486	47.758	56.850	5.322	-	4.886	5.855	80.945	16.671	58.319	29.964	45.375	13.104	34.369
13a	10.283	45.781	53.401	8.454	5.844	-	2.131	89.499	5.582	68.532	14.221	28.718	5.880	24.045
13b	21.415	71.573	81.440	19.593	12.930	2.327	-	128.518	4.192	102.573	27.267	47.608	14.696	41.555
14a	14.895	2.255	1.627	12.778	21.091	22.618	29.382	-	27.449	0.664	9.397	5.586	13.088	6.011
14b	10.641	12.838	14.186	7.666	11.162	3.630	2.429	23.782	-	20.301	4.328	7.388	3.372	7.034
15a	11.127	1.922	1.560	9.304	15.857	18.434	25.731	0.650	26.948	-	8.076	5.118	10.735	5.302
15b	6.746	4.297	5.060	3.717	8.894	4.651	7.587	12.581	6.710	9.599	-	0.905	1.026	1.027
16a	7.580	1.063	1.128	4.766	10.868	6.445	8.353	3.961	5.862	3.375	0.550	-	2.114	0.428
17a	3.115	5.833	7.478	1.302	5.131	2.296	4.068	14.727	3.340	10.213	1.240	3.441	-	2.322
17b	6.625	1.172	1.864	4.132	11.016	9.225	12.595	6.450	8.635	4.377	0.934	0.492	2.429	-

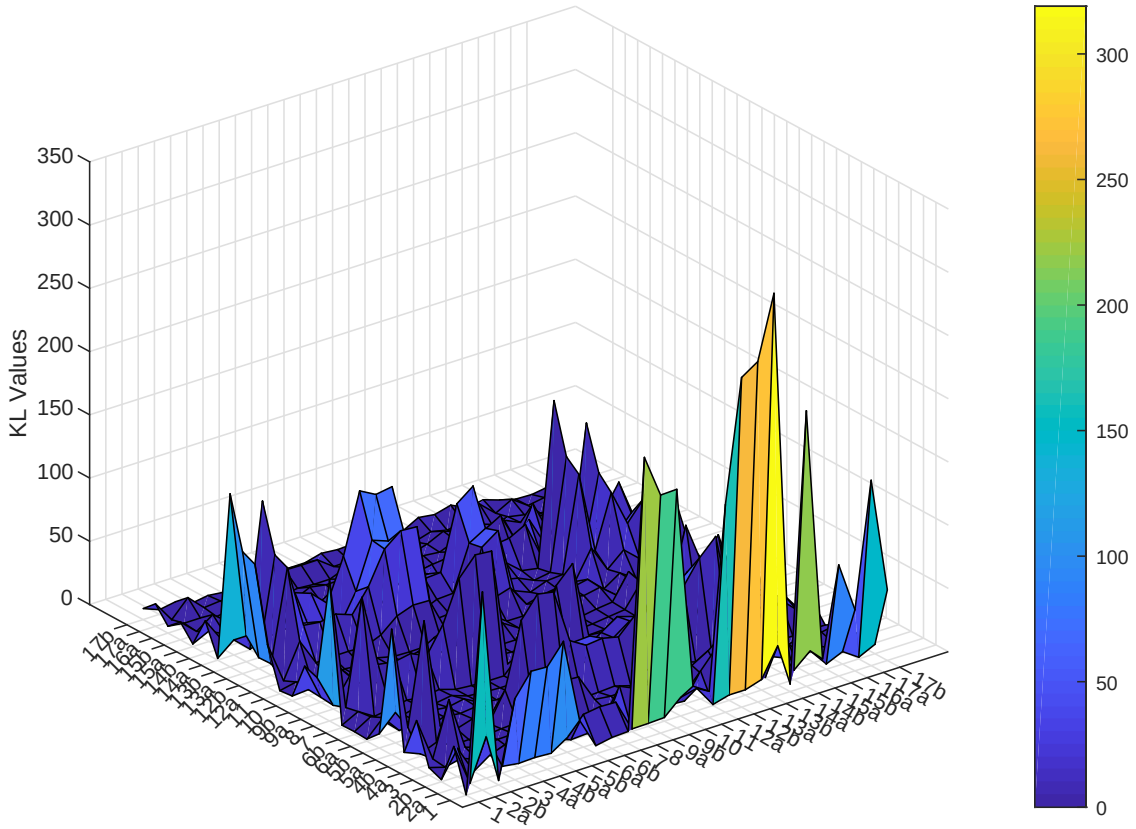

Fig. C.46. A graphical representation of the KL values found between pairing of the data from "Uncorrected" for the nine-substructure case

Appendix D. FIGURES

Appendix D.1. One Substructure

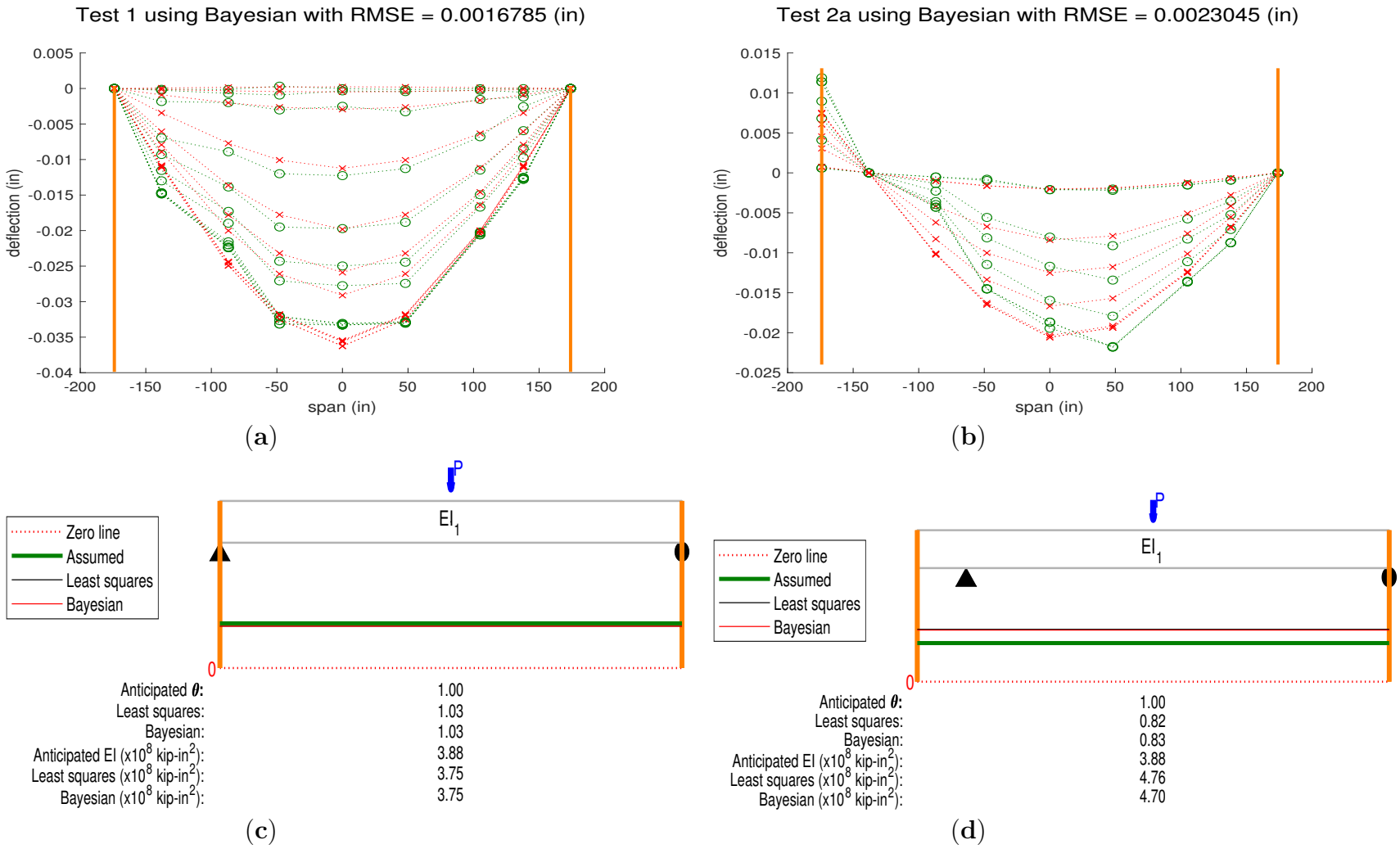

Fig. D.47. Tests 1 and 2a Bayesian analysis deflection comparisons and identification results. Identifications are $\times 10^8$ unless stated otherwise in the substructure result.

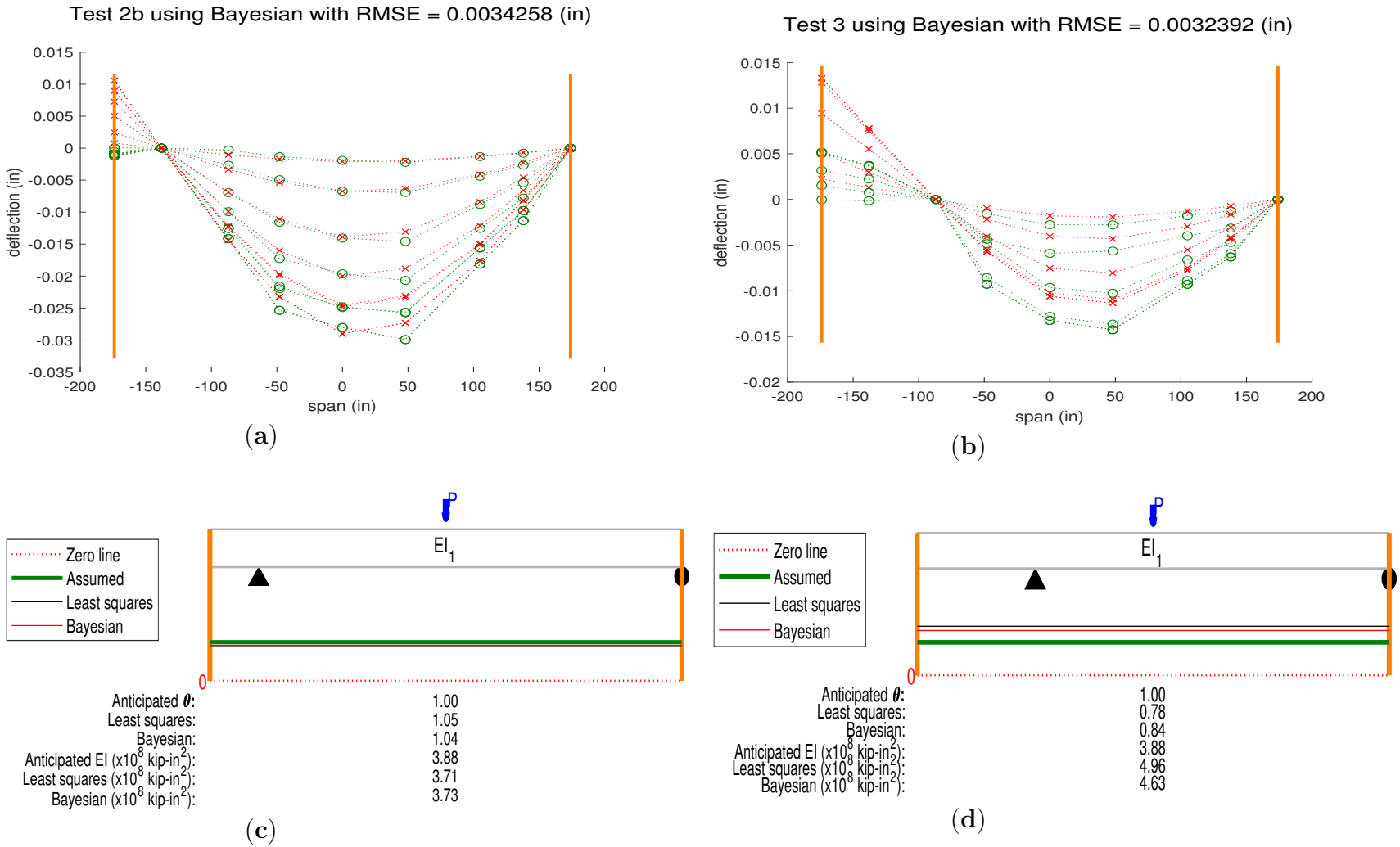

Fig. D.48. Tests 2b and 3 Bayesian analysis deflection comparisons and identification results. Identifications are $\times 10^8$ unless stated otherwise in the substructure result.

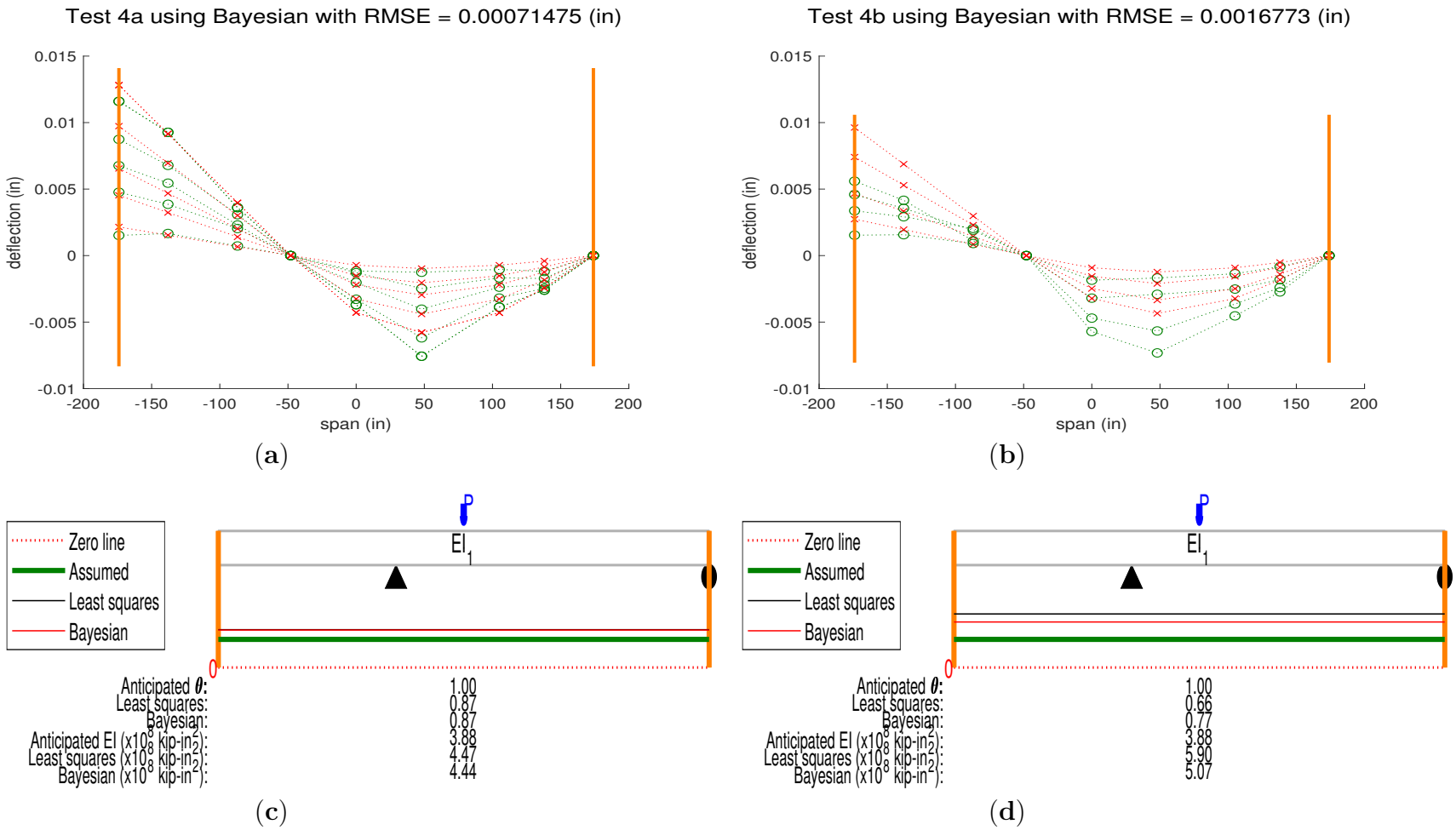

Fig. D.49. Tests 4a and 4b Bayesian analysis deflection comparisons and identification results. Identifications are $\times 10^8$ unless stated otherwise in the substructure result.

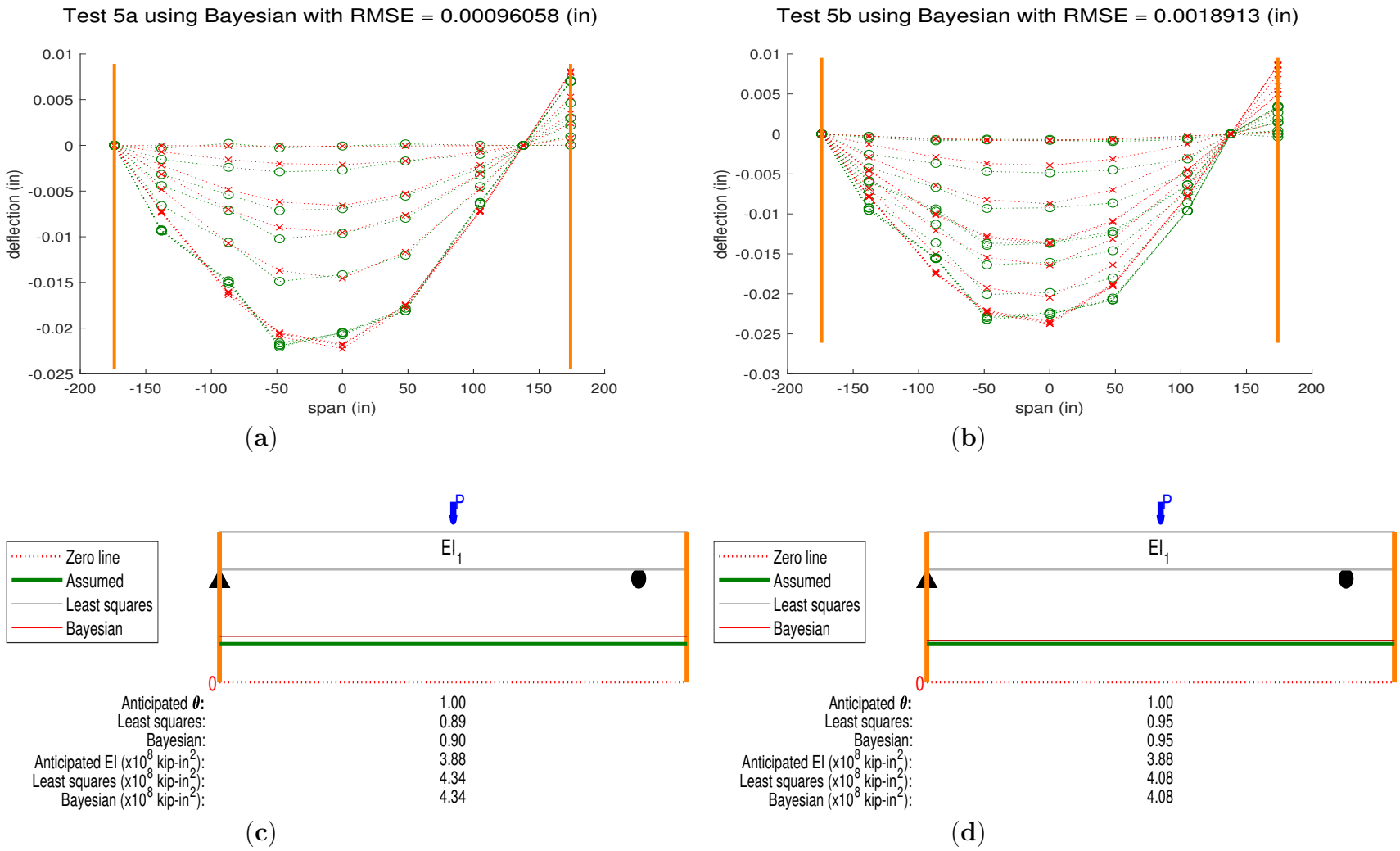

Fig. D.50. Tests 4a and 5b Bayesian analysis deflection comparisons and identification results. Identifications are $\times 10^8$ unless stated otherwise in the substructure result.

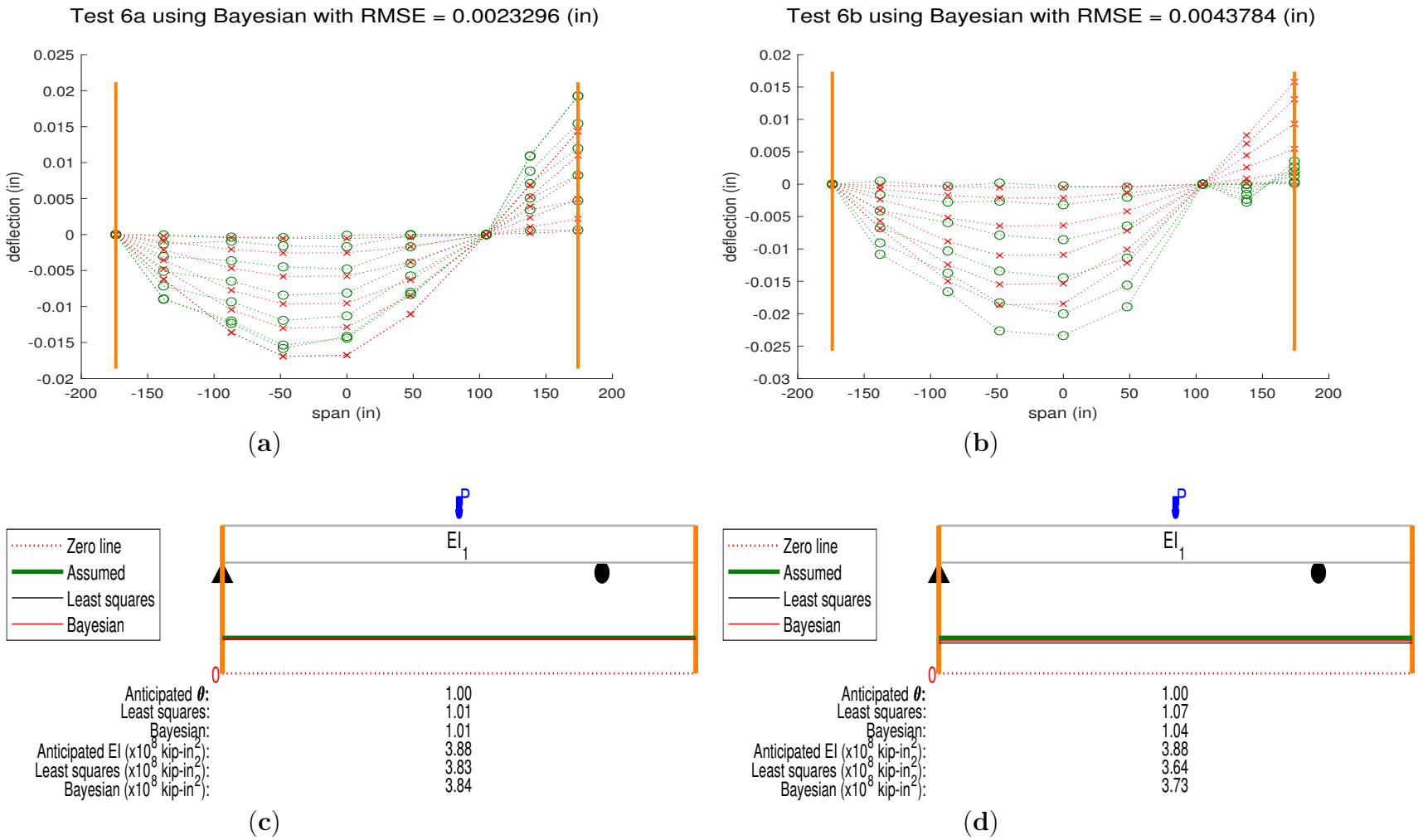

Fig. D.51. Tests 6a and 6b Bayesian analysis deflection comparisons and identification results. Identifications are $\times 10^8$ unless stated otherwise in the substructure result.

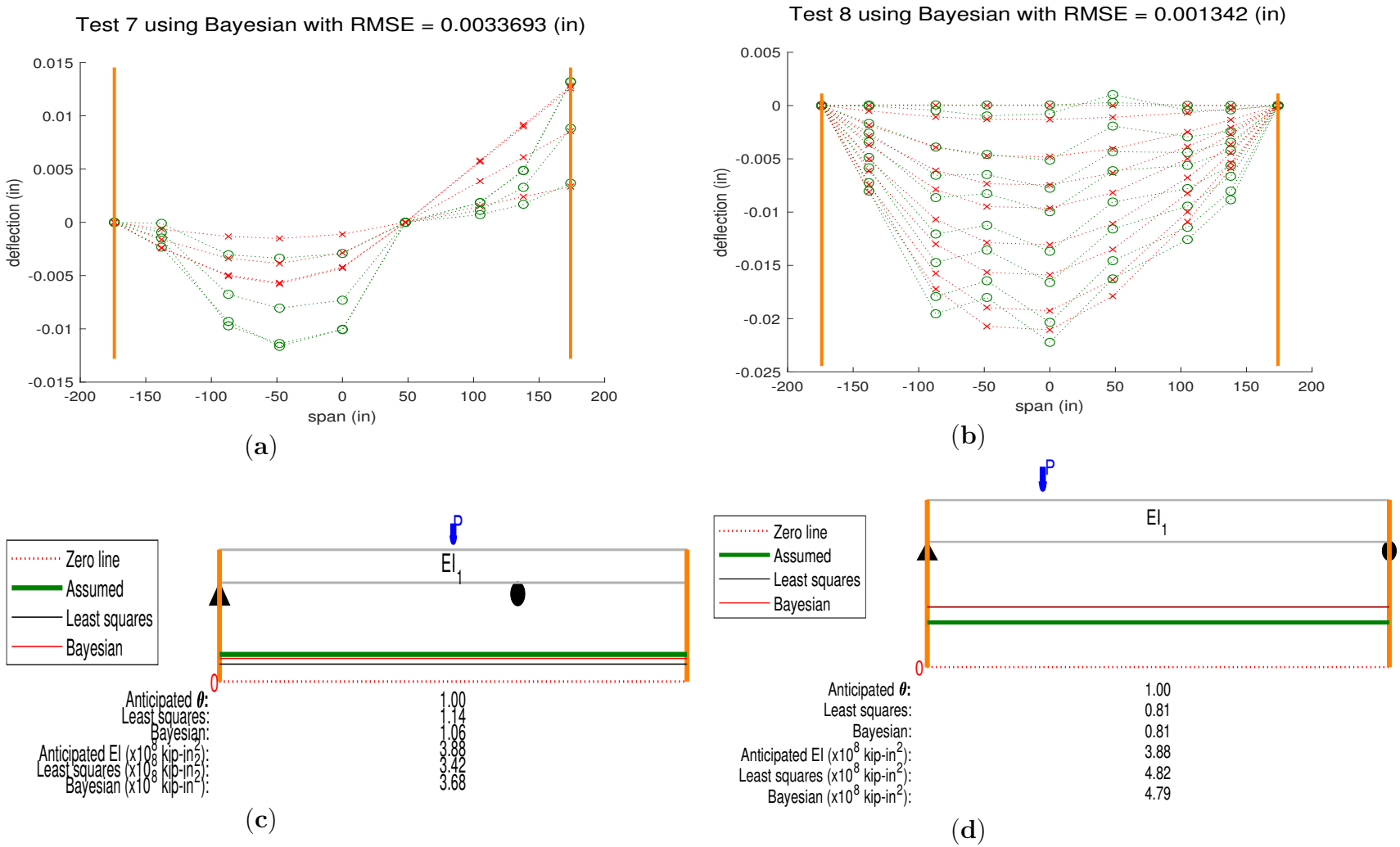

Fig. D.52. Tests 7 and 8 Bayesian analysis deflection comparisons and identification results. Identifications are $\times 10^8$ unless stated otherwise in the substructure result.

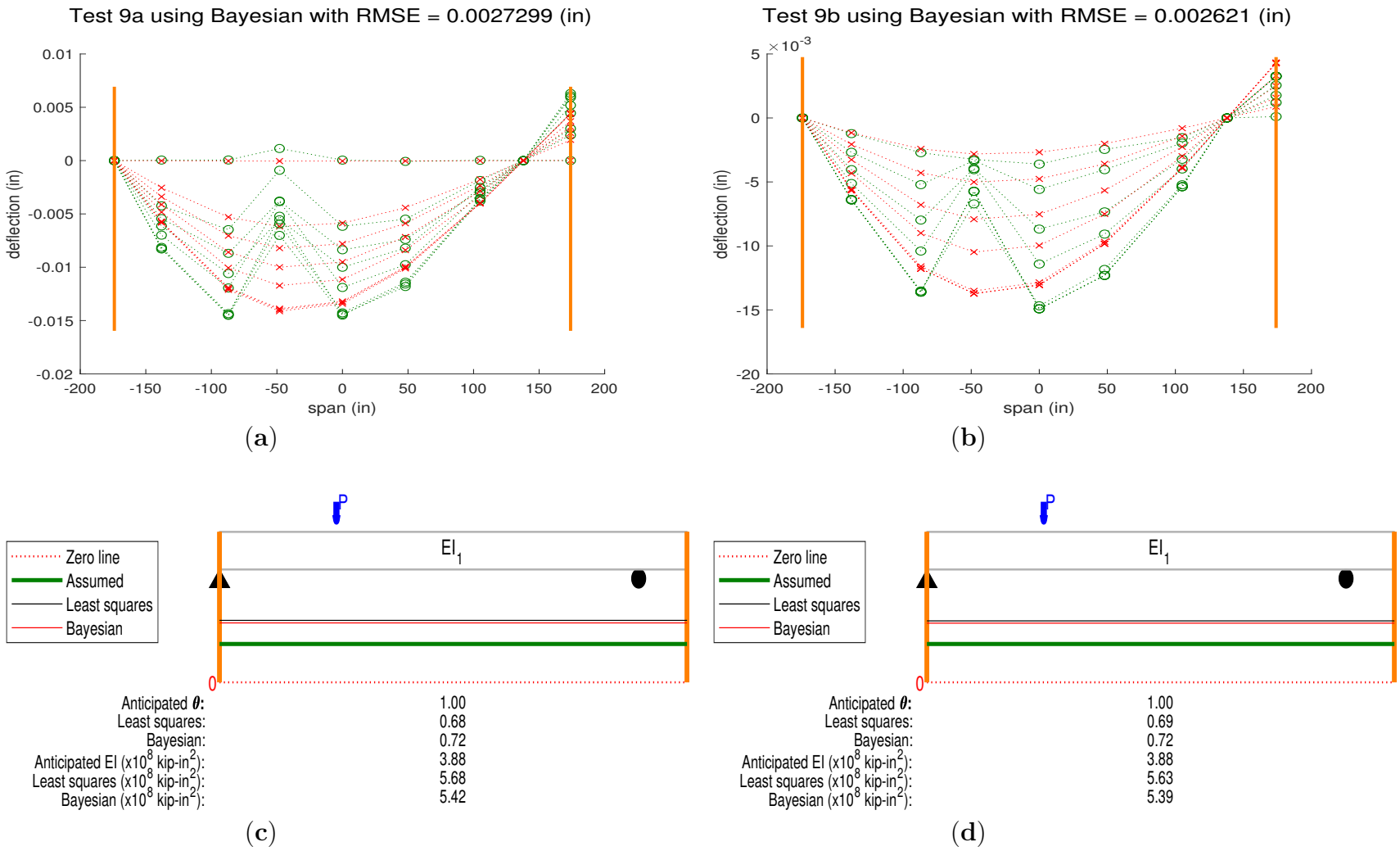

Fig. D.53. Tests 9a and 9b Bayesian analysis deflection comparisons and identification results, identifications are $\times 10^8$ unless stated otherwise in the substructure result.

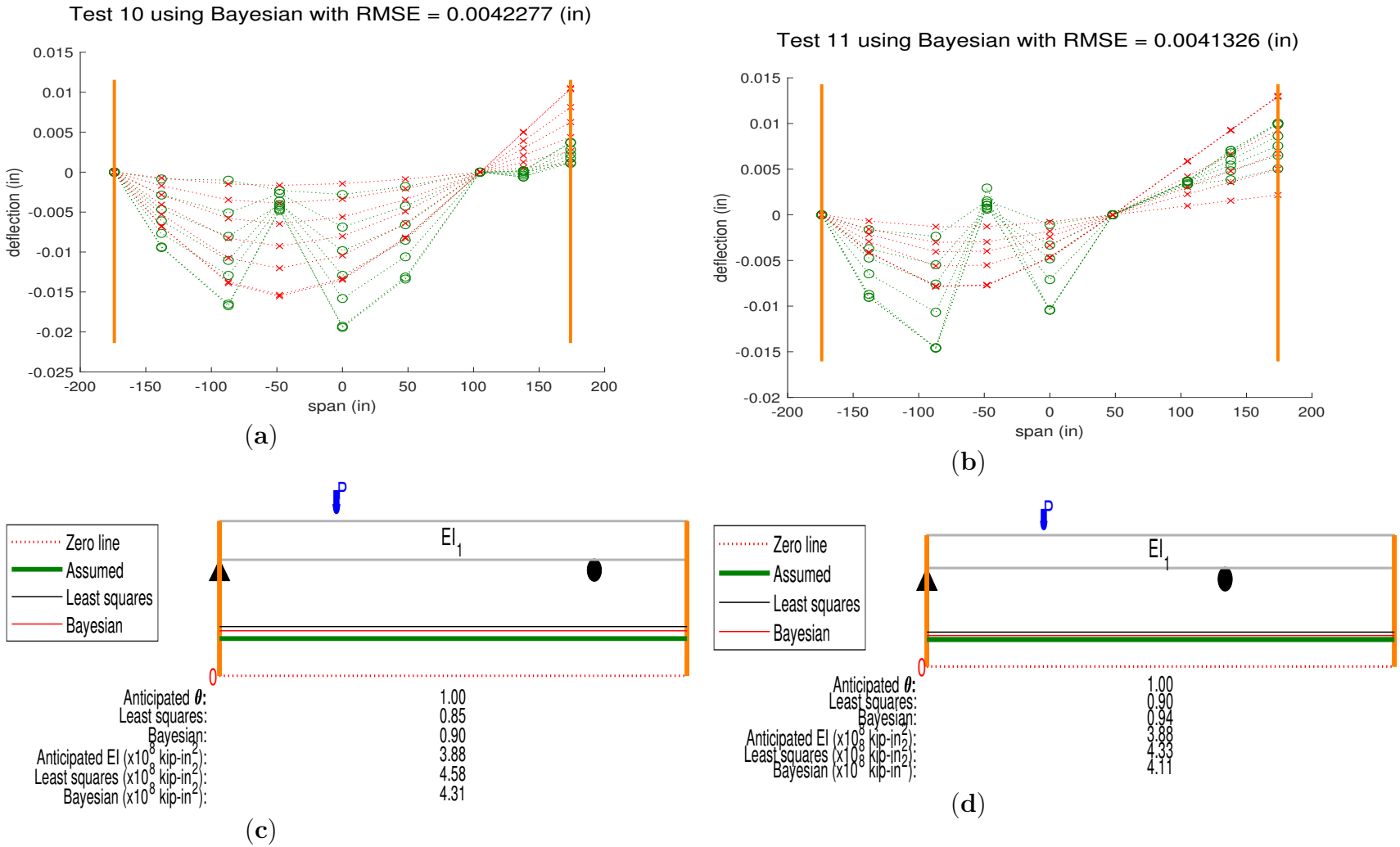

Fig. D.54. Tests 10 and 11 Bayesian analysis deflection comparisons and identification results. Identifications are $\times 10^8$ unless stated otherwise in the substructure result.

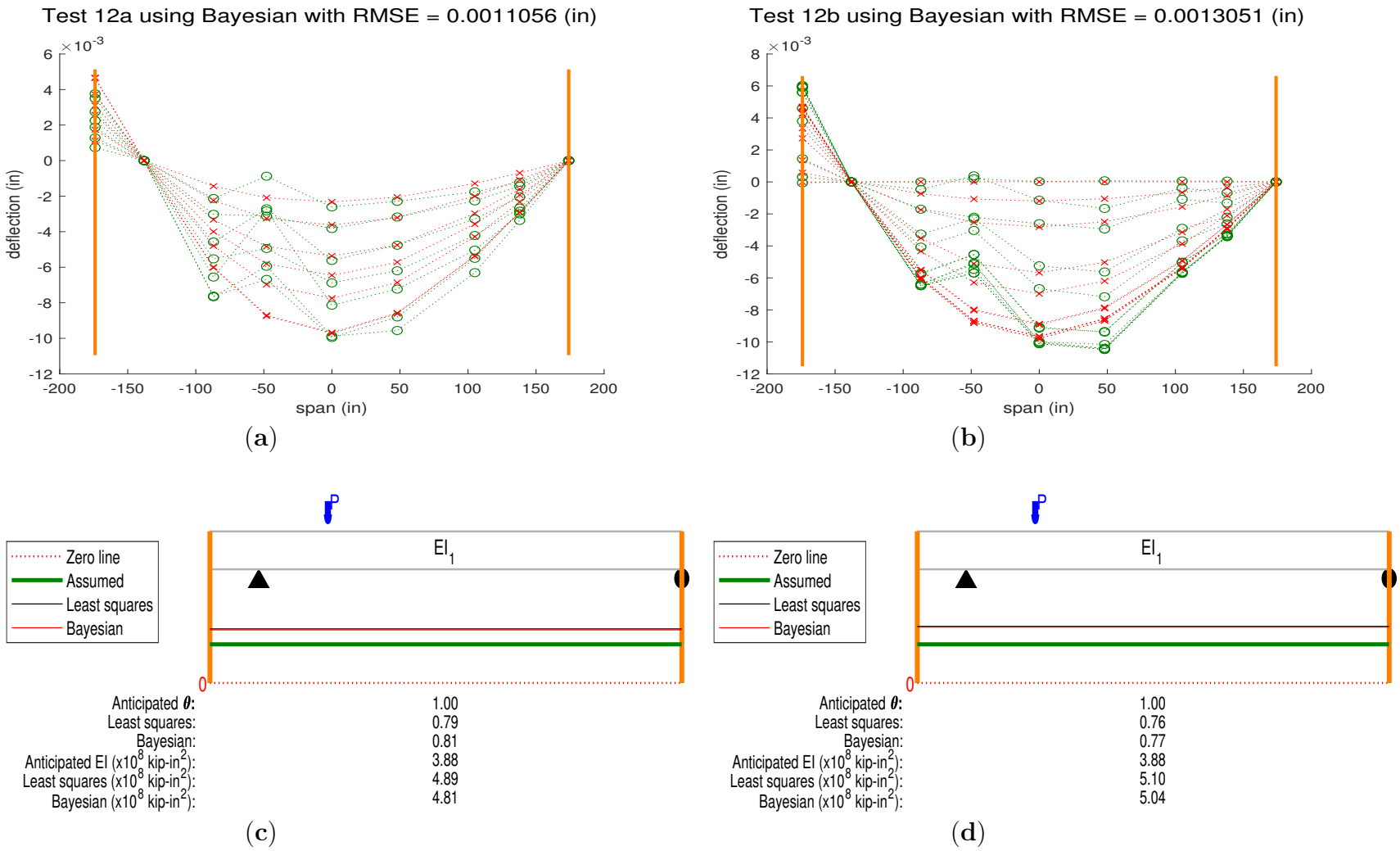

Fig. D.55. Tests 12a and 12b Bayesian analysis deflection comparisons and identification results. Identifications are $\times 10^8$ unless stated otherwise in the substructure result.

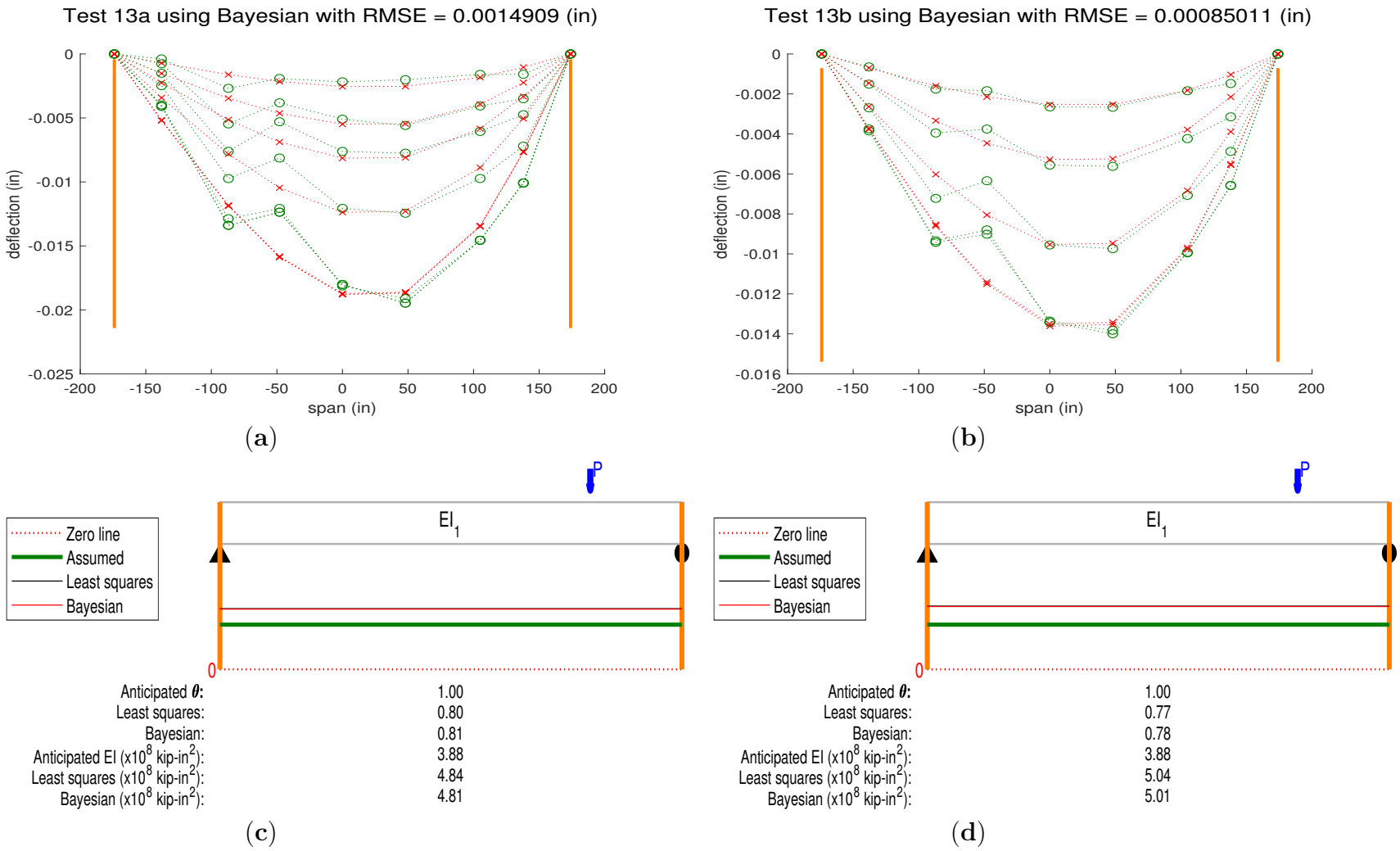

Fig. D.56. Tests 13a and 13b Bayesian analysis deflection comparisons and identification results. Identifications are $\times 10^8$ unless stated otherwise in the substructure result.

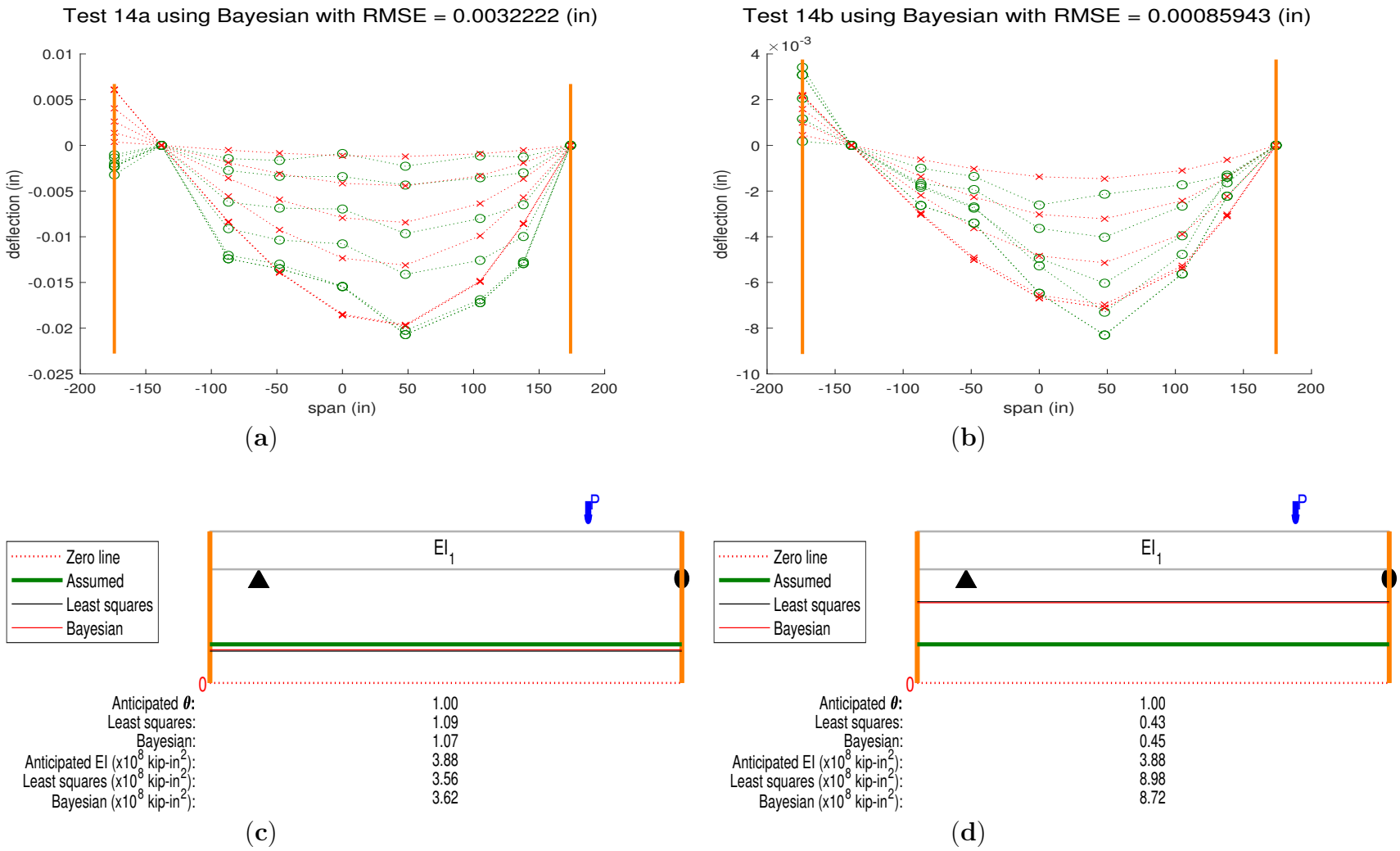

Fig. D.57. Tests 14a and 14b Bayesian analysis deflection comparisons and identification results. Identifications are $\times 10^8$ unless stated otherwise in the substructure result.

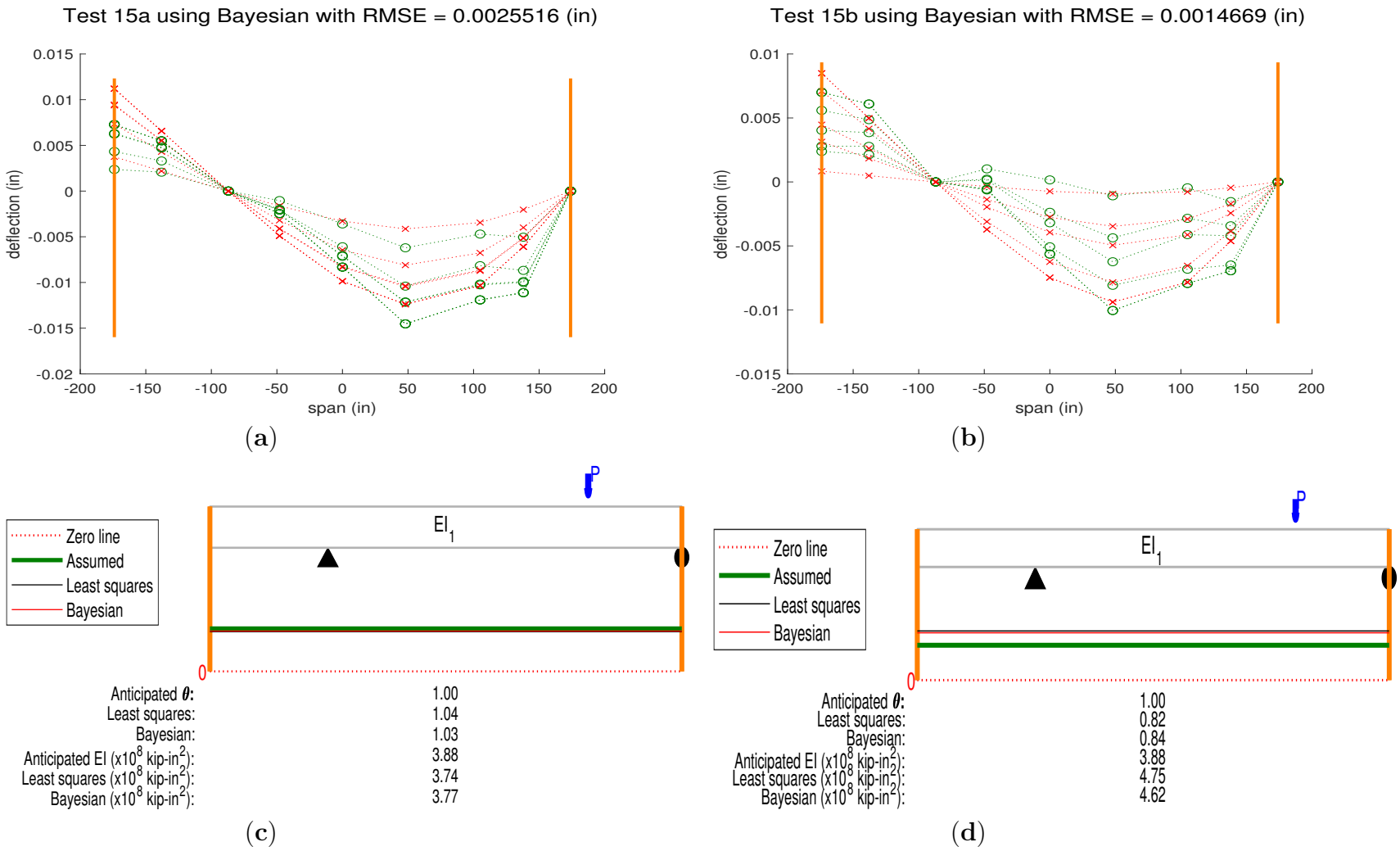

Fig. D.58. Tests 15a and 15b Bayesian analysis deflection comparisons and identification results. Identifications are $\times 10^8$ unless stated otherwise in the substructure result.

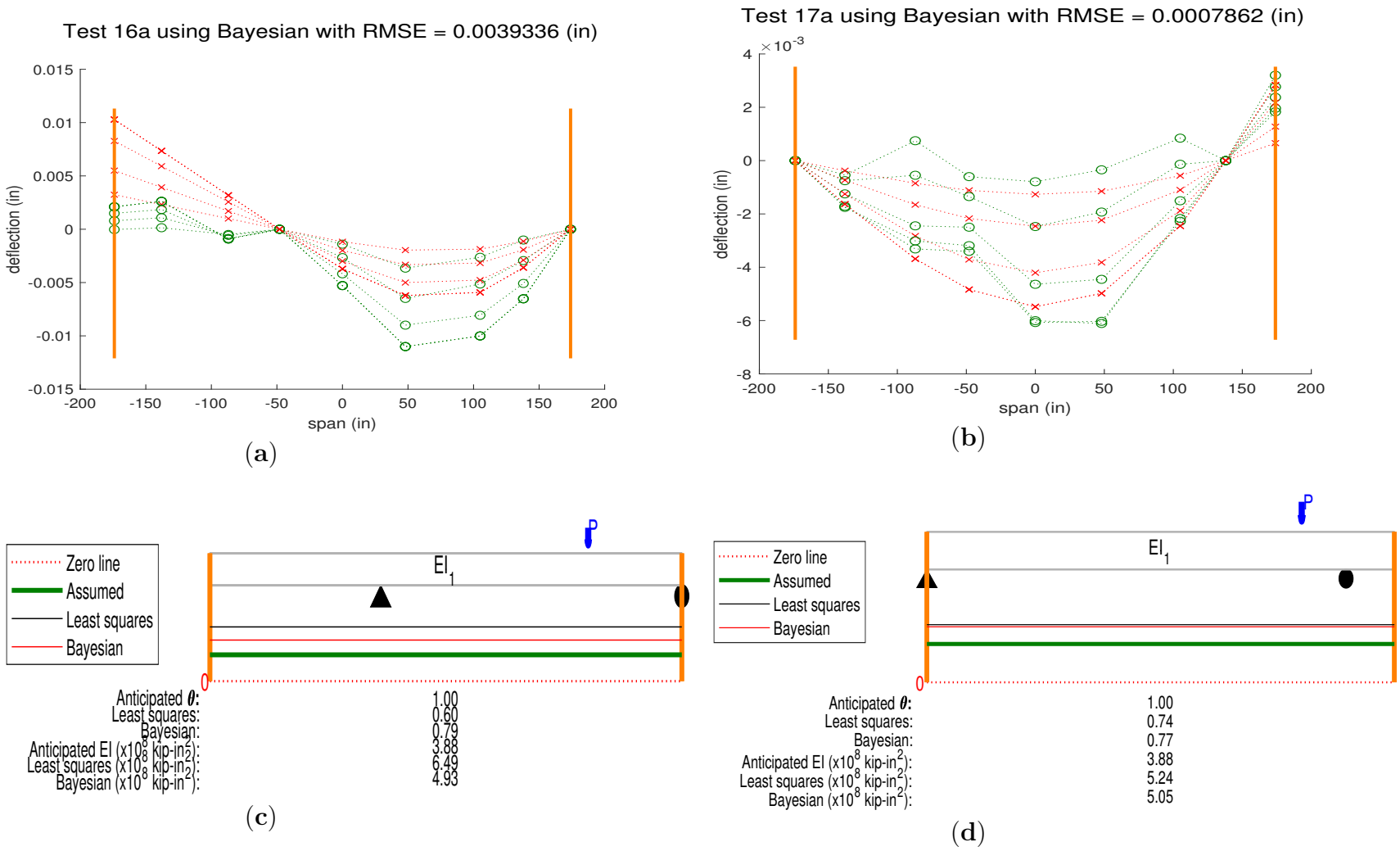

Fig. D.59. Tests 16a and 17a Bayesian analysis deflection comparisons and identification results. Identifications are $\times 10^8$ unless stated otherwise in the substructure result.

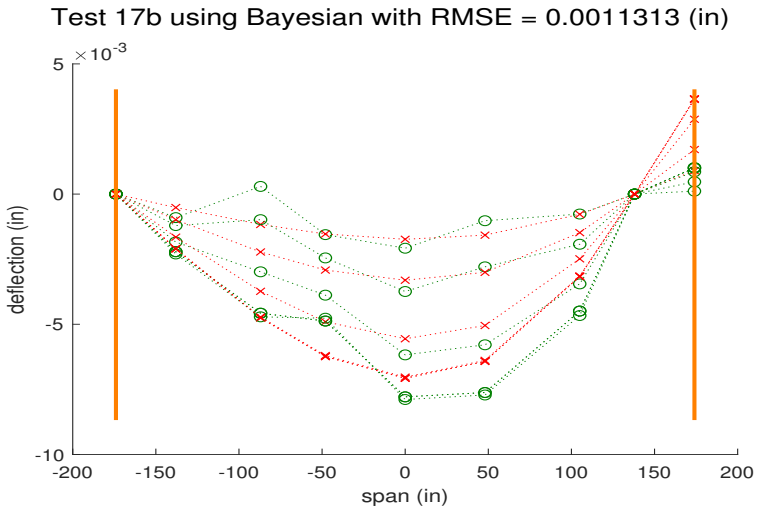

(a)

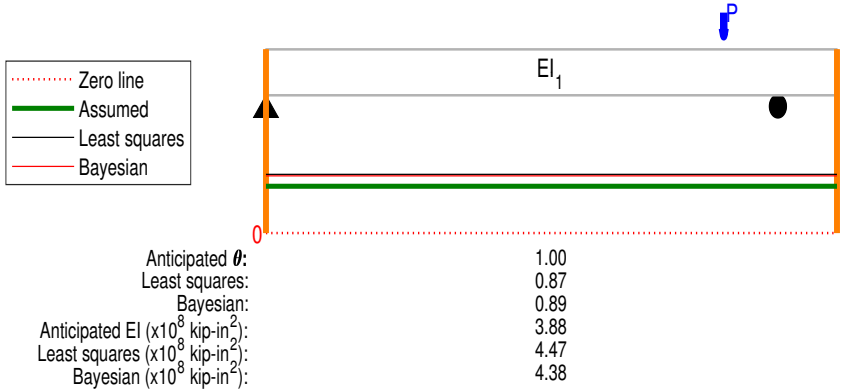

(c)

Fig. D.60. Test 17b Bayesian analysis deflection comparisons and identification results. Identifications are $\times 10^8$ unless stated otherwise in the substructure result.

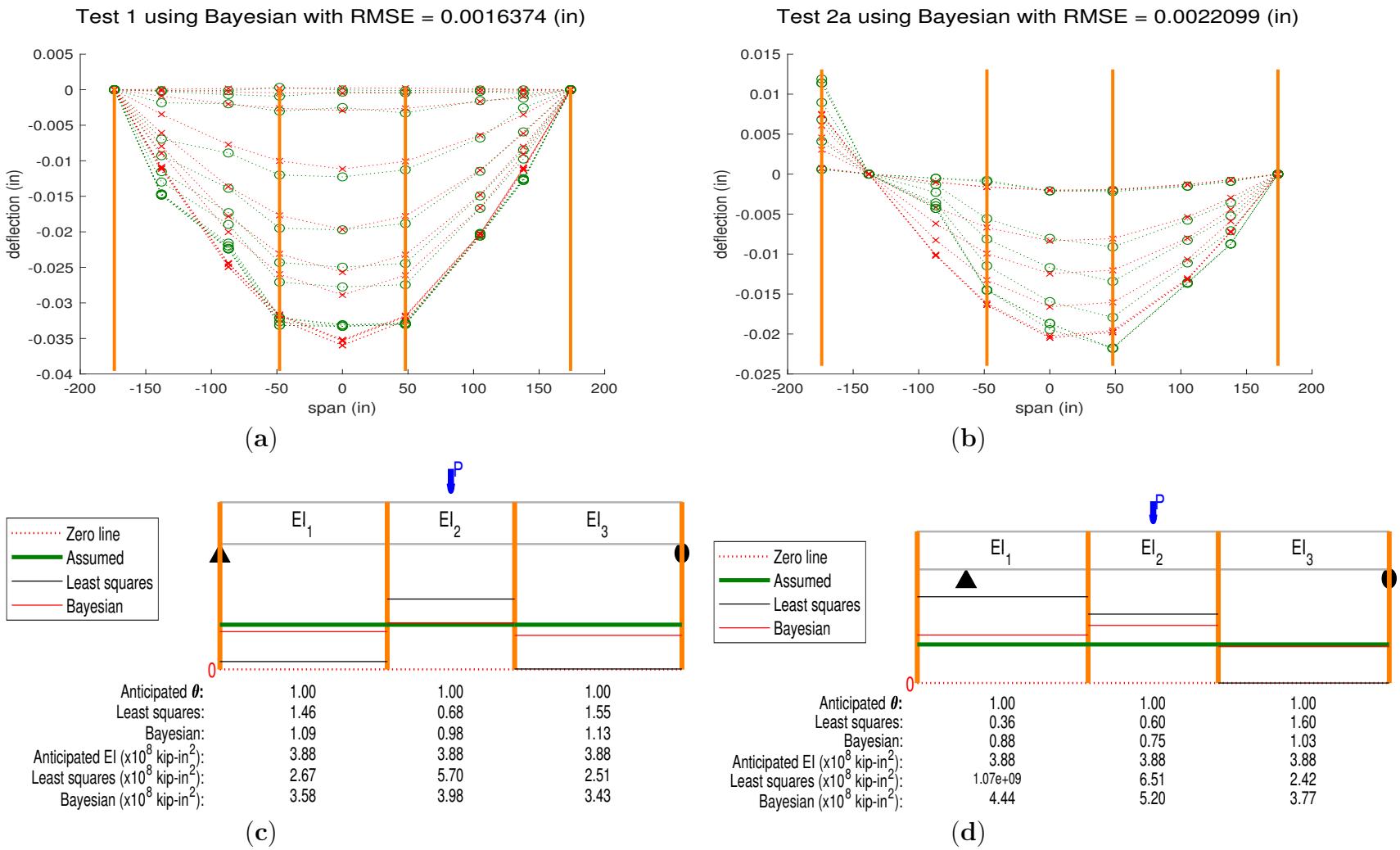

Fig. D.61. Tests 1 and 2a Bayesian analysis deflection comparisons and identification results. Identifications are $\times 10^8$ unless stated otherwise in the substructure result.

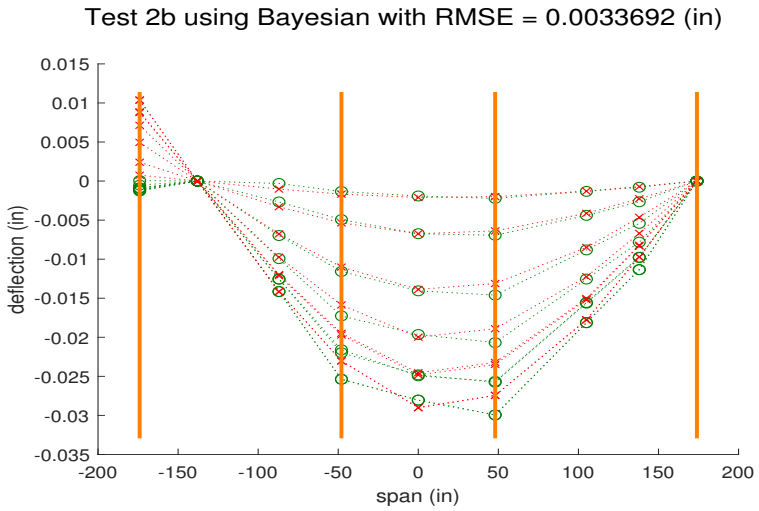

(a)

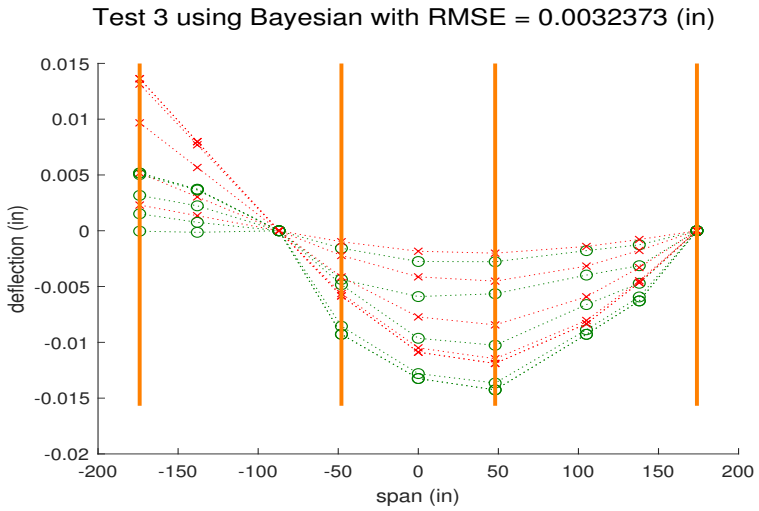

(b)

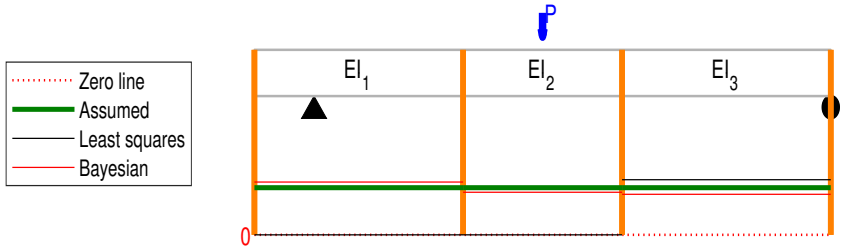

Anticipated θ:	1.00	1.00	1.00
Least squares:	-1.22	1.62	0.91
Bayesian:	0.94	1.05	1.07
Anticipated EI ($\times 10^8$ kip-in^2):	3.88	3.88	3.88
Least squares ($\times 10^8$ kip-in^2):	-3.18e+08	2.40	4.25
Bayesian ($\times 10^8$ kip-in^2):	4.14	3.70	3.62

(c)

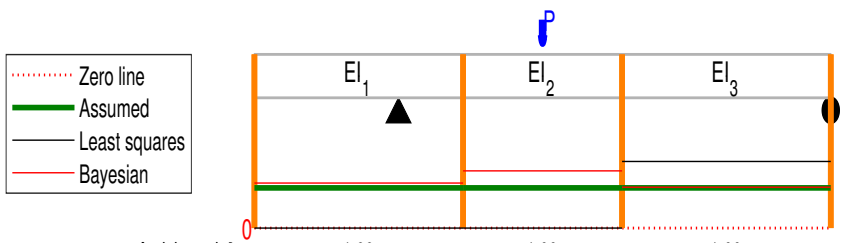

Anticipated θ:	1.00	1.00	1.00
Least squares:	-8.40	1.66	0.71
Bayesian:	0.95	0.81	0.99
Anticipated EI ($\times 10^8$ kip-in^2):	3.88	3.88	3.88
Least squares ($\times 10^8$ kip-in^2):	-4.62e+07	2.34	5.50
Bayesian ($\times 10^8$ kip-in^2):	4.10	4.79	3.91

(d)

Fig. D.62. Tests 2b and 3 Bayesian analysis deflection comparisons and identification results. Identifications are $\times 10^8$ unless stated otherwise in the substructure result.

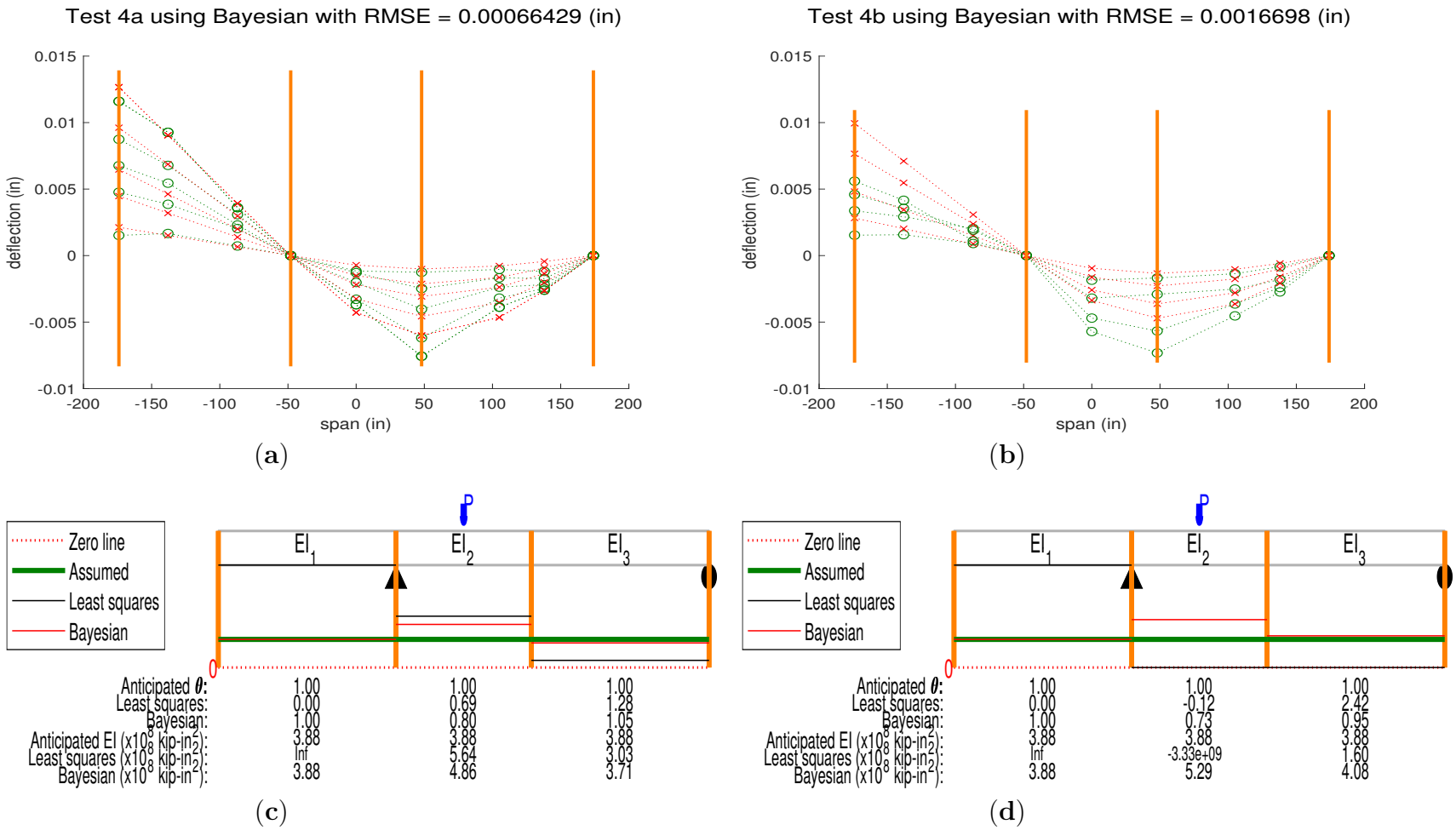

Fig. D.63. Tests 4a and 4b Bayesian analysis deflection comparisons and identification results. Identifications are $\times 10^8$ unless stated otherwise in the substructure result.

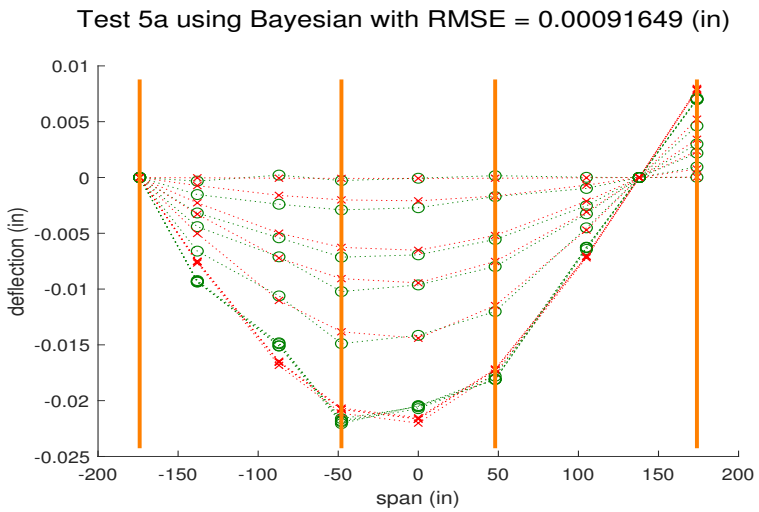

(a)

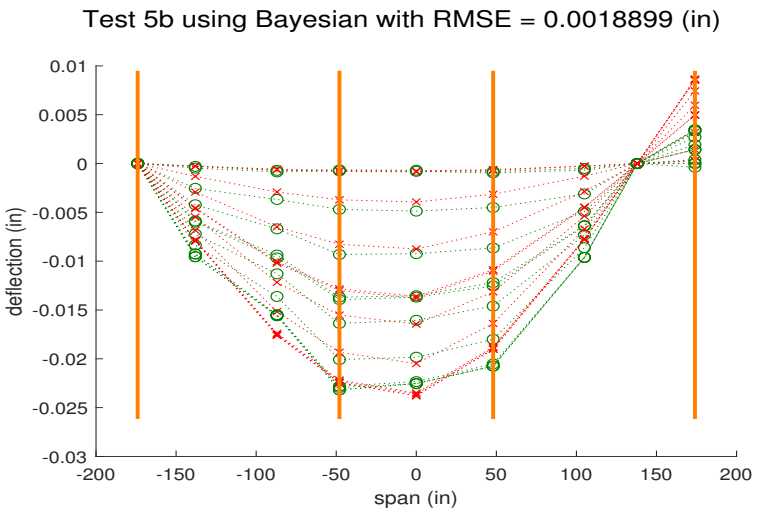

(b)

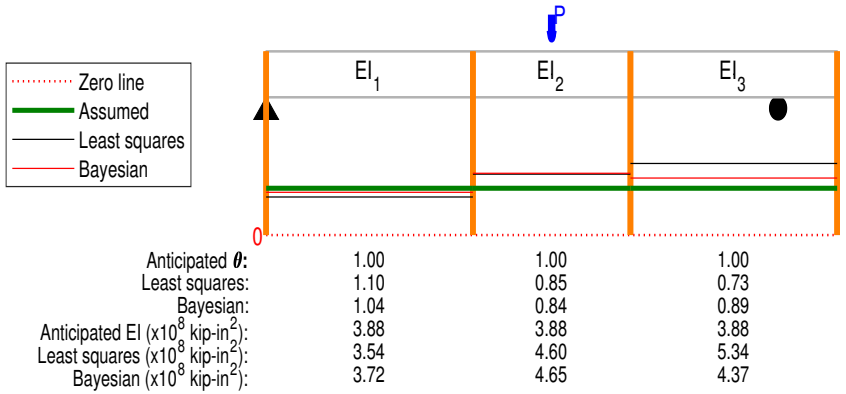

Anticipated $\boldsymbol{\theta}$:	1.00	1.00	1.00
Least squares:	1.10	0.85	0.73
Bayesian:	1.04	0.84	0.89
Anticipated EI ($\times 10^8$ kip-in^2):	3.88	3.88	3.88
Least squares ($\times 10^8$ kip-in^2):	3.54	4.60	5.34
Bayesian ($\times 10^8$ kip-in^2):	3.72	4.65	4.37

(c)

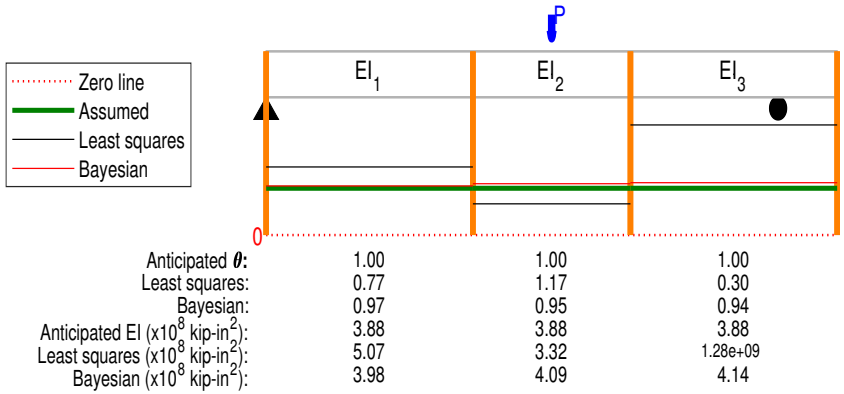

Anticipated $\boldsymbol{\theta}$:	1.00	1.00	1.00
Least squares:	0.77	1.17	0.30
Bayesian:	0.97	0.95	0.94
Anticipated EI ($\times 10^8$ kip-in^2):	3.88	3.88	3.88
Least squares ($\times 10^8$ kip-in^2):	5.07	3.32	1.28e+09
Bayesian ($\times 10^8$ kip-in^2):	3.98	4.09	4.14

(d)

Fig. D.64. Tests 4a and 5b Bayesian analysis deflection comparisons and identification results. Identifications are $\times 10^8$ unless stated otherwise in the substructure result.

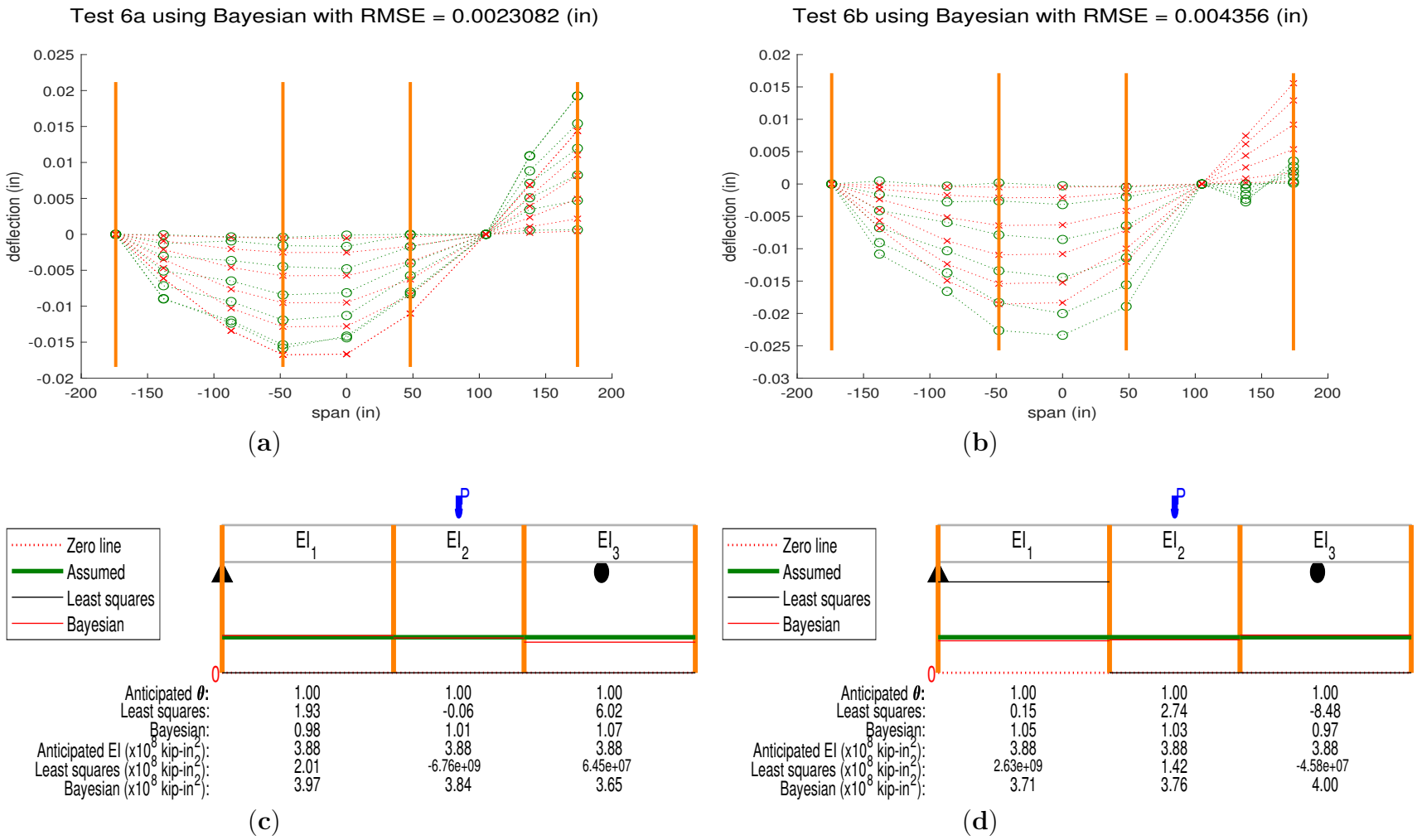

Fig. D.65. Tests 6a and 6b Bayesian analysis deflection comparisons and identification results. Identifications are $\times 10^8$ unless stated otherwise in the substructure result.

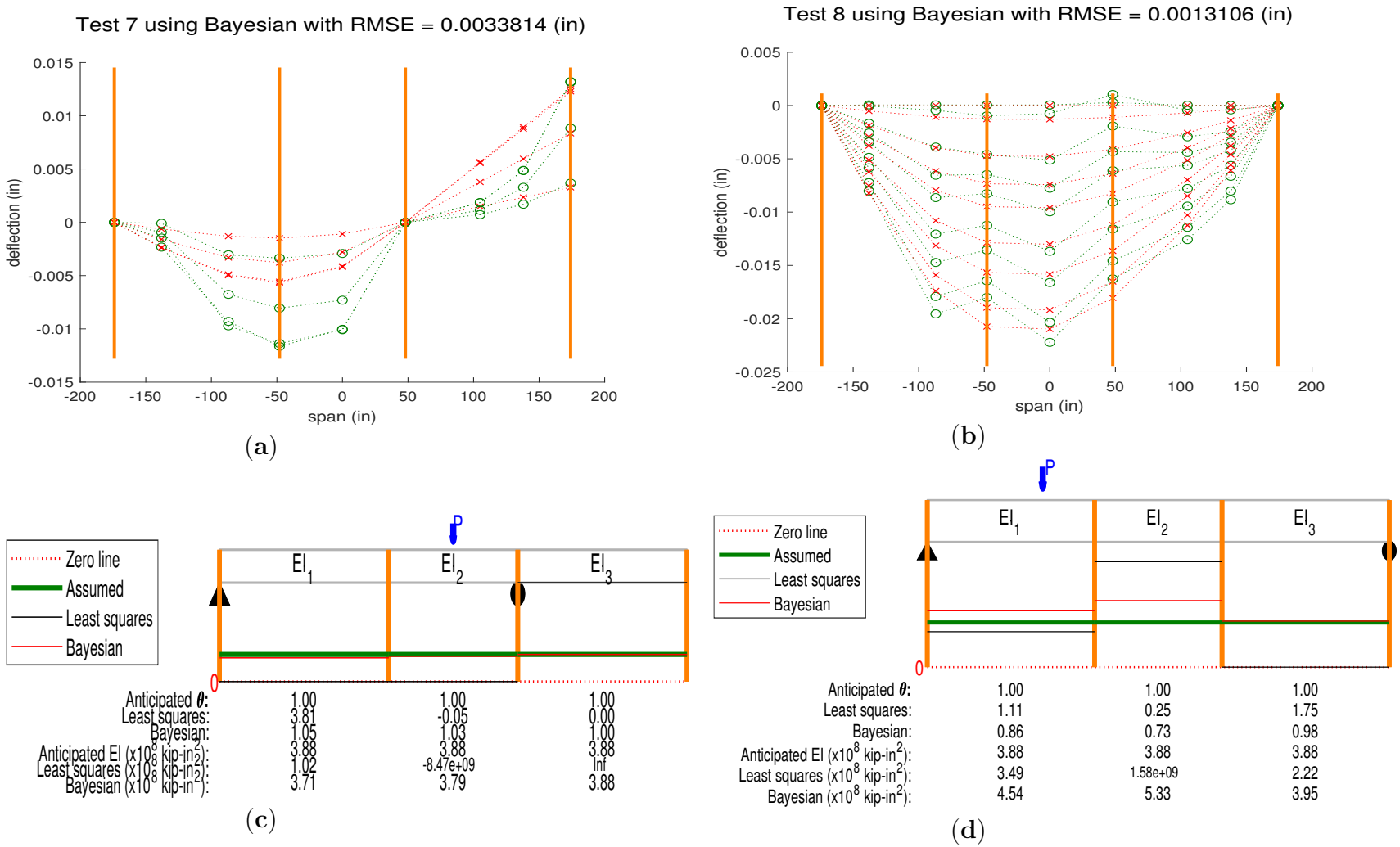

Fig. D.66. Tests 7 and 8 Bayesian analysis deflection comparisons and identification results. Identifications are $\times 10^8$ unless stated otherwise in the substructure result.

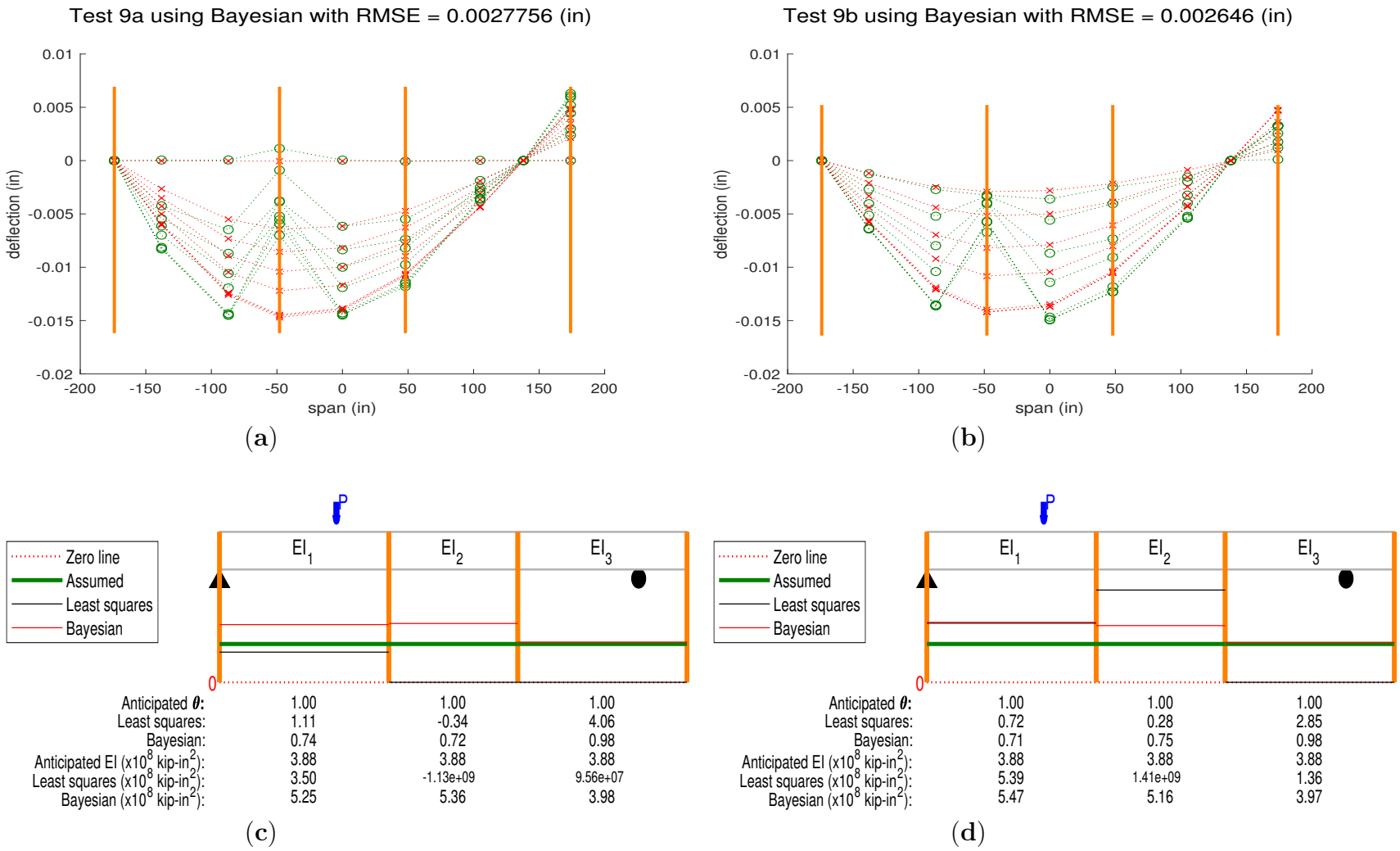

Fig. D.67. Tests 9a and 9b Bayesian analysis deflection comparisons and identification results. Identifications are $\times 10^8$ unless stated otherwise in the substructure result.

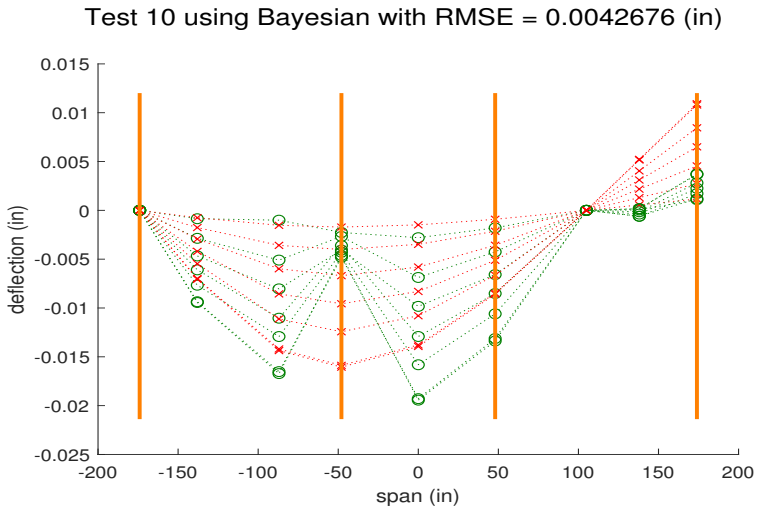

(a)

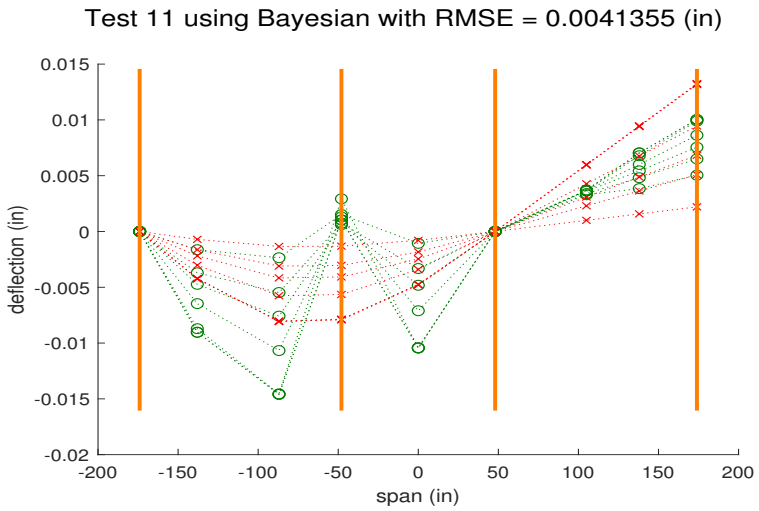

(b)

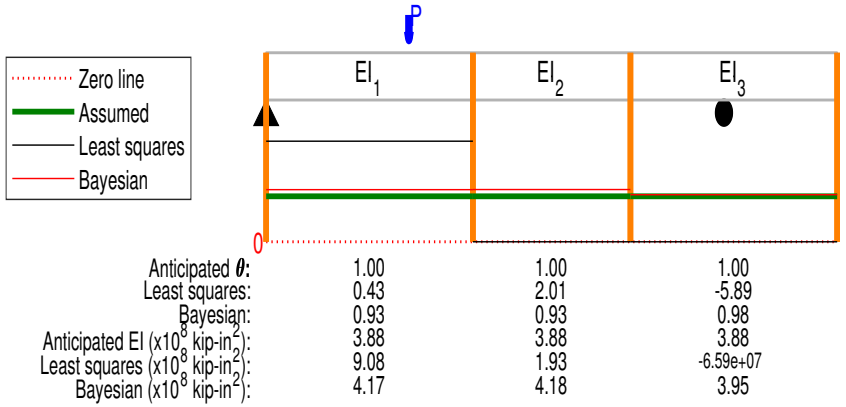

(c)

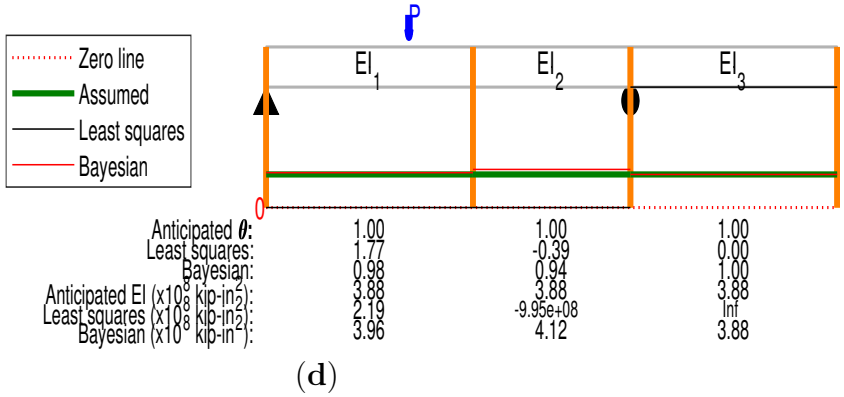

(d)

Fig. D.68. Tests 10 and 11 Bayesian analysis deflection comparisons and identification results. Identifications are $\times 10^8$ unless stated otherwise in the substructure result.

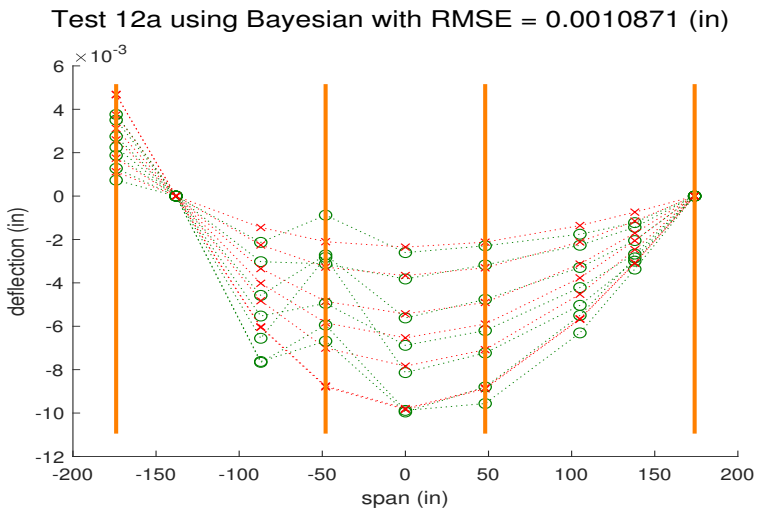

(a)

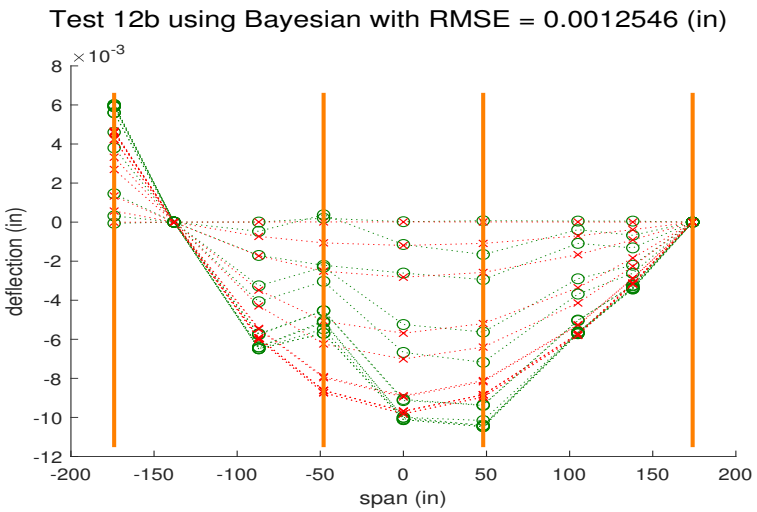

(b)

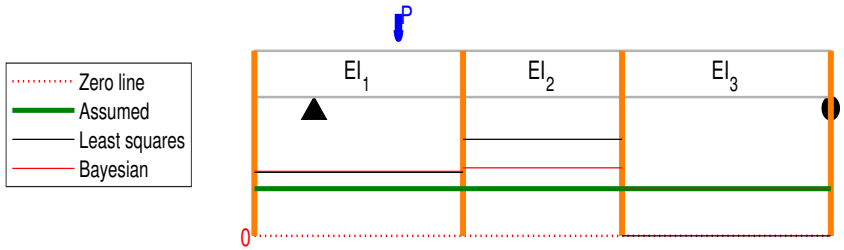

Anticipated θ:	1.00	1.00	1.00
Least squares:	0.82	0.46	1.73
Bayesian:	0.81	0.77	0.99
Anticipated EI ($\times 10^8$ kip-in^2):	3.88	3.88	3.88
Least squares ($\times 10^8$ kip-in^2):	4.73	8.43	2.25
Bayesian ($\times 10^8$ kip-in^2):	4.79	5.03	3.93

(c)

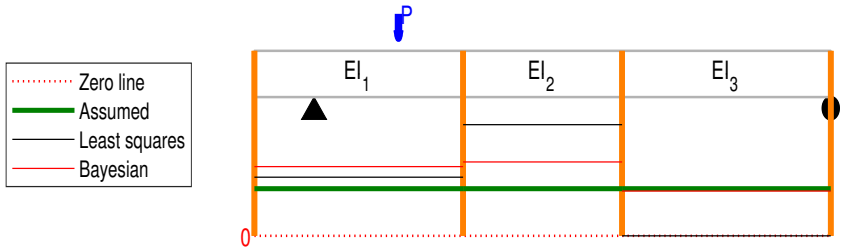

Anticipated θ:	1.00	1.00	1.00
Least squares:	0.87	0.30	1.91
Bayesian:	0.76	0.71	1.03
Anticipated EI ($\times 10^8$ kip-in^2):	3.88	3.88	3.88
Least squares ($\times 10^8$ kip-in^2):	4.44	1.29e+09	2.03
Bayesian ($\times 10^8$ kip-in^2):	5.12	5.48	3.79

(d)

Fig. D.69. Tests 12a and 12b Bayesian analysis deflection comparisons and identification results. Identifications are $\times 10^8$ unless stated otherwise in the substructure result.

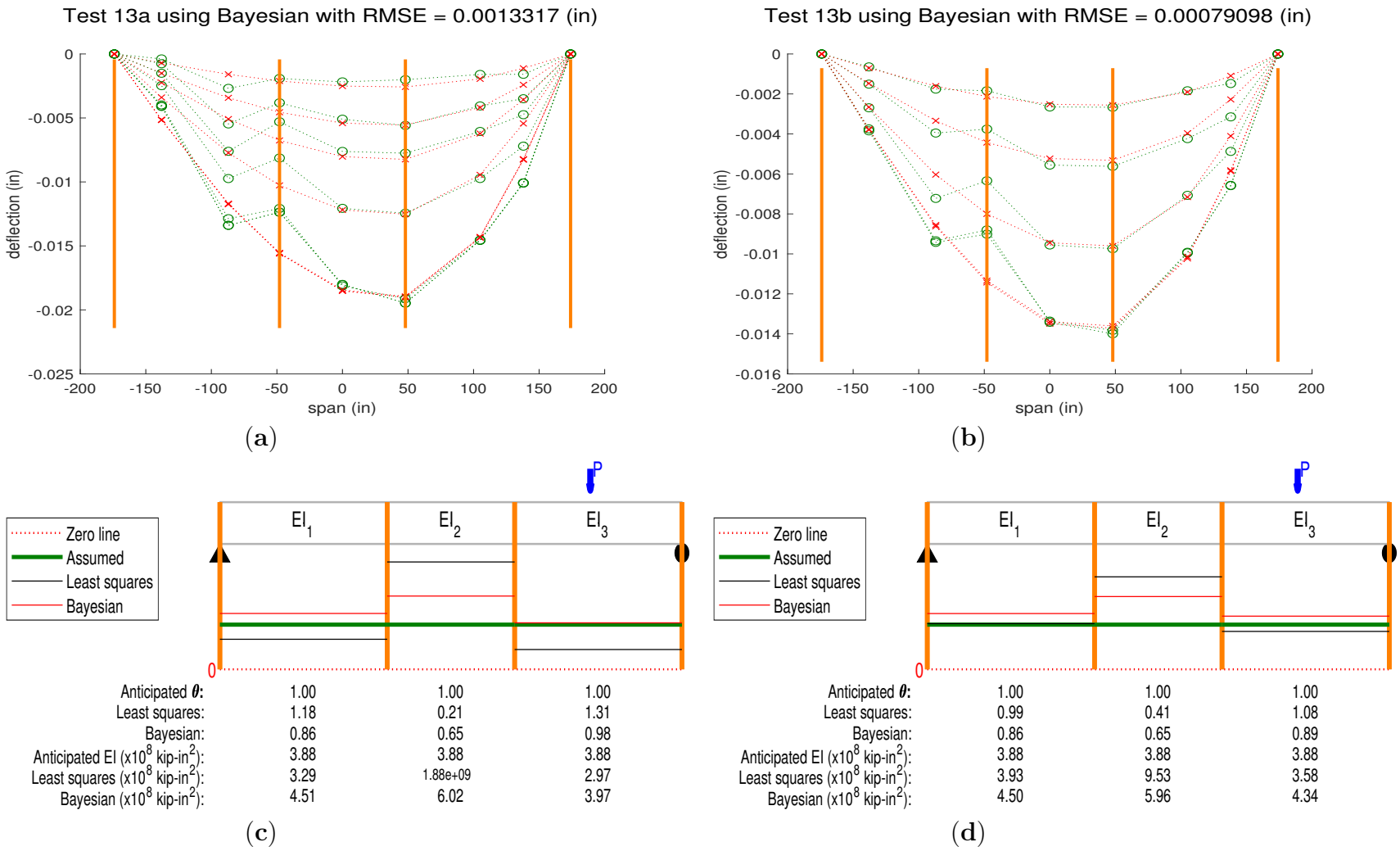

Fig. D.70. Tests 13a and 13b Bayesian analysis deflection comparisons and identification results. Identifications are $\times 10^8$ unless stated otherwise in the substructure result.

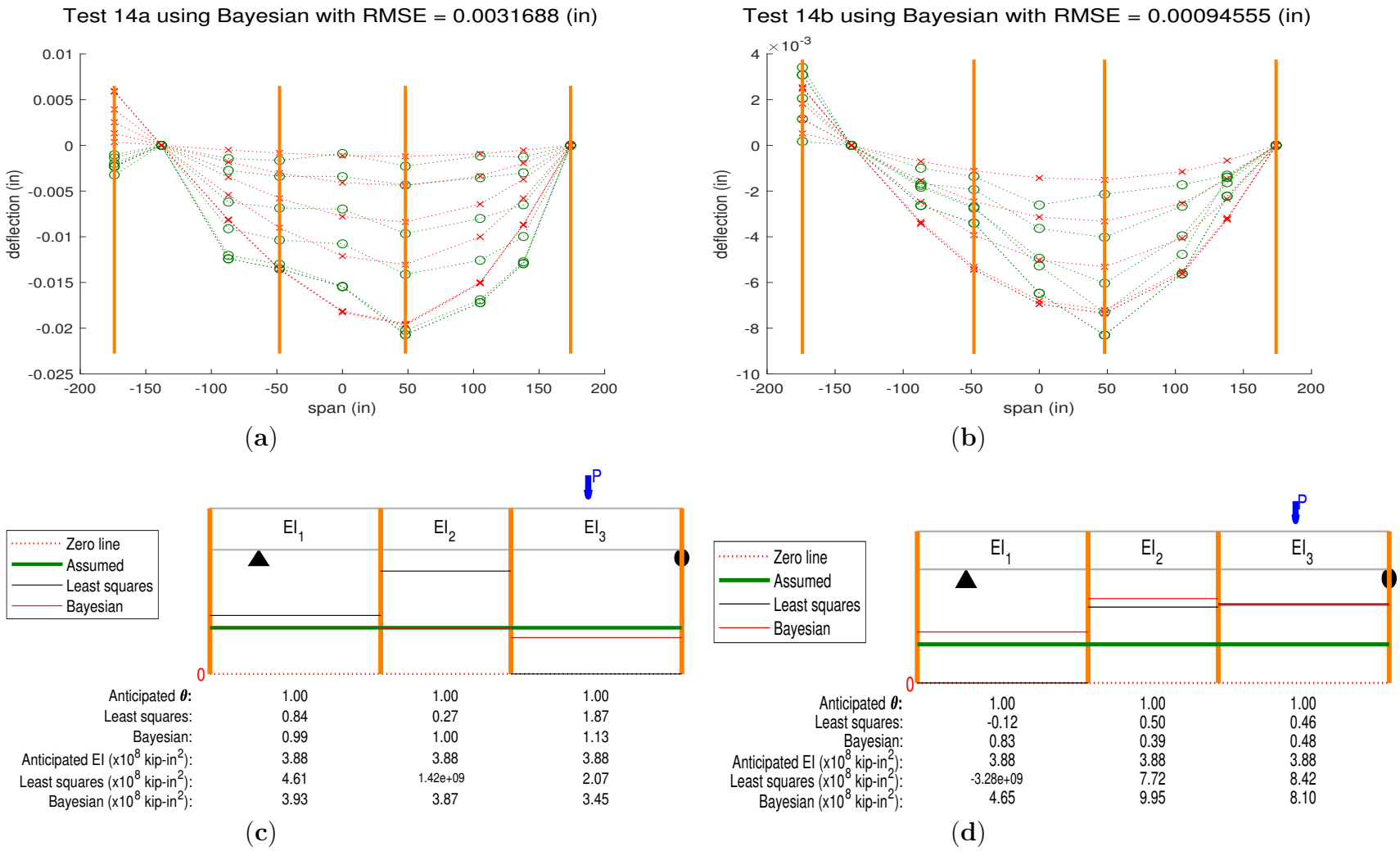

Fig. D.71. Tests 14a and 14b Bayesian analysis deflection comparisons and identification results. Identifications are $\times 10^8$ unless stated otherwise in the substructure result.

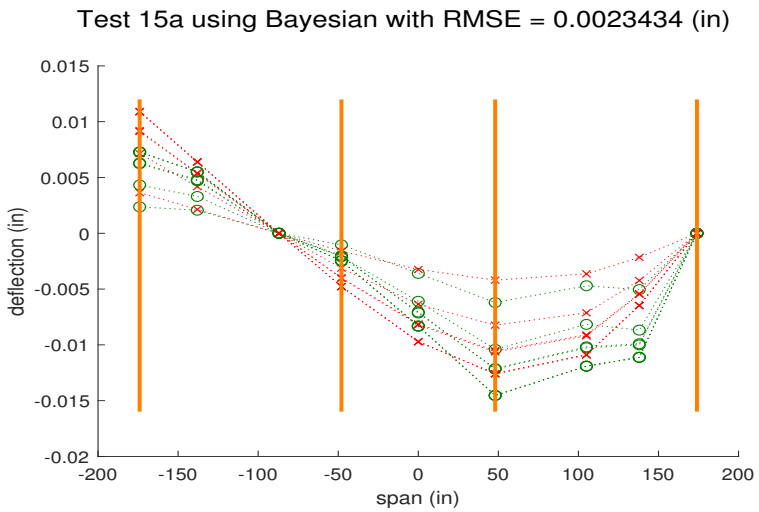

(a)

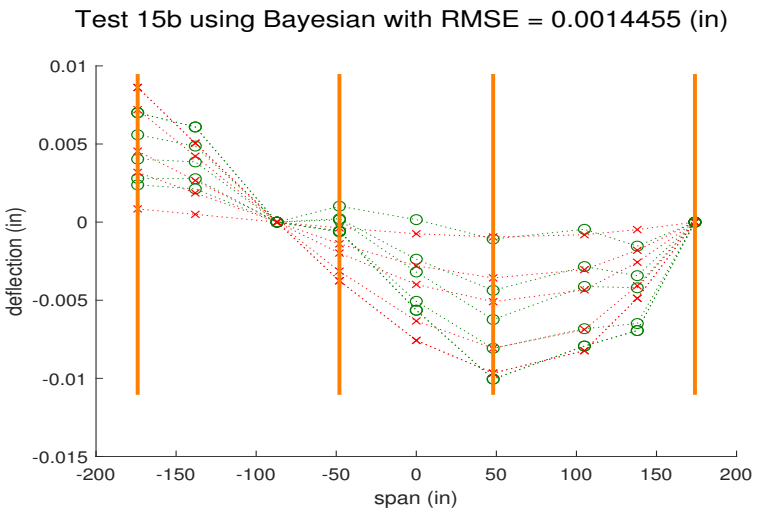

(b)

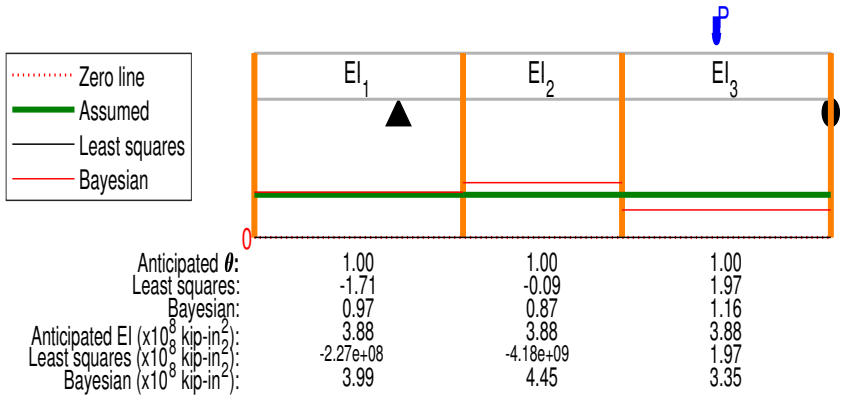

Anticipated θ:	1.00	1.00	1.00
Least squares:	-1.71	-0.09	1.97
Bayesian:	0.97	0.87	1.16
Anticipated EI ($\times 10^8$ kip-in^2):	3.88	3.88	3.88
Least squares ($\times 10^8$ kip-in^2):	-2.27e+08	-4.18e+09	1.97
Bayesian ($\times 10^8$ kip-in^2):	3.99	4.45	3.35

(c)

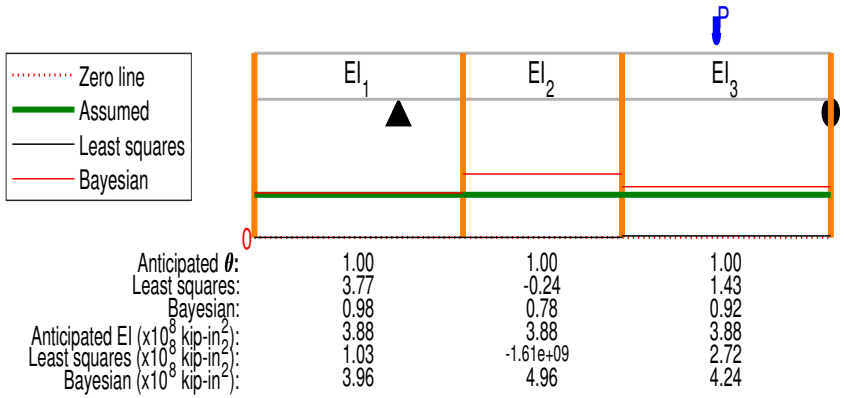

Anticipated θ:	1.00	1.00	1.00
Least squares:	3.77	-0.24	1.43
Bayesian:	0.98	0.78	0.92
Anticipated EI ($\times 10^8$ kip-in^2):	3.88	3.88	3.88
Least squares ($\times 10^8$ kip-in^2):	1.03	-1.61e+09	2.72
Bayesian ($\times 10^8$ kip-in^2):	3.96	4.96	4.24

(d)

Fig. D.72. Tests 15a and 15b Bayesian analysis deflection comparisons and identification results. Identifications are $\times 10^8$ unless stated otherwise in the substructure result.

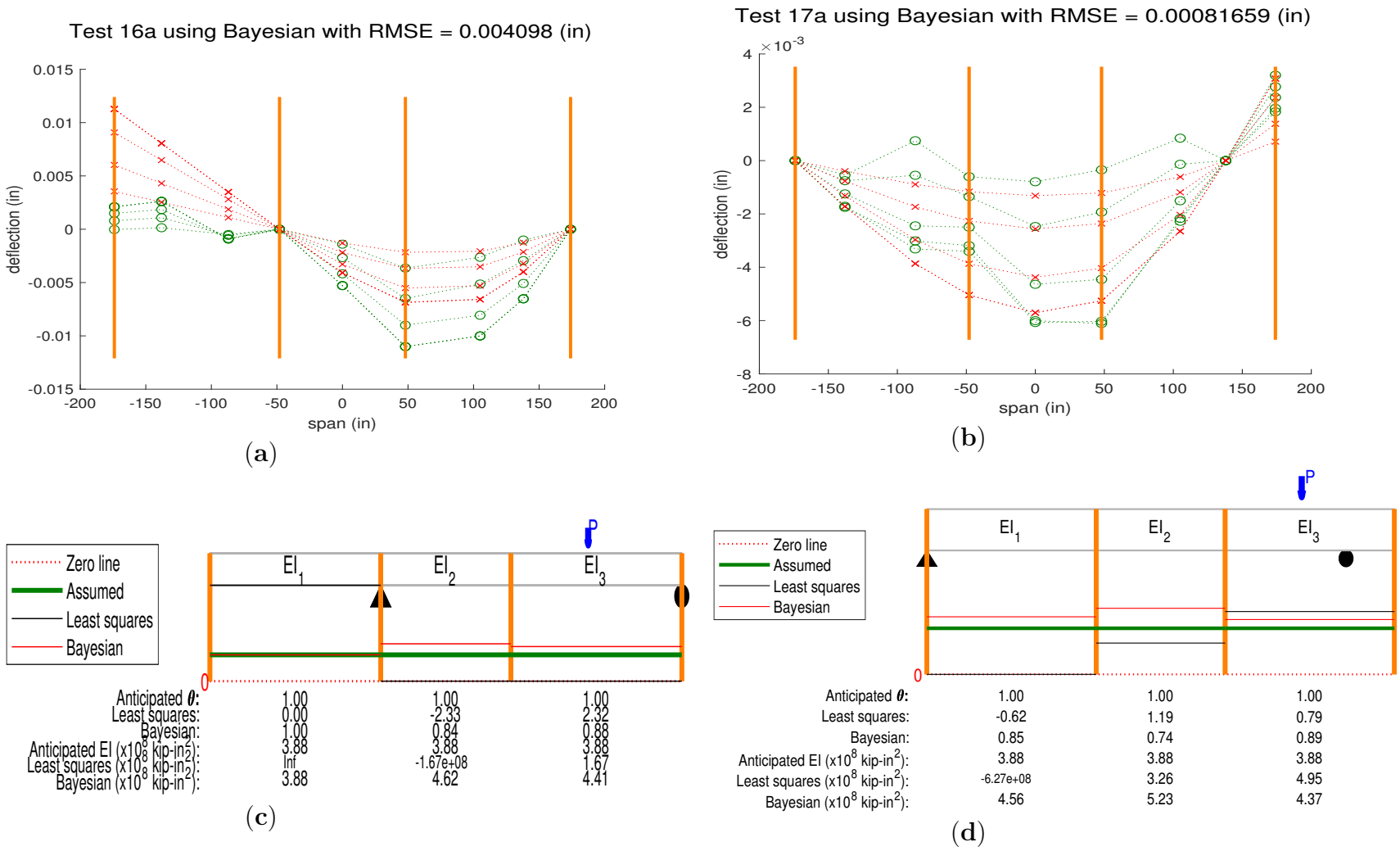

Fig. D.73. Tests 16a and 17a Bayesian analysis deflection comparisons and identification results. Identifications are $\times 10^8$ unless stated otherwise in the substructure result.

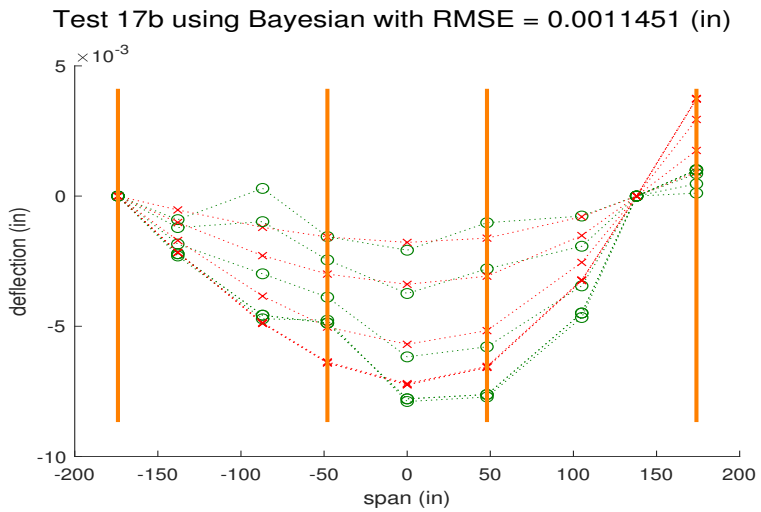

(a)

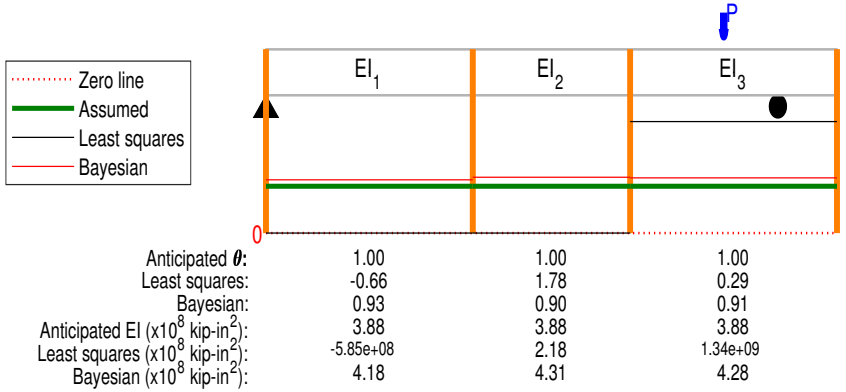

Anticipated θ:	1.00	1.00	1.00
Least squares:	-0.66	1.78	0.29
Bayesian:	0.93	0.90	0.91
Anticipated EI (x10^8 kip-in^2):	3.88	3.88	3.88
Least squares (x10^8 kip-in^2):	-5.85e+08	2.18	1.34e+09
Bayesian (x10^8 kip-in^2):	4.18	4.31	4.28

(c)

Fig. D.74. Test 17b Bayesian analysis deflection comparisons and identification results. Identifications are $\times 10^8$ unless stated otherwise in the substructure result.

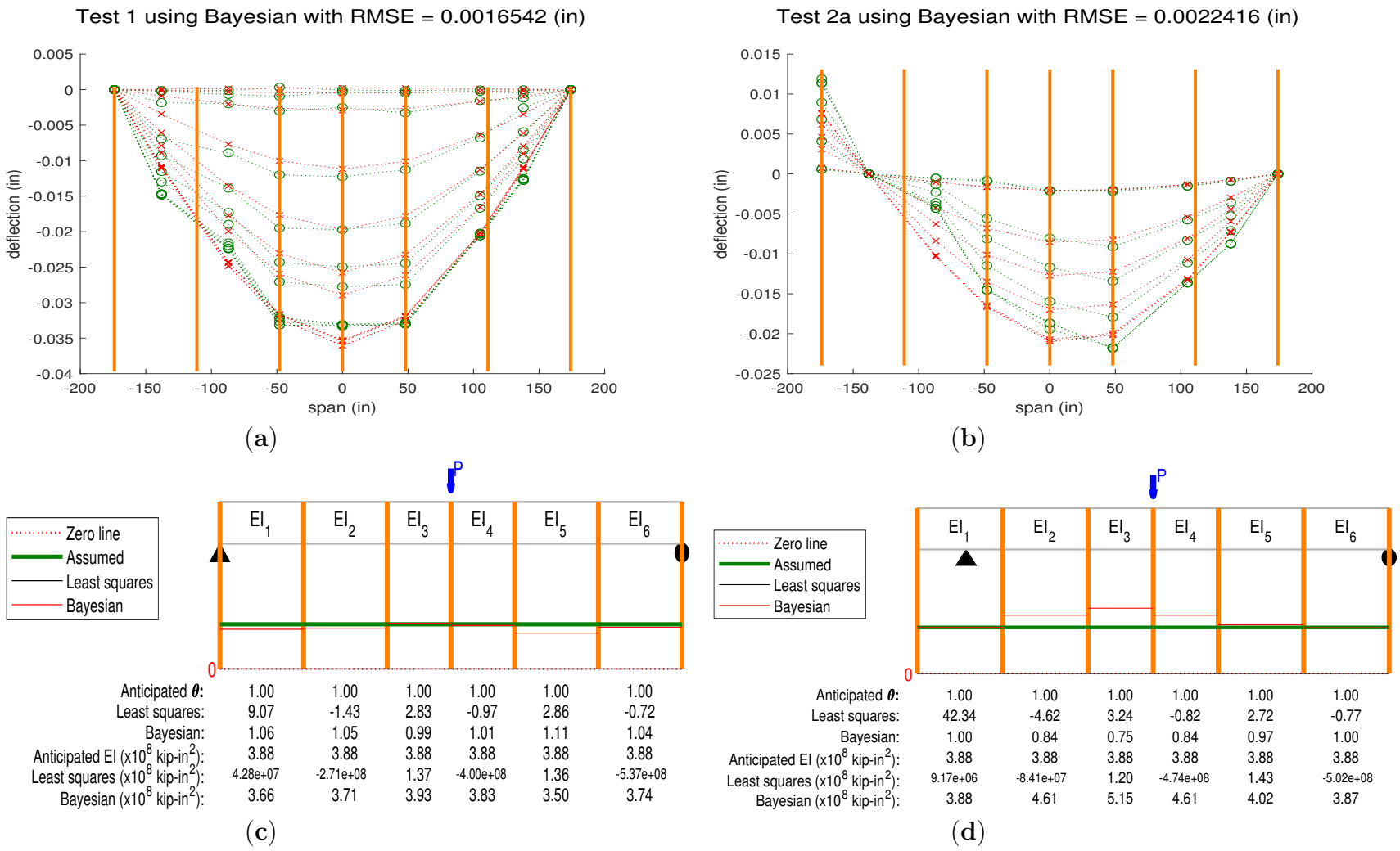

Fig. D.75. Tests 1 and 2a Bayesian analysis deflection comparisons and identification results. Identifications are $\times 10^8$ unless stated otherwise in the substructure result.

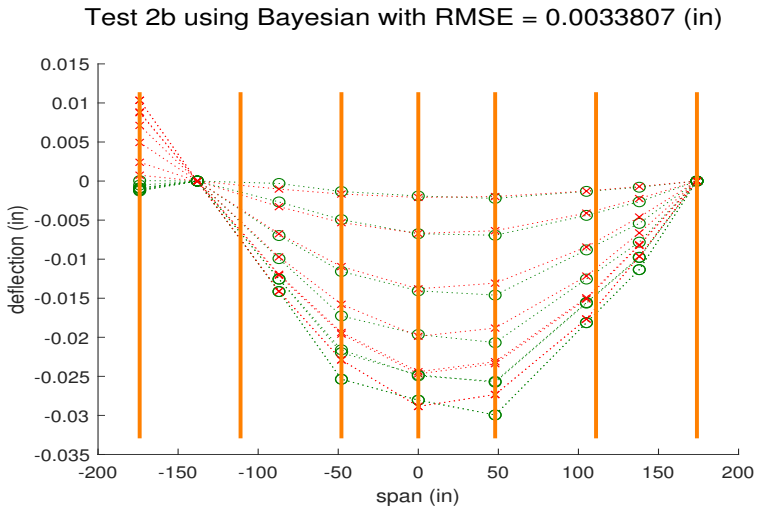

(a)

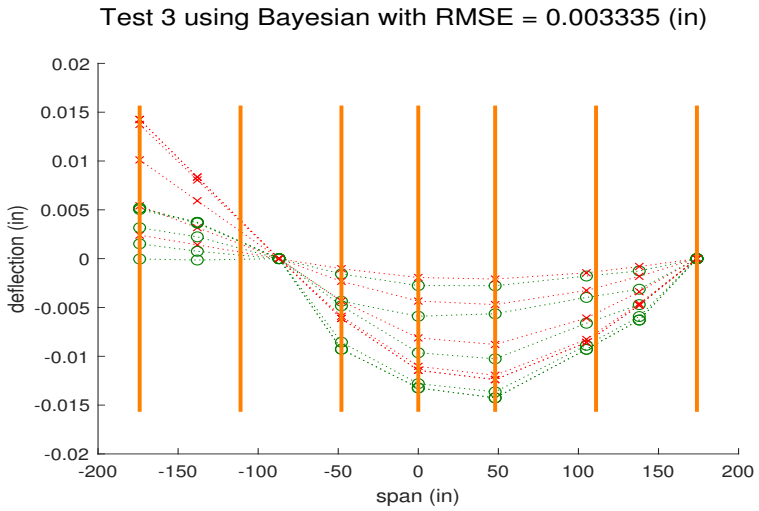

(b)

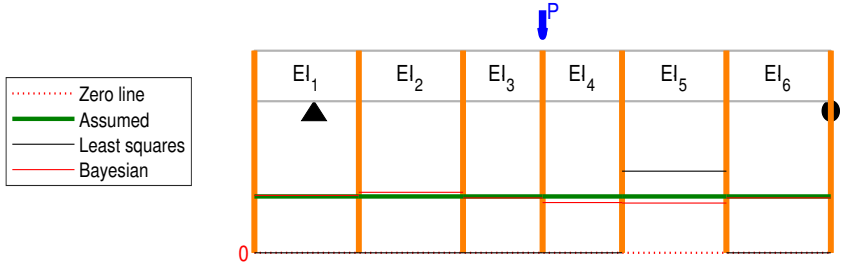

Anticipated θ:	1.00	1.00	1.00	1.00	1.00	1.00
Least squares:	-59.96	4.93	-0.72	2.02	0.73	2.14
Bayesian:	0.99	0.96	1.02	1.06	1.07	1.02
Anticipated EI ($\times 10^8$ kip-in^2):	3.88	3.88	3.88	3.88	3.88	3.88
Least squares ($\times 10^8$ kip-in^2):	-6.48e+06	7.87e+07	-5.43e+08	1.93	5.29	1.82
Bayesian ($\times 10^8$ kip-in^2):	3.93	4.06	3.82	3.65	3.63	3.83

(c)

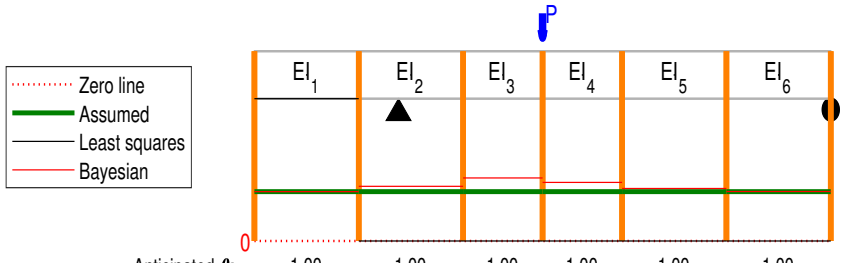

Anticipated θ:	1.00	1.00	1.00	1.00	1.00	1.00
Least squares:	0.00	-15.58	6.42	-2.25	2.82	-0.47
Bayesian:	1.00	0.94	0.85	0.90	0.97	1.00
Anticipated EI ($\times 10^8$ kip-in^2):	3.88	3.88	3.88	3.88	3.88	3.88
Least squares ($\times 10^8$ kip-in^2):	Inf	-2.49e+07	6.05e+07	-1.73e+08	1.38	-8.22e+08
Bayesian ($\times 10^8$ kip-in^2):	3.88	4.12	4.55	4.31	4.02	3.89

(d)

Fig. D.76. Tests 2b and 3 Bayesian analysis deflection comparisons and identification results. Identifications are $\times 10^8$ unless stated otherwise in the substructure result.

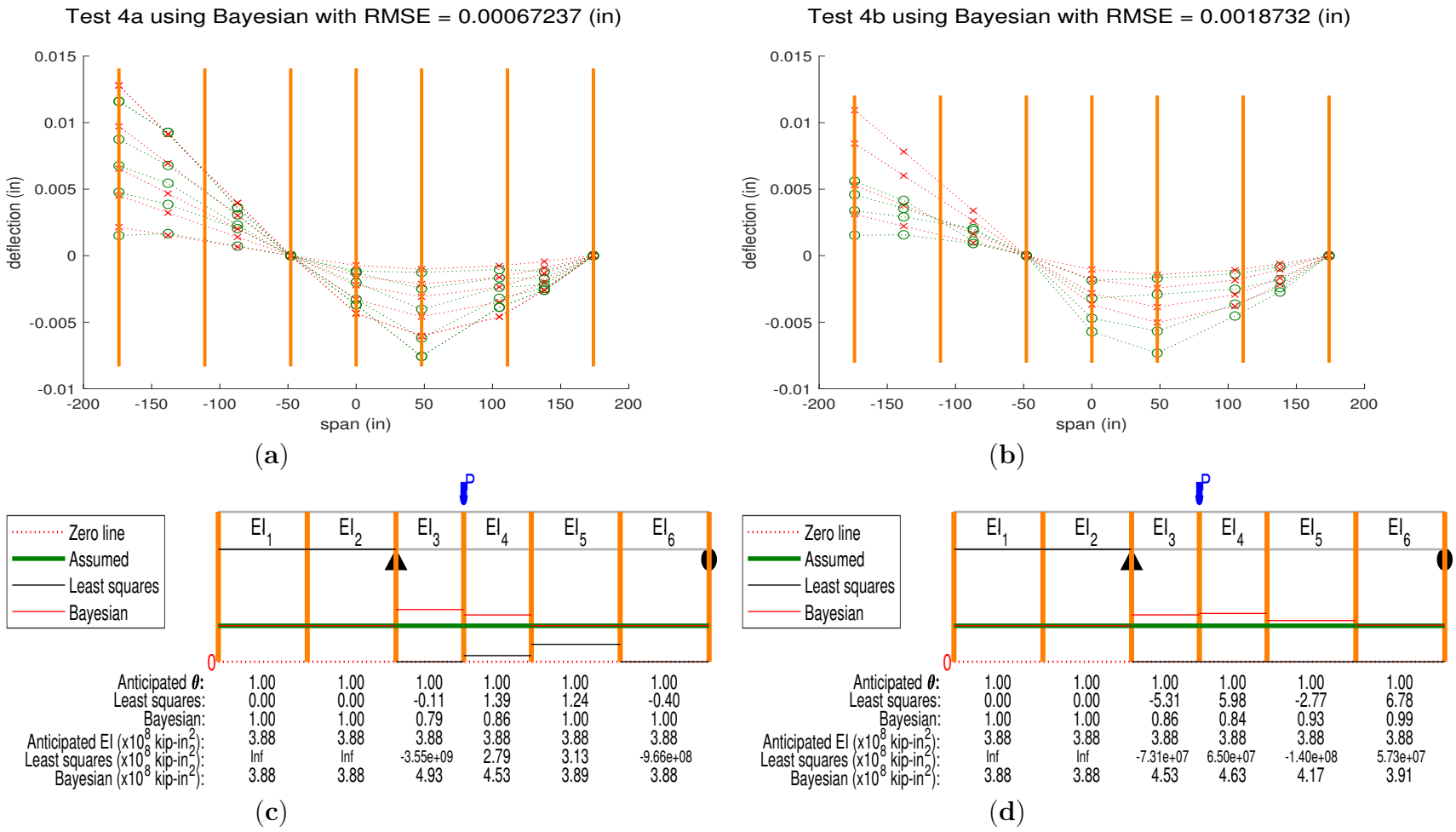

Fig. D.77. Tests 4a and 4b Bayesian analysis deflection comparisons and identification results. Identifications are $\times 10^8$ unless stated otherwise in the substructure result.

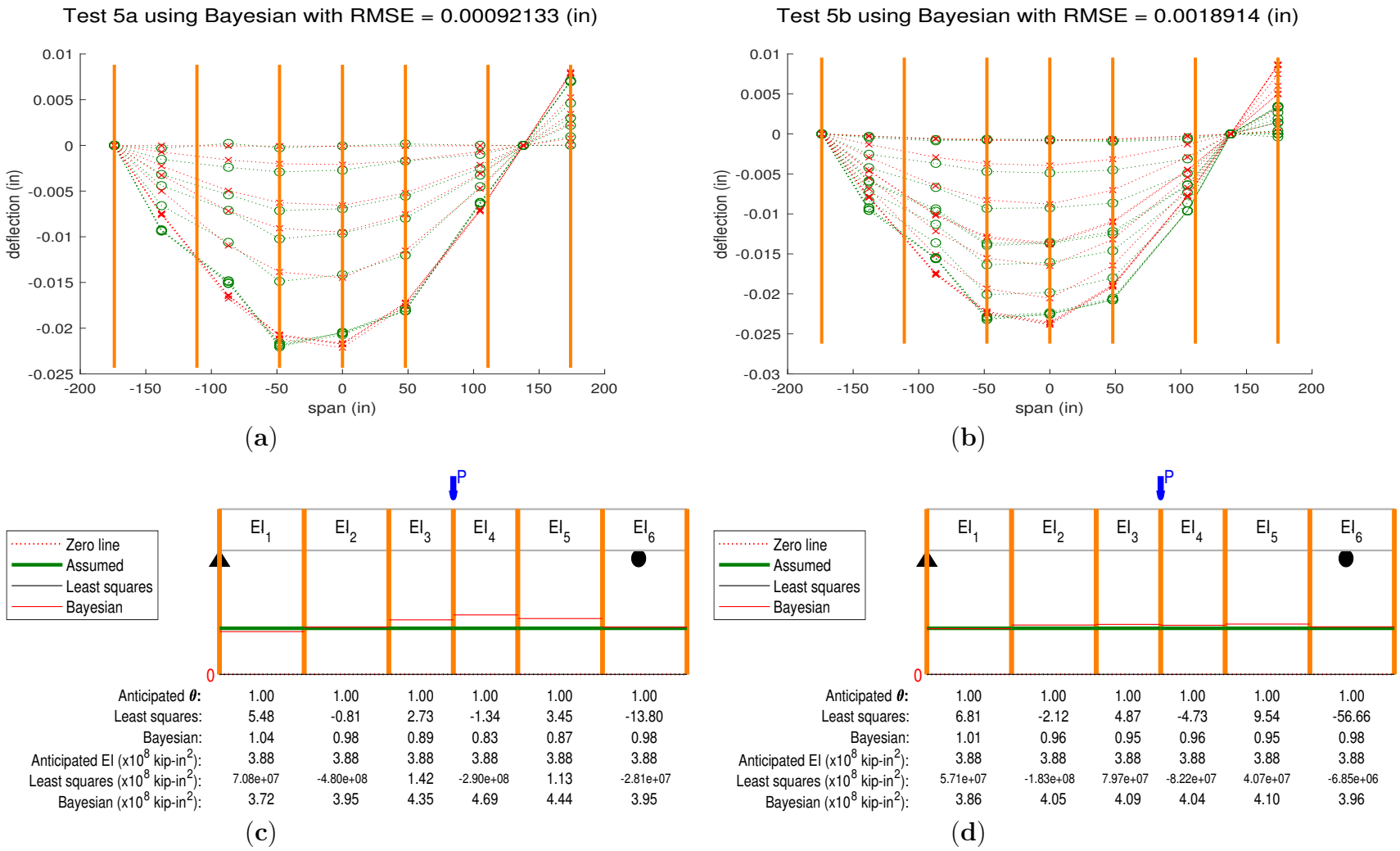

Fig. D.78. Tests 4a and 5b Bayesian analysis deflection comparisons and identification results. Identifications are $\times 10^8$ unless stated otherwise in the substructure result.

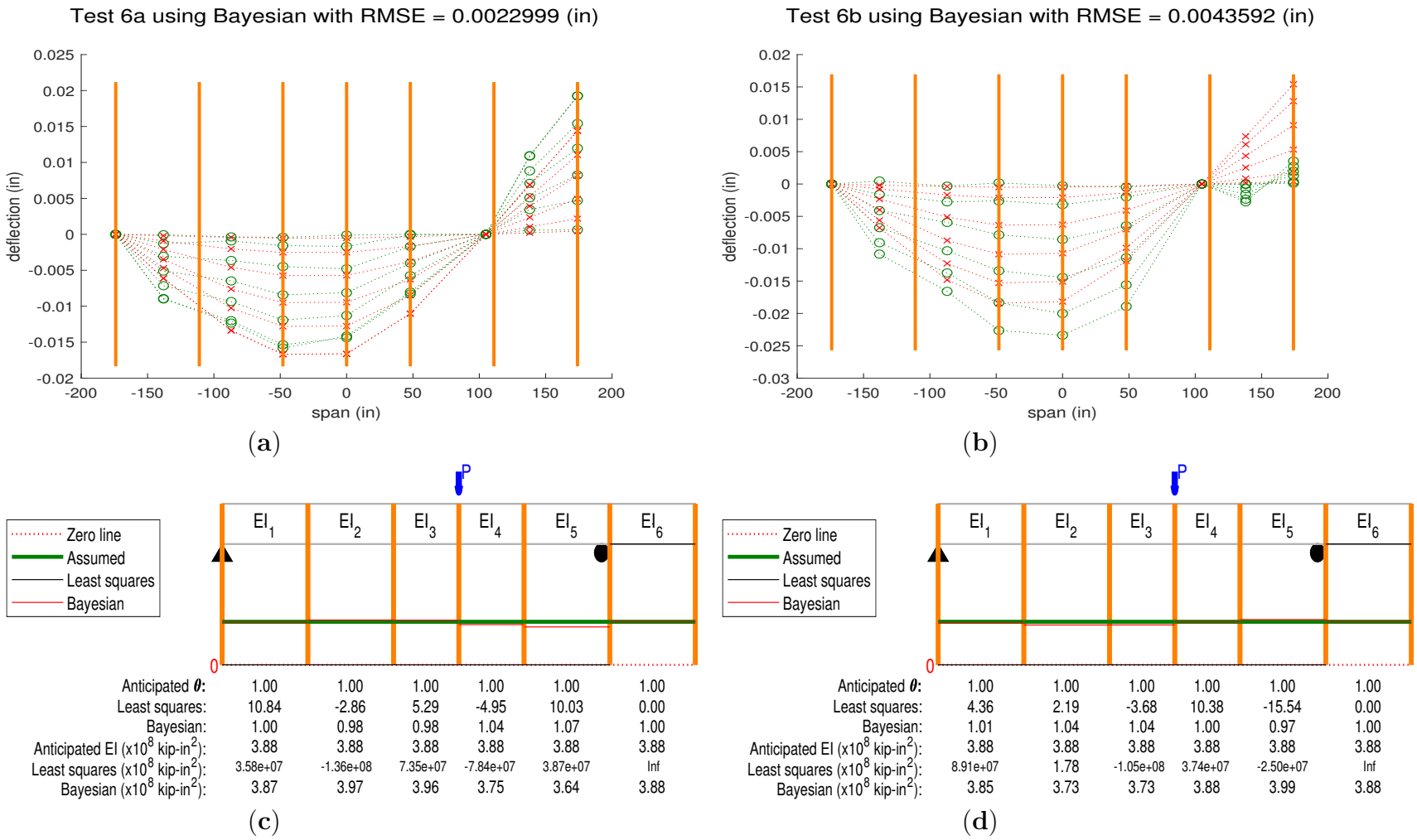

Fig. D.79. Tests 6a and 6b Bayesian analysis deflection comparisons and identification results. Identifications are $\times 10^8$ unless stated otherwise in the substructure result.

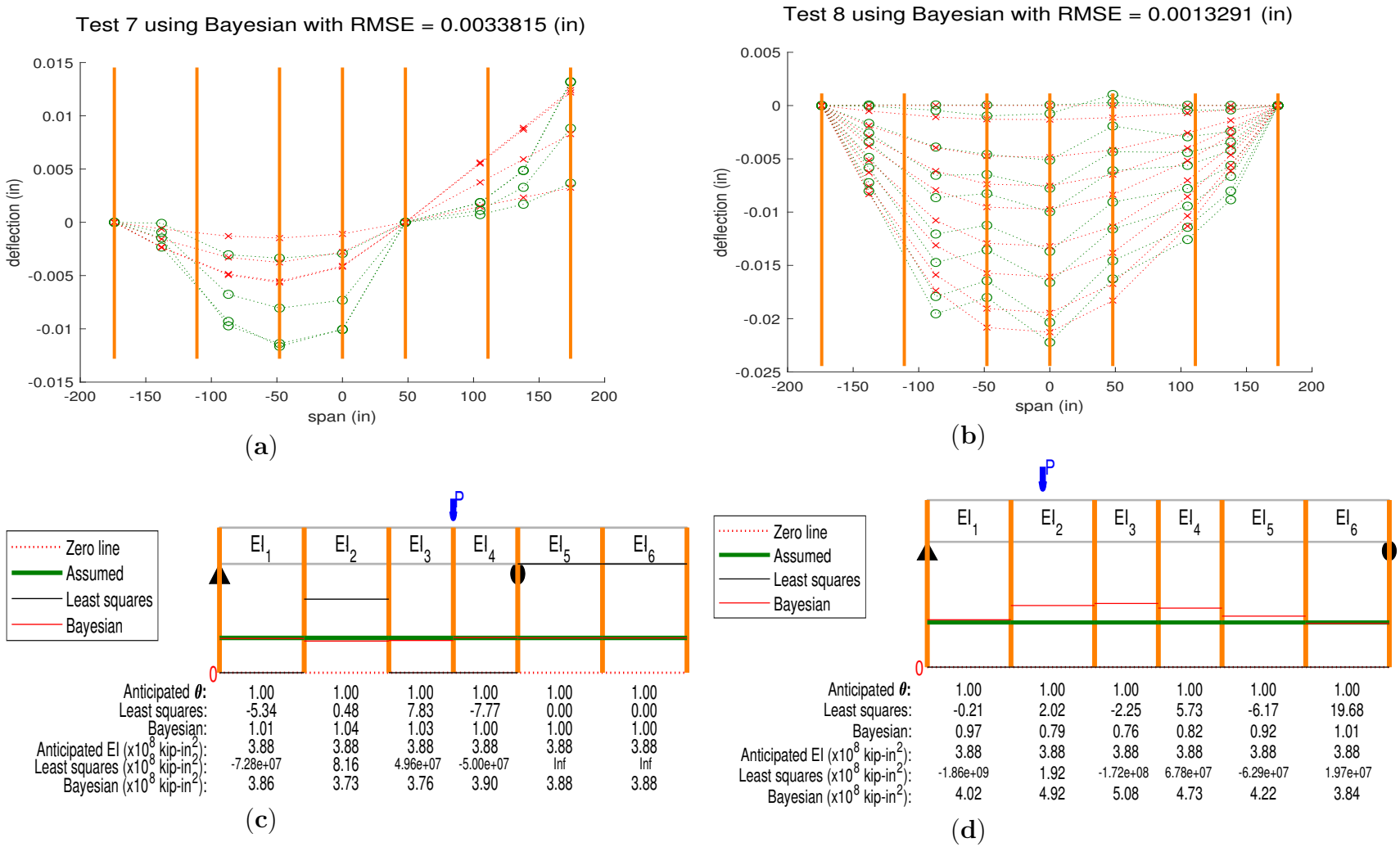

Fig. D.80. Tests 7 and 8 Bayesian analysis deflection comparisons and identification results. Identifications are $\times 10^8$ unless stated otherwise in the substructure result.

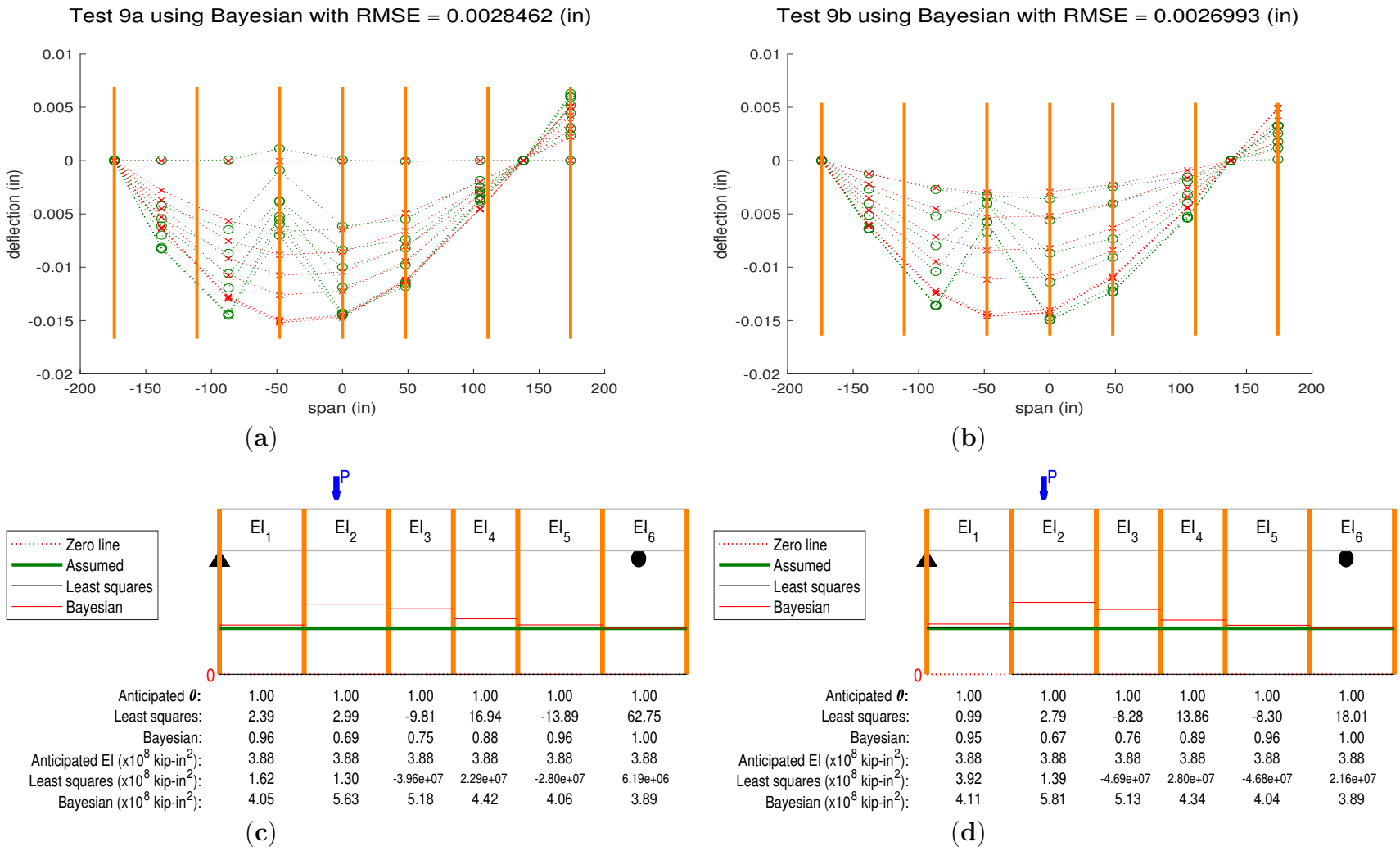

Fig. D.81. Tests 9a and 9b Bayesian analysis deflection comparisons and identification results. Identifications are $\times 10^8$ unless stated otherwise in the substructure result.

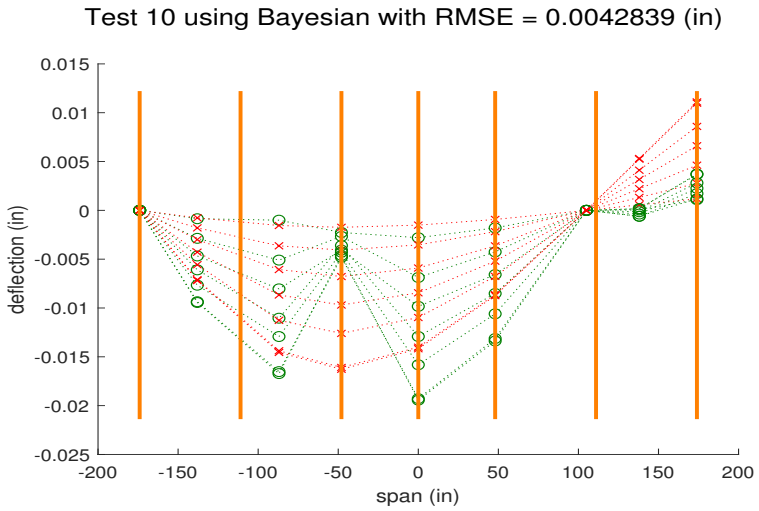

(a)

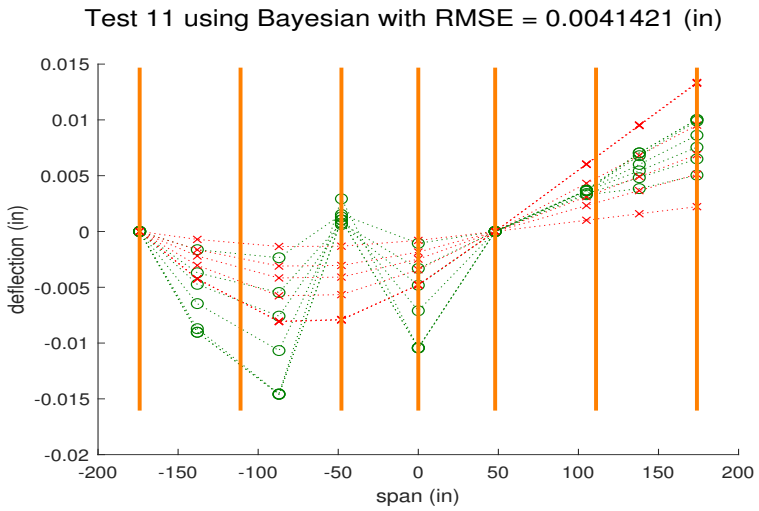

(b)

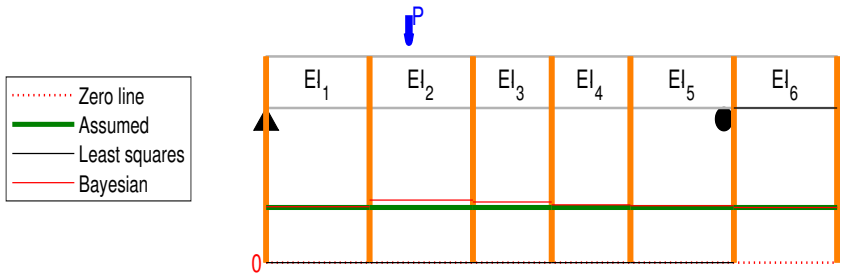

Anticipated θ:	1.00	1.00	1.00	1.00	1.00	1.00
Least squares:	2.61	3.44	-13.52	28.10	-31.19	0.00
Bayesian:	0.99	0.93	0.94	0.97	0.98	1.00
Anticipated EI ($\times 10^8$ kip-in^2):	3.88	3.88	3.88	3.88	3.88	3.88
Least squares ($\times 10^8$ kip-in^2):	1.49	1.13	-2.87e+07	1.38e+07	-1.25e+07	Inf
Bayesian ($\times 10^8$ kip-in^2):	3.91	4.20	4.11	3.99	3.95	3.88

(c)

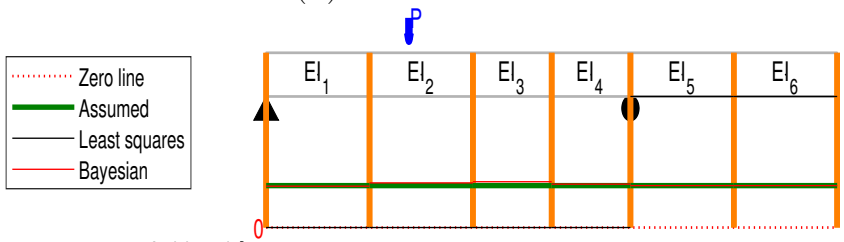

Anticipated θ:	1.00	1.00	1.00	1.00	1.00	1.00
Least squares:	7.21	1.82	-6.05	10.05	0.00	0.00
Bayesian:	1.01	0.97	0.96	0.98	1.00	1.00
Anticipated EI ($\times 10^8$ kip-in^2):	3.88	3.88	3.88	3.88	3.88	3.88
Least squares ($\times 10^8$ kip-in^2):	5.38e+07	2.14	-6.42e+07	3.87e+07	Inf	Inf
Bayesian ($\times 10^8$ kip-in^2):	3.86	4.01	4.06	3.95	3.88	3.88

(d)

Fig. D.82. Tests 10 and 11 Bayesian analysis deflection comparisons and identification results. Identifications are $\times 10^8$ unless stated otherwise in the substructure result.

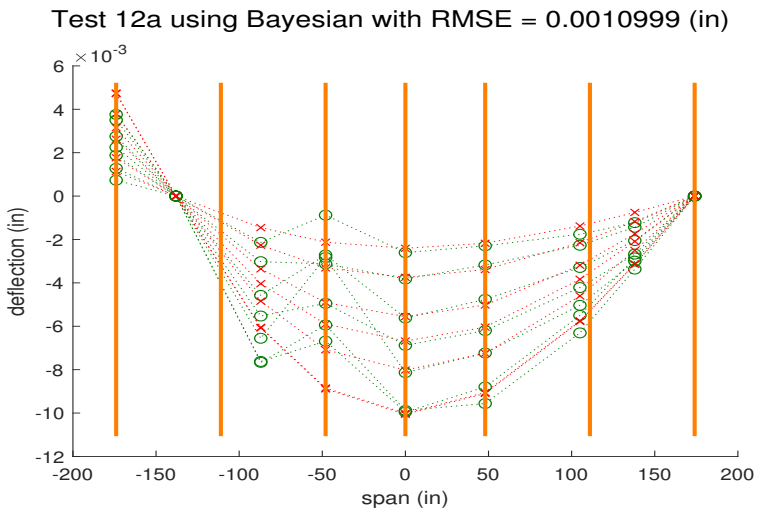

(a)

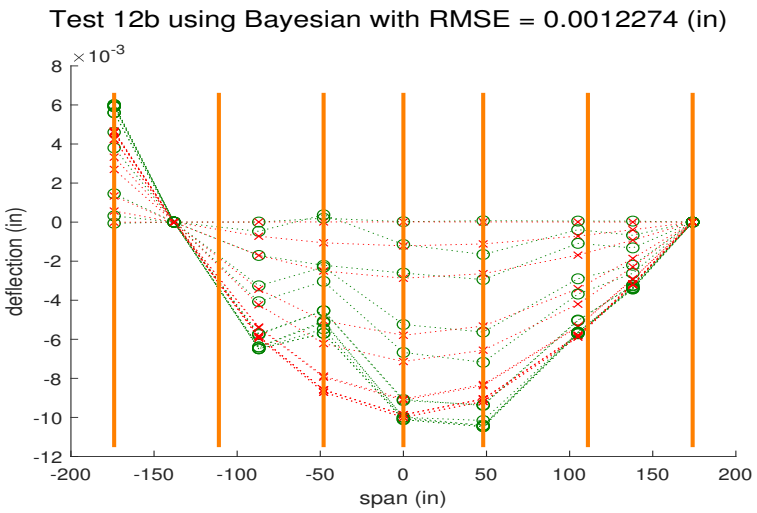

(b)

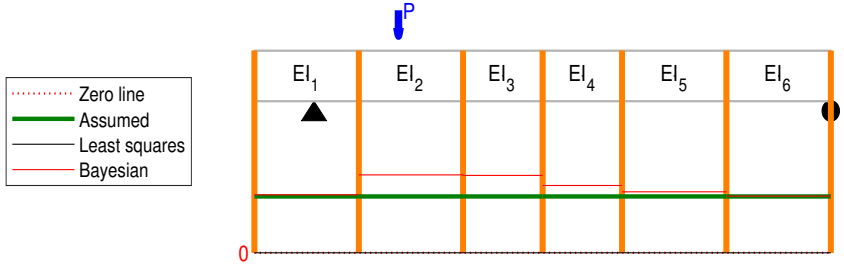

Anticipated **θ**:	1.00	1.00	1.00	1.00	1.00	1.00
Least squares:	-8.96	3.70	-5.86	8.83	-5.01	11.00
Bayesian:	0.98	0.77	0.78	0.88	0.95	1.00
Anticipated EI (x10^8 kip-in^2):	3.88	3.88	3.88	3.88	3.88	3.88
Least squares (x10^8 kip-in^2):	-4.33e+07	1.05	-6.62e+07	4.40e+07	-7.75e+07	3.53e+07
Bayesian (x10^8 kip-in^2):	3.95	5.02	4.99	4.39	4.08	3.90

(c)

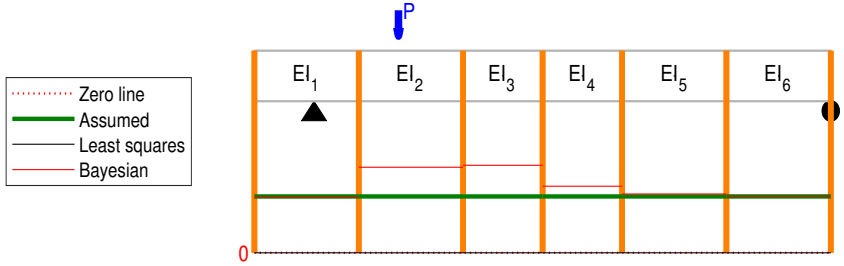

Anticipated **θ**:	1.00	1.00	1.00	1.00	1.00	1.00
Least squares:	4.23	2.04	-5.02	8.66	-4.11	7.50
Bayesian:	1.01	0.69	0.67	0.89	0.97	1.00
Anticipated EI (x10^8 kip-in^2):	3.88	3.88	3.88	3.88	3.88	3.88
Least squares (x10^8 kip-in^2):	9.19e+07	1.90	-7.73e+07	4.49e+07	-9.44e+07	5.18e+07
Bayesian (x10^8 kip-in^2):	3.84	5.60	5.77	4.35	3.99	3.89

(d)

Fig. D.83. Tests 12a and 12b Bayesian analysis deflection comparisons and identification results. Identifications are $\times 10^8$ unless stated otherwise in the substructure result.

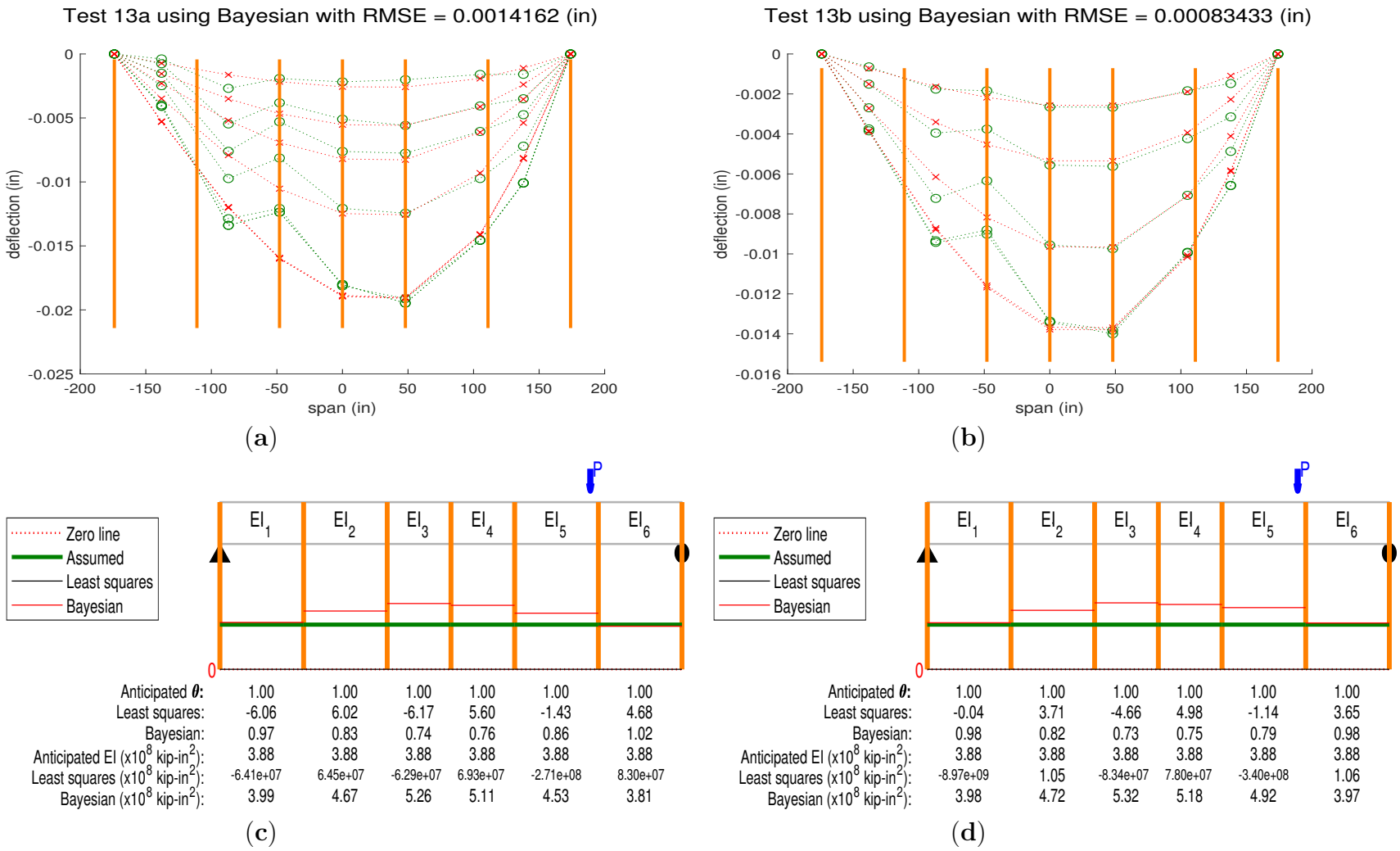

Fig. D.84. Tests 13a and 13b Bayesian analysis deflection comparisons and identification results. Identifications are $\times 10^8$ unless stated otherwise in the substructure result.

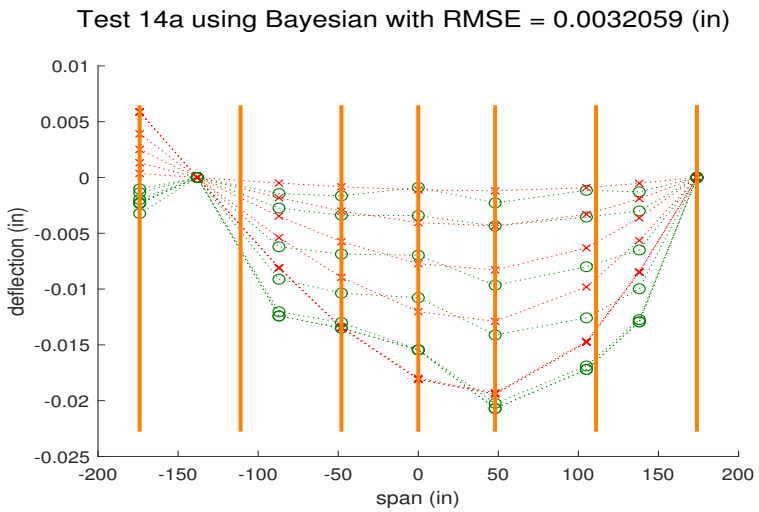

(a)

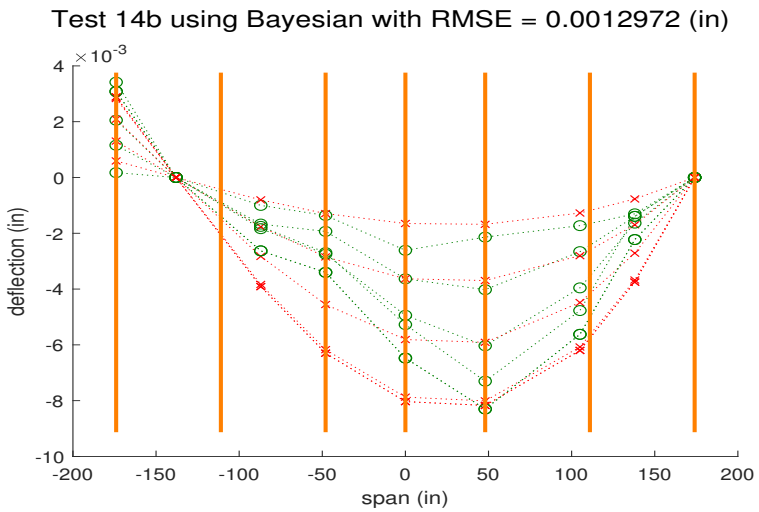

(b)

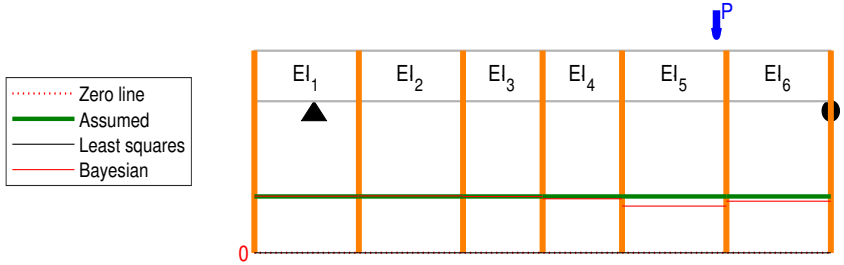

	EI_1	EI_2	EI_3	EI_4	EI_5	EI_6
Anticipated $\boldsymbol{\theta}$:	1.00	1.00	1.00	1.00	1.00	1.00
Least squares:	-147.05	19.18	-10.54	5.91	-1.05	6.12
Bayesian:	1.00	0.99	1.00	1.02	1.10	1.05
Anticipated EI ($\times 10^8$ kip-in^2):	3.88	3.88	3.88	3.88	3.88	3.88
Least squares ($\times 10^8$ kip-in^2):	-2.64e+06	2.02e+07	-3.68e+07	6.57e+07	-3.70e+08	6.35e+07
Bayesian ($\times 10^8$ kip-in^2):	3.89	3.91	3.88	3.79	3.53	3.70

(c)

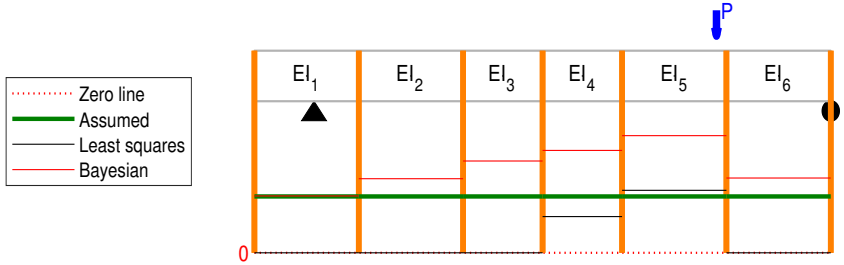

	EI_1	EI_2	EI_3	EI_4	EI_5	EI_6
Anticipated $\boldsymbol{\theta}$:	1.00	1.00	1.00	1.00	1.00	1.00
Least squares:	19.70	-0.38	-0.94	1.21	0.94	-0.99
Bayesian:	0.99	0.81	0.63	0.52	0.36	0.81
Anticipated EI ($\times 10^8$ kip-in^2):	3.88	3.88	3.88	3.88	3.88	3.88
Least squares ($\times 10^8$ kip-in^2):	1.97e+07	-1.01e+09	-4.12e+08	3.21	4.15	-3.92e+08
Bayesian ($\times 10^8$ kip-in^2):	3.90	4.77	6.19	7.52	1.07e+09	4.82

(d)

Fig. D.85. Tests 14a and 14b Bayesian analysis deflection comparisons and identification results. Identifications are $\times 10^8$ unless stated otherwise in the substructure result.

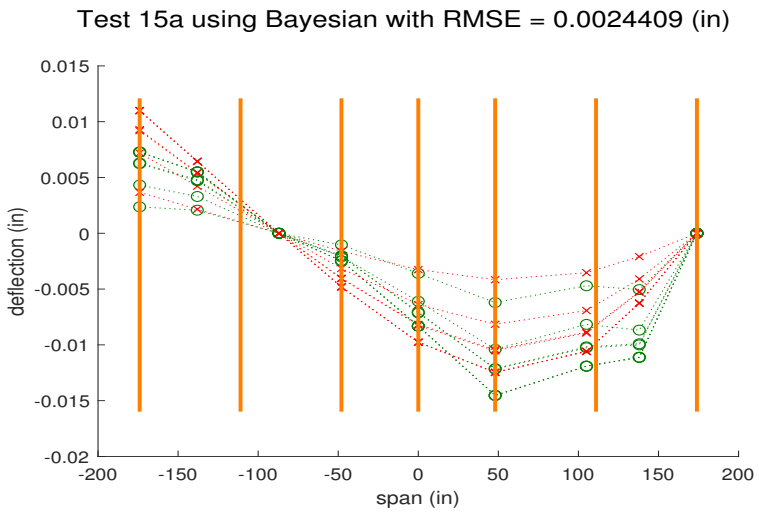

(a)

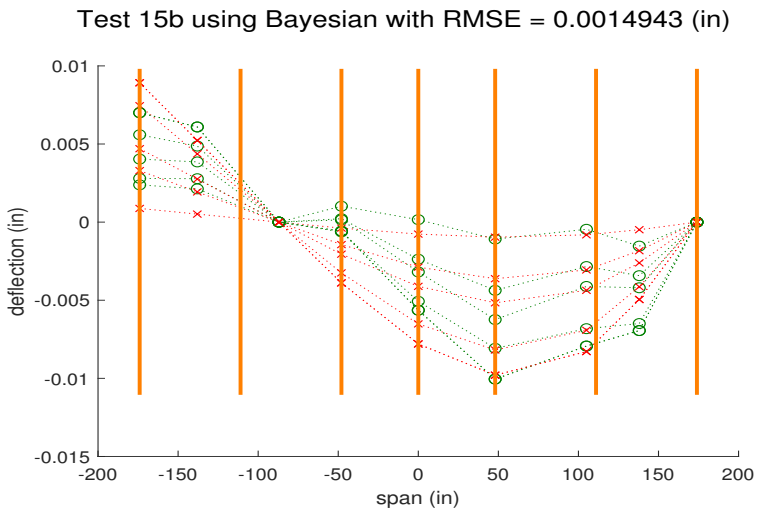

(b)

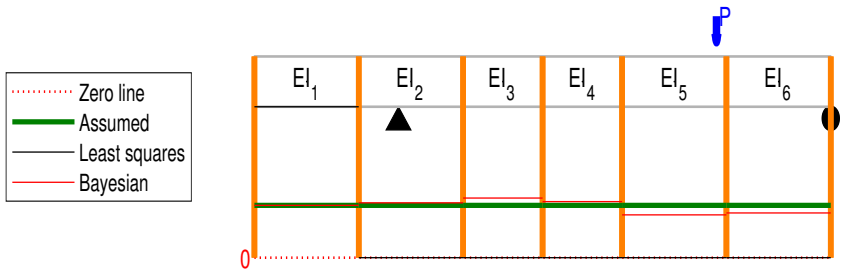

Anticipated θ:	1.00	1.00	1.00	1.00	1.00	1.00
Least squares:	0.00	13.10	-10.81	8.25	-2.35	7.68
Bayesian:	1.00	0.97	0.93	0.96	1.10	1.08
Anticipated EI ($\times 10^8$ kip-in^2):	3.88	3.88	3.88	3.88	3.88	3.88
Least squares ($\times 10^8$ kip-in^2):	Inf	2.96e+07	-3.59e+07	4.71e+07	-1.66e+08	5.06e+07
Bayesian ($\times 10^8$ kip-in^2):	3.88	3.99	4.19	4.04	3.54	3.61

(c)

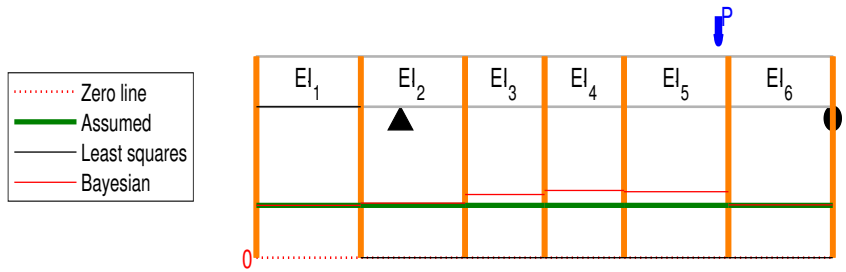

Anticipated θ:	1.00	1.00	1.00	1.00	1.00	1.00
Least squares:	0.00	22.57	-12.97	8.37	-2.25	5.72
Bayesian:	1.00	0.98	0.89	0.85	0.86	1.00
Anticipated EI ($\times 10^8$ kip-in^2):	3.88	3.88	3.88	3.88	3.88	3.88
Least squares ($\times 10^8$ kip-in^2):	Inf	1.72e+07	-3.00e+07	4.64e+07	-1.73e+08	6.79e+07
Bayesian ($\times 10^8$ kip-in^2):	3.88	3.97	4.36	4.58	4.51	3.90

(d)

Fig. D.86. Tests 15a and 15b Bayesian analysis deflection comparisons and identification results. Identifications are $\times 10^8$ unless stated otherwise in the substructure result.

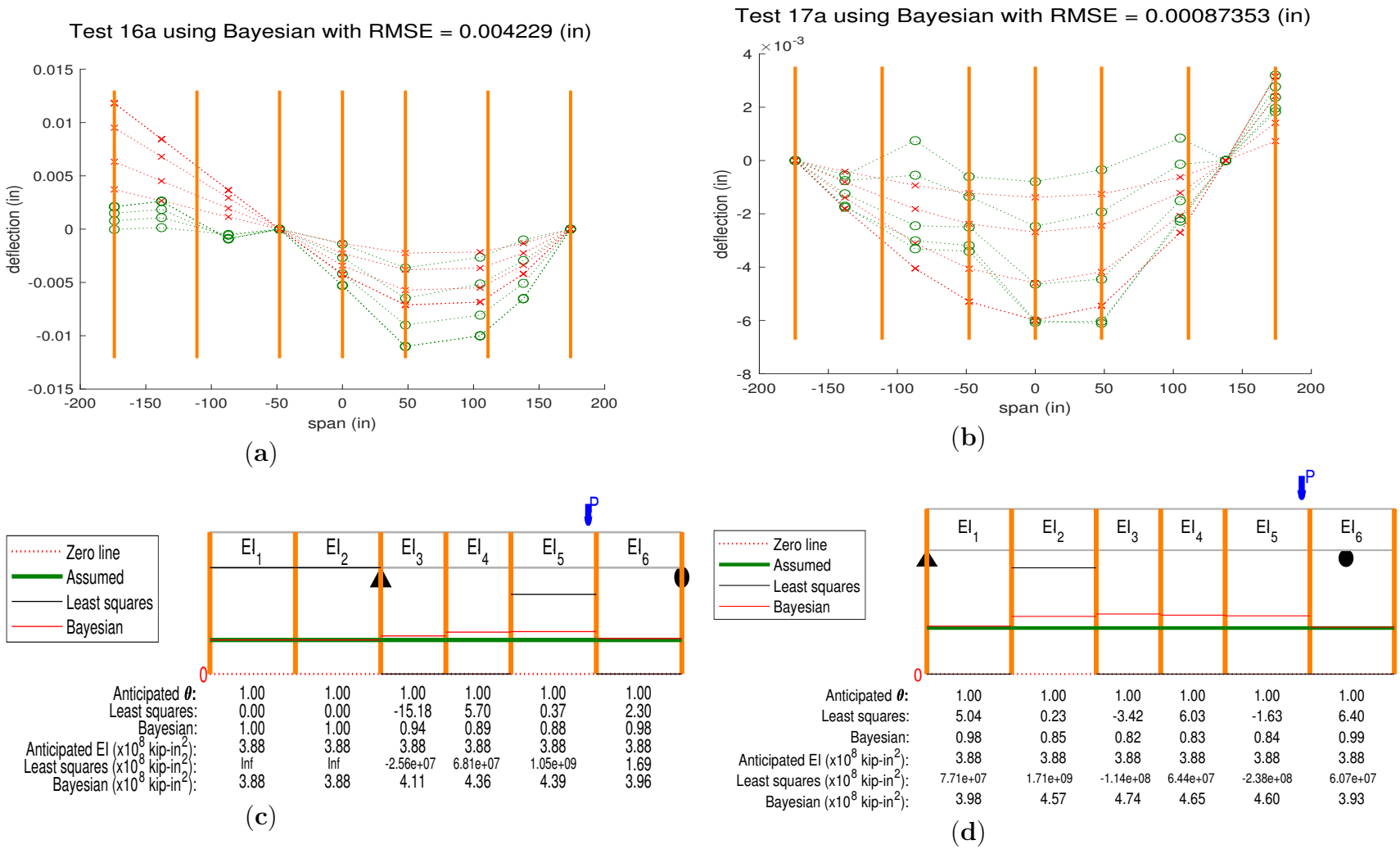

Fig. D.87. Tests 16a and 17a Bayesian analysis deflection comparisons and identification results. Identifications are $\times 10^8$ unless stated otherwise in the substructure result.

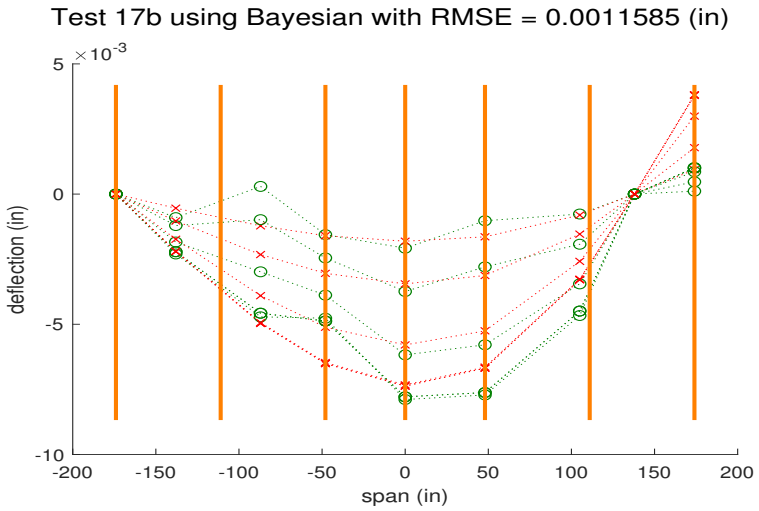

(a)

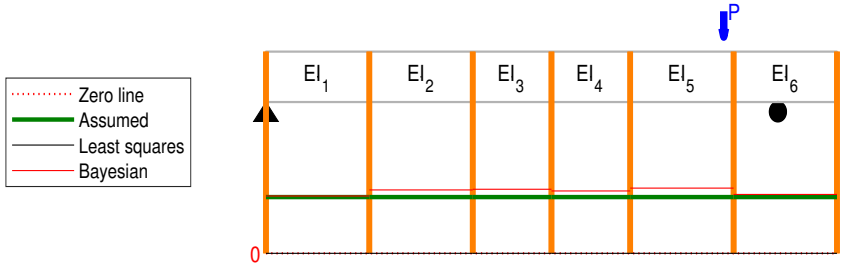

Anticipated $\boldsymbol{\theta}$:	1.00	1.00	1.00	1.00	1.00	1.00
Least squares:	8.50	-2.63	2.72	-1.37	4.07	-14.83
Bayesian:	0.99	0.92	0.92	0.94	0.91	0.97
Anticipated EI ($\times 10^8$ kip-in^2):	3.88	3.88	3.88	3.88	3.88	3.88
Least squares ($\times 10^8$ kip-in^2):	4.57e+07	-1.47e+08	1.43	-2.84e+08	9.53e+07	-2.62e+07
Bayesian ($\times 10^8$ kip-in^2):	3.93	4.20	4.23	4.15	4.29	3.99

(c)

Fig. D.88. Test 17b Bayesian analysis deflection comparisons and identification results. Identifications are $\times 10^8$ unless stated otherwise in the substructure result.

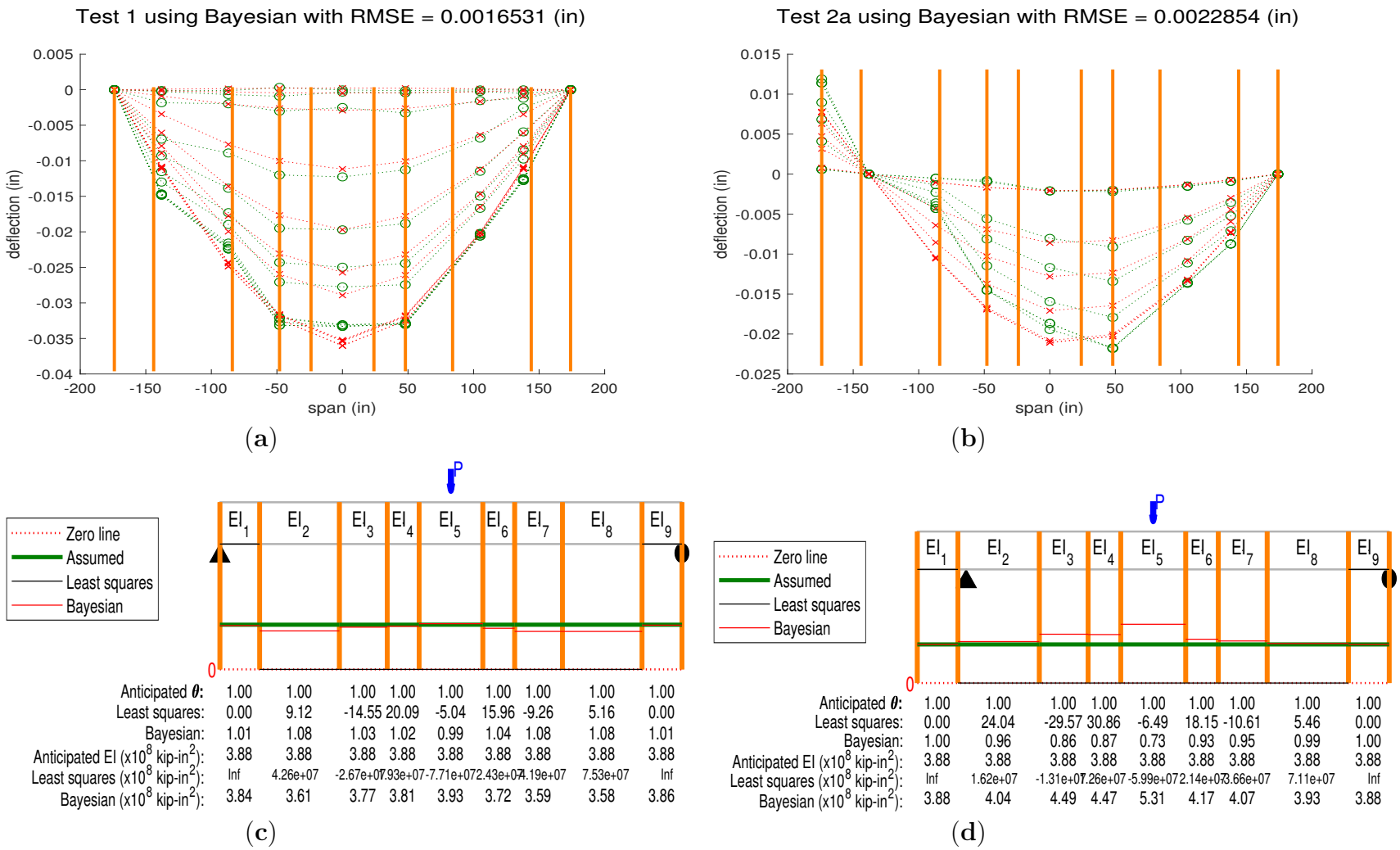

Fig. D.89. Tests 1 and 2a Bayesian analysis deflection comparisons and identification results. Identifications are $\times 10^8$ unless stated otherwise in the substructure result.

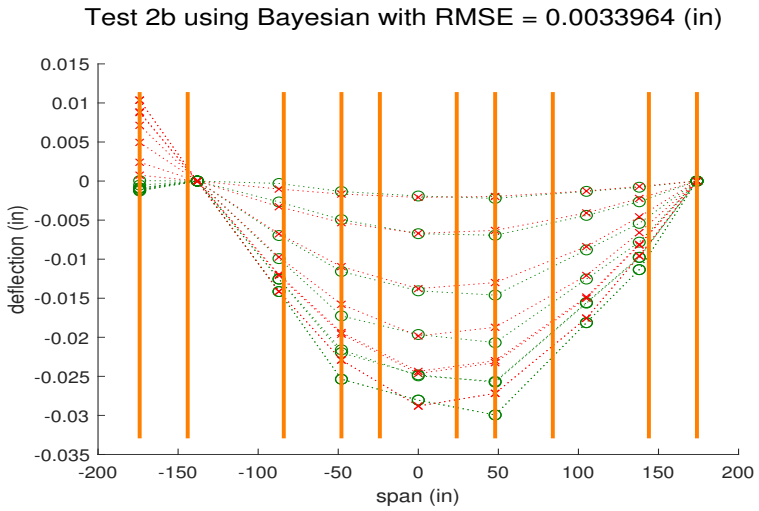

(a)

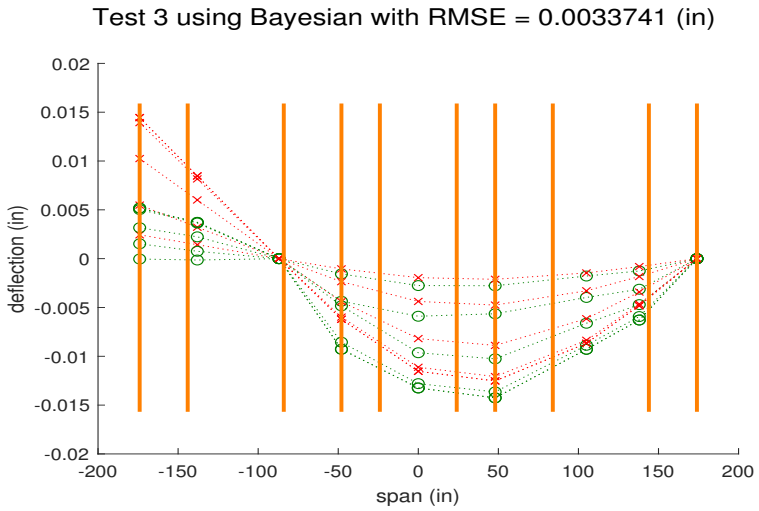

(b)

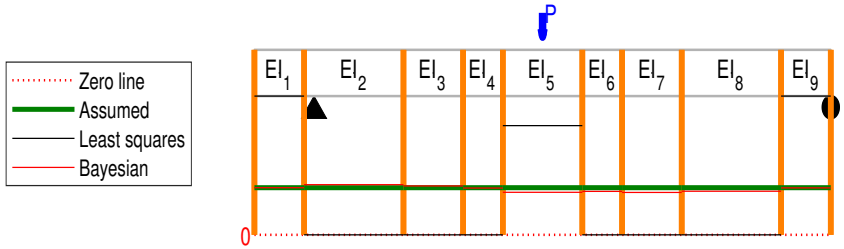

Anticipated θ:	1.00	1.00	1.00	1.00	1.00	1.00	1.00	1.00	1.00
Least squares:	0.00	-28.87	26.86	-17.57	0.32	16.55	-11.33	5.69	0.00
Bayesian:	1.00	0.97	0.98	1.00	1.05	1.04	1.05	1.04	1.00
Anticipated EI ($\times 10^8$ kip-in^2):	3.88	3.88	3.88	3.88	3.88	3.88	3.88	3.88	3.88
Least squares ($\times 10^8$ kip-in^2):	Inf	-1.35e+07	1.45e+07	2.21e+07	1.20e+09	2.35e+07	3.43e+07	6.82e+07	Inf
Bayesian ($\times 10^8$ kip-in^2):	3.88	4.02	3.96	3.87	3.70	3.73	3.69	3.74	3.88

(c)

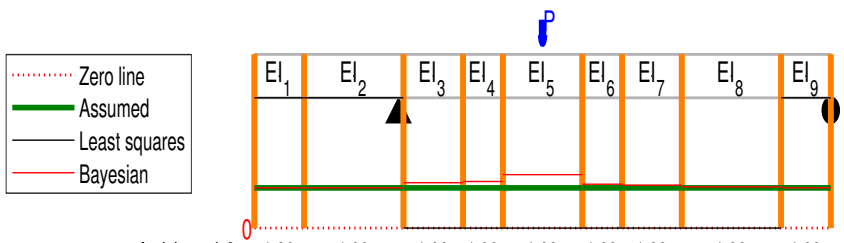

Anticipated θ:	1.00	1.00	1.00	1.00	1.00	1.00	1.00	1.00	1.00
Least squares:	0.00	0.00	-23.44	20.50	-4.12	17.77	-12.65	6.41	0.00
Bayesian:	1.00	1.00	0.94	0.93	0.85	0.96	0.97	0.99	1.00
Anticipated EI ($\times 10^8$ kip-in^2):	3.88	3.88	3.88	3.88	3.88	3.88	3.88	3.88	3.88
Least squares ($\times 10^8$ kip-in^2):	Inf	Inf	-1.66e+07	7.89e+07	-9.42e+07	2.19e+07	3.07e+07	6.05e+07	Inf
Bayesian ($\times 10^8$ kip-in^2):	3.88	3.89	4.12	4.18	4.55	4.05	4.01	3.93	3.88

(d)

Fig. D.90. Tests 2b and 3 Bayesian analysis deflection comparisons and identification results. Identifications are $\times 10^8$ unless stated otherwise in the substructure result.

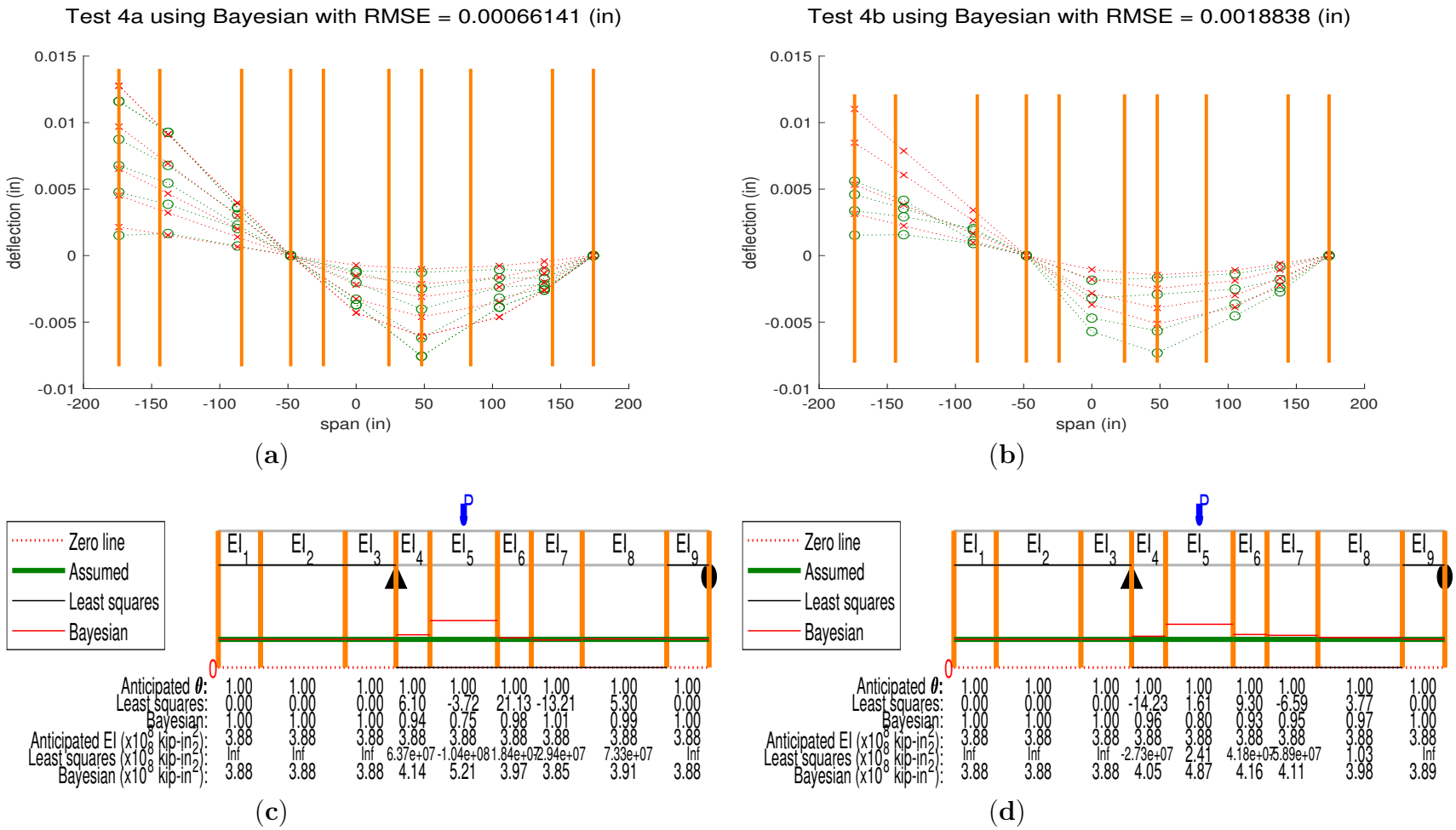

Fig. D.91. Tests 4a and 4b Bayesian analysis deflection comparisons and identification results. Identifications are $\times 10^8$ unless stated otherwise in the substructure result.

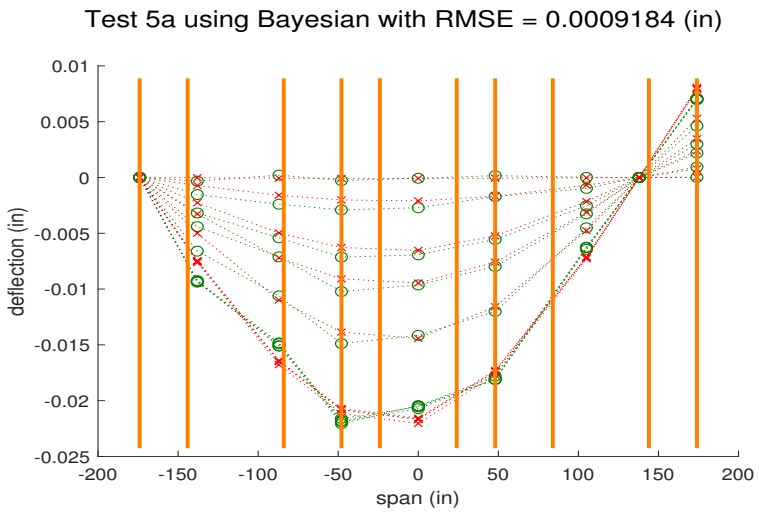

(a)

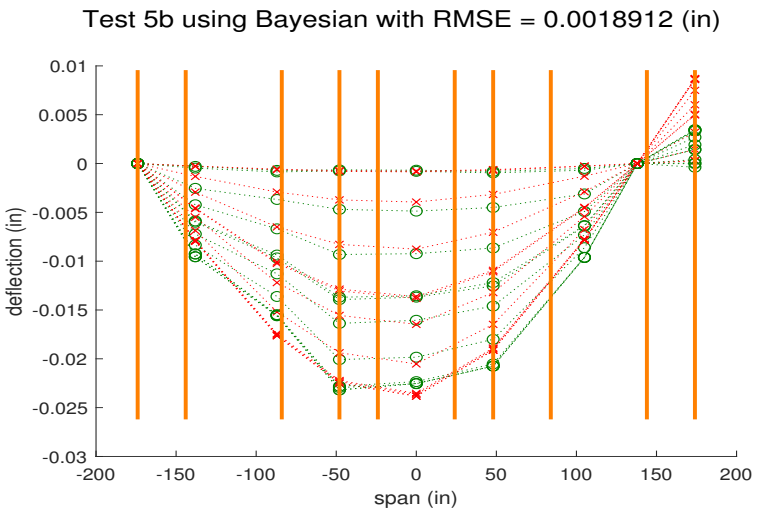

(b)

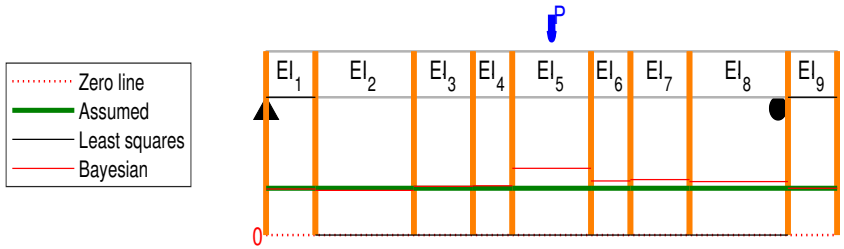

Anticipated θ:	1.00	1.00	1.00	1.00	1.00	1.00	1.00	1.00	1.00
Least squares:	0.00	5.54	-8.75	13.32	-2.33	4.88	-0.26	-0.14	0.00
Bayesian:	1.01	1.02	0.98	0.97	0.78	0.92	0.90	0.93	1.00
Anticipated EI ($\times 10^8$ kip-in^2):	3.88	3.88	3.88	3.88	3.88	3.88	3.88	3.88	3.88
Least squares ($\times 10^8$ kip-in^2):	Inf	7.01e+07	-4.44e+07	2.92e+07	-1.67e+08	7.95e+07	1.48e+09	-2.70e+09	Inf
Bayesian ($\times 10^8$ kip-in^2):	3.85	3.79	3.97	3.99	4.97	4.22	4.29	4.19	3.88

(c)

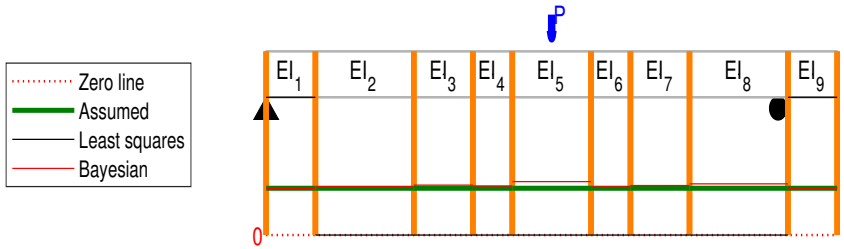

Anticipated θ:	1.00	1.00	1.00	1.00	1.00	1.00	1.00	1.00	1.00
Least squares:	0.00	5.44	-8.89	8.60	10.08	-80.37	83.96	-52.98	0.00
Bayesian:	1.00	0.98	0.97	0.98	0.93	0.98	0.97	0.95	1.00
Anticipated EI ($\times 10^8$ kip-in^2):	3.88	3.88	3.88	3.88	3.88	3.88	3.88	3.88	3.88
Least squares ($\times 10^8$ kip-in^2):	Inf	7.14e+07	-4.37e+07	4.52e+07	3.85e+07	-4.83e+06	6.63e+06	-7.33e+06	Inf
Bayesian ($\times 10^8$ kip-in^2):	3.88	3.95	4.02	3.98	4.19	3.94	4.00	4.08	3.88

(d)

Fig. D.92. Tests 4a and 5b Bayesian analysis deflection comparisons and identification results. Identifications are $\times 10^8$ unless stated otherwise in the substructure result.

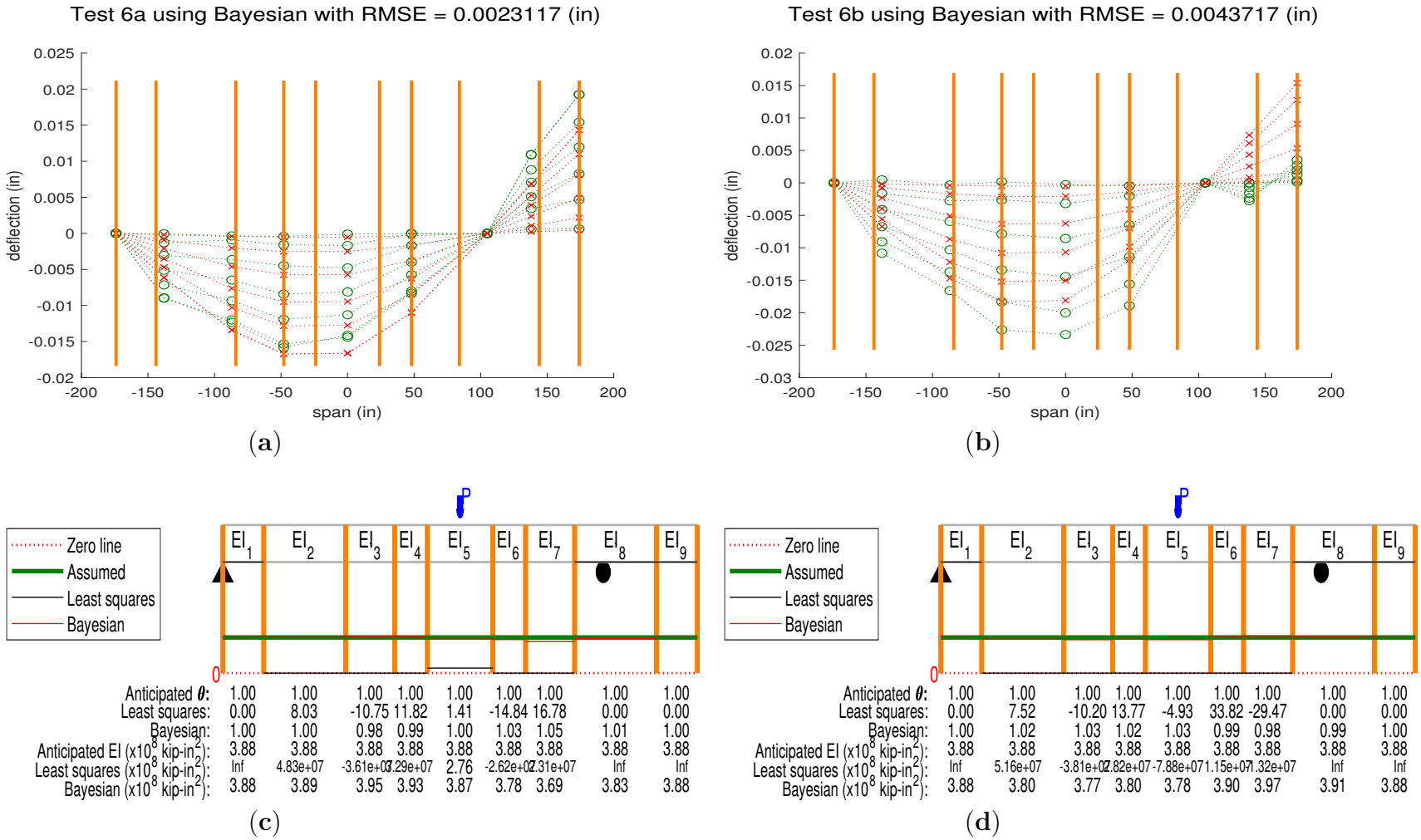

Fig. D.93. Tests 6a and 6b Bayesian analysis deflection comparisons and identification results. Identifications are $\times 10^8$ unless stated otherwise in the substructure result.

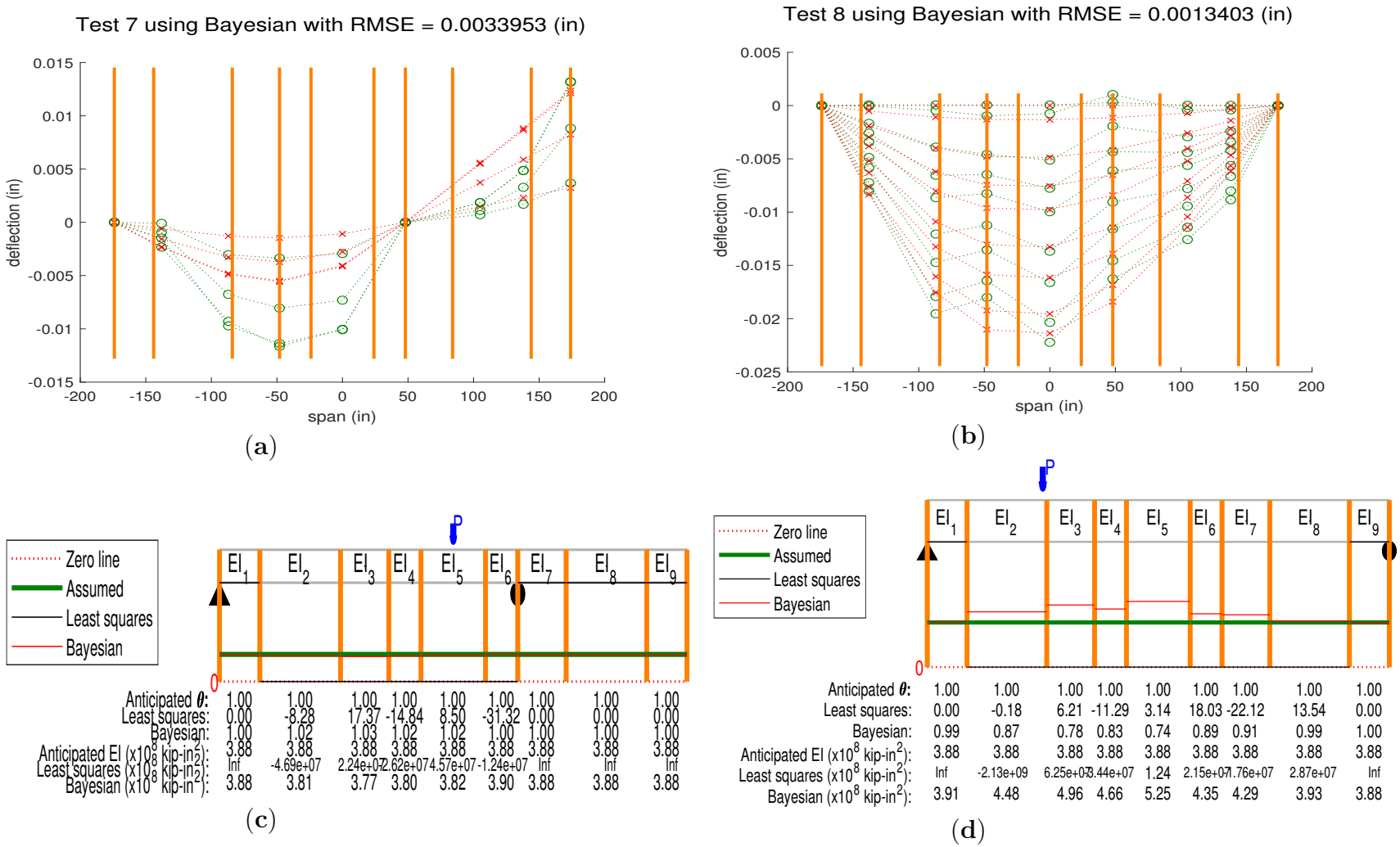

Fig. D.94. Tests 7 and 8 Bayesian analysis deflection comparisons and identification results. Identifications are $\times 10^8$ unless stated otherwise in the substructure result.

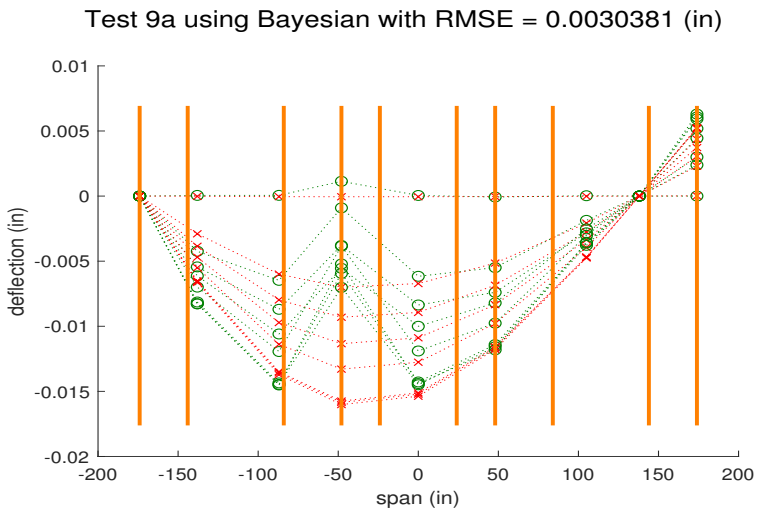

(a)

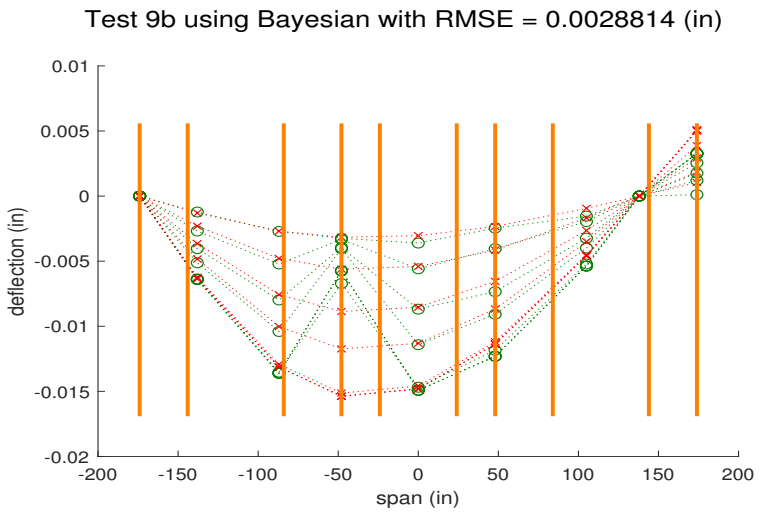

(b)

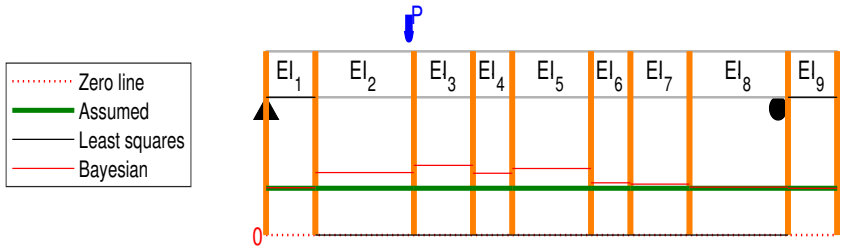

Anticipated θ:	1.00	1.00	1.00	1.00	1.00	1.00	1.00	1.00	1.00
Least squares:	0.00	2.53	4.72	-17.41	2.16	42.63	-41.30	26.19	0.00
Bayesian:	0.99	0.83	0.75	0.84	0.78	0.94	0.95	0.99	1.00
Anticipated EI ($\times 10^8$ kip-in^2):	3.88	3.88	3.88	3.88	3.88	3.88	3.88	3.88	3.88
Least squares ($\times 10^8$ kip-in^2):	Inf	1.53	8.23e+07	-2.23e+07	1.80	9.11e+06	-9.40e+06	1.48e+07	Inf
Bayesian ($\times 10^8$ kip-in^2):	3.91	4.69	5.19	4.65	4.96	4.13	4.07	3.93	3.88

(c)

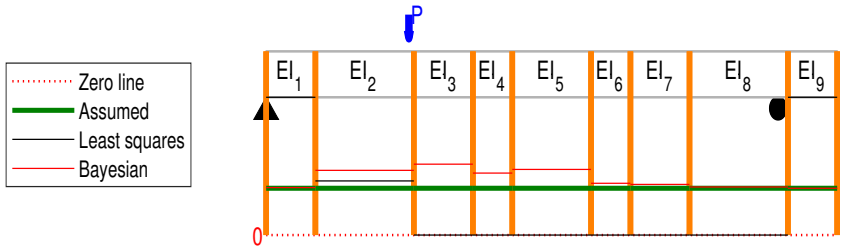

Anticipated θ:	1.00	1.00	1.00	1.00	1.00	1.00	1.00	1.00	1.00
Least squares:	0.00	0.92	7.19	-24.46	16.92	-58.84	57.75	-36.03	0.00
Bayesian:	0.99	0.80	0.74	0.83	0.79	0.95	0.96	0.99	1.00
Anticipated EI ($\times 10^8$ kip-in^2):	3.88	3.88	3.88	3.88	3.88	3.88	3.88	3.88	3.88
Least squares ($\times 10^8$ kip-in^2):	Inf	4.22	5.40e+07	-1.59e+07	2.30e+07	-6.60e+06	6.73e+06	-1.08e+07	Inf
Bayesian ($\times 10^8$ kip-in^2):	3.91	4.83	5.28	4.66	4.90	4.11	4.05	3.94	3.88

(d)

Fig. D.95. Tests 9a and 9b Bayesian analysis deflection comparisons and identification results. Identifications are $\times 10^8$ unless stated otherwise in the substructure result.

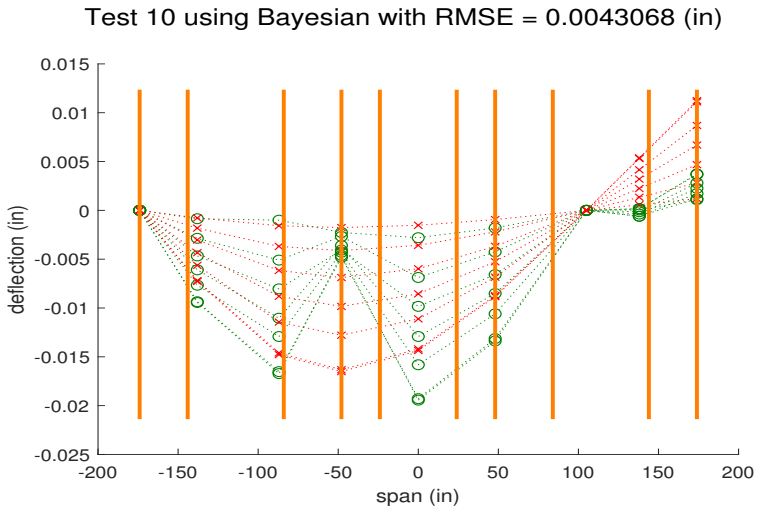

(a)

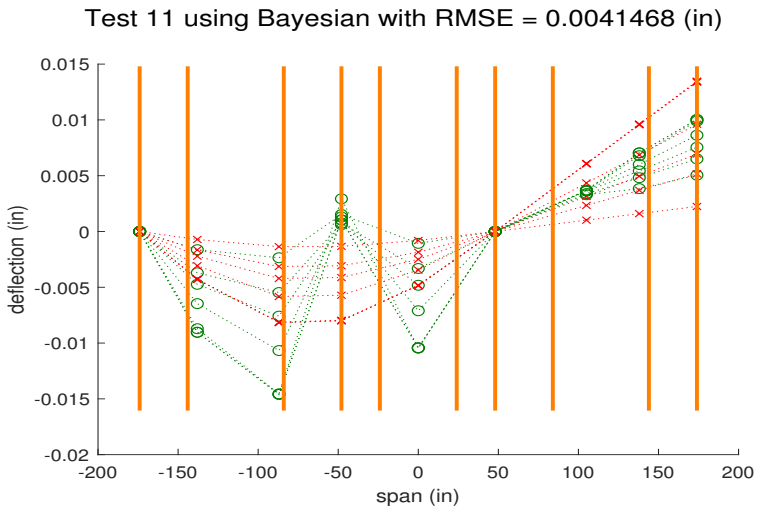

(b)

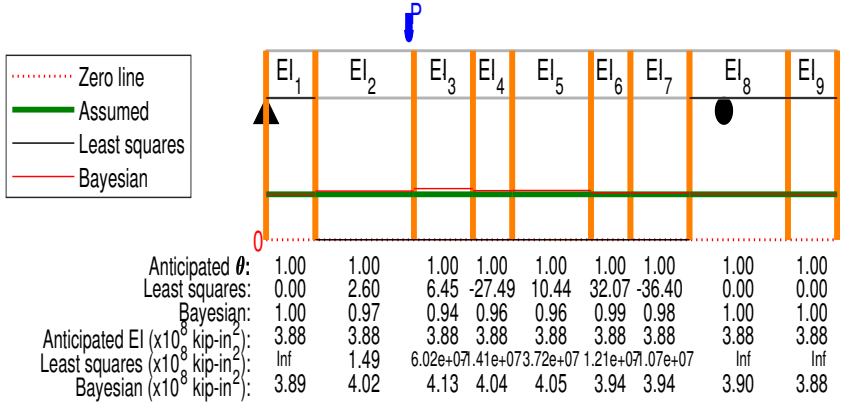

(c)

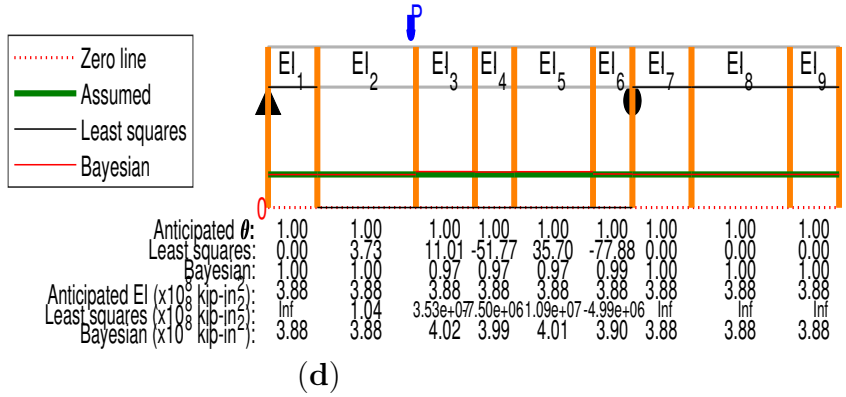

(d)

Fig. D.96. Tests 10 and 11 Bayesian analysis deflection comparisons and identification results. Identifications are $\times 10^8$ unless stated otherwise in the substructure result.

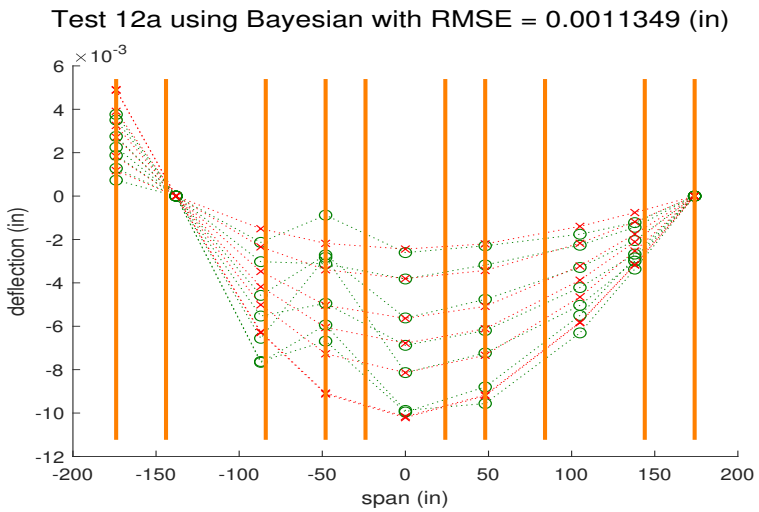

(a)

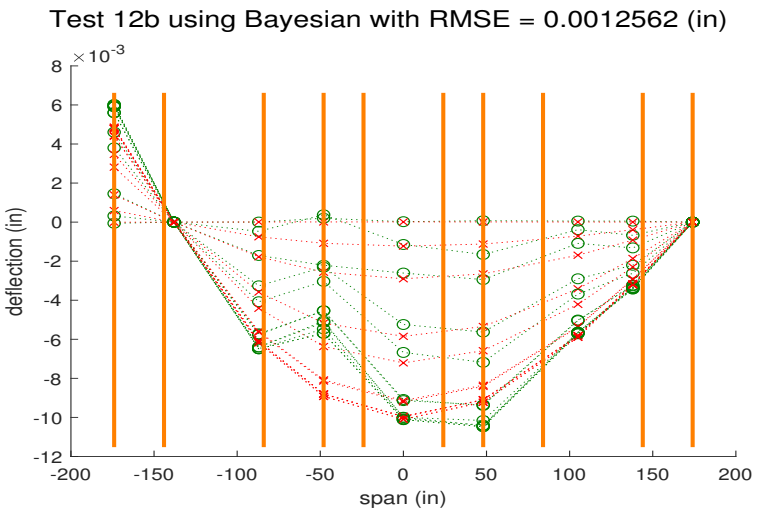

(b)

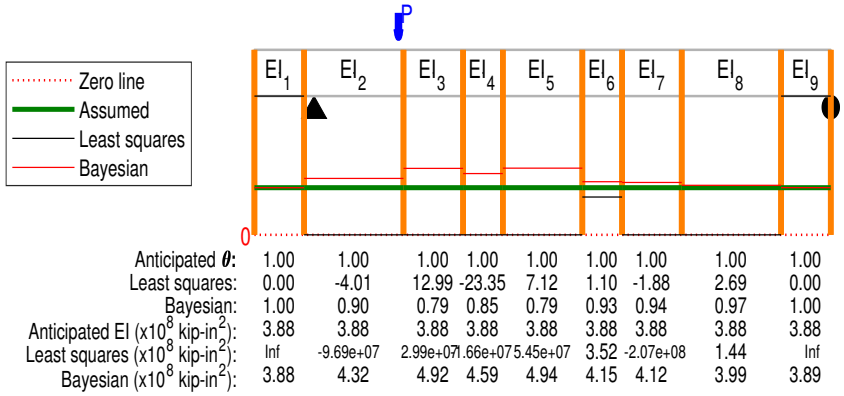

Anticipated θ:	1.00	1.00	1.00	1.00	1.00	1.00	1.00	1.00	1.00
Least squares:	0.00	-4.01	12.99	-23.35	7.12	1.10	-1.88	2.69	0.00
Bayesian:	1.00	0.90	0.79	0.85	0.79	0.93	0.94	0.97	1.00
Anticipated EI ($\times 10^8$ kip-in^2):	3.88	3.88	3.88	3.88	3.88	3.88	3.88	3.88	3.88
Least squares ($\times 10^8$ kip-in^2):	Inf	-9.69e+07	2.99e+07	1.66e+07	5.45e+07	3.52	-2.07e+08	1.44	Inf
Bayesian ($\times 10^8$ kip-in^2):	3.88	4.32	4.92	4.59	4.94	4.15	4.12	3.99	3.89

(c)

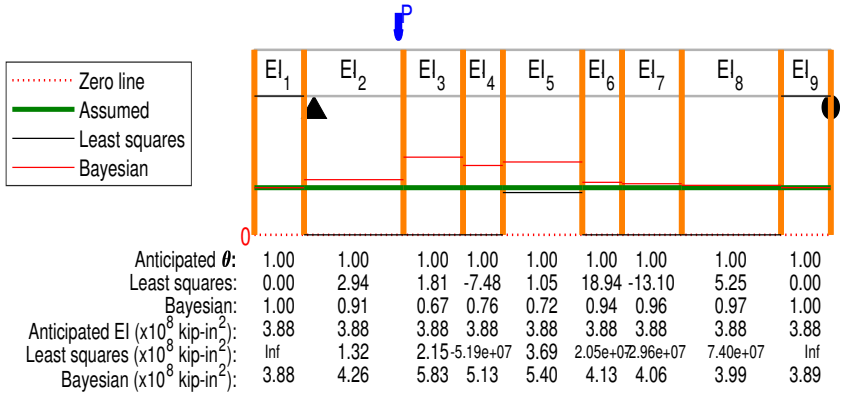

Anticipated θ:	1.00	1.00	1.00	1.00	1.00	1.00	1.00	1.00	1.00
Least squares:	0.00	2.94	1.81	-7.48	1.05	18.94	-13.10	5.25	0.00
Bayesian:	1.00	0.91	0.67	0.76	0.72	0.94	0.96	0.97	1.00
Anticipated EI ($\times 10^8$ kip-in^2):	3.88	3.88	3.88	3.88	3.88	3.88	3.88	3.88	3.88
Least squares ($\times 10^8$ kip-in^2):	Inf	1.32	2.15	-5.19e+07	3.69	2.05e+07	2.96e+07	7.40e+07	Inf
Bayesian ($\times 10^8$ kip-in^2):	3.88	4.26	5.83	5.13	5.40	4.13	4.06	3.99	3.89

(d)

Fig. D.97. Tests 12a and 12b Bayesian analysis deflection comparisons and identification results. Identifications are $\times 10^8$ unless stated otherwise in the substructure result.

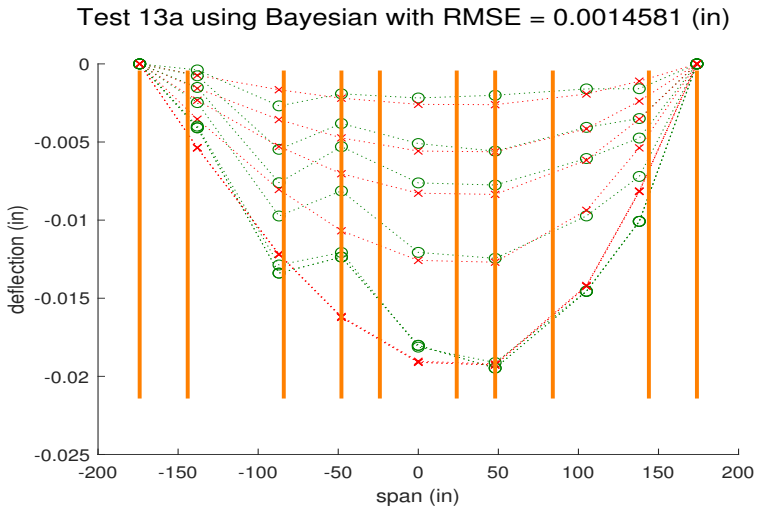

(a)

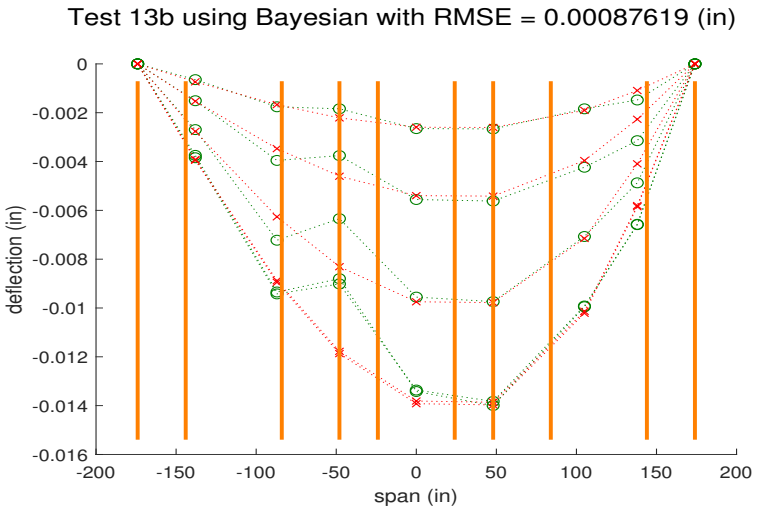

(b)

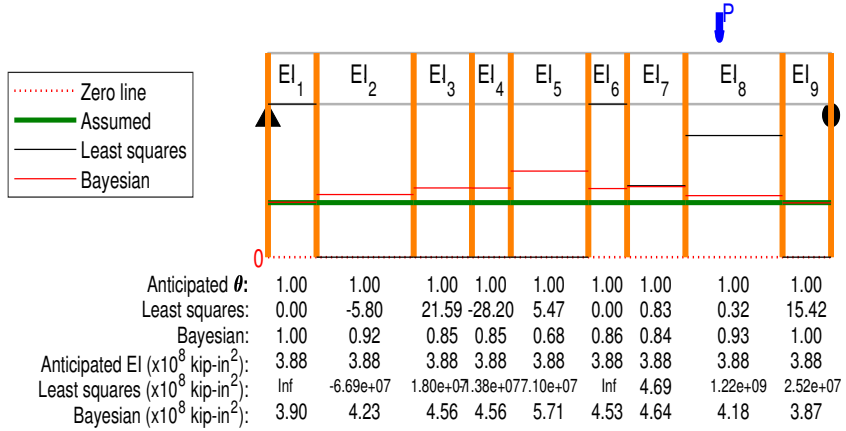

Anticipated θ:	1.00	1.00	1.00	1.00	1.00	1.00	1.00	1.00	1.00
Least squares:	0.00	-5.80	21.59	-28.20	5.47	0.00	0.83	0.32	15.42
Bayesian:	1.00	0.92	0.85	0.85	0.68	0.86	0.84	0.93	1.00
Anticipated EI ($\times 10^8$ kip-in^2):	3.88	3.88	3.88	3.88	3.88	3.88	3.88	3.88	3.88
Least squares ($\times 10^8$ kip-in^2):	Inf	-6.69e+07	1.80e+07	1.38e+07	7.10e+07	Inf	4.69	1.22e+09	2.52e+07
Bayesian ($\times 10^8$ kip-in^2):	3.90	4.23	4.56	4.56	5.71	4.53	4.64	4.18	3.87

(c)

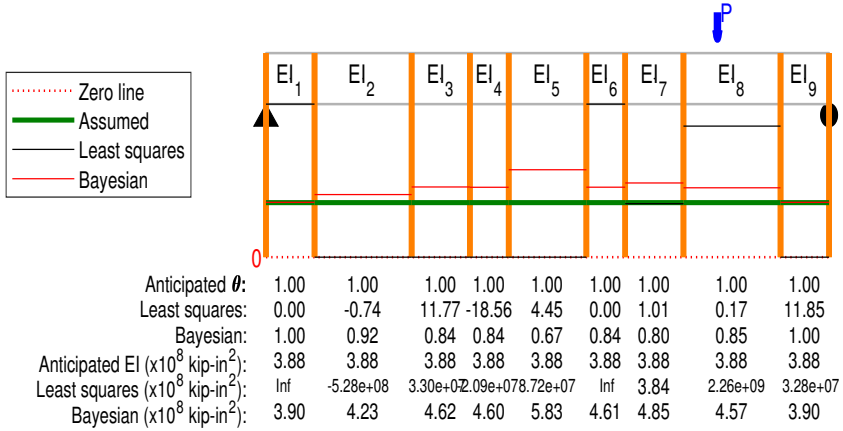

Anticipated θ:	1.00	1.00	1.00	1.00	1.00	1.00	1.00	1.00	1.00
Least squares:	0.00	-0.74	11.77	-18.56	4.45	0.00	1.01	0.17	11.85
Bayesian:	1.00	0.92	0.84	0.84	0.67	0.84	0.80	0.85	1.00
Anticipated EI ($\times 10^8$ kip-in^2):	3.88	3.88	3.88	3.88	3.88	3.88	3.88	3.88	3.88
Least squares ($\times 10^8$ kip-in^2):	Inf	-5.28e+08	3.30e+07	2.09e+07	8.72e+07	Inf	3.84	2.26e+09	3.28e+07
Bayesian ($\times 10^8$ kip-in^2):	3.90	4.23	4.62	4.60	5.83	4.61	4.85	4.57	3.90

(d)

Fig. D.98. Tests 13a and 13b Bayesian analysis deflection comparisons and identification results. Identifications are $\times 10^8$ unless stated otherwise in the substructure result.

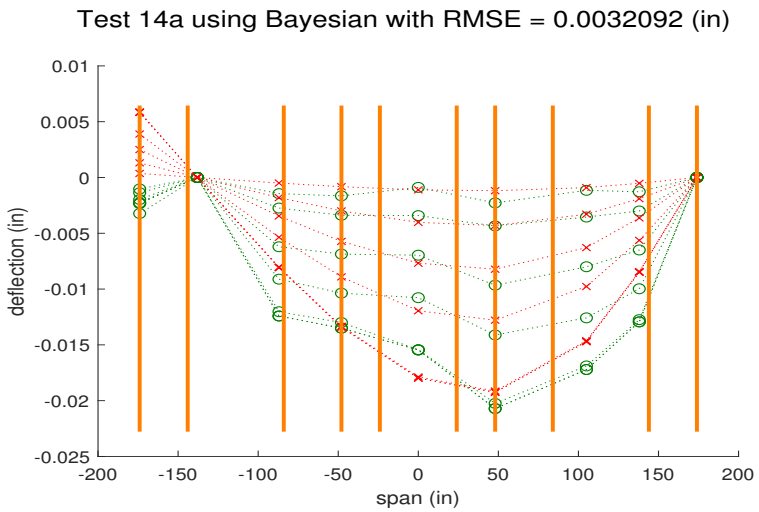

(a)

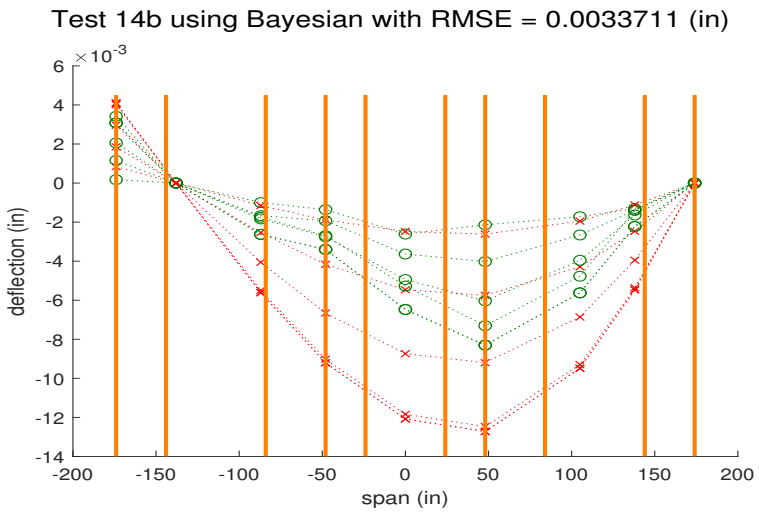

(b)

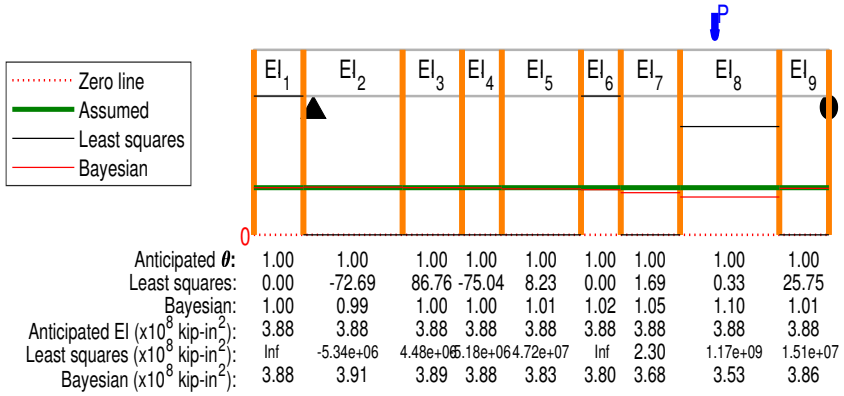

Anticipated θ:	1.00	1.00	1.00	1.00	1.00	1.00	1.00	1.00	1.00
Least squares:	0.00	-72.69	86.76	-75.04	8.23	0.00	1.69	0.33	25.75
Bayesian:	1.00	0.99	1.00	1.00	1.01	1.02	1.05	1.10	1.01
Anticipated EI ($\times 10^8$ kip-in^2):	3.88	3.88	3.88	3.88	3.88	3.88	3.88	3.88	3.88
Least squares ($\times 10^8$ kip-in^2):	Inf	-5.34e+06	4.48e+06	5.18e+06	4.72e+07	Inf	2.30	1.17e+09	1.51e+07
Bayesian ($\times 10^8$ kip-in^2):	3.88	3.91	3.89	3.88	3.83	3.80	3.68	3.53	3.86

(c)

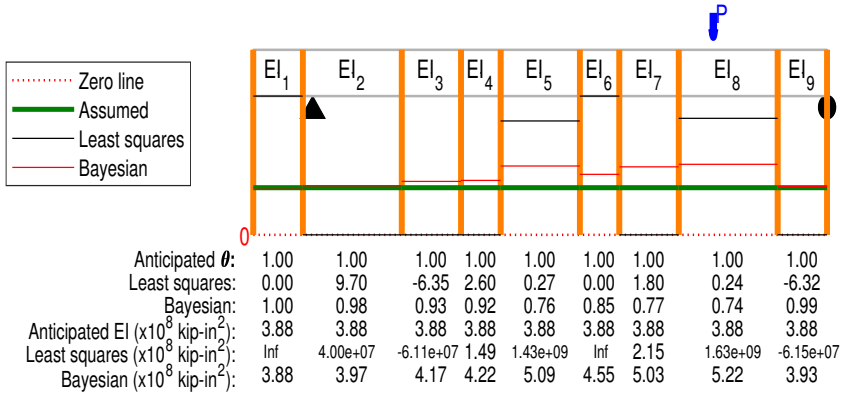

Anticipated θ:	1.00	1.00	1.00	1.00	1.00	1.00	1.00	1.00	1.00
Least squares:	0.00	9.70	-6.35	2.60	0.27	0.00	1.80	0.24	-6.32
Bayesian:	1.00	0.98	0.93	0.92	0.76	0.85	0.77	0.74	0.99
Anticipated EI ($\times 10^8$ kip-in^2):	3.88	3.88	3.88	3.88	3.88	3.88	3.88	3.88	3.88
Least squares ($\times 10^8$ kip-in^2):	Inf	4.00e+07	-6.11e+07	1.49	1.43e+09	Inf	2.15	1.63e+09	-6.15e+07
Bayesian ($\times 10^8$ kip-in^2):	3.88	3.97	4.17	4.22	5.09	4.55	5.03	5.22	3.93

(d)

Fig. D.99. Tests 14a and 14b Bayesian analysis deflection comparisons and identification results. Identifications are $\times 10^8$ unless stated otherwise in the substructure result.

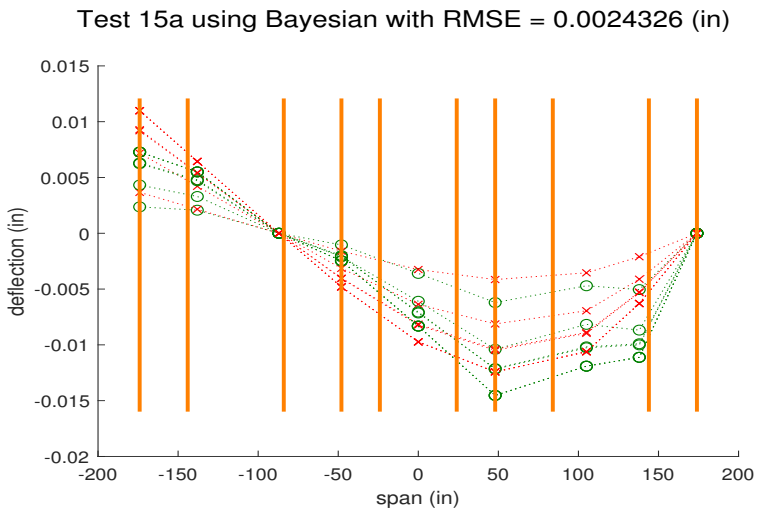

(a)

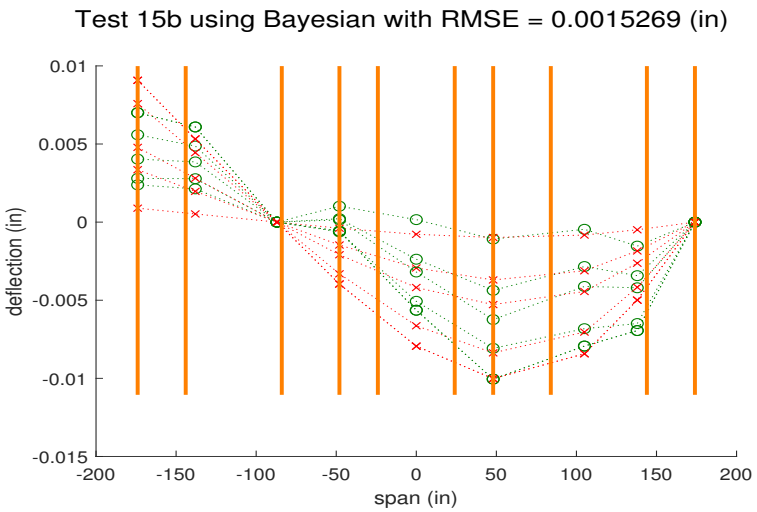

(b)

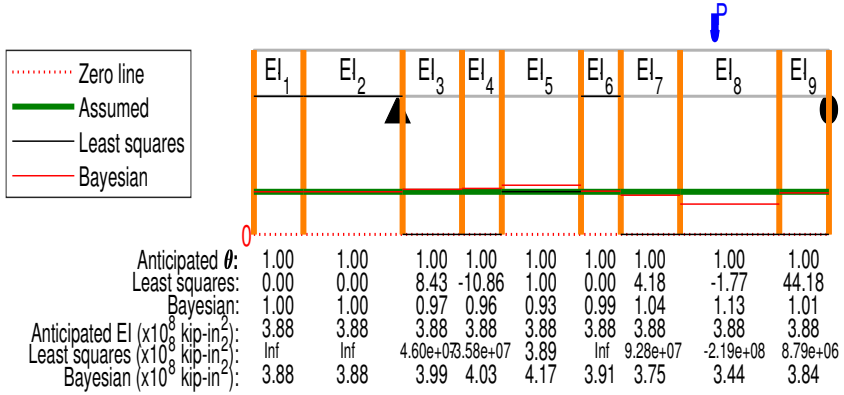

Anticipated θ:	1.00	1.00	1.00	1.00	1.00	1.00	1.00	1.00	1.00
Least squares:	0.00	0.00	8.43	-10.86	1.00	0.00	4.18	-1.77	44.18
Bayesian:	1.00	1.00	0.97	0.96	0.93	0.99	1.04	1.13	1.01
Anticipated EI ($\times 10^8$ kip-in^2):	3.88	3.88	3.88	3.88	3.88	3.88	3.88	3.88	3.88
Least squares ($\times 10^8$ kip-in^2):	Inf	Inf	4.60e+07	3.58e+07	3.89	Inf	9.28e+07	-2.19e+08	8.79e+06
Bayesian ($\times 10^8$ kip-in^2):	3.88	3.88	3.99	4.03	4.17	3.91	3.75	3.44	3.84

(c)

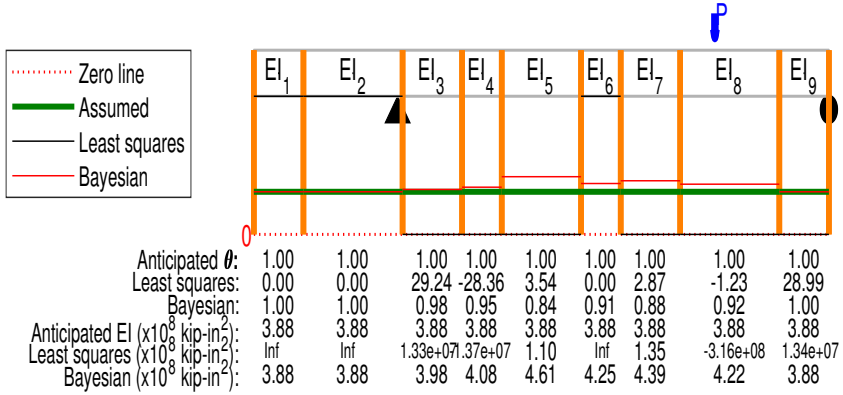

Anticipated θ:	1.00	1.00	1.00	1.00	1.00	1.00	1.00	1.00	1.00
Least squares:	0.00	0.00	29.24	-28.36	3.54	0.00	2.87	-1.23	28.99
Bayesian:	1.00	1.00	0.98	0.95	0.84	0.91	0.88	0.92	1.00
Anticipated EI ($\times 10^8$ kip-in^2):	3.88	3.88	3.88	3.88	3.88	3.88	3.88	3.88	3.88
Least squares ($\times 10^8$ kip-in^2):	Inf	Inf	1.33e+07	1.37e+07	1.10	Inf	1.35	-3.16e+08	1.34e+07
Bayesian ($\times 10^8$ kip-in^2):	3.88	3.88	3.98	4.08	4.61	4.25	4.39	4.22	3.88

(d)

Fig. D.100. Tests 15a and 15b Bayesian analysis deflection comparisons and identification results. Identifications are $\times 10^8$ unless stated otherwise in the substructure result.

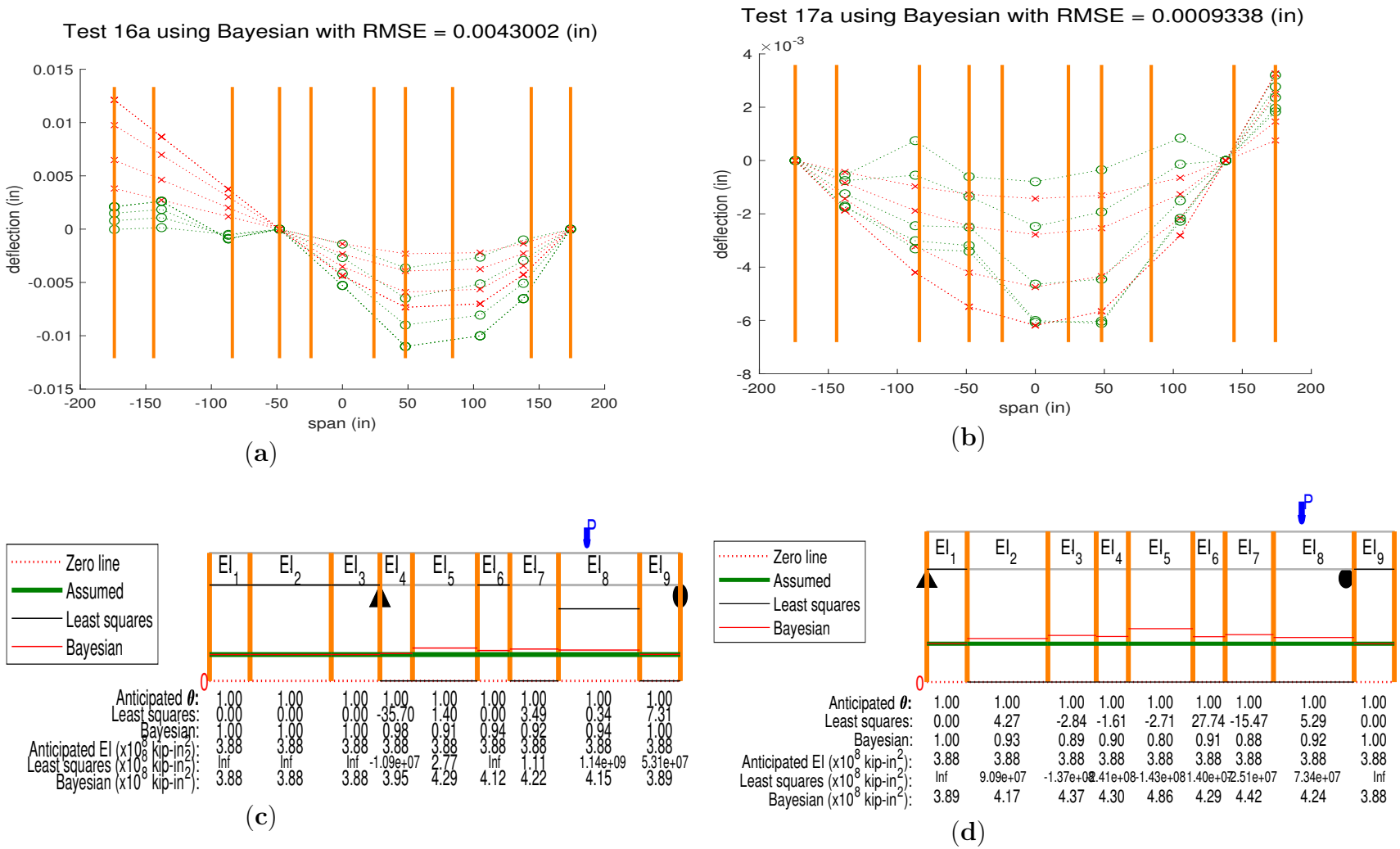

Fig. D.101. Tests 16a and 17a Bayesian analysis deflection comparisons and identification results. Identifications are $\times 10^8$ unless stated otherwise in the substructure result.

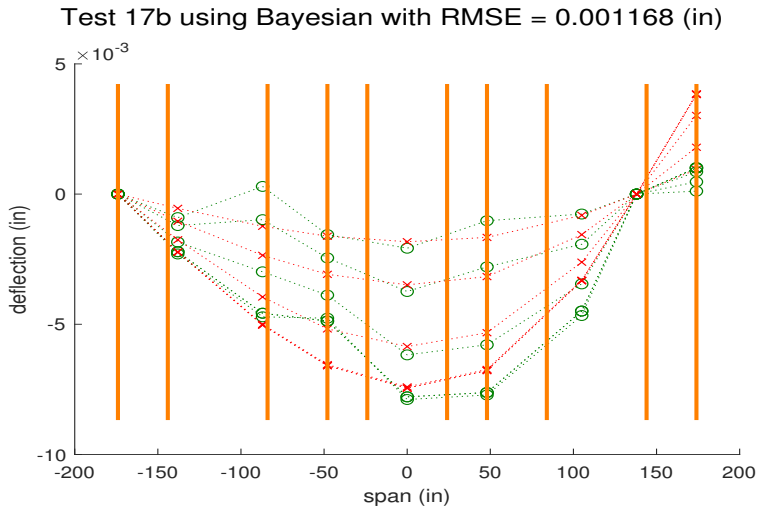

(a)

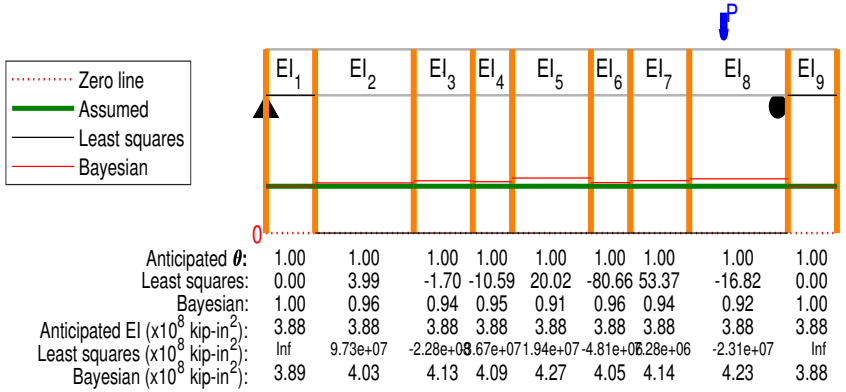

Anticipated θ:	1.00	1.00	1.00	1.00	1.00	1.00	1.00	1.00	1.00
Least squares:	0.00	3.99	-1.70	-10.59	20.02	-80.66	53.37	-16.82	0.00
Bayesian:	1.00	0.96	0.94	0.95	0.91	0.96	0.94	0.92	1.00
Anticipated EI ($\times 10^8$ kip-in^2):	3.88	3.88	3.88	3.88	3.88	3.88	3.88	3.88	3.88
Least squares ($\times 10^8$ kip-in^2):	Inf	9.73e+07	-2.28e+08	3.67e+07	1.94e+07	-4.81e+06	7.28e+06	-2.31e+07	Inf
Bayesian ($\times 10^8$ kip-in^2):	3.89	4.03	4.13	4.09	4.27	4.05	4.14	4.23	3.88

(c)

Fig. D.102. Test 17b Bayesian analysis deflection comparisons and identification results. Identifications are $\times 10^8$ unless stated otherwise in the substructure result.

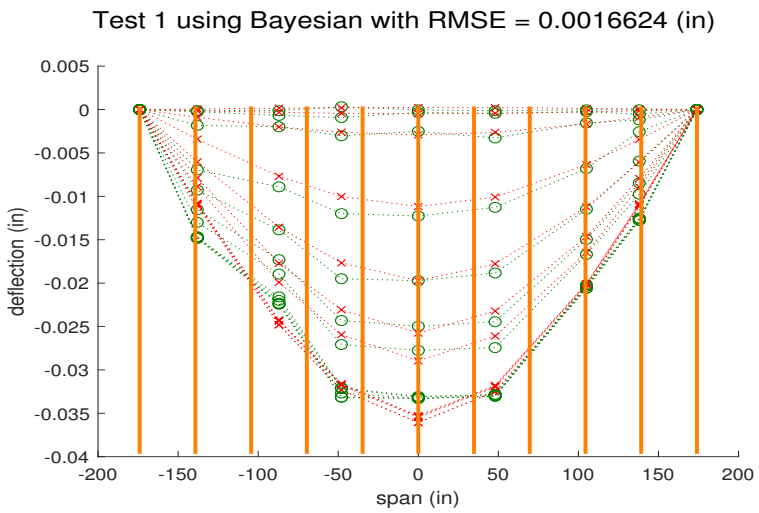

(a)

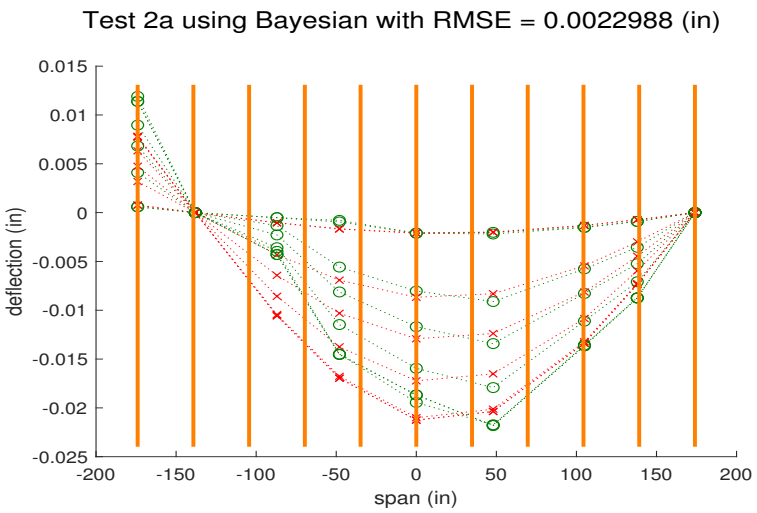

(b)

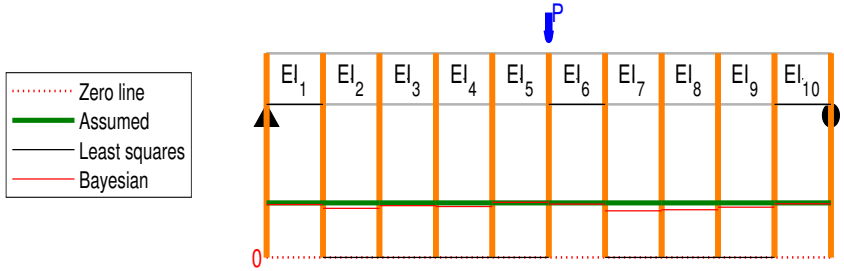

Anticipated $\boldsymbol{\theta}$:	1.00	1.00	1.00	1.00	1.00	1.00	1.00	1.00	1.00	1.00
Least squares:	0.00	13.37	-7.42	4.88	-0.31	0.00	4.04	-3.35	6.04	0.00
Bayesian:	1.02	1.06	1.03	1.04	0.99	1.01	1.08	1.07	1.04	1.01
Anticipated EI ($\times 10^8$ kip-in^2):	3.88	3.88	3.88	3.88	3.88	3.88	3.88	3.88	3.88	3.88
Least squares ($\times 10^8$ kip-in^2):	Inf	2.90e+07	-5.23e+07	7.95e+07	-1.25e+09	Inf	9.61e+07	-1.16e+08	6.43e+07	Inf
Bayesian ($\times 10^8$ kip-in^2):	3.82	3.68	3.78	3.74	3.91	3.84	3.59	3.63	3.72	3.85

(c)

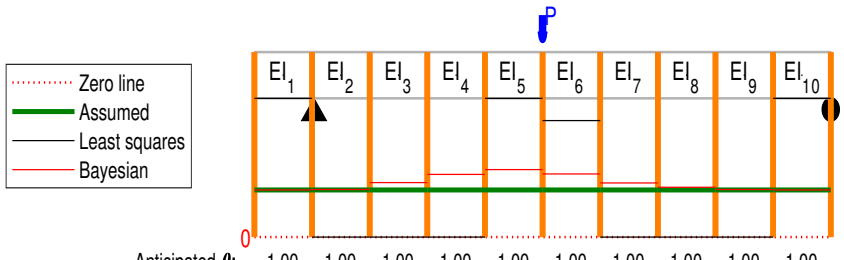

Anticipated $\boldsymbol{\theta}$:	1.00	1.00	1.00	1.00	1.00	1.00	1.00	1.00	1.00	1.00
Least squares:	0.00	37.98	-13.69	4.43	0.00	0.10	4.30	-4.01	6.40	0.00
Bayesian:	1.00	1.00	0.92	0.83	0.78	0.83	0.92	0.97	1.00	1.00
Anticipated EI ($\times 10^8$ kip-in^2):	3.88	3.88	3.88	3.88	3.88	3.88	3.88	3.88	3.88	3.88
Least squares ($\times 10^8$ kip-in^2):	Inf	1.02e+07	-2.84e+07	8.77e+07	Inf	3.92e+09	9.03e+07	-9.68e+07	6.07e+07	Inf
Bayesian ($\times 10^8$ kip-in^2):	3.88	3.90	4.22	4.68	4.99	4.71	4.21	4.00	3.90	3.88

(d)

Fig. D.103. Tests 1 and 2a Bayesian analysis deflection comparisons and identification results. Identifications are $\times 10^8$ unless stated otherwise in the substructure result.

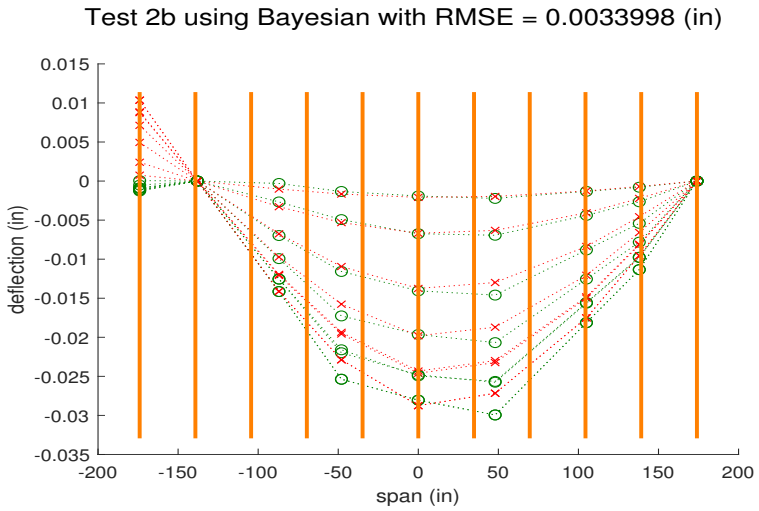

(a)

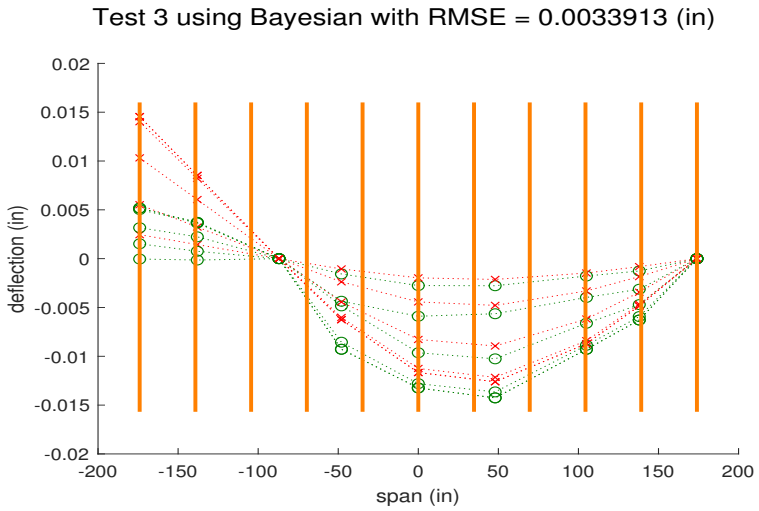

(b)

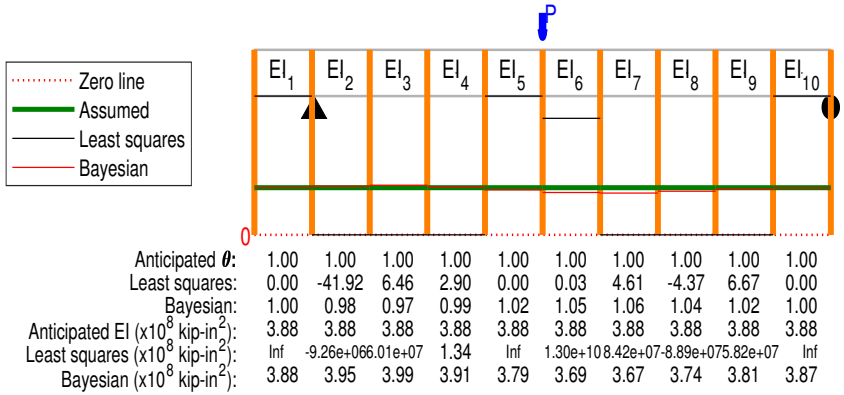

(c)

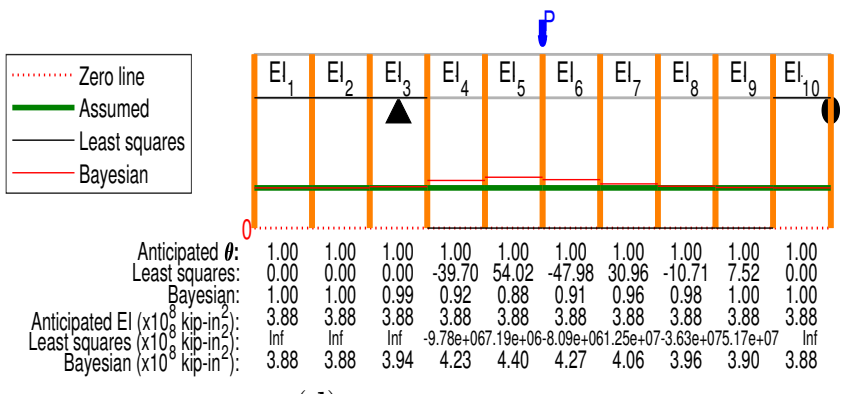

(d)

Fig. D.104. Tests 2b and 3 Bayesian analysis deflection comparisons and identification results. Identifications are $\times 10^8$ unless stated otherwise in the substructure result.

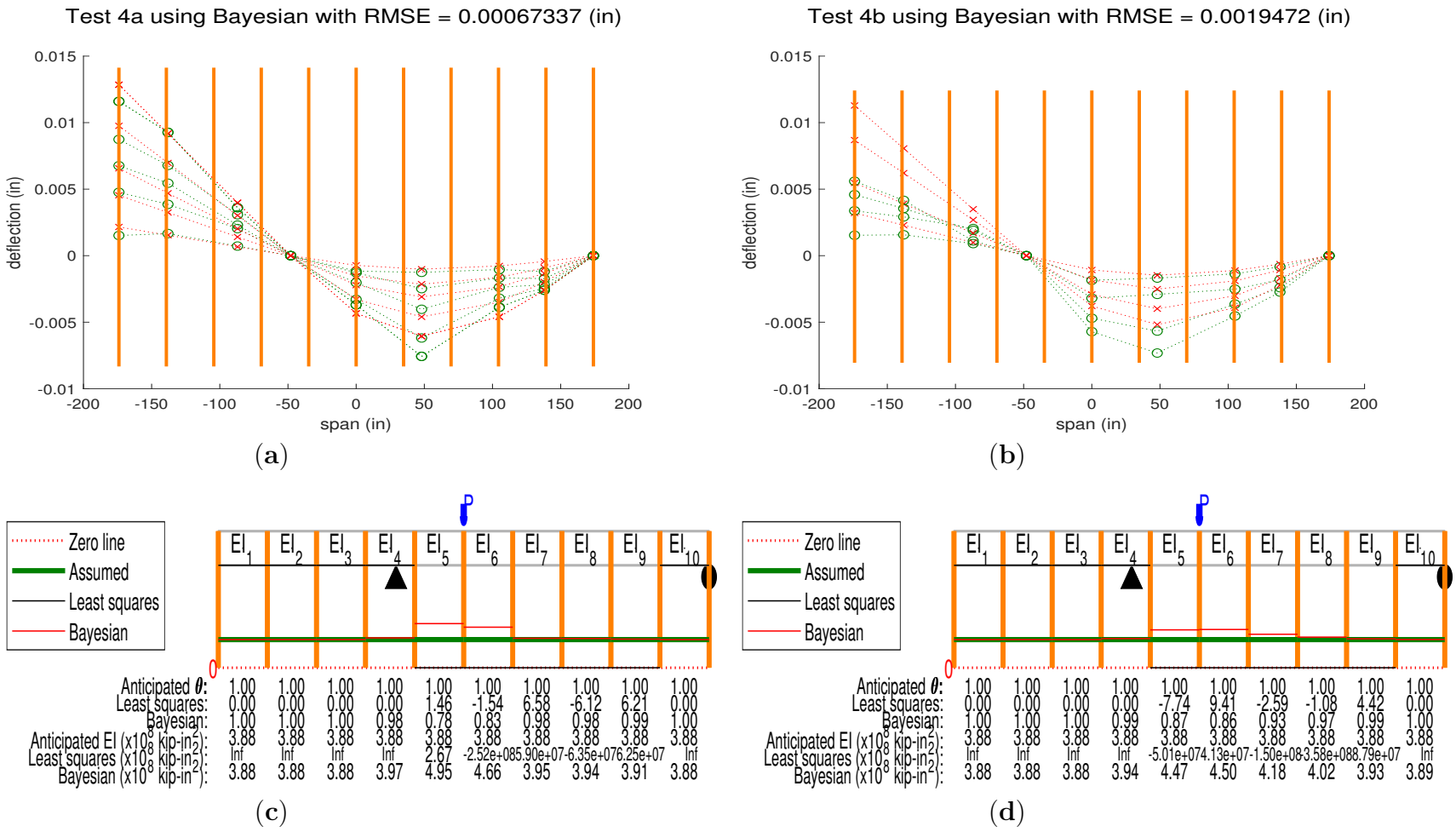

Fig. D.105. Tests 4a and 4b Bayesian analysis deflection comparisons and identification results. Identifications are $\times 10^8$ unless stated otherwise in the substructure result.

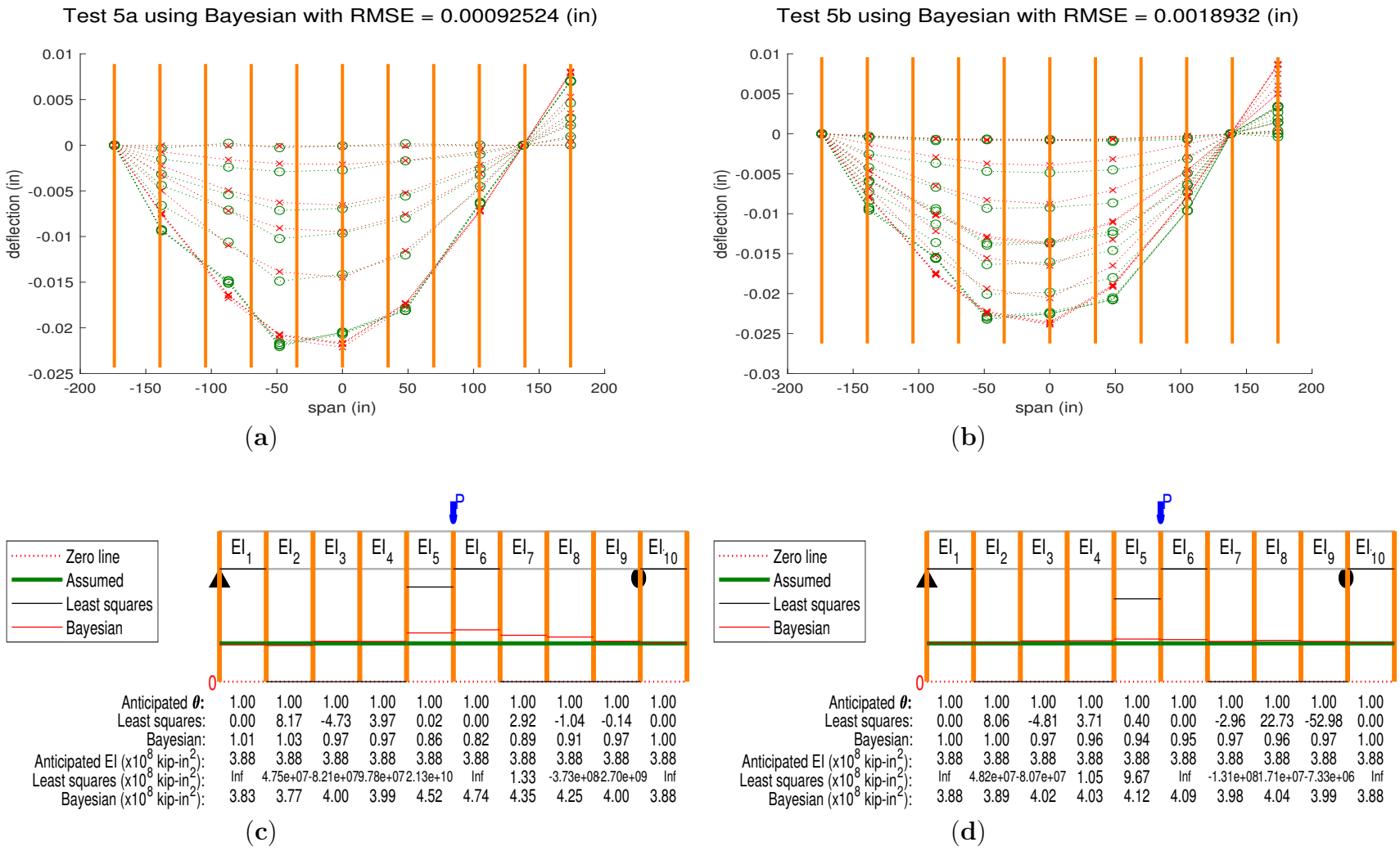

Fig. D.106. Tests 4a and 5b Bayesian analysis deflection comparisons and identification results. Identifications are $\times 10^8$ unless stated otherwise in the substructure result.

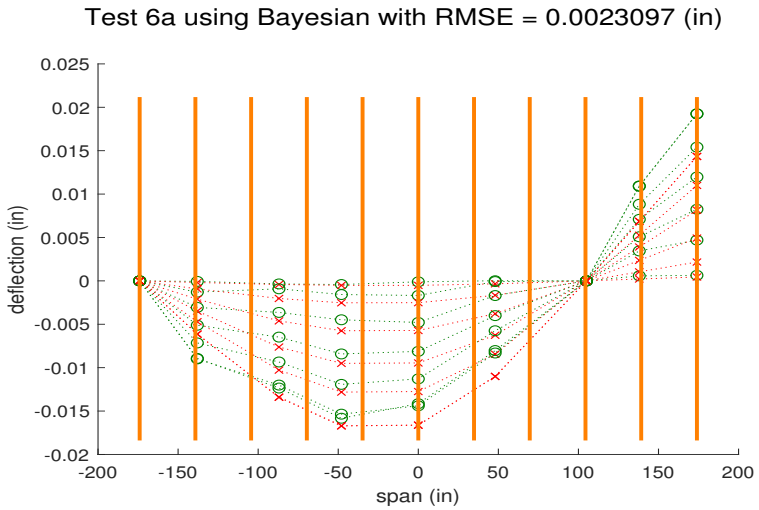

(a)

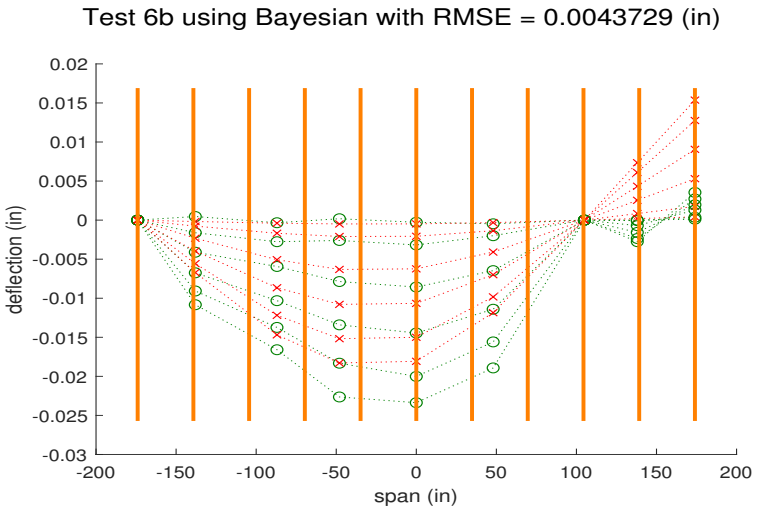

(b)

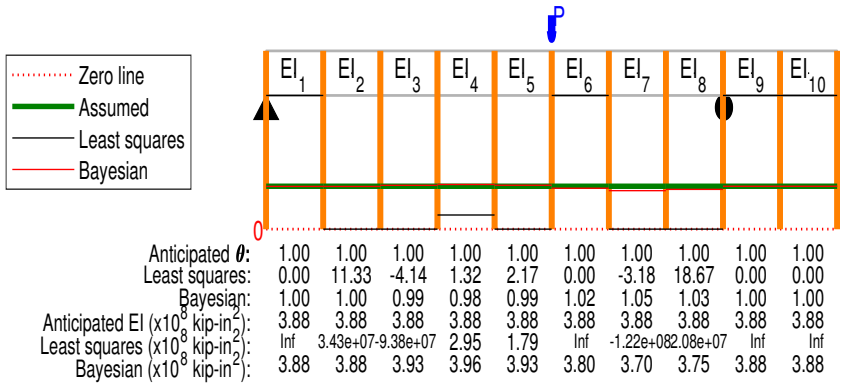

Anticipated θ:	1.00	1.00	1.00	1.00	1.00	1.00	1.00	1.00	1.00	1.00
Least squares:	0.00	11.33	-4.14	1.32	2.17	0.00	-3.18	18.67	0.00	0.00
Bayesian:	1.00	1.00	0.99	0.98	0.99	1.02	1.05	1.03	1.00	1.00
Anticipated EI ($\times 10^8$ kip-in^2):	3.88	3.88	3.88	3.88	3.88	3.88	3.88	3.88	3.88	3.88
Least squares ($\times 10^8$ kip-in^2):	Inf	3.43e+07	-9.38e+07	2.95	1.79	Inf	-1.22e+08	2.08e+07	Inf	Inf
Bayesian ($\times 10^8$ kip-in^2):	3.88	3.88	3.93	3.96	3.93	3.80	3.70	3.75	3.88	3.88

(c)

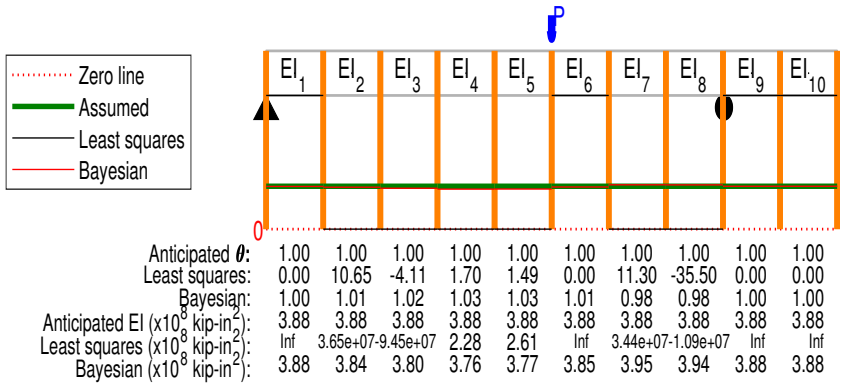

Anticipated θ:	1.00	1.00	1.00	1.00	1.00	1.00	1.00	1.00	1.00	1.00
Least squares:	0.00	10.65	-4.11	1.70	1.49	0.00	11.30	-35.50	0.00	0.00
Bayesian:	1.00	1.01	1.02	1.03	1.03	1.01	0.98	0.98	1.00	1.00
Anticipated EI ($\times 10^8$ kip-in^2):	3.88	3.88	3.88	3.88	3.88	3.88	3.88	3.88	3.88	3.88
Least squares ($\times 10^8$ kip-in^2):	Inf	3.65e+07	-9.45e+07	2.28	2.61	Inf	3.44e+07	-1.09e+07	Inf	Inf
Bayesian ($\times 10^8$ kip-in^2):	3.88	3.84	3.80	3.76	3.77	3.85	3.95	3.94	3.88	3.88

(d)

Fig. D.107. Tests 6a and 6b Bayesian analysis deflection comparisons and identification results. Identifications are $\times 10^8$ unless stated otherwise in the substructure result.

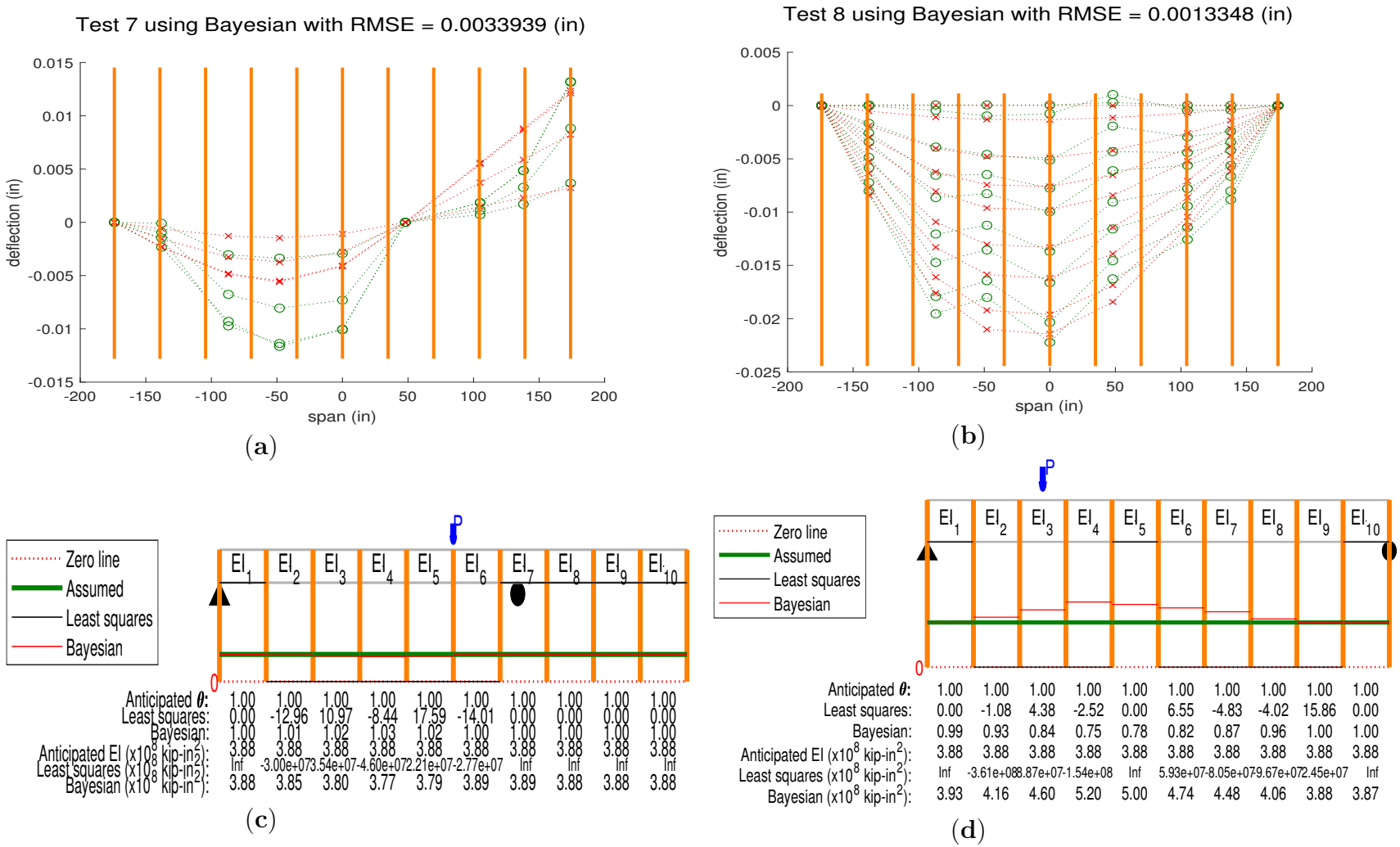

Fig. D.108. Tests 7 and 8 Bayesian analysis deflection comparisons and identification results. Identifications are $\times 10^8$ unless stated otherwise in the substructure result.

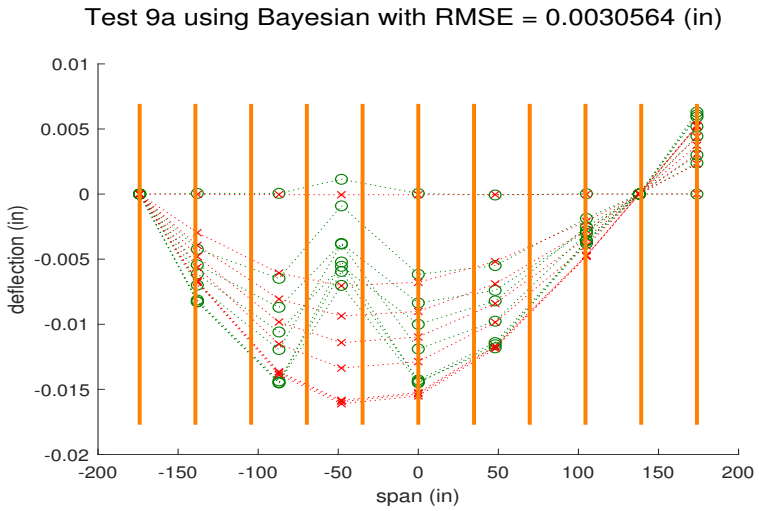

(a)

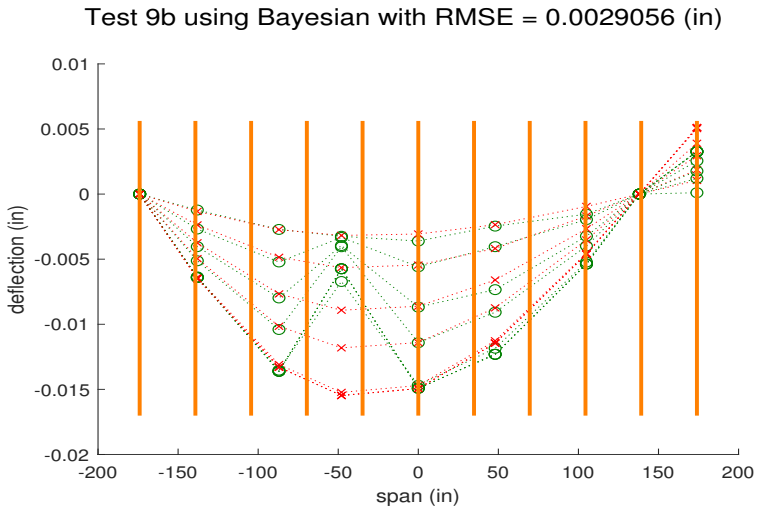

(b)

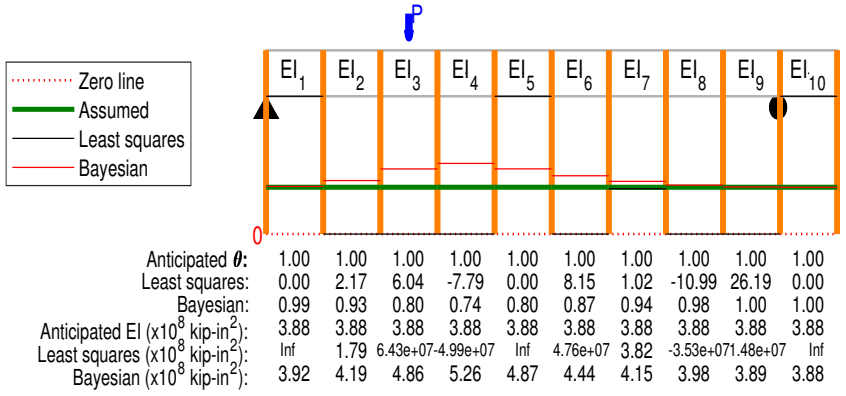

Anticipated $\boldsymbol{\theta}$:	1.00	1.00	1.00	1.00	1.00	1.00	1.00	1.00	1.00	1.00
Least squares:	0.00	2.17	6.04	-7.79	0.00	8.15	1.02	-10.99	26.19	0.00
Bayesian:	0.99	0.93	0.80	0.74	0.80	0.87	0.94	0.98	1.00	1.00
Anticipated EI ($\times 10^8$ kip-in^2):	3.88	3.88	3.88	3.88	3.88	3.88	3.88	3.88	3.88	3.88
Least squares ($\times 10^8$ kip-in^2):	Inf	1.79	6.43e+07	-4.99e+07	Inf	4.76e+07	3.82	-3.53e+07	1.48e+07	Inf
Bayesian ($\times 10^8$ kip-in^2):	3.92	4.19	4.86	5.26	4.87	4.44	4.15	3.98	3.89	3.88

(c)

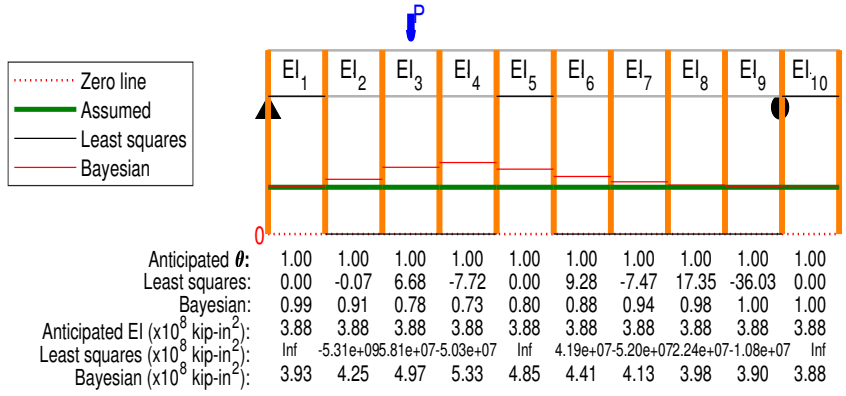

Anticipated $\boldsymbol{\theta}$:	1.00	1.00	1.00	1.00	1.00	1.00	1.00	1.00	1.00	1.00
Least squares:	0.00	-0.07	6.68	-7.72	0.00	9.28	-7.47	17.35	-36.03	0.00
Bayesian:	0.99	0.91	0.78	0.73	0.80	0.88	0.94	0.98	1.00	1.00
Anticipated EI ($\times 10^8$ kip-in^2):	3.88	3.88	3.88	3.88	3.88	3.88	3.88	3.88	3.88	3.88
Least squares ($\times 10^8$ kip-in^2):	Inf	-5.31e+09	5.81e+07	-5.03e+07	Inf	4.19e+07	-5.20e+07	2.24e+07	-1.08e+07	Inf
Bayesian ($\times 10^8$ kip-in^2):	3.93	4.25	4.97	5.33	4.85	4.41	4.13	3.98	3.90	3.88

(d)

Fig. D.109. Tests 9a and 9b Bayesian analysis deflection comparisons and identification results. Identifications are $\times 10^8$ unless stated otherwise in the substructure result.

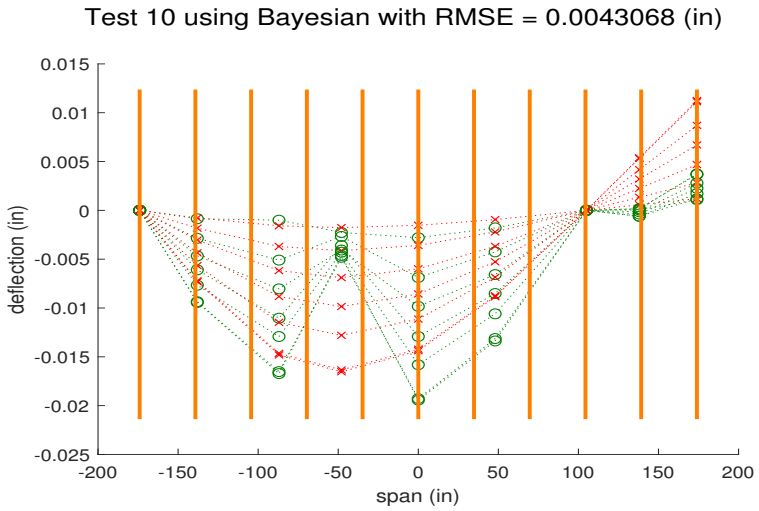

(a)

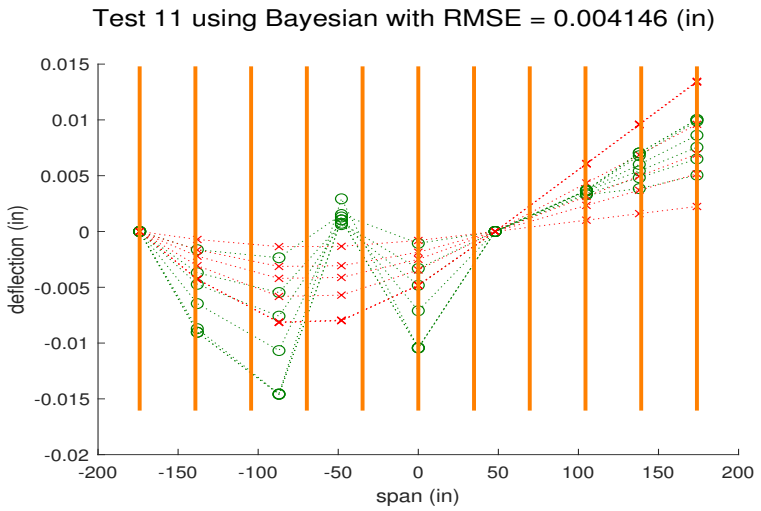

(b)

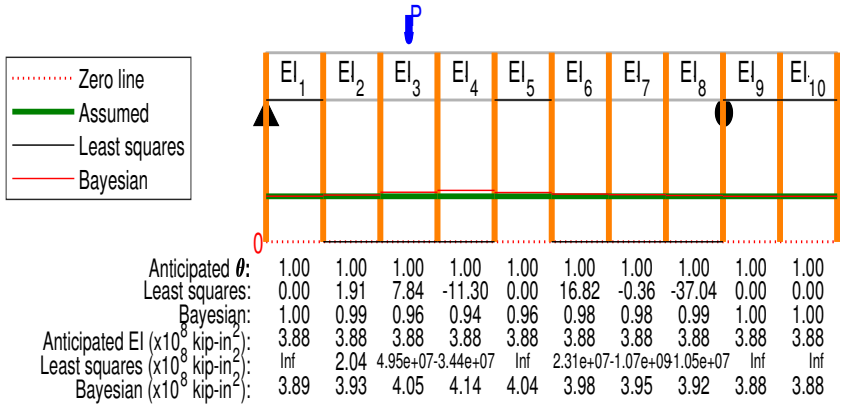

(c)

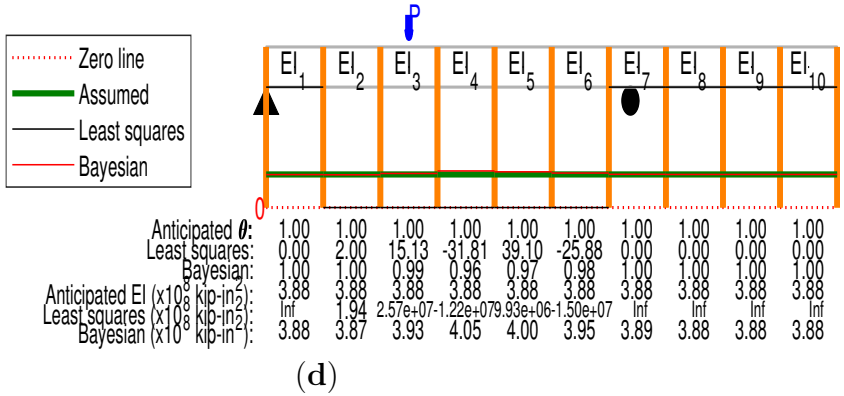

(d)

Fig. D.110. Tests 10 and 11 Bayesian analysis deflection comparisons and identification results. Identifications are $\times 10^8$ unless stated otherwise in the substructure result.

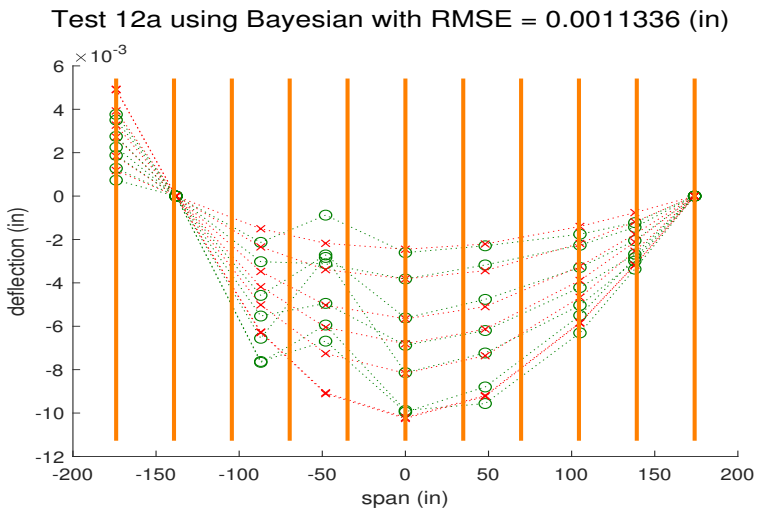

(a)

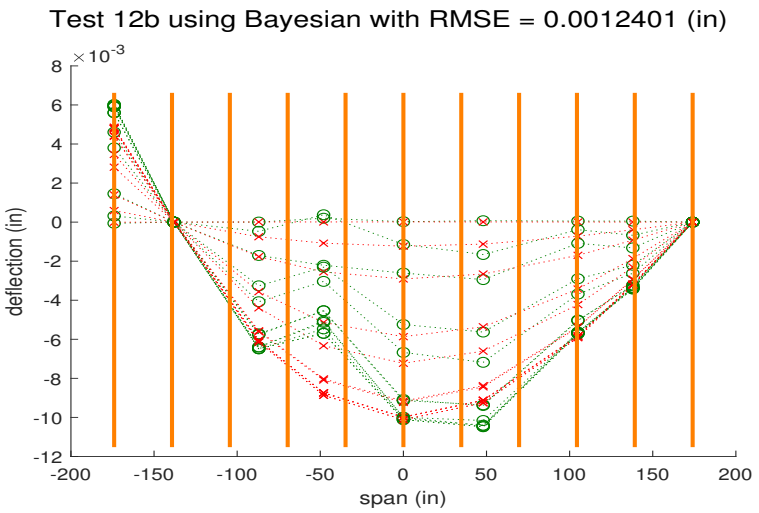

(b)

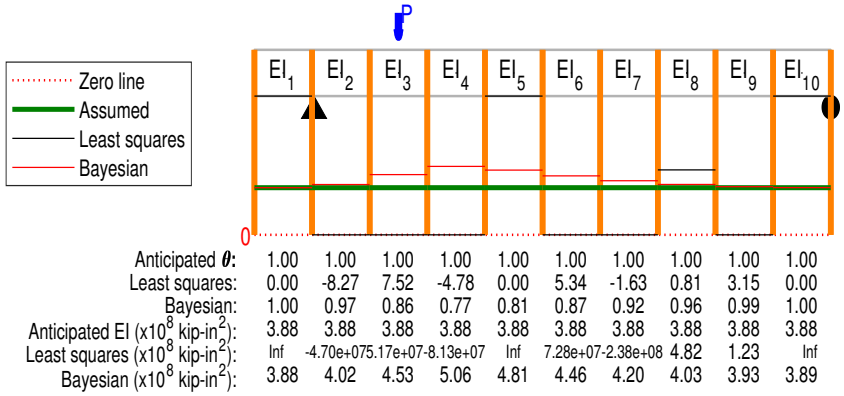

Anticipated θ:	1.00	1.00	1.00	1.00	1.00	1.00	1.00	1.00	1.00	1.00
Least squares:	0.00	-8.27	7.52	-4.78	0.00	5.34	-1.63	0.81	3.15	0.00
Bayesian:	1.00	0.97	0.86	0.77	0.81	0.87	0.92	0.96	0.99	1.00
Anticipated EI ($\times 10^8$ kip-in^2):	3.88	3.88	3.88	3.88	3.88	3.88	3.88	3.88	3.88	3.88
Least squares ($\times 10^8$ kip-in^2):	Inf	-4.70e+07	5.17e+07	-8.13e+07	Inf	7.28e+07	-2.38e+08	4.82	1.23	Inf
Bayesian ($\times 10^8$ kip-in^2):	3.88	4.02	4.53	5.06	4.81	4.46	4.20	4.03	3.93	3.89

(c)

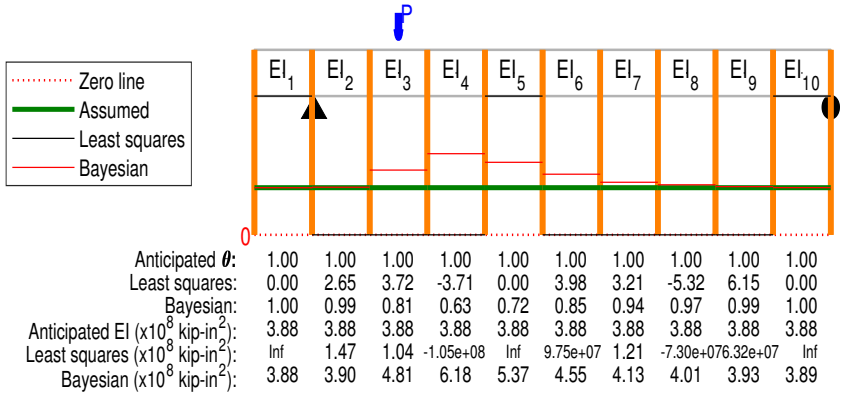

Anticipated θ:	1.00	1.00	1.00	1.00	1.00	1.00	1.00	1.00	1.00	1.00
Least squares:	0.00	2.65	3.72	-3.71	0.00	3.98	3.21	-5.32	6.15	0.00
Bayesian:	1.00	0.99	0.81	0.63	0.72	0.85	0.94	0.97	0.99	1.00
Anticipated EI ($\times 10^8$ kip-in^2):	3.88	3.88	3.88	3.88	3.88	3.88	3.88	3.88	3.88	3.88
Least squares ($\times 10^8$ kip-in^2):	Inf	1.47	1.04	-1.05e+08	Inf	9.75e+07	1.21	-7.30e+07	6.32e+07	Inf
Bayesian ($\times 10^8$ kip-in^2):	3.88	3.90	4.81	6.18	5.37	4.55	4.13	4.01	3.93	3.89

(d)

Fig. D.111. Tests 12a and 12b Bayesian analysis deflection comparisons and identification results. Identifications are $\times 10^8$ unless stated otherwise in the substructure result.

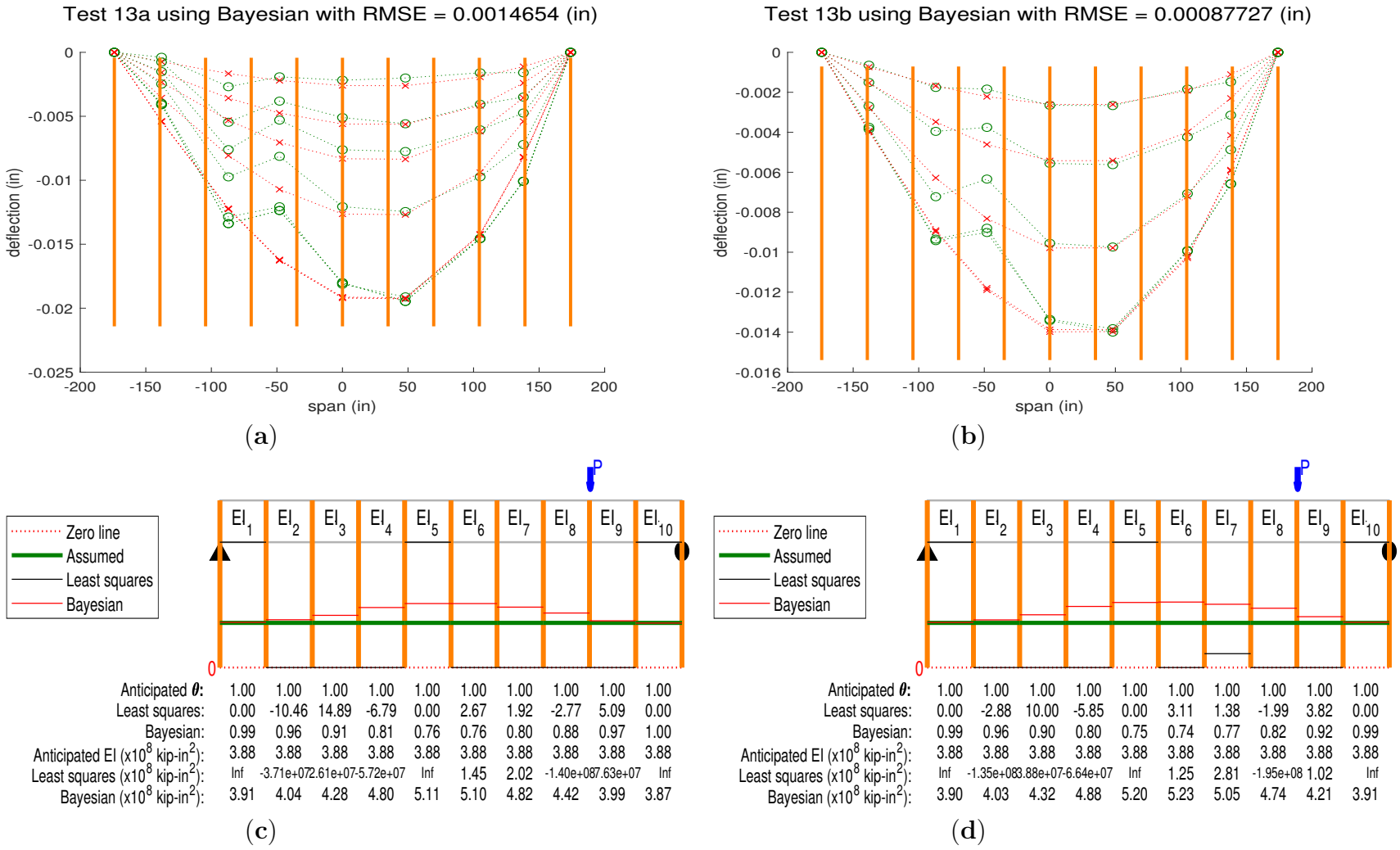

Fig. D.112. Tests 13a and 13b Bayesian analysis deflection comparisons and identification results. Identifications are $\times 10^8$ unless stated otherwise in the substructure result.

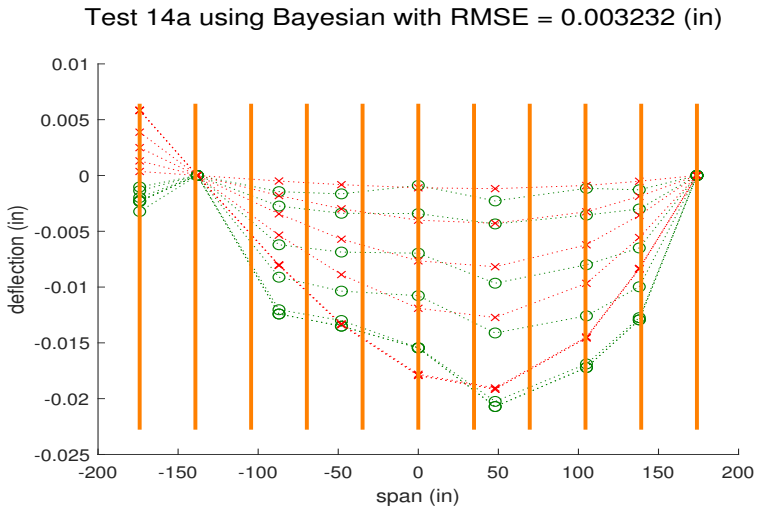

(a)

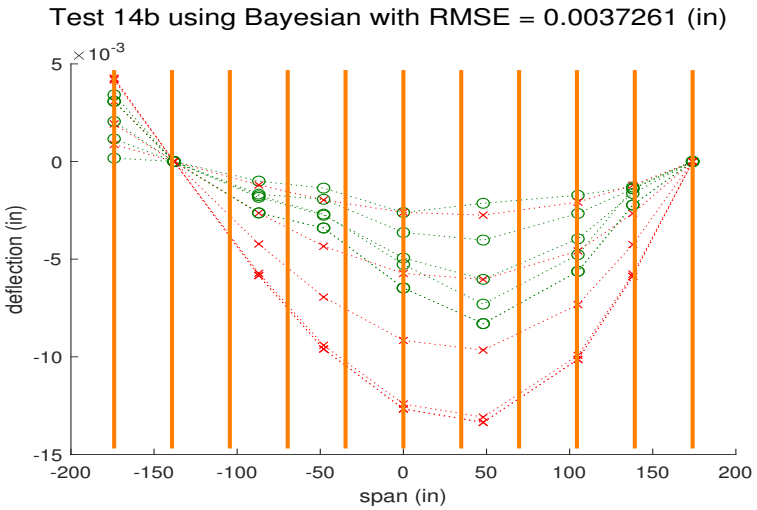

(b)

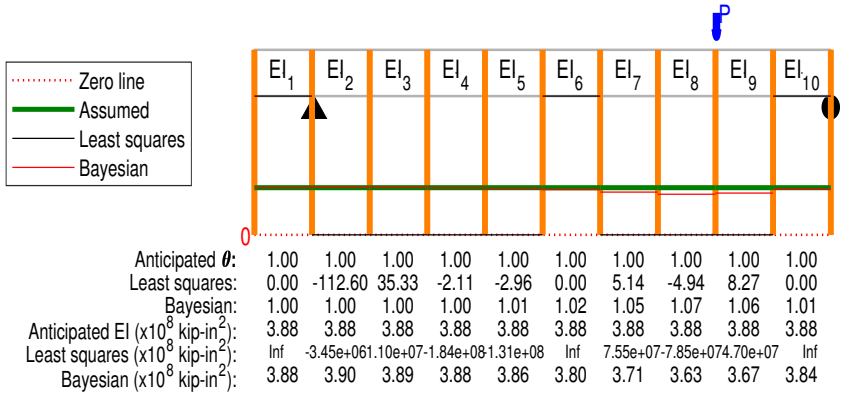

Anticipated θ:	1.00	1.00	1.00	1.00	1.00	1.00	1.00	1.00	1.00	1.00
Least squares:	0.00	-112.60	35.33	-2.11	-2.96	0.00	5.14	-4.94	8.27	0.00
Bayesian:	1.00	1.00	1.00	1.00	1.01	1.02	1.05	1.07	1.06	1.01
Anticipated EI ($\times 10^8$ kip-in^2):	3.88	3.88	3.88	3.88	3.88	3.88	3.88	3.88	3.88	3.88
Least squares ($\times 10^8$ kip-in^2):	Inf	-3.45e+06	1.10e+07	-1.84e+08	1.31e+08	Inf	7.55e+07	-7.85e+07	4.70e+07	Inf
Bayesian ($\times 10^8$ kip-in^2):	3.88	3.90	3.89	3.88	3.86	3.80	3.71	3.63	3.67	3.84

(c)

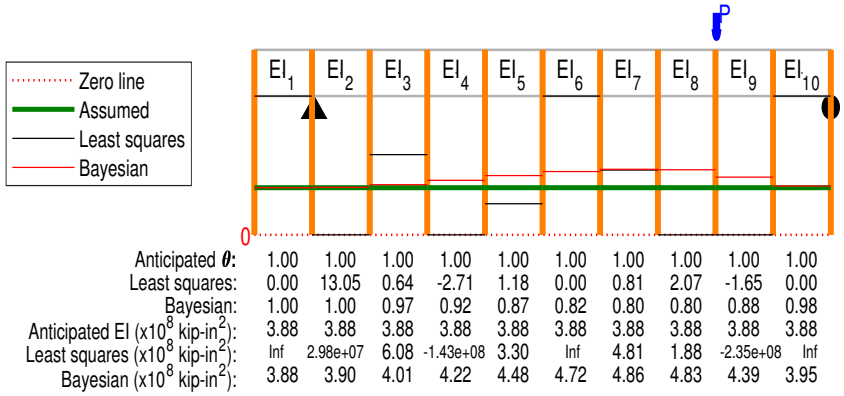

Anticipated θ:	1.00	1.00	1.00	1.00	1.00	1.00	1.00	1.00	1.00	1.00
Least squares:	0.00	13.05	0.64	-2.71	1.18	0.00	0.81	2.07	-1.65	0.00
Bayesian:	1.00	1.00	0.97	0.92	0.87	0.82	0.80	0.80	0.88	0.98
Anticipated EI ($\times 10^8$ kip-in^2):	3.88	3.88	3.88	3.88	3.88	3.88	3.88	3.88	3.88	3.88
Least squares ($\times 10^8$ kip-in^2):	Inf	2.98e+07	6.08	-1.43e+08	3.30	Inf	4.81	1.88	-2.35e+08	Inf
Bayesian ($\times 10^8$ kip-in^2):	3.88	3.90	4.01	4.22	4.48	4.72	4.86	4.83	4.39	3.95

(d)

Fig. D.113. Tests 14a and 14b Bayesian analysis deflection comparisons and identification results. Identifications are $\times 10^8$ unless stated otherwise in the substructure result.

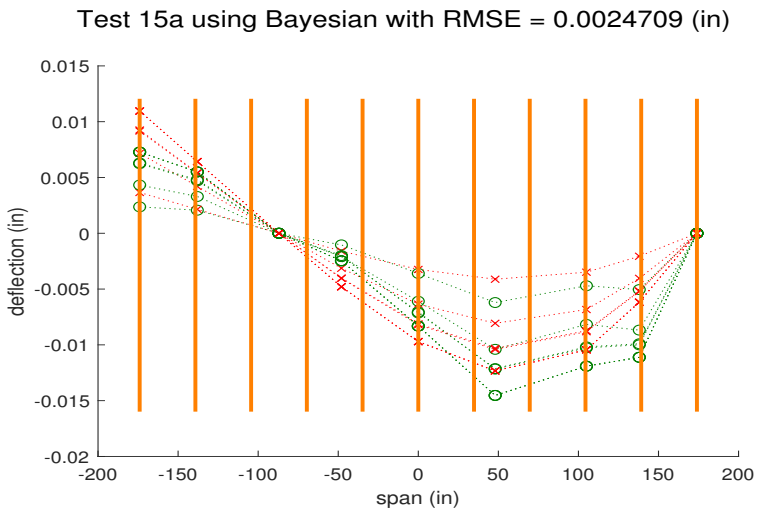

(a)

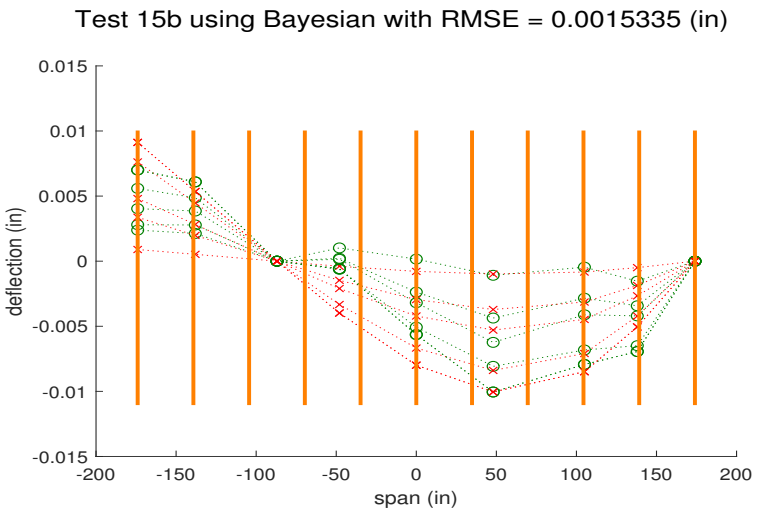

(b)

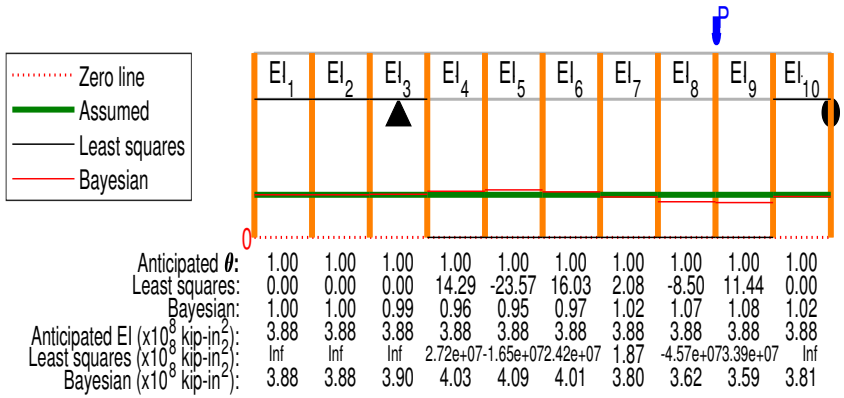

	EI_1	EI_2	EI_3	EI_4	EI_5	EI_6	EI_7	EI_8	EI_9	EI_{10}
Anticipated θ:	1.00	1.00	1.00	1.00	1.00	1.00	1.00	1.00	1.00	1.00
Least squares:	0.00	0.00	0.00	14.29	-23.57	16.03	2.08	-8.50	11.44	0.00
Bayesian:	1.00	1.00	0.99	0.96	0.95	0.97	1.02	1.07	1.08	1.02
Anticipated EI ($\times 10^8$ kip-in^2):	3.88	3.88	3.88	3.88	3.88	3.88	3.88	3.88	3.88	3.88
Least squares ($\times 10^8$ kip-in^2):	Inf	Inf	Inf	2.72e+07	-1.65e+07	2.42e+07	1.87	-4.57e+07	3.39e+07	Inf
Bayesian ($\times 10^8$ kip-in^2):	3.88	3.88	3.90	4.03	4.09	4.01	3.80	3.62	3.59	3.81

(c)

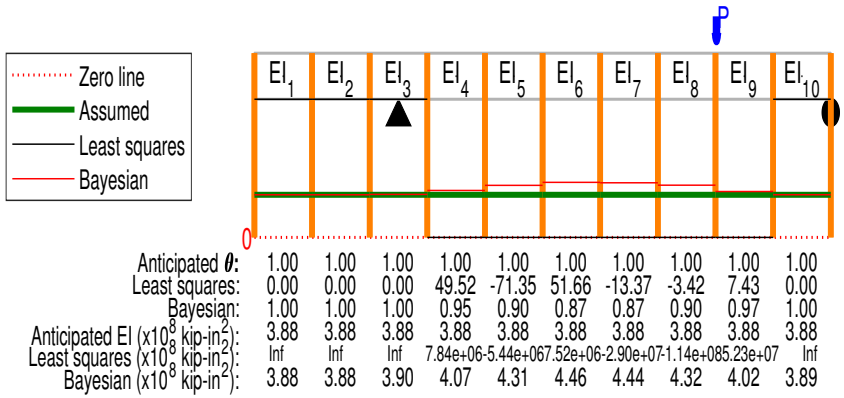

	EI_1	EI_2	EI_3	EI_4	EI_5	EI_6	EI_7	EI_8	EI_9	EI_{10}
Anticipated θ:	1.00	1.00	1.00	1.00	1.00	1.00	1.00	1.00	1.00	1.00
Least squares:	0.00	0.00	0.00	49.52	-71.35	51.66	-13.37	-3.42	7.43	0.00
Bayesian:	1.00	1.00	1.00	0.95	0.90	0.87	0.87	0.90	0.97	1.00
Anticipated EI ($\times 10^8$ kip-in^2):	3.88	3.88	3.88	3.88	3.88	3.88	3.88	3.88	3.88	3.88
Least squares ($\times 10^8$ kip-in^2):	Inf	Inf	Inf	7.84e+06	-5.44e+06	7.52e+06	-2.90e+07	-1.14e+08	5.23e+07	Inf
Bayesian ($\times 10^8$ kip-in^2):	3.88	3.88	3.90	4.07	4.31	4.46	4.44	4.32	4.02	3.89

(d)

Fig. D.114. Tests 15a and 15b Bayesian analysis deflection comparisons and identification results. Identifications are $\times 10^8$ unless stated otherwise in the substructure result.

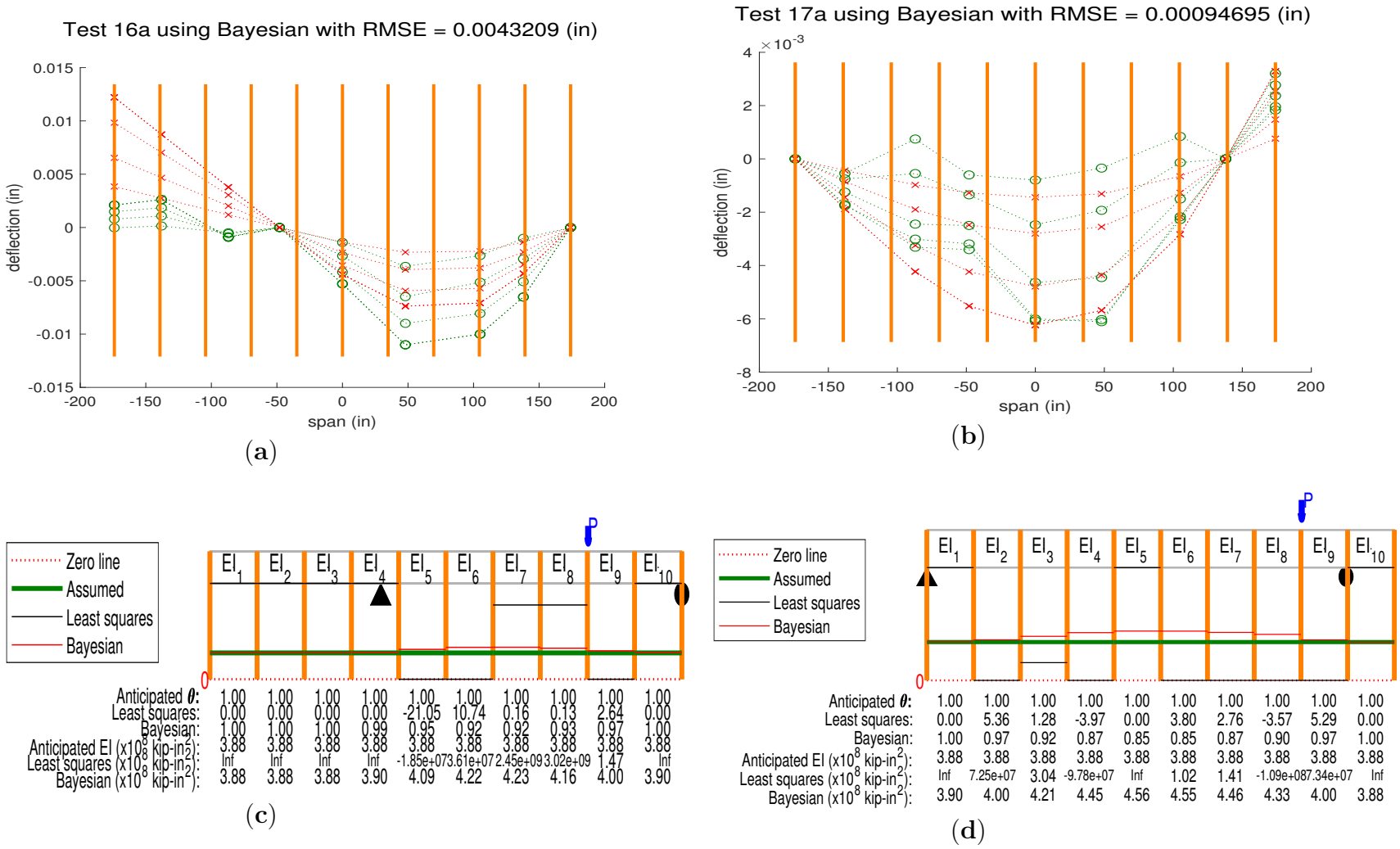

Fig. D.115. Tests 16a and 17a Bayesian analysis deflection comparisons and identification results. Identifications are $\times 10^8$ unless stated otherwise in the substructure result.

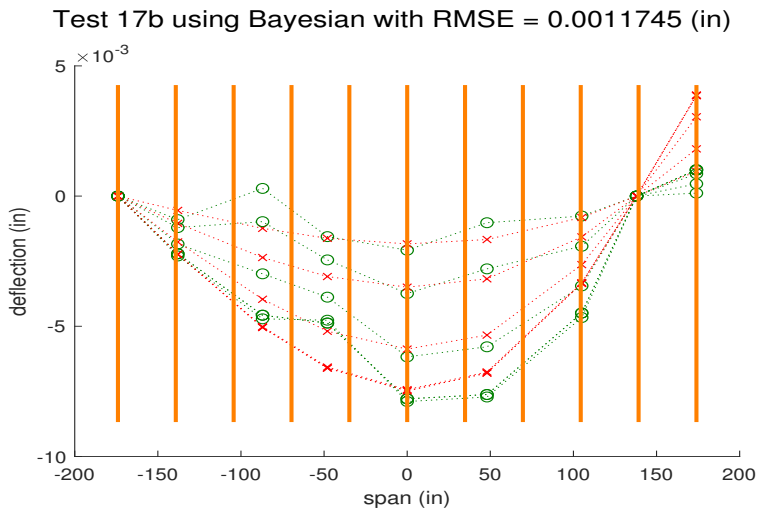

(a)

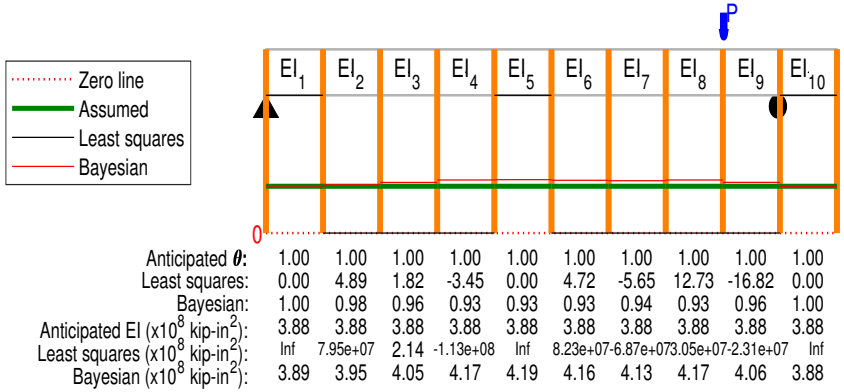

Anticipated θ:	1.00	1.00	1.00	1.00	1.00	1.00	1.00	1.00	1.00	1.00
Least squares:	0.00	4.89	1.82	-3.45	0.00	4.72	-5.65	12.73	-16.82	0.00
Bayesian:	1.00	0.98	0.96	0.93	0.93	0.93	0.94	0.93	0.96	1.00
Anticipated EI ($\times 10^8$ kip-in^2):	3.88	3.88	3.88	3.88	3.88	3.88	3.88	3.88	3.88	3.88
Least squares ($\times 10^8$ kip-in^2):	Inf	7.95e+07	2.14	-1.13e+08	Inf	8.23e+07	-6.87e+07	3.05e+07	-2.31e+07	Inf
Bayesian ($\times 10^8$ kip-in^2):	3.89	3.95	4.05	4.17	4.19	4.16	4.13	4.17	4.06	3.88

(c)

Fig. D.116. Test 17b Bayesian analysis deflection comparisons and identification results. Identifications are $\times 10^8$ unless stated otherwise in the substructure result.

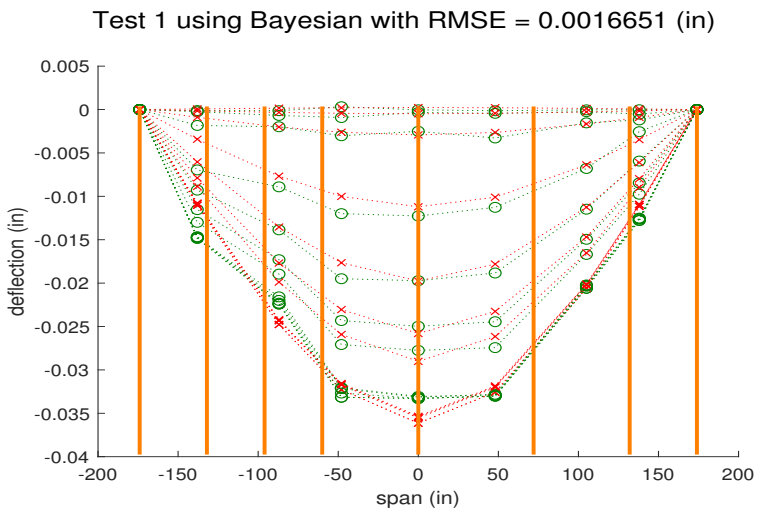

(a)

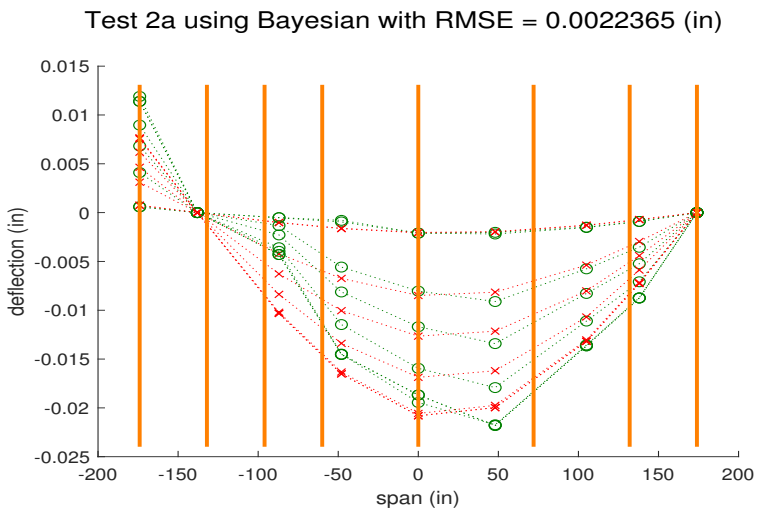

(b)

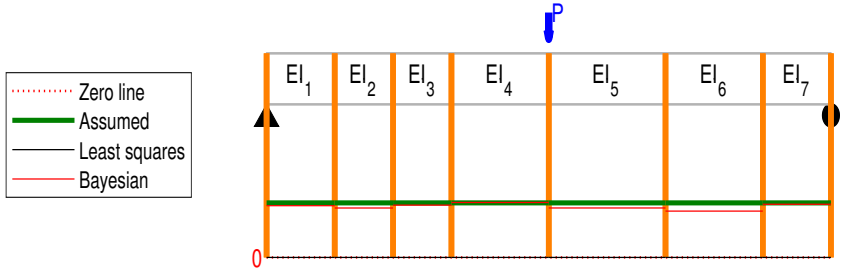

Anticipated $\boldsymbol{\theta}$:	1.00	1.00	1.00	1.00	1.00	1.00	1.00
Least squares:	105.73	-52.74	20.93	-1.67	1.95	-0.04	7.70
Bayesian:	1.03	1.05	1.02	1.00	1.05	1.08	1.01
Anticipated EI ($\times 10^8$ kip-in^2):	3.88	3.88	3.88	3.88	3.88	3.88	3.88
Least squares ($\times 10^8$ kip-in^2):	3.67e+06	-7.36e+06	1.86e+07	-2.33e+08	1.99	-1.11e+10	5.05e+07
Bayesian ($\times 10^8$ kip-in^2):	3.78	3.69	3.80	3.90	3.69	3.58	3.83

(c)

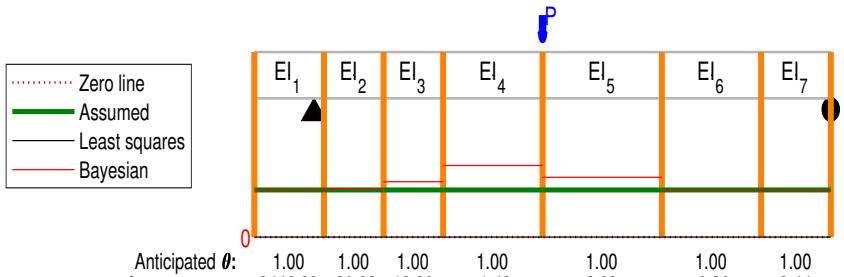

Anticipated $\boldsymbol{\theta}$:	1.00	1.00	1.00	1.00	1.00	1.00	1.00
Least squares:	2446.99	-80.92	18.86	-1.49	2.08	-0.36	8.44
Bayesian:	1.00	0.99	0.91	0.73	0.86	1.00	1.00
Anticipated EI ($\times 10^8$ kip-in^2):	3.88	3.88	3.88	3.88	3.88	3.88	3.88
Least squares ($\times 10^8$ kip-in^2):	1.59e+05	-4.80e+06	2.06e+07	-2.61e+08	1.87	-1.07e+09	4.60e+07
Bayesian ($\times 10^8$ kip-in^2):	3.88	3.92	4.27	5.30	4.51	3.87	3.87

(d)

Fig. D.117. Tests 1 and 2a Bayesian analysis deflection comparisons and identification results. Identifications are $\times 10^8$ unless stated otherwise in the substructure result.

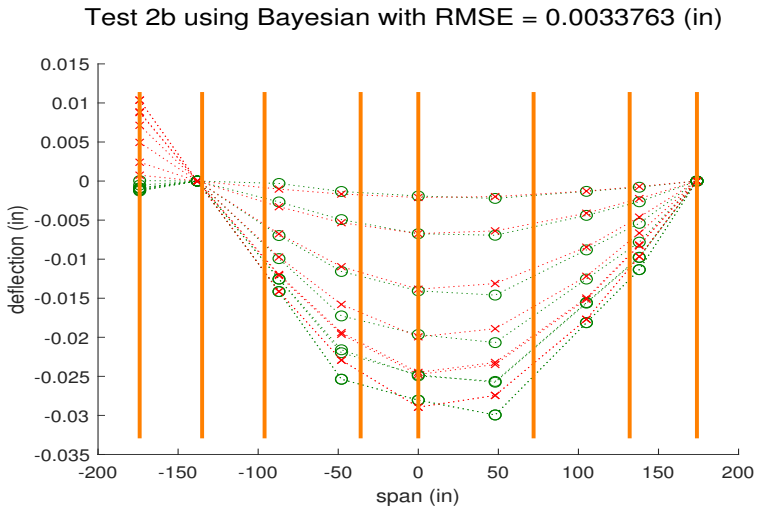

(a)

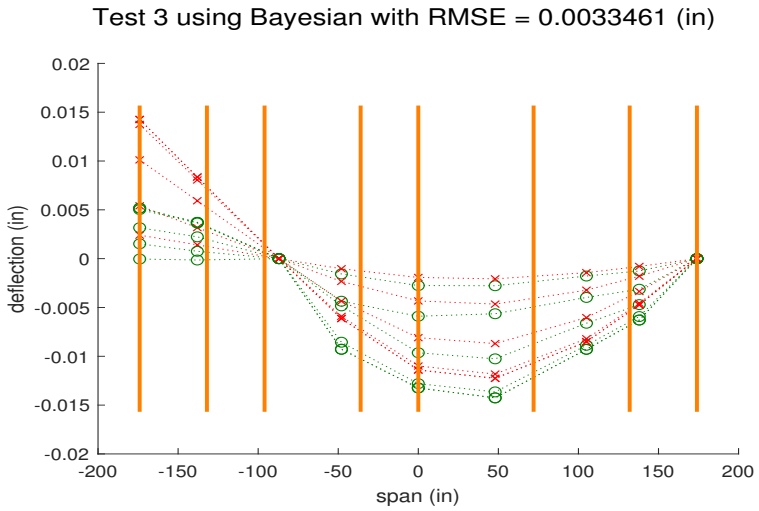

(b)

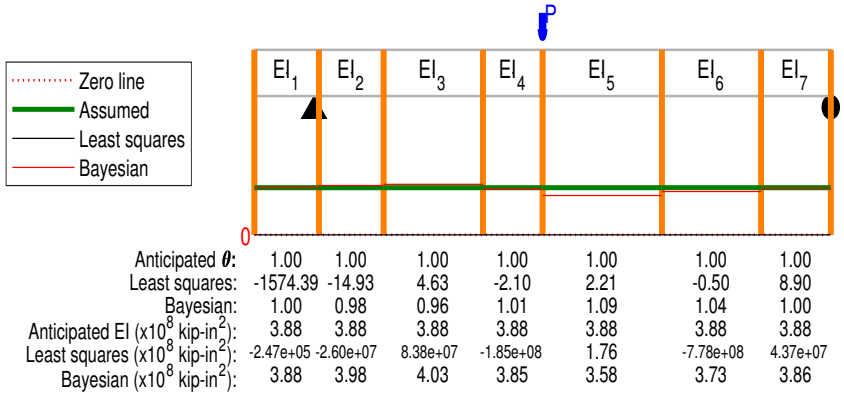

(c)

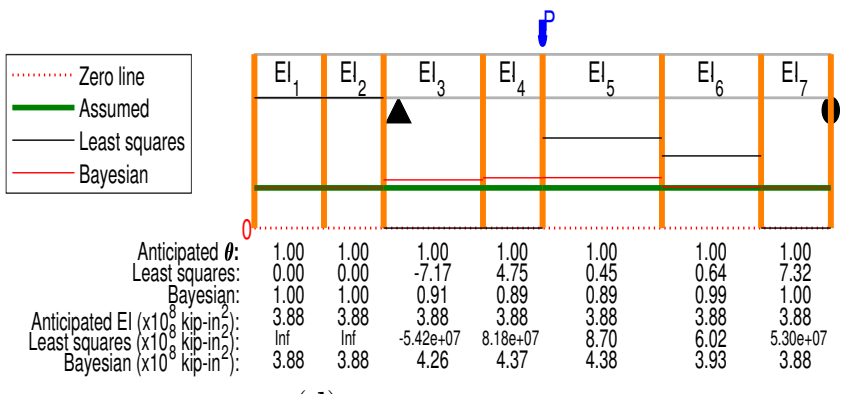

(d)

Fig. D.118. Tests 2b and 3 Bayesian analysis deflection comparisons and identification results. Identifications are $\times 10^8$ unless stated otherwise in the substructure result.

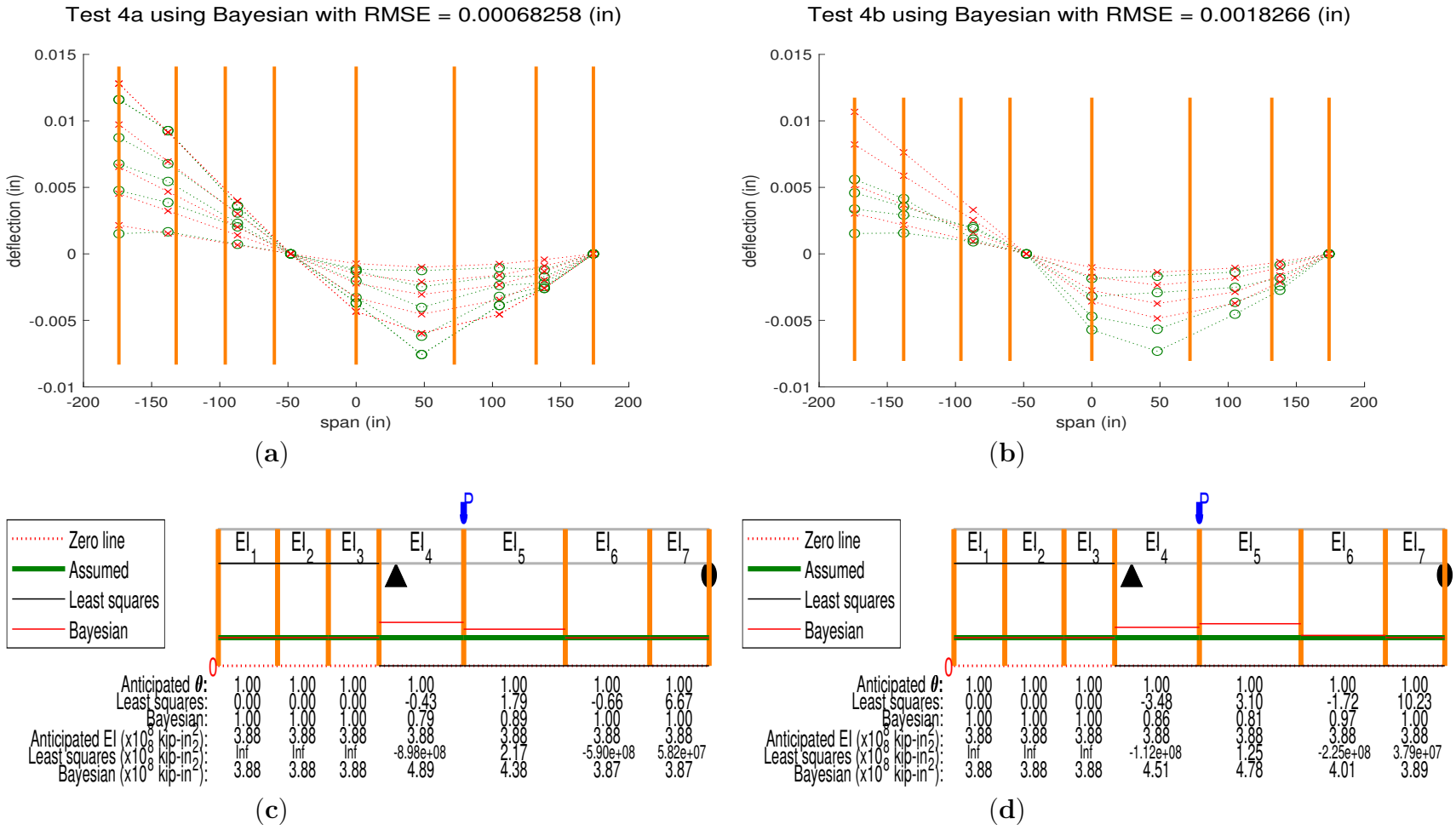

Fig. D.119. Tests 4a and 4b Bayesian analysis deflection comparisons and identification results. Identifications are $\times 10^8$ unless stated otherwise in the substructure result.

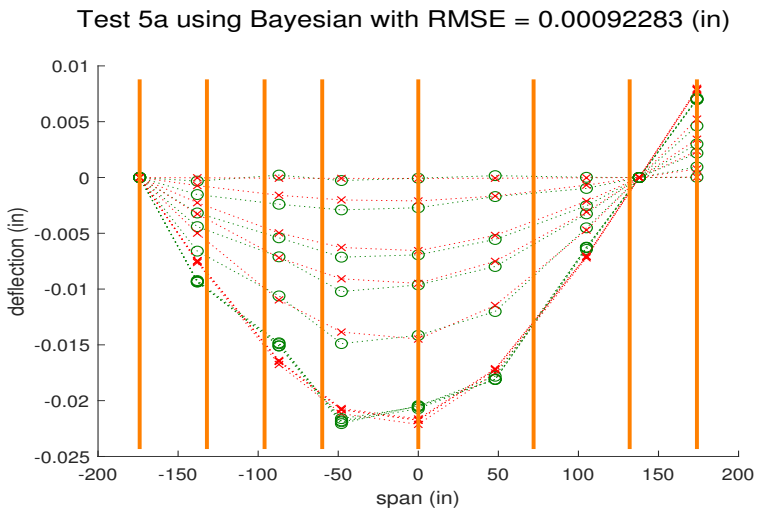

(a)

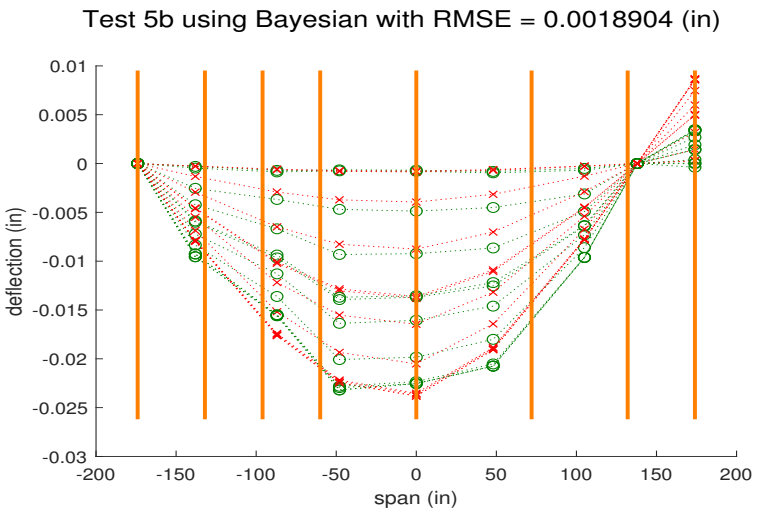

(b)

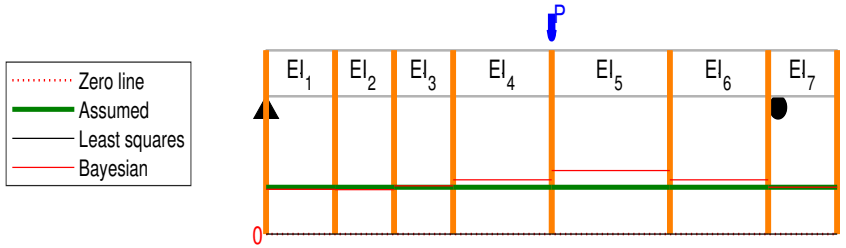

Anticipated θ:	1.00	1.00	1.00	1.00	1.00	1.00	1.00
Least squares:	81.08	-42.61	17.50	-1.24	1.73	-0.69	5.58
Bayesian:	1.02	1.03	0.98	0.92	0.82	0.92	1.00
Anticipated EI ($\times 10^8$ kip-in^2):	3.88	3.88	3.88	3.88	3.88	3.88	3.88
Least squares ($\times 10^8$ kip-in^2):	4.79e+06	-9.11e+06	2.22e+07	-3.14e+08	2.24	-5.63e+08	6.96e+07
Bayesian ($\times 10^8$ kip-in^2):	3.80	3.78	3.94	4.23	4.76	4.23	3.89

(c)

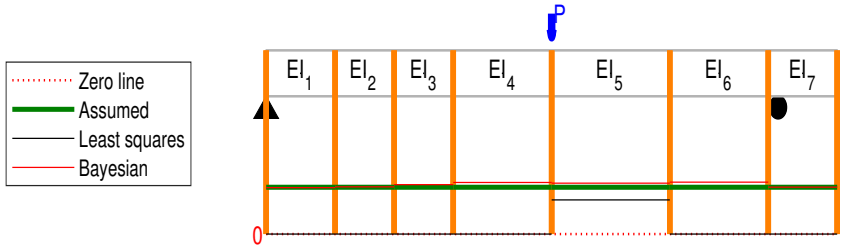

Anticipated θ:	1.00	1.00	1.00	1.00	1.00	1.00	1.00
Least squares:	71.47	-36.72	14.64	-0.67	1.14	4.08	-650.65
Bayesian:	1.00	1.00	0.97	0.95	0.96	0.94	1.00
Anticipated EI ($\times 10^8$ kip-in^2):	3.88	3.88	3.88	3.88	3.88	3.88	3.88
Least squares ($\times 10^8$ kip-in^2):	5.43e+06	-1.06e+07	2.65e+07	-5.79e+08	3.41	9.51e+07	-5.97e+05
Bayesian ($\times 10^8$ kip-in^2):	3.87	3.90	4.00	4.10	4.07	4.11	3.89

(d)

Fig. D.120. Tests 4a and 5b Bayesian analysis deflection comparisons and identification results. Identifications are $\times 10^8$ unless stated otherwise in the substructure result.

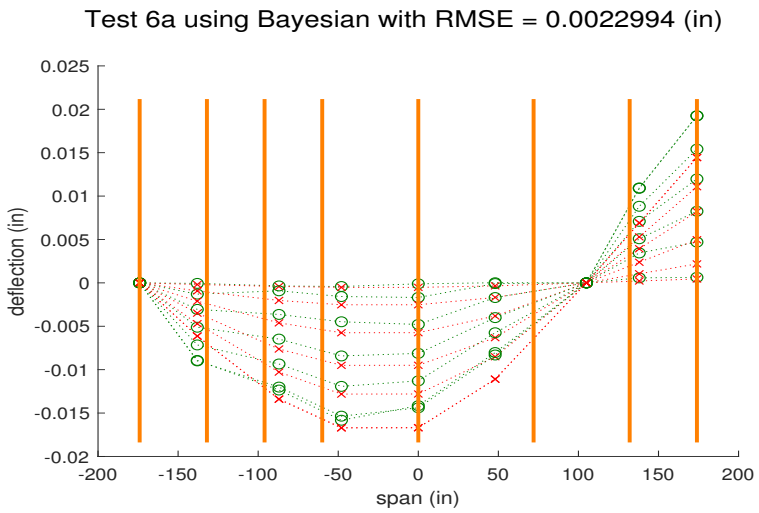

(a)

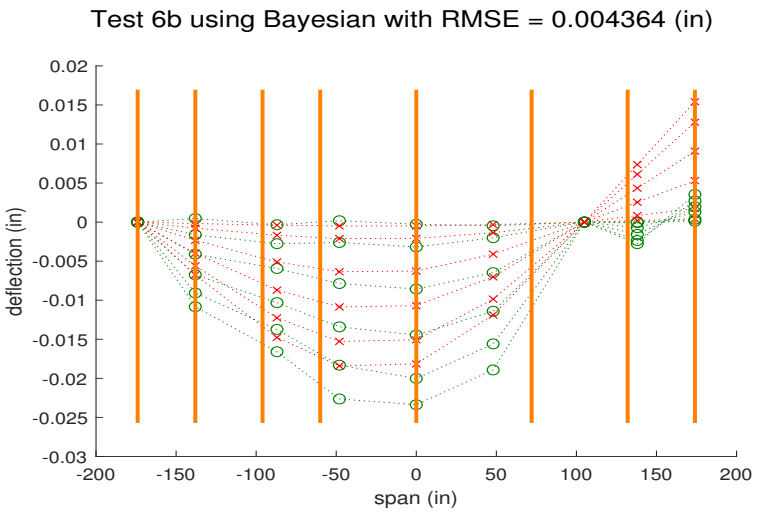

(b)

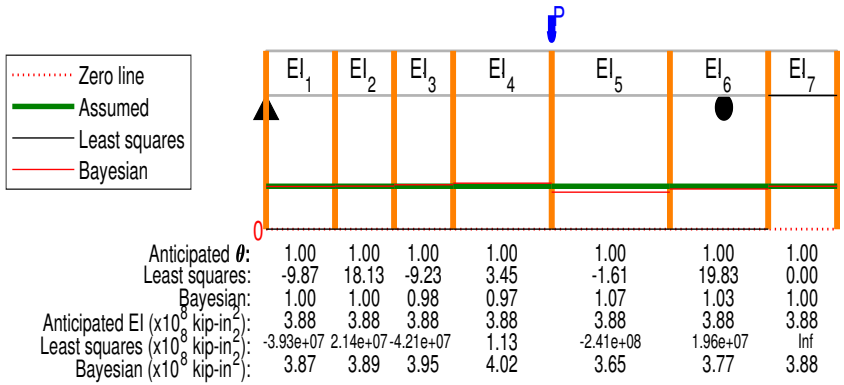

Anticipated θ:	1.00	1.00	1.00	1.00	1.00	1.00	1.00
Least squares:	-9.87	18.13	-9.23	3.45	-1.61	19.83	0.00
Bayesian:	1.00	1.00	0.98	0.97	1.07	1.03	1.00
Anticipated EI ($\times 10^8$ kip-in^2):	3.88	3.88	3.88	3.88	3.88	3.88	3.88
Least squares ($\times 10^8$ kip-in^2):	-3.93e+07	2.14e+07	-4.21e+07	1.13	-2.41e+08	1.96e+07	Inf
Bayesian ($\times 10^8$ kip-in^2):	3.87	3.89	3.95	4.02	3.65	3.77	3.88

(c)

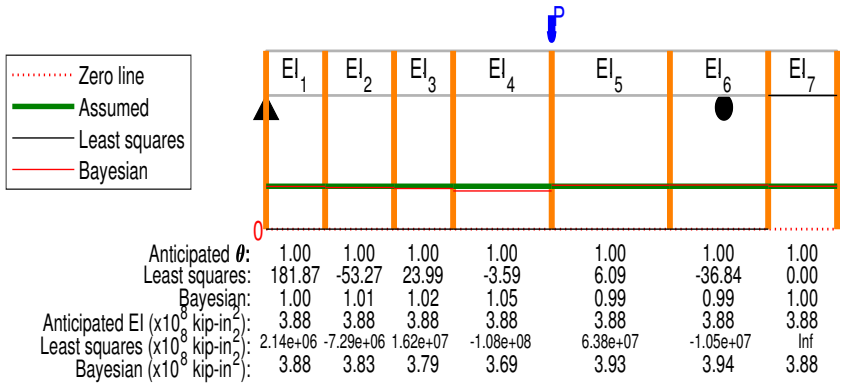

Anticipated θ:	1.00	1.00	1.00	1.00	1.00	1.00	1.00
Least squares:	181.87	-53.27	23.99	-3.59	6.09	-36.84	0.00
Bayesian:	1.00	1.01	1.02	1.05	0.99	0.99	1.00
Anticipated EI ($\times 10^8$ kip-in^2):	3.88	3.88	3.88	3.88	3.88	3.88	3.88
Least squares ($\times 10^8$ kip-in^2):	2.14e+06	-7.29e+06	1.62e+07	-1.08e+08	6.38e+07	-1.05e+07	Inf
Bayesian ($\times 10^8$ kip-in^2):	3.88	3.83	3.79	3.69	3.93	3.94	3.88

(d)

Fig. D.121. Tests 6a and 6b Bayesian analysis deflection comparisons and identification results. Identifications are $\times 10^8$ unless stated otherwise in the substructure result.

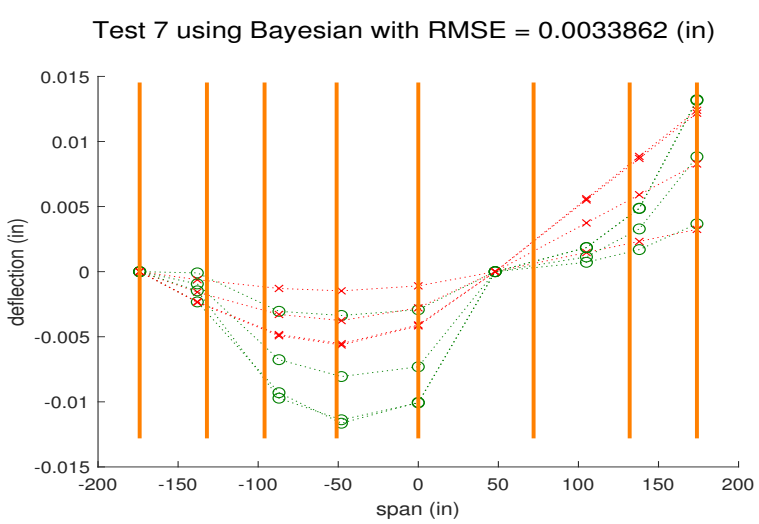

(a)

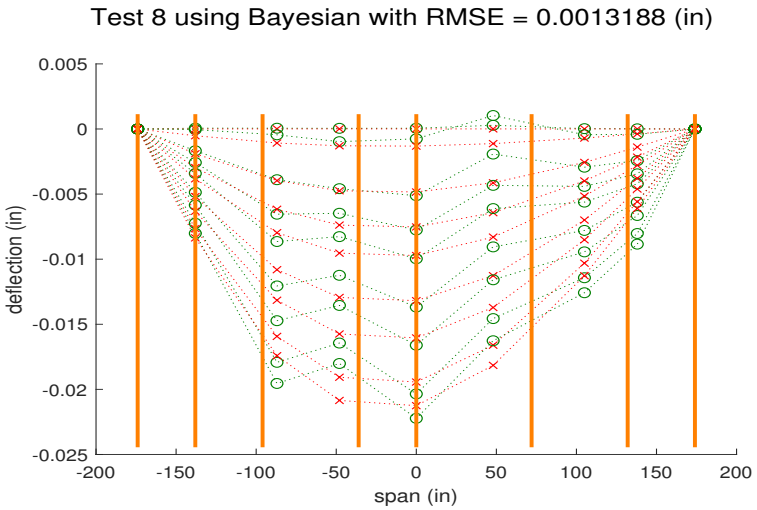

(b)

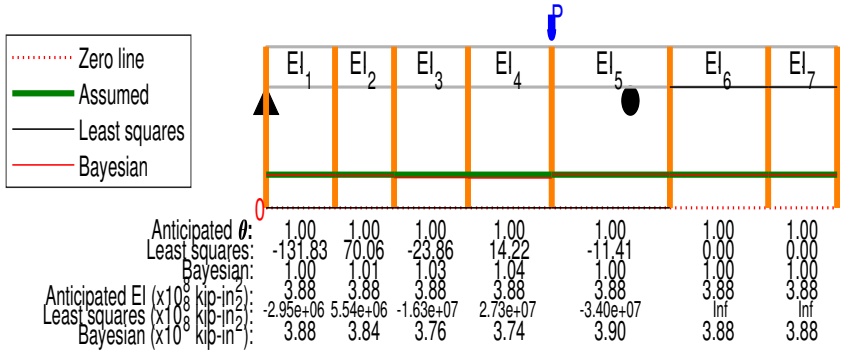

Anticipated θ:	1.00	1.00	1.00	1.00	1.00	1.00	1.00
Least squares:	-131.83	70.06	-23.86	14.22	-11.41	0.00	0.00
Bayesian:	1.00	1.01	1.03	1.04	1.00	1.00	1.00
Anticipated EI ($\times 10^8$ kip-in^2):	3.88	3.88	3.88	3.88	3.88	3.88	3.88
Least squares ($\times 10^8$ kip-in^2):	-2.95e+06	5.54e+06	-1.63e+07	2.73e+07	-3.40e+07	Inf	Inf
Bayesian ($\times 10^8$ kip-in^2):	3.88	3.84	3.76	3.74	3.90	3.88	3.88

(c)

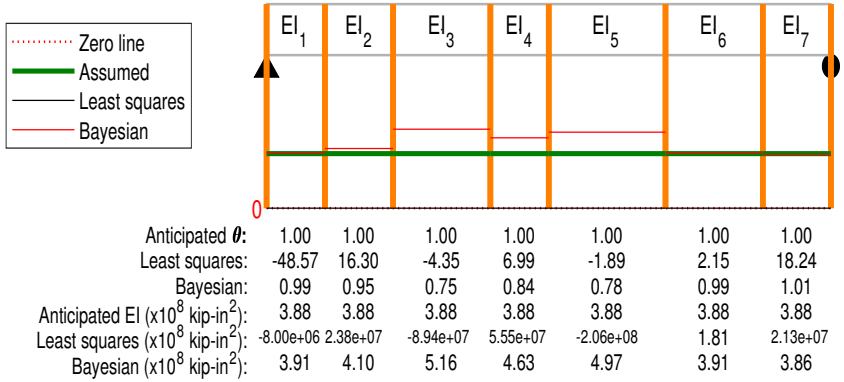

Anticipated θ:	1.00	1.00	1.00	1.00	1.00	1.00	1.00
Least squares:	-48.57	16.30	-4.35	6.99	-1.89	2.15	18.24
Bayesian:	0.99	0.95	0.75	0.84	0.78	0.99	1.01
Anticipated EI ($\times 10^8$ kip-in^2):	3.88	3.88	3.88	3.88	3.88	3.88	3.88
Least squares ($\times 10^8$ kip-in^2):	-8.00e+06	2.38e+07	-8.94e+07	5.55e+07	-2.06e+08	1.81	2.13e+07
Bayesian ($\times 10^8$ kip-in^2):	3.91	4.10	5.16	4.63	4.97	3.91	3.86

(d)

Fig. D.122. Tests 7 and 8 Bayesian analysis deflection comparisons and identification results. Identifications are $\times 10^8$ unless stated otherwise in the substructure result.

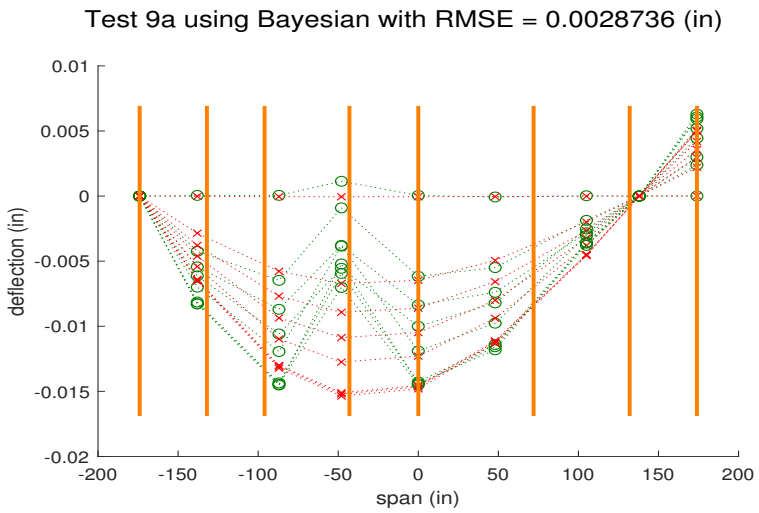

(a)

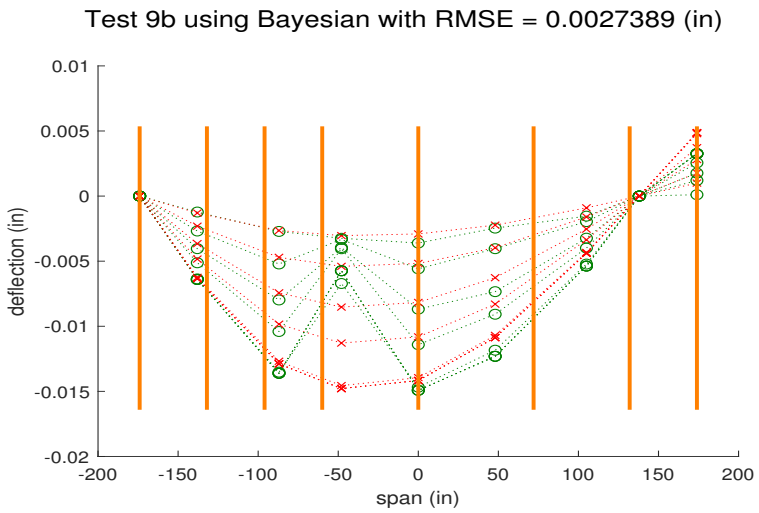

(b)

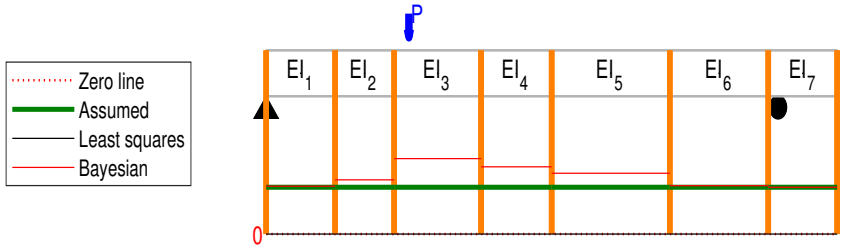

	EI_1	EI_2	EI_3	EI_4	EI_5	EI_6	EI_7
Anticipated $\boldsymbol{\theta}$:	1.00	1.00	1.00	1.00	1.00	1.00	1.00
Least squares:	-45.10	31.79	-9.92	3.87	2.20	-2.63	328.01
Bayesian:	0.99	0.92	0.69	0.78	0.85	0.98	1.00
Anticipated EI ($\times 10^8$ kip-in^2):	3.88	3.88	3.88	3.88	3.88	3.88	3.88
Least squares ($\times 10^8$ kip-in^2):	-8.61e+06	1.22e+07	-3.92e+07	1.00	1.76	-1.48e+08	1.18e+06
Bayesian ($\times 10^8$ kip-in^2):	3.93	4.23	5.67	5.01	4.59	3.95	3.88

(c)

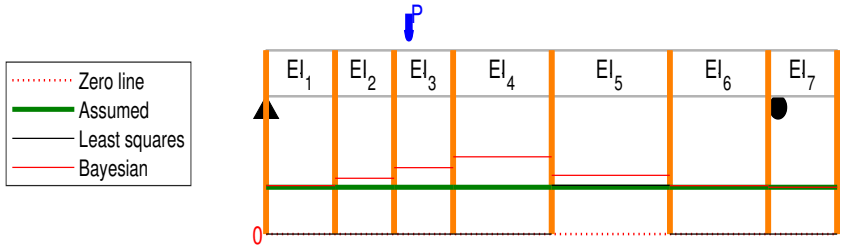

	EI_1	EI_2	EI_3	EI_4	EI_5	EI_6	EI_7
Anticipated $\boldsymbol{\theta}$:	1.00	1.00	1.00	1.00	1.00	1.00	1.00
Least squares:	-120.16	76.72	-33.34	5.09	0.98	3.06	-445.43
Bayesian:	0.98	0.90	0.78	0.67	0.87	0.98	1.00
Anticipated EI ($\times 10^8$ kip-in^2):	3.88	3.88	3.88	3.88	3.88	3.88	3.88
Least squares ($\times 10^8$ kip-in^2):	-3.23e+06	5.06e+06	-1.16e+07	7.63e+07	3.97	1.27	-8.72e+05
Bayesian ($\times 10^8$ kip-in^2):	3.95	4.31	4.95	5.84	4.47	3.95	3.88

(d)

Fig. D.123. Tests 9a and 9b Bayesian analysis deflection comparisons and identification results. Identifications are $\times 10^8$ unless stated otherwise in the substructure result.

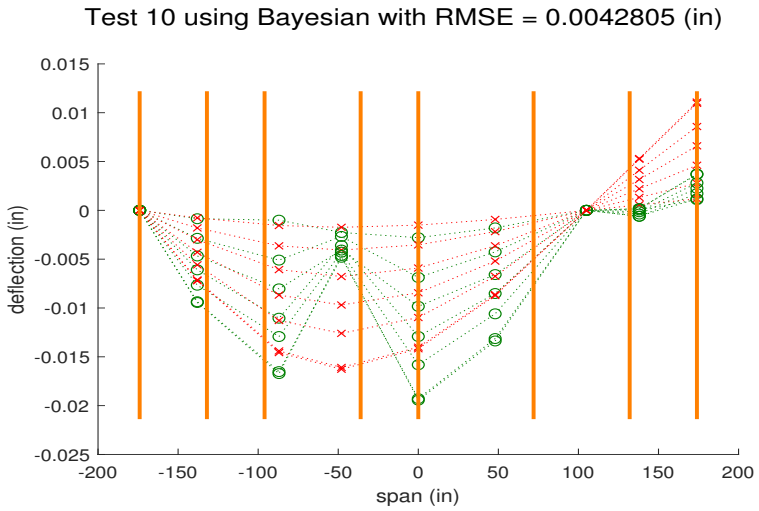

(a)

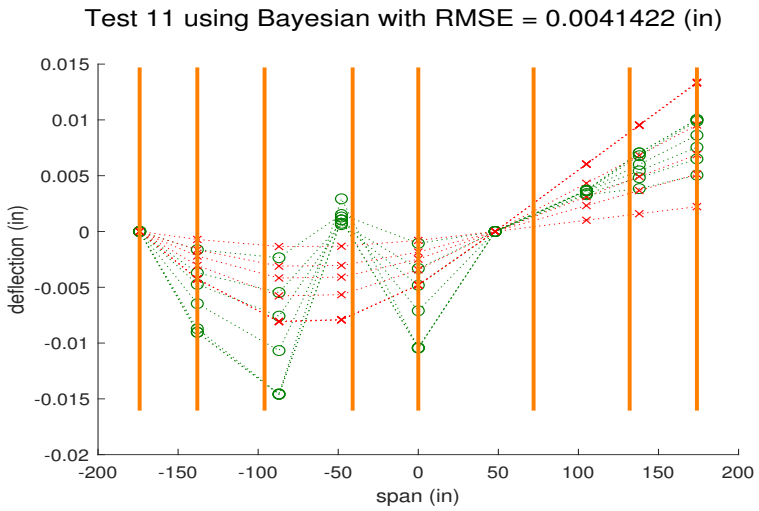

(b)

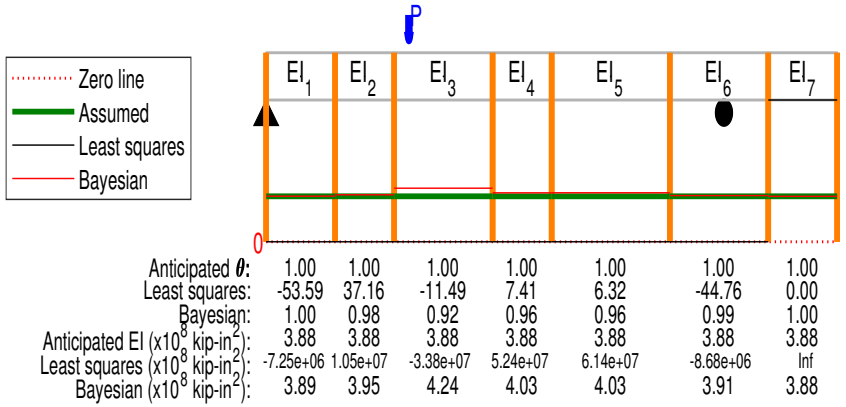

(c)

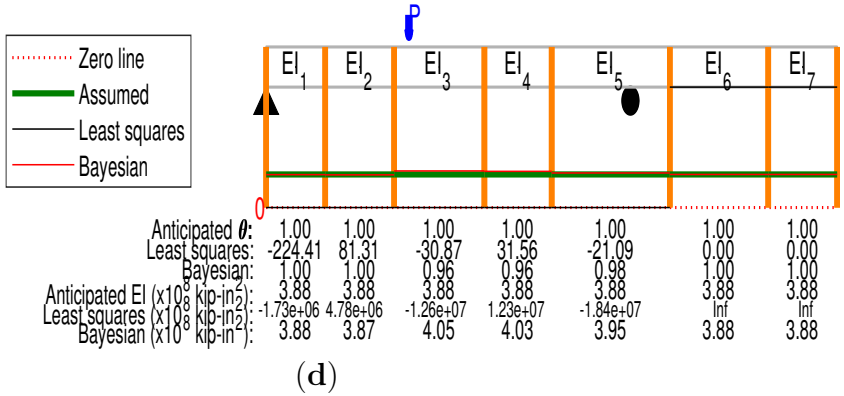

(d)

Fig. D.124. Tests 10 and 11 Bayesian analysis deflection comparisons and identification results. Identifications are $\times 10^8$ unless stated otherwise in the substructure result.

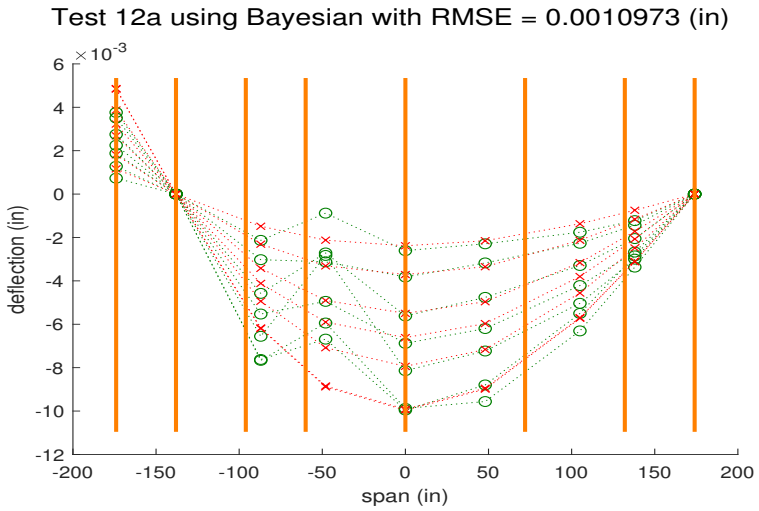

(a)

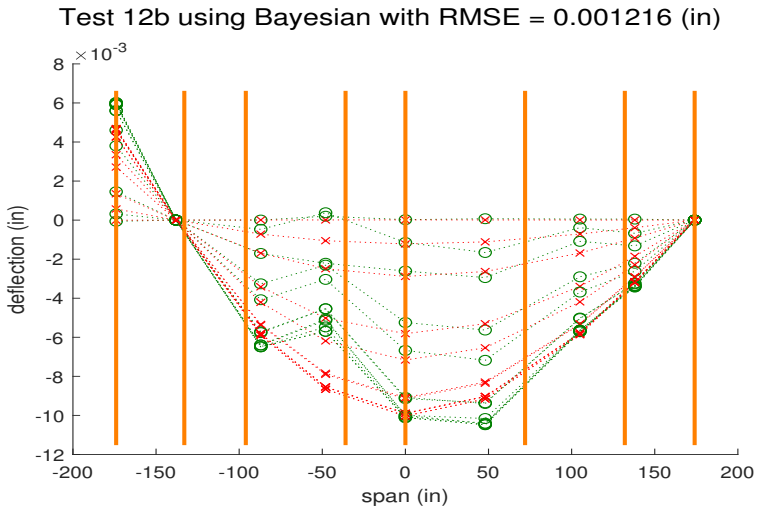

(b)

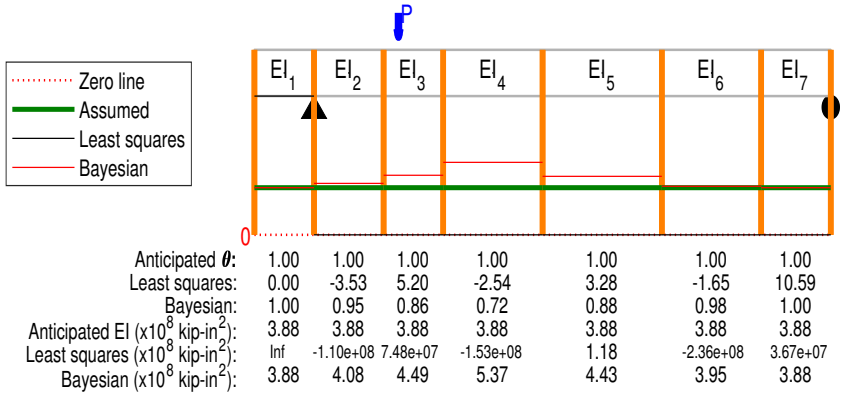

(c)

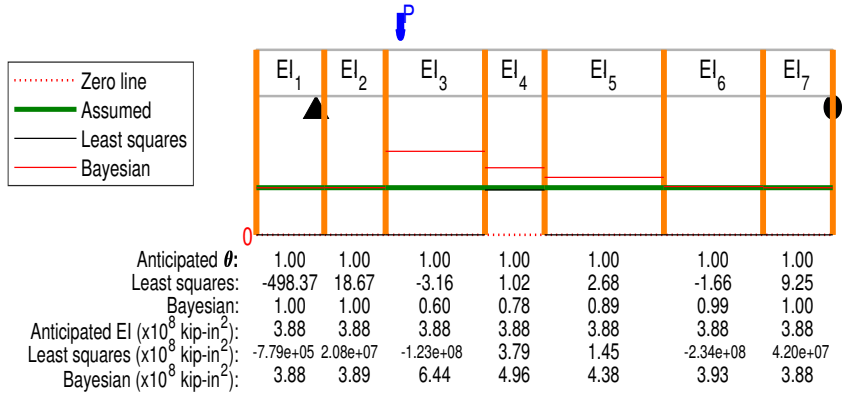

(d)

Fig. D.125. Tests 12a and 12b Bayesian analysis deflection comparisons and identification results. Identifications are $\times 10^8$ unless stated otherwise in the substructure result.

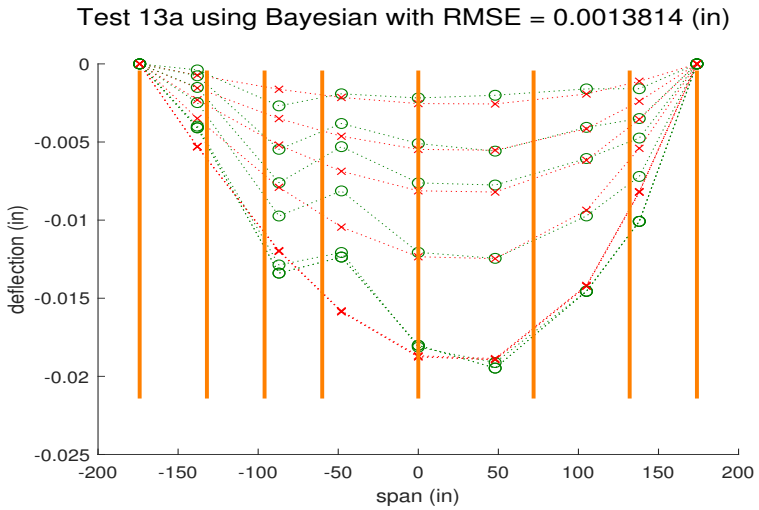

(a)

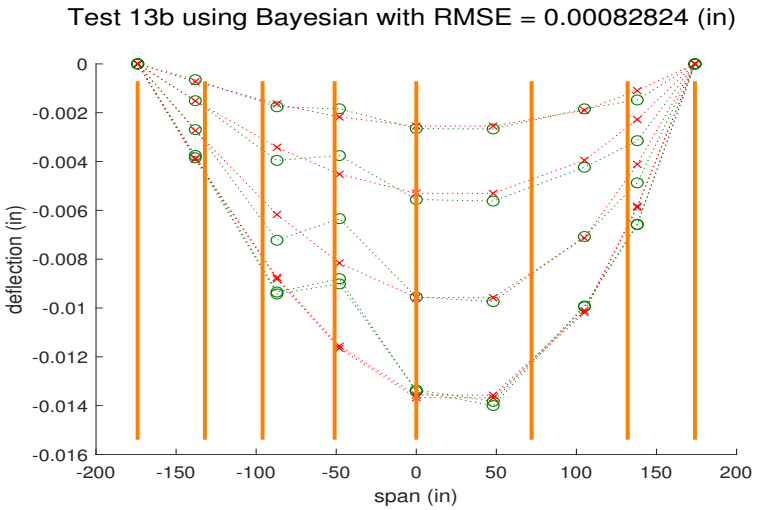

(b)

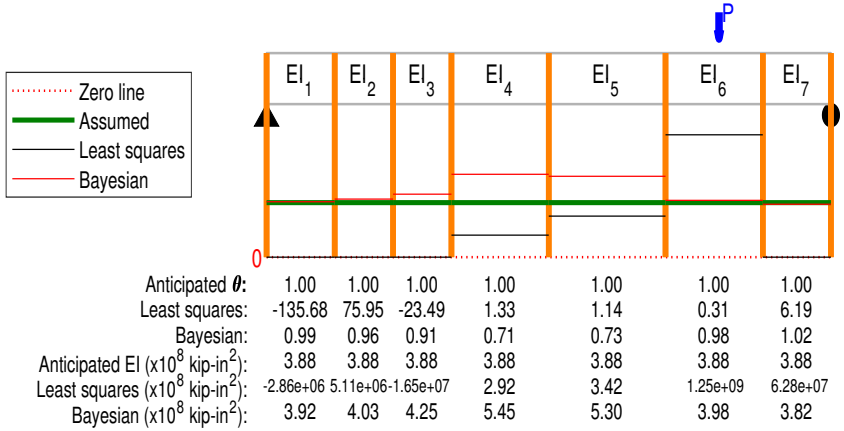

Anticipated θ:	1.00	1.00	1.00	1.00	1.00	1.00	1.00
Least squares:	-135.68	75.95	-23.49	1.33	1.14	0.31	6.19
Bayesian:	0.99	0.96	0.91	0.71	0.73	0.98	1.02
Anticipated EI ($\times 10^8$ kip-in^2):	3.88	3.88	3.88	3.88	3.88	3.88	3.88
Least squares ($\times 10^8$ kip-in^2):	-2.86e+06	5.11e+06	-1.65e+07	2.92	3.42	1.25e+09	6.28e+07
Bayesian ($\times 10^8$ kip-in^2):	3.92	4.03	4.25	5.45	5.30	3.98	3.82

(c)

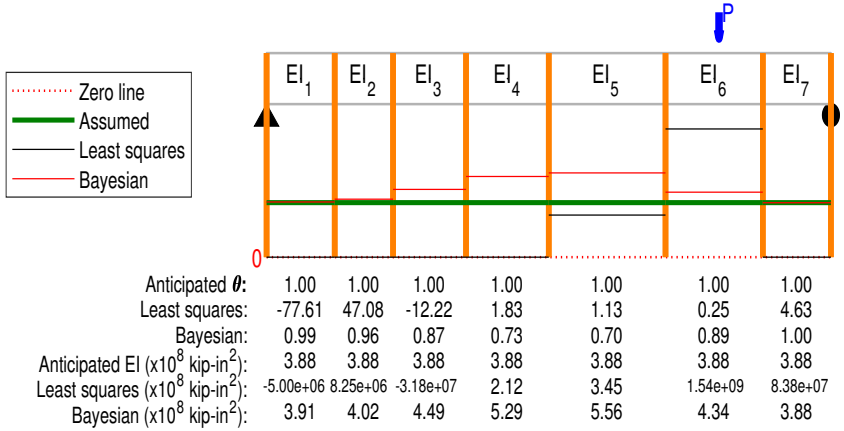

Anticipated θ:	1.00	1.00	1.00	1.00	1.00	1.00	1.00
Least squares:	-77.61	47.08	-12.22	1.83	1.13	0.25	4.63
Bayesian:	0.99	0.96	0.87	0.73	0.70	0.89	1.00
Anticipated EI ($\times 10^8$ kip-in^2):	3.88	3.88	3.88	3.88	3.88	3.88	3.88
Least squares ($\times 10^8$ kip-in^2):	-5.00e+06	8.25e+06	-3.18e+07	2.12	3.45	1.54e+09	8.38e+07
Bayesian ($\times 10^8$ kip-in^2):	3.91	4.02	4.49	5.29	5.56	4.34	3.88

(d)

Fig. D.126. Tests 13a and 13b Bayesian analysis deflection comparisons and identification results. Identifications are $\times 10^8$ unless stated otherwise in the substructure result.

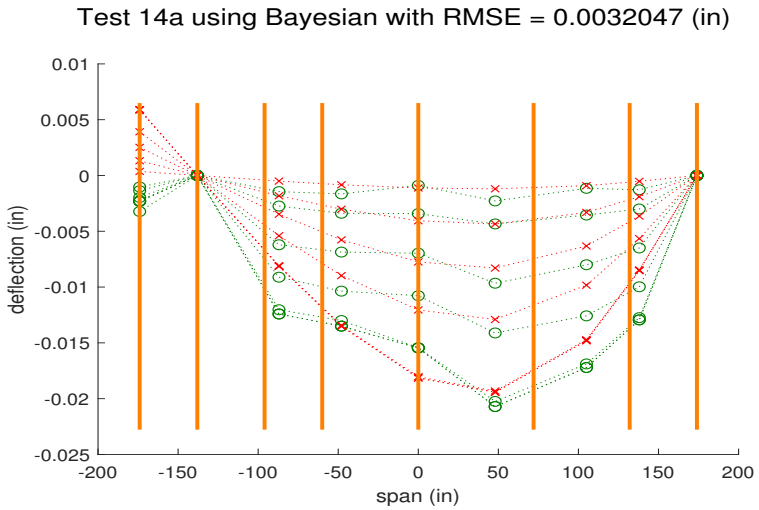

(a)

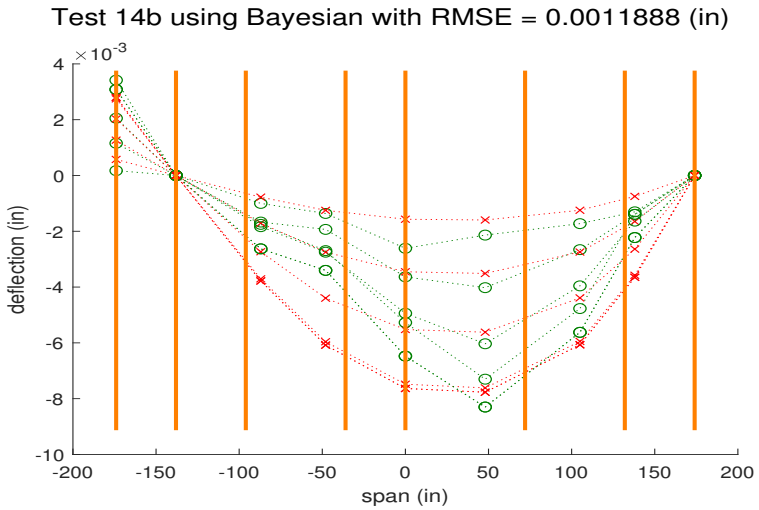

(b)

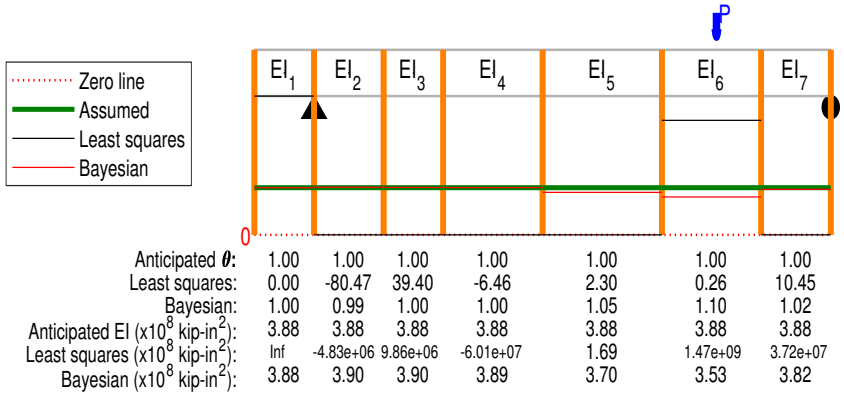

Anticipated θ:	1.00	1.00	1.00	1.00	1.00	1.00	1.00
Least squares:	0.00	-80.47	39.40	-6.46	2.30	0.26	10.45
Bayesian:	1.00	0.99	1.00	1.00	1.05	1.10	1.02
Anticipated EI ($\times 10^8$ kip-in^2):	3.88	3.88	3.88	3.88	3.88	3.88	3.88
Least squares ($\times 10^8$ kip-in^2):	Inf	-4.83e+06	9.86e+06	-6.01e+07	1.69	1.47e+09	3.72e+07
Bayesian ($\times 10^8$ kip-in^2):	3.88	3.90	3.90	3.89	3.70	3.53	3.82

(c)

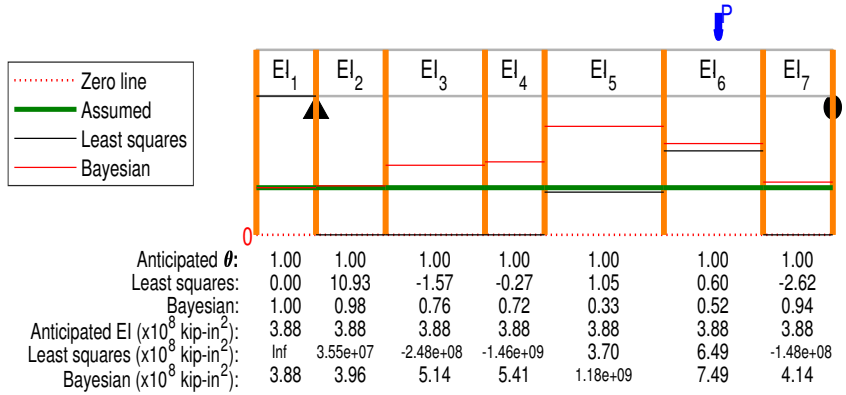

Anticipated θ:	1.00	1.00	1.00	1.00	1.00	1.00	1.00
Least squares:	0.00	10.93	-1.57	-0.27	1.05	0.60	-2.62
Bayesian:	1.00	0.98	0.76	0.72	0.33	0.52	0.94
Anticipated EI ($\times 10^8$ kip-in^2):	3.88	3.88	3.88	3.88	3.88	3.88	3.88
Least squares ($\times 10^8$ kip-in^2):	Inf	3.55e+07	-2.48e+08	-1.46e+09	3.70	6.49	-1.48e+08
Bayesian ($\times 10^8$ kip-in^2):	3.88	3.96	5.14	5.41	1.18e+09	7.49	4.14

(d)

Fig. D.127. Tests 14a and 14b Bayesian analysis deflection comparisons and identification results. Identifications are $\times 10^8$ unless stated otherwise in the substructure result.

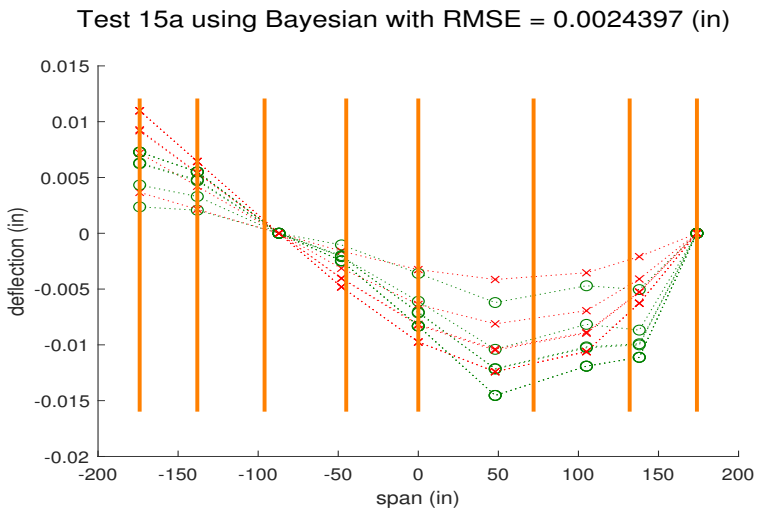

(a)

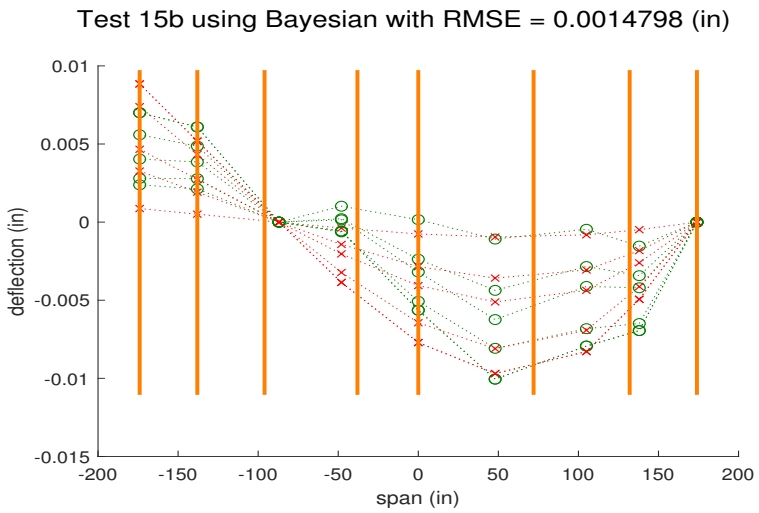

(b)

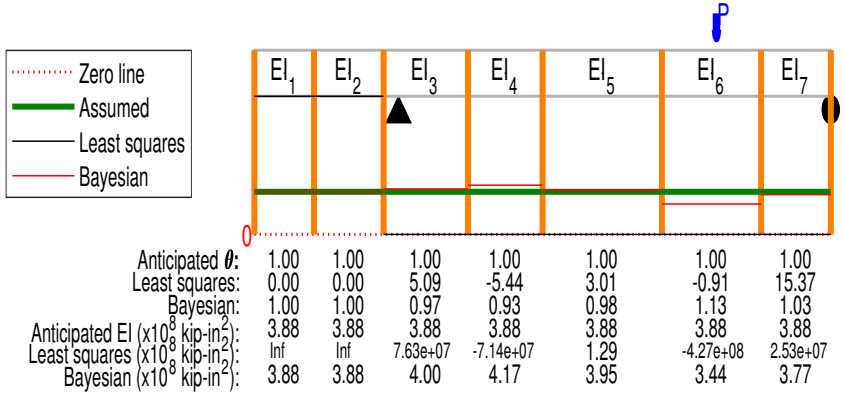

Anticipated θ:	1.00	1.00	1.00	1.00	1.00	1.00	1.00
Least squares:	0.00	0.00	5.09	-5.44	3.01	-0.91	15.37
Bayesian:	1.00	1.00	0.97	0.93	0.98	1.13	1.03
Anticipated EI ($\times 10^8$ kip-in^2):	3.88	3.88	3.88	3.88	3.88	3.88	3.88
Least squares ($\times 10^8$ kip-in^2):	Inf	Inf	7.63e+07	-7.14e+07	1.29	-4.27e+08	2.53e+07
Bayesian ($\times 10^8$ kip-in^2):	3.88	3.88	4.00	4.17	3.95	3.44	3.77

(c)

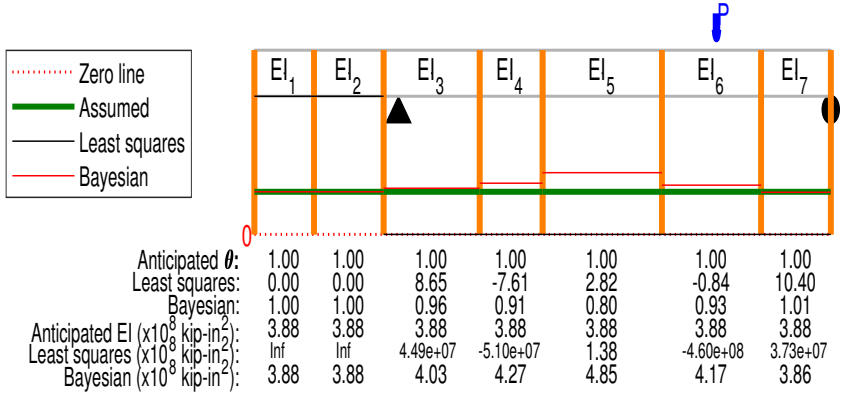

Anticipated θ:	1.00	1.00	1.00	1.00	1.00	1.00	1.00
Least squares:	0.00	0.00	8.65	-7.61	2.82	-0.84	10.40
Bayesian:	1.00	1.00	0.96	0.91	0.80	0.93	1.01
Anticipated EI ($\times 10^8$ kip-in^2):	3.88	3.88	3.88	3.88	3.88	3.88	3.88
Least squares ($\times 10^8$ kip-in^2):	Inf	Inf	4.49e+07	-5.10e+07	1.38	-4.60e+08	3.73e+07
Bayesian ($\times 10^8$ kip-in^2):	3.88	3.88	4.03	4.27	4.85	4.17	3.86

(d)

Fig. D.128. Tests 15a and 15b Bayesian analysis deflection comparisons and identification results. Identifications are $\times 10^8$ unless stated otherwise in the substructure result.

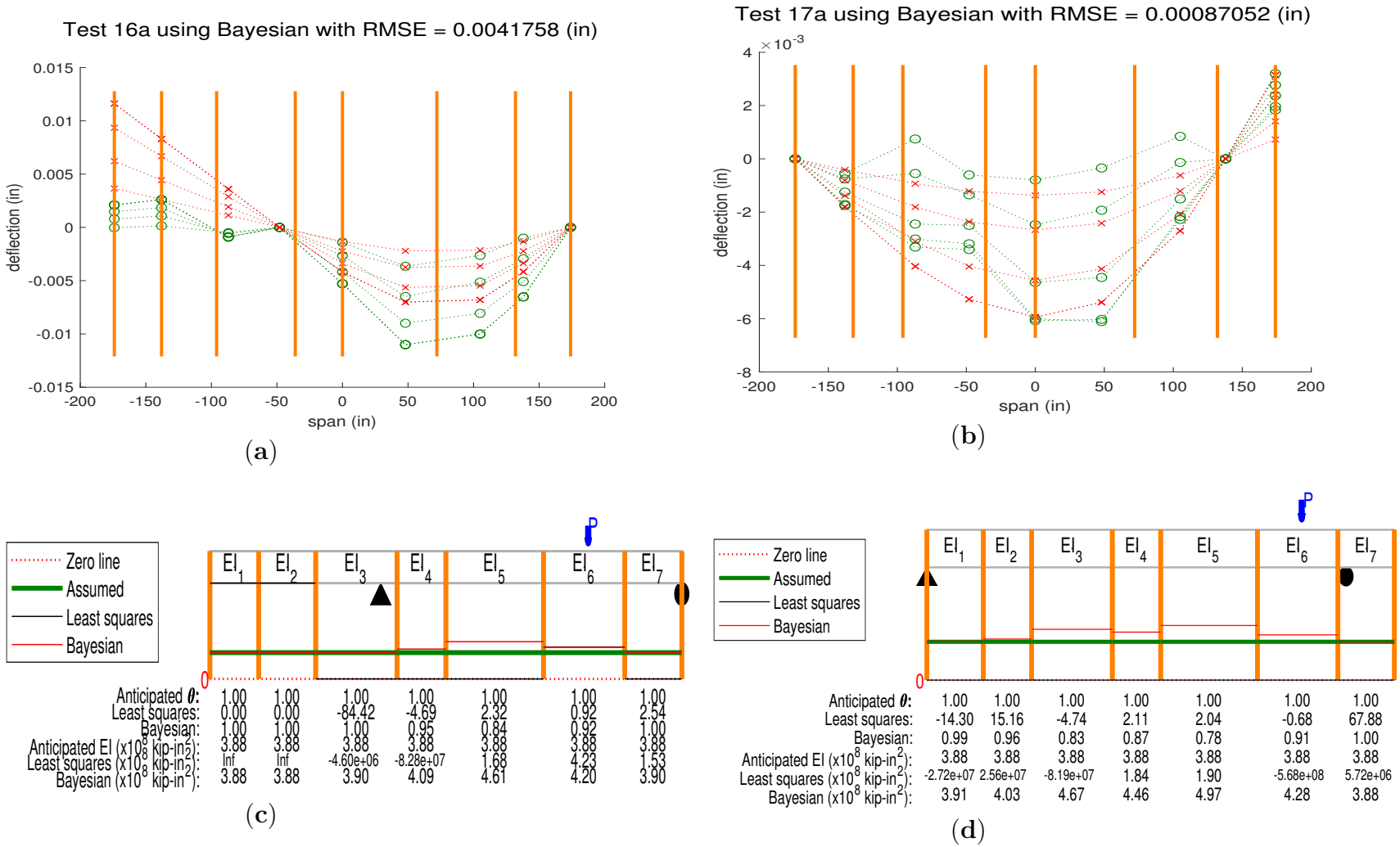

Fig. D.129. Tests 16a and 17a Bayesian analysis deflection comparisons and identification results. Identifications are $\times 10^8$ unless stated otherwise in the substructure result.

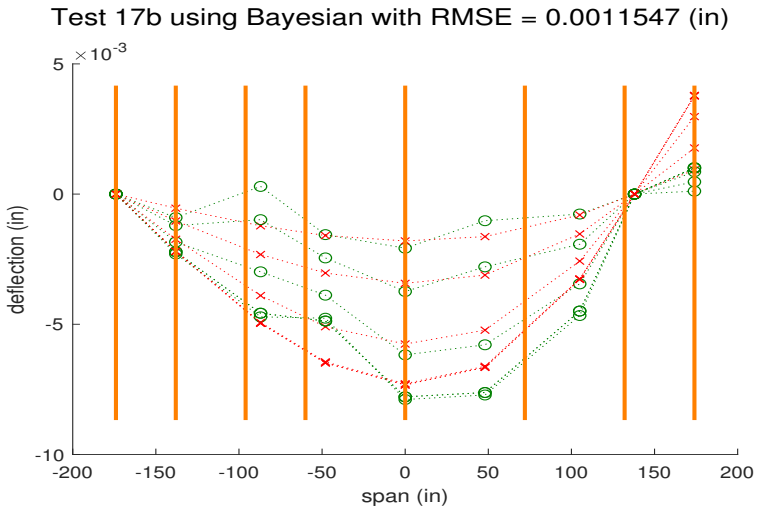

(a)

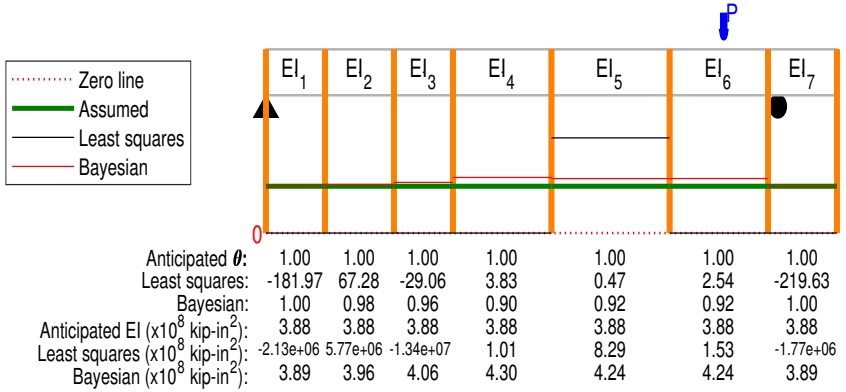

(c)

Fig. D.130. Test 17b Bayesian analysis deflection comparisons and identification results. Identifications are $\times 10^8$ unless stated otherwise in the substructure result.

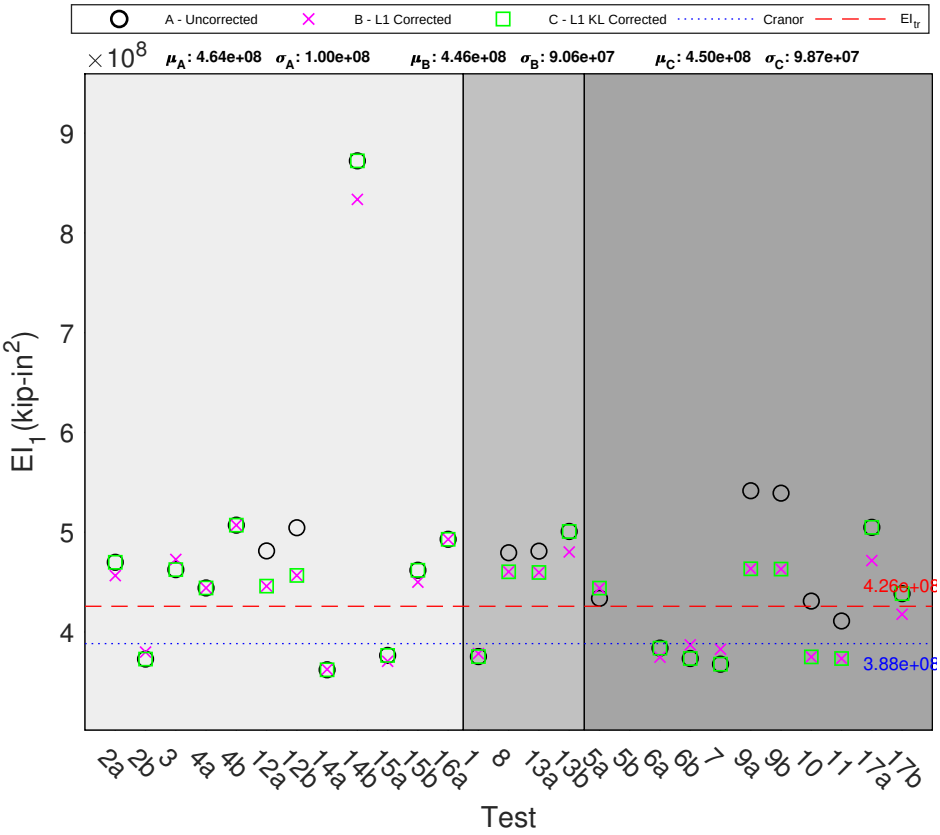

Fig. D.131. One EI value for Girder A when Bayesian analysis was applied: Distribution of EI identification for each test based on category

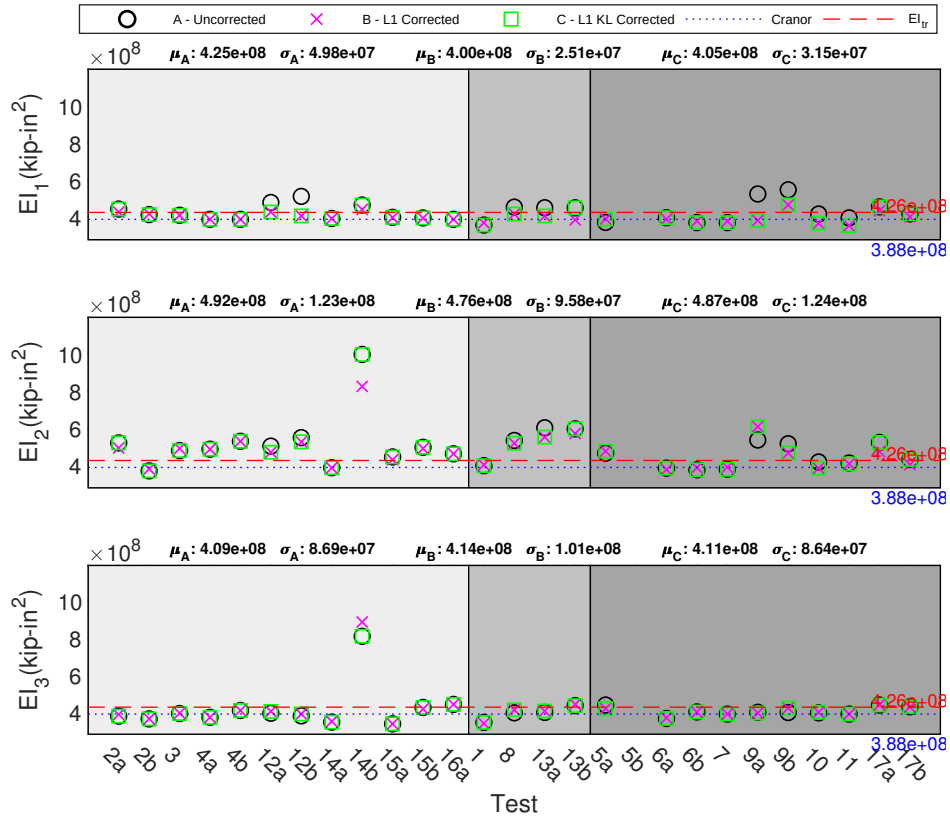

Fig. D.132. Three EI values for Girder A when Bayesian analysis was applied: Distribution of EI identification for each tet based on category

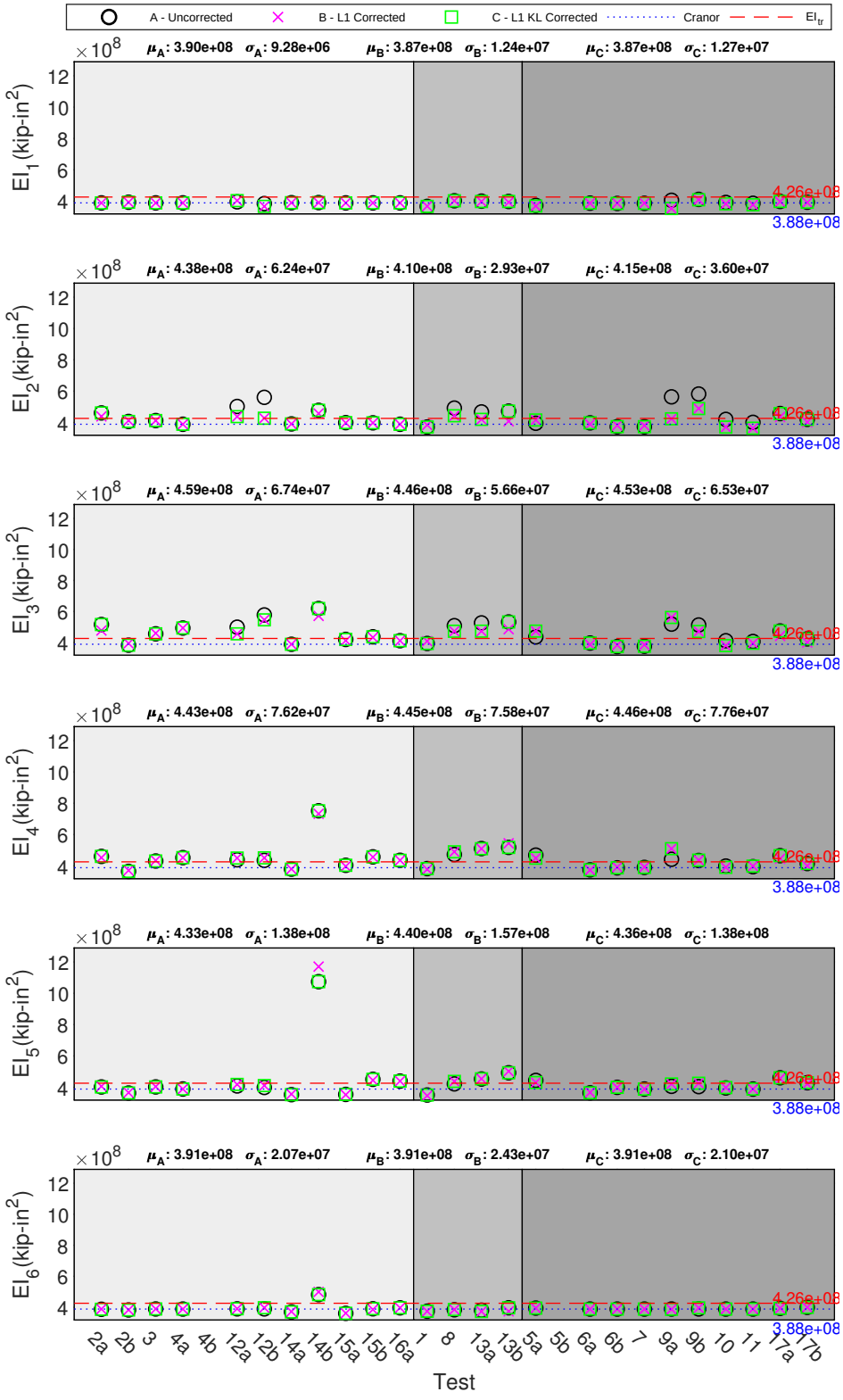

Fig. D.133. Six EI values for Girder A when Bayesian analysis was applied: Distribution of EI identification for each test based on category

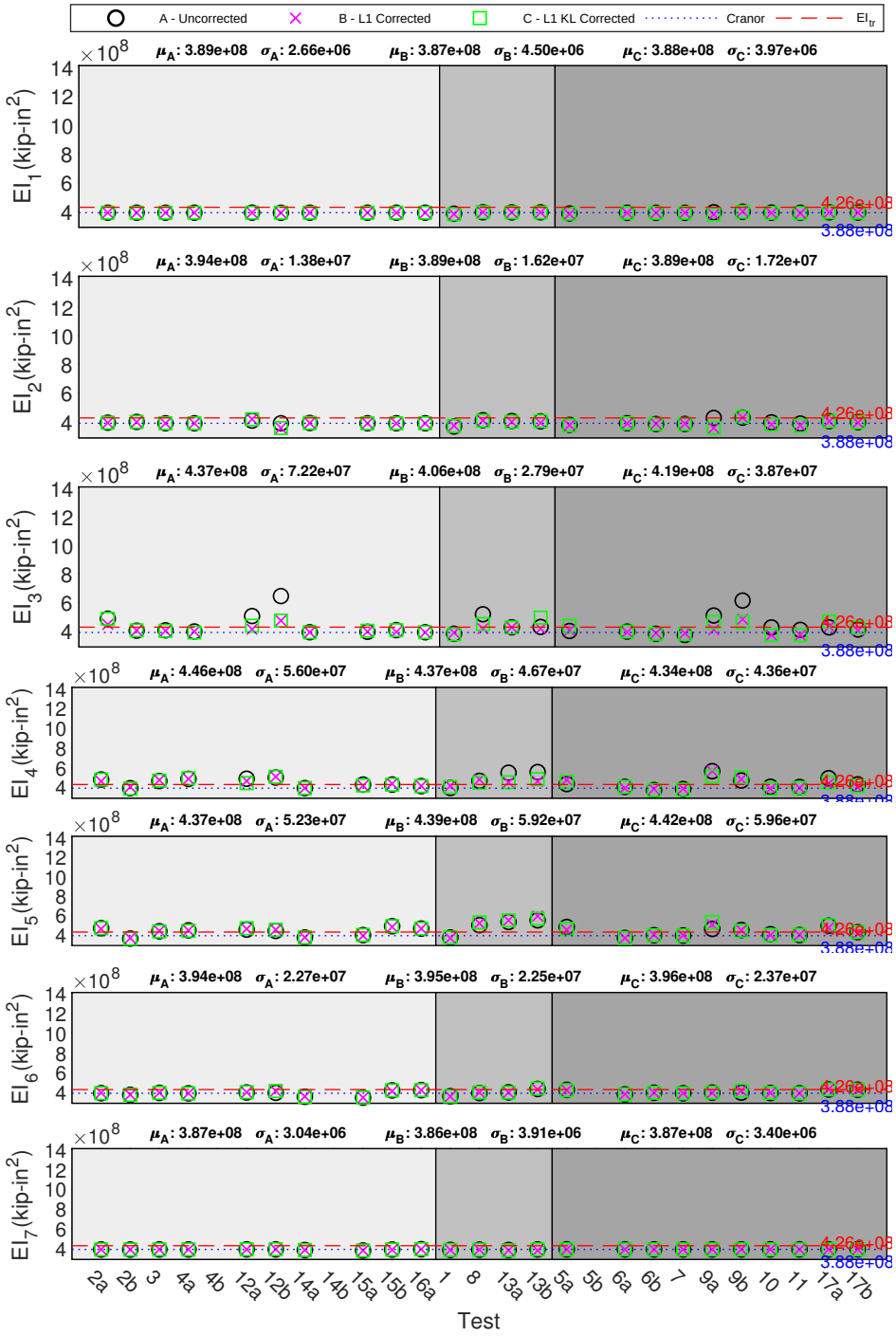

Fig. D.134. Seven arbitrary EI values for Girder A when Bayesian analysis was applied: Distribution of EI identification for each test based on category

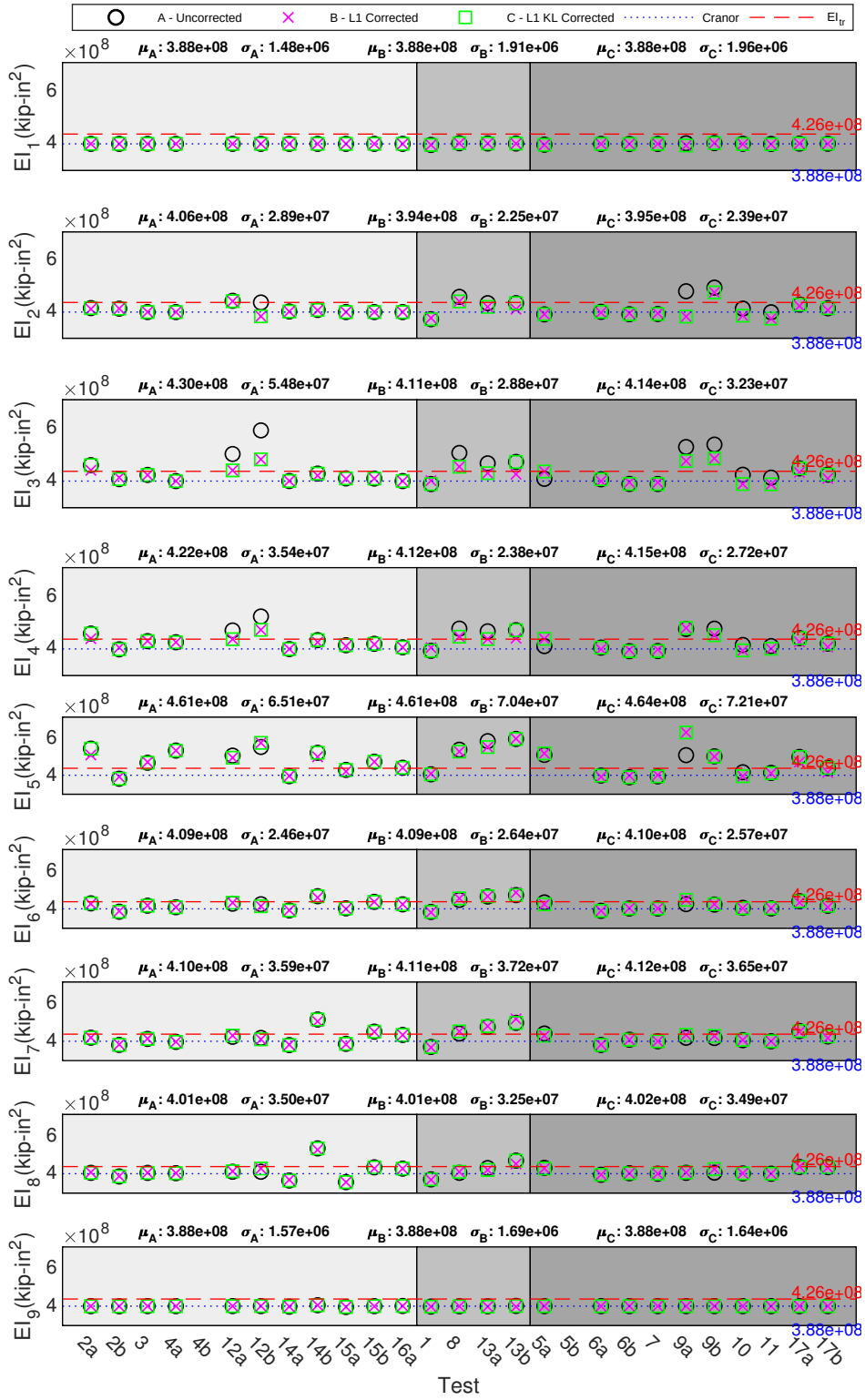

Fig. D.135. Nine EI values for Girder A when Bayesian analysis was applied: Distribution of EI identification for each test based on category

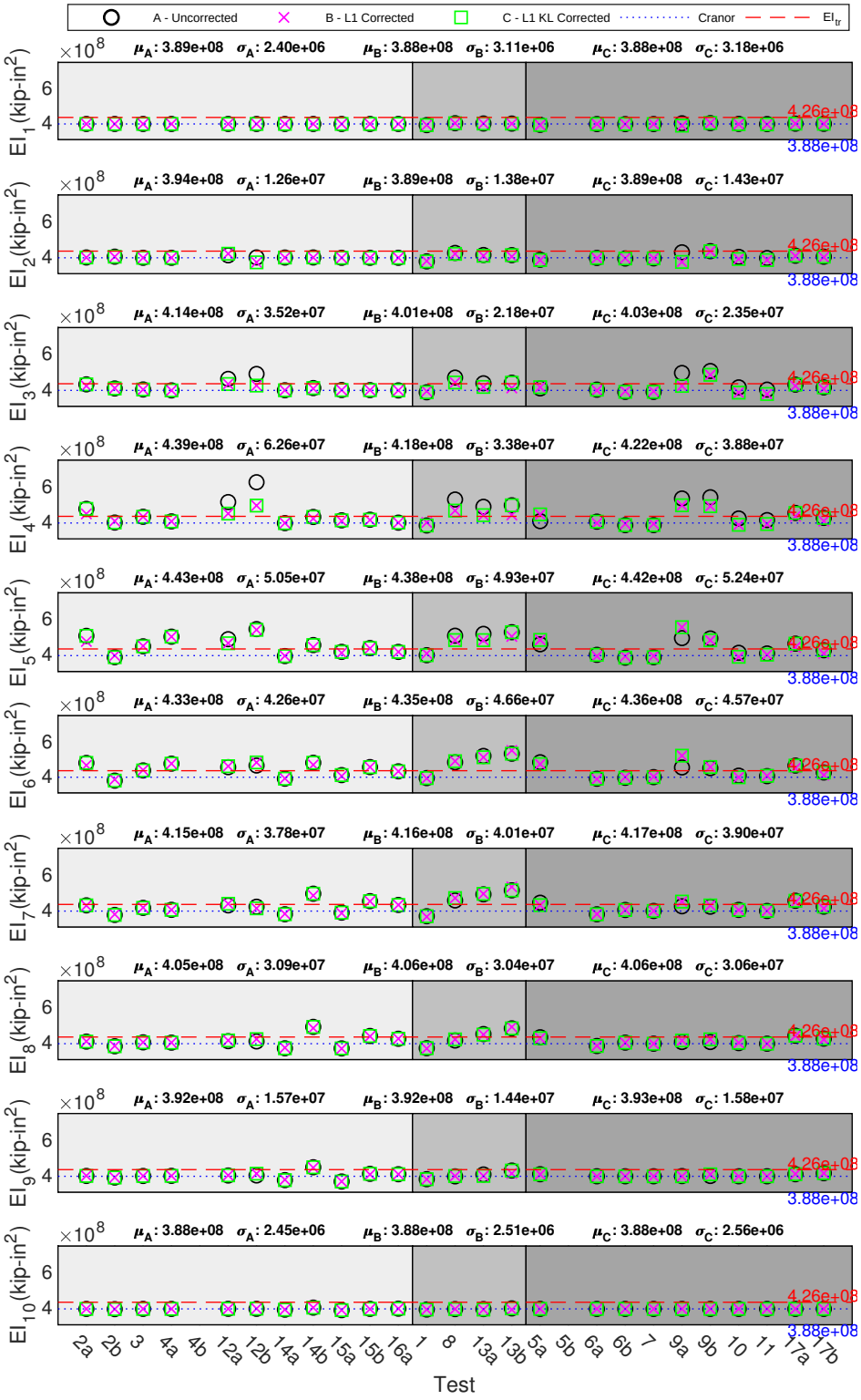

Fig. D.136. Ten EI values for Girder A when Bayesian analysis was applied: Distribution of EI identification for each test based on category

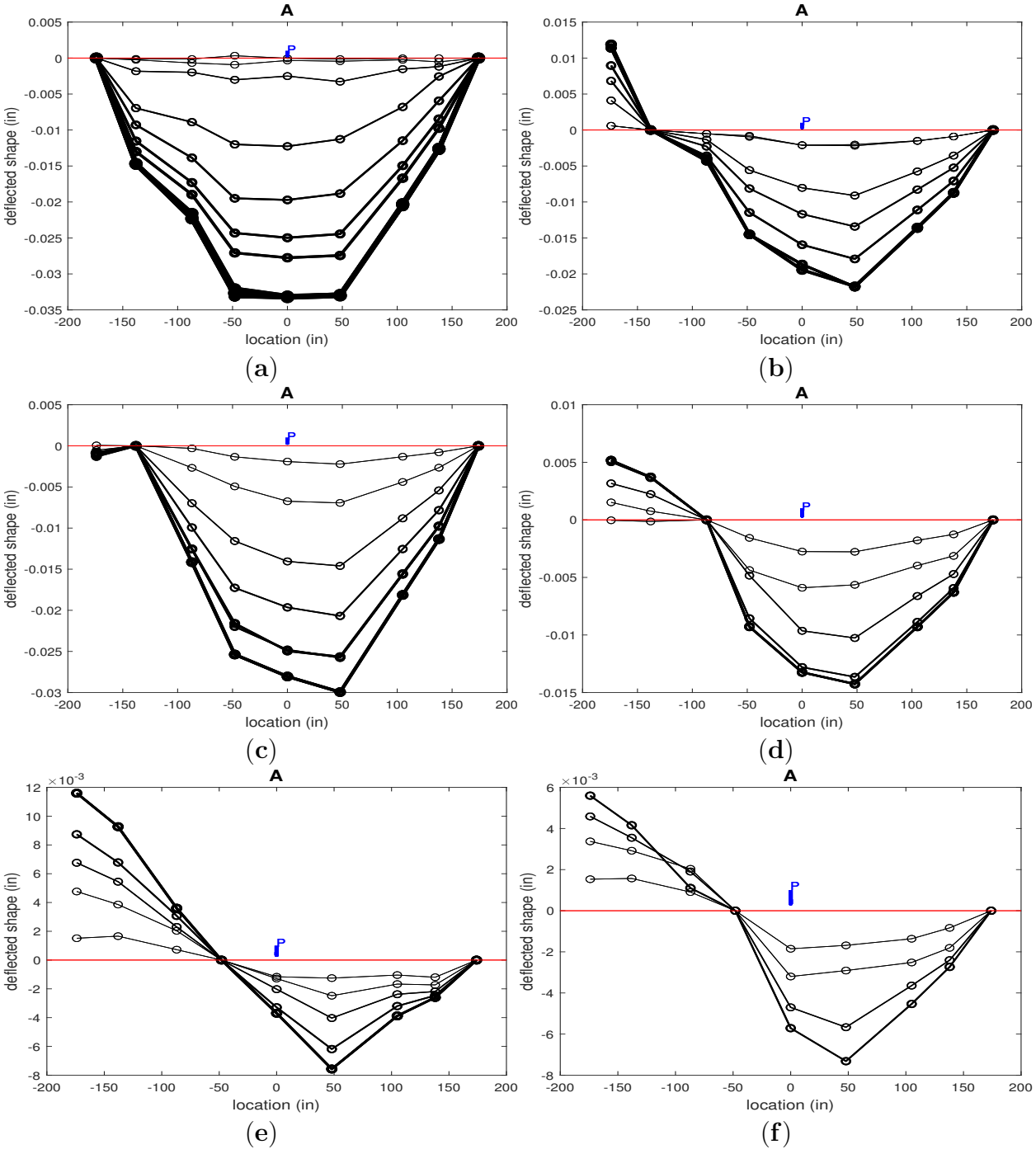

Fig. D.137. Deflected shapes with corresponding load location and zero deflection line for tests 1 (a), 2a (b), 2b (c), 3 (d), 4a (e), and 4b (f).

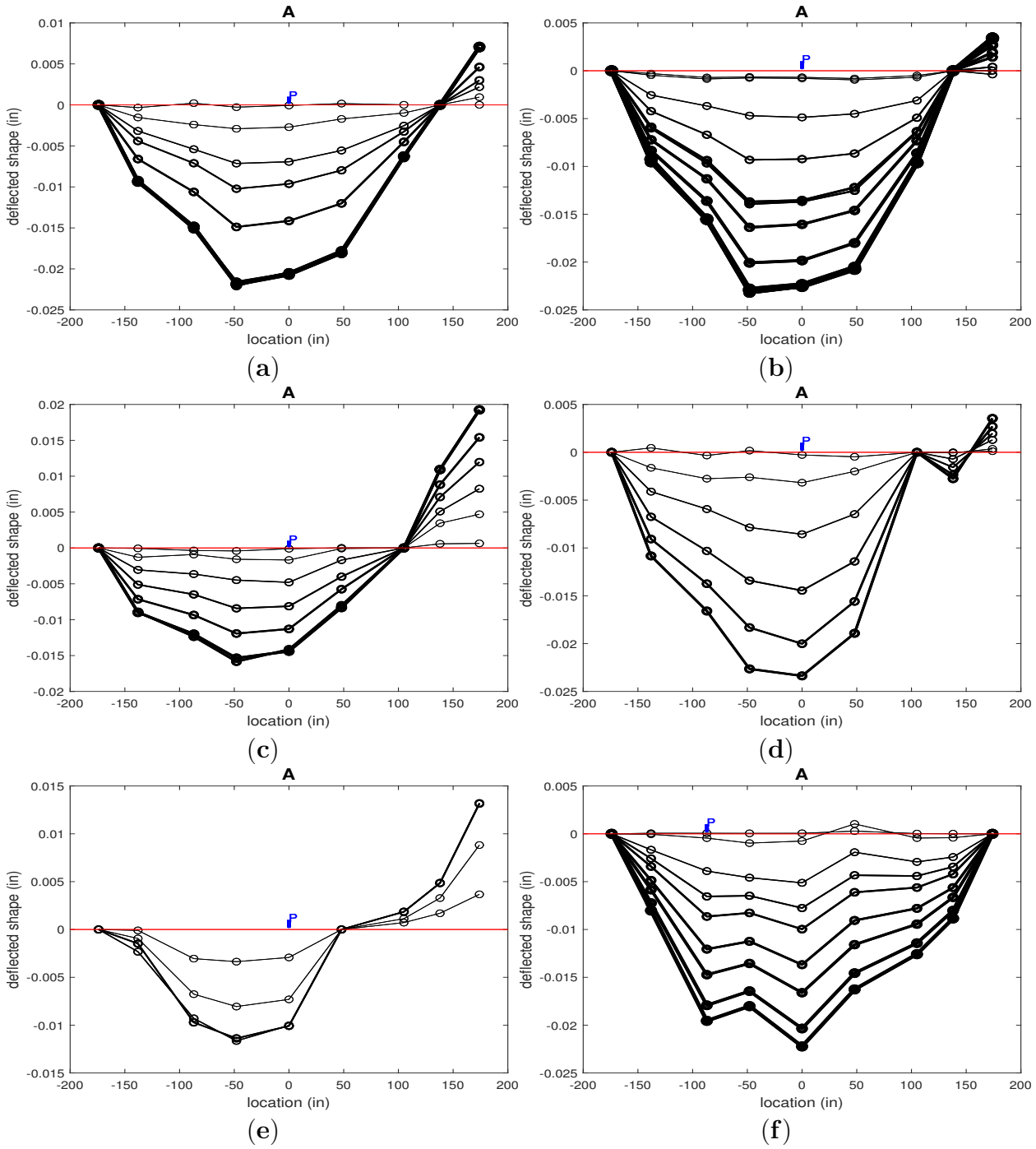

Fig. D.138. Deflected shapes with corresponding load location and zero deflection line for tests 5a (a), 5b (b), 6a (c), 6b (d), 7 (e), and 8 (f).

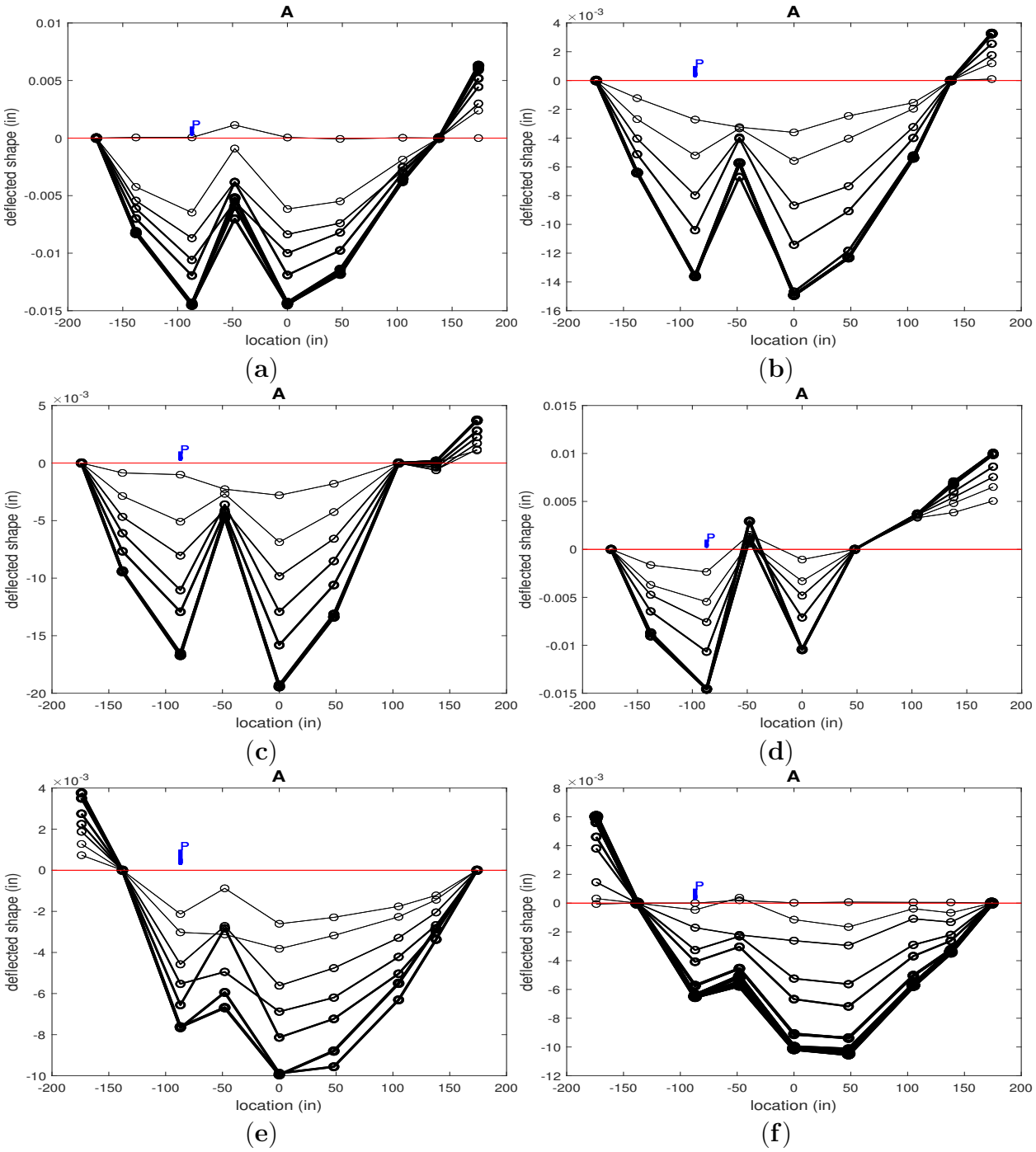

Fig. D.139. Deflected shapes with corresponding load location and zero deflection line for tests 9a (a), 9b (b), 10 (c), 11 (d), 12a (e), and 12b (f).

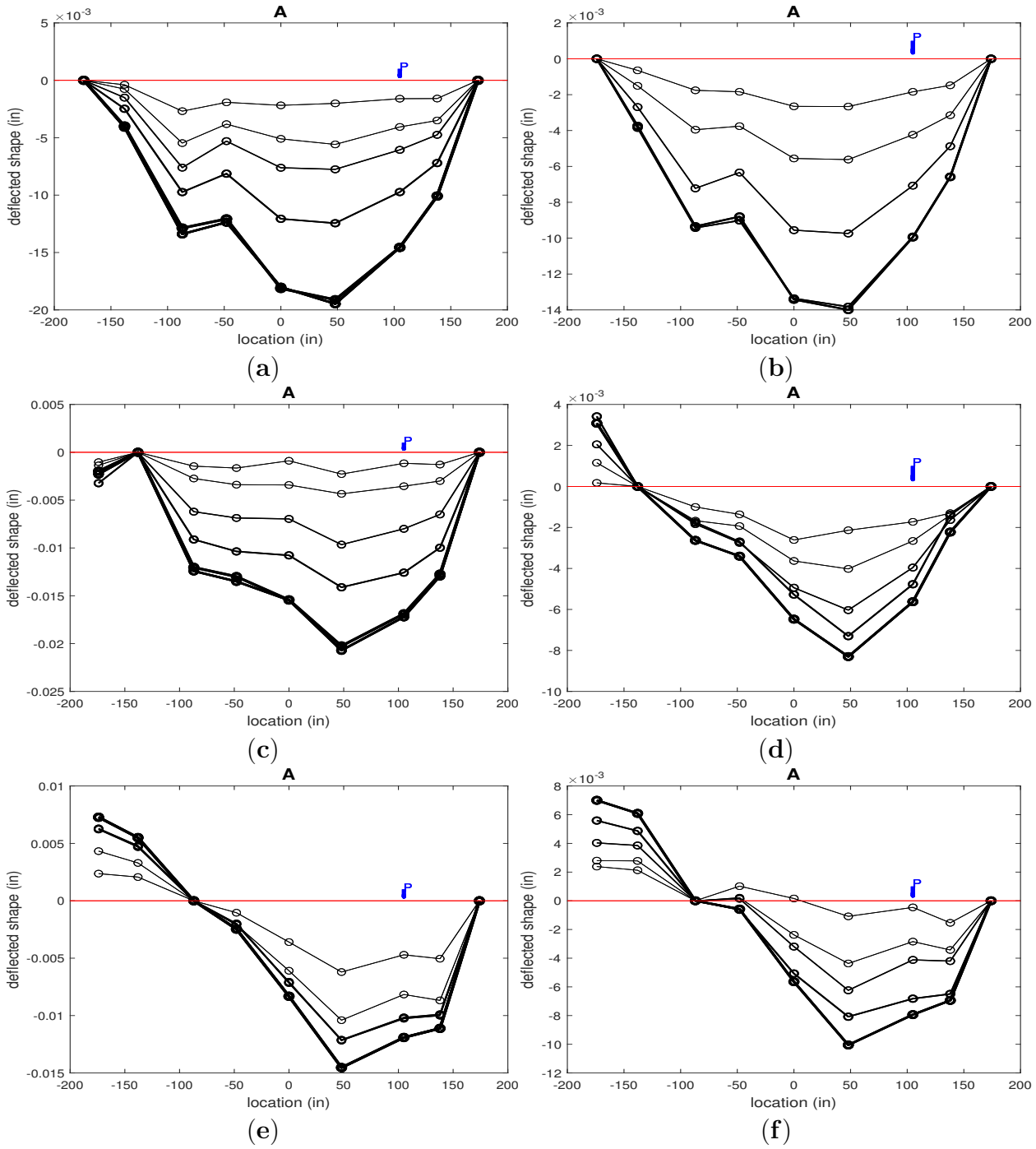

Fig. D.140. Deflected shapes with corresponding load location and zero deflection line for tests 13a (a), 13b (b), 14a (c), 14b (d), 15a (e), and 15b (f).

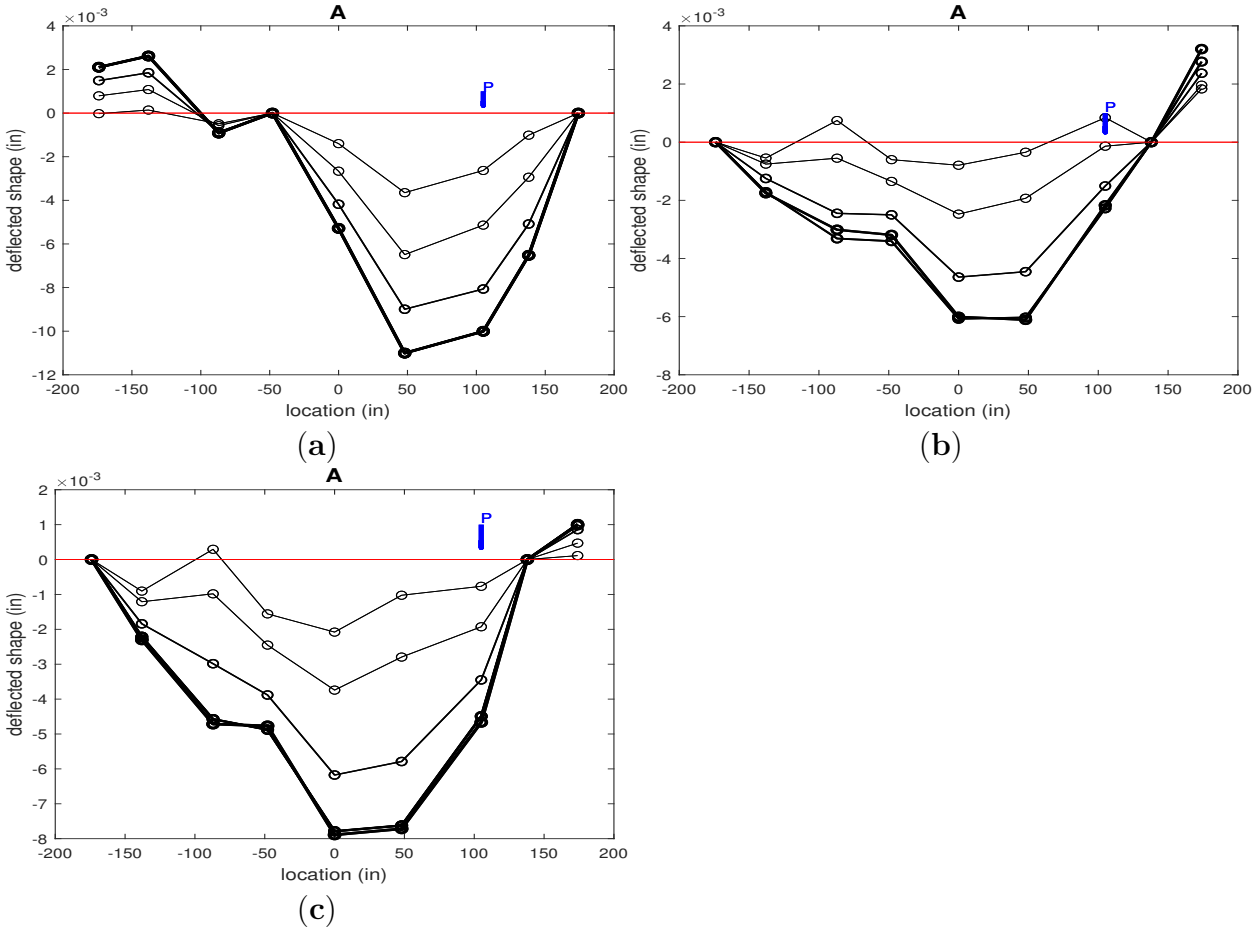

Fig. D.141. Deflected shapes with corresponding load location and zero deflection line for tests 16a (a), 17a (b), 17b (c).

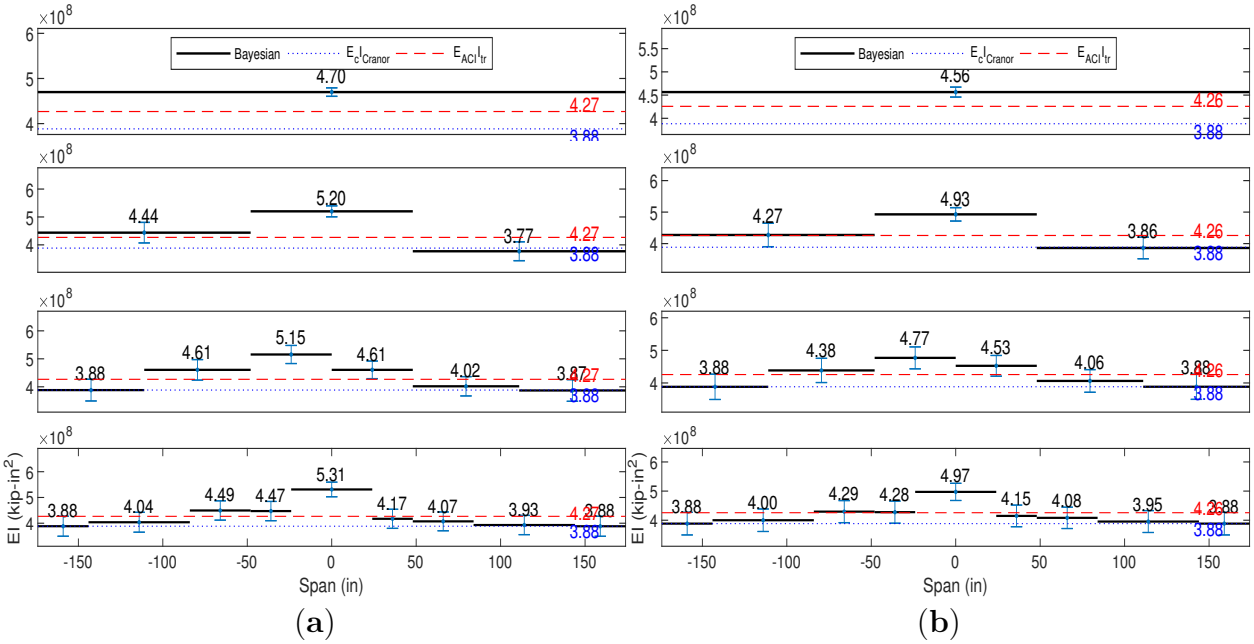

Fig. D.142. Test 2a Bayesian piecewise *EI* identification for categories *Uncorrected* (a) and *L*1 *Corrected* (b).

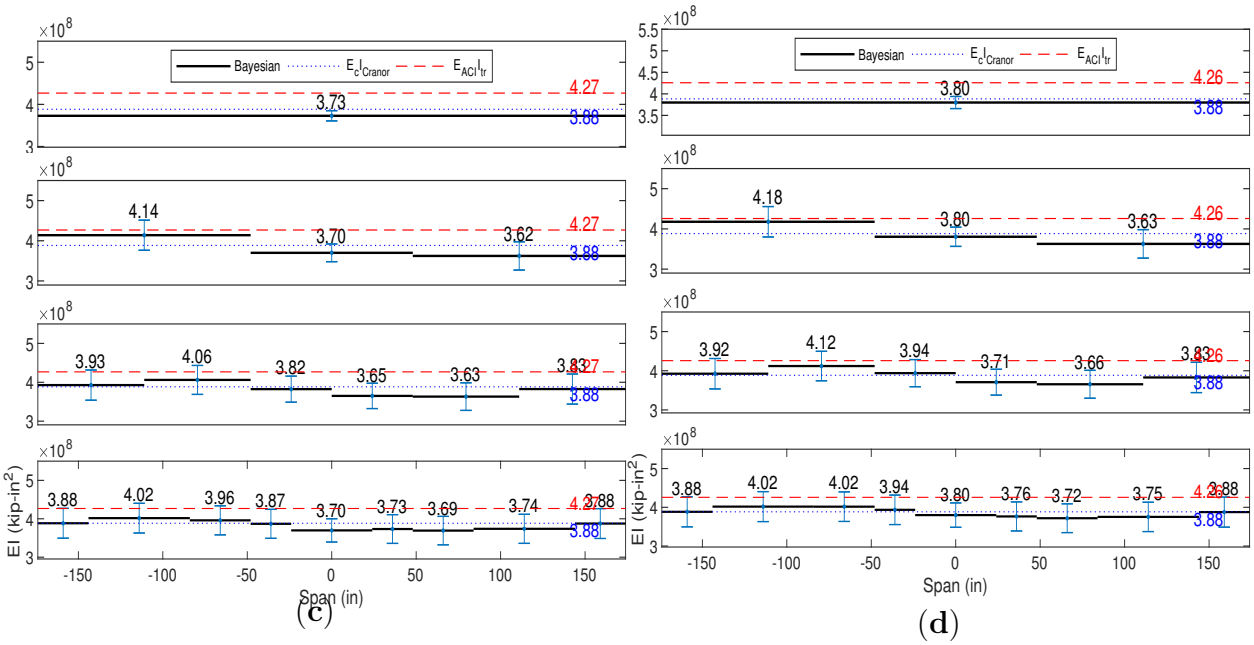

Fig. D.143. Test 2b Bayesian piecewise *EI* identification for categories *Uncorrected* (c) and *L*1 *Corrected* (d).

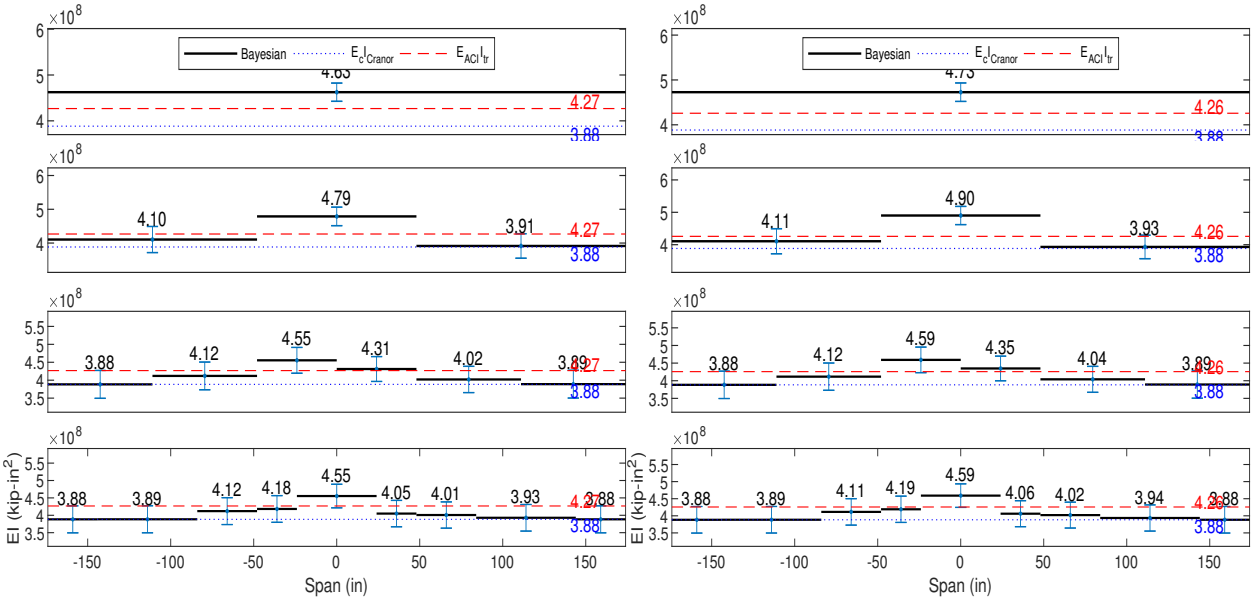

Fig. D.144. Test 3 Bayesian piecewise EI identification for categories *Uncorrected* (a) and *L*1 *Corrected* (b).

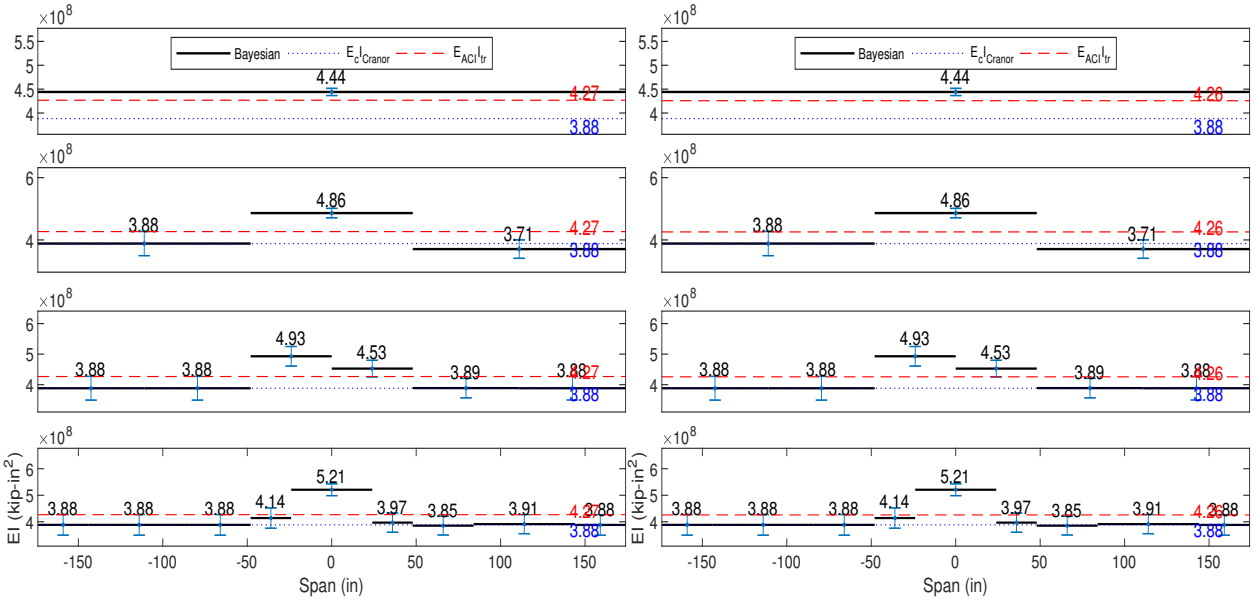

Fig. D.145. Test 4a Bayesian piecewise EI identification for categories *Uncorrected* (c) and *L*1 *Corrected* (d).

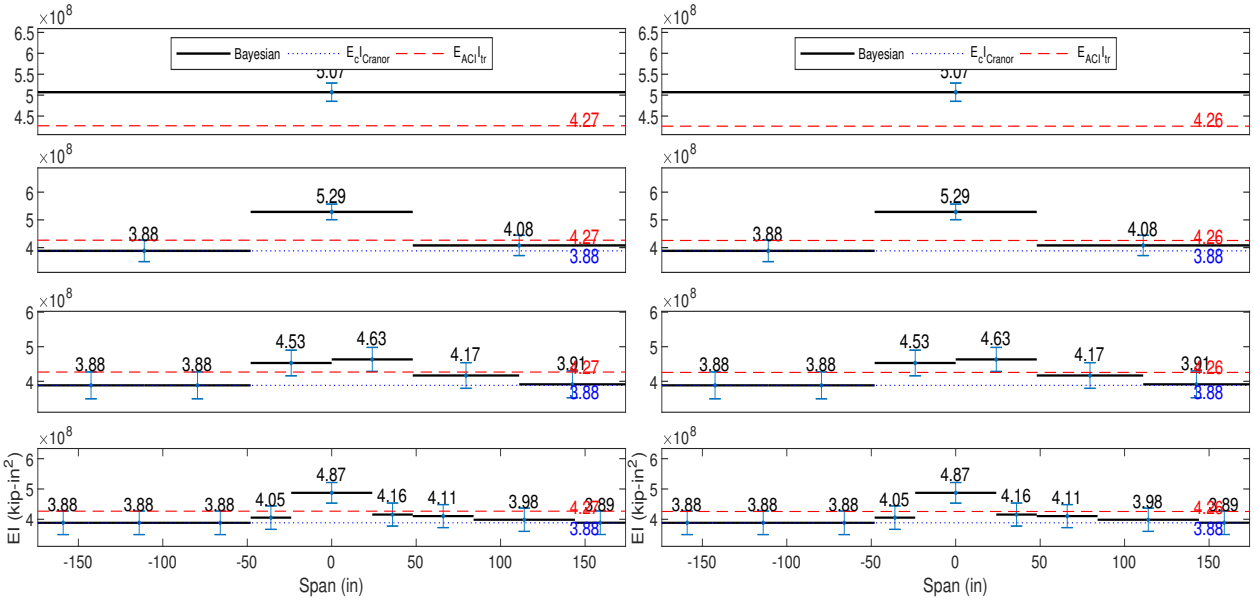

Fig. D.146. Test 4b Bayesian piecewise EI identification for categories *Uncorrected* (a) and $L1$ *Corrected* (b).

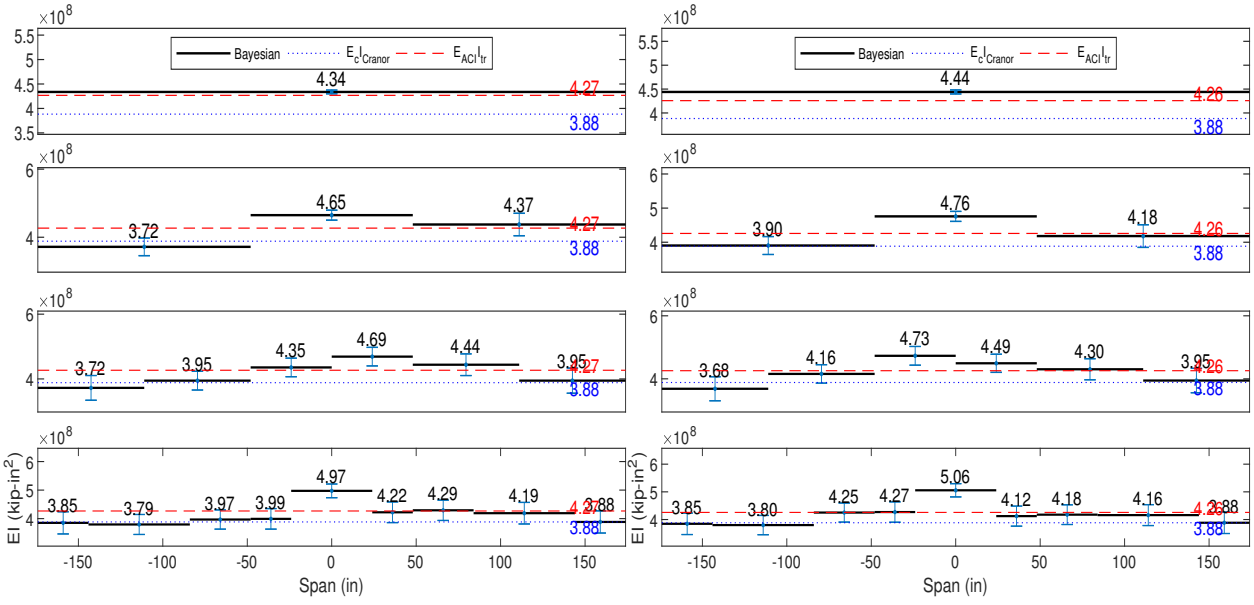

Fig. D.147. Test 5a Bayesian piecewise EI identification for categories *Uncorrected* (c) and $L1$ *Corrected* (d).

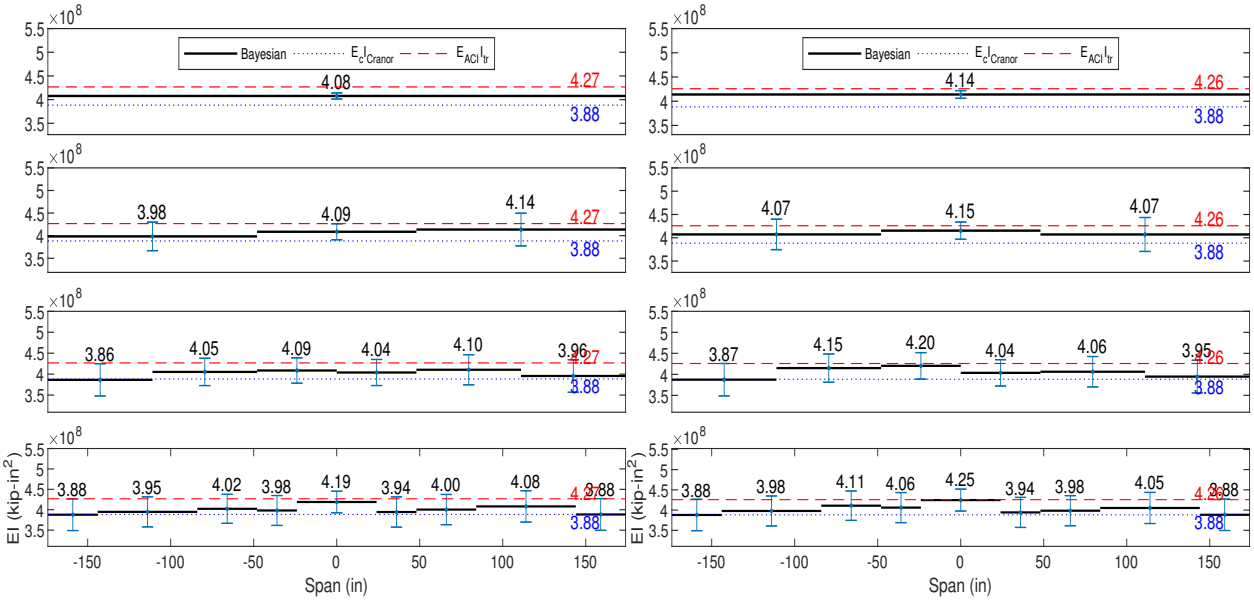

Fig. D.148. Test 5b Bayesian piecewise EI identification for categories *Uncorrected* (a) and $L1$ *Corrected* (b).

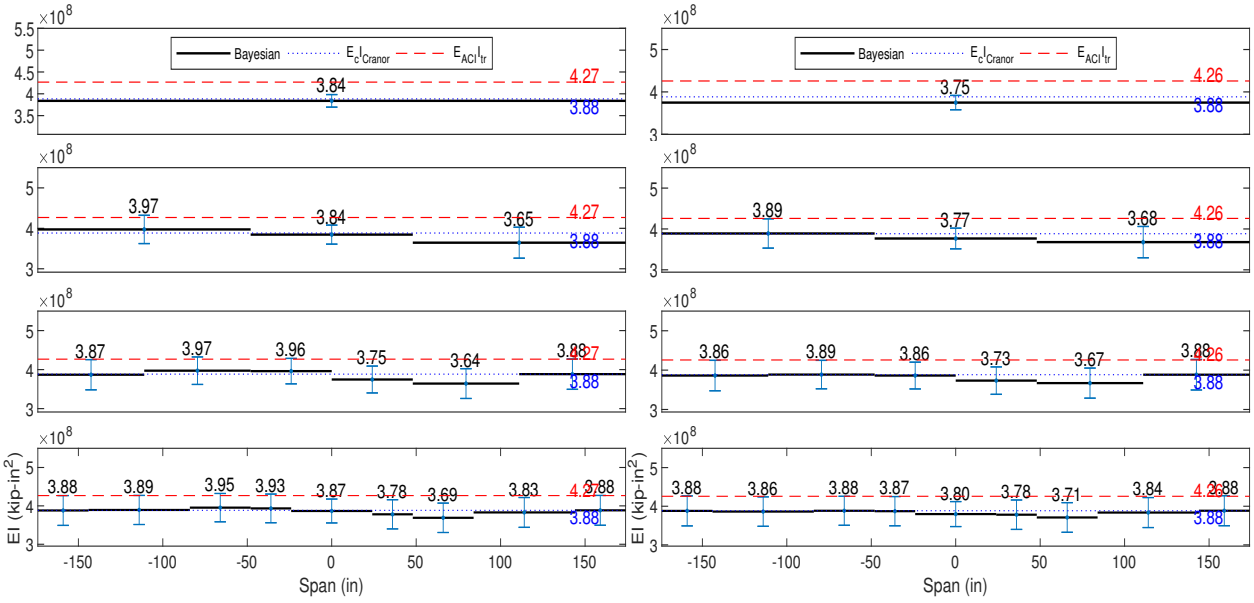

Fig. D.149. Test 6a Bayesian piecewise EI identification for categories *Uncorrected* (c) and $L1$ *Corrected* (d).

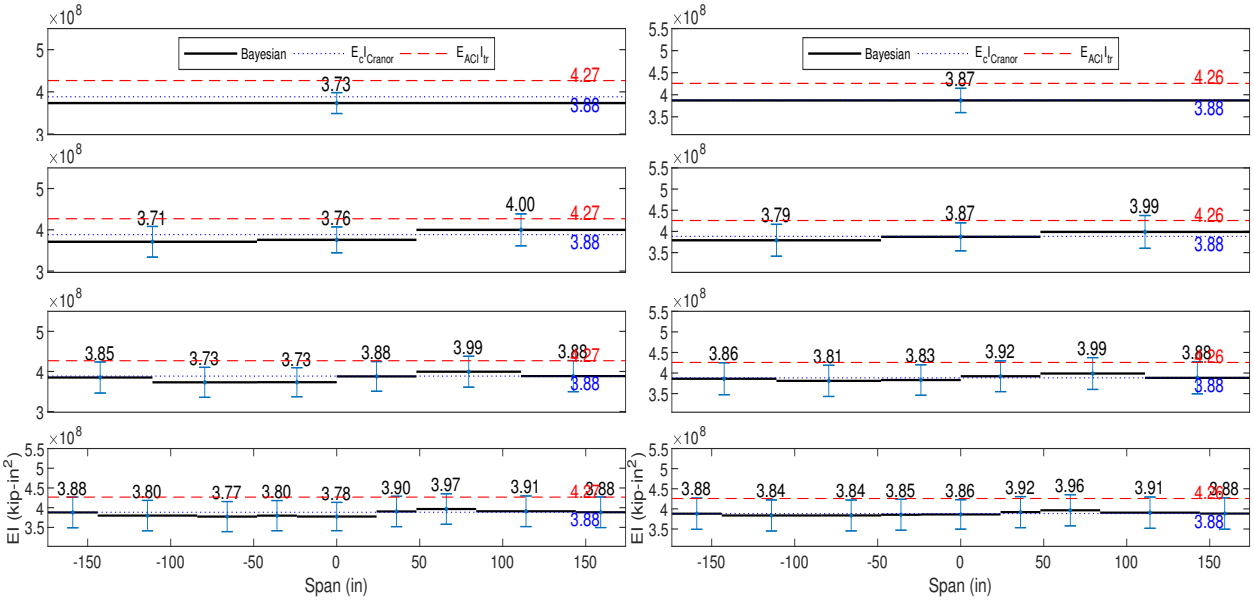

Fig. D.150. Test 6b Bayesian piecewise EI identification for categories *Uncorrected* (a) and $L1$ *Corrected* (b).

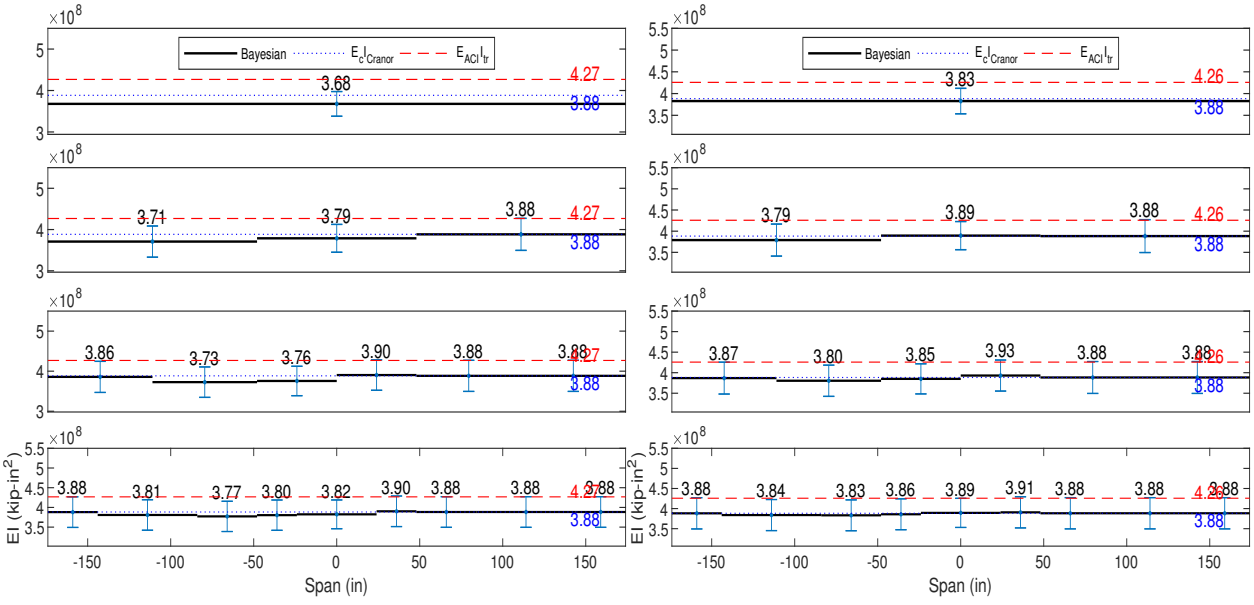

Fig. D.151. Test 7 Bayesian piecewise EI identification for categories *Uncorrected* (c) and $L1$ *Corrected* (d).

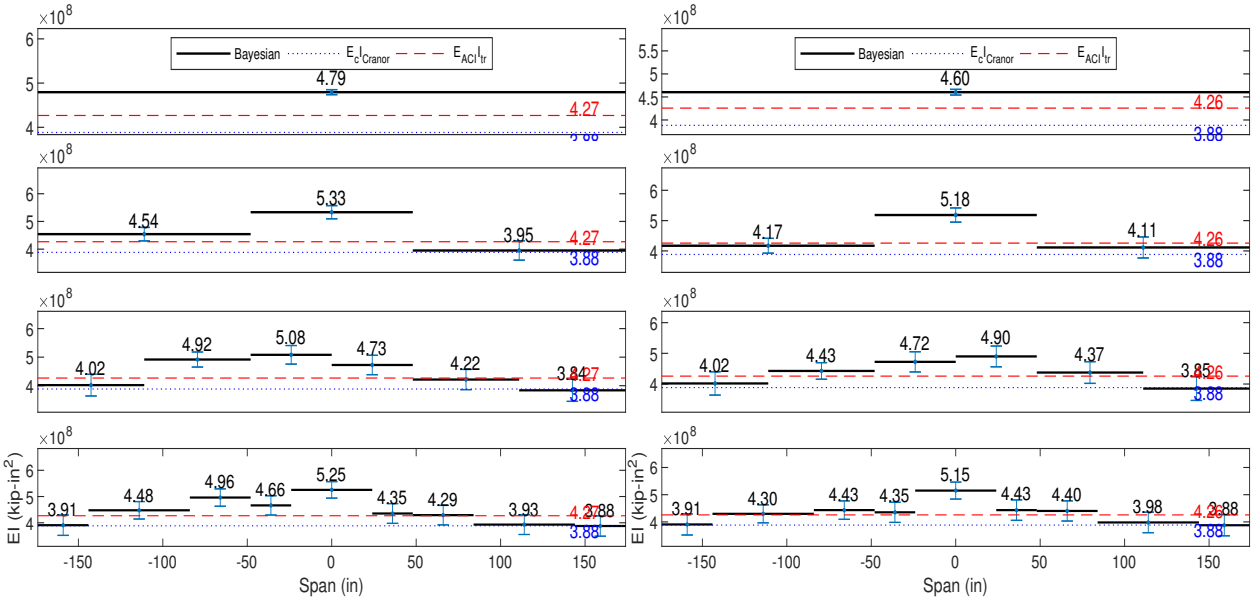

Fig. D.152. Test 8 Bayesian piecewise EI identification for categories *Uncorrected* (a) and *L*1 *Corrected* (b).

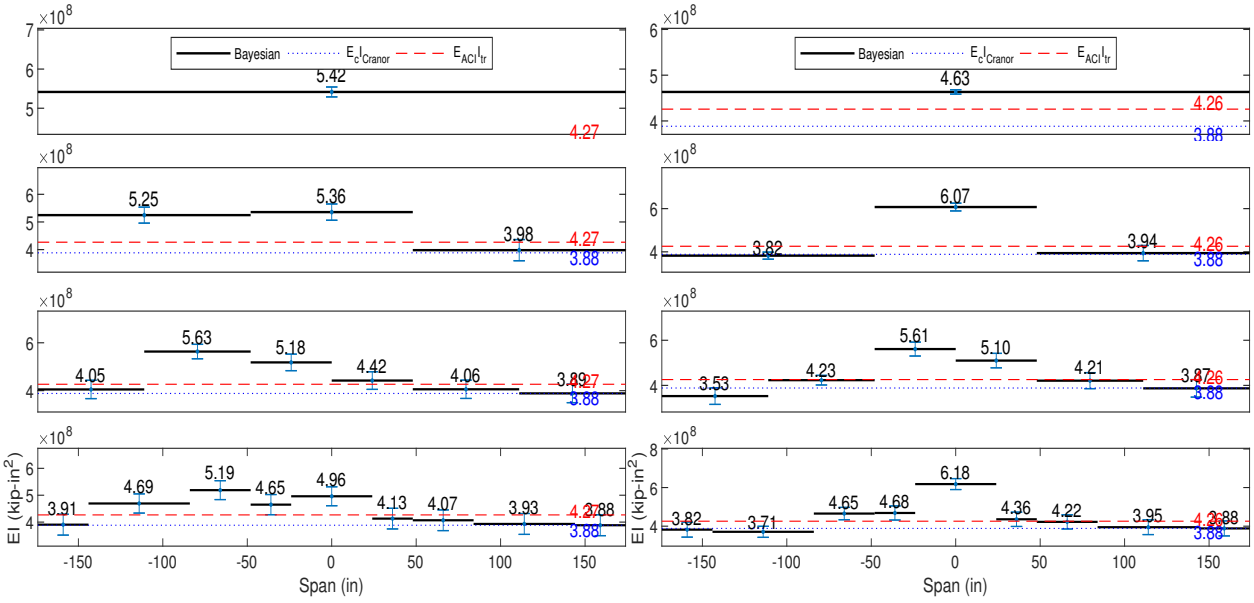

Fig. D.153. Test 9a Bayesian piecewise EI identification for categories *Uncorrected* (c) and *L*1 *Corrected* (d).

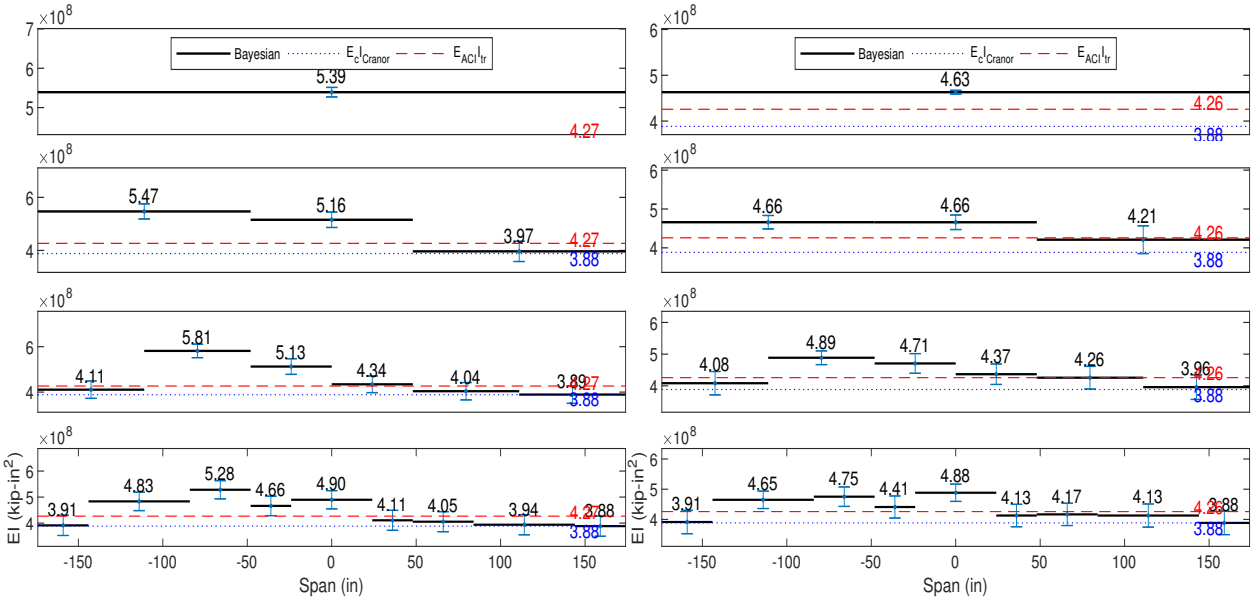

Fig. D.154. Test 9b Bayesian piecewise EI identification for categories *Uncorrected* (a) and $L1$ *Corrected* (b).

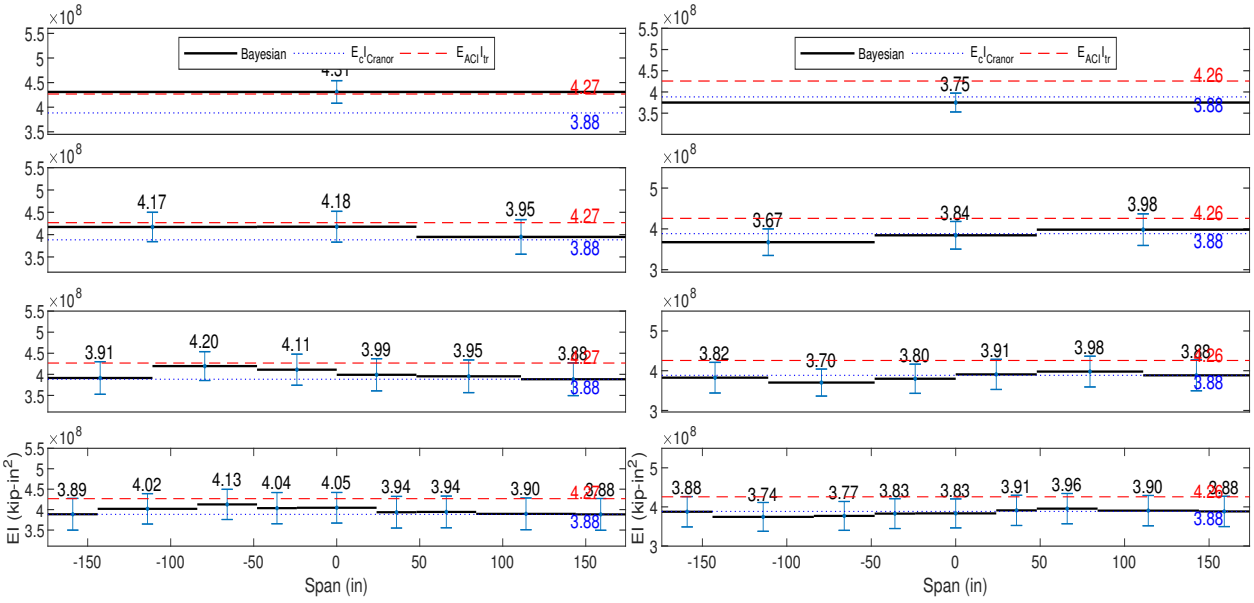

Fig. D.155. Test 10 Bayesian piecewise EI identification for categories *Uncorrected* (c) and $L1$ *Corrected* (d).

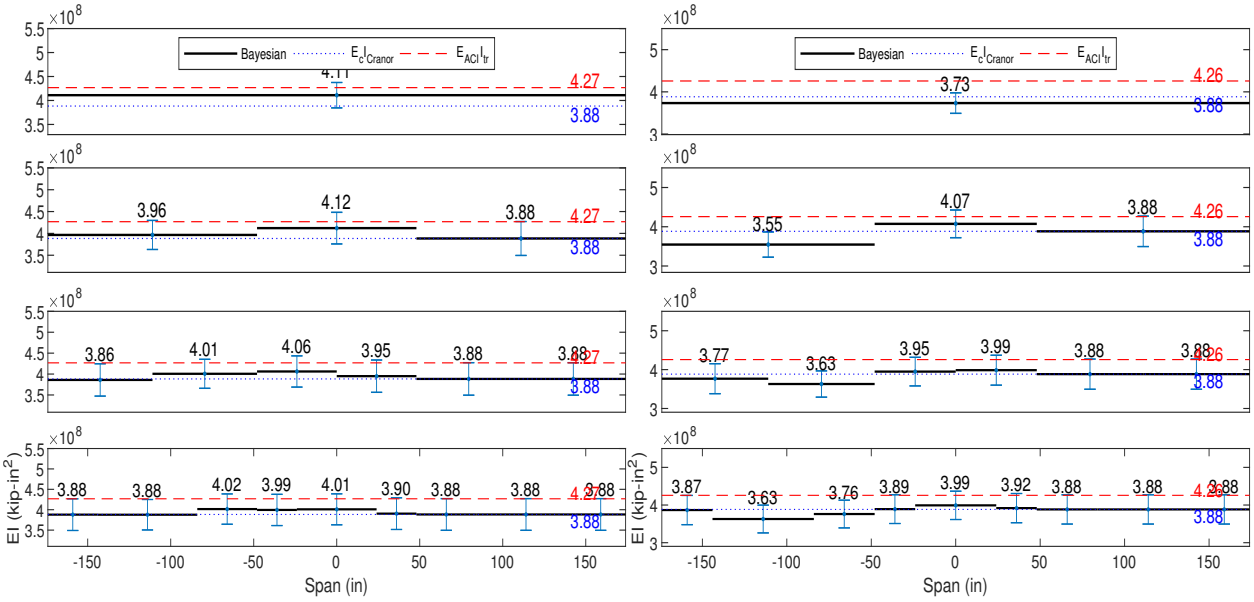

Fig. D.156. Test 11 Bayesian piecewise *EI* identification for categories *Uncorrected* (a) and *L*1 *Corrected* (b).

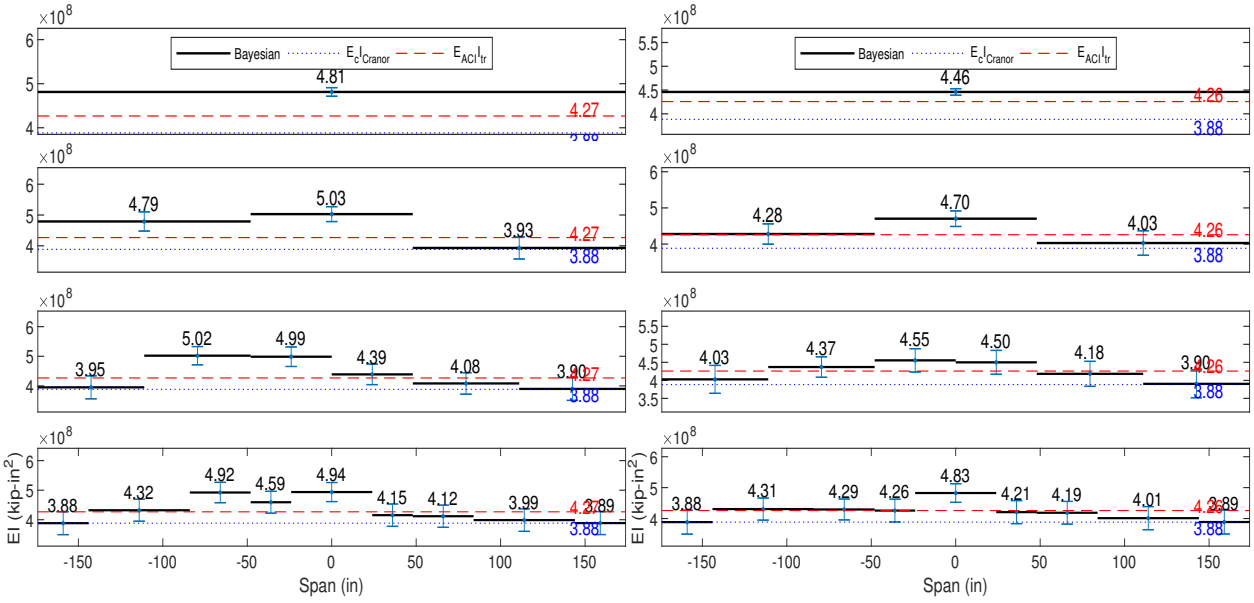

Fig. D.157. Test 12a Bayesian piecewise *EI* identification for categories *Uncorrected* (c) and *L*1 *Corrected* (d).

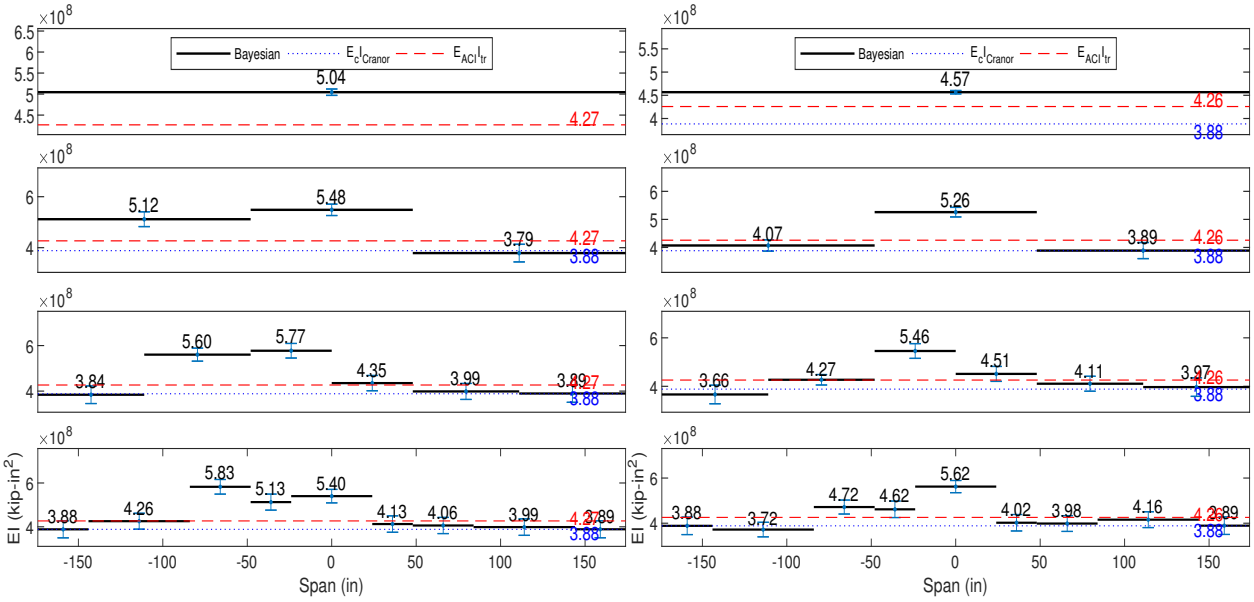

Fig. D.158. Test 12b Bayesian piecewise *EI* identification for categories *Uncorrected* (a) and *L*1 *Corrected* (b).

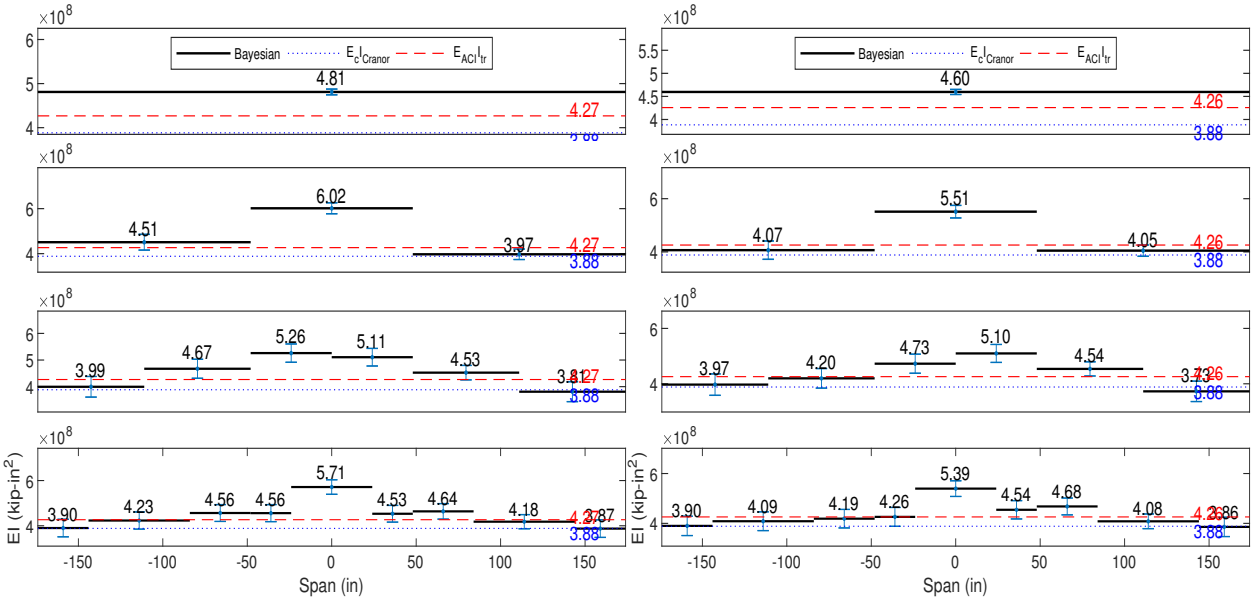

Fig. D.159. Test 13a Bayesian piecewise *EI* identification for categories *Uncorrected* (c) and *L*1 *Corrected* (d).

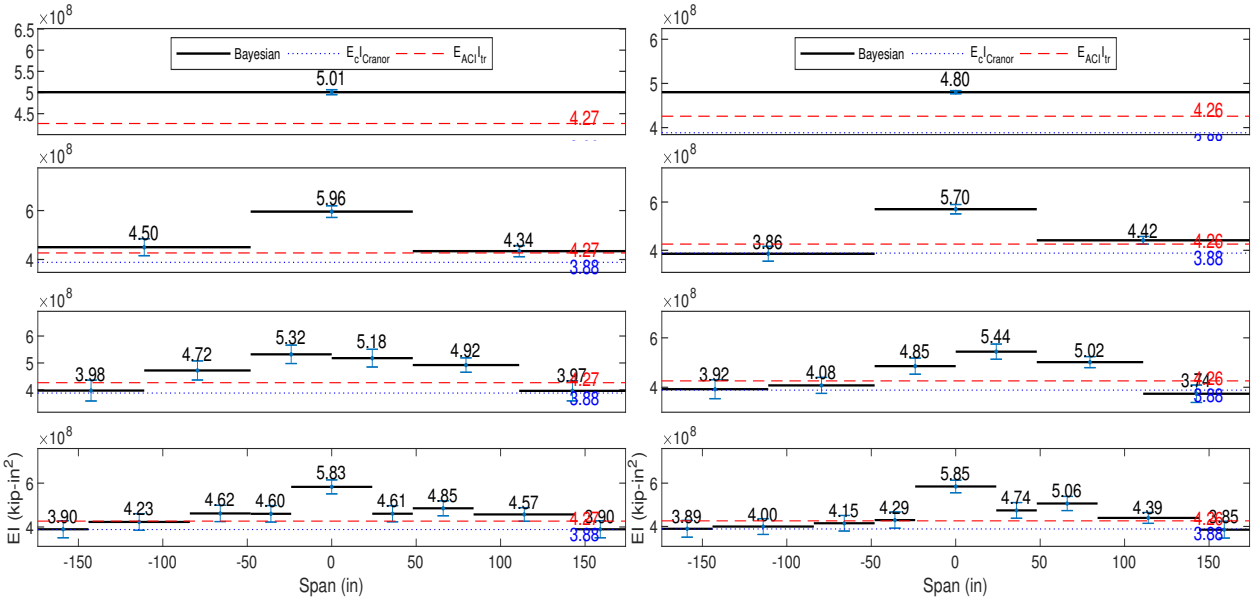

Fig. D.160. Test 13b Bayesian piecewise EI identification for categories *Uncorrected* (a) and $L1$ *Corrected* (b).

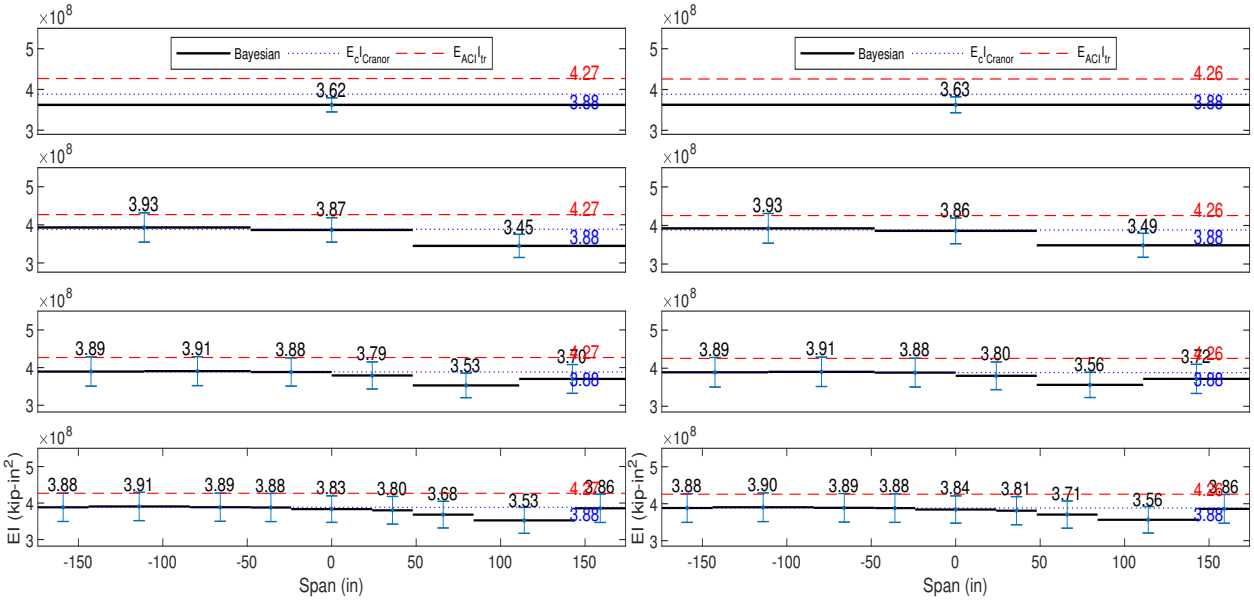

Fig. D.161. Test 14a Bayesian piecewise EI identification for categories *Uncorrected* (c) and $L1$ *Corrected* (d).

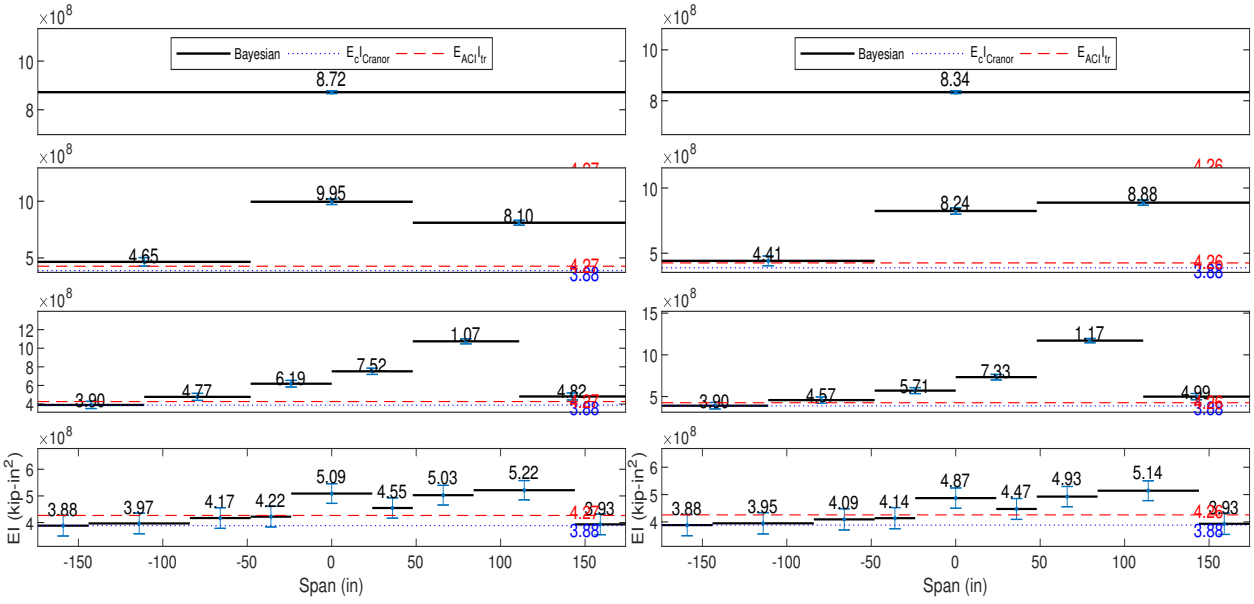

Fig. D.162. Test 14b Bayesian piecewise *EI* identification for categories *Uncorrected* (a) and *L*1 *Corrected* (b).

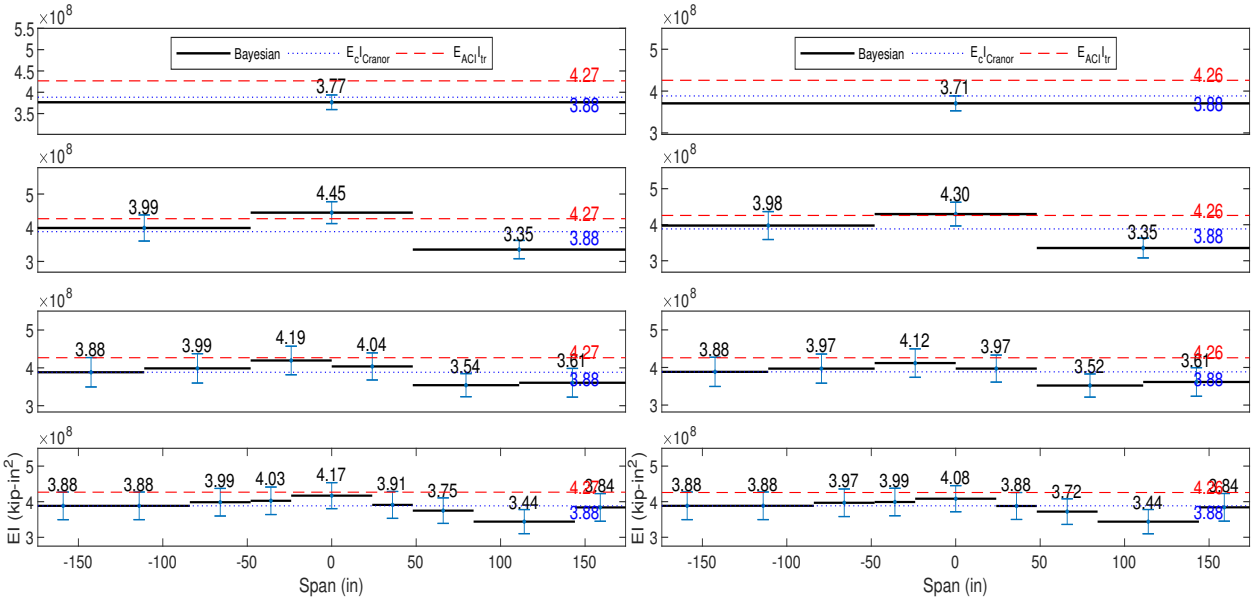

Fig. D.163. Test 15a Bayesian piecewise *EI* identification for categories *Uncorrected* (c) and *L*1 *Corrected* (d).

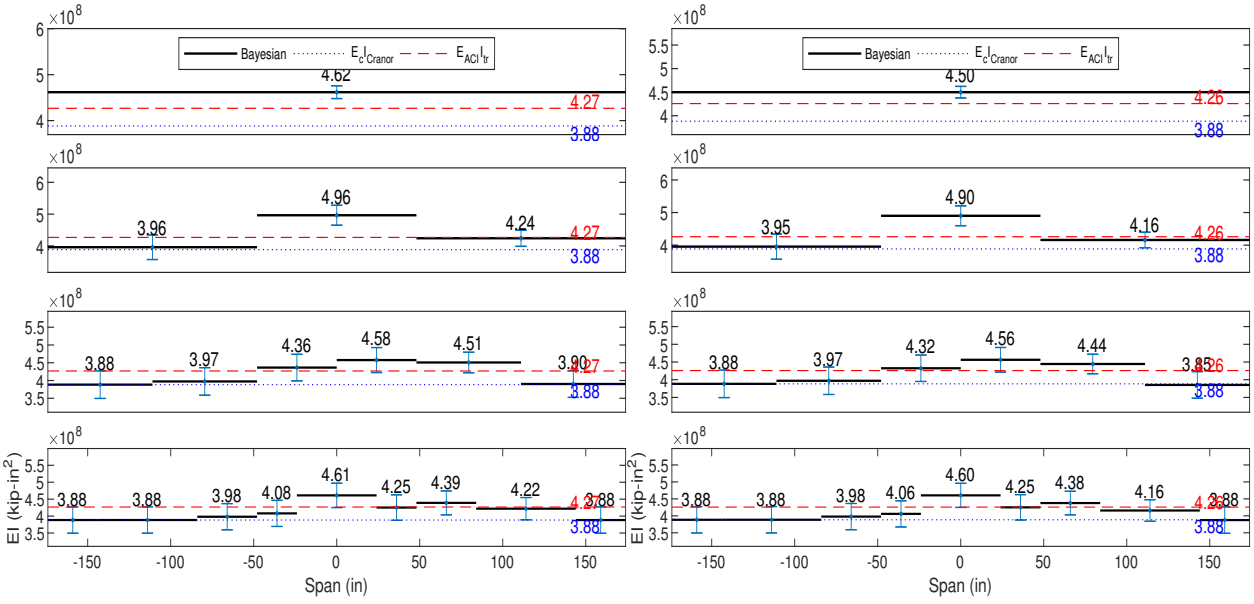

Fig. D.164. Test 15b Bayesian piecewise EI identification for categories *Uncorrected* (a) and $L1$ *Corrected* (b).

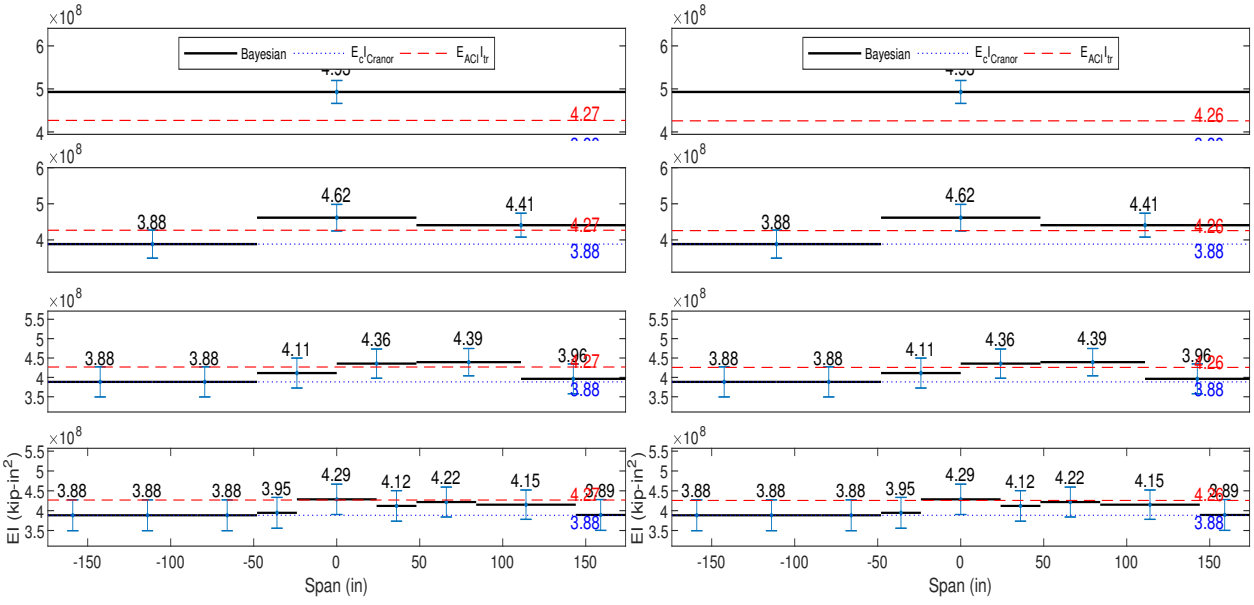

Fig. D.165. Test 16a Bayesian piecewise EI identification for categories *Uncorrected* (c) and $L1$ *Corrected* (d).

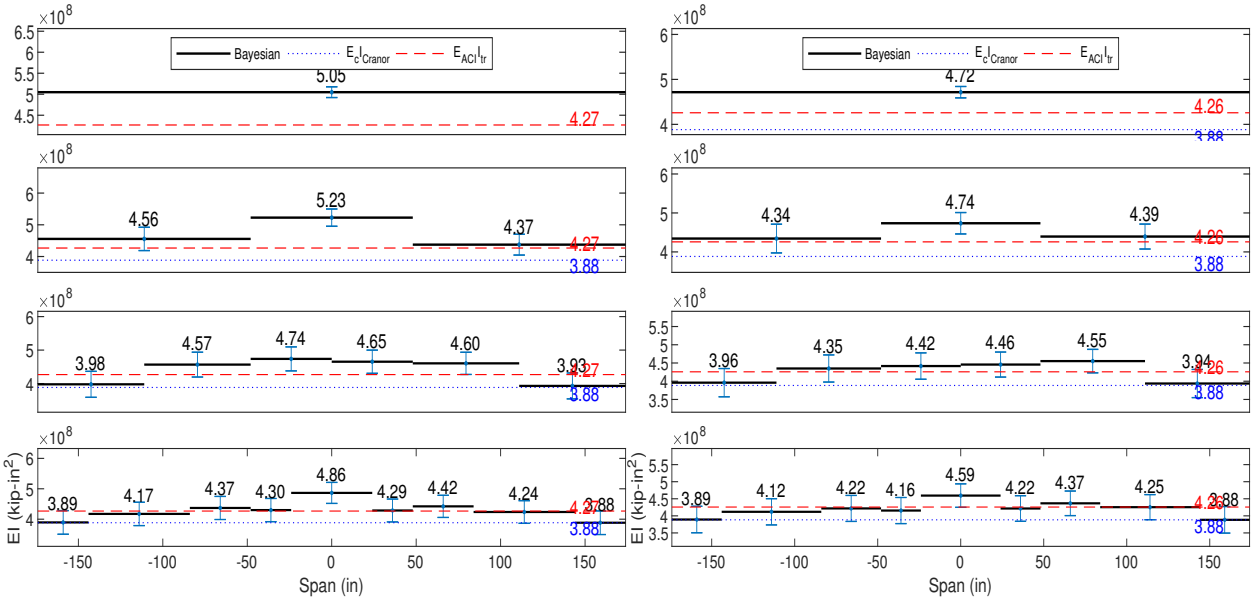

Fig. D.166. Test 17a Bayesian piecewise EI identification for categories *Uncorrected* (a) and $L1$ *Corrected* (b).

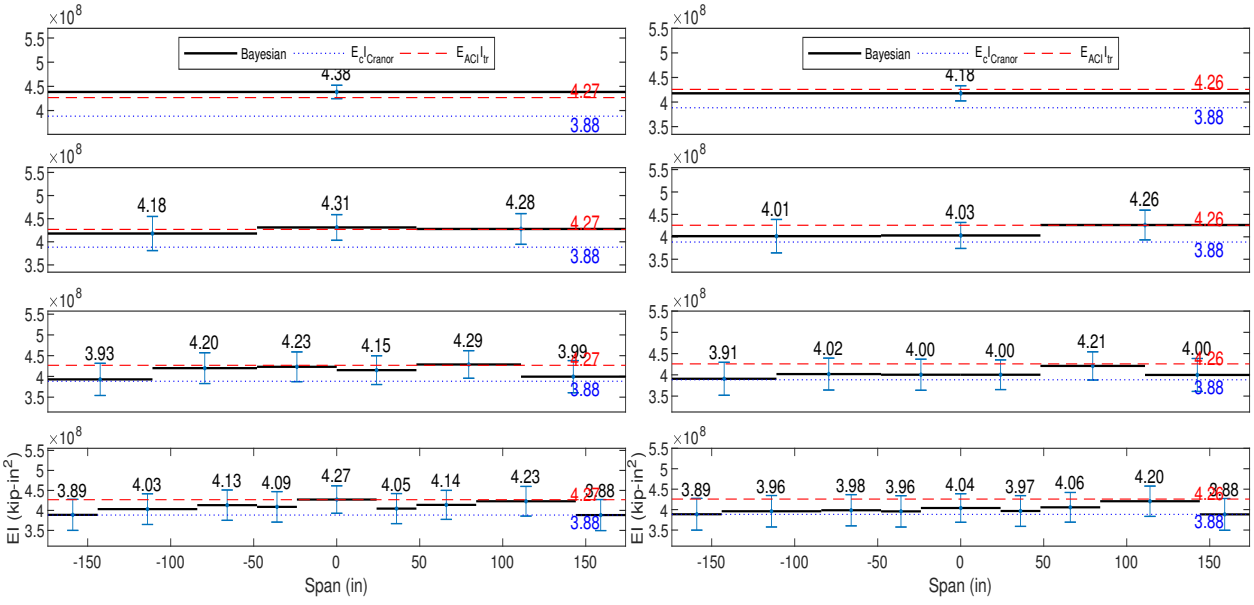

Fig. D.167. Test 17b Bayesian piecewise EI identification for categories *Uncorrected* (c) and $L1$ *Corrected* (d).